



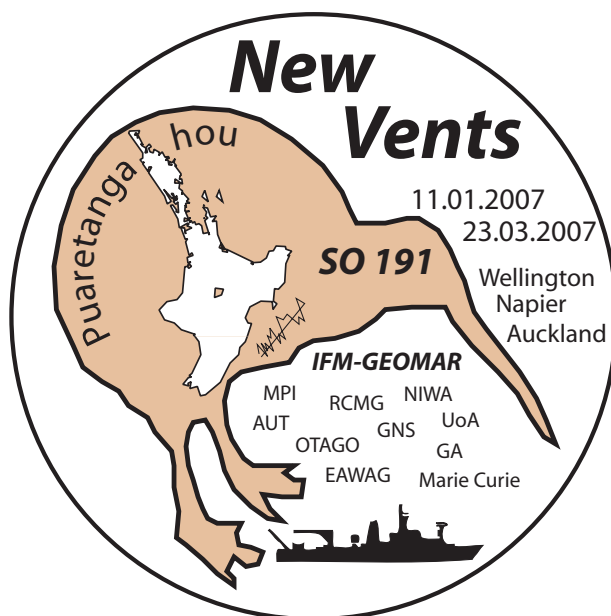
IFM-GEOMAR

Leibniz-Institut für Meereswissenschaften
an der Universität Kiel

**FS Sonne
Fahrtbericht / Cruise Report SO 191
New Vents**

"Puaretanga Hou"

Wellington - Napier - Auckland
11.01. - 23.03.2007



Berichte aus dem Leibniz-Institut
für Meereswissenschaften an der
Christian-Albrechts-Universität zu Kiel

Nr. 9
April 2007



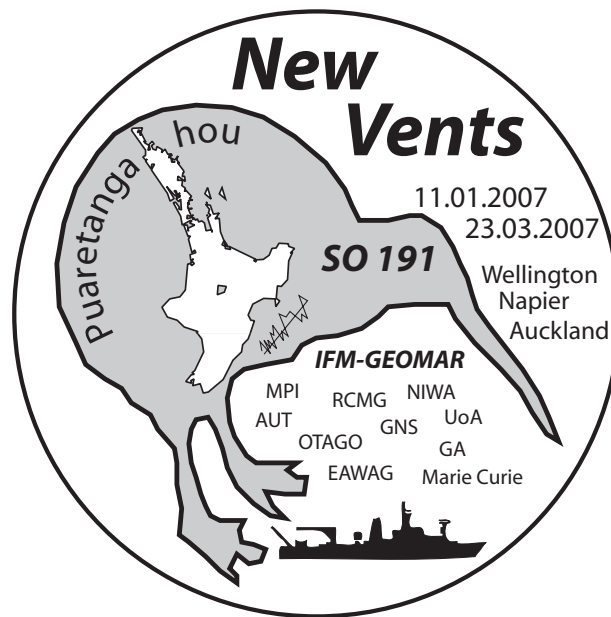
IFM-GEOMAR

Leibniz-Institut für Meereswissenschaften
an der Universität Kiel

FS Sonne Fahrtbericht / Cruise Report SO 191 New Vents

"Puaretanga Hou"

Wellington - Napier - Auckland
11.01. - 23.03.2007



Berichte aus dem Leibniz-Institut
für Meereswissenschaften an der
Christian-Albrechts-Universität zu Kiel

Nr. 9, April 2007

ISSN Nr.: 1614-6298



IFM-GEOMAR

Leibniz-Institut für Meereswissenschaften
an der Universität Kiel

Das Leibniz-Institut für Meereswissenschaften
ist ein Institut der Wissenschaftsgemeinschaft
Gottfried Wilhelm Leibniz (WGL)

The Leibniz-Institute of Marine Sciences is a
member of the Leibniz Association
(Wissenschaftsgemeinschaft Gottfried
Wilhelm Leibniz).

Herausgeber / Editor:

Jörg Bialas, Jens Greinert, Peter Linke, Olaf Pfannkuche

IFM-GEOMAR Report

ISSN Nr.: 1614-6298

Leibniz-Institut für Meereswissenschaften / Leibniz-Institute of Marine Sciences

IFM-GEOMAR
Dienstgebäude Westufer / West Shore Building
Düsternbrooker Weg 20
D-24105 Kiel
Germany

Leibniz-Institut für Meereswissenschaften / Leibniz-Institute of Marine Sciences

IFM-GEOMAR
Dienstgebäude Ostufer / East Shore Building
Wischhofstr. 1-3
D-24148 Kiel
Germany

Tel.: ++49 431 600-0
Fax: ++49 431 600-2805
www.ifm-geomar.de

Content:	page
1 Summary	3
2 Introduction	4
2.1 Aim of the Project	4
2.2 Regional Geologic–Tectonic Setting	5
2.3 Previous Investigations	7
3. Participants	10
3.1 Scientists	10
3.1.1 Scientists of Leg 1	10
3.1.2 Scientists of Leg 2	10
3.1.3 Scientists of Leg 3	11
3.2 Crew	12
3.2.1 Crew of Leg 1	12
3.2.2 Crew of Leg 2	12
3.2.3 Crew of Leg 3	13
4. Narratives	13
4.1 Cruise Narrative of Leg 1	13
4.2 Cruise Narrative of Leg 2	15
4.3 Cruise Narrative of Leg 3	17
5 Scientific Equipment	21
5.1 Shipboard Equipment	21
5.1.1 Navigation	21
5.1.2 Simrad EM120 Multibeam	21
5.1.3 PARASOUND	23
5.1.4 ADCP	23
5.1.5 CTD (Conductivity-Temperature-Depth) operations	23
5.1.6 OFOS	24
5.2 Computer Facilities	24
5.2.1 OBH/S Computer Facilities	24
5.2.2 Leg 1: NIWA, GNS Science, and University of Otago	25
5.3 Geophysical Instrumentation	25
5.3.1 Airguns	25
5.3.2 Seismic Streamer	27
5.3.3 OBH/OBS Seismic Instrumentation	29
5.4 Sidescan sonar	31
5.5 CSEM – Controlled Source Electro-Magnetics	33
5.6 Magnetotelluric Instrumentation	37
5.7 Geological Instrumentation	39
5.7.1 THP Temperature Sensors	39
5.7.2 Coring devices	40
5.8 ROV “GENESIS”	40
5.9 Thermistor Moorings	42
5.10 Surface Methane Concentrations: Equilibrator Measurements	42
5.11 Water Column Methane Analyses	43
5.12 Radon (²²² Rn) Measurements	44
5.13 Lander Deployments	44
5.14 Foraminiferal and Metazoan Biology	49
5.15 Microbial Ecology	50
5.16 Geochemical Investigations	51
5.17 Carbonate Sampling Program	53
6 Work completed and first results	53
6.1 Hydroacoustics	53
6.2 DTS-1 Operations	54
6.2.1 Builder’s Pencil	54

6.2.2	Wairarapa.....	56
6.2.3	Uruti Ridge	61
6.2.4	LM9 area	62
6.2.5	Rock Garden	64
6.3	Seismic Studies	66
6.3.1	Builder’s Pencil (P01)	66
6.3.2	LM-9 (P05)	72
6.3.3	Uruti (P04).....	74
6.3.4	Wairarapa (P03).....	79
6.4	CSEM - Controlled Source Electro- Magnetics	84
6.5	Heatflow.....	86
6.6	OFOS Surveys.....	88
6.7	ROV Deployments	91
6.8	Methane Measurements	95
6.8.1	Surface Methane Concentrations: Equilibrator Measurements	95
6.8.2	CTD and Water Column Methane Measurements	97
6.8.3	OBM Measurements at Seismic Profile P05.....	108
6.9	Thermistor Moorings	109
6.10	Lander Deployments.....	113
6.11	Foraminiferal and Metazoan Biology	120
6.12	Microbial Ecology	122
6.13	Geochemistry	125
6.14	Radon Measurements	131
6.15	Carbonates.....	132
7	Regional Work	134
7.1	Multichannel Seismic Reflection Study	134
7.2	Higher-Resolution Imaging for Gas Hydrates.....	136
7.3	Controlled Source Electro-Magnetics – Ingo’s Site.....	136
8	Acknowledgements.....	138
9	References:	138
10.	Appendices	140
10.1	List of Gears and Biogeochemical Parameters determined.....	141
10.3	List of Porewater Sampling Sites and Collected Sub-samples.....	144
10.4	CSEM Measure Points	146
10.5	Table of OBS Deployments	147
10.6	Maps of Coring Stations	148
10.7	Map of Lander and Mooring Stations.....	151

1 Summary

During cruise SO191 with R/V SONNE three scientific legs were carried out along the Hikurangi Margin offshore the Eastcoast of the North Island of New Zealand. Here a large number of cold seeps were already known from previous cruises, which had been in part investigated by bathymetric, seismic and geochemical analysis. Nevertheless a wide range of questions according the build up, life time, internal structure, long term behaviour, etc. is still waiting for an answer, not only regarded to this area but to other occurrences of seeps world wide. Therefore the project NewVents, funded by the German Federal Ministry of Education and Science (BMBF), set out to achieve further insight into such seeps sites with a multidisciplinary approach applying the most recent available technologies in a combined effort at this location.

Based on previous observations provided by GNS and NIWA three major areas along the Hikurangi Margin were identified for investigation during the three cruise legs. From Wairarapa at the Southern tip of the North Island up to LM-9 and further north to Rock Garden, at the northern tip of Hawkes Bay sites with several active seeps were chosen, which should represent the variety of such locations along the margin.

The 1st leg was dedicated to acoustic investigations as a presite survey for the following detailed sampling by the geochemical and biological groups. Supported by existing bathymetric maps and additional high resolution mapping detailed maps of the morphology of the investigation areas were provided. Based on these maps successful profile planning could be done, which resulted into well placed OBS and Methane sensor deployment right on top of active seep sites. Three high resolution seismic networks were recorded by multichannel streamer and Ocean Bottom Seismometers. Thanks to the good data quality detailed velocity depth information will be available as well as high resolution image of the sediment interfaces. Due to the dense grid spacing small scale variations within sediment structures and gas/hydrate related reflectivity will be precisely mapped in 3D. Together with deep towed sidescan sonar observations active seep locations and the involved seafloor alteration could be mapped in great detail. The integration of high frequency images achieved from shipboard Parasound and deep towed subbottom profiler with the deeper penetrating airgun seismic images enabled to follow fluid pathways through the entire sediments towards the seafloor. Already from shipboard processing seismic and sidescan images and maps could be provided with clear identification of gas fronts and active seep locations, which were used to precisely identify sampling locations for the following legs. Five regional seismic lines complete the seismic coverage for the tectonic understanding of the processes at the Hikurangi Margin.

The detailed bathymetric and side scan sonar mapping performed during leg 1 was continued during leg 2 as it proved to be an excellent working basis for the thorough sampling program which mainly contributed to the GEOTECHNOLOGY collaborative projects COMET and MUMM II. High resolution side scan sonar mapping and video surveys of morphological suspicious areas previously detected provided a clear image of the spatial dimensions of the chemoherms in the different working areas. At these sites beside cemented carbonate blocks and chemoautotrophic communities dark sediment patches were found which proved to be densely colonized with polychaetes. This novel manifestation of cold seep activity was studied in great detail with all sampling gear including the video-guided observatories. High resolution CTD and rosette profiles yielded complex snapshots of the methane distribution in the water column. Thermistor moorings were deployed to gain information on the physical microstructure and stability of the water column, both of which have an impact on the stratification/distribution and retention time within it.

Leg 3 continued the investigations of leg two mainly in the frame work of the BMBF collaborative projects COMET and MUMM II. The sites surveyed and selected during leg 2 were revisited and studied in detail. Station works concentrated to the region of Okamere Ridge and Rock Garden off Napier and the Wairarapa Region off the southern tip of the Northern Island. Investigations focused on the measurement of benthic boundary layer bio-geochemical fluxes, fluid and gas flows and the investigations of specific ecosystems such as anoxic chemosynthetically based sediment communities. As a new instrument a ROV was employed during the cruise to study methane seeps in fine scale resolution and to make in situ measurements. All other instruments were already deployed during leg two.

2 Introduction

2.1 Aim of the Project

The overriding aim of the cruise SO191 **New-Vents** was the detailed investigation of different cold vent and gas hydrate sites at the Hikurangi Margin on the east coast of New Zealand (Figure 2.1.1).

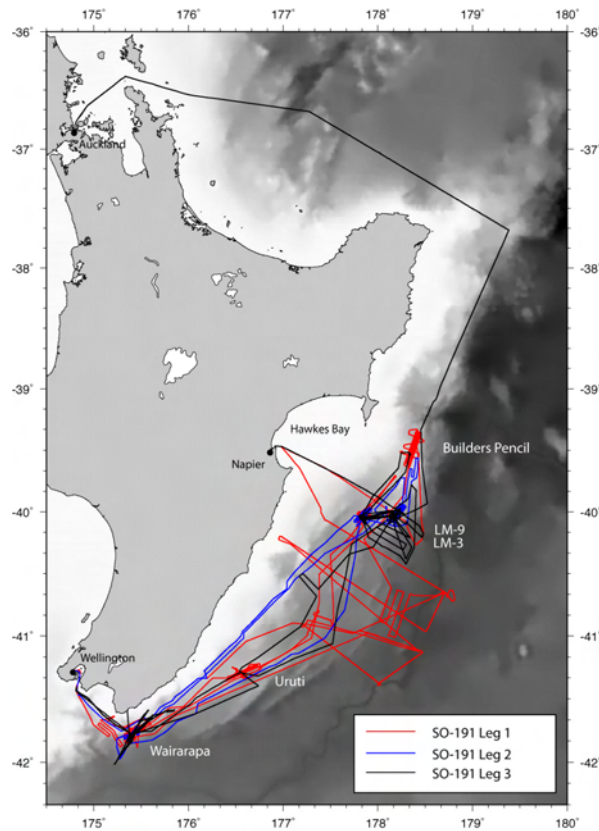


Figure 2.1.1: Map of the east coast of New Zealand; tracks of cruise SO191 are given in individual colors; major working sites are identified with their regional acronyms.

Target of the investigation was to study whether and how surface and sub-surface expressions of cold vents and related gas hydrates are connected to different geological, bathymetrical and geochemical conditions. A broad range of geophysical, geological, geochemical and biological investigations were carried out to complete a very detailed investigation of the working areas from a large scale (seismic) to a very small scale (microbiology). These investigations included:

- 1: OBH/OBS and multi-channel seismic (MSC); deep-tow streamer seismic,
- 2: bathymetric and side-scan sonar mapping, hydroacoustic water column investigations and visual seafloor observations,
- 3: geochemical analyses of the water column, sediment and pore water; oceanographic investigations of the water column and current regime measurements,
- 4: carbonate sampling of vent-induced chemoherm structures,
- 5: biological and microbiological sampling.

Active cold vents and surface-near gas hydrates were identified by use of morphological, geochemical, geophysical and visual expressions which unambiguously indicate the presence of upward-migrating and expelling fluids (typically enriched in methane) and gas hydrate. These expressions are:

- the occurrence of subsurface BSR structures
- differences in the backscattering behaviour of side-scan sonar investigations
- the formation of massive, morphologically expressed carbonate chemoherms as well as pockmark structures
- hydroacoustically detectable disturbances in the water column (flares), where free gas is released from the seafloor
- strongly increased methane concentrations in the water column
- the settlement of vent-specific fauna (e.g. clams, tube worms, bacteria) that indicate the release of geochemically reduced species (particularly CH_4 , H_2S)

All of these expressions were known from several sites within the working area offshore Hawks Bay (Figure 2.1.1; e.g. Lewis & Marshall, 1996). However, few studies investigated these sites in greater detail. During cruise SO191 *New-Vents*, a more or less complete set of all available state-of-the-art observations and sampling techniques currently used for cold vent and gas hydrate research were available to address the overall aims:

- to enhance the global data base for cold vent and gas hydrate occurrences
- to identify different gas hydrate and cold vent facies around New Zealand, which allow an easier understanding and generalisation of cold vent and gas hydrate occurrences in general
- to link the active submarine cold vents with the known fossil vent sites on land for a better understanding of the Hikurangi Margin evolution
- to establish a database which can be used to check whether the investigated surface expressions can be used as an additional indicator for future oil, gas or even gas hydrate exploration around New Zealand
- to collect gas hydrate and to investigate the occurrence, distribution and the amount of gas hydrate in the sediment for large-scale estimates of the gas hydrate quantity
- to investigate the hazard potential of gas hydrate-induced submarine land slides, both natural or man-made
- to study the faunal assemblages present at the studied vent sites
- to investigate whether the natural methane release has an impact on the methane concentration in the atmosphere

A first insight into the acquired database is given in chapter 6. "Work completed and first results".

2.2 Regional Geologic–Tectonic Setting

The Hikurangi margin is characterised by the oblique subduction of the Pacific Plate beneath the North Island of New Zealand (Figure 2.2.1). The convergence rate varies from 45 mm/yr in the north, to 38 mm/yr in the northern South Island region. North of New Zealand, normal-thickness ocean crust of the Pacific Plate is being subducted beneath the Kermadec Ridge along the Kermadec Trench, which reaches >8 km water depth. In contrast, along the Hikurangi margin, the subducting plate comprises the Hikurangi Plateau, an anomalously thick (10-15 km) region of oceanic crust. As a consequence of the buoyancy of this subducting crust, the Hikurangi Trough at the toe of the subduction margin is anomalously shallow, lying at about 3 km of water depth. Mountain building associated with oblique continental collision processes occur in the South Island, where both the Pacific Plate, including the Chatham Rise, and the Australian Plate are continental crust.

Along the Hikurangi margin, the degree of obliquity between the plate motion vector and the orientation of plate boundary increases to the south, resulting in a greater component of the total plate motion being accommodated by strike-slip faults, and a lesser component by the subduction zone. These strike slip faults occur largely on land, except in the south where several such faults extend offshore into the Hikurangi margin. Large-scale tectonic rotations of the eastern North Island also accommodate a significant component of the oblique convergence across the plate boundary.

The Hikurangi margin started to develop as a subduction zone some 25 Myr ago. Prior to that the region was tectonically passive, with relatively thin Paleogene sequences overlying thick Cretaceous sediments and a basement framework of Mesozoic greywacke rocks. With the onset of subduction, the older passive margin sequences became tectonically imbricated by widespread thrust faulting, and thick sequences of Miocene to Recent sediments were deposited and deformed. These sequences occur in an uplifted and exposed forearc basin, and in basins beneath the upper continental slope. Sediments deposited in the trench by the Hikurangi Channel system have been accreted, and where this is an important process have substantially widened the margin. Lower slope occur basins between thrust-faulted ridges and contain variable thickness of sediments deposited on top of the accretionary wedge. Some of these slope basins have been deformed by thrust faults that have continued their activity behind the active deformation front in the Hikurangi Trough. The thrust-faulted ridges are sites of focussed deformation.

The thickness of turbidite sediments in the Hikurangi Trough generally decreases away from their source in the south. They are > 5 km thick near Cook Strait, and about 1.0-1.5 km thick north of Hawke's Bay. Beneath the trench-fill sequence, the surface of the Hikurangi Plateau is relative smooth with low relief south of Hawke's Bay, and rough with >3 km of relief north of Hawke's Bay. The combination of relatively thin trench-fill sediment in the north, relatively higher subduction rate, and rough topography of the subducting plate promotes the occurrence of tectonic erosion processes at the continental margin. This section of the margin is about 50-60 km in width, has a relative steep gradient, and there are numerous impact scars and major landslides associated with subducted

seamounts and ridges. Conversely, relatively thick trench fill sediment and smooth subducting plate in the centre of the margin promotes the processes of rapid frontal accretion of trench fill sediments. Here the margin reaches 150 km in width, and represents one of Earth's classical, large accretionary wedges. This wedge has an extremely low taper, e.g. gentle surface gradient and low angle subduction fault beneath it. Its geometry is comparable to the well studied Barbados and Nankai Trough systems. Such accretionary wedges are characterised by complex deformation of accreted and subducted sediments, high pore pressures, significant fluid flow associated with porosity reduction and deformation, widespread gas hydrates, and fluid expulsion associated with unique biological communities.

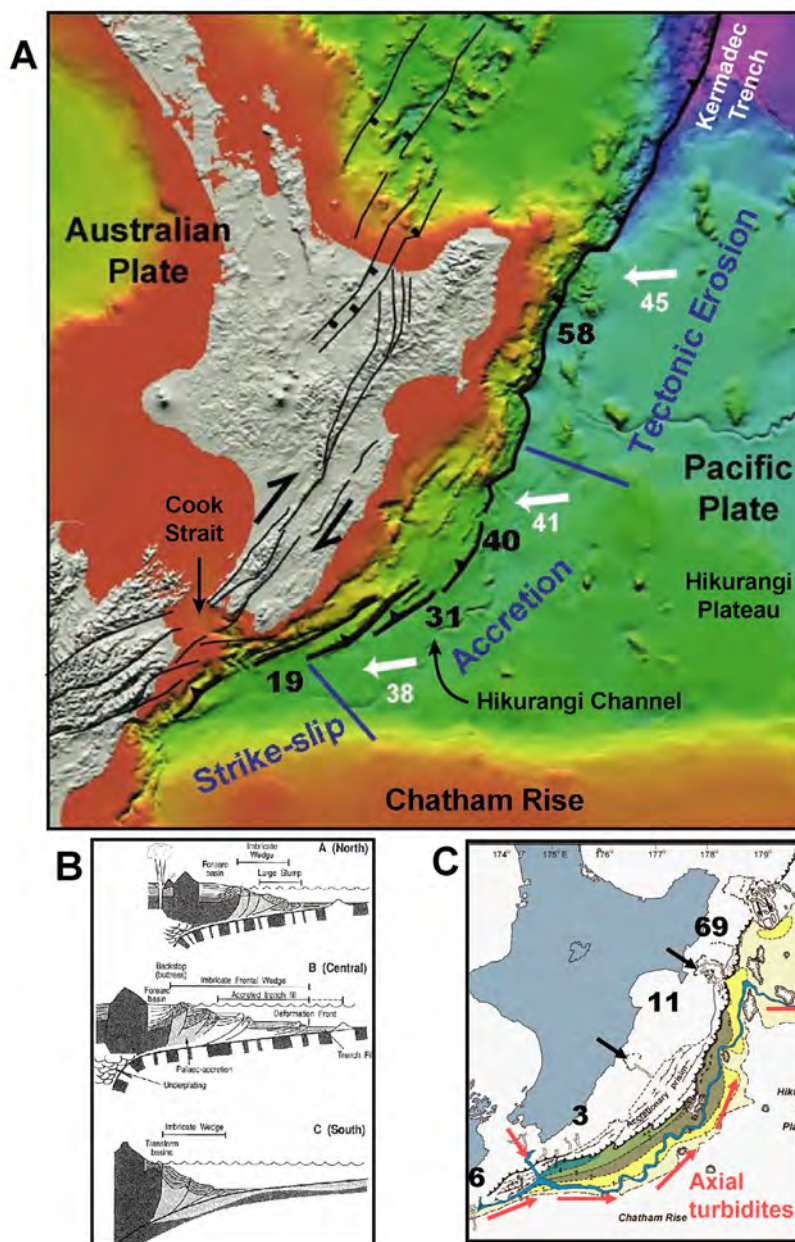


Figure 2.2.1: Regional geological and tectonic setting of the Hikurangi margin subduction zone. (A) Major tectonic components, showing thrust deformation front along the Hikurangi Trough and Kermadec Trench, strike-slip faults along the axial ranges of North Island and northeastern South Island, and back-arc extensional rifting in the Taupo Volcanic Zone and offshore southern Havre Trough. Dominant styles of subduction tectonics are indicated along the Hikurangi margin by the three broad divisions. White arrows are Nuvel-1A relative Pacific-Australian plate motion rates in mm/yr (DeMets et al., 1994). Black numbers are modelled estimates of the relative motion of the eastern North Island margin relative to the subducting Pacific Plate (Wallace et al., 2004). (B) Schematic geological cross-sections of the three broad divisions indicated in (A) (Lewis and Pettinga, 1993). (C) Map showing thickness of trench-fill turbidites (small black numbers in km), and principal sedimentary distributary systems. Large black numbers are current sediment yields from land (Mt/yr) (Hicks, NIWA data).

There is ample evidence of widespread fluid flow in the Hikurangi margin. This includes the occurrence of direct hydrocarbon indicators in industry seismic reflection data, more than 300 oil, gas

and mud expulsion sites on land, widespread marine gas hydrates, acoustic flares at submarine seep sites associated with chemosynthetic fauna and authigenic sediments, and numerous fluid related features interpreted in side-scan sonar images.

2.3 Previous Investigations

There exists reasonably good bathymetric coverage of the margin, albeit of variable quality. In the early 1990's large parts of the margin were surveyed by the French research vessel *L'Atalante* using a SIMRAD EM12Dual system. Large sectors of the margin not surveyed by *L'Atalante*, particularly in the central section, were covered by Hawaii MR1 side-scan sonar, which also provided poorer quality bathymetry data. Since the late 1990's some localised areas and vessel transits have been surveyed with a SIMAD 30 kHz EM300 multibeam system on NIWA's vessel *Tangaroa*, providing high quality bathymetry in these areas. On the continental shelf, bathymetric contours at 10 m have been constructed by NIWA using analogue and digital data, much of which was collected by the NZ Royal Navy Hydrographic Office for safe navigation purposes.

The coverage and quality of seismic reflection data is highly variable. The best data exists on the continental shelf and upper slope, and has been collected to industry standards by various oil companies and the NZ Ministry for Economic Development (MED). These modern surveys follow reconnaissance surveys by various oil companies in the 1970s. Low fold data from several areas have also been collected by NIWA, GNS Science and the former NZ Department of Scientific Research (DSIR), as part of Government-funded research contracts. Prior to this survey, the best quality regional seismic lines crossing the central margin included the *SP Lee* profile acquired by DSIR in 1983 (Davey et al., 1985), the NIGHT and CM05#38 profiles acquired on the *MV GECO Resolution* and *MV Multiwave* by GNS Science, and the CM05#1 profile acquired by Crown Minerals (MED). The regional survey lines planned as part of this survey were designed to infill significant gaps in the margin, while providing a large scale tectonic framework for the detailed studies at seep sites.

Gas Hydrates

Bottom simulating reflections (BSRs), as proxies for gas hydrates, were first identified in seismic data from the Hikurangi margin in the early 1980s (Katz, 1981). In the 1990s, BSRs were mapped along the southern part of the margin, mostly based on high-speed streamer data collected by the R/V *L'Atalante* during the French/New Zealand GeodyNZ campaign. Earlier analyses of BSRs focussed on heatflow (Townend, 1997; Henrys et al., 2003) (Figure 2.3.1). Most of New Zealand's current gas hydrate funding is energy related. Attempts are now being made to locate gas hydrate "sweet spots", locations where gas hydrates may be sufficiently concentrated for future gas production. In 2006, the first-ever cruise dedicated to studying gas hydrates off New Zealand, was conducted on the R/V *Tangaroa* (TAN0607, 20/6-3/7/06) in an international collaboration between GNS Science, NIWA, the U.S. Naval Research Laboratory, the Universities of Hawaii, Otago, Rochester and Auckland, and individual scientists from other institutions (CHARMNZ, CH₄ Hyrates on the Accretionary Margins of New Zealand).

Gas hydrate "sweet spots" on the Hikurangi Margin

It has been noticed that the strength of BSRs on the Hikurangi margin varies significantly (Pecher and Henrys, 2003; Henrys et al., submitted), more than on many other continental margins. BSRs appear strongest where geologic structures favour fluid migration such as anticlines, layer outcrops, and fault systems (Figure 2.3.2).

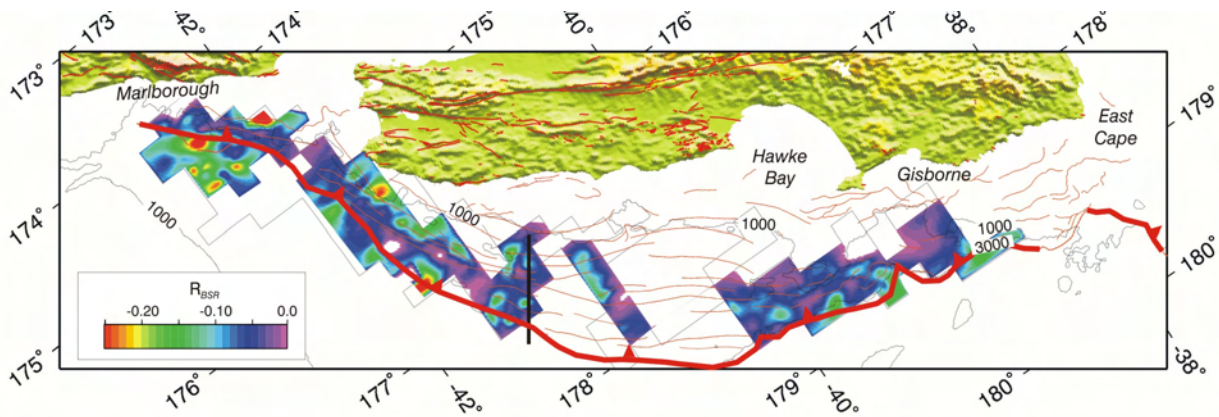


Figure 2.3.1: Heatflow from the depth of BSRs on the Hikurangi margin. Thin lines are seismic tracks. Note the wide-spread occurrence of BSRs – the gap in the centre of the figure reflects a gap in seismic coverage (that has been filled by regional MCS lines during the SO191 cruise). Thick black line is seismic track shown in Figure 2.3.2.

BSR strength itself is not a reliable parameter for quantifying gas hydrates. However, a strong BSR, as a proxy for free gas at the base of gas hydrate stability, does indicate that methane flux into the system is exceeding a threshold, the critical methane flux, leading to the release of gas out of solution (Xu and Ruppel, 1999). Given the lack of any geochemical data until 2006, it was therefore concluded that the best first-order candidates for possible gas hydrate “sweet spots” would be locations where strong BSRs coincide with structures that favour fluid flow focussing (Pecher and Henrys, 2003).

Two geochemical and heatflow profiles were acquired during the CHARMNZ campaign across a potential “sweet spot” beneath an anticline. Seismic data reveal high-amplitude anomalies in the regional gas hydrate stability fiend beneath this anticline (Figure 2.3.3). The high amplitudes may be caused by free gas (Crutchley et al., 2006), perhaps indicating a fluid-flow related upward-warping of the local hydrate stability field. A controlled-source electromagnetic would be ideally suited to study whether significant amounts of gas hydrates are present above these anomalies. More generally, our knowledge of the sources and migration paths of gas on the Hikurangi margin needs to be enhanced to understand gas hydrate formation on this margin, its potential link to the underlying petroleum system, and the conditions that may lead to elevated gas hydrate concentrations.

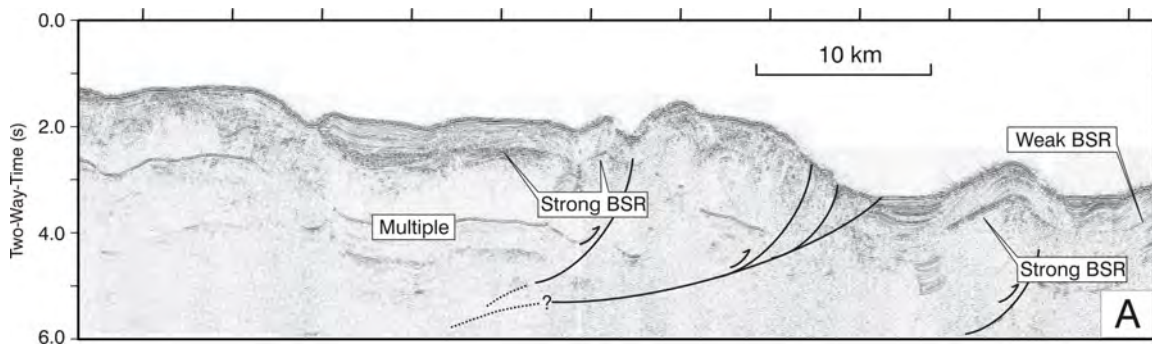


Figure 2.3.2: Seismic profile across the Hikurangi margin (Figure 2.3.1 for location), showing correlation of strong BSRs with layer outcrops (left), faults (centre), and anticlines (right). BSRs are weaker in the basins between anticlines, if present at all.

Erosion of the seafloor at the top of the gas hydrate stability zone

Rock Garden is an uplifted ridge that appears to be eroded at ~600 m water depth. Pinchouts of BSRs at the edges of its plateau-like crest (Figure 2.3.4) and theoretical phase boundary considerations in combination with water temperature data suggest that most likely, erosion is linked to the top of gas hydrate stability in the ocean. A combination of two mechanisms that may cause seafloor erosion during ridge uplift has been proposed (Pecher et al., 2005): (1) An upward migrating base of gas hydrate stability with respect to the seafloor caused by depressurization during uplift may lead to overpressure and sliding. After sliding, water depth and hence, hydrate stability, increases again and the process may repeat itself during continued uplift. (2) Gas hydrates are predicted to repeatedly form and dissociate close to the seafloor because of water temperature fluctuations. Resulting pore volume contraction and expansion may cause a frost-heave-like weakening of the seafloor.

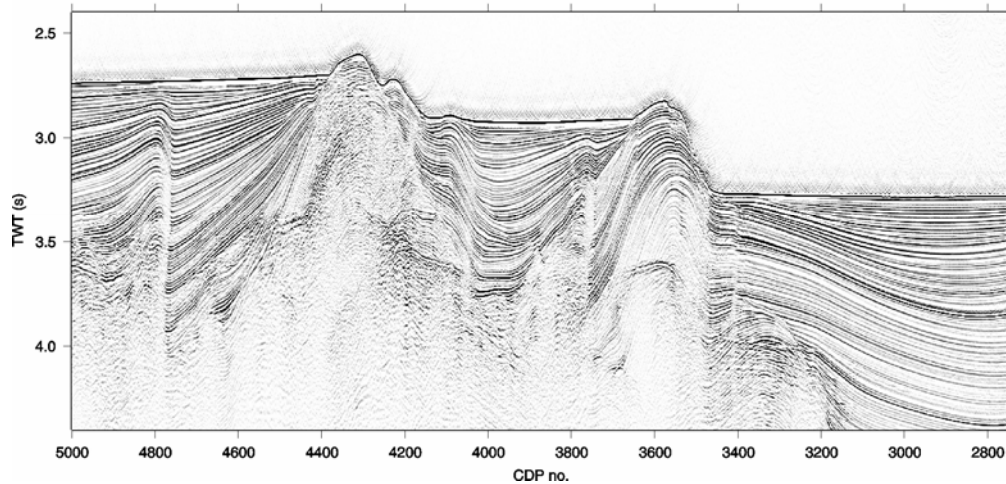


Figure 2.3.3: High-amplitude anomaly in industry-style seismic data beneath an anticline at CDP 4400, CDP spacing is 6.25 m. BSRs on either side of this anomaly mark the regional base of gas hydrate stability. The anomaly is likely to be caused by free gas in the regional hydrate stability zone (after Crutchley et al., 2006).

Seismic data collected during the CHARMNZ survey indicate numerous shallow gas pockets beneath the seafloor. The buoyancy of gas beneath lower-permeability hydrate-bearing sediments may lead to significant overpressure, sufficient for hydrofracturing (Hornbach et al., 2004; Liu and Flemings, 2006) and potentially contributing to sediment weakening and hence, seafloor erosion. The feasibility of these possible erosion mechanisms is being modelled. Sediment samples from Rock Garden for measurement of physical properties, would be very helpful for constraining the models. The composition of gas for hydrate formation is also needed for assessing hydrate stability.

Gas hydrates and vents

Numerous vent sites have been discovered on the Hikurangi margin in the past decades (e.g., Lewis and Marshall, 1996), mostly by coincidence. It is clear by now, that parts of the margin are inundated by vents releasing methane. The strong link between BSRs and features that lead to fluid-flow focussing makes the Hikurangi margin an excellent target to study the relation between gas hydrates and fluid expulsion. This is best documented by the fact that the first-ever gas hydrate sample from the Hikurangi Margin was recovered close to a vent site (Wairarapa Site, R/V *Tangaroa*, 11/2006).

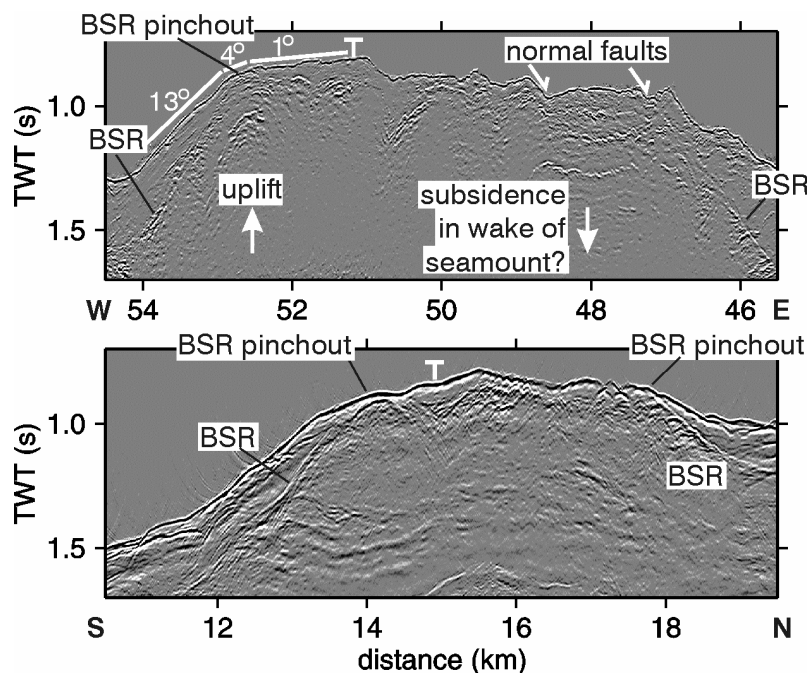


Figure 2.3.4: Seismic profiles across Eastern Rock Garden. A flattening of the top of the ridge coincides with BSR pinchouts (after Pecher et al., 2005).

3. Participants

3.1 Scientists

3.1.1 Scientists of Leg 1

Name	Given Name	Affiliation	Discipline
Bialas	Joerg	IFM-GEOMAR	Chief Scientist
Barnes	Philip	NIWA	MCS seismic
Crutchley	Gareth	OTAGO	MCS processing
Gerring	Peter Kenneth	NIWA	MCS technician
Greinert	Jens	GNS	Flare imaging, bathymetry
Hagen	Claudia	IFM-GEOMAR	OBS seismic
Jones	Andrew	GA	DeepTow Sidescan
Jung	Claudia	IFM-GEOMAR	OBS seismic
Keen	David	GNS	CSEM technician
Klaucke	Ingo	IFM-GEOMAR	DeepTow Sidescan
Krabbenhöft	Anne	IFM-GEOMAR	OBS seismic
Lamarche	Geoffroy	NIWA	MCS seismic
Netzeband	Gesa	IFM-GEOMAR	DeepTow streamer
Pecher	Ingo	HW	MCS seismic
Petersen	Joerg	SFB574	Sidescan
Rohde	Anne-Dörte	IFM-GEOMAR	OBS seismic
Schroeder	Patrick	SFB574	DeepTow technician
Schwalenberg	Katrin	BGR	CSEM
Steffen	Klaus	IFM-GEOMAR	Airgun technician
Sticher	Annemarie	IFM-GEOMAR	OBS seismic
Wilcox	Steve	NIWA	MCS technician

3.1.2 Scientists of Leg 2

Name	Given Name	Affiliation	Discipline
Linke	Peter	IFM-GEOMAR	Chief Scientist
Bannert	Bernhard	Oktopus	Video-electronics
Bowden	David	NIWA	OFOS, Macrofauna
Boyd	Sheree	AUT	Macrofauna
Crowe	Michelle	GNS	Water column chemistry
Domeyer	Bettina	IFM-GEOMAR	Porewater geochemistry
Eisenhauer	Anton	IFM-GEOMAR	Carbonates, Radon
Faure	Kevin	GNS	Methane
Greinert	Jens	GNS	Flare Imaging, bathymetry
Haeckel	Matthias	IFM-GEOMAR	Porewater geochemistry
Hütten	Edna	TePapa	Geochemistry
Kilner	Jeremy	OTAGO	Parasound, Hydrosweep
Krieger	Kristin	BIOLAB	Porewater geochemistry
Kriwanek	Sonja	IFM-GEOMAR	Lander geochemistry
McGinnis	Daniel	EAWAG	CTD, Moorings
Müller	Daniel	IFM-GEOMAR	Porewater geochemistry
Petersen	Asmus	IFM-GEOMAR	Lander & corer technology
Queisser	Wolfgang	IFM-GEOMAR	Lander & corer technology
Santillano	Daniel	MPI	Microbiology
Schneider v. Deimling	Jens	IFM-GEOMAR	CTD, Methane
Schott	Thorsten	Oktopus	SideScanSonar technician
Sommer	Stefan	IFM-GEOMAR	BIGO, BWS, Meiofauna
Treude	Tina	MPI Bremen	Microbiology
Türk	Matthias	IFM-GEOMAR	Lander electronics
Weinrebe	Willi	IFM-GEOMAR	SideScanSonar
Wegener	Gunter	MPI Bremen	Microbiology
Zemke-White	William Lindsey	AUT	Macrofauna

3.1.3 Scientists of Leg 3

Name	Given Name	Affiliation	Discipline
Pfannkuche	Olaf	IFM-GEOMAR	Chief Scientist
Arnds	Julia	MPI Bremen	Microbiology
Bausch	Marlene	Uni Bremen	Porewater geochemistry
Beier	Viola	MPI Bremen	Microbiology
Boone	Dries	RCMG	ROV
Cordts	Dethlev		Journalist
De Batist	Marc	RCMG	Heat flow, ROV
Greinert	Jens	GNS	Flare Imaging, Bathymetry
Haeckel	Matthias	IFM-GEOMAR	Porewater geochemistry
Kipfer	Rolf	EAWAG	CTD, noble gases
Krieger	Kristin	BIOLAB	Porewater geochemistry
Kriwanek	Sonja	IFM-GEOMAR	Lander geochemistry
Kröger	Kerstin	NIWA	Macrofauna
Liebetrau	Volker	IFM-GEOMAR	Carbonates, Radon
Linke	Peter	IFM-GEOMAR	Lander technology
Marquardt	Matthias	IFM-GEOMAR	Porewater geochemistry
Martin	Ruth Ann	UoA	Benthic Foraminifera
Naudts	Lieven	RCMG	Head of ROV Team
Niemann	Helge	MPI	Microbiology
Poort	Jeffrey	RCMG	ROV
Queisser	Wolfgang	IFM-GEOMAR	Lander & corer technology
Schneider v. Deimling	Jens	IFM-GEOMAR	CTD, Methane
Sommer	Stefan	IFM-GEOMAR	BIGO, BWS, Meiofauna
Stange	Karen	IFM-GEOMAR	Porewater geochemistry
Thurber	Andrew	USCD	Macrofauna
Türk	Matthias	IFM-GEOMAR	Lander electronics

Affiliation/Addresses:

AUT:	Auckland University of Technology, 24 St. Paul Street, Private Bag 92006, Auckland 1020, New Zealand
BGR:	Bundesanstalt für Geowissenschaften und Rohstoffe, Hannover, Germany
BIOLAB:	Kieler Str. 51, 24596 Hohenwestedt, Germany
EAWAG:	Swiss Federal Institute of Environmental Science and Technology (Eawag) Swiss Federal Institute of Technology (ETH) Ueberlandstr. 133 CH-8600 Duebendorf, Switzerland
GA:	Geoscience Australia, Sidney, Australia
GNS:	Institute of Geology and Nuclear Sciences LTD, P.O. Box 30-368, Lower Hutt, New Zealand
HW:	Heriot-Watt University, Edinburgh, Great Britain
IFM-GEOMAR:	Leibniz Institute of Marine Sciences Wischhofstr. 1-3. 24148 Kiel, Germany
MPI-Bremen:	Max Planck Institut für Mikrobiologie Bremen, Celsiusstr. 1 28359 Bremen Germany
NIWA:	National Institute for Water and Atmosphere LTD, 301 Evans Bay Parade, Greta. Point PO Box 14901, Kilbirnie, Wellington, New Zealand
OKTOPUS	GmbH, Wischhofstr. 1-3, 24148 Kiel, Germany
OTAGO:	The University of Otago, Otago, New Zealand
RCMG:	Renard Centre of Marine Geology, Department of Geology and Soil Science Ghent University, Krijgslaan 281 s.8, B-9000 Gent
TePapa:	Museum of New Zealand – Te Papa Tongarewa, Cable Street, Wellington, New Zealand PO Box 467, Wellington, New Zealand
UoA:	University of Auckland Geology Department, Private Bag 92019, Auckland, New Zealand
USCD:	University of California, San Diego, 9500 Gilman Drive, La Jolla, California 92093-0218, USA

3.2 Crew

3.2.1 Crew of Leg 1

Name	Given Name	Rank
Meyer	Oliver	Master
Korte	Detlef	Chief Mate
Büchele	Ulrich	2 nd Mate
Göbel	Jens	2 nd Mate
Walther	Anke	Surgeon
Lindhorst	Norman	Chief Engineer
Rex	Andreas	2 nd Engineer
Buß	Jörg	2 nd Engineer
Zebrowski	Darius	Electrician
Angermann	Rudolf	Chief Electrician
Leppin	Jörg	Electrician
Eglof	Frank	System Operator
Zeitz	Holger	Motorman
Rosemeyer	Rainer	Motorman
Wieden	Wilhelm	Chief Cook
Oryszewski	Kryzstof	2 nd Cook
Grübe	Gerlinde	Chief Steward
Rudnicki	Gabriel	2 nd Steward
Jahns	Winfried	Bosum
Hödl	Werner	A. B.
Bierstedt	Torsten	A. B.
Schrapel	Andreas	A. B.
Dehne	Dirk	A. B.
Decker	Jens	A. B.
Fricke	Ingo	A. B.
Förster	Tino	Trainee

3.2.2 Crew of Leg 2

Name	Given Name	Rank
Mallon	Lutz	Master
Korte	Detlef	Chief Offc.
Göbel	Jens Christian	2 nd Offc.
Meyer	Oliver	1 st Offc.
Lindhorst	Norman	Chief Eng.
Rex	Andreas	2 nd Eng.
Buss	Jörg	2 nd Eng.
Zebrowski	Dariusz	Electr.
Großmann	Matthias	System Manager
Angermann	Rudolf	Ch. El. Eng.
Egloff	Frank	Syst.-Man.
Walther	Anke	Doc
Rosemeyer	Rainer Franz	Fitter
Zeitz	Holger	Motorman
Marcinkowski	Przemyslaw	Motorman
Wieden	Wilhelm	Cook
Oryszewski	Krzysztof	2 nd Cook
Slotta	Werner	Ch. Stwd.
Rudnicki	Gabriel	2 nd Stwd.
Jahns	Winfried	Bosun
Fricke	Ingo	A.B.
Hödl	Werner	A.B.
Etzdorf	Detlef	A.B.
Dehne	Dirk	A.B.
Schrapel	Andreas	A.B.
Bierstedt	Torsten	A.B.

3.2.3 Crew of Leg 3

Name	Given Name	Rank
Mallon	Lutz	Master
Korte	Detlef	Chief Offc.
Göbel	Jens Christian	2 nd Offc.
Aden	Nils-Arne	2 nd Offc.
Lindhorst	Norman	Chief Eng.
Rex	Andreas	2 nd Eng.
Klinder	Klaus Dieter	2 nd Eng.
Rieper	Uwe	Electr.
Großmann	Matthias	System Manager
Angermann	Rudolf	Ch. El. Eng.
Egloff	Frank	Syst.-Man.
Walther	Anke	Doc
Rosemeyer	Rainer Franz	Fitter
Zeitz	Holger	Motorman
Marcinkowski	Przemyslaw	Motorman
Wieden	Wilhelm	Cook
Tiemann	Frank	Cook
Slotta	Werner	Ch. Stwd.
Rudnicki	Gabriel	2 nd Stwd.
Jahns	Winfried	Bosun
Bierstedt	Torsten	A.B.
Drumm	Christian	A.B.
Etzdorf	Detlef	A.B.
Hödl	Wernder	A.B.
Noack	Robert	Trainee
Schrapel	Andreas	A.B.

4. Narratives

4.1 Cruise Narrative of Leg 1

R/V SONNE arrived on the 09th Jan. 2007 in the port of Wellington, New Zealand after two weeks of transit from Darwin, Australia. Although the official charter time of project SO-191 New Vents did start on 11th Jan. 2007 an official reception took place onboard during the 10th Jan. The German Ambassador at Wellington, New Zealand, together with the ships owner and operating company Reederei Forschungsschiffahrt (RF) and the Institute of Geological and Nuclear Sciences Limited (GNS) invited to “attend a function on board the RV SONNE to mark the start of major geo-science investigations of New Zealand’s offshore region in 2007”. The function was held onboard R/V SONNE when docked at the Aotea Quay in Wellington. A group of 62 invited guests came together to express their wishes for a successful cruise and to take the opportunity of being guided through one of Germany’s largest research vessels. The overall public interest in the scientific co-operation between Germany and New Zealand is best documented by Radio interviews broadcasted and newspaper reports published about the cruise the day after. Although the Minister of Science and could not attend the meeting his representative expressed the ongoing strong interest of New Zealand into the German – New Zealand contract of scientific and technical co-operation.

On the 11th Jan. 21 scientists from four different countries (Germany, New Zealand, Great Britain, and Australia) boarded R/V SONNE to participate in the first Leg of cruise SO191. After installation of streamer winch provided by NIWA and further container operations the laboratories onboard R/V SONNE were occupied and instruments were set up. As OBS and airgun equipment was already used on the previous cruise parts of the installation remained and was reactivated now.

R/V SONNE left the port of Wellington on Friday the 12th Jan. at 08:00 hrs and headed towards the first working area, south of Hawkes Bay. During the transit a short bathymetric grid was sailed above the Wairarapa working area in preparation for the coming deep towed operations. The set up of equipment in the laboratories could not be completed during the previous day and was continued. During routine testing of installed equipment it turned out that the short baseline navigation system failed. Three integrated circuits were burned and could not be replaced by onboard available spare parts. An immediate help request to the product company in France resulted in express shipping of

spare boards. This was necessary as the USBL positioning of the deep towed sidescan and streamer is essential to the following legs to achieve best as possible seafloor locations for the probes.

A velocity sound profile and test of the acoustic releases for the ocean bottom stations were successfully completed on the 13th. Unfortunately the deployment of the NIWA streamer failed despite several attempts. Bathymetric profiling above an area where mud volcanoes are assumed and transit towards the northern most working area around LM-1 and Builders Pencil was done instead.

Between 17:00 and 20:00 on the 14th 10 OBS were deployed in the region of flare site 1 reported by Lewis and Marshal and the large Builders Pencil mussel field. Until the 16th 23:00 hrs 130 nm of deep towed sidescan were obtained together with 14 s GI-gun shots. Unfortunately the deep towed streamer failed after three attempts and MCS data were only acquired by a 100 m long mini streamer. During the 17th deployment of 6 MT stations was done, interrupted by a successful test of the NIWA surface streamer. As the last MT station was located only 30 nm off the port of Napier it was decided to use this opportunity to pick up the iXSea spare parts for the USBL navigation system.

On 18th Jan. 02:00 hrs deployment of 2 G-gun clusters and the 600 m streamer started the regional MCS survey. It turned out that the Airgun array could be fired at 20 s with a remaining pressure of 180 bar. Profiling of three MCS lines across the slope of the margin started at the southern tip of Hawkes Bay. The survey was completed on 19th Jan. 2007. After transit to the trench at 41°S 6 OBS were deployed. The NIWA streamer and the 1000 cinch Arigun Array were used to record additional three MCS lines. Due to strong winds and a cross over of streamer and guns the last line could not be completed to match with elder seismic lines (SP-Lee, CM38) from this region. All 6 OBS could be recovered without problems.

As NIWA had announced to deploy 2 moorings on the two Towers seep sites of the Wairarapa field at 26th Jan. we had to transit to this area next. At 22:00 hrs on the 21st Jan. the deployment of the CSEM equipment started. 23 measurements were completed crossing the seep sides at the South Tower. At 16:00 hrs on the 22nd 16 OBS were deployed in the Wairarapa field. Instruments close to the Tower seep sides and at the elevated cone were equipped with Methane sensors. Due to high winds (>20 m/s) and rough seas it became to dangerous to deploy the 2 t weight of the deep towed sidescan. As well the GI-gun could not be operated in the high level swell. It was decided to hide closer to the coast and wait until the wind and seas had calm down again. With reduced winds bathymetry profiling was carried out until deployment of the Sidescan could be prepared in the morning of the 23rd. Before the POSIDONIA calibration took place. At 13:00 the deep towed sidescan was deployed again. Within 24 hrs of operation four sites with flares were observed in the online monitor already. OBS recovery started 15:00 hrs of the 24th Jan. After 6 hrs all instruments were recovered and the deployment of the CSEM equipment started. Due to uncertain wind directions a Sw-NE profile was scheduled first, but it turned out after a few hours that the direction of the wind changed and SONNE could not be kept on position while towing the deep sea cable. On short notice an alternate profile was designed crossing the seep sites in SE-NW direction. This line could be completed until 14:00 hrs on the 25th Jan. Well before the announced mooring deployment by NIWA should take place.

After eight hours transit SONNE reach the survey area of the Uruti site. Ship speed was reduced to 8 kn max as the Posidonia antenna was kept deployed to avoid additional calibration procedures. Another set of 16 OBS were deployed until 26th, 02:30 hrs. Deployment of the Sidescan had become routine and the profiling started at 04:00 hrs. Unfortunately failures in power transmission made it necessary to recover the instrument at 23 hrs. By this time the major targets for the sidescan had been crossed already and it was decided to complete the lines with airgun shots serving for the mini streamer and the OBS only. At 14:00 hrs on 27th all OBS were recovered and SONNE could set course for the next CSEM deployment. All transits were chosen to add new coverage to the existing bathymetry map, if possible.

At 21:00 hrs the CSEM equipment was deployed for a line at 40° 50' S in water depth of about 2000 m. About 5000 m of cable were laid out to enable higher power transmission as deeper targets identified on existing New Zealand MCS data should be imaged. The expected increase in wind speed of 30 kt did not happen and the line could be completed without problems at 15:00 hrs.

Transit towards site LM9 was done parallel to previous tracks in order to accomplish the bathymetric map. At 23:20 hrs deployment of 12 OBS started and at 04:00 hrs on 29th Jan. the sidescan was deployed again. Again problems with the power supply were reported 10 hrs later. At this time half of the planned survey was done and the area of major interest has already been covered by the sidescan. It was decided not to deploy the system again but to complete the strike line with mini streamer and GI gun as this line was the major OBS line. This work was completed at 18:20. During recovery of the mini streamer, which was deployed through the boom of the magnetometer as usual, it was washed underneath the ships hull and got stuck in the rudder. Even attempts with the ships

working boat did not succeed to get the remaining chain of hydrophones cleared. The streamer was broken into parts. Recovery of the OBS was completed at 01:20 hrs. After additional bathymetry profiles the CSEM was deployed again at 07:00 hrs. As the site dimension are smaller than the others this measurement could be completed 16:00 hrs.

After 5 hrs transit the NIWA streamer and the GI gun were deployed another time at 22:00 hrs. Goal was to accomplish a tie line between the regional line, which was interrupted at 19th Jan., and the elder CM38 profile. Luckily the strong wind and wave state which would not have allowed to run the GI gun had decreased well enough. When the line was completed SONNE set course further south and steamed for 100 nm towards the Wairarapa area again.

At 11:00 hrs on the 31st streamer and GI gun were deployed a last time. A MCS line should accomplish the previous work in this area following the course of the earlier CSEM experiment. Due to remaining time this line could be extended across a neighbouring bathymetric high, which seem to contain free gas as well, as indicated by well pronounced BSR reflections.

At 16:00 hrs on the 31st Jan. this final profile was completed and the scientific work was continued with multibeam bathymetry recordings until early morning of the 01st Februar 2007 when course was set to the pilot station (Figure 4.1.1). Scientific work stopped at that time.

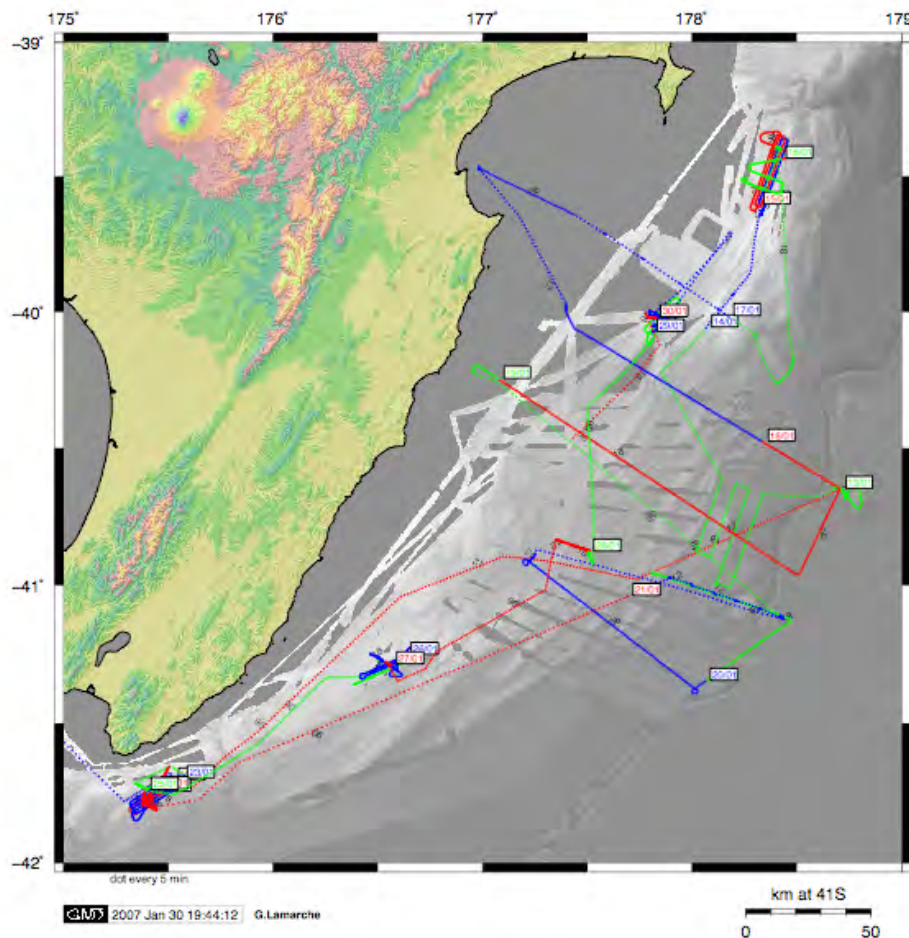


Figure 4.1.1: Cruise track leg 1

4.2 Cruise Narrative of Leg 2

Since transits to the working areas of all three legs of SONNE cruise 191 are short, work on setting up the equipment for the ambitious scientific programme already started on 31 January 2007 with unloading three containers in a shed at Wellington Centre Port. An advance party of five assembled the four video-guided lander systems that were to be deployed during cruise legs 2 and 3.

Because of the different thematic approaches, after a short scientific and nautical briefing the scientific crew and equipment were exchanged almost completely during the port call in Wellington. The vessel also took provisions. This could all be achieved within the scheduled length of the port call thanks to the competent cooperation between the ship's crew and land crew. Loading was already completed when the main body of the scientific crew arrived. RV SONNE could sail on time at 1:00 pm on 3 February.

To provide the scientific crew with time for securing the substantial array of equipment and setting up the laboratories, 'Rock Garden' was chosen as the first working area. Having successfully calibrated

the underwater navigation system POSIDONIA on the 4th Feb., mapping with the already installed side scan sonar could start without delay during the night until noon of the 5th. This was followed by 2 CTD casts. Water column sampling yielded a methane maximum near the seafloor, which replicates findings of earlier expeditions. Subsequent OFOS profiling confirmed 'Rock Garden' to be just that, it does not lend itself to sediment sampling.

Thus station work was relocated to the fluid expulsion/seep area 'LM 9' published by Lewis and Marshall. First TV-guided multicorer deployments yielded the first sediments of the cruise followed by gravity corer and video-guided boxcorer deployments during the 6th.

Apart from cemented carbonate blocks, chemoautotrophic communities directly related to seep fluids (Pogonophora, Vestimentifera, Calyptogena and Mytiliid bivalves as well as some bacterial mats) were found during 3 nocturnal OFOS profiles on the 7th.

After this survey, a sampling programme with CTD, multicorer and bottom water sampler (BWS) was conducted on the 8th followed by nocturnal DTS-profiles at LM 9.

On the 9th sampling of water and sediments was continued with deployments of the CTD, BWS, TV-grab, gravity corer and boxcorer followed by a CTD-programme at night.

The working programme of the 10th included a multicorer deployment, HS/PS profiles, and TV-grab deployments, unfortunately without success due to failures of the telemetry.

On the 11th the Fluid Flux Observatory (FLUFO) was deployed after another failure of the TV-grab. After this deployment, a multicorer and a gravity corer were deployed on a reference site, followed by nocturnal OFOS profiles in the western part of the LM 9 working area. After a CTD-cast a thermistor mooring was deployed on the 12th followed by sampling with the BWS, multicorer, TV-grab and boxcorer. On the 13th gravity corer and box corer deployments followed a nocturnal CTD programme. After the recovery of the FLUFO Lander and the thermistor mooring and a final CTD cast at the mooring position RV SONNE started the transit with a bathymetric profil to the southernmost working area.

RV SONNE arrived at Wairarapa in the evening of the 14th with large swell conditions which made it impossible to use the multicorer. Even the deployment of OFOS was extremely difficult in this sea state.

On 15 February an intense sediment sampling programme with multicorer, boxcorer and gravity corer was conducted at a seep site named Northern Tower, followed by a series of CTD casts at the summit (TUI) in the NE of the Wairapa working area during the night.

As the wind speed increased rapidly in the morning of 16 February 2007, the GasQuant lander was rapidly prepared and deployed on the summit where gas flares have been repeatedly detected in the water column. An attempt to deploy the multicorer had to be stopped as the wave action tripped the cores already close to the sea surface. All scientific worked had to be stopped due to the deteriorating wind and wave conditions.

In the morning of the 17th the weather improved and we were able to conduct a CTD cast with a HS/PS profile for flare imaging. After this, a sampling programme with a multicorer, 2 short gravity corer and 2 unsuccessful box corer deployments due to the hard ground was conducted, followed by another CTD cast and a nocturnal OFOS programme.

The morning of the 18th started with a CTD cast followed by a deployment of a thermistor mooring at the TUI reference site and a FLUFO deployment at the Northern Tower. After this, the GasQuant Lander was recovered from the TUI summit. At this position a physical CTD and another thermistor mooring was deployed and the multicorer was used to recover sediments at the Northern Tower. Furthermore, we were finally able to retrieve a huge block of authigenic carbonate and cold seep fauna with the TV-grab.

During the night another deployment of the deep-towed side scan sonar was performed using both frequencies (75 and 410 kHz) in the working area Wairarapa. The remarkably increased resolution showed many new gas flares, dredge marks and chemoherms which were investigated in greater details during nocturnal OFOS profiles.

The morning of the 19th started with a CTD cast and a deployment of the Biogeochemical Observatory (BIGO) followed by 2 TV-grab deployments at the Northern Tower. During the night an intense CTD programme was performed at TUI. After 2 TV-grab deployments in the morning of the 20th, FLUFO was recovered and sampling continued with TV-grab and gravity coring. On the 21st we performed TV-MUC deployments, recovery of moorings and BIGO under excellent weather conditions. Start of transit with bathymetric profiles back to working area LM 9.

RV SONNE arrived at LM 9 in the evening of 22 February and sampled the seep site Bear's Paw by TV-grabs. After another OFOS profile the gravity corer and TV-MUC were deployed to recover the last sediments of this leg. During the night OFOS was towed in the Rock Garden area and on 24

February we deployed the fluid flux observatory (FLUFO) and 2 thermistor moorings scheduled for recovery on the third leg. After the recovery of 3 of 6 magnetotelluric bottom stations (OBMT) which had been deployed on leg 1 RV SONNE headed for Napier where we arrived at 9:00 am on 25 February 2007 (Figure 4.2.1).

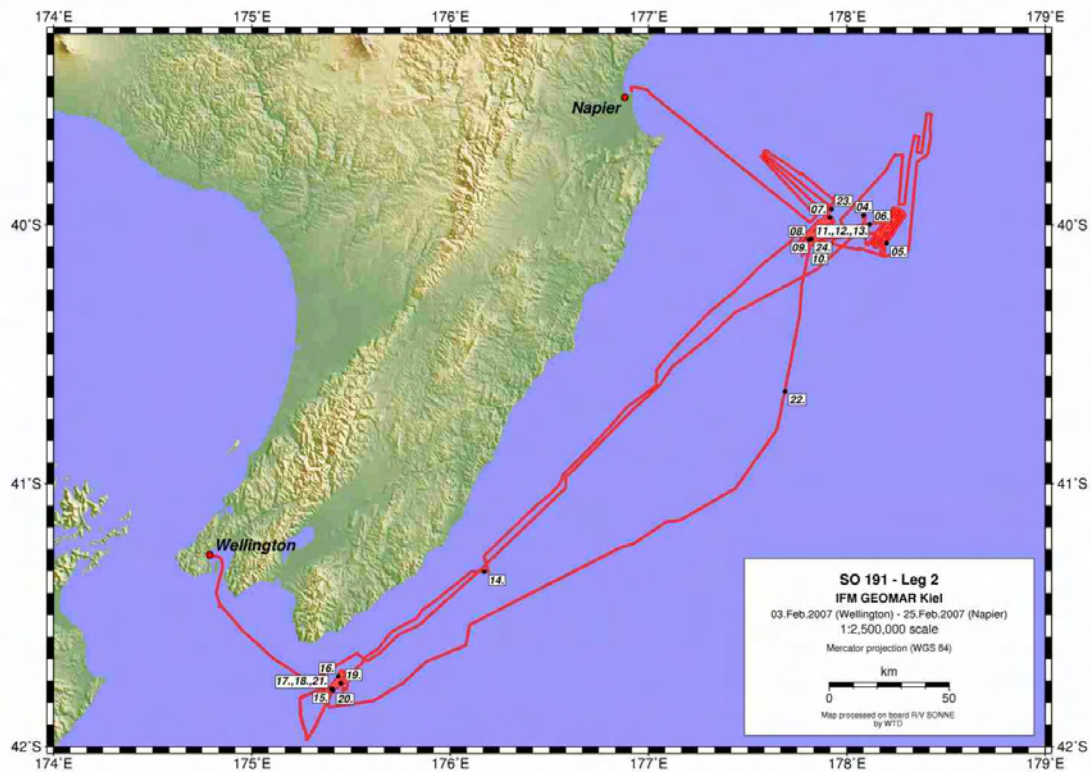


Figure 4.2.1: Cruise track Leg 2

4.3 Cruise Narrative of Leg 3

Tuesday, 27-02-2007

In the course of the day we performed tests with the Belgian Cherokee ROV which was installed during the harbour stay in Napier. The tests included a deployment in the harbour basin. At 18:00h local time R/V SONNE left Napier and headed eastwards towards the Rock Garden site already visited at leg 2. During the transit we mapped the sea floor with the multi-beam.

Wednesday, 28-02-2007

We started station work in the early morning with the recovery of an OBMT mooring followed by a CTD/Ro cast and the recovery of two additional OBMT moorings (Stat. 182-85). In the course of the day we took sediment samples with two TV-multiple corer casts (Stat. 186-87) and deployed the BIGO lander (Stat. 188) at station Bear's Paw. In the evening we made 3 towed CTD/Ro transects for methane analysis in the benthic boundary layer (Stat. 189-91).

Thursday, 01-03-2007

The CTD/Ro transects were finished in the morning. A first test ROV dive followed during mid day (Stat. 192). In the afternoon a sequence of four gravity corer casts was taken (Stat. 193-96) followed by two TV-multiple corer casts in the evening (Stat. 197-98). Afterwards the ship steamed to station Builder's Pencil 30nm north of Bear's Paw.

Friday, 02-03-2007

At Builder's Pencil we surveyed some pockmark like bottom structures with the OFOS (Stat 199) and performed a CTD/Ro cast (Stat 200). We then returned to Bear's Paw where we took another CTD/Ro for Helium analysis (Stat 201). In the afternoon we retrieved the FLUFO lander which was moored at the end of leg 2 (Stat. 202). The evening was spent with two TV-multiple corer casts (Stat. 203-204). The planned giant TV-grab sampling had to be cancelled since the LWL was damaged and 1200m had to be cut off and stored on deck. We therefore changed to multi beam mapping during the night. (Stat. 205)

Saturday, 03-03-2007

After the multi beam survey we steamed to station Rock Garden where we deployed the ROV (Stat. 206). The dive was very successful as we could detect a cluster of methane seeps on the seabed which released vigorous bubble streams. We then headed back to Station Bear's Paw where we retrieved the BIGO lander during the afternoon (Stat. 207). With another TV-multiple corer sample (Stat. 208) we finished our activities at Bear's Paw and steamed Back to Rock Garden where we deployed the GasQuant Lander near the newly discovered methane seeps (Stat. 209).

Sunday 04-03-2007

We spent the night with two transects with a towed CTD/Ro (Stat. 210-211). In the morning a ROV survey (Stat 212) followed which had to be cancelled since long lines from a tuna fishing vessel blocked our way. Another ROV survey of a mussel colony colonizing a carbonate platform followed in several miles distance (Stat 213). The evening was dedicated to TV-multiple corer sampling (Stat. 214-16) and a gravity corer cast (Stat. 217) from "rain drop" sites (patches of black sediments) near the methane seeps.

Monday, 05-03-2007

During the night we steamed to Station Moa where we took a TV-grab sample (Stat. 218) of carbonate rocks populated with cold water coral reefs of the genus Lophelia. The rest of the night and the early morning were spent with another multi beam survey (Stat. 219) which was finished at Rock Garden where we retrieved the GasQuant lander (Stat. 220). During the afternoon we took two multiple corer samples from the methane seeping area (Stat. 221-22). In the evening we deployed the FLUFO lander at the same position (Stat. 223). A TV-grab (Stat. 224) was taken at the LM-3 site in Rock Garden. In the late evening we surveyed mussel beds with the ROV at the same locality (Stat. 225) and measured temperature anomalies.

Tuesday; 06-03-2007

During the night we changed position again to Station Moa where we drove a CTD/Ro (Stat. 226) and took a TV-grab sample from hard bottom (Stat. 227). Later on we headed back to position LM-3 where we deployed the BIGO Lander on a rain drop site (Stat. 228). Station work at LM-3 was finished with two more TV-grab samples (Stat. 229-30). In the evening we changed position to station Kaka where we took two TV-multiple corer samples (Stat. 231-32).

Wednesday, 07-03-2007

Station work continued during the night with two gravity corer samples at LM-9 (Stat. 233) and Moa (Stat. 234). Afterwards we headed back to LM-3 for a CTD/Ro survey (Stat. 235-236). In the morning we deployed the ROV and inspected the moored landers FLUFO and BIGO, the later was located directly at the gas seeping site. (Stat. 237) Further activities were a TV-grab sample (Stat. 238) a gravity corer cast (Stat. 239) and the successful retrieval of the FLUFO Lander (Stat. 240). Station work continued at Kaka with TV-multiple corer casts (Stat. 241-42) and a gravity corer (Stat. 243). Another gravity corer sample was taken at the nearby LM-9 site (Stat- 244).

Thursday, 08-03-2007

During the night we returned to LM-3 where we made another methane plume survey at the seep site with the CTD/Ro (Stat. 245). A ROV survey came next to sample water directly from the gas seep with NISKIN bottles integrated into the ROV's tool sled (Stat. 246). The day was occupied with several lander operations: the deployment of GasQuant (Stat. 247) and FLUFO (Stat. 248) and the retrieval of BIGO (Stat.249). During the evening we started with a series of gravity corer cast with temperature logging devices on the liner to measure heat flow (Stat. 250-53).

Friday, 09-03-2007

The rest of the night was spent with a multi beam survey (Stat. 254). During the morning we retrieved two moorings with thermistors which were deployed on leg 1. After each retrieval operation we drove a CTD-profile (Stat. 254-56). We then returned to the gas seep and d retrieved the GasQuant lander moored on the previous day (Stat. 257). Station work at LM-3 went on with three TV-multiple corer casts (Stat. 258-60). Afterwards we steamed to Station Kaka for two more TV-multiple corer samples (Stat. 261-62).

Saturday, 10-03-2007

We returned to Rock Garden to measure methane with yoyo-CTD/Ro casts (Stat. 263-64). In the morning we retrieved the FLUFO lander (Stat. 265) We finished station work in the Rock Garden area with three gravity corer samples at LM-3 (Stat 266-68) Afterwards we took course to the Wairarapa site some 150miles to the south at the eastern entrance of the Cook Strait. En route we made a multi beam survey (Stat. 269). During the night we deviated from our course for a CTD/Ro cast at the Uruti Ridge (Stat. 270) afterwards we returned to our track and continued our multi beam survey towards Wairarapa (Stat. 271).

Sunday, 11-03-2007

We arrived at Wairarapa in the morning and started station work at the Pukeko site with an OFOS transects (Stat. 272). We changed position to the North Tower site to sample sediments with the TV-multiple corer (Stat. 273-74) and for a CTD/Ro cast (Stat 275). During the late afternoon and evening the BIGO lander (Stat. 276) and the FLUFO lander (Stat. 277) were deployed at a rain drop site at North Tower. In the late evening we started a series of gravity corer casts for heat flow measurements (Stat.278-79).

Monday, 12-03-2007

During the night we interrupted our heat flow measurements for two CTD/Ro casts (Stat. 280-81). Afterwards we continued our transect for heat flow measurement with three more gravity corer casts (Stat. 282-284). Three more gravity corer samples for the Geochemistry group were taken during mid day (Stat 285-87). In the evening we deployed a lander with a micro-electrode profiling device (Profiler lander) at a rain drop site (Stat. 288). Next came three TV- multiple corer samples (Stat. 289-91).

Tuesday, 13-03-2007

During the night we drove an OFOS (Stat 292) which was followed by two CTD/Ro casts (Stat. 293-94) until the morning. During the morning the weather started to deteriorate and we were only able to take two gravity corer samples for geochemical analyses (Stat 294-296). At 13:07h wind speeds reached Bft 9 and we were forced to abandon station work.

Wednesday 14-03-2007

The storm persisted and prevented any station works.

Thursday, 15-03-2007

During the night the storm calmed down and we started station work again with the retrieval of the three landers: Profiler, BIGO and FLUFO (Stat. 297-99). Two CTD/Ro casts (Stat. 300-01) followed during the day. Next came a gravity corer cast (Stat. 302) followed by another CTD/Ro (Stat. 303) and a series of three additional gravity corer casts (Stat. 304-6).

Friday, 16-03-2007

After the completion of station 306 we left the Wairarapa area and steamed through the Cook Strait to Wellington pilot station where we took over an airfreight delivery with spare parts for the ROV navigation system from the pilot boat. We returned to the Wairarapa area to continue our station works with the deployment of the Profiler and BIGO lander (Stat. 307-308). During the day a considerable swell developed which impeded our station plans since we had to cancel the planned ROV and TV-grab stations. Instead we drove two TV-Multiple corers (Stat.309). Only one cast was successful since the release mechanism of the core seals was prematurely triggered by bottom contact of the gear through the swell.

Saturday, 17-03-2007

During the night we managed to perform three CTD/Ro casts (Stat 310-312). Meanwhile the weather conditions deteriorated again and we had to stop station work at 06:48h. Wind speeded up rapidly in the course of the morning blowing with Bft 10 with peaks of Bft 11 to 12.

Sunday, 18-03-2007

During the night the storm calmed down and in the morning we had a slack period of about four hours before a new front travelled through our area. We were able to retrieve the Profiler and the BIGO Lander (Stat. 313-14) and took a final a TV-multiple corer sample (Stat. 315). With the wind rising

again we left Wairarapa and steamed north to the Rock Garden area on a multi beam profiling course. We stopped at Uruti Ridge and took a TV-grab sample of carbonate rocks (Stat. 316). Afterwards we continued our transit to Rock Garden on the multi beam profiling track (Stat. 317).

Monday, 19-03-2007

We arrived in the Rock Garden area in the morning and made a ROV dive at the gas seeps to measure temperature anomalies and to take water samples from the seep outflows (Stat 318). In the course of the day we took 3 CTD/Ro samples at the Faure Site (Stat. 319-321) follows by a multi-beam survey (Stat 322). The evening was dedicated again to CTD/Ro sampling (Stat. 323-324). During the night we continued our multi beam survey (Stat 325)

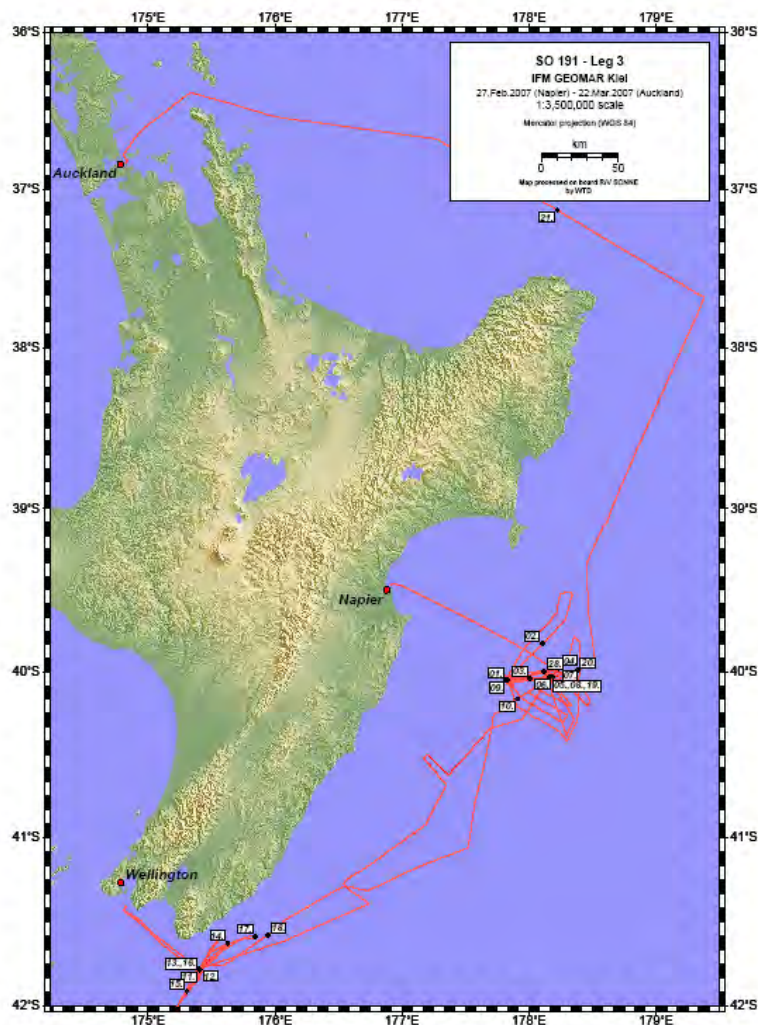


Figure 4.3.1: Cruise track Leg 3.

Tuesday, 20-03-2007

Station 325 was finished in the morning and with this the Station work of SONNE191 leg3 was completed. We stayed at the end of the station for some hours to shift gear on the working deck and to prepare the transit to Auckland. In the early afternoon we left the Rock Garden area and headed towards under fair weather conditions Auckland.

Wednesday, 21-03-2007

We continued on our transit to Auckland.

Thursday, 22-03-2007

We arrived at Auckland in the morning and unloaded our equipment during the day.

Friday, 23-03-2007

With the disembarkment of the scientists and the discharge of the airfreight in course of the morning, cruise SONNE 191 leg 3 ended.

5 Scientific Equipment

5.1 Shipboard Equipment

5.1.1 Navigation

A crucial prerequisite for all kinds of marine surveys is the precise knowledge of position information (latitude, longitude, altitude above/below a reference level). Since 1993 the global positioning system (GPS) is commercially available and widely used for marine surveys. It operates 24 satellites in synchronous orbits, thus at least 3 satellites are visible anywhere at any moment (Seeber, 1996). The full precision of this originally military service yields positioning accuracy of a few meters. In the past this was restricted to military forces and inaccessible to commercial users (Blondel and Murton, 1997). Since about 2000 the full resolution is generally available (with an accuracy in the order of 15 m). As the one of the targets of this cruise was to provide high resolution positioning information of seeps sites, which cover usually only a few tens of meters for the following geologic and geochemical sampling, the operation of the differential (DGPS) option was requested.

GPS-values as well as most other cruise parameters are continuously stored in the navigation database, and are distributed via the DVS- ("data distribution system") on the ship's network.

5.1.2 Simrad EM120 Multibeam

J. Greinert, A. Jones, J. Kilner

Knowing the depth and morphology of the seafloor is essential for cold seep research. It is important for deploying and towing gear at/over the seafloor and of course gives a detailed insight into tectonic and sedimentary developments.

System

The EM120 system is a multibeam echosounder (with 191 beams) providing accurate bathymetric mapping up to depths higher than 11000 m. This system is composed of two transducer arrays fixed on the hull of the ship, which send successive frequency coded acoustic signals (11.25 to 12.6 kHz). Data acquisition is based on successive emission-reception cycles of this signal. The emission beam is 150° wide across track, and 2° along track direction. The reception is obtained from 191 overlapping beams, with widths of 2° across track and 20° along it. The beam spacing can be defined as equidistant or equiangular, and the maximum seafloor coverage fixed or not. The echoes from the intersection area (2°x 2°) between transmission and reception pattern, produce a signal from which depth and reflectivity are extracted.

For depth measurements, 191 isolated depth values are obtained perpendicular to the track for each signal. Using the 2-way-travel-time and the beam angle known for each beam, and taking into account the ray bending due to refraction in the water column by sound speed variations, depth is estimated for each beam. A combination of phase (for the central beams) and amplitude (lateral beams) is used to provide a measurement accuracy practically independent of the beam pointing angle. The raw depth data need then to be processed to obtain depth-contour maps. In the first step, the data are merged with navigation files to compute their geographic position, and the depth values are plotted on a regular grid to obtain a digital terrain model (*DTM*). In the last stage, the grid is interpolated, and finally smoothed to obtain a better graphic representation.

Together with depth measurements, the acoustic signal is sampled each 3.2 ms and processed to obtain a cartographic representation, commonly named mosaic, where grey levels are representative of backscatter amplitudes. These data provide thus information on the sea-floor nature and texture; it can be simply said that a smooth and soft seabed will backscatter little energy, whereas a rough and hard relief will return a stronger echo.

Method

During SO191 a swath width of 120 or 100° was usually used for mapping. The system kept running during the entire time regardless if the ship steamed or was on station. New raw data files were started about every hour. Data processing occurred by a very simplified procedure using MB Systems 5.0.7. After setting the sound velocity file for each raw data file the data were processed and XYZ data were exported excluding data during the time the ships speed was slower than 3km/h (Figure 5.1.1.1).

Data editing was performed via the 3D editing tool in Fledermaus. The edited XYZ data were gridded and displayed with GMT 4.1.3. The sound velocity profile used was recorded during a TANGAROA cruise in November 2006 (Figure 5.1.2.2).

```
#!/bin/bash -f
# doing MB data processing during SO191
#
# copy all new data from the
# windows/D/SO191_all data directory into /home/Jens/SO191_1
#-----
# write all new .all files in a datalist file by typing
ls *.all > datalist.mb-1
# create parameter files with mbset and add the svp file
mbset -ldatalist.mb-1 -PSVPFILE:TAN06-07_svp.txt
#-----
# run mbprocess (which applies the correct svp and is doing
# all the calculations
mbprocess -F-1 -ldatalist.mb-1 -V
#
# the result are *.mb56 files
#-----
# write the processed files in a datalist file by typing
ls *.mb56 > datalistp.mb-1
#export the xyz data via mblast
mblast -ldatalistp.mb-1 -F-1 -OXY-z -M0/190 -S3 -V >>
SO191_#1.xyz
```

Figure 5.1.1.1: MB Script for multi beam data processing during SO191.

Explicit mapping surveys were planned mostly during transit times. The 5 study areas, Wairarapa, Uruti Ridge, LM-9, Rock Garden and Builders Pencil were mapped parallel to the side scan surveys during Leg 1.

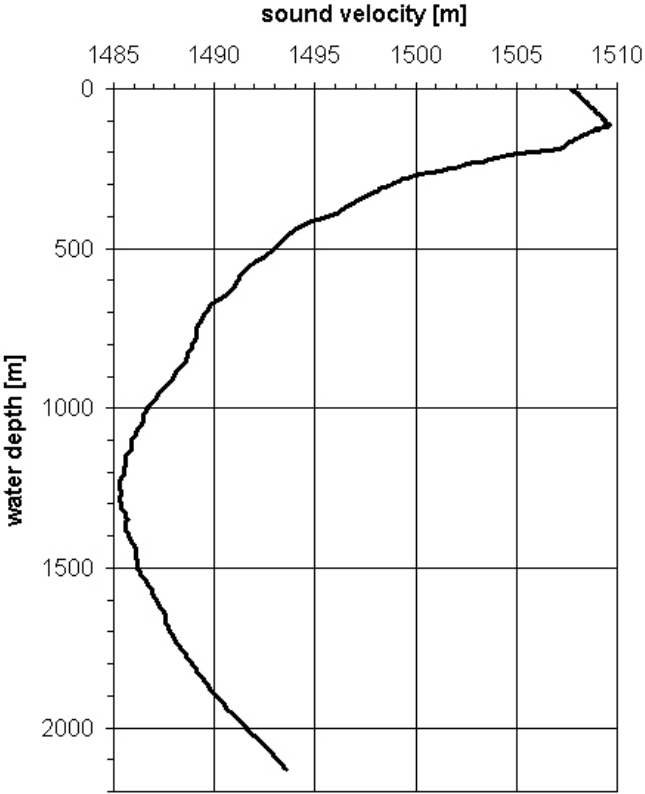


Figure 5.1.2.2: Sound velocity profile used during the multi beam processing

5.1.3 PARASOUND

The PARASOUND system works both as a low-frequency sediment echosounder and as a high-frequency narrow beam sounder to determine the water depth. It utilizes the parametric effect, which produces additional frequencies through nonlinear acoustic interaction of finite amplitude waves. If two sound waves of similar frequencies (here 18 kHz and e.g. 22 kHz) are emitted simultaneously, a signal of the difference frequency (e.g. 4 kHz) is generated for sufficiently high primary amplitudes. The new component travels within the emission cone of the original high frequency waves, which are limited to an angle of only 4° for the equipment used. Therefore, the footprint size of 7% of the water depth is much smaller than for conventional systems and both vertical and lateral resolution are significantly improved.

The PARASOUND system is permanently installed on the ship. The hull-mounted transducer array has 128 elements within an area of 1 m by 2 m. It requires up to 70 kW of electric power due to the low degree of efficiency of the parametric effect. In 2 electronic cabinets, beam formation, signal generation and the separation of the primary (18, 22 kHz) and secondary frequencies (4 kHz) is carried out. Since the two-way travel time in the deep sea is long compared to the length of the reception window of up to 266 ms, the PARASOUND System sends out a burst of pulses at 400 ms intervals, until the first echo returns. The coverage in this discontinuous mode is dependent on the water depth and also produces non-equidistant shot distances between bursts.

In addition to the analog recording features with the b/w DESO 25 device, the PARASOUND System is equipped with the digital data acquisition system ParaDigMA, developed at the University of Bremen. The data is stored on removable hard disks using the PS3 format. The 486-processor based PC allows for buffering, transfer and storage of the digital seismograms at very high repetition rates. Of the emitted series of pulses, usually only every second pulse can be digitized and stored, resulting in recording intervals of 800 ms for a given pulse sequence. The seismograms were sampled at a frequency of 40 kHz, with a typical registration length of 266 ms for a depth window of ~200 m. The source signal was a band limited, 2-6 kHz sinusoidal wavelet with a dominant frequency of 4 kHz and duration of 1 period (250 μ s total length). Data was stored on DAT-tapes using Windows NT backup software.

5.1.4 ADCP

D. McGinnis

The R/V SONNE is equipped with a deep water hull-mounted ADCP (Ocean Surveyor RD Instruments). The Ocean Surveyor ADCP is designed for long-range three-dimensional current profiling, and includes backscatter profiling. The RDI 4-beam system allows bottom-tracking which enables visually observing bottom features, and allows the RDI to track the ship position and speed based on bottom readings. The ADCP is a 38.4 kHz system with a 30° beam angle. The maximum profiling range is up to 1000 m deep, with user selectable 16 or 24 meter vertical resolution (bin size). Manufacturers specifications list the precision at 23 – 30 cm/s with accuracy of $\pm 1.0\%$ and ± 0.5 cm/s. The maximum ping rate for the 38.4 kHz system is 0.4 pings/s with a velocity range of 5 – 9 m/s.

5.1.5 CTD (Conductivity-Temperature-Depth) operations

K. Faure, D. McGinnis, R. Kipfer, J. Schneider v. Deimling

The goals of the CTD program were to; (1) provide real-time information for water sampling by monitoring the METS sensor and hydrographic characteristics of the water column at each station, (2) provide a sampling platform for the collection of water samples, and (3) map the distribution of (methane) signals within a previously identified survey area (information from side scan sonar, historical, etc.), and (4) attempt to determine the input mechanism of subsurface methane (diffusive, bubble or plume). The success of the CTD operations on this scientific voyage is undoubtedly indebted to a METS sensor, possibly the only one of a kind, that is very sensitive to change (by as low as 3-5 nM) in water CH₄ content and a relatively rapid recovery after exposure to high concentrations (discussed further below). Each of these objectives was successfully completed. 72 CTD stations were occupied during the cruise, which consisted mainly of vertical casts and discrete water samples have been taken for various analysis like δ^{13} CH₄, radon (IFM-GEOMAR), microbiology (MPI, GNS) and noble gases (EAWAG).

Submarine venting is a major source of methane to the ocean. Methane is also one of the most commonly used chemical tracers for shipboard detection of cold water vents, mainly because of its relative ease of shipboard measurement, low CH₄ background concentrations in deep seawater, and

its relatively short residence time (c. 10 days) in plumes rising above vent sources. A total of 1301 samples were collected and analysed for CH₄ during the SO191-2,3 legs. Duplicate samples were collected for later carbon isotope analysis of dissolved CH₄ from samples which had high CH₄ concentrations. Water that was identified to have high CH₄ concentration using the head-space GC method were sampled for later carbon isotope measurement by extracting dissolved gases using the vacuum-extraction method.

All casts used a high-precision *SeaBird 911plus* CTD equipped with a CAPSUM METS sensor or a CONTROS methane sensor, DO, conductivity and temperature sensor. The *911plus* samples at 24 hz with a temperature accuracy was better than 0.001°C; accuracy of the conductivity cell is nominally 0.0003 S/m. Water samples were collected and CH₄ analyses determined by GC on-board using mainly a head-space equilibration extraction method and also to a lesser extent a vacuum extraction system. The bottom contact alarm allowed us to safely lower the CTD to within 3-5 m of the bottom. The rosette holds twenty four 10 litre Niskin bottles, however, Niskin bottle 13 failed to work throughout the SO191-2/3 survey.

5.1.6 OFOS

D. Bowden

The OFOS (Ocean Floor Observation System) towed camera platform of the RV Sonne was used at all study locations to make real-time video observations of the seabed and to take higher-resolution time-lapse digital still images for later analysis. OFOS carries colour and monochrome CCD video cameras and, for this voyage, a 4 mp digital stills camera. An array of 3 red lasers (10 mw) allows image scaling and ranging: 2 lasers are parallel at 20cm spacing for scaling; the third, central, laser is set at an angle of 8.8° to the plane of the parallel lasers to give a visual indication of altitude. When all 3 lasers are in line, the camera is 3 m above the seabed. Video is streamed to the surface via fibre-optic cable for real-time viewing and is recorded to hard disc with later DVD backup. During SO191, all video was also recorded to miniDV digital tapes. Still images are recorded in camera and downloaded at the surface. OFOS has an integral SIMRAD DHT 163 hydro acoustic transponder for tracking but after initial trials the more precise IXSEA Posidonia system was used.

OFOS transects were planned on the basis of existing information (e.g. NOAA/NIWA TAN0616, Lewis & Marshall 1996) and data from acoustic surveys conducted during SO191. Thus, surveys at progressively finer spatial scales (multibeam, Parasound, deep-towed side-scan sonar) defined the location of potential seep sites at which OFOS was then deployed for visual ground-truthing and biological observations. High-resolution side-scan sonar images were particularly important for the detection of carbonate formations. All OFOS deployments were planned, tracked, and annotated using the OFOP (Ocean Floor Observation Protocol) software developed by J. Greinert.

Spatially-referenced observations of substratum type and benthic fauna in the video image were recorded in real time, using OFOP, with emphasis on seep-associated fauna, carbonate rock formations, bacterial patches, and sulphidic sediments. Still images were examined after the deployment to confirm faunal identifications and will be used later to make estimates of relative abundance. Combining the spatial distribution data from the video with quantitative data from the stills will allow analysis of faunal distributions in relation to physical characteristics of the habitat.

5.2 Computer Facilities

5.2.1 OBH/S Computer Facilities

A. Krabbenhoft, J. Petersen, J. Bialas

The experiments and investigations during SO191 required special computing facilities in addition to the existing shipboard systems. For programming of ocean bottom stations, processing and interpretation of seismic data and analysis of magnetics, several PC-workstations and a dedicated PC-laptop were installed by the wide angle group of IFM-GEOMAR.

Due to the large amount of data transfer IFM-GEOMAR installed a workstation cluster onboard comprising the systems listed in Tab. 5.2.1.1.

In addition to these computers, several laptops were used and two Macintosh computers for the seismic modeling and interpretation with the forward modeling program MacRay. For plotting and printing one Kyocera Mita FS6020 Postscript Laserprinter (papersize A3 and A4) as well as the shipboard color plotters were available.

Tab. 5.2.1.1: List of workstations available for OBS and bathymetry processing

1	"caicos"	INTEL Pentium 4 3.2 GHz	2 CPU, 1 GB memory	375 GB disks, 4x PCMCIA	Windows XP Linux (Suse 10.1)
2	"potosi"	INTEL Pentium 4 3.2 GHz	2 CPU, 1 GB memory	375 GB disks, 4x PCMCIA	Windows XP Linux (Suse 10.1)
3	"crimea"	AMD Duron 700 MHz	1 CPU, 128 MB memory	68 GB disks, 6x PCMCIA	Windows XP Linux (Suse 9.3)
4	"roorise"	AMD Duron 700 MHz	1 CPU, 128 MB memory	68 GB disks	Windows XP Linux (Suse 10.1)

The workstation cluster was placed in the Magnetiklabor. The huge amount of data and thus data transfer required a high-performance network, which was accomplished by a switched twisted-pair ethernet. A 24-port ethernet switching-hub (3COM-SuperstackII 3300) with an uplink connection of 100 Mbps maintained the necessary network performance. A shipboard router was used to allow for communication between the IFM-GEOMAR and the shipboard network in order to keep the shipboard network undisturbed by the workstation cluster. This provided the additional benefit of a simplified network configuration. The workstations used the same IP-addresses and network configuration as at IFM-GEOMAR so no further setup work was necessary. Sharkoon 250 GB usbdisks were used as backup system. They were ext3 formatted to allow for backup of files larger than 2 GB, typical sizes for seismic data files. This network setup showed a reliable and stable performance, and no breakdowns were observed.

5.2.2 Leg 1: NIWA, GNS Science, and University of Otago

Several Linux workstations from NIWA, GNS Science and the University of Otago, were used for processing and interpretation of the regional seismic lines and for re-processing of TAN0607 data that will help guiding sampling in Legs 2 and 3. NIWA's computers in the Reinlabor were fully integrated into the vessel's network, while the other computers were mostly used in a separate intranet in the Magnetik Labor. A summary of the computers' specifications and main software packages is given below.

	Technical Specifications	Main software
NIWA	Intel I Pentium, 4CPU, 1.5 GB Ram	ArcGIS, ArcMap
	HP nc6220, Pentium 1.8 Ghz, 2Gb RAM	MS Word, Geographix Seisvision (Seismic interpretation), Adobe Illustrator
	HP-Compact. Pentium LINUX operating system	Globe Claritas, GMT
GNS		
zephyr	Dell Dimension 5150, Dual processor, 2 GB RAM	Globe Claritas
essex	Dell Dimension 8300, Single processor, 512 MB RAM	Globe Claritas
U Otago		
gareth	Toshiba T7200 notebook (Linux/Windows), Dual processor, 2 GHz, 2 GB RAM	Globe Claritas

5.3 Geophysical Instrumentation

5.3.1 Airguns

K. Steffen, J. Petersen, J. Bialas

G-gun Cluster

For the regional investigations 4 G-guns manufactured by *Sercel Marine Sources Division* (former *SODERA*) and *Seismograph Services Inc.* were used as seismic sources. The guns were set up in two clusters, carried by a 5 m long frame (Figure 5.3.1), four floats were adjusted to tow the guns at 4 m water depth. All guns were fired through the IFM-GEOMAR LongShot airgun source controller

manufactured by *RealTime* using the shipboard photo trigger of the *Preussag* telemetry system (see External Trigger below).

Each cluster comprises two 520 cinch (8 l) G-guns (Figure 5.3.1.1) and the cluster arrangement provides a good primary to bubble signal ratio. Operating 4 guns provides a total volume of 32l, and results in high energy radiated from the multiple guns and the high working pressure. Usually, the G-guns are operated at 210 bar. For this purpose a second compressor was set up by RF onboard SONNE to increase the 140 bar pressure from the onboard *Leobersdorfer*. However, due to chosen shot interval of 20s, the pressure could only be built up to about 180 bar. The single delay times of the guns kept constant during this time and hence should provide a consistent shape of the source signal.

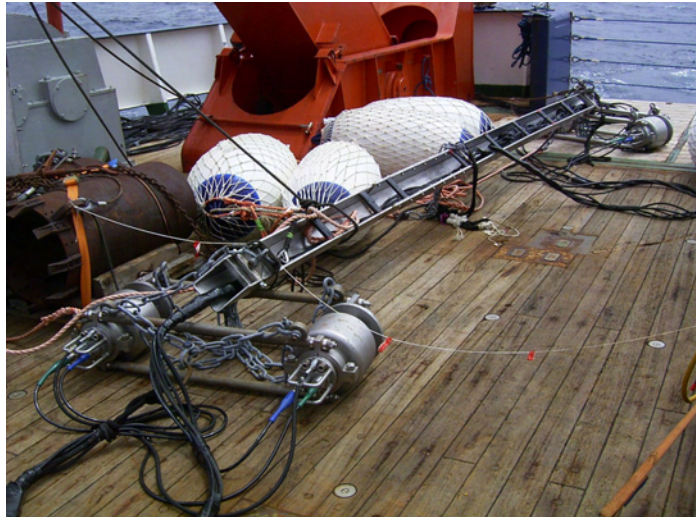


Figure 5.3.1.1: Picture of a 5 m long G-gun Cluster carrier. Two G-gun clusters are mounted below the carrier, while four Polyform floatation are visible on the left hand side

The gun carrier was deployed and towed through the inside of the A-frame. For lifting purposes winches on top of the A-frame were used. First the winch of the A-frame lifted the gun carrier, which was then guided behind the aft of the vessel. Here the towing winch took over the weight while the back of the carrier already tipped into the water. Now the hoisting rope was attached to the towing rope and finally the entire carrier was lowered into the water. Meanwhile four F11 size *Polyform* buoys were pushed into the water, acting as floatation for the frame. Towing depth was 4 m during SO191-1 cruise.

GI-gun

For the high-resolution seismics GI-gun manufactured by *Sercel Marine Sources Division* with a volume of 5.5l (250 cinch generator chamber, 105 cinch injector chamber) was used. It was operated in harmonic mode. The compressed air was supplied by the same compressors as for the G-guns with a pressure of 210 bar. The profiles were acquired with a shot interval of 14s. The GI-gun was attached with chains to a steel frame and towed at the starboard side approx. 22 m behind the stern in a depth of 3.5 m. The setup with the floatation is shown in Figure 5.3.1.2.

External trigger during SO191-1

Since the replacement of the old *Atlas* ANP navigation system on the bridge by the new DSHIP system from *Werum* GPS controlled seismic trigger signals are no longer available. Therefore the control device of the digital camera used with the *Preussag* OFOS telemetry system was used to provide a trigger signal for the airgun shots. The impulse was delivered to the *LongShot* trigger box. The trigger pulses from the OFOS system, necessary for subsequent data processing and instrument location, were stored on a MBS recorder and displayed in real time to double check. For this process the same time basis was used as for the OBH. A test of the timing reliability of the *LongShot* trigger box was performed consisting of a synchronous recording of the OFOS trigger signal and the Clock Time Break (CTB) of the *Longshot* device, i.e. a TTL pulse that is 5 ms wide and representing the aim-point or the time when the guns are firing. This aim-point was set to be 60 ms after the OFOS trigger pulse, but the test resulted in a delay of 155 ms pointing to an additional internal delay of the *Longshot* trigger box. After careful analysis of the direct arrivals and multiples in the seismic data, a delay of 135 ms with respect to the OFOS trigger pulse was determined, thus indicating a time shift of 20 ms of the airgun firing time given by the CTB

pulse. Exact position calculation for the shot time should be done by later post-processing using shot time and UTC time values stored with GPS coordinates in the ship's data base.



Figure 5.3.1.2: GI-gun mounted below the carrier to which a Polyform floatation is attached.

5.3.2 Seismic Streamer

P. Barnes, P.K. Gerring, S. Wilcox, G. Lamarche

MCS data were acquired using a new GeoEel system from Geometrics. The system includes a digital streamer and a PC-based controller system. The controller enables staff to perform quality control and recording data on tape or hard discs. Three depth controllers were fitted on the streamer on channels 1, 17 and 25. Depth is directly controlled from the board. A safety recovery unit is attached to channel 25 in case the streamer is cut (e.g., shark bytes). A tail rope was used after an unsuccessful trial with a tail buoy demonstrated that the latter provided too much tension on the streamer and damaged 2 sections. The original setting was a length of 600 m, with a 12.5 m group spacing. Each group consists of 16 Benthos geopoint (see Figure 5.3.2.1, Table 5.3.2.1).

A gun array of 4 x 520 in³ was used for lines 1 to 6 and a GI gun in 250/105 in³ for lines 8 to 10.

Problems with the first two sections of the streamer required them to be disconnected, and the MCS data were recorded on 4 sections, i.e. leaving 32 groups at 12.5 m interval.

Acquisition Shot records were recorded in SEG-D revision 1 format on hard disc and DLT tape. An ASCII string in the shot file header contains all navigation information: time, source longitudes and latitudes in degree, min and in UTM-60, ship longitude and latitude in degrees, minutes and UTM60, vessel speed over ground, full date. Example below:

Example of SEG-D revision 1 navigation string (one line no carriage return): 12:32:18,Source, 40°57.5695'S, 177°15.9910'E, 5465705.56 N,522428.17 E,Ship,40°57.6094'S, 177°15.9632'E, 5465631.86 N, 522388.92 E, 4.8knots, Tuesday, 30 January 2007.

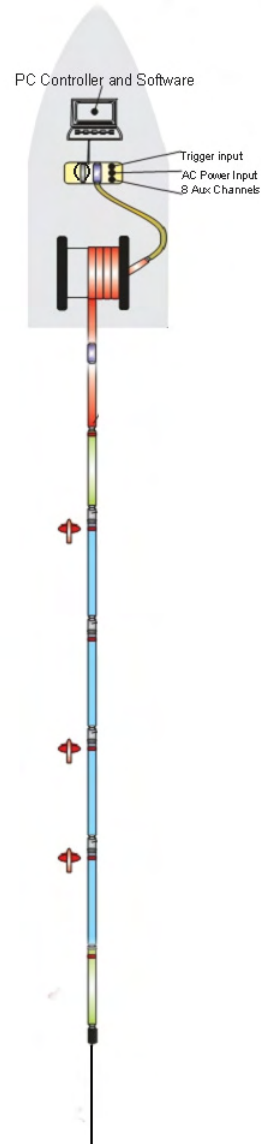
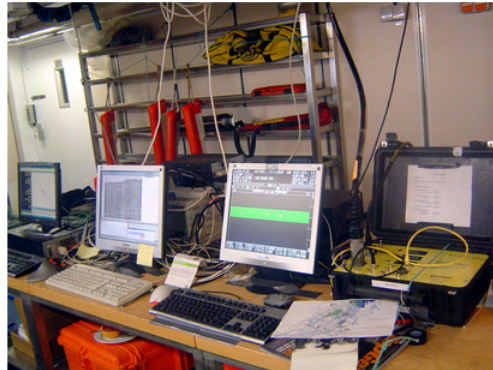
Multi-Channel Seismic (MCS) processing sequence

We used the Globe Claritas software from GNS Sciences to apply a simple processing sequence to the data. This enabled us to undertake quality control and an onboard preliminary interpretation of the seismic profiles.

We used a desktop PC under Linux operating system and connected on the ship network. The raw shot file was transferred across the network onto the linux box.

Acquisition Parameters

Shot Interval	20 seconds (nominally 50m @ 5 knots)
CDP	6.25m
Fold	4
Number of channels	32
Group interval	12.5m
Hydrophones per group	16 Benthos Geopoint
Source	2000 cu inch @ 175 bar (4 x 500 cu inch G guns)



Components:














-  Streamer Power Supply Unit (SPSU)
-  Deck Cable
-  170 m Tow Cable
-  Repeater Module
-  25m Stretch Section
-  A/D Digitizer Module
-  Depth Control Bird
-  100m 8-channel Active Section
-  Digital Connector Pair
-  Analog/Digital Combo Connector Pair
-  Bird Coil
-  Tail Swivel
-  Tail Buoy

Figure 5.3.2.1: The Geometrics GeoEel Streamer and acquisition system.

The processing consisted of:

- 1 – reading SEG-D formatted shot gather and reformatting in extended Claritas SEG-Y format.
- 2 – A single channel section is plotted using trace #3. A broad band-pass filter and a AGC (Automatic Gain Control, 500 ms sliding window) are applied before plotting. (Figure 5.3.2.2)
- 3 – Editing of bad traces (trace #14 is consistently noisy),
- 4 – Compensation for loss of energy by applying a correction for spherical divergence.
- 5 – Definition of a Frequency domain filter. So as to preserve high frequencies in the top part and enhance low frequencies in the deeper part the frequency function varies with depth:

0-800 ms below seafloor	Band-Pass	20-25	150-250 Hz
1100-2000 ms below seafloor	Band-Pass	10-20	110-200 Hz
2250-9000 ms below seafloor	Band-Pass	7-15	80-140 Hz
- 6 – Add geometry and sort into CDP gather. So as to increase the lateral coherency the CDP binning was set at 12.5 m. Trace location was based on ship position with the estimated gun and traces offsets (See Table 5.3.2.1)
- 7 – Apply Normal Move-Out correction using a simple velocity function, and stack traces with a root-square normalisation of amplitudes.
- 8 – Finite difference time migration (Figure 5.3.2.3). A velocity model was built before migration, based on maximum of the semblance functions. Although very crude, because of the lack of offset provided by the streamer, this proved a good first approximation for attenuating the hyperbolae and replacing dipping events in true time position. We have not undertaken any depth migration. Velocity in sediments ~2300 m/s, Velocity along decollement ~3500 m/s.

Table 5.3.2.1 – Acquisition geometry for MCS data – regional lines.

First offset	105 m
Last offset	493 m
Nominal shot spacing (20 s firing rate at 5 knots)	50 m
Group spacing	12.5 m
Hydrophones per group	16 Benthos Geopoint
nominal CDP fold	4
CDP binning	12.5 m
Resulting nominal CDP fold	8
Maximum CDP fold	10

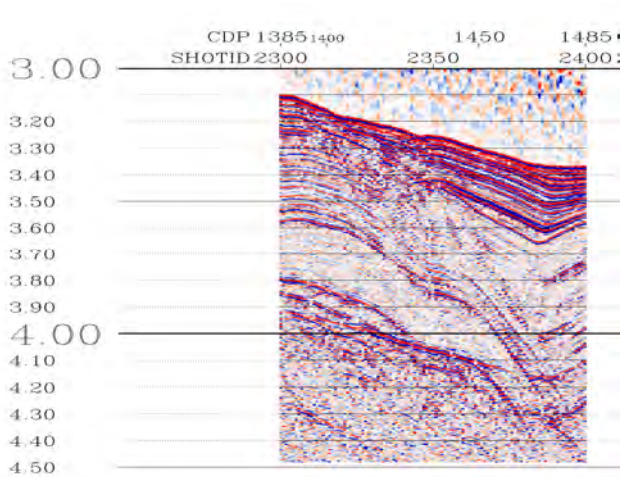


Figure 5.3.2.2. Extract of single channel section SO191-1. To compare with next figure (migrated section)

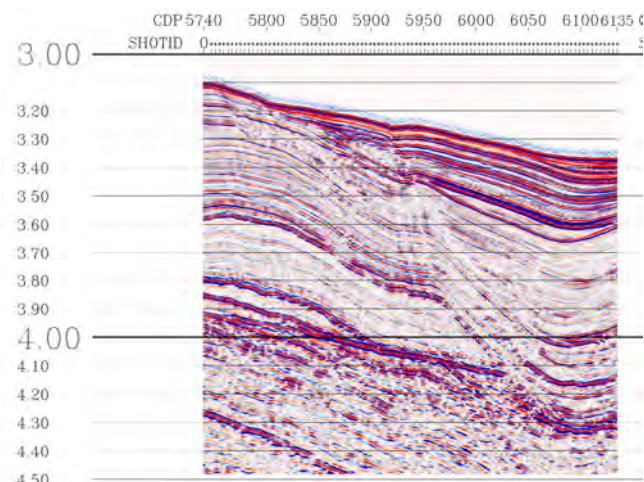


Figure 5.3.2.3. Extract of migrated section SO191-1. To compare with previous figure (single channel)

A total of 9 lines were acquired (Line 7 was curtailed and not recorded), with lines 1, 3, 4, 6, 9 and 10 being dip lines and lines 2, 5 and 8 being strike lines acquired to tie adjacent seismic profiles (Table 5.3.2.2).

Table 5.3.2.2: Acquisition parameters for MCS regional lines.

Line	First shot	Last shot	First CDP	Last CDP	Approx. length
1	1000	3529	458	10752	134 km
2	4000	4785	100	3291	41 km
3	4786	7774	185	12449	155 km
4	10000	11099	100	4545	57 km
5	11100	12060	100	4041	50 km
6	12169	13860	100	6959	90 km
8	15240	15649	100	1765	20 km
9	20000	20560	100	1382	16 km
10	20520	20999	100	1179	14 km

5.3.3 OBH/OBS Seismic Instrumentation

A. Krabbenhoef, J. Petersen, J. Bialas, G. Netzeband, P. Schroeder, C. Jung, C. Hagen, A. Sticher, A.-D. Rohde

The IFM-GEOMAR Ocean Bottom Seismometer 2002

The first IFM-GEOMAR Ocean Bottom Hydrophone was built in 1991 and tested at sea in January 1992. This type of instrument has proved to have a high reliability; more than 4000 successful deployments were conducted since 1991. A total of 16 OBS instruments were available for SO191-1. Altogether 60 sites were deployed for wide angle seismic profiles during the SO191-1 cruise.

The IFM-GEOMAR Ocean Bottom Seismometer 2002 (OBS-2002, Figure 5.3.3.1) is a new design based on experiences gained with the IFM-GEOMAR Ocean Bottom Hydrophone (OBH; Flueh and Bialas, 1996) and the IFM-GEOMAR Ocean Bottom Seismometer (OBS, Bialas and Flueh, 1999). For system compatibility the acoustic release, pressure tubes, and the hydrophones are identical to

those used for the OBH. Syntactic foam is used as floatation body again but compared to the IFM-GEOMAR OBH/S in a less expensive cylinder shape. The entire frame can be dismantled for transportation, which allows storage of more than 50 instruments in one 20" container. Upon cruise preparation onboard all parts are screwed together within a very short time. Four main floatation cylinders are fixed within the system frame, while additional disks can be added to the sides without changes. The basic system is designed to carry a hydrophone and a small seismometer for higher frequency active seismic profiling. The sensitive seismometer is deployed between the anchor and the OBS frame, which allows good coupling with the sea floor. The three-component seismometer (*KUM*) is housed in a titanium case, modified from a package built by Tim Owen (Cambridge) earlier. Geophones of 4.5 Hz natural frequency were used. The signals of the sensors are recorded by use of the *Marine Broadband Seismic Recorder (MBS)*, which are manufactured by *SEND GmbH* and specially designed for short-time high-resolution recordings due to their high precision internal clock. While deployed to the seafloor the entire system rests horizontally on the anchor frame. After releasing its anchor weight the instrument turns 90° into the vertical and ascends to the surface with the floatation on top. This ensures a maximally reduced system height and water current sensibility at the ground (during measurement). On the other hand the sensors are well protected against damage during recovery and the transponder is kept under water, allowing permanent ranging, while the instrument floats at the surface.

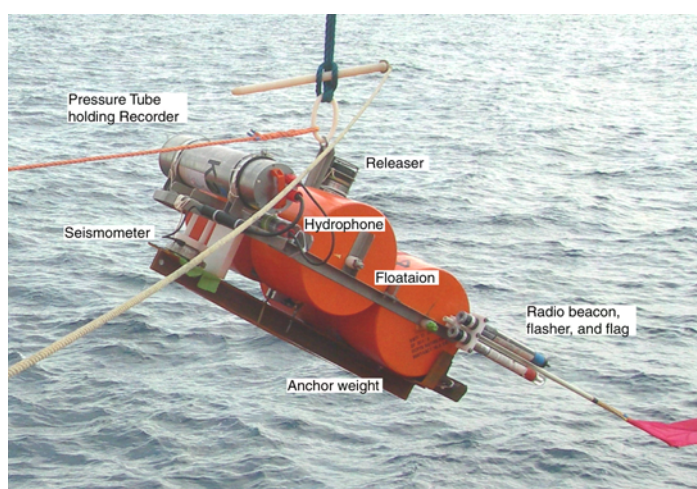


Figure 5.3.3.1: The IFM-GEOMAR Ocean Bottom Seismometer design 2002

Marine Broadband Seismic Recorder (MBS)

The so-called *Marine Broadband Seismic recorder (MBS)*; Bialas and Flueh, 1999), manufactured by *SEND GmbH*, was developed based upon experience with the DAT-based recording unit Methusalem (Flueh and Bialas, 1996) over previous years. This recorder involves the PCMCIA technology enabling static flash memory cards to be used as non-powered storage media. In addition, a data compression algorithm is implemented to increase data capacity. The power consumption of 1.5 W allows to use rechargeable batteries during short time deployments. Depending on the sampling rate, data output could be in 16 to 18 bit signed data. Based on digital decimation filtering, the system was developed to serve a variety of seismic recording requirements. Therefore, the bandwidth reaches from 0.1 Hz for seismological observations to the 50 Hz range for refraction seismic experiments and up to 10 kHz for high resolution seismic surveys.

During SO191-1 cruise the bandwidth of 250 Hz was used for the regional profiles, whereas it was set to 1000 Hz for the closely spaced instruments, that were deployed for the high-resolution network along with the deep towed System.

The basic system of the recorder is adapted to the required frequency range by setting up the appropriate analogue front module. Alternatively, 1, 2, 3 or 4 analogue input channels may be processed. The time base is based on a DTCXO with a 0.05 ppm accuracy over temperature. Setting and synchronising the time as well as monitoring the drift is carried out automatically by synchronisation signals (DCF77 format) from a GPS-based coded time signal generator. After software pre-amplification the signals are low-pass filtered using a 5-pole Bessel filter with a -3 dB corner frequency of 10 kHz. Then each channel is digitised using a sigma-delta A/D converter at a resolution of 22 bits producing 32-bit signed digital data. After delta modulation and Huffman coding the samples are saved on PCMCIA storage cards together with timing information. Up to four 1 GB

storage cards may be used. Data compression allows increase of this capacity. After recording the flashcards need to be copied to a PC workstation using the SEND2X software package. After decompression of the data output to disks can be done in SEG-Y or PASSCAL compatible data format.

Reflection seismic data acquisition (mini-streamer)

In addition to the ocean bottom seismic recorders for cruise SO191-1 a 4 channel mini-streamer was used. The streamer was deployed along the profiles, where the OBH/S profiles were conducted together with the DeepTow system. The streamer was manufactured by *S.I.G. (Service et Instruments de Geophysique, France)*. The system comprises several parts: four 12 m long active sections with 24 hydrophones spaced at 0.5 m. The lead-in cable is 150 m long and directly connected to the lab. The individual hydrophones are omnidirectional and have a flat frequency response from 10 to 1000 Hz. The sensitivity is -90 dB, re $1\text{V}/\mu\text{bar}$, ± 1 dB. Two preamplifiers were available, one with 32 dB and one with 35.5 dB gain. During the first deployment the 35.5 dB preamplifier was used. Due to the large (clipped) amplitudes the preamplifier was exchanged with the 32 dB version, which avoided the amplitudes from clipping on the following profiles of SO191-1 cruise. The hydrophones are mounted in an oil filled polyurethane pipe of 25 mm diameter, with a nominal density of 1.13 g/cm^3 . The tow depth can be controlled by supplying the lead-in cable with air or water and the depth can be monitored at the depth monitor integrated in the system with the power supply. Following experiments on cruise SO190 additional iron bars had been attached to the streamer. During the SO191-1 cruise it was towed at a depth of 9 m. The streamer had to be deployed and recovered manually.

A four channel MBS data logger (s.a.) was used to record the seismic signals of the G-gun clusters and GI-gun. Direct water wave arrival and reflection signals could be well observed using the online display capabilities of the MBS device (s.a.) already.

Due to the close distance between the GI-gun and the towing cable for the DeepTowedSystem at the stern of RV SONNE it was decided to use the portside magnetometer boom on the Backdeck. Deployment and towing was guided through the large diameter rolls of the IFM-GEOMAR magnetometer to avoid strong bending. With 7 m offset to the vessel the streamer was towed in safe distance to the port G-gun array.

Due to the inflexible stiffness of the additional iron bars the parts of the leadin cable need to be hand guided through the large diameter roll on the magnetometer boom. Therefore the boom was swung towards the ship when recovery of the streamer starts. During the final recovery strong currents and wind moved the remaining part of the streamer towards the stern of the vessel where it got stuck in the rudder. No attempt to pull it out was successful, even trials from the deployed work boat did help. During the work boat trials the streamer was broken into parts. Only 35 of 96 hydrophones could be recovered.

5.4 Sidescan sonar

I. Klaucke, W. Weinrebe, J. Petersen

Detailed geoacoustic mapping of asphalt volcanism and related fluid-escape structures have been targeted using the DTS-1 sidescan sonar system (Figure 5.4.1) operated by IfM-GEOMAR, Kiel. The DTS-1 sidescan sonar is a dual-frequency, chirp sidescan sonar (*EdgeTech Full-Spectrum*) working with 75 and 410 kHz centre frequencies. The 410 kHz sidescan sonar emits a pulse of 40 kHz bandwidth and 2.4 ms duration (giving a range resolution of 1.8 cm), and the 75 kHz sidescan sonar provides a choice between two pulses of 7.5 and 2 kHz bandwidth and 14 and 50 ms pulse length, respectively. They provide a maximum across-track resolution of 10 cm. With typical towing speeds of 2.5 to 3.0 kn and a range of 750 m for the 75 kHz sidescan sonar, maximum along-track resolution is on the order of 1.5 metres. In addition to the sidescan sonar sensors, the DTS-1 contains a 2-16 kHz chirp subbottom profiler providing a choice of three different pulses of 20 ms pulse length each. The 2-10 kHz, 2-12 kHz or 2-15 kHz pulse gives a nominal vertical resolution between 6 and 10 cm. The sidescan sonar and the subbottom profiler can be run with different trigger modes, internal, external, coupled and gated triggers. Coupled and gated trigger modes also allow specifying trigger delays. The sonar electronics provide four serial ports (RS232) to attach up to four additional sensors. One of these ports is used for a Honeywell attitude sensor providing information on heading, roll and pitch and a second port is used for a pressure sensor. Finally, there is the possibility of recording data directly in the underwater unit through a mass-storage option with a total storage capacity of 30 Gbyte (plus 30 Gbyte emergency backup).

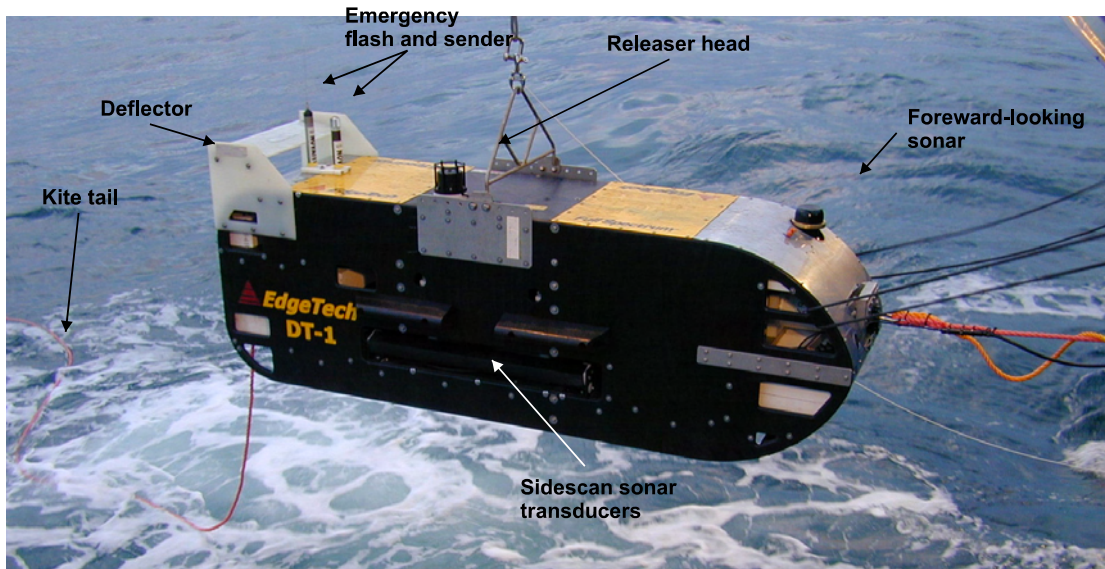


Figure 5.4.1: A picture of the DTS-1 sidescan sonar towfish. The forward-looking sonar is no longer mounted.

The sonar electronic is housed in a titanium pressure vessel mounted on a towfish of 2.8 m x 0.8 m x 0.9 m in dimension (Figure 5.4.1). The towfish houses a second titanium pressure vessel containing the underwater part of the telemetry system (*SEND DSC-Link*). In addition, a releaser capable to work with the USBL positioning system *POSIDONIA (IXSEA-OCEANO)* with separate receiver head, and an emergency flash and radio beacon (*NOVATECH*) are included in the towfish. Since 2006 the towfish houses a *SEA&SUN* pressure sensor. The towfish is also equipped with a deflector at the rear in order to reduce negative pitch of the towfish due to the weight of the depressor and buoyancy of the towfish.

The towfish is connected to the sea cable via the depressor through a 45-m long umbilical cable (Figure 5.4.2). The umbilical cable is tied to a buoyant rope that takes up the actual towing forces. An additional rope has been taped to the buoyant rope and serves to pull in the instrument during recovery.

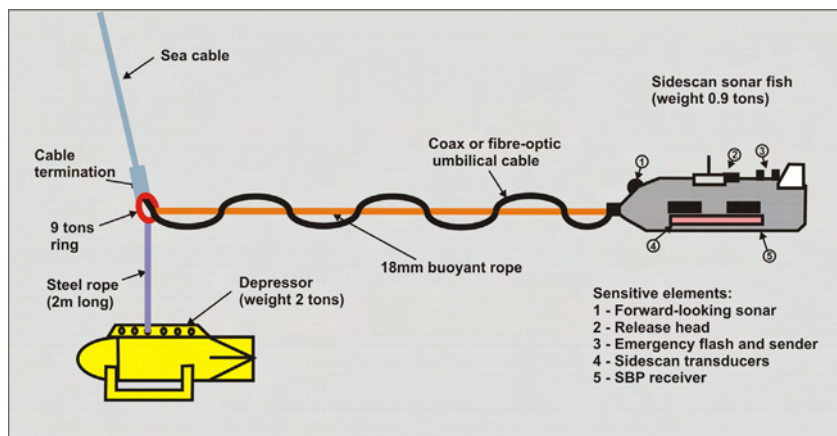


Figure 5.4.2: The DTS-1 towing configuration.

The main operations of the DTS-1 sidescan sonar are run using *HydroStar Online*, the multibeam bathymetry software developed by *ELAC Nautik GmbH* and adapted to the acquisition of *EdgeTech* sidescan sonar data. This software package allows onscreen presentation of the data, of the tow fish's attitude, and the tow fish's navigation when connected to the *POSIDONIA* USBL positioning system. It also allows setting the main parameters of the sonar electronics, such as selected pulse, range, power output, gain, ping rate, and range of registered data. *HydroStar Online* also allows activating data storage either in XSE-format on the *HydroStar Online* PC or in JSF-format underwater on the full-spectrum deep-water unit *FS-DW*. Simultaneous storage in both XSE and JSF-formats is also possible. Accessing the underwater electronics directly via the surface full-spectrum interface-unit *FS-IU* and modifying the sonar.ini file of the *FS-DW* allows changing additional settings such as trigger mode. The *FS-IU* also runs *Jstar*, a diagnostic software tool that also allows running some

basic data acquisition and data display functions. *HydroStar Online* creates a new XSE-file when a file size of 20 MB is reached, while a new JSF-file is created every 40 MB. How fast this file size is reached depends on the amount of data generated, which depends on the use or not use of the high-frequency (410 kHz) sidescan sonar. The amount of data generated is also a function of the sidescan sonar and subbottom pulses and of the data window that is specified in the initialisation file (sonar.ini) on the *FS-DW*. The data window specifies the range over which data are sampled.

5.5 CSEM – Controlled Source Electro-Magnetics

K. Schwalenberg, D. Keen, P. Schroeder

Marine controlled source electromagnetic (CSEM, Figure 5.5.1) is a relatively new application to derive the electrical properties of the upper seafloor to a depth of 1 or 2 km. The physical parameter, the electrical conductivity or its reciprocal, the electrical resistivity of marine sediments is mainly controlled by the amount of conductive seawater in the available pore space, and thus depends on the porosity. It is in the order of 1-2 Ohm*m for the first hundred meters below seafloor. The conductivity of seawater on the seafloor varies between 3 and 3.5 S/m and is mainly a function of temperature and salinity. In recent years marine CSEM became increasingly attractive to the offshore hydrocarbon industry because of the potential to image the presence of natural hydrocarbons such as oil, gas and gas hydrates in the sub-seafloor sediments. Within the reservoir, the conductive pore water is replaced by resistive hydrocarbon. As a consequence, the apparent resistivity measured on the seafloor is enhanced, if hydrocarbon is formed in sufficient quantities. Here, it complements seismic methods, which provide structural information, but are often ambiguous whether the reservoir is filled with oil, gas or water.

Within the “New Vent” project, marine CSEM has been applied to investigate the electrical signature of several gas seep sites along the Hikurangi Margin. Marine CSEM has been employed for the first time within a German project as well as off the coastlines of New Zealand.

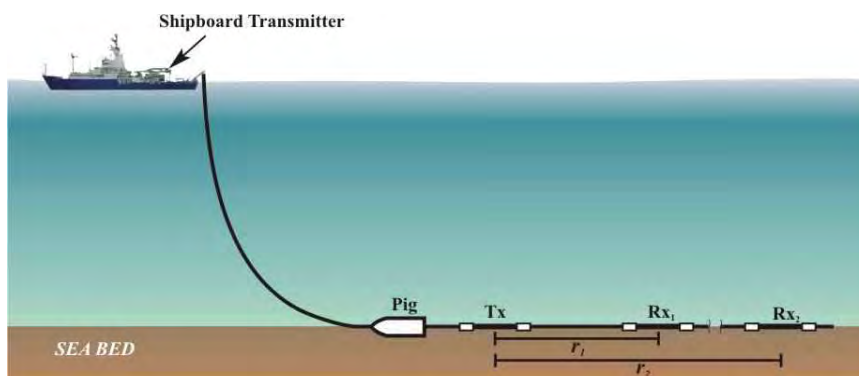


Figure 5.5.1: Geometry of the CSEM System

Instrumentation

The instrument used is a bottom towed electric dipole-dipole system designed and built at the University of Toronto to investigate the resistivity structure of the upper seafloor to a depth of a few hundred meters. The instrumentation has been successfully used so far to explore gas hydrate deposits and cold vent sites on the Cascadia Margin off the coast of Vancouver Island, Western Canada (Yuan and Edwards, GRL 2000, Schwalenberg et al., First Break 2005) and is now available at IFM-Geomar in Kiel. On the seafloor, it consists of a transmitter dipole, Tx (124m long), and two receiver dipoles, Rx1 and Rx2, at distances r_1 and r_2 , which are towed inline behind the transmitter dipole (Figure 5.5.1). A heavy weight (pig) is attached to the front of the array to keep it in straight alignment on the seafloor during the deployment. The pig hosts the electrical connection from the deep tow cable to the transmitter cable Tx. RV Sonne is equipped with a 7.5km long coaxial cable. Pieces of copper braid are coiled around each end of the transmitter cable and serve as transmitter electrodes. The two receivers are identical in construction and consist of pieces of 15m long heavy-duty rubber hose to protect a pair of silver/silver chloride electrodes mounted inside both ends of the rubber hose. Each receiver is equipped with a self-contained electrical unit attached to the front end of the rubber hose to enhance and store the signal coming from the electrodes. The units contain an Onset Tattletale data logger, model TT8, with a 12 bit A/D converter, a synchronous clock with a 10 MHz crystal, and an analog filter board. They are powered by C-cell battery packs with a lifetime of about 36h for the chosen experimental set-up. Similar electronics to those attached to the receiver

arrays are used on-board to monitor the signal coming from the transmitter. Transmitter and receiver dipoles are mechanically connected with simple rope of sufficient traction (Figure 5.5.2).

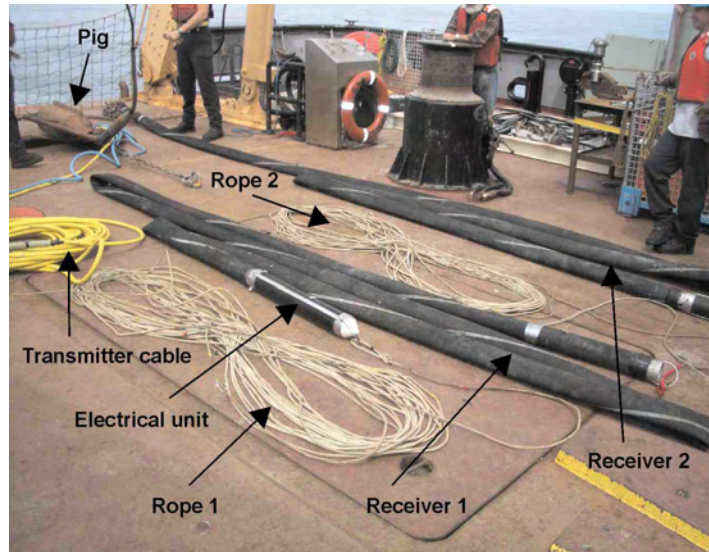


Figure 5.5.2: Parts of the CSEM Instrument. Photo taken on Canadian Coastguard Ship J.P. Tully.

The system is operated in the time domain. The source signal is generated on-board. It has a square wave form with a period of 3.36 s taken from the clock board of the unit used to monitor the transmitted current in the lab. The signal from the clock is used as logic input into a signal driver box which controls polarity and size of the signal. The signal from the driver box is passed on as external reference to the transmitter box which has a maximum output of 15A and 600V. The output of the transmitter box is sent through the deep tow cable to the transmitter dipole on the seafloor where it propagates along two pathways to the receivers towed behind. One pathway is through the conductive seawater, the other is through the more resistive sediments. A third path, namely through the air, has to be considered when the water depth is comparable or less than the transmitter receiver separation. At the receivers, AC coupled time windows are recorded at a sampling rate of 0.819 ms, each 59000 samples long, and stored on 512MB flash cards. The TT8 can handle positive inputs between 0 and 4096 mV. Therefore the input signal is shifted by 2V and gain factors are chosen appropriately to the expected size of the signal.

The CSEM system is operated as a "black box". After launching the recording software to the data logger no communication is possible during the experiment. Once the array is mechanically and electrically connected and lined up on deck it can be deployed in the water and lowered to the seafloor by paying out the deep tow cable.

The instrument is towed along profiles making measurements from site to site. This can be achieved by moving the ship while reeling the deep tow cable in and out. To obtain clean data it is important that the array on the seafloor is stationary during the measurement. A sophisticated solution has been found by paying out a working length of 300m cable while the ship is holding position during measurements on site and taking in the same working length while moving the ship from site to site in between measurements. Taking in cable has the effect of pulling the array forward on the seafloor. Paying out cable, in contrast, gives additional slack and allows the ship to move about a ship length during measurements.

Instrument relocation

Instrument relocation has been a problem in recent deployments. The position of the pig on the seafloor has been calculated from a simple Pythagoras approximation using the GPS positions of the ship, water depths and the length of the deep tow cable being paid out. However, the true shape of the deep tow cable in water describes a catenary and the estimated error involved maybe in the order of 100m in 1200m water depth and cable length of 3000m. This time an acoustic release transponder was attached to the pig and the distance from the ship to the pig through the water was determined acoustically (Figure 5.5.3). Then the distance between pig and ship on the seafloor results from Pythagoras and should be accurate to an order of 10m. The dimensions of the array itself have been measured and the points of measurements are assigned midpoint between transmitter dipole and receiver dipole.

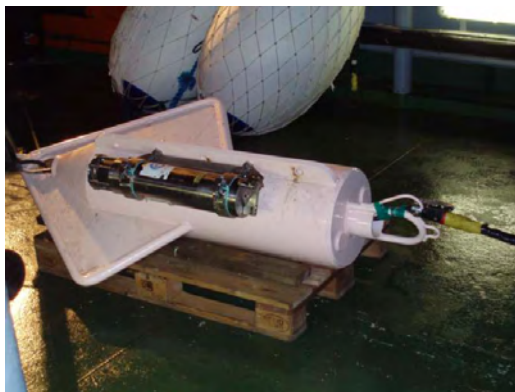


Figure 5.5.3: Pig and acoustic release transponder

Technical data

Transmitter Source

Geophysical Current Transverter DPS Model 042GND03,

Owner: University of Toronto

Manufacturer: Digital Predictive Systems Inc., Mississauga, Canada

Input: 400-460V, 3 Phase 60Hz

Output: Max +- 600 Volts, +- 15 Amps, 9kW

Dimensions: 70x70x71 cm, Weight 110kg

Transmitter Set-up

Input power for the transmitter source was provided by a 380V to 440V transformer on RV Sonne (Figure 5.5.4). The reference signal for the transmitter was taken from the 3.36sec pin on the clock board of the unit recording the transmitter signal in the lab. The clock board outputs square wave forms switching between 0 and ~3V at periods from 25.6 micro sec to 54975 sec or 15.27 h of an oven-heated 10 MHz crystal divided down by factors of two. The reference signal from the clock is fed into a signal driver box, which interprets and amplifies the signal either analog or digital and sends the output to the current transmitter box. The output of the current transmitter box is connected to a current monitor box from where the signal is passed on to the slip ring at the winch and to the coaxial cable where it is sent down through the cable to the transmitter dipole on the seafloor. The signal which is passed on to the coaxial cable is also recorded by the transmitter unit in the lab.

Transmitter dipole

The Transmitter dipole is an approximately 126m long side armored sidescan cable with three coaxial cables and three conductors. The cable is mantled with yellow garden hose for protection and to inhibit current backflow through the armoring. Transmitter electrodes are 50cm pieces of tinned copper braid coiled around each end of the transmitter cable. The electrode at the close end of the transmitter dipole (close to the pig) directly connects to either the shield or the conductor of the coaxial cable. The electrode at the far end connects to the conductors of the side scan cable and to either the conductor or the shield of the coaxial cable.

Receiver Assemblies

Heavy duty rubber hose, length 15m, diameter ~10cm

Pair of non-polarisable Ag-AgCl electrodes, made by Woods Hole Oceanographic Institution (WHOI)

Plastic tube, stainless steel frame, aluminium pressure cylinder

Onset data logger, model Tattletale TT8, 12 bit ADC

Each receiver dipole consists of a length of about 15m heavy duty rubber hose with a diameter of 10cm. A non-polarisable Ag-AgCl electrode made by Woods Hole Oceanographic Institution (WHOI) is mounted inside a plastic holder at each end of the rubber hose. The electrical recording unit resides in a pressure cylinder placed into a torpedo shaped frame mounted to the closer end of each rubber hose.

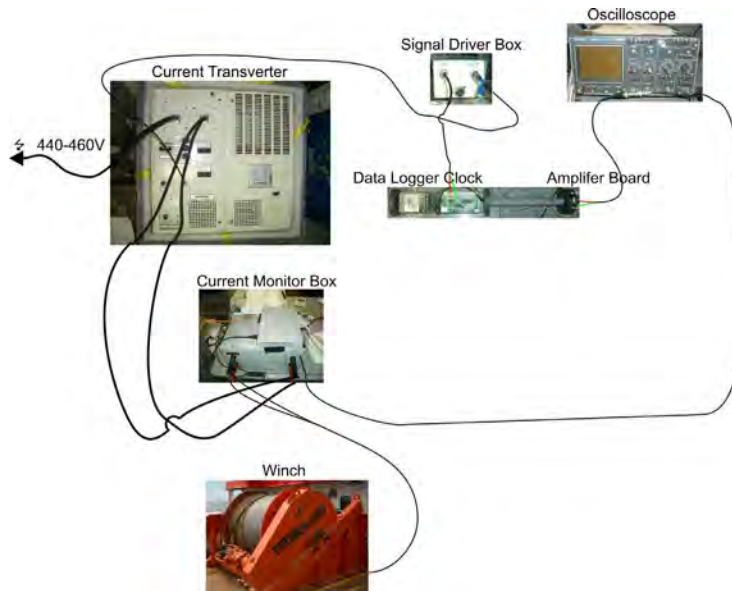


Figure 5.5.4: Schematic of the transmitter set-up.

Data Analysis

The data collected at the two receivers are time series of finite length of the voltage difference between electrodes. Each window is 59,000 samples long which fits the size of the buffer of the Tattletale data logger. This agrees with a window length of ~ 48 sec at a sampling rate of 819microsec. The data have been corrected for DC offsets and gain factors. A high pass filter at the input of the signal is causing the asymptotic decay of the otherwise square wave form of the signal. Data examples from profile Waira I collected at Rx1 and Rx2 are shown in Figure 5.5.5. Data processing includes a conditional stacking process of all half periods recorded at a site. The stacking criteria have been inferred from the cross correlation of adjacent half periods. Depending on data quality, the stacking depths are between some tens and more than 400 for all data collected during the cruise. Examples for the data quality achieved through conditional stacking are shown in Figure 5.5.6. The source signal has been recorded with a similar set-up as the receiver data. The source signal used in the data analysis is obtained through conditional stacking of all half periods for the respective experiment.

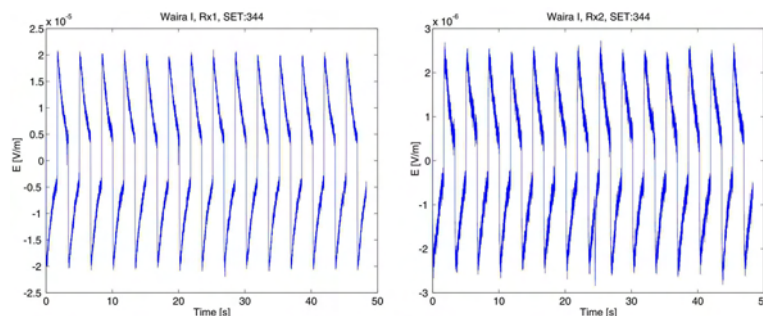


Figure 5.5.5: Examples of time series recorded at Rx1 (left) and Rx2 (right) along Waira I. Each window has 59,000 samples and is about 48s long (sampling rate: 819 microseconds). The asymptotic decay is caused by a high pass filter on the analog circuit of the input. Data have been corrected for DC offsets and gain factors.

1D Inversion

Software provided by C. Scholl, University of Toronto, has been used to calculate one-dimensional layered resistivity models from the data. The inverse code is based on programs composed by N. Edwards, University of Toronto. Two inverse strategies can be applied: Occam and Marquardt inversion. In the first case, a smooth model, minimum structure strategy is implied, while in the second a damping factor is considered to regularize the solution which may also result in a smooth model structure. The Marquardt technique also allows to fix single model parameters during the inversion. Input data are the conditional stacked time series for each site, at chosen, logarithmically spaced time steps and the respective data errors (standard deviations), the source signal, water depth and water conductivity (both fixed in the inversion), and layer resistivities and thicknesses of the

starting model. To calculate the apparent resistivity profile, the only model parameter is the resistivity of the lower halfspace, i.e. sediment section.

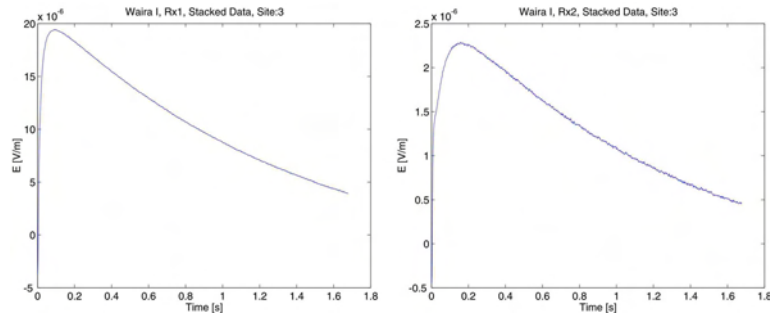


Figure 5.5.6: Examples of conditional stacked data, Site 3 on profile Waira I.

5.6 Magnetotelluric Instrumentation

P. Schroeder

For testing a newly constructed system for seafloor magnetotelluric measurements, six ocean bottom magnetotelluric (OBMT) instruments were deployed on cruise SO 191-1.

This instrument measures the natural temporal geomagnetic and geoelectric (telluric) field variations in a period range from $T = 0.2 \text{ s} - \text{DC}$ (Possible sampling rates are 10Hz, 5Hz, 1Hz and 1/60Hz.).

The OBMT-System is constructed at IFM-Geomar according to Ocean Bottom Seismometers. The recording instrument inside the titanium cylinder is designed and constructed by MAGSON GmbH and contains:

- a three component fluxgate magnetometer,
- two E-field channels for recording the electric field in two components,
- a dual axes tilt meter for measuring pitch and roll,
- a realtime Clock (RTC), and
- a temperature sensor.

The instrument is equipped with an internal data logger for instrument control and data storage on compact flash cards. The OBMT-System is a free falling system with a non-magnetic anchor made of aluminium and concrete to avoid distortion of data due to induction effects, and has an acoustic release for recovery. A photo showing the instrument upon deployment is shown in Figure 5.6.1, a sketch is given in Figure 5.6.2.

Fluxgate Sensor:

The magnetic field is measured with a vector compensated ring core fluxgate sensor. It consists of two crossed ring cores, three pick-up coils and a tri-axial Helmholtz coil system for field feedback. The vector compensation reduces the cross field influence on the measurement. Scale values and non-orthogonality depend only on stability of the feedback coil system. Because of stable temperature conditions on seafloor, the use of the three component mini sensor without additional support materials is applicable. Thermal expansion coefficient of the feedback coil system is about 24ppm/°C. Noise level of ring cores is in the order of $10\text{pT}/\sqrt{\text{Hz}} @ 1\text{Hz}$.

Digital Fluxgate Magnetometer Principle:

The main property of the digital fluxgate magnetometers is the direct digitization of the second harmonic of the excitation frequency, which contains the magnetic field information. Filters and phase-sensitive demodulators are not used. Analog-to-digital conversion close to the sensor reduces the amount of analogue parts, which often cause drift problems or show deviations in the component values, and it highly increases the robustness against environmental influences (e.g. temperature change and electromagnetic disturbances). These considerations lead to the design of mainly digital sensor electronics. First, the sensor output (sense) signal is amplified by an instrumentation amplifier. Next, it is digitized by a 16-bit analogue-to-digital converter exactly in the minimum and maximum of the second harmonic of the excitation frequency.

The FPGA (Field Programmable Gate Array) calculates the difference between both measurements and stores the result in an accumulator. This measurement will be repeated for a programmable number of excitation periods. A FPGA internal RISC (Reduced Instruction Computer) processor calculates from the accumulated ADC (Analog/Digital Converter) values and the last set DAC

(Digital/Analog Converter) feedback value the magnetic field value, transmits the results to the data logger and calculate a new set of DAC feedback values.

The feedback system is driven by two 16bit DA-Converters for each component, the first one to compensate the Earth's field and the second one to operate the sensor in a reduced range. Therefore two measurement modes are available. The full range mode covers the whole Earth's magnetic field range and the variometer mode works in a limited range of +/-2.000nT. The reason to separate the field compensation into coarse and fine range is the differential nonlinearity (DLN) of the DA-Converter. Reduced operation range in variometer mode guarantees, that non-linearity is smaller than the resolution. Using a higher internal sampling rate and cascaded DA-Conversion the dynamic range corresponds with 24bit. The resolution on the background of the Earth's field is still 10pT.

Ocean Bottom MT electronics:

The electronics consists of magnetometer electronics, electric (E-) field measurement, tilt and temperature measurement and the data logger with real time clock (RTC) and power management. B- and E- field will be measured in time synchrony, triggered by the 1Hz signal of the RTC. The internal data acquisition rate is 100Hz. Dependent on the selected storage frequency, data output as well as system time, inclination, temperature and instrument status are stored on the flash disk. Furthermore, data logging and instrument control with an external unit via RS232 is possible. Optionally, a time table may be programmed to determine settings of mode, sampling rate and format for any time chosen. This option allows, as an example, a broadband recording at shallower depth from high frequent sampling in the beginning switching automatically to long period measurements, since it may save disk capacity and battery.

Electric field sensors

Electric field fluctuations are determined by measuring the potential difference (U) between pairs of electrodes, which are connected via shielded cable to form a dipole and fixed nearby the ground at known distances (d) round about 10m apart: $E=U/d$.

In this system we use 4 unpolarizable Ag-AgCl electrodes for probing the electric field (2x two dipoles). Two dipoles are required in order to ascertain the two horizontal components of the electric field. They are configured orthogonal to each other being fixed to four tubes of each 5 m length (see Figure 5.6.1).

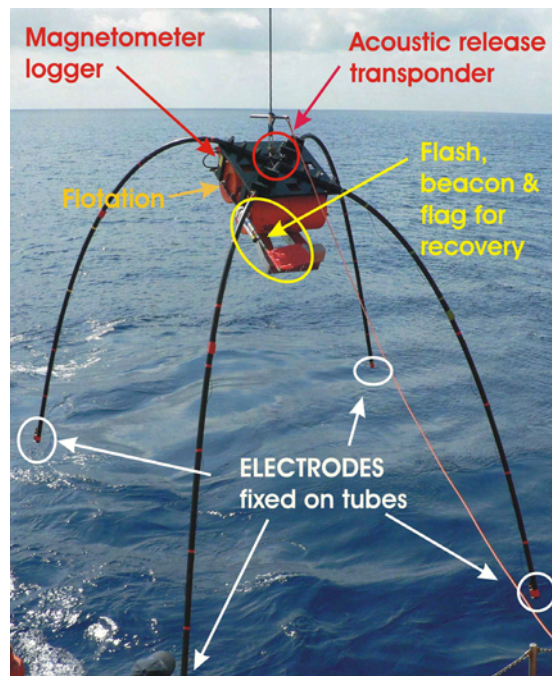


Figure 5.6.1 Photograph of an OBMT being deployed

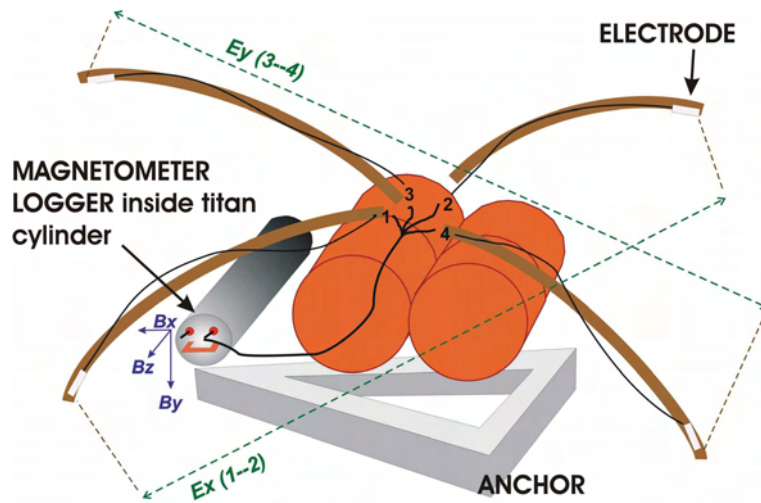


Figure 5.6.2. Sketch of an OBMT

5.7 Geological Instrumentation

5.7.1 THP Temperature Sensors

J. Poort, L. Naudts, D. Boone, J. Greinert, M. De Batist

Heat flow and thermal gradient data provide first-order constraints for the thermal modelling of geodynamical processes such as subduction or rifting processes. On a local scale geothermal data may also identify active faults and seepage areas. The near-surface thermal regime can be strongly disturbed at faults and seeps due to upflowing warm fluids and formation and dissociation of gas hydrates. During SO191 Leg 3 it was aimed to characterize the geothermal setting of the seep environments of the Hikurangi Margin. We used THP temperature sensors that were attached to the gravity corer of the R/V Sonne (Figure 5.7.1). The THP temperature sensors (NKE product) are autonomous temperature data loggers. Arbitrarily attached at different depth intervals of a coring device, they will provide temperature and thermal gradients along the sediment core down to the depth to which the corer penetrated. Five sensors were connected to a gravity corer of 3 m long and over an active length of 2 meters. First sensor was placed at 40 cm from the core catcher, the interval distance of the sensors was set at 0.5 m.

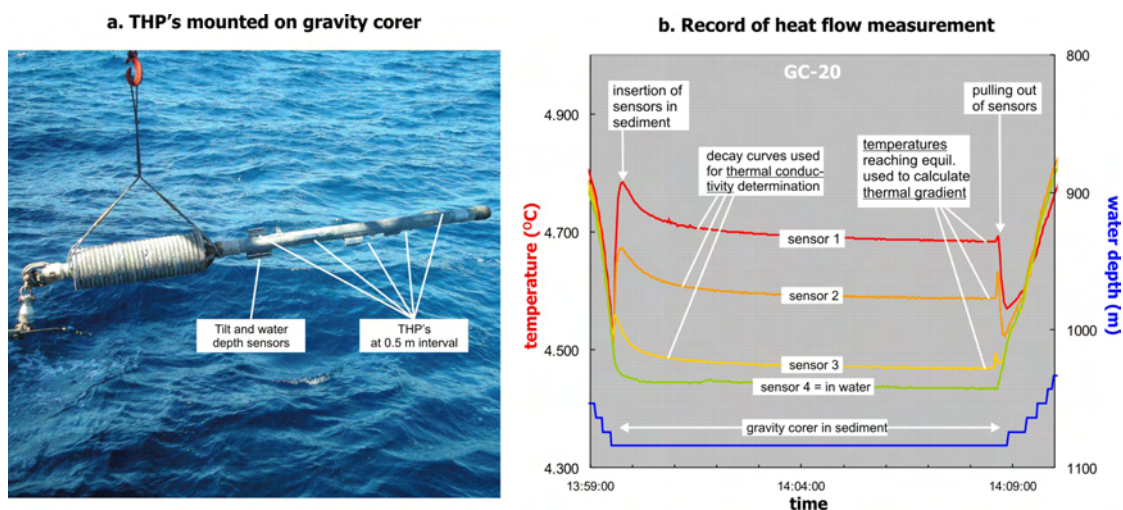


Figure 5.7.1: (a) Gravity corer with mounted THP temperature sensors ready for lowering. (b) Example of an in-situ temperature record with the different parts used to obtain geothermal parameters tagged.

The corer was kept in the sediment for a period of 6–8 min at each station, during which time the sediment temperatures, at a lateral distance of 6 cm away from the corer, were recorded at a time interval of 2-5 sec. The angle of tilting of the corer was registered with a tilt meter with accuracy of 1°. Data was downloaded upon arrival of the corer on-board. The THP thermistors have an accuracy of 0.007 °C and a resolution of 0.0007 °C at 20 °C.

Equilibrium temperatures are obtained by extrapolation from the transient temperature curves. Thermal gradients are calculated by incorporating inter-calibration data at large water depth in each

station. Thermal conductivity of the sediments will be estimated from the heat friction decay curves that results from the penetration of the data-loggers. The product of the thermal gradient with the thermal conductivity in each interval will give us heat flow values.

5.7.2 *Coring devices*

Sediment samples were collected from a variety of coring equipment including:

- TV guided Multicore (TV-MUC)
- TV guided Grab (TV-G)
- TV guided box-core (TV-BC)
- Box core without video (BC)
- Gravity Core (GC)

Whereas the TV-MUC proved to be the most reliable video-guided sampling tool, we lost during Leg 2 a lot of station time with the TV-grab due to malfunction of the connectors which needed replacement. Nevertheless, the TV-grab was very useful for the sampling of large carbonate blocks. The video-guided deployment of the box corer was very difficult as expected, since the mechanics and the movement of the gear during deployment jeopardize cables and connectors needed for the video and power transmission. Therefore, the box core was used with video on Leg 3. The gravity corer was used without the coring rack and was equipped either with plastic foil for rapid pore water and gas hydrate sampling or with plastic liner for noble gas subsampling and archive purposes.

5.8 **ROV “GENESIS”**

L. Naudts, J. Poort, D. Boone, J. Vercruyssen, W. Versteeg, J. Greinert, M. De Batist

The Remotely Operated Vehicle (ROV) “Genesis”, deployed by the Renard Centre of Marine Geology (RCMG) of Ghent University (Belgium), was acquired in 2006 thanks to an Impulsfinanciering of the Special Research Fund of Ghent University. It is a fully-electric sub-Atlantic CHEROKEE ROV that is depth-rated up to 2000 m with a maximum payload of 60 kg for extra instrumentation. The ROV can be operated in 2 modes: ‘live boating’ or ‘TMS’. The ‘live boating’ mode is a deployment of the ROV ‘over the side’ with a tether of 500 m. The second operation mode is with the Tether Management System (TMS). In this mode, the deck-container with winch (1600 m of fibre-optic cable) is used to lower the ROV within the TMS-cage from the ship’s deck to 30-40 m above the seafloor. The ROV can then freely survey the seafloor connected to the TMS with a tether cable of 200 m. The latter operation mode was used during SO191-3. All ROV-operations were conducted from the control unit in the deck-container (Figure 5.8.1).

The standard instrumentation of the ROV consists of 5 cameras (Kongsberg) and lights: a forward-looking black-and-white camera, a forward-looking color camera, a forward-looking color still camera, a rear-looking black-and-white camera and a TMS-mounted black-and-white camera. The ROV contains an alti-, depth-, pan- and tilt-meter and a compass. For object detection a forward-looking “Super Seeking Sonar System” (325 or 675 kHz) is used. A 5-function manipulator arm is used for sampling and measuring. Retrieved samples or additional instrumentation can be stored in a sample tray (Figure 5.8.2). Meter-scale positioning and navigation of the ROV takes place with a ship-mounted IXSEA GAPS system and 2, ROV-mounted and TMS-mounted, transponders (IXSEA). This calibration-free Global Acoustic Positioning System (GAPS) is a portable Ultra Short Base Line (USBL) with integrated Inertial Navigation System (INS) and Global Positioning System (GPS). During SO191-3, only the transponder on the ROV was used. The GAPS was deployed from the ship’s moon pool and used the DGPS signal from the ship (Figure 5.8.3). Navigation of the ROV and online display of the ships and ROV position was done via the OFOP software. In addition to the position data, ROV specific data like heading, depth, view direction, roll and pitch were stored via a serial link from the decks unit to OFOP.

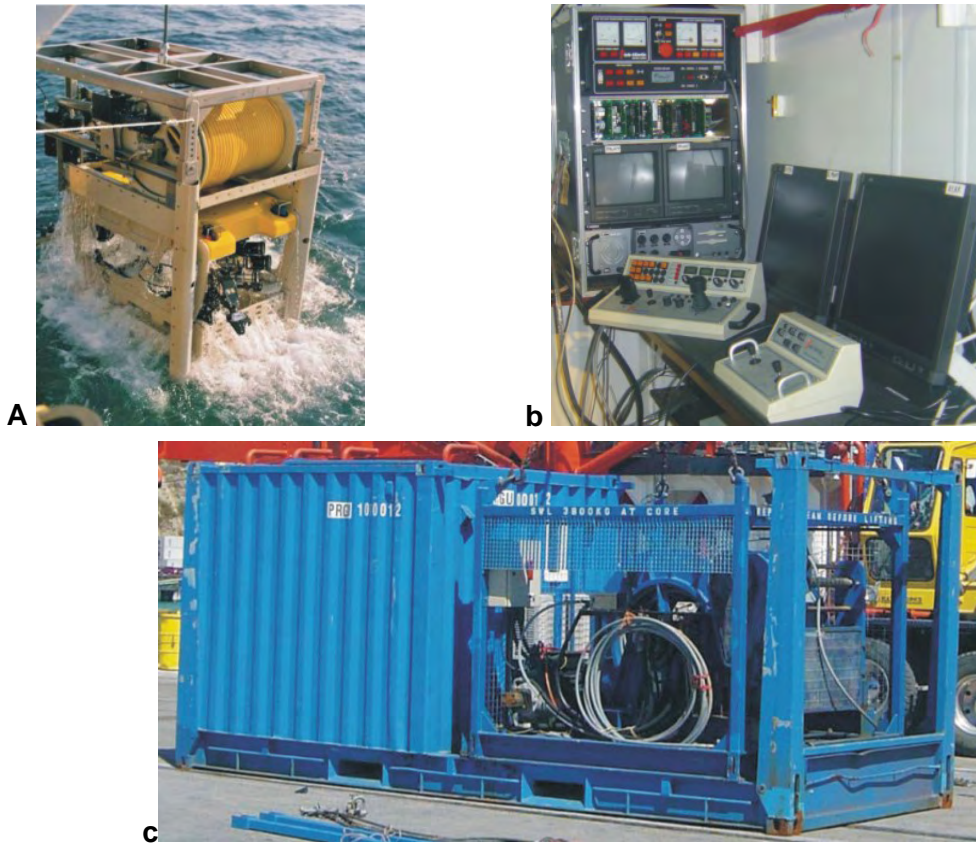


Figure 5.8.1: (a) Retrieval of the ROV within the TMS. (b) Control unit in the deck-container. (c) Deck-container with winch

Additional instrumentation implemented during SO191-3 consisted of:

- a THP thermistor (MICREL) for measuring the sediment-temperature,
- a CTD probe (FSI; provided by IFM-GEOMAR) for measuring the bottom-water physical characteristics,
- 2 Niskin bottles (5 liter) (provided by IFM-GEOMAR) for bottom-water sampling.

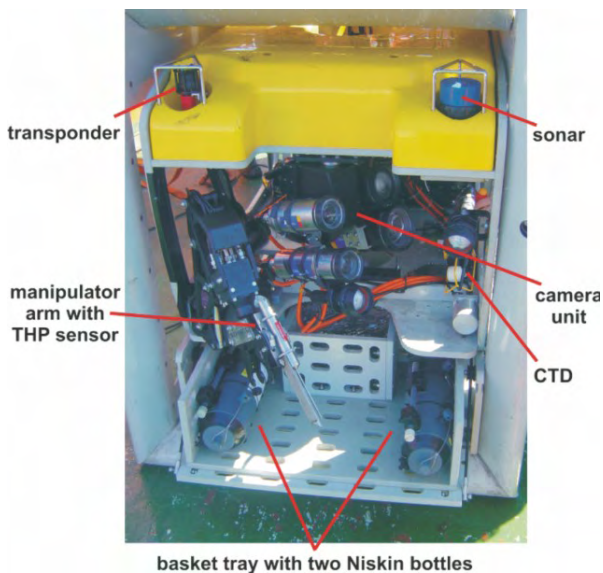


Figure 5.8.2: Front view of the ROV with indication of the installed instrumentation during SO191-3.

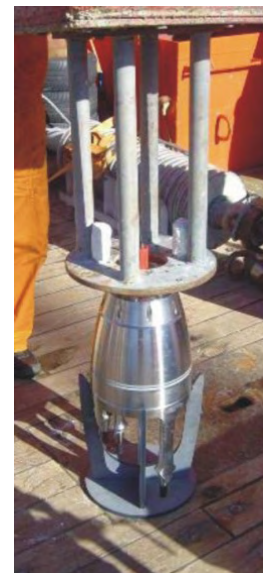


Figure 5.8.3: GAPS positioning system as was mounted during SO191-3.

5.9 Thermistor Moorings

D. McGinnis

As of 24 Feb. 07, five thermistor moorings were deployed: one at LM9 and four at Wairarapa site (See map from CTD section for locations; see Tables 1&2 for thermistor types and locations). TM2 and TM3 were deployed at approximately the same time as a reference and a seep-location mooring. TM4 and TM5 were also deployed at Bear Paw on 23 Feb as a reference and seep mooring, respectively. All moorings consisted of temperature loggers (thermistors) which continuously record water temperature at fixed locations. The high-resolution thermistors (TR-1050) also measure temperature fluctuations associated with turbulence.

Additionally, thermistors were installed on the leg of the bottom-water sampler on two occasions to aid in resolving the BBL dynamics.

Technical description

TR-1000 thermistors – are manufactured by Richard Brancker Research, Ltd. And recorded temperature at a 30 second interval. The loggers record temperatures between -5° to $+35^{\circ}$ with a time constant of 30 seconds, an accuracy of $\pm 0.05^{\circ}\text{C}$ and a resolution of 0.002°C .

TR-1050 thermistors – are also manufactured by Brancker Research, Ltd. and recorded temperature at a 2 second interval. The loggers record temperatures in the range of -5° to $+35^{\circ}$ with a time constant of <3 seconds, an accuracy of $\pm 0.002^{\circ}\text{C}$ and a resolution of $<0.00005^{\circ}\text{C}$.

One thermistor also recorded pressure, and two recorded DO. The quality of the DO data is questionable, which may be associated with the large depths.

5.10 Surface Methane Concentrations: Equilibrator Measurements

J. Greinert

One question in seep research is “Does methane released from seeps reach the atmosphere?” To answer this question continuous measurements of the methane concentration at the sea surface are needed and were undertaken during SO191 with the “Equilibrator System”(Figure 5.10.1). The system ran continuously during the entire cruise, with a small delay of one week at the beginning. During the third leg, the membrane of the air pump broke and was replaced. Minor gaps in data recording are caused either by necessary maintenance work (changing gas bottles or replacing drying material) or mis-operation.

The seawater-air Equilibrator System is based on gas chromatography [Weiss, 1981; Rehder et al., 2001]. CH_4 and CO_2 were measured. Air samples were sucked in from above the bridge approximately 10m above the sea surface. Water was pumped at a high flow rate by a pump installed in the moon pool of SONNE at 6.5m water depth. Tow calibration gas 1 (CG1 = 1.8991 ppmV and CG2 9.78 ppmV CH_4) were measured as well to correct for pressure changes over time. The sucked-in water is equilibrated in a counter flow of air in a closed system (about 80ml) for 9.5min before 2ml of the equilibrated air is injected into the GC. N_2 is used as carrier, gas separation is provided by a 4 m 1/8-inch stainless steel packed column filled with Porapak QS (mesh 50/80); methane is detected using an FID.

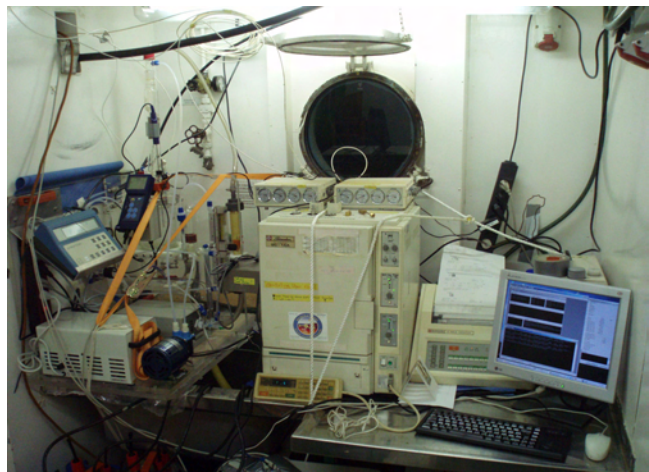
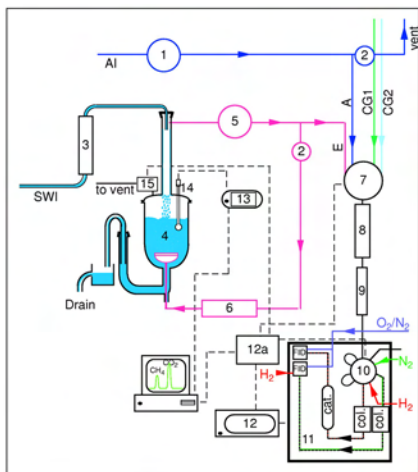


Figure 5.10.1: Scheme of the Equilibrator...

... and the real thing.

Two ml samples of either, calibration gas, air, or air equilibrated with a continuous flow of seawater are automatically injected into the GC and measured. The sequence used for the analysis of the gas in general is CG1-W-W-A-W-W-CG2-W-W-A-W-W. Where CG1 and CG2 are calibration gases, W is the air equilibrated with surface seawater, and A is the atmospheric air sample. Peak integration is performed using a Shimadzu CR6A integrator. The integrated peak area, water temperature in the equilibration system, pH, GPS data and CTD data of the surface water and weather data are stored online by the CH₄-Equi-Log software.

5.11 Water Column Methane Analyses

K. Faure, D. McGinnis, R. Kipfer, J. Schneider v. Deimling

For onboard methane analysis, samples were collected directly from Niskin bottles, into 140 ml syringes immediately after the CTD was recovered. In the head-space GC method (Faure et al., 2006) methane is extracted from the samples by adding 40 ml of N₂ to 100 ml of seawater and vigorously agitating for about 2 minutes to reach an equilibrium between the CH₄ in the water and in the gas phase. The syringe headspace gas is injected directly into a robust SRI 8610C GC via a drierite column to remove excess moisture. The sample gases are separated using a 15 metre, 0.53 mm ID, 0.5 µm Porapak Q column and measured using a flame ionization detector. Methane concentrations are reported in nanomoles per liter (nM), corrected for temperature and atmospheric pressure at the time of measurement. The lower limit of determination for dissolved CH₄ is c. 0.3 nM. A combined analytical and sampling error of ca. 8 % was calculated from replicate samples within a CH₄ concentration range 1-15 nM.

A modified vacuum extraction method described by Lammers and Suess (1994) was also used (Rehder, 1998). A measured amount of water (about 1600 ml) is filled into pre-evacuated 2200 ml glass bottles, which are closed with custom designed valve caps to minimise the possibility of air leaks. A calibrated Flowmeter (ENGOLIT Flow-Control 100S DMK) was used to determine the exact water volume that was transferred into the glass bottles. Water transferred into pre-evacuated bottles results in almost quantitative degassing. One millilitre of this gas was extracted with a syringe and injected into a CE Instruments gas chromatograph (GC8000). The GC was calibrated using Matheson standard gas with CH₄ concentrations of 9.78 and 100 ppm. Two methods have been applied to obtain the total amount of methane in nanomoles per litre. In the first method, the gas volume extracted from a known amount of water was used to determine the total amount of methane. In a second method, it was assumed that the water was saturated with nitrogen and argon, the oxygen was measured in the water (using an O₂ sensor), and the total amount of methane calculated.

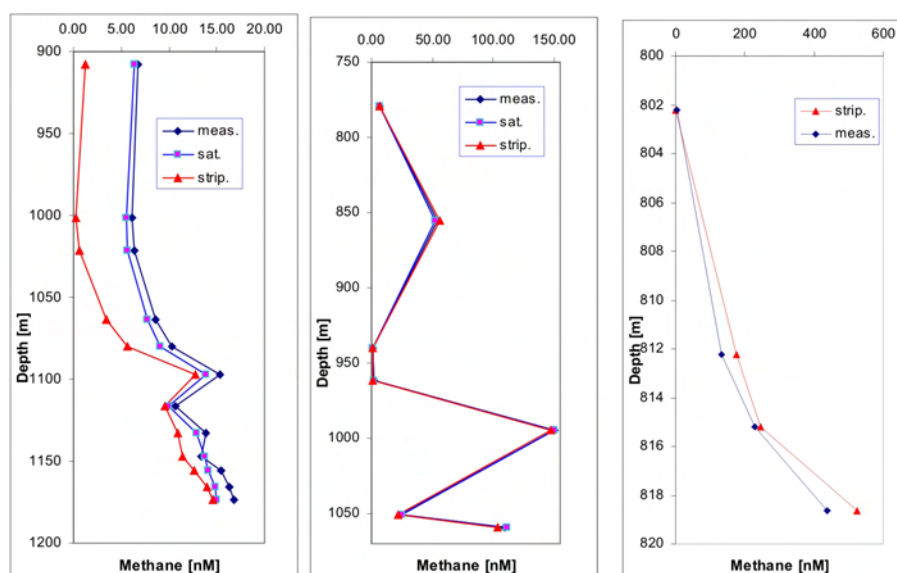


Figure 5.11.1: Methane concentrations determined by three different methods applied to weak (a, CTD-9), medium (CTD-6) and high (CTD-34) concentration samples at different sites. The bluish curves derive from the vacuum extraction measurement whereas the red curves were obtained from the headspace equilibrium method.

A comparison of results from the vacuum extraction and headspace analysis revealed excellent agreement (Figure 5.11.1), despite the quite different methodology and GCs used in the analyses. At lower CH₄ concentrations (<10 nM) the headspace method is about 5 nM lower, however, at higher

concentrations there is excellent agreement. The advantage of the headspace analysis method is that the equipment is easily set-up, water samples are easily and quickly collected from the Niskin bottles and extraction and measurement is rapid (~ 4 minutes per sample). The disadvantage of the headspace method is that it is not possible to collect gas samples for later isotope analyses, whereas with the vacuum extraction method it is possible. Having the two methods available on-board ship has been very useful.

5.12 Radon (^{222}Rn) Measurements

A. Eisenhauer, V. Liebetrau

On board SO191-2 ^{222}Rn depth profiles of sediment cores were performed in order to study gas transport through marine sediments of different marine settings. The goal of the study is the determination of advection and diffusion rates in vent and non-vent site settings.

^{222}Rn is a member of the ^{238}U decay chain and directly produced by the decay of ^{226}Ra in the marine sediments. Because ^{238}U is enriched in sediments its production is depth dependent and increases as a function of the sedimentary height below the water column. ^{222}Rn is an excellent tracer in order to determine diffusion and advection rates because as a radioactive rare-gas it is chemically inert and decays away with a half-life of about 3.5 days ($\lambda=0.0001374$ 1/min). Thus the time dependent transport of ^{222}Rn can be observed as a function of time and sediment depth directly on board of a ship while performing liquid-scintillation-alpha counting (Purkl and Eisenhauer, 2004). The results from ^{222}Rn depth profile measurements can then be compared and applied to other gases of interest (e.g. CH_4) supplied from the sediments to the water column.

Sediments for ^{222}Rn measurements are usually collected with the TV-MUC. From the MUC sediments are sub-sampled in about two or three 30 cm long cylinders (2.5 cm diameter). ^{222}Rn -fluxes out of the cylinders are then determined by a time controlled measurement of the activity above the sediment column and as a function of sediment depth (usually 25 cm). In order to determine the ^{222}Rn activity all samples (pore water, sediments) are mixed with a certain amount of a liquid scintillation material. Latter material is back extracted from the sediments or pore water samples by centrifugation and then counted in a Alpha/Beta-Liquid scintillation counter (Purkl and Eisenhauer, 2004).

5.13 Lander Deployments

S. Sommer, P. Linke, O. Pfannkuche, J. Greinert, J. Schneider v Deimling

Occurrence of gas hydrates and gas seepage from Hikurangi margin sediments has been inferred from BSR structures (Henry et al. 2003), methane derived carbonates, gas flares in the water column (Faure et al. 2006), and the presence of seep fauna (Lewis & Marshall 1996). Apart from these geophysical findings and sporadic observations by fishermen and scientific dredge samples, detailed geochemical studies are missing. The activity of the Hikurangi margin methane seeps in terms of seabed methane emission is not investigated. Nor is our understanding of biological processes and organisms involved in the benthic methane cycling and emission very well constrained.

In sedimentary environments dominated by slow pore water flow and diffusion but also in freshwater systems and soils (cf. Reeburgh 2003) microbial methanotrophy has been early recognised as an important control mechanism for the methane flux across the sediment water interface (Reeburgh et al 1993, Valentine et al. 2001). These microbial processes embedded within a complex network of biogeochemical reactions and interactions with meio- and macro benthic communities control the emission of methane across the sediment water interface representing an important "benthic filter", (Figure 5.13.1). Via anaerobic methane oxidation the energy bound in methane is transferred to sulphide. High fluxes of methane and sulphide sustain chemosynthetically driven production of autochthonous organic carbon, which potentially enters the benthic food web. For methane seep locations, such as the Hydrate Ridge (Sahling et al. 2002), mud volcanoes seaward of the Barbados accretionary prism (Olu et al. 1997), or in the northern Gulf of Mexico (Mac Donald et al. 2003) often dense mats of sulphide oxidising bacteria of the genus *Beggiatoa*, *Thiothrix*, and abundant macrobenthic communities consisting of vestimentiferan tube worms and bivalve mollusks of the genera *Calypptogena* and *Acharax* were reported.

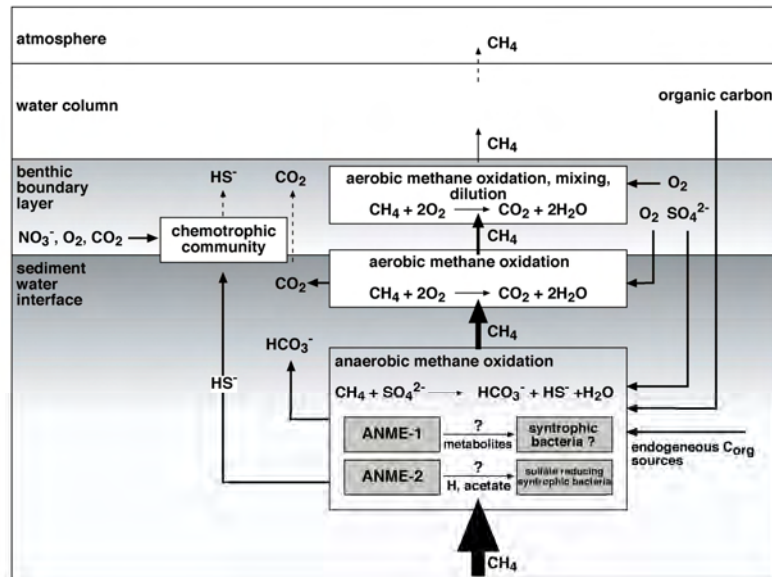


Figure 5.13.1: Schematic diagram of the “Benthic Filter” in Hydrate Ridge seep sediments (Sommer et al. 2006)

Due to the limited availability of appropriate in situ technology, still, the fraction of methane and other volatile carbon compounds leaving the sediment after fluids and gases have been passing through the sediment matrix and benthic communities and the amount of carbon being retained in the sediment, either as carbonates or as biomass, is not very well quantified. So far only a few in situ measurements of seabed methane emission (Torres et al 2002, Linke et al 2005, Sommer et al 2006) exists, other studies mostly rely on model calculations (e.g. Luff and Wallmann 2003, Treude et al. 2003). For cold seep sites at Hydrate Ridge characterised by sediments containing shallow gas hydrates and various fluid flow velocities from below, great inconsistency exists between emission rates measured in situ and fluxes derived from numerical modelling of pore water gradients. Moreover extreme spatial and temporal variability exists at cold seep sites, which makes it very difficult to estimate overall methane flux into the bottom water. Methane bubble release from seeps is transient and thus influences flux estimates significantly. Furthermore the knowledge about the temporal bubble release activity will help to understand the control mechanism for fluid release. These might be tides, changing currents, or filling and emptying of a gas reservoir close to the seafloor surface (short-term variations) or in deeper sediment horizons (variations are probably longer). Furthermore, the composition of microbial and macrobenthic communities differ greatly between the various seep locations.

The aims of our studies were

- To determine the spatial variability of in situ fluxes of methane (dissolved and free gas), oxygen, nitrate, ammonium, sulphate, and sulphide at different cold seep sites at the Hikurangi margin.
- To identify organisms and biogeochemical processes, which are involved in the turnover and release of methane across the sediment water interface at these cold seep sites. To determine the efficiency of this benthic filter to restrain methane carbon and other volatile short chain hydrocarbons in the sediment.

Seabed methane emission (free gas or dissolved), turnover and flux rates of oxygen, sulfate, sulfide, nitrate and ammonium are measured in situ using GasQuant, the Biogeochemical Observatory (BIGO) and the Fluid-Flux Observatory (FLUFO). Parallel investigations are conducted using the multiple corer and the Bottom Water Sampler (BWS). Additionally, first tests were conducted with an in situ profiler equipped with micro sensors.

GasQuant, BIGO and FLUFO used during this cruise belong to the series of the GEOMAR modular lander system (Pfannkuche and Linke 2003). Within the integrated projects LOTUS and COMET (BMBF), embedded within the gas hydrate initiative of the GEOTECHNOLOGIEN programme FLUFO and BIGO were specifically designed to measure benthic turnover and flux along a wide range of different fluid flow velocities. As free gas from several bubble releasing holes in a seep area cannot be measured simultaneously with one chamber or video-equipped lander, a hydroacoustic lander, GasQuant, was developed at IFM-GEOMAR.

GasQuant

Bubbles even very small in size can be easily detected by hydroacoustics even if they occur in great distances from the transducer (depending on the frequency used). Bubbles which are not in resonance with the used frequency and at ambient pressure can also be detected by their strong backscattering of the echo signal. In fact, the GasQuant's frequency (180 kHz) was chosen to avoid resonance effects at the expected bubble size distribution (~ 1 mm to 20mm in diameter) and the pressure in up to 1000m water depth, (Greinert and Nützel, 2004, 1000m is the depth rating of the transducer). Although flux quantification are possible as outlined by Greinert and Nützel (2004) the system used could not be calibrated properly to provide real flux measurements. Nevertheless it allowed very accurate monitoring of the spatial distribution, the temporal variability and relative flux differences between seeps.

GasQuant builds on a 'normal' multibeam Seabeam 1000 system, which was modified by L3-Communication ELAC-Nautik (Kiel, Germany) to run as a stand-alone system operating in a sonar-like mode. The main difference from a seafloor mapping multibeam system is the horizontal orientation of the swath. The swath consists of 21 beams with 1.5° vertical and 3° horizontal beam width, covering a total swath angle of 63° (Figure 5.13.2). The transducer is mounted into a cardanic frame that keeps the hydroacoustic swath horizontally even if the lander stands slightly tilted. The transducer is fixed at ~3m above the seafloor; taking the 1.5° vertical beam angle the signal hits the seafloor in more than 200m distance.

A modified version of HydrostarOnline (standard multibeam recording software for Seabeam 1000 series) was used as recording software. The received signal is converted from analogue to digital every 128 μ s; this corresponds to a water cell thickness of about 9.6 cm (at 1500 m/s sound velocity) along the beam (lateral resolution) for one data sample. During the measurements, the pulse length was 1 ms and the ping rate was 4 sec. With 1 ms pulse length but 128 μ s sampling rate the data are over sampled as will be shown later. The signal is TVG-corrected and automatically gains adjustments by the system itself as it is stored as raw data. Overall: 512 samples are recorded for each beam covering a distance between 14 and 63 m away from the transducer. In total, 10752 samples were recorded monitoring an area of 2,075 m² for each ping (Figure 5.13.2).

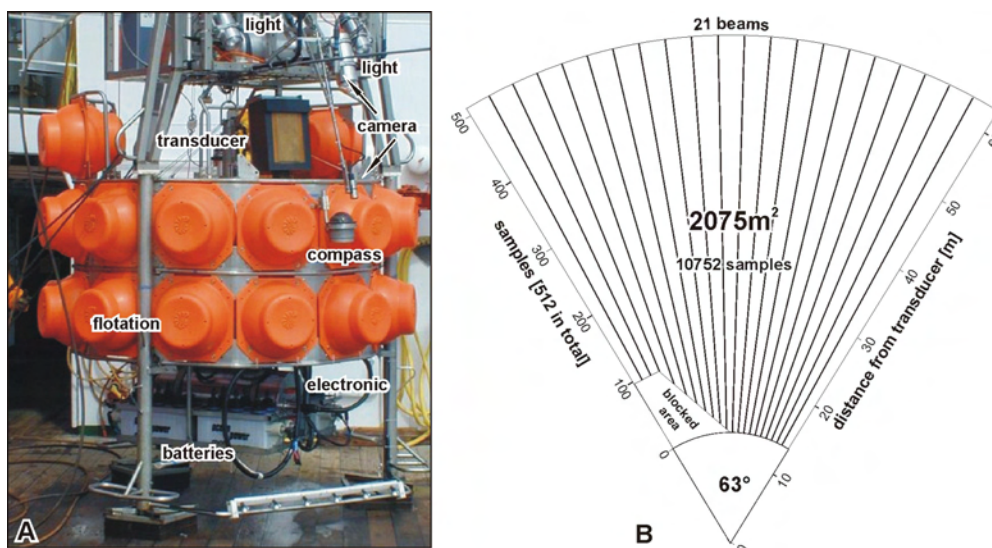


Figure 5.13.2: A: Photo of the GasQuant lander attached to the launcher system ready for deployment. B: Size of the hydroacoustic swath showing the 21 beams and positions of the finally analysed samples per beam. Due to the technical block depth setting of the system during the time of the measurements no correct data have been recorded from the blocked area.

GasQuant data processing

The data processing described below mainly uses a simple approach for filtering and bubble release event detection based on moving averages of different window width, bandpass filtering, interactive background corrections and automatically and visually defined thresholds. These processing steps were implemented into a self-written software package that reads the binary data stored in XSE format.

Data were plotted in two different ways to find potential seep sites. Swath plots, color coded x (sample), y (beam) and amplitude images were used to get potential seep positions. Plots showing the amplitude of each ping for one specific sample over time, following called trace, were used to verify these seep positions. Bubble release events (*bre*) for swath plots were detected by calculating

the moving average (*ma*) over many values/pings (*v*; here typically between 301 and 2001 samples; or the entire trace) from one specific trace and comparing it to the mean of a few consecutive amplitude values (target window *tw*; here typically 4) in the middle of the moving average window. The respective mean amplitude value was counted as a bubble release event if it was more than twice the standard deviation (*std*; calculated over the entire trace) above the moving average [1]. Using an average of a few samples [2] was done to eliminate spike values in the trace.

$$Bre \text{ is true if: } tw > ma + 2 * std \quad [1]$$

$$tw_n = \sum_n^{n+4} v_n / 4 \quad [2]$$

$$ma_n = \sum_{n-150}^{n+150} v_n / 301 \quad [3]$$

$$std = \sqrt{n_{\text{-max}} \sum_1^{n_{\text{-max}}} v - \left(\sum_1^{n_{\text{-max}}} v \right)^2 / n_{\text{-max}}^2} \quad [4]$$

with n = number of amplitude value in trace

Although swath plots give very good indication of possible seeps, detailed visual studies of trace plots are needed as confirmation and for those seeps which are less active (e.g. those which were active only once during the time of observation). For this, traces were smoothed by moving averages or bandpass filtering before plotting.

Biogeochemical Observatory (BIGO)

BIGO allows the experimental simulation of different environmental conditions (oxygen content/organic influx) inside the benthic chambers under in situ conditions and represents an ideal experimental platform to study the kinetics of prominent biogeochemical reactions and threshold levels involved in the regulation of seabed methane emission. BIGO contains two benthic chambers which were slowly driven into sediment 1-2 hours after the observatory has been placed at the seafloor. In order to measure interfacial fluxes under natural conditions in one benthic chamber of BIGO, hitherto referred to as “EX Chamber”, the oxygen concentration inside this chamber was maintained at the ambient oxygen level by use of a gas exchange system. This gas exchange system provides oxygen from a reservoir filled with oxygenated sea water. Similarly to the artificial gill system by Morse et al (1999) the gas exchange is facilitated across a silicone tubing. The functional principle of BIGO including a description of an earlier prototype of this gas exchange system has been described by Sommer et al (2006) and Sommer et al. (subm.). In order to record temporal variability of interfacial fluxes the water body inside the second chamber, hitherto referred to as “CO Chamber”, was replaced with ambient water at defined time intervals. By this means high amounts of methane or other substances such as ammonia which have accumulated inside the chamber will approach the outside level and flux measurements can be “re-started” in the same chamber.

Fluid Flux Observatory (FLUFO)

The Fluid-Flux-Observatory (FLUFO) is designed to identify and quantify the impact and overall relevance of the complex physico-chemical controlling mechanisms on the effective discharge rates of fluids and dissolved chemical species related to the decomposition of gas hydrates. Like BIGO it carries 2 benthic chambers each equipped with a syringe sampler to obtain sediment and water samples. FLUFO is equipped with a FLUFO module (Meerestechnik Bremen/TUHH) to measure aqueous and gaseous discharge rates (Figure 5.13.3). This flux chamber has an opening to the surrounding bottom water to avoid back pressure effects during the flux measurements, whereas the backup chamber is closed with a conventional lid. After deployment a permeability test is performed in the FLUFO chamber to check the sealing of the chamber and measure the permeability in-situ. Sediment cores were taken for grain size analyses after recovery of the incubated sediments. Furthermore, two up-looking acoustic current profilers (2 MHz Nortek Aquadopp and 300 KHz RDI ADCP) were mounted to measure the current regime above the lander, which was additionally equipped with a storage CTD (RBR), a methane sensor (Contros) and an in situ pump (EAWAG).

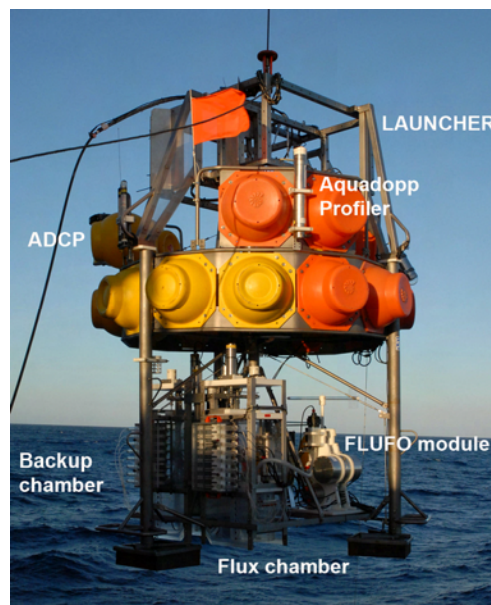
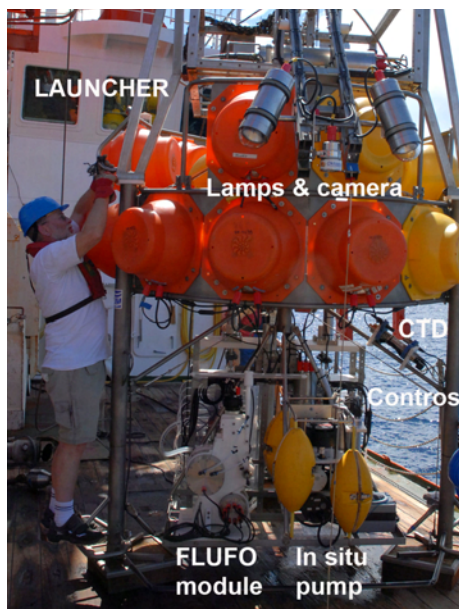


Figure 5.13.3: Fluid-Flux Observatory prepared for deployment with the Launcher. The front and back view show the different modules integrated into the FLUFO observatory.

Bottom Water Sampler (BWS)

The frame of one lander was modified as a bottom water sampler by exchanging the instrument frame against a lance with 14 sampling ports. These ports were connected to 2 syringe samplers which enable to take a total of 16 water samples. The vertical distance of the sampling ports above the sediment water interface can be freely adjusted in 1, 2, 4, 5 and 10 cm intervals up to a maximum distance of about 100 cm. During the deployment the BWS remains firmly connected with the launcher. It carries a second video camera in view of the sampling ports for visual control of the water sampling. This is to avoid sampling of water masses containing a high proportion of re-suspended sediment particles after sediment disturbance when the lander has been placed at the seafloor. The sampling is initialized from the surface telemetry unit and activates one syringe after the other. The whole sampling takes approximately 2 minutes. Furthermore, the BWS was equipped with a small down-looking acoustic current profiler (2 MHz Nortek Aquadopp) and a storage CTD (FSI) to record the physical environmental parameters during sampling.

Biogeochemical, biological analyses

Sediment samples

Sediment samples for the measurement of methane, pore water chemistry (total alkalinity, ammonium, nitrate, sulphate, sulphide, bromide, ICP), pigments, meiofauna, and physical properties were taken immediately after recovery of the sampling gear and processed in a cool container at a temperature regime of 6-8 °C. Photos were taken from the surface and the vertical structure of almost all sediment samples.

In sediment cores from MUC casts and Lander deployments oxygen, sulphide and pH micro-profiles were measured under ex situ conditions in the cool container.

A micro-respiration system (Unisense, DK) was used to measure the respiration rate of ampharetid polychaetes originating from the rain drop sites at the fringe of the carbonate structures. Their spatial distribution and abundance was determined using photographs and subsequent image analysis. Samples of selected ampharetids were deep frozen (- 40 °C) for latter biomass determination (C/N, dry-weight) as well as for analyses of stable isotope composition ($^{12/13}\text{C}$ and $^{14/15}\text{N}$) of their tissues in cooperation with the Kompetenz-Zentrum für stabile Isotope in Göttingen (KOSI).

Sediments for latter meiofauna analyses were taken from MUC deployments and sub-samples of the sediments retrieved by the landers. The sediment cores were sectioned in 1 cm intervals down to a depth of 10 cm. The respective sediment slices were deep frozen for latter analyses of abundance, biomass, taxonomic composition, determination of C/N content and stable isotopic composition of selected organisms.

Methane concentrations in the sediment were determined on board by headspace analysis. For the determination of methane concentration in sediments 2 times 1 cm depth intervals, which have been taken in the same liner with a cut off syringe, were pooled in a 20 ml headspace vial. This vial

contained 6 ml saturated NaCl and 1.5 g NaCl to stop microbial activity and to degas the sample. During the measurement series several blanks have been measured. Within 24 hours methane concentrations were determined using a GC 8000TOP CE Instruments equipped with a Poraplot Q 30m 0.32mm column. Prior to GC measurements samples were equilibrated for 2 h in a shaking table. Calibration was conducted using a 10 ppm, 100 ppm and 10000 ppm standard. For a detailed description of the methods used for pore water analysis see http://www.ifm-geomar.de/index.php?id=mg_analytik&L=O.

Water samples

Syringe water samples (volume 46- 47 ml) retrieved during deployments of BIGO, FLUFO and the BWS were immediately after recovery transferred into the cool room. From these samples sub-samples for the determination of methane, oxygen (Winkler), pH, and geochemistry (sulphate, sulphide, nitrate, ammonium, total alkalinity and ICP) were taken. Geochemical parameters were not determined for the BWS water samples. During the BIGO deployments oxygen and temperature was additionally recorded using in situ using optodes (Tengberg et al. 2006) in the two benthic chambers, the reservoir and in the ambient sea water.

For the determination of methane concentrations in the water samples, 10ml of the syringe water sample was transferred into a 20 ml head space vial which contained 3g NaCl to stop microbial activity and to strip off the methane from the water. For the measurement of the methane concentration the same GC as deployed for the sediment samples was used.

pH was determined in the water samples using a standard pH electrode (WTW Sentix 81), which has been calibrated in seawater buffer solutions (BIS & Amphy) under consideration of the temperature. Between the measurements the electrode was stored in an artificial seawater solution (35‰).

5.14 Foraminiferal and Metazoan Biology

D. Bowden, S. Boyd, K. Kröger, R. Martin, A. Thurber, L. Zemke-White

Methane-based ecosystems harbour a diverse group of eukaryotes which harness chemosynthetic production to fuel a biomass that is far greater than that in adjacent habitats. Although well documented in the northeast Pacific and many Atlantic Ocean locations, our knowledge of seeps in the southern Pacific Ocean is restricted to very few sites. An area with well documented fossil methane seep fauna, and yet little known about its extant fauna, is New Zealand; prior to 2006 our knowledge of this seep fauna was limited to a few species of bivalve. The goal of our research is to 1) describe the megafauna and macrofauna (retained on a 300 micron sieve) that inhabit these unique habitats; 2) build a food web utilizing lipid and stable isotopic patterns for the metazoan fauna which will address the microbial metabolic pathways which fuel this ecosystem; 3) use both species assemblage patterns and genetic analyses to place the New Zealand seep fauna in a global context; 4) compare foraminiferal assemblages within the Hikurangi margin microhabitats as well as with other seeps globally; 5) use stable isotope and trace element analyses of foraminifera tests to identify methane sources, assess early diagenetic alteration, and detect hydrate dissociation.

Sediment samples were collected from a variety of sampling equipment including:

- TV guided Multicore (TV-MUC)
- Gravity Core (GC)
- TV guided box-core (TV-BC)
- Box core (BC)
- TV guided Grab (TV-G)

During leg 2 sediment samples taken from the equipment (Table 6.11.1) were rinsed through sieves with 500µm and 300µm mesh. All macrofauna collected were catalogued on NIWA (National Institute of Water and Atmosphere) catch forms, preserved in either 10% formalin, 70% ethanol, or frozen depending on the type of specimen. Once catalogued, each sample was entered into the NIWA database on board the Sonne. The samples will be lodged with NIWA at the New Zealand National Archive for Marine Invertebrates.

Sediment slabs for burrow analysis

Plastic boxes (20x30x8cm) were pushed into the face of the box cores, the slabs were cut from the box core and stored in the cold-room for x-ray. Multicore samples were kept for the same analysis. Samples were collected during leg three of RV SONNE cruise 191 using 15 TV-guided multicore, six TV-guided grab, four gravity corer, and four lander deployments (Table 6.11.2).

TV Guided Grab

Mega fauna was sampled via the TV guided grab. Sediments that were collected were sieved on a 300µm sieve and preserved for later identification. Rocks that were collected had visible epibionts removed, and were sprayed with filtered seawater (FSW). This seawater was then sieved and visible animals were removed. Rocks were left overnight in FSW, which was then filtered and again had animals removed both by naked eye as well as dissecting scope. Animals were sorted into putative species and preserved for later identification using either formalin or ethanol according to phylum. In the instance that a sufficient sample was collected, a subset was frozen for later food web analyses (stable isotopes and lipids).

TV Guided Multicore

Multicore samples were split (by core tube) into three processing schemes 1) quantitative megafaunal community samples, 2) live sorting for genetic and food web analyses, 3) foraminiferal processing. Quantitative megafaunal samples were vertically sectioned into 0-1, 1-2, 2-3, 3-5, 5-7, 7-10, and 10-20cm fractions. The >5cm fractions were sieved on 300µm sieves and all were preserved in 10% buffered formalin for later sorting and identification. The live sort cores were immediately sliced into the same vertical fractions, sieved on 300µm sieves and sorted at sea (<36hours from collection) to putative species using a dissecting microscope. Each species was photographed and reference samples were preserved in formalin while those for genetic analyses were frozen or preserved in 95% ethanol. Samples for carbon and nitrogen stable isotope analyses were placed directly in pre-weighed tin boats, or frozen for later lipid analyses. Foraminiferal cores were sliced at either 0.5cm or 1cm intervals for the majority of their length and stained with Rose Bengal in 4% formalin. Preserved samples were sieved on a 63µm sieve and dried prior to examination.

Lander deployments

Mud collected by the lander team that was not utilized for their analyses were sieved on a 300µm sieve and either placed in 1) 10% formalin 2) 95% EtOH for later genetic analyses or 3) live sorted and treated as described in the multicore section. Foraminiferal samples were again stained with rose bengal, sieved and dried for examination.

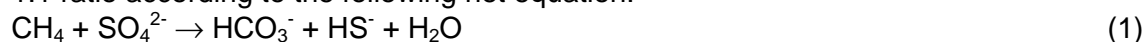
Gravity Corer

Three gravity cores were sampled at high resolution for foraminiferal analysis. Two-centimeter slices were taken continuously from 0-10 cm (0-2cm, 2-4cm, etc.), then every 5 cm to 50 cm deep in the core, every 10 cm to 100 cm in the core, and every 20 cm to the bottom of the core. In addition, one core (Station 250) was only qualitatively sampled due to the disturbed nature of the core. These samples were stained and sieved as above.

5.15 Microbial Ecology

J. Arnds, V. Beier, H. Niemann, D. Santillano, T. Treude, G. Wegener

Ocean margin research of the last decade has provided evidence for a variety of fascinating ecosystems associated with fluid, gas and mud escape structures. These so-called cold seeps are colonized by enormous biomasses of bacterial mats, chemosynthetic fauna and associated animals. Cold seep systems support a variety of microhabitats such as surface and subsurface sediments, carbonate precipitates and symbiotic megafauna including tubeworm aggregations and bivalve beds. Subsurface seep sediments harbour a great diversity of hydrocarbon degrading communities of anaerobic bacteria and archaea along fluid and gas escape pathways. The seep-related micro and mega fauna thrive along- and shape gradients of electron donors such as methane and sulphide as well as electron acceptors such as oxygen and sulphate. Furthermore, the metabolic products (e.g., bicarbonate and sulphide) of seep-microbes provide the base of the food web thereby fuelling the vast amount of biomass that is typically found at many seeps. In this context, specialised, symbiotic archaea and sulphate reducing bacteria (SRB) mediating the anaerobic oxidation of methane (AOM) with sulphate are of particular importance (Boetius et al. 2000) because the activity of these communities reduces the efflux of methane to the hydro- and potentially to the atmosphere where it strongly contributes to the green house effect. During AOM, methane and sulphate are consumed in a 1:1 ratio according to the following net equation:



However, the activity of AOM communities is regulated by the availability of methane and sulphate, which in return is regulated by the fluid and/or gas flux as well as bioirrigation activities (Treude et al. 2003, Niemann et al. 2006). Many cold seeps are furthermore characterised by enormous carbonate

precipitates which may serve as a hard substrate for sessile megafauna or as habitat structure for fish species (Niemann et al. 2005). The driving mechanisms leading to the precipitation are largely unknown but an increase in alkalinity during AOM was suggested as a one mechanism. The aim of our investigations during cruise SO191 leg 2 and 3 was to study geo-microbial processes in sediments of the cold-seeps at the Hikurangi Margin east of New Zealand. Of special interest was the investigation of the activity, identity and abundance of chemosynthetic, microbial communities mediating AOM sulphate reduction (SR), aerobic oxidation of methane (Mox) and sulphide oxidation (Sox) in the sediment.

Table 5.15.1. List of investigated parameters and applied methods. Samples for methane and sulphate concentrations as well as porosity were taken in parallel to those obtained by the geochemistry group of M. Haeckel or to complete their data set.

Parameter	Method
AOM rates	radiotracer incubations (^{14}C -methane)
MOx rates	radiotracer incubations (^{14}C -methane)
SR rates	radiotracer incubations (^{35}S -sulphate)
CH_4 concentration	gas chromatography
Porosity	weighing, drying
SO_4^{2-} concentrations	ion chromatography
microbial abundance	Counts with 4',6'-diamidino-2-phenylindole (DAPI), acridine orange (AODC), fluorescence in situ hybridization (FISH), quantitative polymerase chain reaction (q-PCR) and biomarker analyses
microbial identification and diversity	FISH, DNA, RNA and biomarker analyses

For our investigations of sediment samples from the various sampling areas (Tab. 10.2), we applied a transdisciplinary approach using a suite of different biogeochemical, microbiological and molecular methods (Tab. 5.15.1). Sediments for sampling were recovered with a multiple-corer (MUC), gravity corer (GC), TV-grab, and the BIGO-lander (Tab. 10.2). Directly after sampling, MUC cores were transferred to a cold room (2°C) and sampled for the various parameters. GC and TV-grabs were sampled on deck. Radiotracer incubations were carried out at *in situ* temperature in the dark for 24 h (sediment) to 8 days (water samples) and then fixed in NaOH (AOM, Mox) or ZnAc (SR). Sediments for DNA, q-PCR and biomarker analysis were frozen at -20°C. Sediments for RNA analysis were fixed with RNA later[®] for 4 h at 4°C and then frozen at -20°C. Samples for FISH analysis were fixed in formalin/seawater for 4 h at 4°C, subsequently washed in PBS and stored in PBS/ethanol at -20°C. All further analysis will be conducted in the home laboratories.

5.16 Geochemical Investigations

M. Haeckel, K. Krieger, B. Domeyer, E. Hütten, M. Bausch, M. Marquardt, D. Müller

The geochemical analyses of the porewaters and sediments of cold seeps at the Hikurangi margin, New Zealand, aim at the investigation and characterization of the compositions, sources, and fluxes of the expelled fluids and gases as well as the determination of the amount and rates of formation of methane hydrates. We also plan to combine the geochemical characteristics with the biological as well as the geophysical information. Therefore, a comprehensive geochemical dataset has been collected on the SO 191 cruise onboard RV SONNE. Onboard, the collected samples were analysed for their content of NH_4^+ , PO_4^{3-} , SiO_4^{4-} , H_2S , Cl^- , Br^- , SO_4^{2-} , NO_3^- , and alkalinity. In addition, sub-samples were taken for further shore-based analyses (Helium isotopes, CH_4 headspace, ICP-AES, ion chromatography, isotope analyses, porosity determination, and CNS element analyses).

The geochemistry group investigated a total of 8 different seep sites and 2 reference sites for their geochemical characteristics, giving a total of 57 cores and 939 samples. The sampling locations were chosen based on seismic and hydroacoustic studies on Leg 1 as well as video observations during video sled (OFOS) surveys on Leg 2 and TV-MUC deployments on Legs 2 and 3 that suggested potential fluid and gas seepage. Onboard, we focussed on the chemical analyses of the composition of the pore fluids.

The observed biogeochemical characteristic of the collected porewaters appears to be similar in the investigated areas at the Hikurangi margin: Rock Garden, Okamere Ridge, and Wairarapa. In general, the porewater signatures seem to be related to characteristic features observed at the seafloor, such as black sediment spots, clam shells, carbonates, vestimentifera, and 'normal'

sediment cover and these are common to all three areas. Hence, only a few porewater data sets typical for these seafloor features are presented and discussed in more detail in section 6.10.

Sediment and porewater sampling

Surface and subsurface sediment samples were retrieved using a TV-guided multi-corer (TV-MUC), a gravity corer (GC), and deployments of benthic chamber landers (BIGO – biogeochemical observatory and FLUFO – fluid flux observatory). From the benthic chambers, push cores were taken as well as in situ bottom water samples collected by syringes at certain time intervals during the deployment at the seafloor. The sediment of the MUCs and lander chambers were extruded out of the plastic liners and cut into 1-2 cm thick slices. In case of the GCs, 2-3 cm thick slices were taken in approximately 20-40 cm intervals. Subsequently, the porewater was extracted using a low pressure-squeezer (argon at 1-4 bar). While squeezing the porewater was filtered through 0.2 µm cellulose acetate Nuclepore filters and collected in recipient vessels. About 5 ml of each wet sediment slice was collected for porosity analyses. For concentration and isotope analyses of hydrocarbons, a defined sediment volume of 3 cm³ was sampled into a glass vial containing 3 ml 0.1 M NaOH solution, tightly crimped, and suspended. The above procedures were performed at approximately in situ temperature of 4°C in a cold room onboard the ship.

All samples – the squeeze cakes, wet sediment, and additional porewaters – for analyses subsequent to the cruise at the shore-based laboratories were stored refrigerated.

The samples for He isotope analyses on porewaters were extracted from pre-drilled MUC and GC liners and directly from the bottom water according to the method described by Brennwald et al. (2003). To enable atmospheric-free sediment sampling, copper vials were mounted to the liners and subsequently the sediment was squeezed through the copper vials. Having the copper vials sufficiently rinsed with sediment they were crimped and stored at room temperature. At the shore-based laboratory at the ETH in Zurich (CH) the porewater will be extracted from the sediment by degassing them in an extraction vessel and subsequently analysed by standard MS technique.

Porewater analyses

Analyses for the nutrients NH₄⁺, PO₄³⁻, SiO₄⁴⁻, and H₂S were completed onboard using a Hitachi UV/VIS spectrophotometer. The respective chemical analytics follow standard procedures (Grasshoff et al., 1999), i.e. ammonium was measured as indophenol blue, phosphate and silicate as molybdenum blue, and sulfide as methylene blue. Since high sulfide contents (> 1 mM) interfere with the reactions of NH₄⁺, PO₄³⁻, and SiO₄⁴⁻, these sub-samples were acidified with 20 µl of HCl and bubbled with argon to strip any H₂S prior to the analysis.

The total alkalinity of the porewater was determined by titration with 0.02 N HCl using the Tashiro indicator, a mixture of methyl red and methylene blue. The titration vessel was bubbled with nitrogen to strip any CO₂ and H₂S produced during the titration. The IAPSO seawater standard was used for the calibration of the method. The porewater contents of chloride, bromide, sulphate, and nitrate were determined by ion-chromatography. We used a Metrohm ion-chromatograph equipped with a conventional anion-exchange column and carbonate-bicarbonate solution as an eluent. While chloride and sulphate were measured with a conductivity detector, nitrate and bromide were measured with a UV detector. Again, the IAPSO seawater standard was used for calibration.

A list of the measured properties is presented in Table 5.16.1 including an estimate of the analytical precision. Table 10.3 lists the sub-samples and number of total samples collected from each core.

Table 5.16.1: Analytical methods for measuring porewater parameters.

Parameter	Method	Detection limit	analytical error (accuracy)
H ₂ S	Photometer	1 µmol/l	3 µmol/l
NH ₄ ⁺	Photometer	2 µmol/l	5 µmol/l
PO ₄ ³⁻	Photometer	1 µmol/l	5 µmol/l
SiO ₄ ⁴⁻	Photometer	1 µmol/l	5 µmol/l
Cl ⁻	ion chromatography	< 1 µmol/l	1%
Br ⁻	ion chromatography	1 µmol/l	1%
SO ₄ ²⁻	ion chromatography	< 1 µmol/l	1%
NO ₃ ⁻	ion chromatography	1 µmol/l	1%
Alkalinity	Titration	0.01 meq/l	0.02 meq/l

5.17 Carbonate Sampling Program

A. Eisenhauer, V. Liebetrau

The precipitation of calcium carbonate (CaCO_3) polymorphs (aragonite and calcite) is one of the major chemical side effects of increased alkalinity during AOM (Anaerobic Oxidation of Methane) activity. The more or less formation of CaCO_3 directly reflects the stoichiometric amount of CH_4 and SO_4^{2-} consumption at vent sites. In general terms, the higher the abundance of cold seep carbonates the higher the related AOM activity.

The vent site carbonates are excellent archives for the reconstruction of past AOM activity and CH_4 -fluxes. Furthermore, vent site carbonates preserve proxy information on vent site fluid and pore water composition, pore water temperature and the microbiological composition of the AOM consortia. Latter information can be embedded in a time frame by precise carbonate dating using U/Th-dating methods (cf. Teichert et al., 2003). Furthermore, the past environmental conditions can be determined by the measurement of distinct elemental ratios (Sr/Ca, Mg/Ca, etc.), isotope ratios ($\delta^{13}\text{C}$, $\delta^{18}\text{O}$, $\delta^{44/40}\text{Ca}$, $\delta^{34}\text{S}$, etc.) and biomarker composition.

6 Work completed and first results

6.1 Hydroacoustics

J. Greinert

Hydroacoustic mapping was performed during the entire cruise. Transit tracks between the different stations were chosen to enlarge the existing bathymetric map. Based on existing data from GNS (Figure 6.1.1) the areas of major interest along the Hikurangi margin could be almost completely covered.

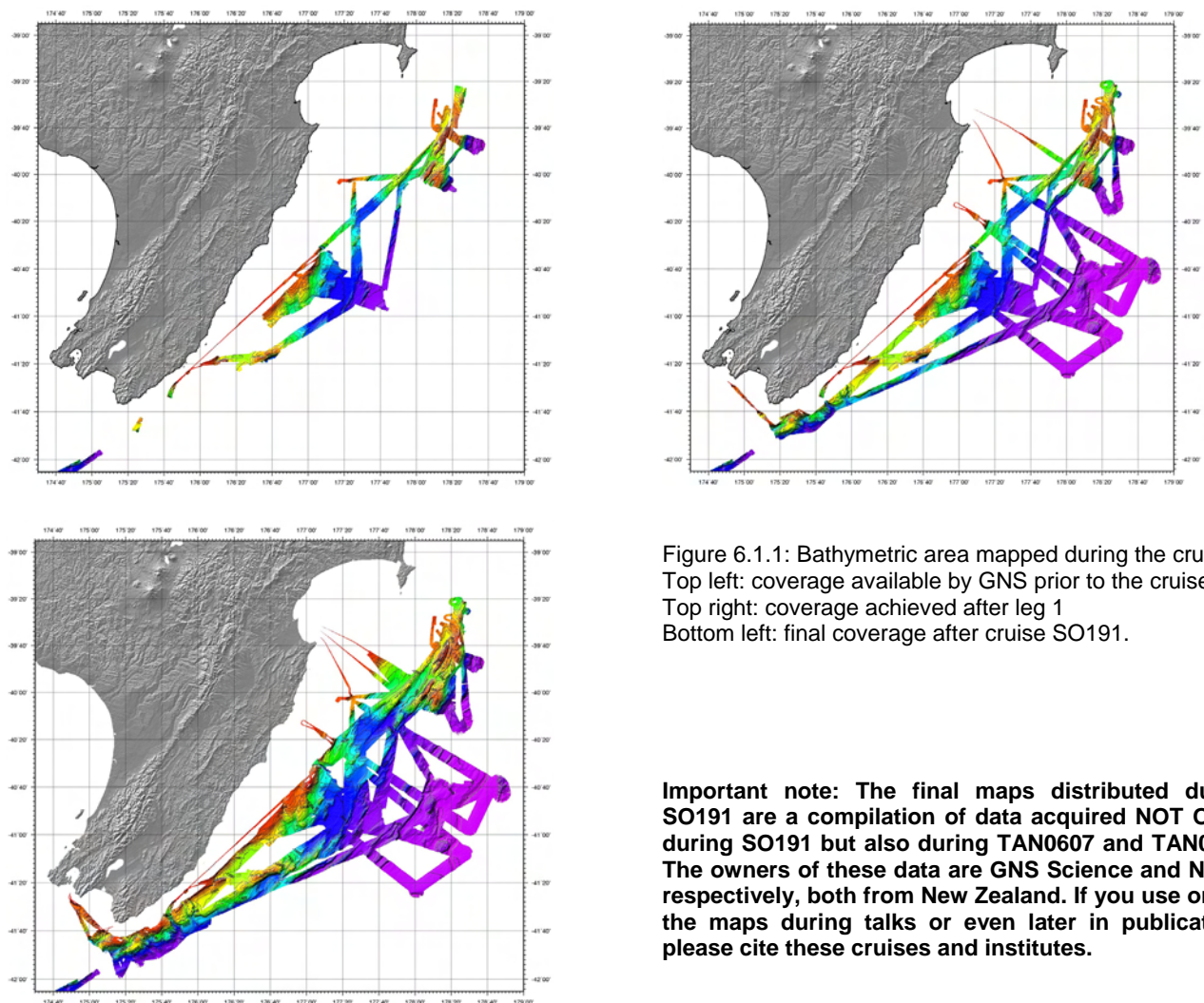


Figure 6.1.1: Bathymetric area mapped during the cruise. Top left: coverage available by GNS prior to the cruise Top right: coverage achieved after leg 1 Bottom left: final coverage after cruise SO191.

Important note: The final maps distributed during SO191 are a compilation of data acquired NOT ONLY during SO191 but also during TAN0607 and TAN0616. The owners of these data are GNS Science and NIWA, respectively, both from New Zealand. If you use one of the maps during talks or even later in publications please cite these cruises and institutes.

6.2 DTS-1 Operations

I. Klauke, W. Weinrebe, J. Petersen, A. Jones and watchstanders

Sidescan sonar mapping of potential cold seeps offshore New Zealand's North Island was carried out during the first and second leg of cruise SO191. While the first leg was dedicated to map four main areas with 75 kHz sidescan sonar, the second leg complemented the 75 kHz surveys of the first leg, added an additional fifth area of investigation with 75 kHz sidescan sonar, and carried out high-resolution investigations of two sites using 410 kHz sidescan sonar. The sidescan sonar data were processed onboard using the software package *Caraibes v3.2*. The subbottom profiler data were processed with in-house shell scripts based on *Seismic UNIX* and *GMT*.

6.2.1 Builder's Pencil

The area known as Builder's Pencil was surveyed using 75 kHz sidescan sonar from 14/01/2007 at 06:00 UTC until 16/01/2007 at 02:00 UTC. The deployment consisted of 5 NNE-SSW trending profiles and four crossing profiles with a general W-E orientation (Figure 6.2.1.1). The Posidonia USBL system was not running properly during this survey and the navigation of the towfish was consequently obtained using the ship's position and a layback method that generally gives good results except during turns. Processing of the sidescan sonar data onboard revealed a mismatch between adjoining profiles. This mismatch could be attributed to an inversion of the port and starboard sidescan sonar transducers and was corrected for all subsequent deployments.

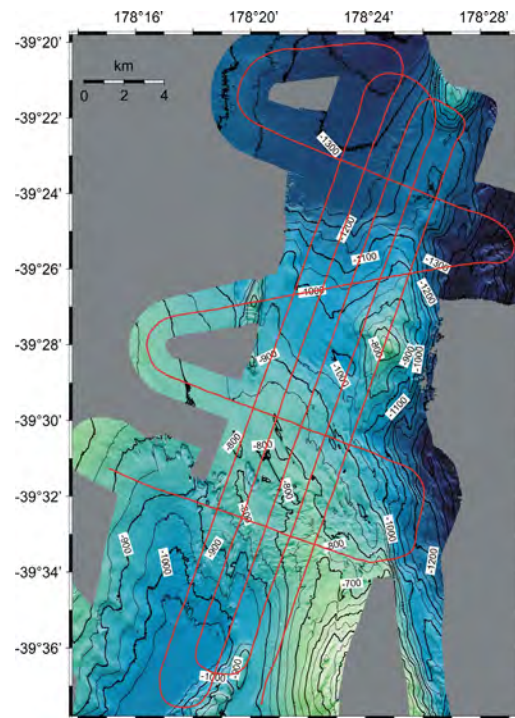


Figure 6.2.1.1: Bathymetry and cruise track of the Builder's Pencil working area.

75 kHz sidescan sonar data from the Builder's Pencil reveal a large number of structures that display high backscatter intensity. However, in many places the sedimentary basement crops out or is covered by only minimal recent sediment cover. A distinction between basement outcrops and "hardgrounds" due to the precipitation of authigenic carbonates is difficult without ground-truthing information.

The subbottom profiler data that have been collected concurrently with the sidescan profiles clearly indicate that sedimentary basement is cropping out in many areas (Figure 6.2.1.3, Figure 6.2.1.4). Profiles running over the area shown in figure 6.2.1.2 do show small elevation on the seafloor, but they are also underlain by a continuous reflection. This reflection almost precludes the structures from being recent chemoherms related to ascending fluids from below. There are locations where this reflector is much weaker and speculations about this reflector being some sort of BSR are possible.

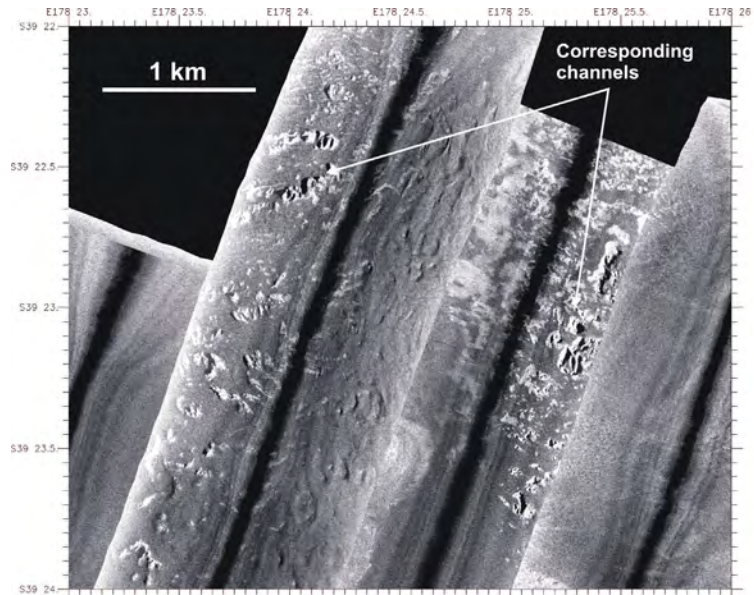


Figure 6.2.1.2: Mosaic of 75 kHz sidescan sonar data from the northern end of the Builder's Pencil area. Please note that individual profiles have to be mirrored along the nadir (black line in the middle of the profiles) in order to match. The origin of the high backscatter (= light tones) patches is not known.

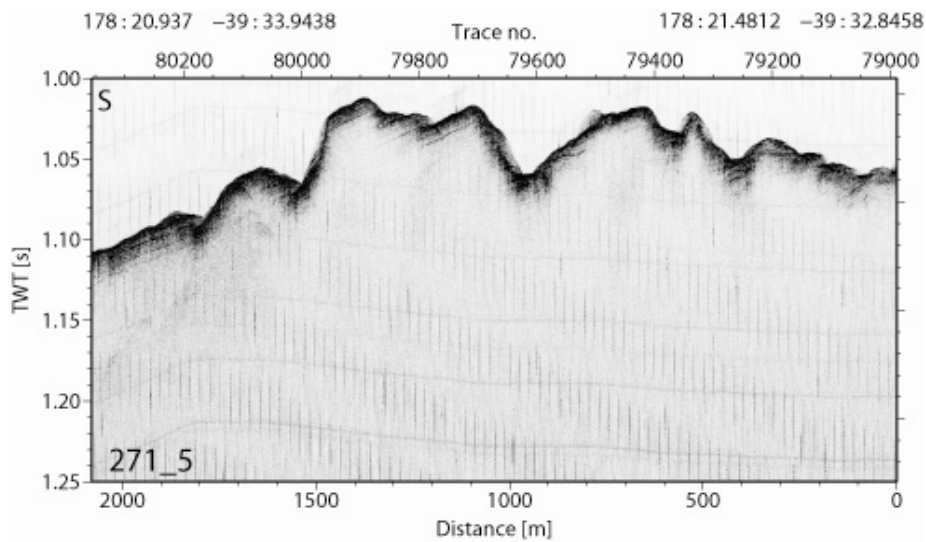


Figure 6.2.1.3: 2-10 kHz Chirp subbottom profile showing outcrops of basement structures with almost no recent sediment cover.

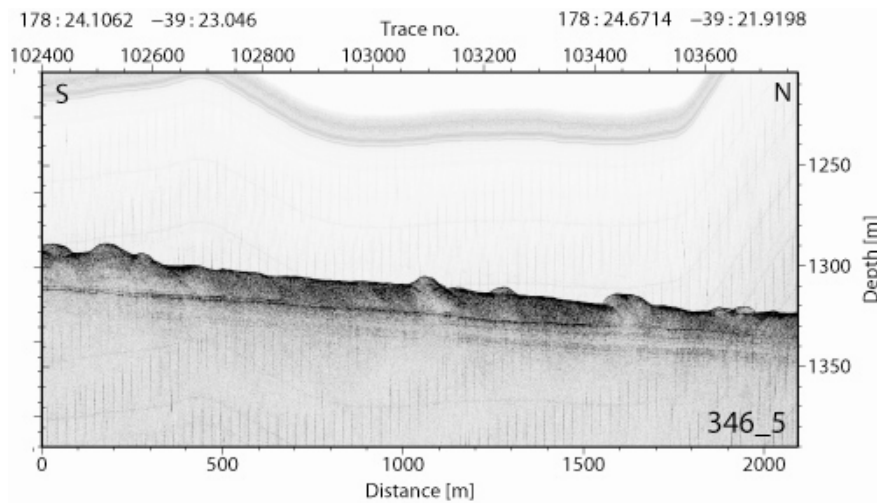


Figure 6.2.1.4: 2-10 kHz Chirp subbottom profile showing small elevations on the seafloor underlain by a continuous reflector. This reflector is disrupted underneath one of the structures at the northern end of the profile.

6.2.2 Wairarapa

The Wairarapa Area was mapped in leg 1 by a sidescan-sonar survey (DTS-2) using the low-frequency mode (75 kHz). This deployment lasted from 23/01/2007 at 00:00 UTC until 24/01/2007 at 02:00 UTC. Five NE-SW trending profiles together with one additional N-S profile have been obtained (Figure 6.2.2.1). Unfortunately, due to a computer failure about 15 minutes of data were missed during the central profile and USBL data were again not available for this survey.

The Wairarapa working area consists of one broad NE-SW trending ridge with a flat-topped, dome-shaped elevation in the Northeast. This ridge is surrounded by erosive sediment pathways and the ridge is covered by recent fine-grained sediments from either hemipelagic sedimentation or turbidity-current overspill. Two locations in the southwest of the survey area and at the summit of the dome-shaped elevation show distinct areas of high backscatter intensity that can be related to fluid venting. In addition two locations have shown gas flares in the raw sidescan sonar data (Figure 6.2.2.2).

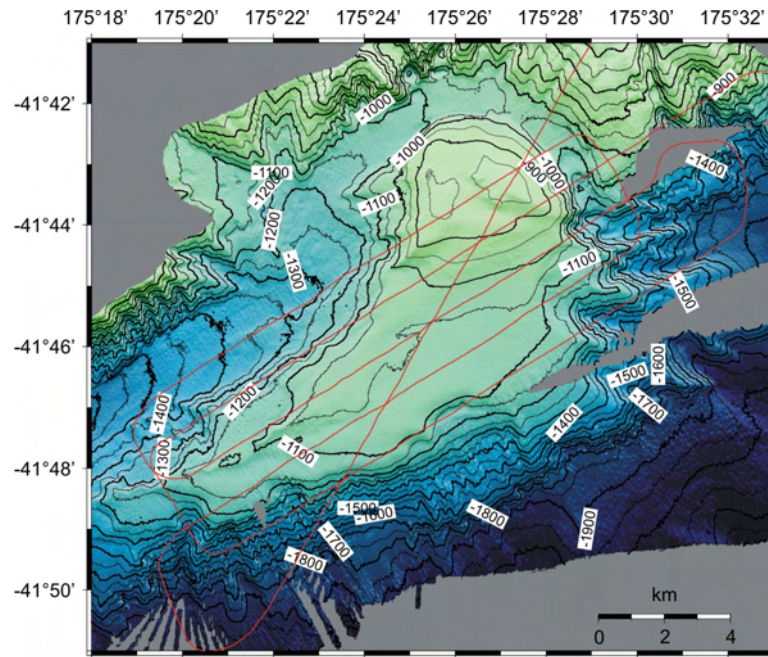


Figure 6.2.2.1: Bathymetry and cruise track of the Wairarapa working area during leg 1.

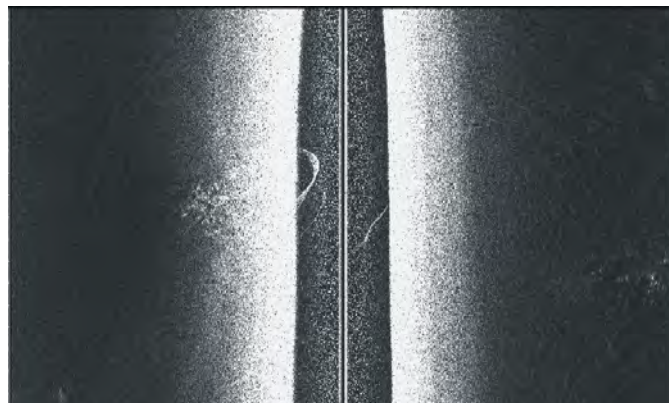


Figure 6.2.2.2: Raw sidescan sonar image showing a distinct high backscatter anomaly in the water column (central black area) that can be attributed to gas bubbles.

The gas flares area associated high backscatter intensities on the seafloor of processed sidescan data (Figure 6.2.2.3) and most likely the result of authigenic carbonate precipitates at the seafloor. The distribution of the high backscatter intensities is rather patchy, and isolated, small (10-20 metres across) occurrences are observed in addition to the main seep site. In the vicinity of the seep a small band (100 metres across) of dune-like structures has been observed and could also be related to seep activity. Sediment bedforms due to the current regime in the area should have a more

widespread distribution, but sediment creeps due to fluid-expulsion at the seep site can also explain the observed feature.

In addition to these seep locations similar high backscatter patches have been observed at the northern flat-topped cone (Figure 6.2.2.4). However, at this location the raw sidescan sonar data did not show gas flares in the water column. On the other hand the potential seep sites are larger and show more relief judging from the extent of shadows. The seeps at this location could be older and not yet active any more or erosion has exposed more of the deeper structure of the seep site. There are no indications for sediment outflows at either of these seep sites.

The subbottom profiler data from the Wairarapa area show the presence of gas fronts in the subsurface. Some profiles show a distinct three-fold stratigraphic succession with roughly 10-m thick successions of relatively reflective data sediment packages overlying an almost transparent unit (Figure 6.2.2.5). The lower contact of the transparent unit shows a high amplitude contact with the gas front. The gas front in itself probably comes to the surface at the seep sites, but extends for much wider area close to the surface surrounding the seep visible on the sidescan sonar data.

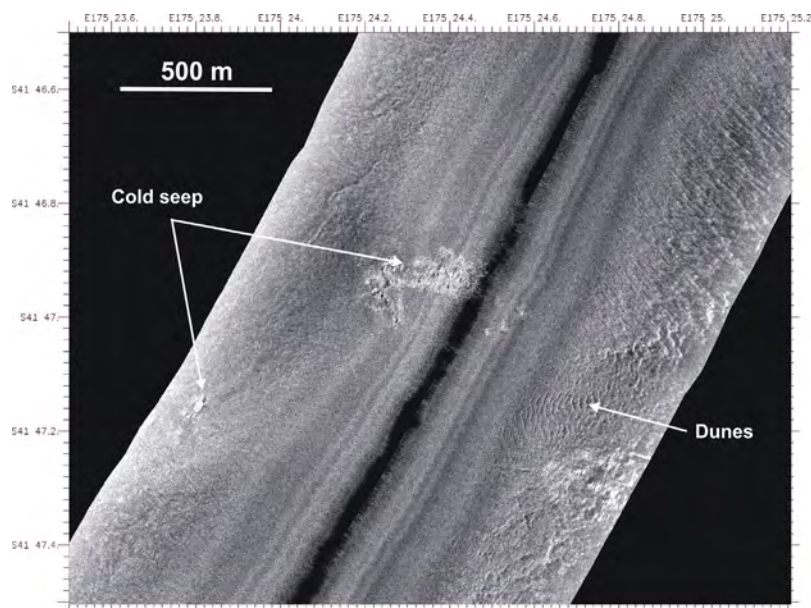


Figure 6.2.2.3: Processed sidescan sonar profile showing several patches of high backscatter intensity that are attributed to authigenic carbonate precipitates at the seafloor. Note the presence of dune-like features that are NOT the result of mudflows from the seeps site.

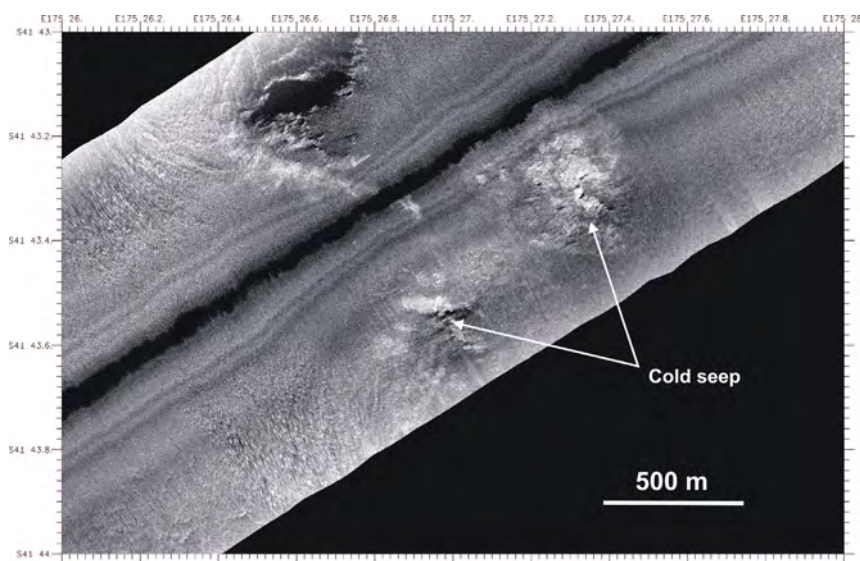


Figure 6.2.2.4: Processed sidescan sonar profile showing several patches of high backscatter intensity at the northern dome of the Wairarapa area.

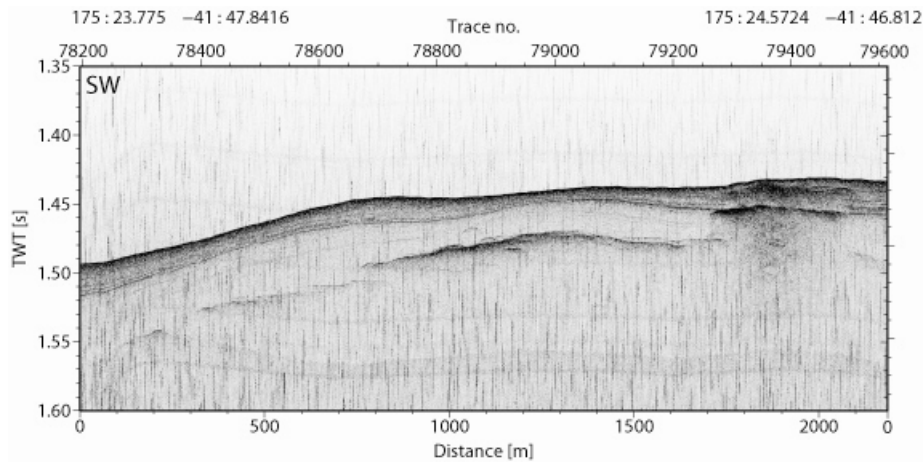


Figure 6.2.2.5: 2-10 kHz Chirp subbottom profile across the cold seep shown in figure 6.2.7. The seep area is characterised by several layers of high amplitude reflections that are most likely due to gas in the sediments.

To gain higher a resolution and more detailed images of the area, parts of the Wairarapa area were resurveyed in leg 2 using the high-frequency mode (410 kHz). This survey (DTS-8) was run on February 18, 2007 from 13:02 to 23:52 UTC. Figure 6.2.2.6 shows the tracks and the bathymetry of the detailed survey. The narrow swath imposed by the high-frequency mode resulted in the planned tow-fish tracks being separated by only 300 m; however, because of strong deep-water currents it was not possible to keep the tow-fish constantly on the planned track. The towing depth for this high-frequency survey was 10 to 20 m above the seafloor.

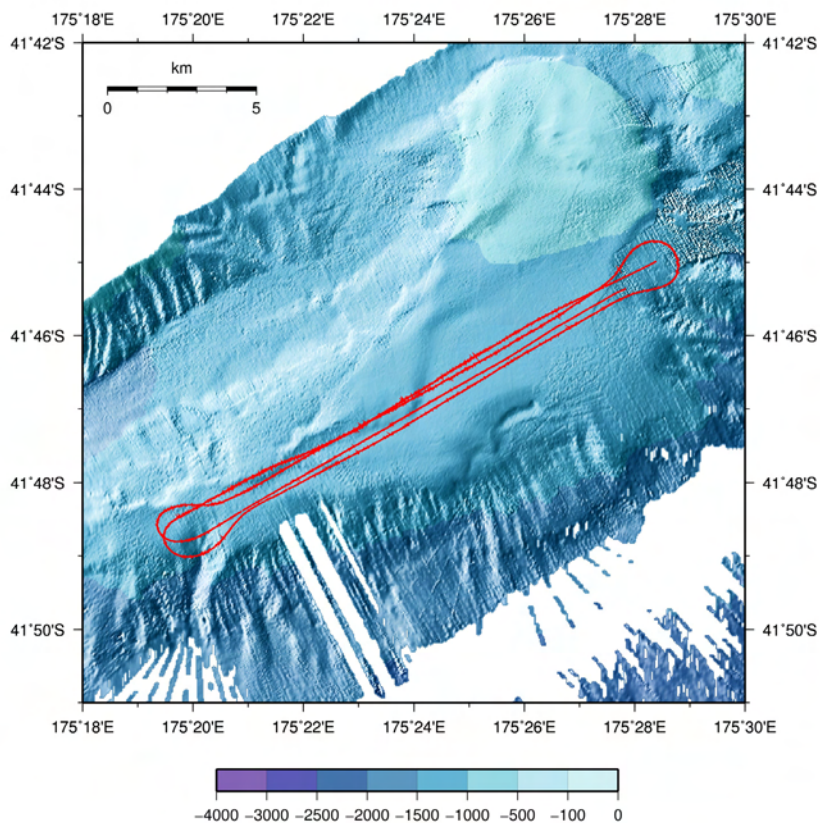


Figure 6.2.2.6: Cruise-track of 410 kHz sidescan survey of the Wairarapa area

In order to get a better control on tow-fish depth above the ground, the 75 kHz sidescan signal and the sub-bottom profiler with a 2 – 10 kHz pulse were used in addition to the 410 kHz mode. As all three signals are operated without synchronisation their pulses are recorded in all three windows resulting in noise; however, due to their systematic generation they can be easily identified as artefacts. Despite the low altitude tow depth the 75 kHz swath covered 1,500 m of seafloor, resulting in major profile overlaps. Therefore many areas of the ocean floor have been ensonified up to four times within the space of a few hours. Of interest is how seafloor features differ in appearance across the four profiles, which is most likely caused by the varying tow-fish altitude across the various profiles resulting in pings with slightly different grazing angles. Figures 6.2.2.7 to 6.2.2.9 give examples of the same surveyed feature during the four different profiles. At position 175°23.4'E, 41°46.8'S a very

distinct flare can be observed on profiles 1, 2, and 4. This position is just outside the range of profile 3. The outline of the flare changes over time as viewed in the different profiles. Detailed inspection of the mosaics yields several smaller flares in the area (Figure 6.2.2.8). Other remarkable features include, distinct dredge marks, single cones, and distinct rough surface areas that may represent carbonate structures on the seafloor. Figure 6.2.2.10 shows the sidescan mosaics of the 4 areas draped over the bathymetry of the Wairarapa area in a perspective view.

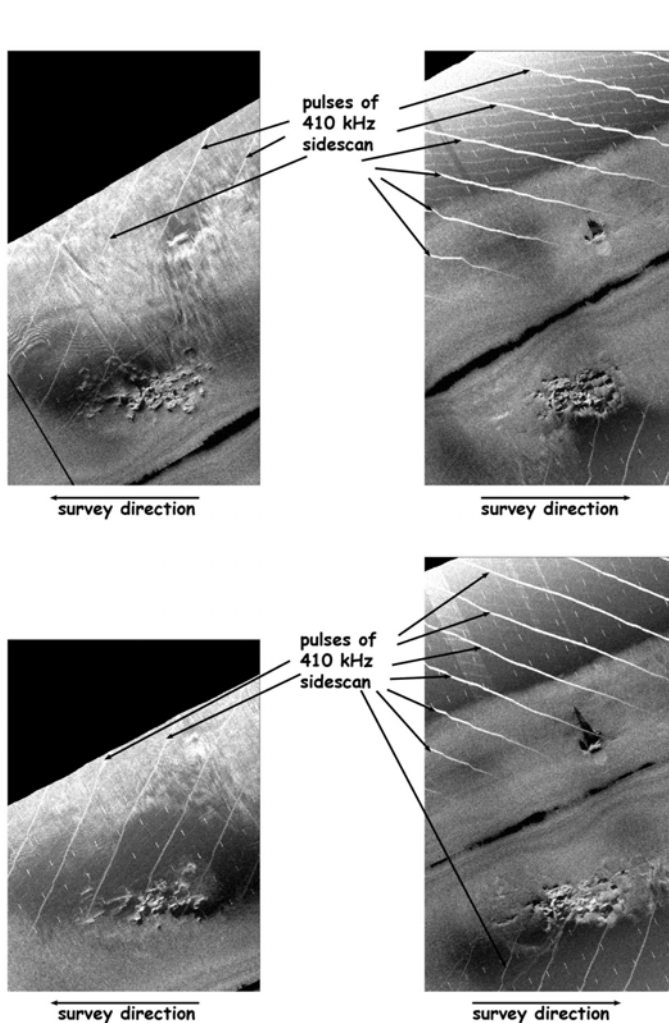


Figure 6.2.2.7: Series of 75 kHz sidescan profiles at lateral incidence over the same area of the seafloor. Between each profiles there are approximately 4 hours.

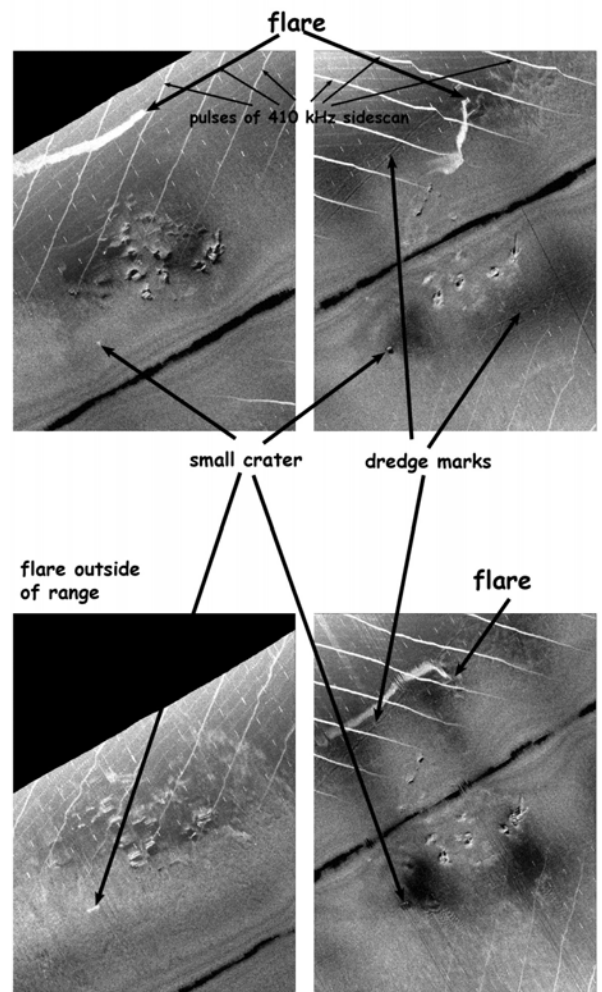


Figure 6.2.2.8: Series of 75 kHz sidescan profiles at lateral incidence over the same area of the seafloor. Between each profiles there are approximately 4 hours. Note the different orientation of the flare.

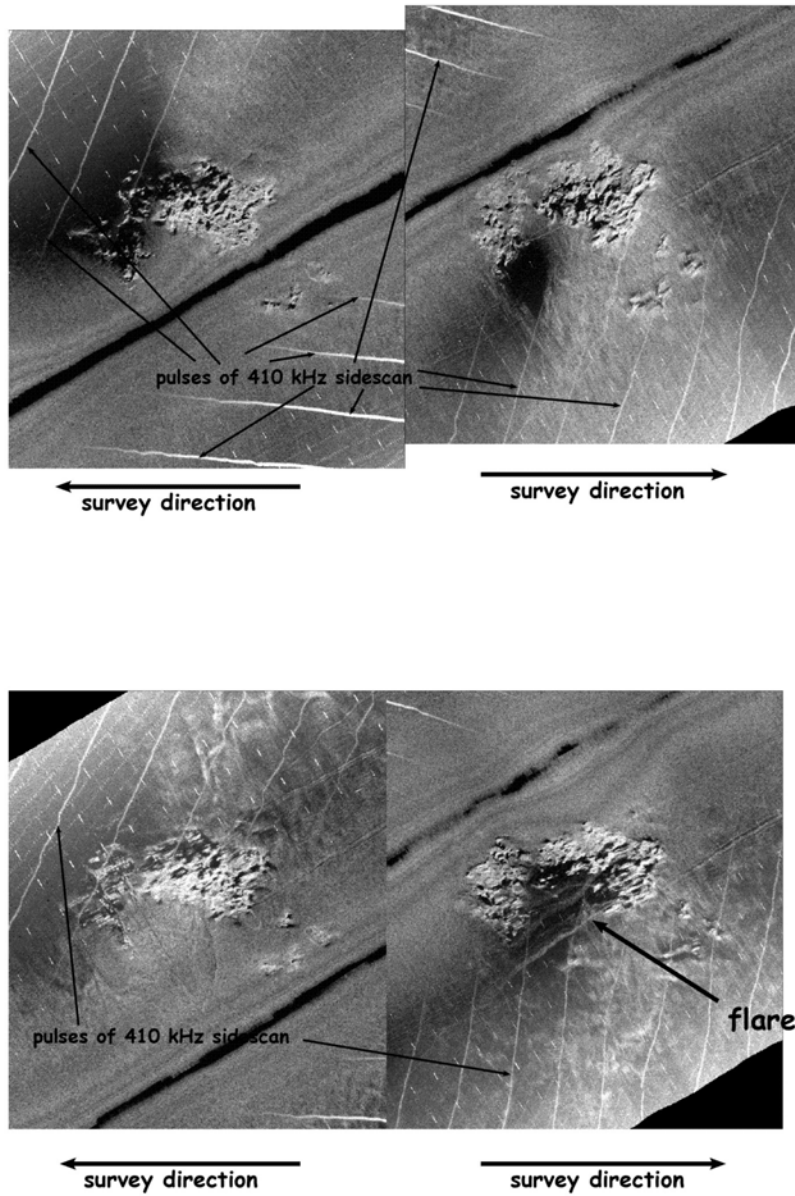


Figure 6.2.2.9: Series of 75 kHz sidescan profiles at lateral incidence over the same area of the seafloor. Between each profiles there are approximately 4 hours. Depending on data acquisition geometry some of the potential chemoherm structures are imaged differently.

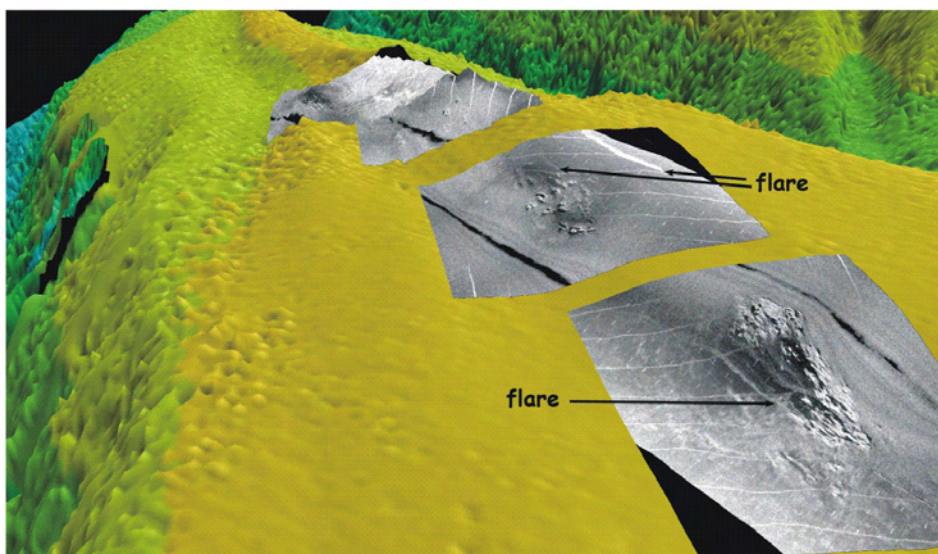


Figure 6.2.10: Perspective view of 75 kHz sidescan sonar data draped over the bathymetry of the Wairarapa survey area..

6.2.3 Uruti Ridge

The Uruti Ridge area (Figure 6.2.3.1) was mapped with 75 kHz sidescan sonar during the first leg between 25/01/2007 at 09:00 UTC and 26/01/2007 at 01:15 UTC. The deployment consisted of three NE-SW trending profiles. A fourth profile was planned but the deployment was cut short due to a broken cable connection. During this deployment Posidonia USBL navigation was available providing a lateral resolution of a few tens of metres.

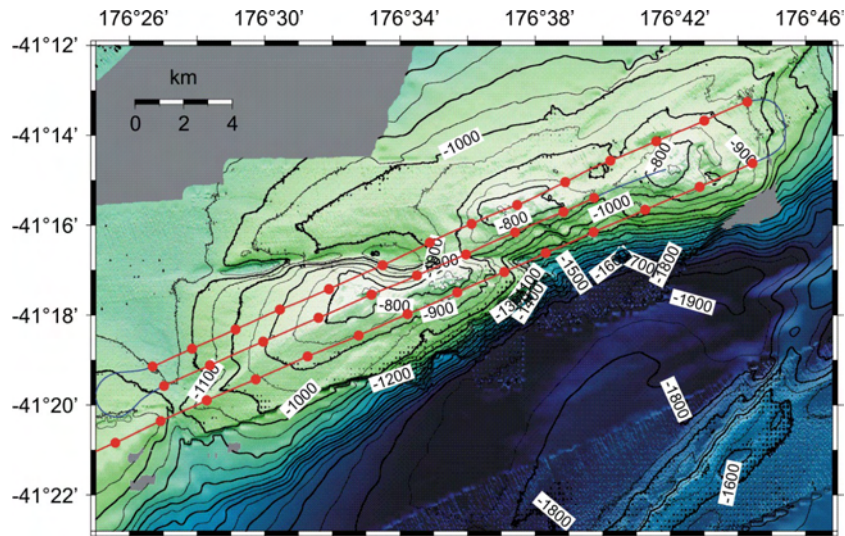


Figure 6.2.3.1: Bathymetry and cruise track for the sidescan sonar deployment over Uruti Ridge during leg 1.

The sidescan sonar data from Uruti Ridge show a number of high backscatter areas associated with small-scale relief as indicated by shadows on the sidescan mosaic (Figure 6.2.3.2). Whether these high backscatter areas correspond to basement outcrops of chemoherm structures associated with fluid venting is not clear from the sidescan data alone. However subbottom profiler data from the area (Figure 6.2.3.3) do indicate localised areas of increased amplitudes that could correspond to gas charged sediments or gas hydrates. The Uruti Ridge area is also cut into two parts by a regional fault that is well imaged with sidescan sonar data (Figure 6.2.3.2), where the fault trace appears as a gullied escarpment.

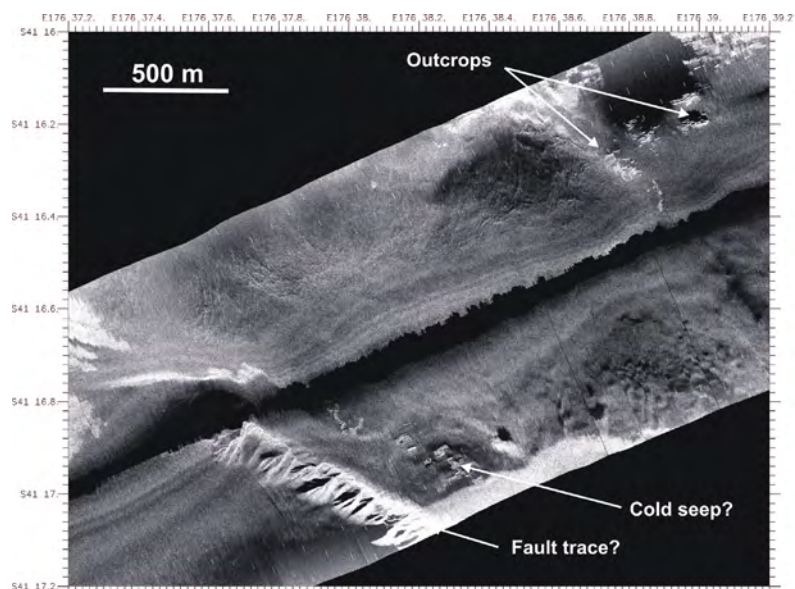


Figure 6.2.3.2: 75 kHz sidescan sonar profile from the Uruti Ridge area showing potential cold seep sites that are characterised by high backscatter intensity (=light areas). Also shown is the trace of a major fault.

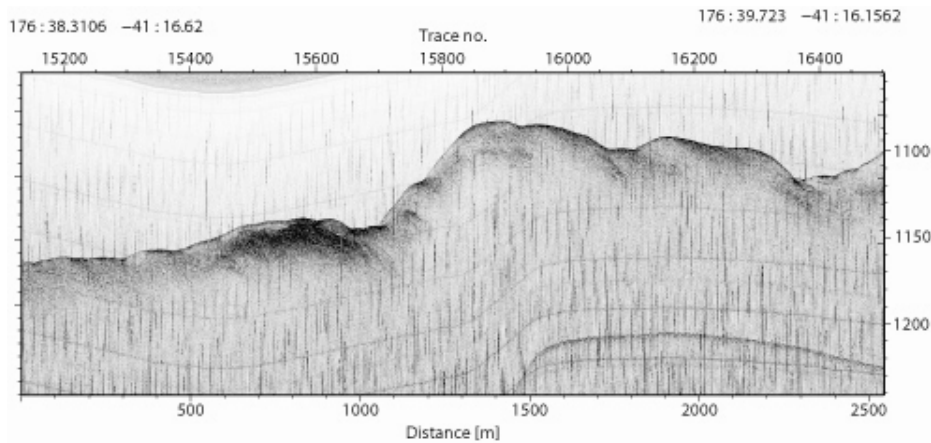


Figure 6.2.3.3: 2-10 kHz chirp profile over Uruti Ridge. The high amplitudes around ping number 15600 could indicate the presence of cold venting at this location.

6.2.4 LM9 area

Two sidescan-sonar surveys were conducted in the LM9 area during legs 1 and 2. Acquisition of DTS-4 on leg 1 was cut short because of a cable failure resulting in only two profiles being surveyed. DTS-6 on leg 2 aimed to complete the sidescan-sonar survey of the LM9 area left incomplete from DTS-4. Survey DTS-6 was run on February 6, 2007 from 12:24 to 19:01 UTC. Figure 6.2.4.1 shows the track of survey DTS-4 plotted on the bathymetry of the area. During this survey the sidescan was operated in low-frequency mode (75 kHz) with the sub-bottom profiler set to a chirp pulse of 2 – 10 kHz.

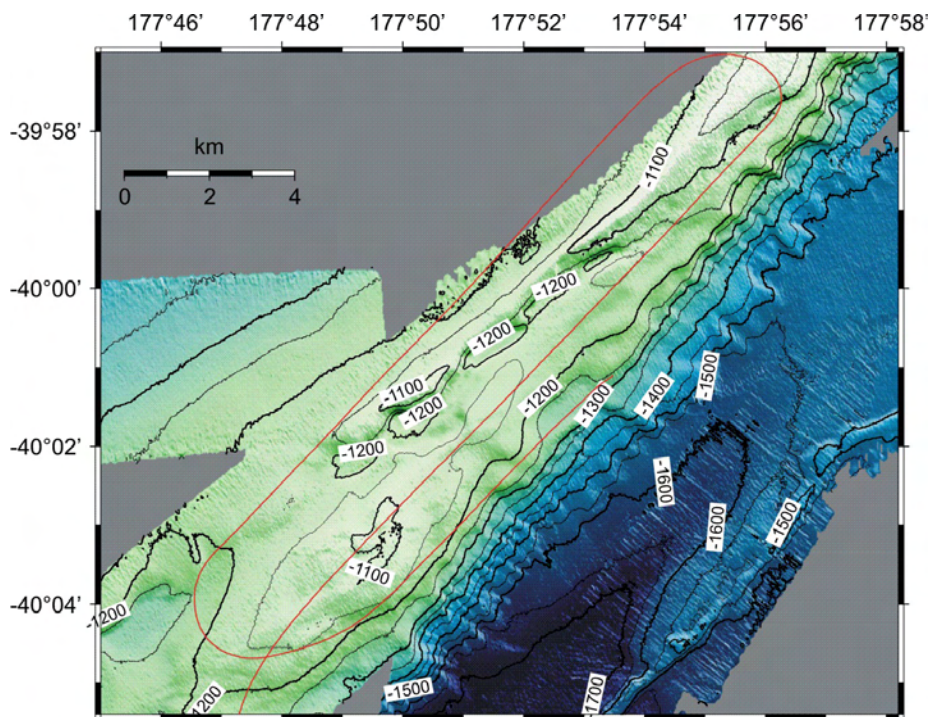


Figure 6.2.4.1: Bathymetry and cruise-track of the 75 kHz sidescan survey of the LM9 area during leg 1. The continuation of the profile and the remaining gap was closed during DTS-6 survey of the second leg.

The sidescan sonar data obtained during leg one show a variety of structures that are probably related to fluid venting. These include isolated areas of high backscatter intensity and peculiar rimmed structures that resemble collapse structures observed elsewhere (Figure 6.2.4.2). Although mud pies in other areas of the world display similar features, there are no indications for recent mud flow activity within the LM9 area. The seep sites are particularly well imaged because they occur within otherwise featureless sediments (Figure 6.2.4.3). In order to determine the exact morphology of the seeps, however, further processing of the data will be required, as some of the aspect ratios may be wrong to navigation errors (Figure 6.2.4.3). In addition the extent of the seeps at depth and maybe even their location at the seafloor, are probably related to the depositional facies. Subbottom profiler records

clearly indicate high amplitudes that are likely related to gas charged sediments or gas hydrates to be at least partly controlled by bedding (Figure 6.2.4.4).

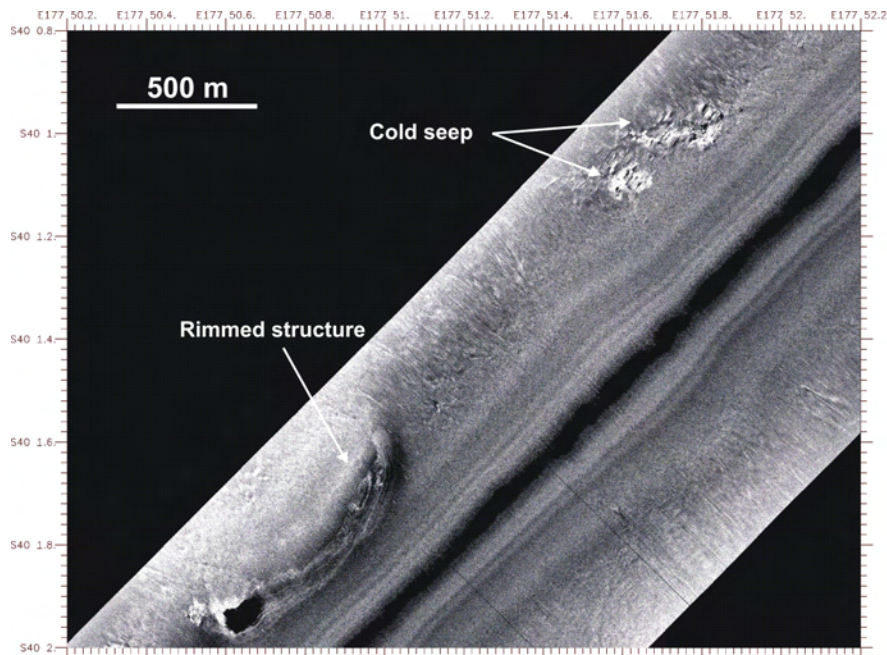


Figure 6.2.4.2: 75 kHz sidescan sonar profile showing two different cold seep locations in the LM9 area.

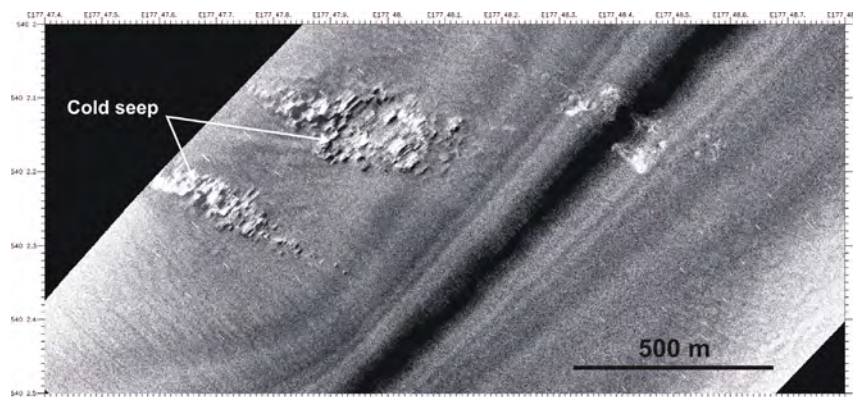


Figure 6.2.4.3: 75 kHz sidescan sonar profile showing several different cold seep locations in the LM9 area. The slightly elongated aspect of the structures at far range might be a processing artefact.

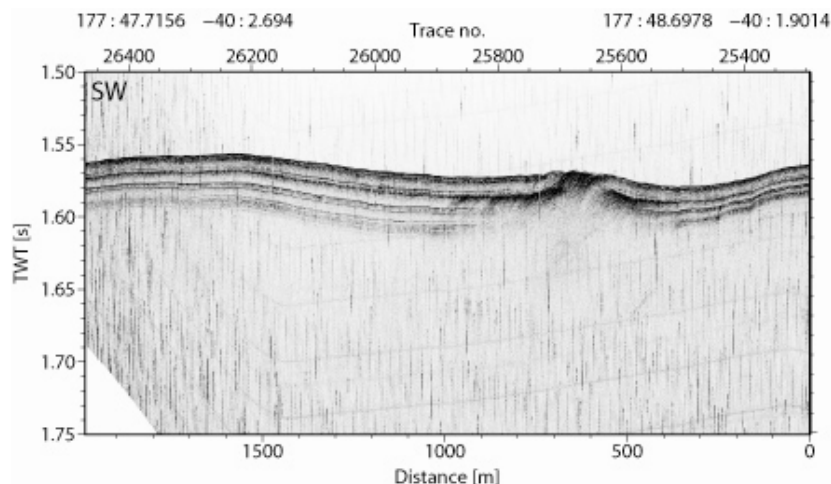


Figure 6.2.4.4: 2-10 kHz Chirp profile over a cold seep in the LM9 area. Please note the high amplitudes that both reach the seafloor and spread laterally along bedding planes.

Survey DTS-7 was acquired from 12:20 to 18:58 UTC on February 8, 2007, the sidescan was operated in high-frequency mode (410 kHz). In this mode the system is towed 10 to 20 m above the seafloor, which requires full attention of the operators and winch crew. The maximum swath range is

150 m either side of the tow-fish. The sub-bottom profiler is only available if the 75 kHz sidescan is operating, hence no sub-bottom profiler data were recorded. Four profiles were recorded during this survey. Figure 6.2.4.5 displays these tracks overlying bathymetry. Data were processed yielding a pixel size of 25 cm in the final mosaics. Figures 6.2.4.6 and 6.2.4.7 show examples from this high frequency survey, the profiles are characterised by large extents of featureless seafloor with occasional structural features.

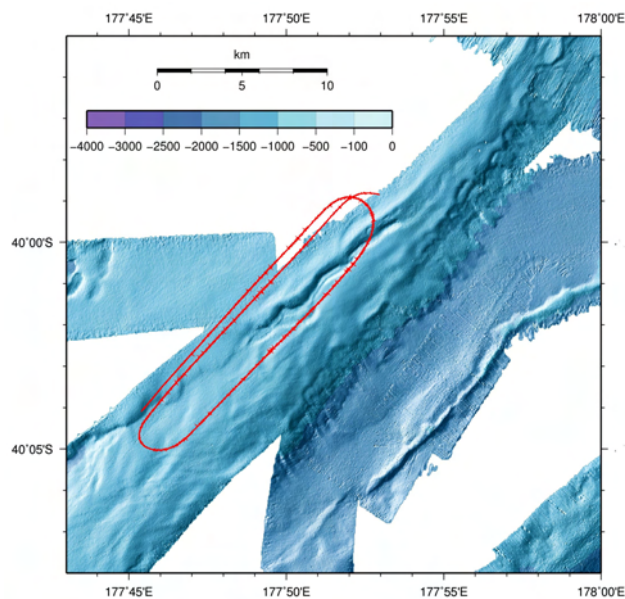


Figure 6.2.4.5: Bathymetry and cruise-track of the 410 kHz sidescan survey of the LM9 area during leg 2.

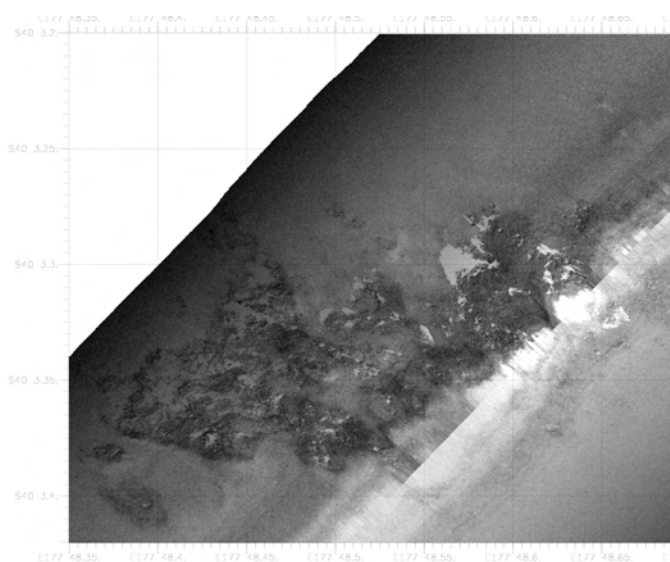


Figure 6.2.4.6: Detail of 410 kHz sidescan sonar image showing a cold seep area at the LM9 site. Pixel size is 0.25 metres and high backscatter is shown in dark tones.

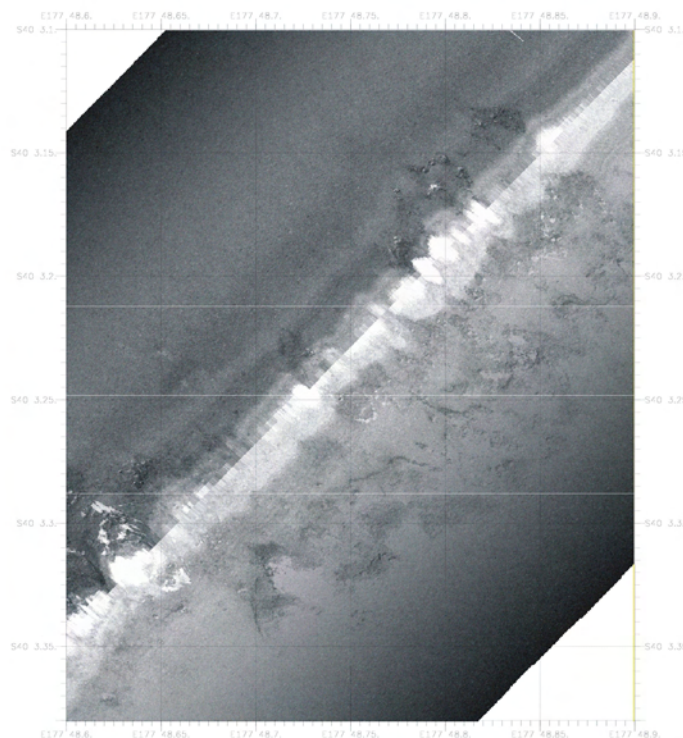


Figure 6.2.4.7: Detail of 410 kHz sidescan sonar image showing a cold seep area at the LM9 site. High backscatter is shown in dark tones.

6.2.5 Rock Garden

Survey DTS-5 was run in the “Rock Garden” area from February 4, 2007 – 04:23 UTC until February 5, 2007 – 00:30 UTC. In total six profiles, each about 7 nm in length, were mapped with the 75 kHz sidescan-sonar and the 2-10 kHz sub-bottom profiler. The area is quite hilly with an average water

depth of 1000 m. During acquisition the DTS-1 system was flown approximately 100 m above the seafloor. The port and starboard swathes were recorded with a reduced number of samples (6000 instead of 13000) because of setup error, resulting in a reduced swath range of only 350 m to each side. Figure 6.2.5.1 shows the track of the tow fish on the seafloor as recorded by the Posidonia USBL system and the bathymetry of the area. All components of the system worked without failure resulting in excellent data quality. The data were processed with *Caraibes* version 3.2. Data processing comprised; merging of checked and smoothed navigation, slant range correction, merging to mosaics and contrast enhancement. Figures 6.2.5.2 and 6.2.5.3 are two examples of the processed data from survey DTS-5.

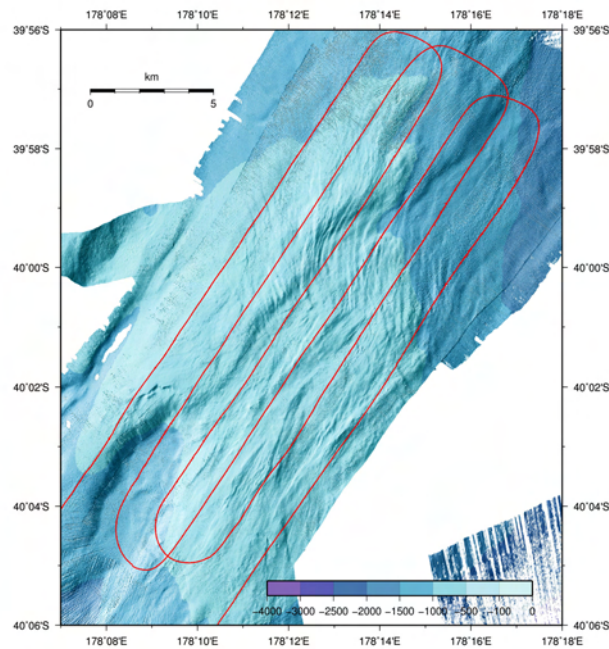


Figure 6.2.5.1: Bathymetry and cruise-track of the sidescan sonar survey in the Rock Garden area.

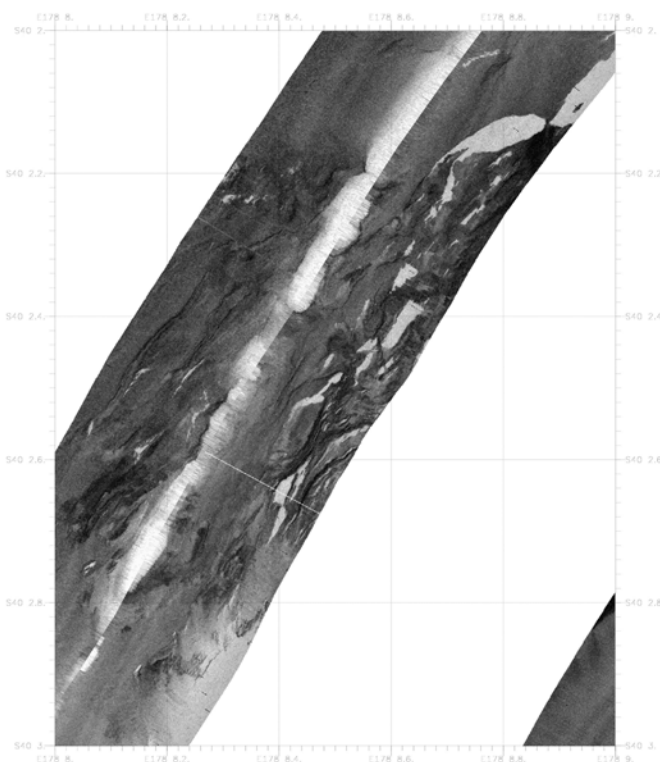


Figure 6.2.5.2: 75 kHz sidescan sonar profiles of the Rock Garden area. Swath width is 560 metres and high backscatter intensity is shown in dark tones.

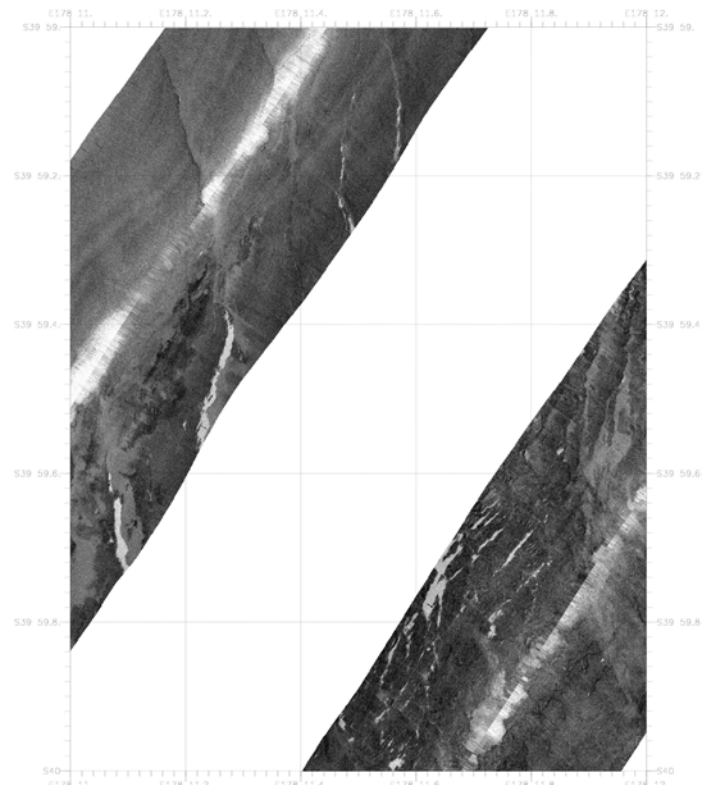


Figure 6.2.5.3: 75 kHz sidescan sonar profiles of the Rock Garden area. Swath width is 560 metres and high backscatter intensity is shown in dark tones. Note the image of several N-S stretching faults in the survey area.

6.3 Seismic Studies

A. Krabbenhoeft, J. Petersen, J. Bialas, G. Netzeband, P. Schroeder, C. Jung, C. Hagen, A. Sticher, A.-D. Rohde

6.3.1 Builder's Pencil (P01)

In the area of Builder's Pencil (-39°36' S/178°15' E to -39°21' S/178°30' E, Figure 6.3.1.1), 10 OBSs were deployed, and nine profiles were shot with lengths between 10 km and 28 km. P012 and P015 (Figures 6.3.1.2 and 6.3.1.3) are shown below.

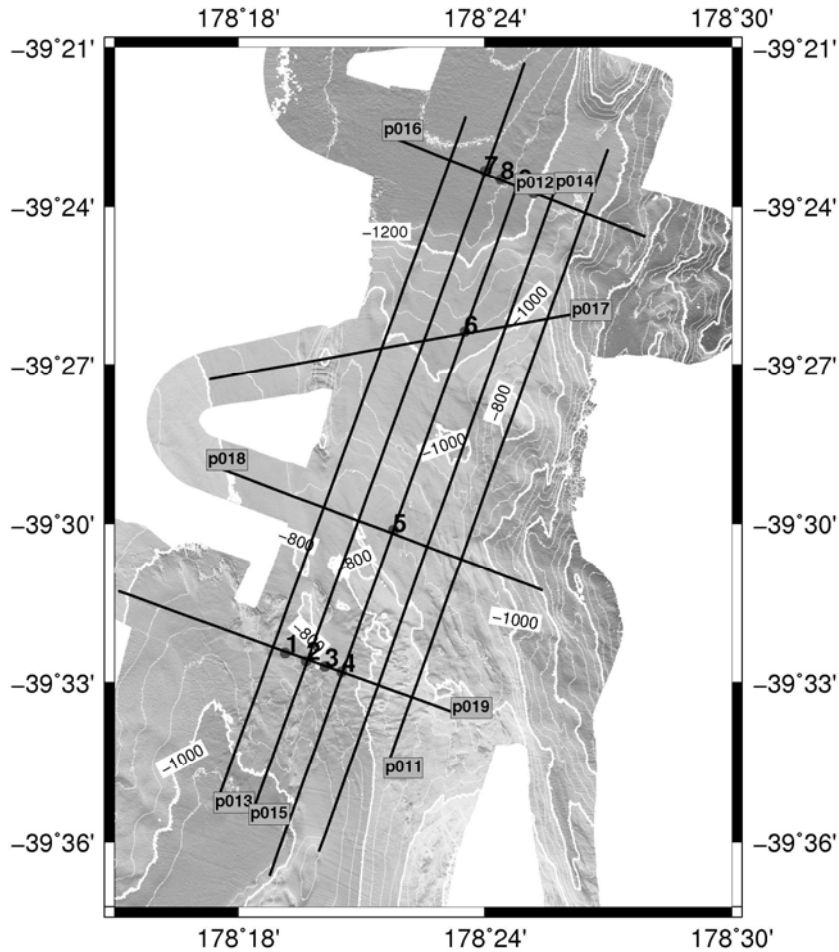


Figure 6.3.1.1 Map of the area of 'Builder's pencil'. Grey dots correspond to OBS locations, black lines to seismic lines.

On the southern end of line P012 (Figure 6.3.1.2), the seafloor appears comparatively uneven, it features many small bulges of 100 – 200 m in diameter, accompanied by strong diffractions. The sediments underneath appear well stratified, interrupted by small faults. A BSR is observed about 300 ms TWT below the seafloor, concordant to the sediment layers. Towards the north, from km -8, the seafloor becomes smoother. Between km -13 and km -7, the sediment layers terminate against a steep reflection, inclining from 2.2s TWT almost to the seafloor. From km -7 to the north, only the upper 200 ms TWT below the seafloor show stratified sediments. The BSR is weaker, but now discordant. Hence, this steep reflection divides P012 into two parts, proper stratification of almost 1s TWT, concordant BSR, bumpy seafloor to the south and hardly any stratification, discordant BSR and smooth seafloor to the north. At km -24, km 23, km-18.5 and km -16, a very weak blanking beneath the seafloor can be observed. If these are vent sites, they are either old, inactive vents or just show very little activity at the moment.

On line P015 (Figure 6.3.1.3), parallel to P012, the same structures are observed, but slightly altered. The steep reflection in the centre of the profile, here between km 12 – km 18, continues northward and it evidently corresponds to the top of a buried mound. To the northern end of P015 it declines and forms the basis of a sediment basin. The BSR appears very clearly within the mound area, at about 500 ms below the seafloor. Further north, it can be traced underneath the sediment basin at up to 1s below the seafloor, but it is very weak. The seafloor is smooth, except for many tiny humps in the sediment basin at the north, which are probably related to gas/fluid escape.

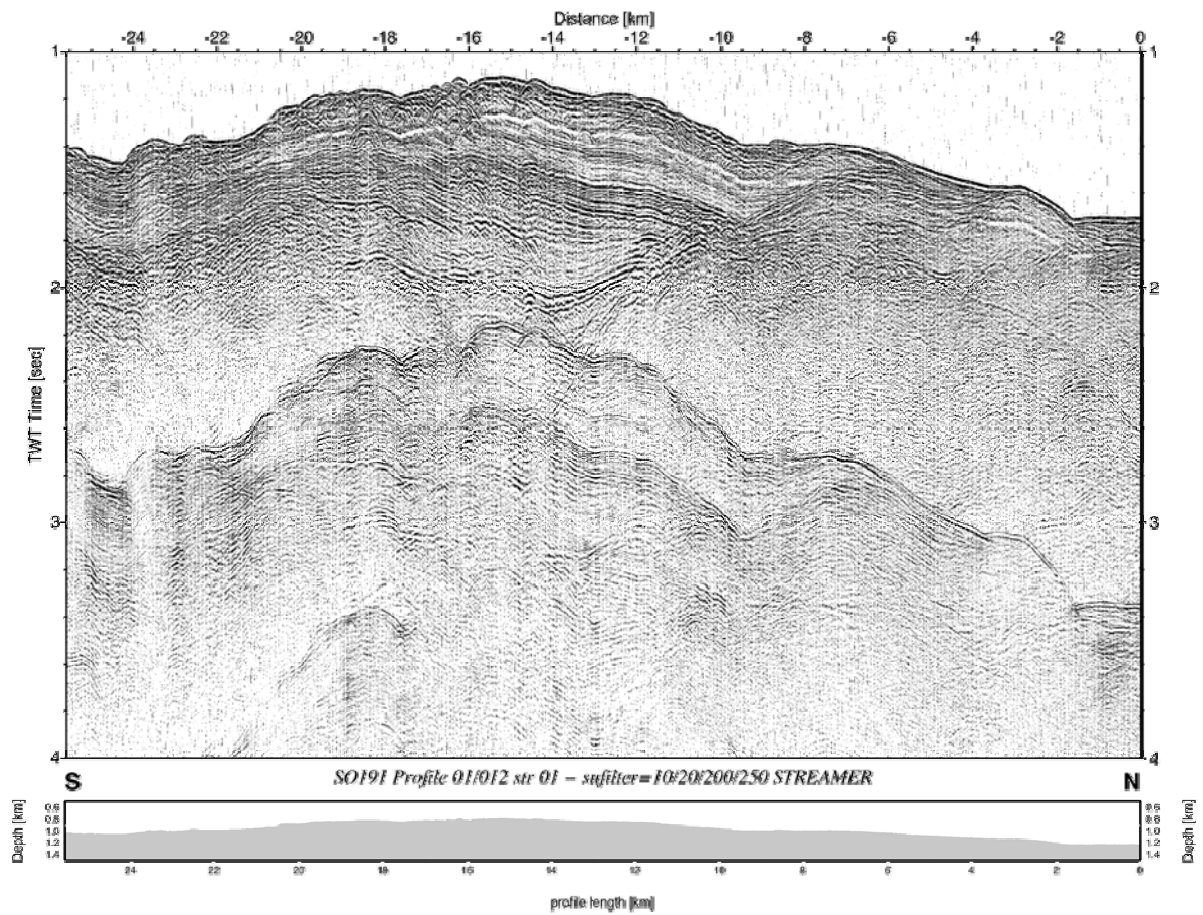


Figure 6.3.1.2: Stack multichannel seismic streamer recorded on profile P012

The Parasound data (Figure 6.3.1.3a) show that these humps are 30 – 200m in diameter and have an average height of about 5 m. The seafloor appears very bright, while the reflections below are quite weak, which suggests that these humps could consist of carbonate deposits associated with venting.

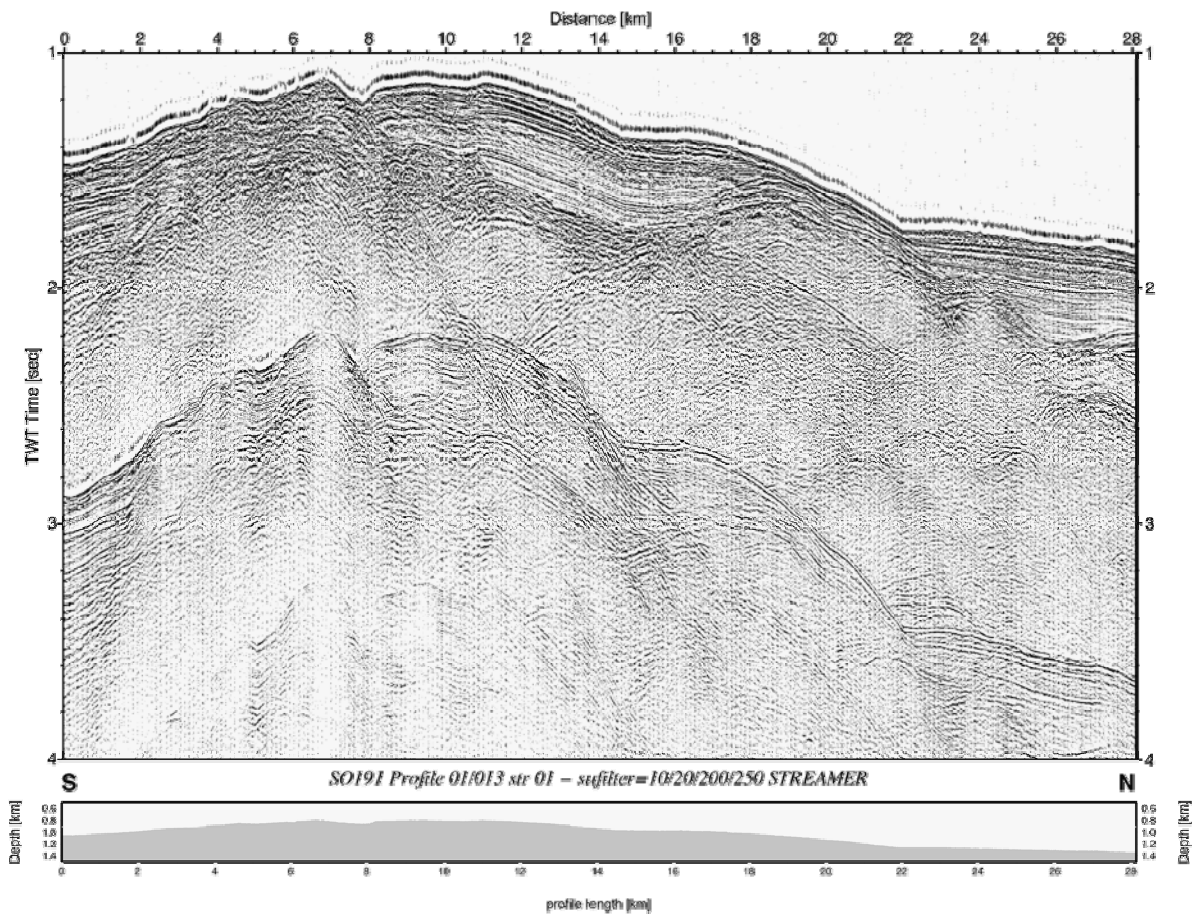


Figure 6.3.1.3: Stack of multichannel seismic streamer recorded on profile P015

Figures 6.3.1.4, 6.3.1.5, 6.3.1.6, 6.3.1.7 present data examples of the OBS recordings. They show a number of reflections and refractions from the first 1,5s below the seafloor.

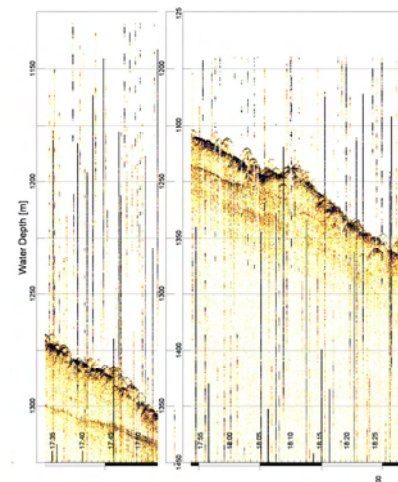


Figure 6.3.1.3a: Parasound image of a hump structure recorded on profile P015

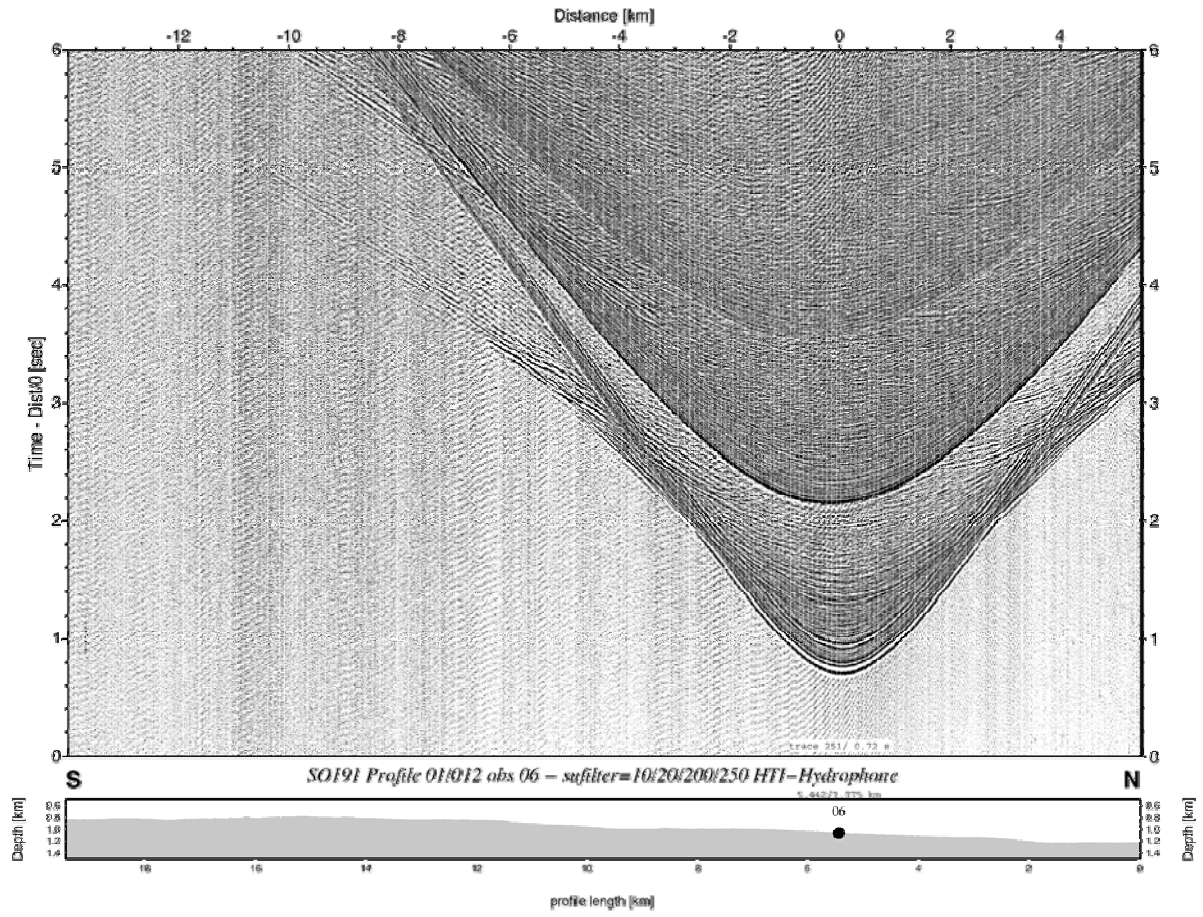


Figure 6.3.1.4: Hydrophone section of OBS06 on profile P012

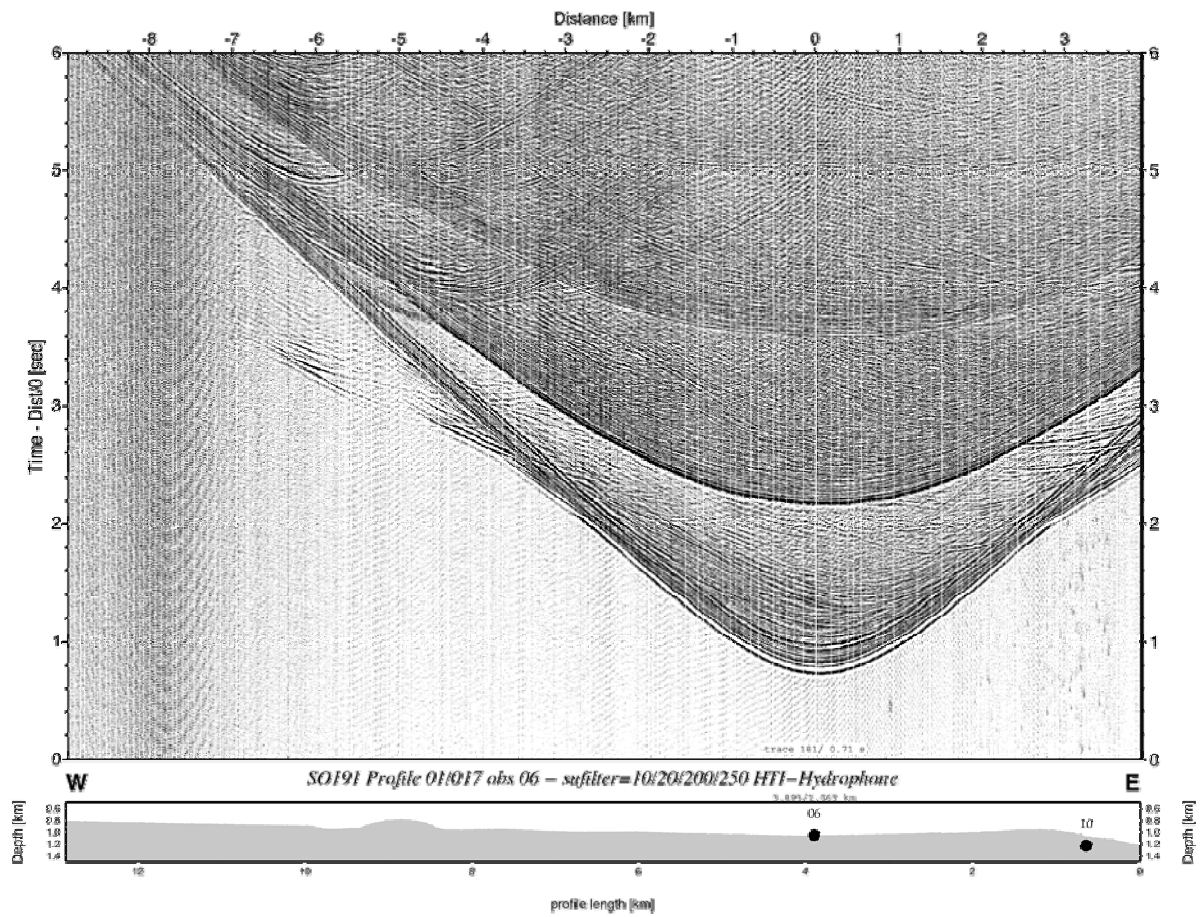


Figure 6.3.1.5: Hydrophone section of OBS06 recorded on profile P017

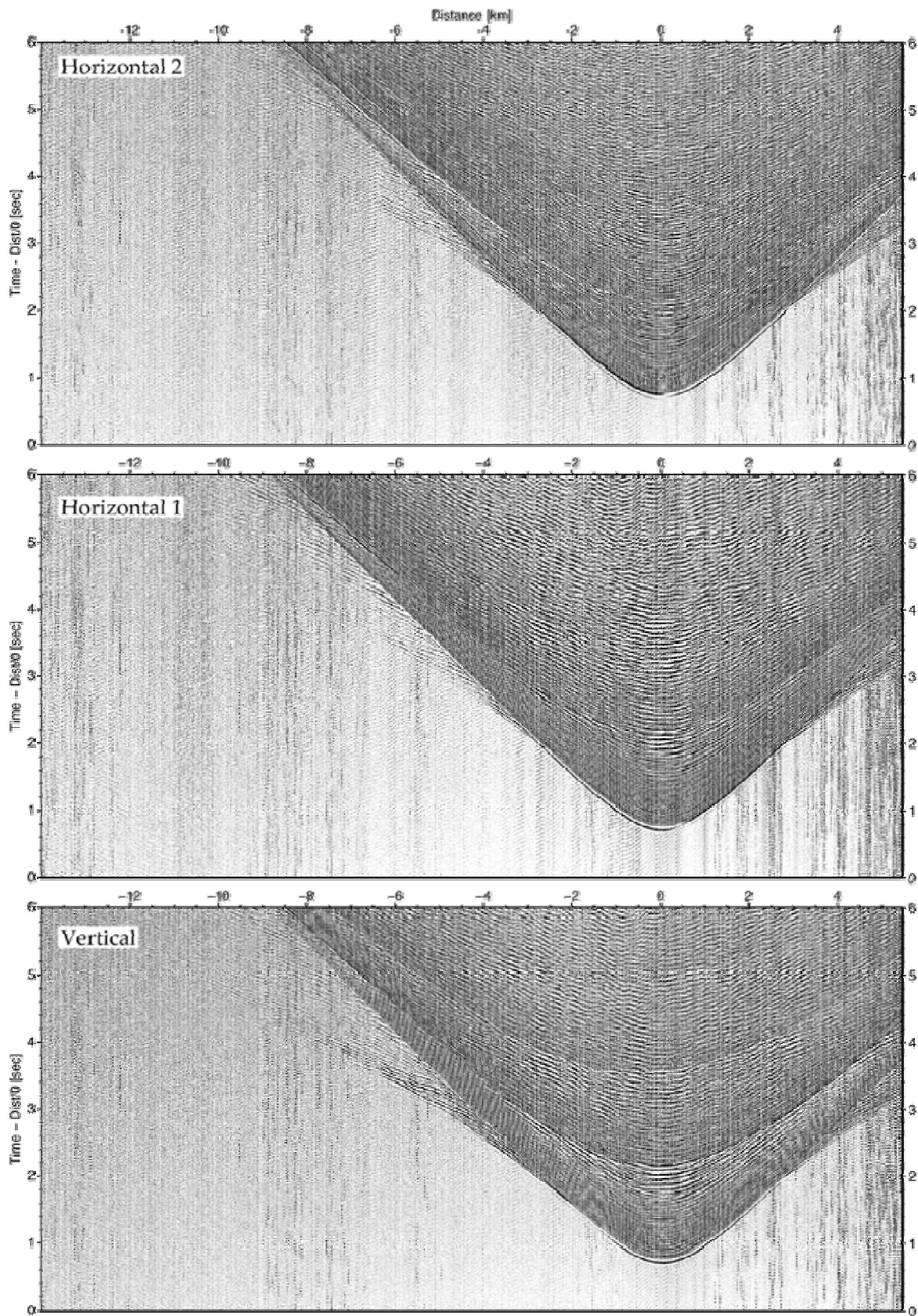


Figure 6.3.1.6: Seismometer section of OBS06 on profile P012

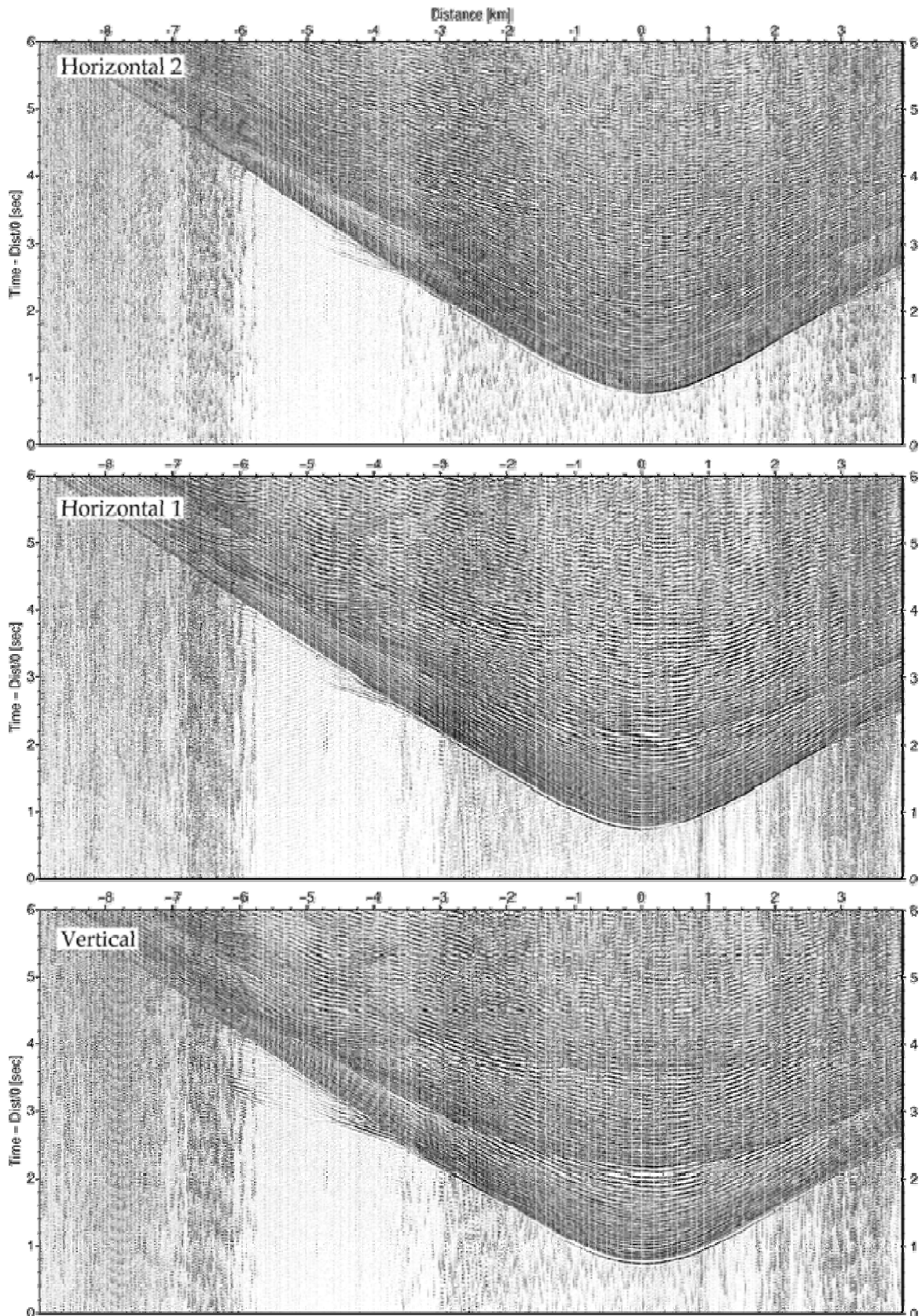
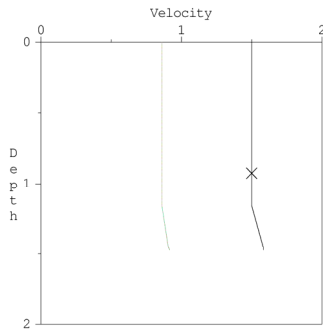


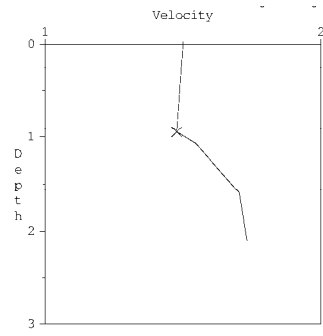
Figure 6.3.1.7: Seismometer section of OBS06 on profile P017

Figures 6.3.1.8 and 6.3.1.9 show 1-D velocity-depth functions derived from OBS04 on Line P012, OBS05 on line P012 and OBS07 on line P015.



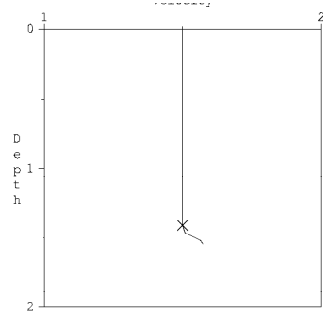
Wed Jan 31 04:55:59 2007
Model File: 01204_besser.mod

Figure 6.3.1.8: 1-D velocity-depth functions on line P012
Left: OBS04.



Wed Jan 31 06:04:09 2007
Model File: 01205.mod

Right OBS05.



Wed Jan 31 05:00:22 2007
Model File: 01507.mod

Figure 6.3.1.9: 1-D velocity-depth function from OBS07 on line P015.

6.3.2 LM-9 (P05)

In the area of LM-9 (-40°06' S/177°45' E to -39°57' S/178° E, see Figure 6.3.2.1), 16 OBSs were deployed, and 4 seismic profiles were shot with lengths between 6 km and 8 km. The lines P053 and P054 (Figs 6.3.2.2 and 6.3.2.3) are shown below.

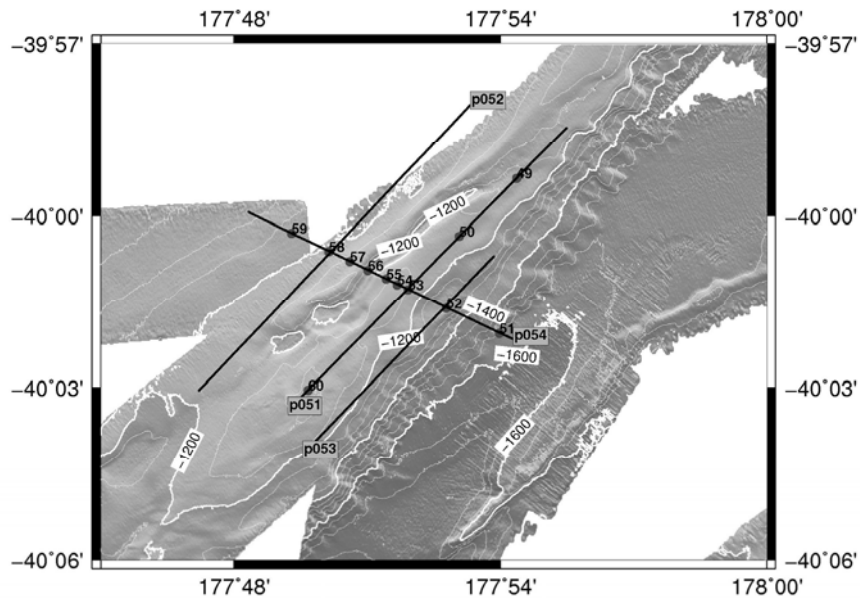


Figure 6.3.2.1 Map of the area of LM-9. Grey dots correspond to OBS locations, black lines to seismic lines.

On line P053 (Figure 6.3.2.2), the sedimentation pattern looks a bit chaotic, only few reflections can be traced for a couple of km. The otherwise flat seafloor is interrupted by two little mounds, about 1 km in diameter and 30 m high. There are no other signs of gas or fluid venting.

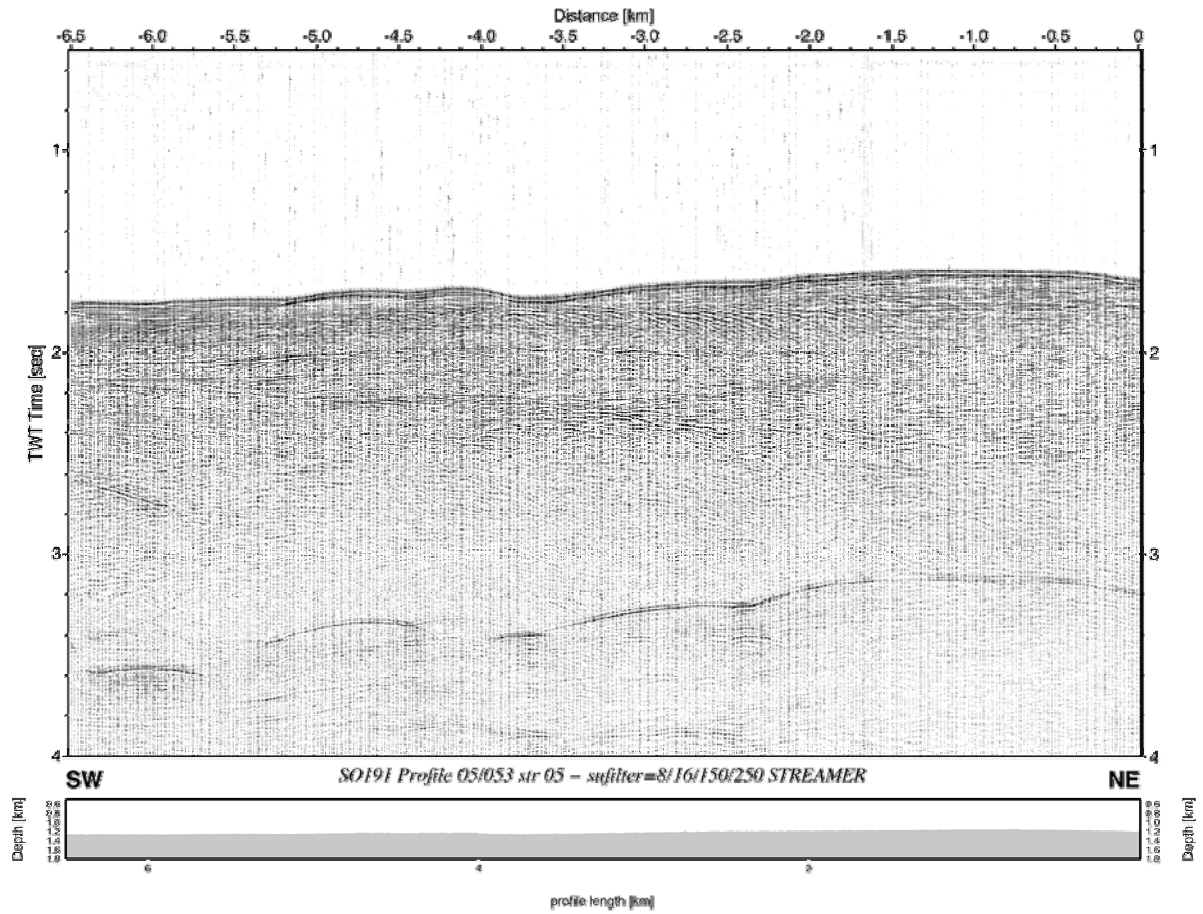


Figure 6.3.2.2 Stack of multichannel seismic streamer recorded on profile P053

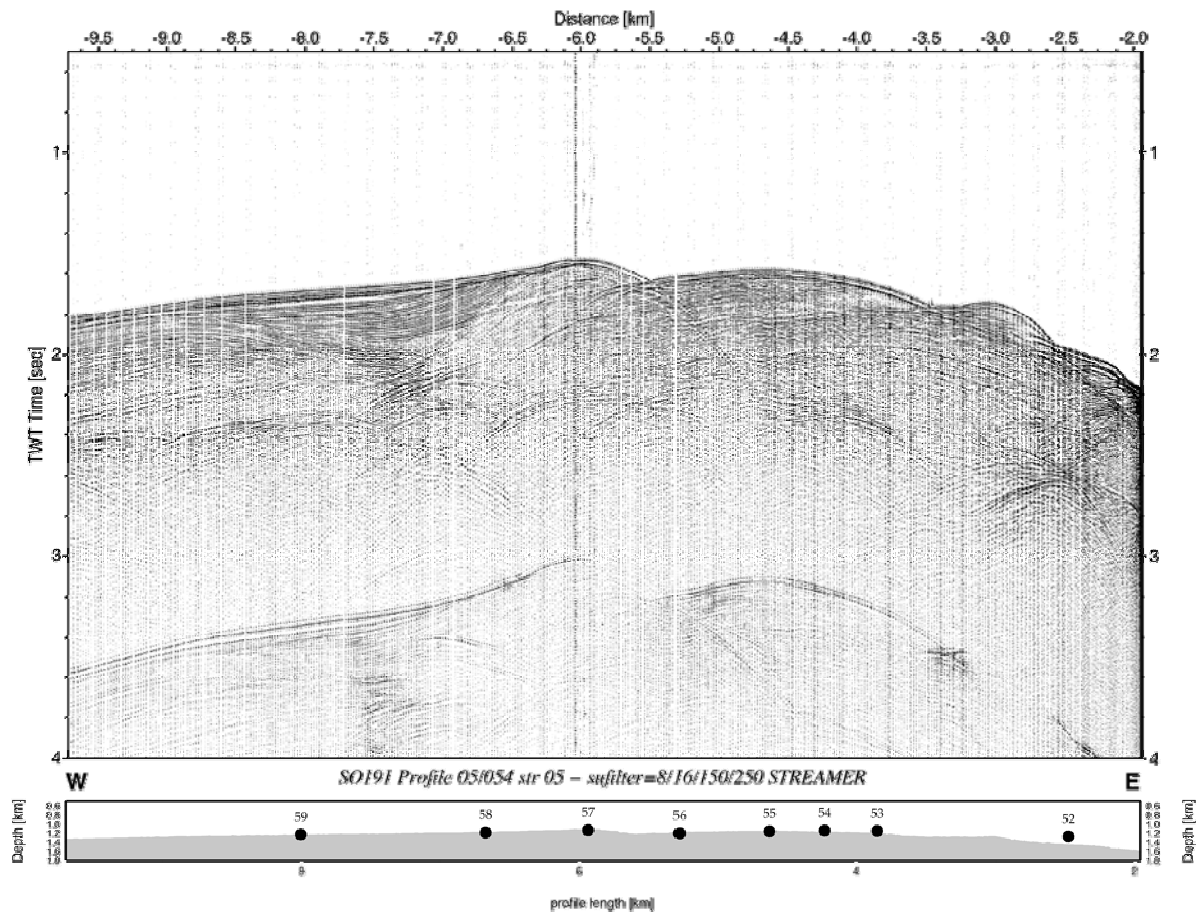


Figure 6.3.2.3 Stack of multichannel seismic streamer recorded on profile P054

P054 (Figure 6.3.2.3) shows the same irregular reflection pattern, except for a small sediment basin between km -9 and km -6.5. The ridge in the centre of the basin is well expressed and the sediments in the small basin terminate against its flank.

6.3.3 Uruti (P04)

In the Uruti area (-41°24' S/176°24' E to -41°12' S/176°48' E, see Figure 6.3.3.1), 16 OBSs were deployed, and 5 seismic profiles were shot with lengths between 11 km and 29 km, of which P041 and P045 (Figs 6.3.3.2 and 6.3.3.3) are shown below.

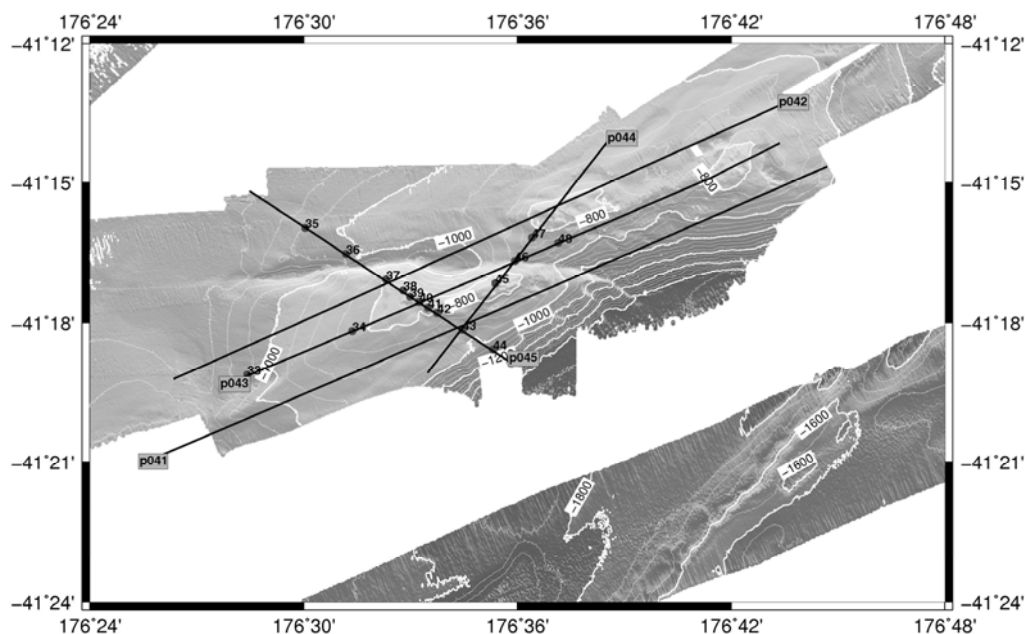


Figure 6.3.3.1 Map of the Uruti area. Grey dots correspond to OBS locations, black lines to seismic lines.

Line P041 (Figure 6.3.3.2) shows well stratified sediments below the seafloor for at least 1 s TWT. These sediment layers dip to the southeast and pinch out at the seafloor until the centre of the line at about km 14. In this part of line P041, the seafloor becomes very bumpy and a BSR can be seen between km 11 to km 17 at about 1.5 s TWT. Only 200ms below another reflection is detected, which cross-cuts the stratigraphy. It is a bit weaker and can only be observed between km 12 and km 16. From km 18 on to the NE of line P041, the BSR is very faint and hard to detect, because it follows the same dip as the layering.

On line P045 (Figure 6.3.3.3) the seafloor is mostly smooth with the exception of two mounds, about 30 -40 m high and 1 km in diameter, at km -4.5 and km -3.5. Blanking below these mounds indicate that these probably vent sites. A BSR is observed between km -9 and km -6, and then again from the vent sites to the Southeast end of the line. Beneath the vent sites the BSR is absent.

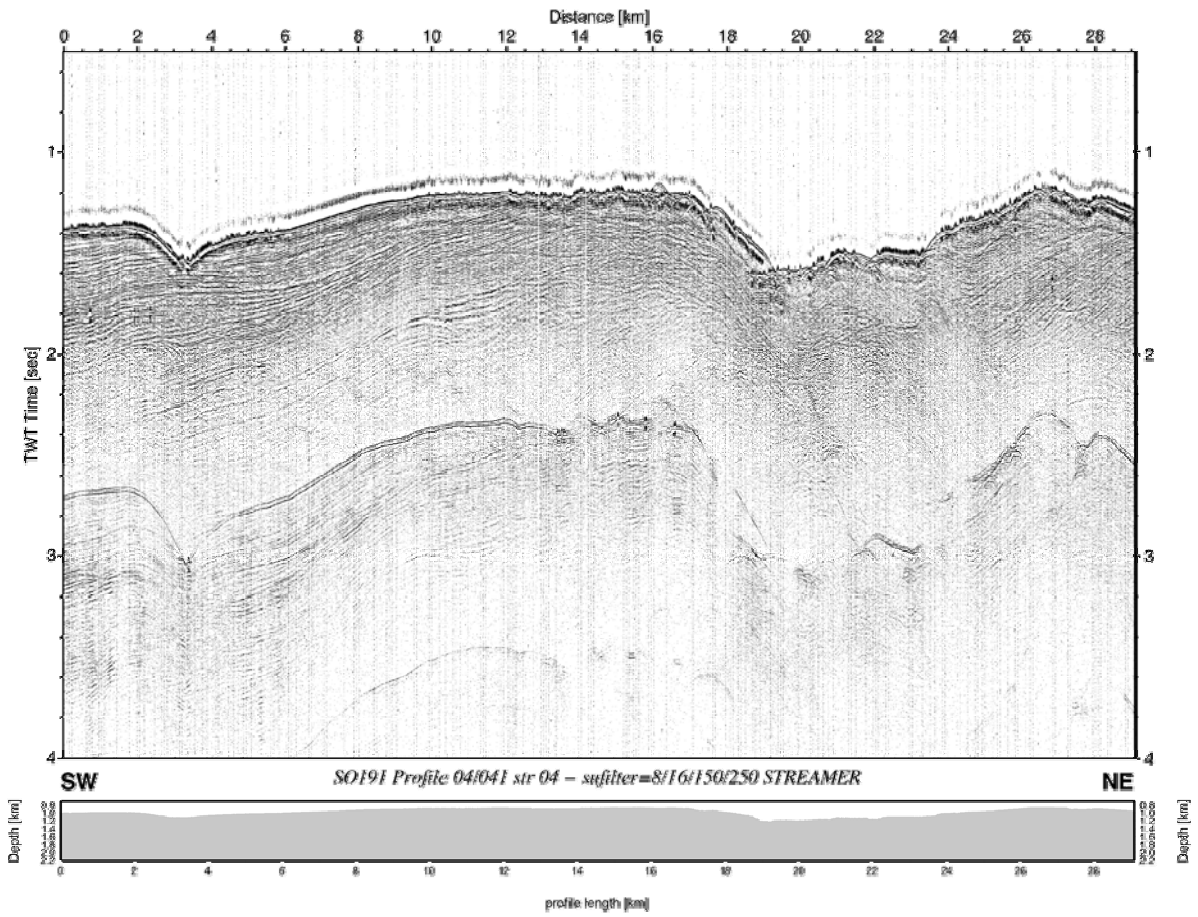


Figure 6.3.3.2: Stack of multichannel streamer recorded on line P041

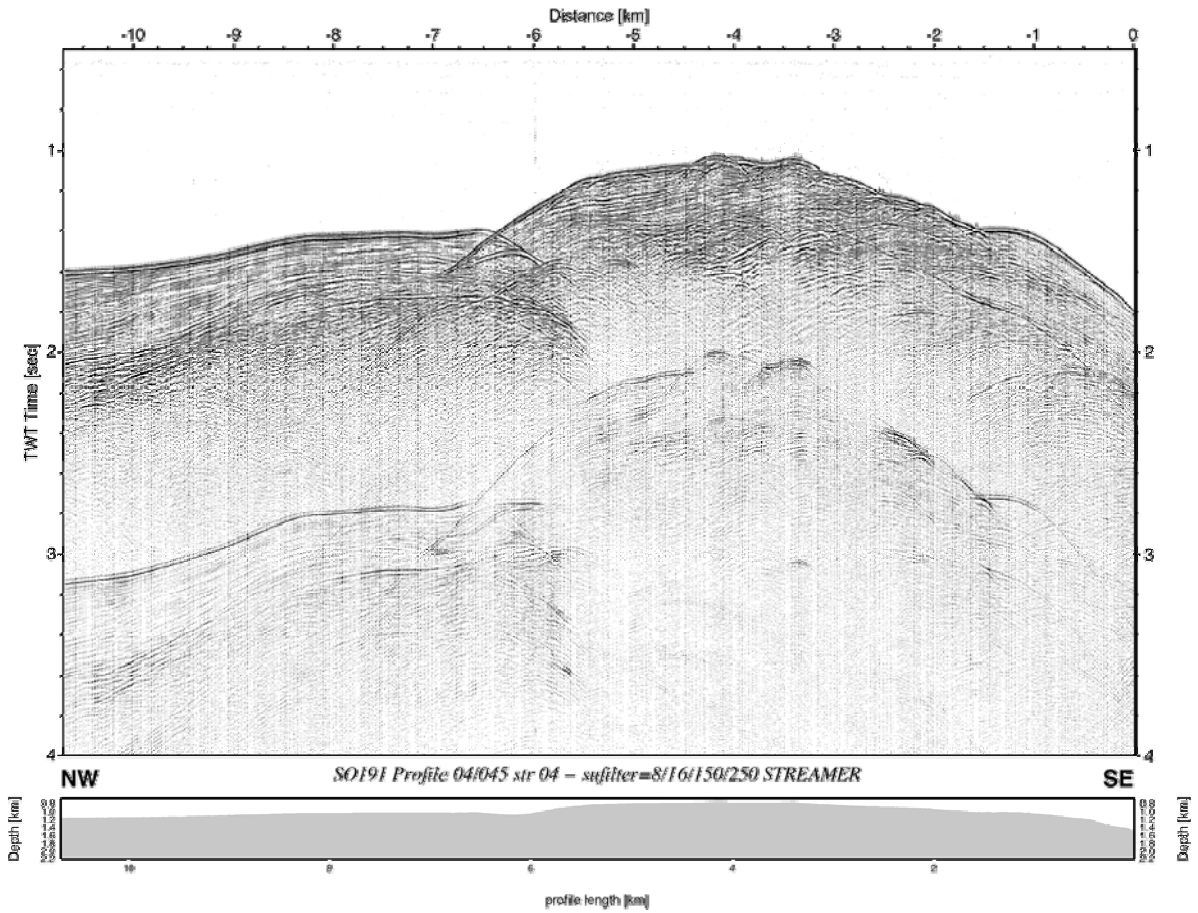


Figure 6.3.3.3: Stack of multichannel streamer recorded on line P045

Figures 6.3.3.4, 6.3.3.5, 6.3.3.6, 6.3.3.7 present data examples of the OBS recordings. A number of reflections can be seen between the first arrival and the multiple.

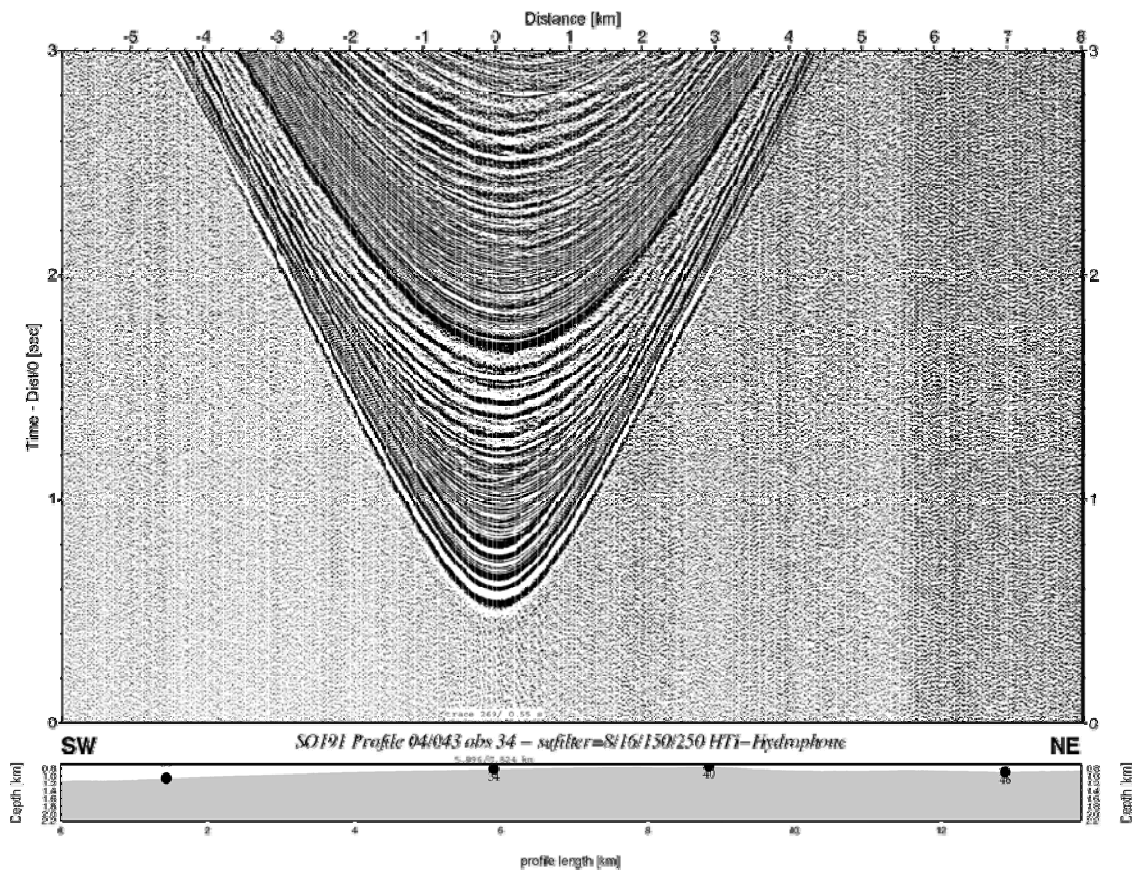


Figure 6.3.3.4: Record section of the hydrophone recorded by OBS 34 on line P043

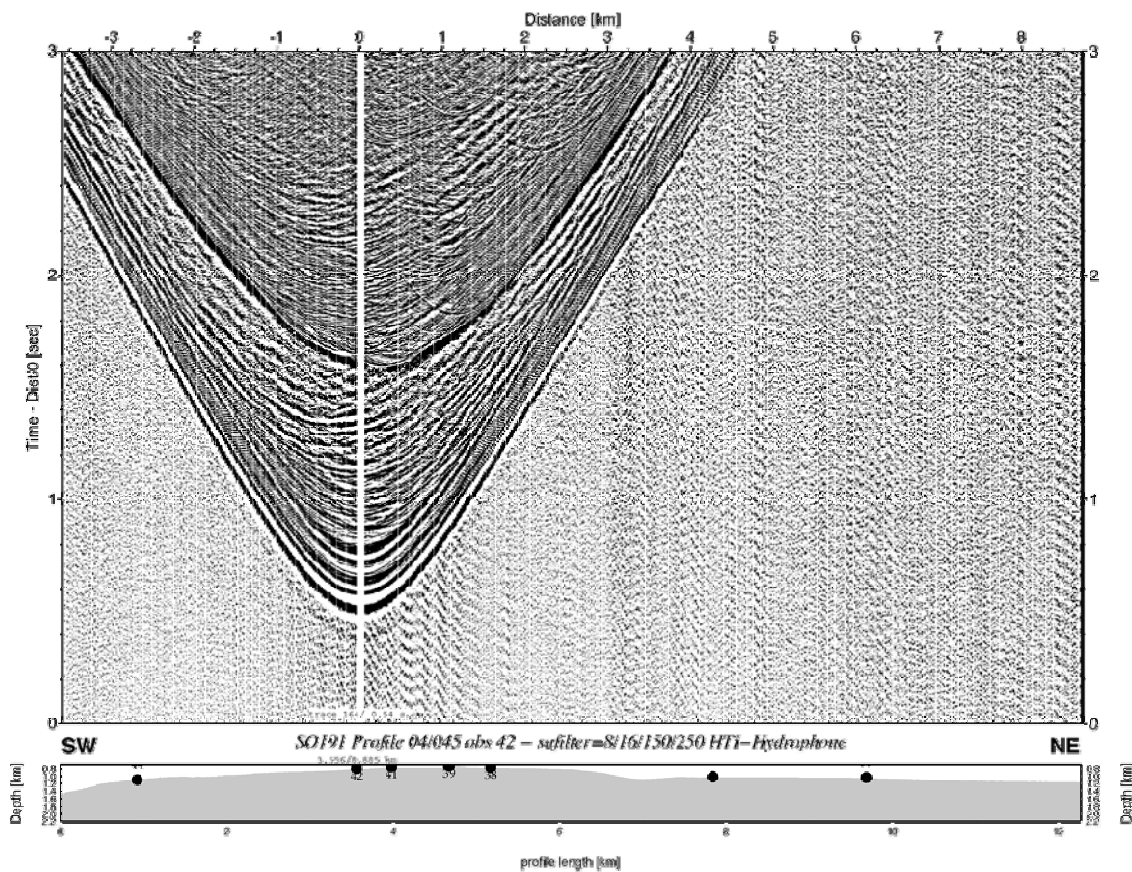


Figure 6.3.3.5: Record section of the hydrophone of OBS 42 recorded on line P045

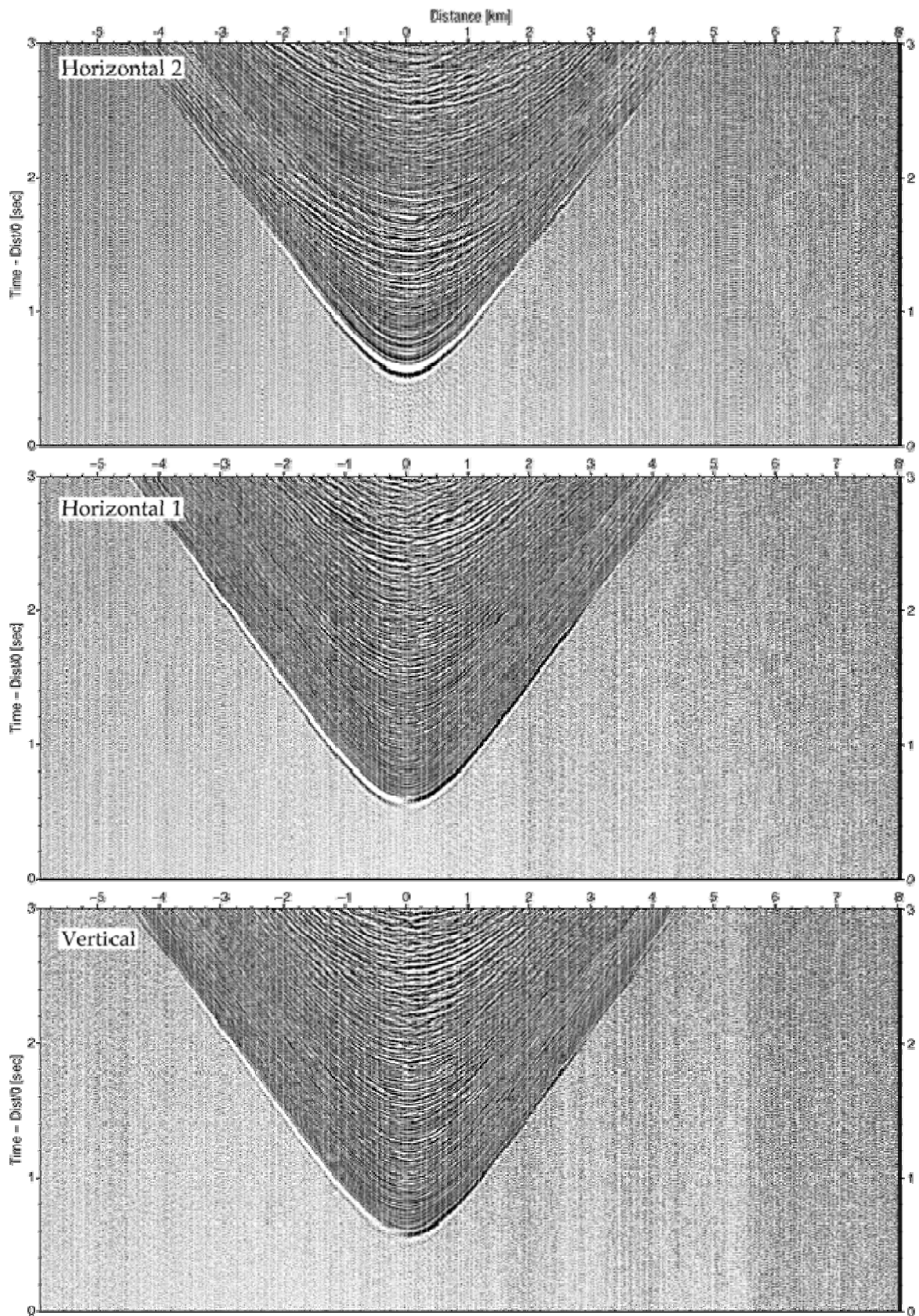


Figure 6.3.3.6: Record sections from the seismometer of OBS 34 recorded on line P043

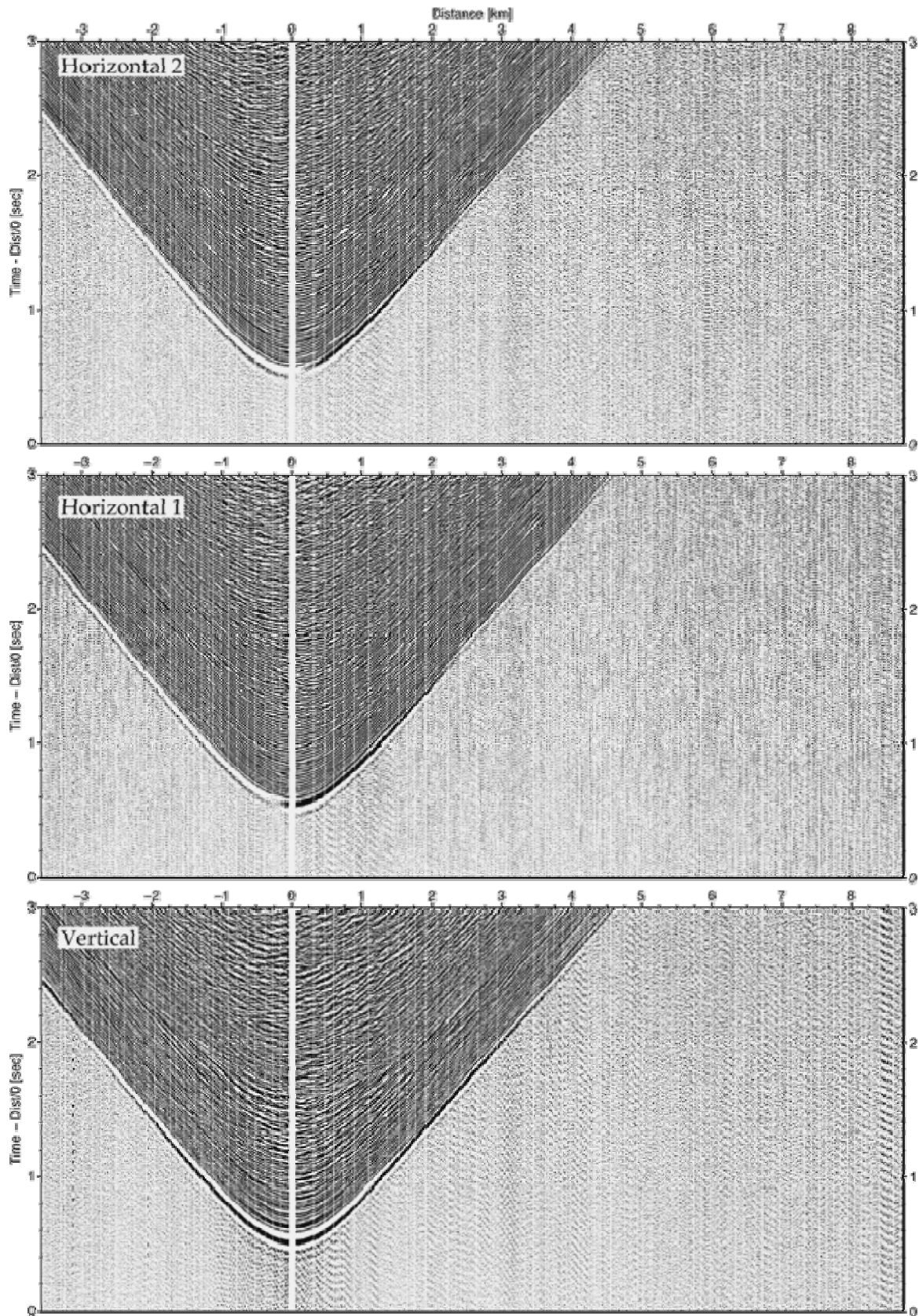


Figure 6.3.3.7: Record sections of the seismometer of OBS 42 recorded on line P045

6.3.4 Wairarapa (P03)

In the area of Wairarapa (-41°52' S/175°15' E to -41°39' S/175°36' E, see Figure 6.3.4.1) a number of active vent sites were expected. 16 OBSs were deployed and six profiles were shot with lengths between 13 km and 20 km. Two of these (P035 and P036, Figs 6.3.4.2 and 6.3.4.3) are shown below.

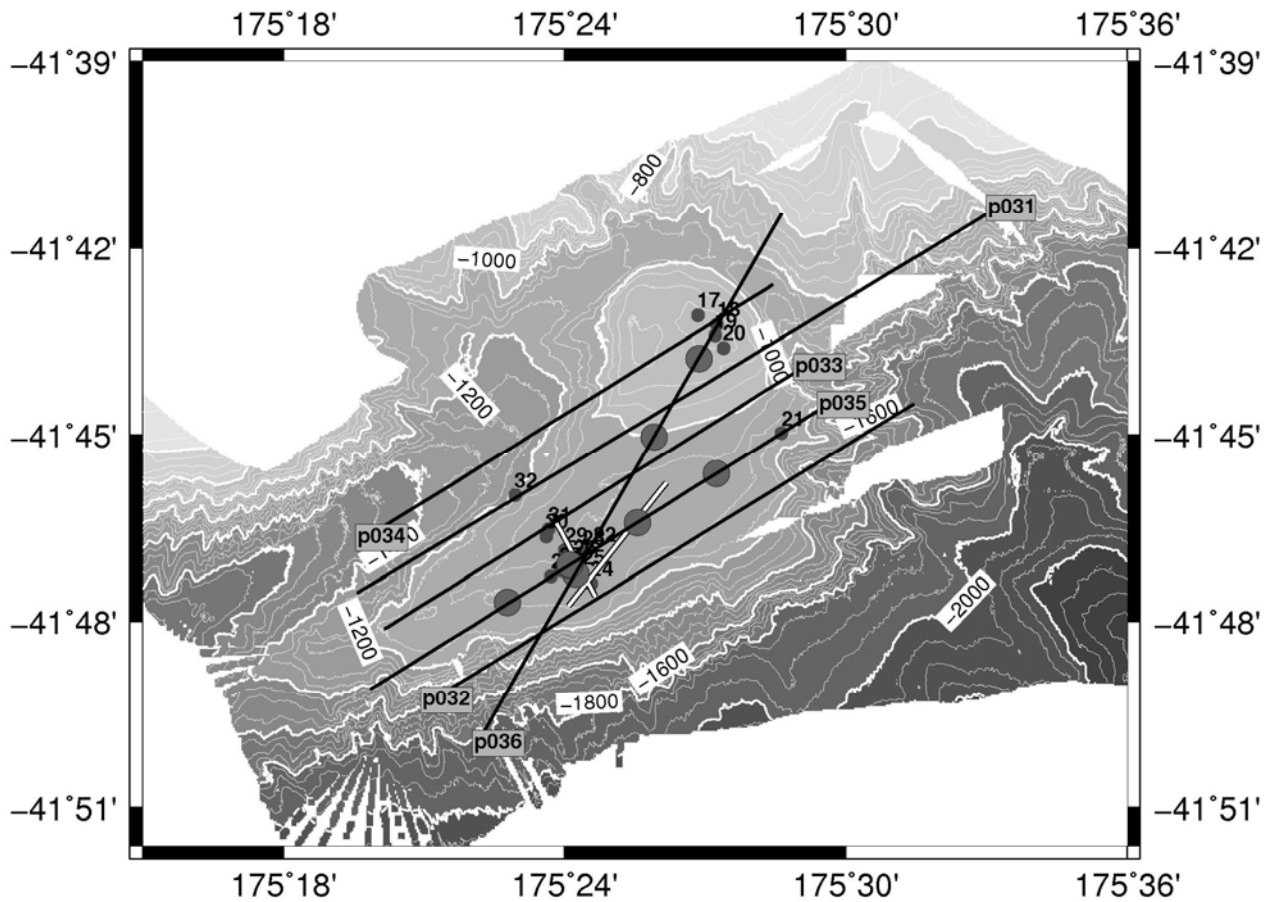


Figure 6.3.4.1 Map of Wairarapa area. Small grey dots correspond to OBS locations, black lines to seismic lines. Big grey circles denote vent locations. White lines mark the CSEM profiles.

On line P035 (Figure 6.3.4.2), a prominent BSR is observed in the south west. At -20 km offset, this BSR is obscured by blanking, which continues all the way up to the seafloor. Here the reflection patterns of the stratigraphy of the upper 0.5s TWT are disturbed and the reflections are bent upwards for about 200 – 300 m. Following the profile to the NE, the BSR is visible again until km 18, where the reflections again become distorted and bent upwards for a length of about 600m. These sites are considered possible vent sites, where fluids and/or gas rises. The upward bending of the reflection horizons could be caused by the fluid transport or it could just be a velocity effect, because the fluids/gas would have a lower velocity than the surrounding sediments. Two more quite prominent vent sites are observed on line P035, at km -15.5 and km-13. The blanking at these sites is not as pronounced as at km -20.

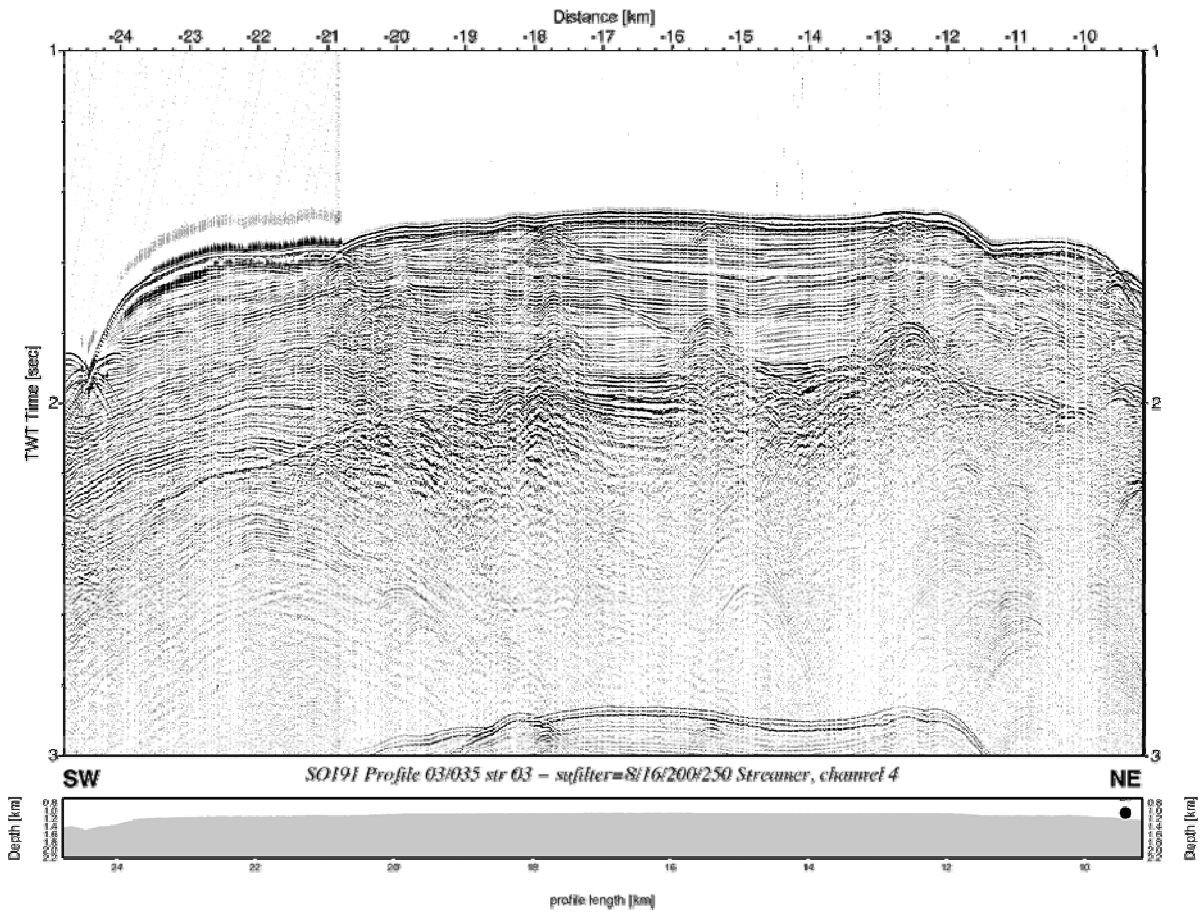


Figure 6.6.3.2: Record section from str-03 Streamer, channel 4, Profile 035.

Figure 6.3.4.2: Stack of multichannel streamer recorded on line P035

The BSR reappears at the very NE of line P035 at km -12. Inbetween, very strong reflections are observed at BSR level and up to 300ms TWT beneath. They indicate a sharp velocity contrast, which could be caused by free gas beneath the gas hydrate stability zone.

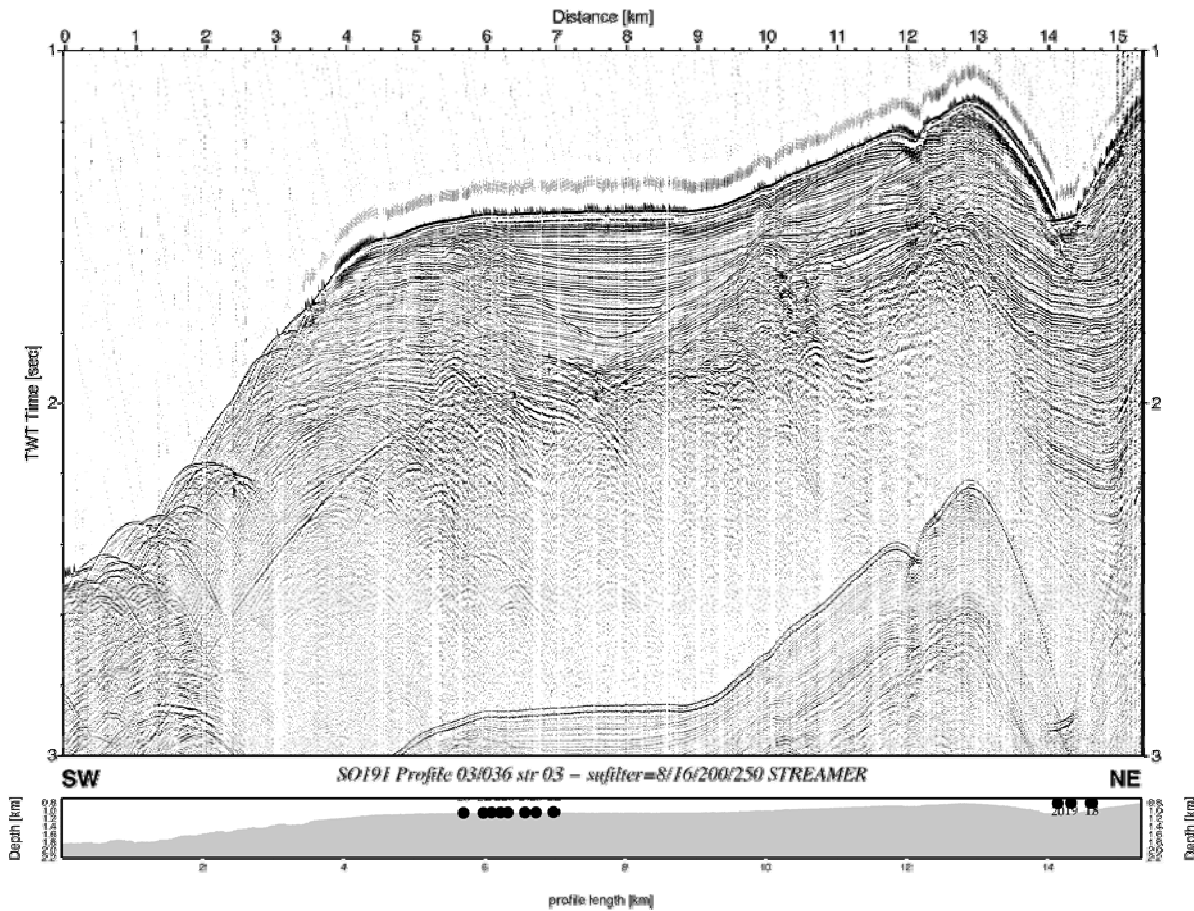


Figure 6.3.4.3: Record section from str-03 STREAMER, Profile 036.

Figure 6.3.4.3: Stack of multichannel streamer recorded on line P036

Profile P036 (Figure 6.3.4.3) features a clear BSR in the SW, inclining steeply towards the NW, although not as steeply as the seafloor. Vent sites similar to those on P035 (Figure 6.3.4.2) are observed at km 5.5, km 6.3 and km 10. The BSR is only visible up to the first vent site at km 5.5. Between km 9 and km 12, a reflection which is cross-cutting the stratigraphy is detected, which terminates at the seafloor in a small depression. This could be the continuation of the BSR. It could also be a fluid path, which conducts fluids and/or gas to the seafloor. A similar feature, but less prominent, is observed between km 8.5 and km 10, terminating at the vent site at km 10. While an assembly of bright reflections at BSR level, are observed in the centre of line P035 (Figure 6.3.4a), these are absent on P036 (Figure 6.3.4.3). A peculiar feature can be seen between km 6 and km 9, where a reflection cuts the stratigraphy in a basin-like shape. A change in the reflectivity is not observed.

The coordinates of the vent sites have been picked on P035 and P036:

P035	km -20	175.40386143	-41.78738421
P035	km -18	175.43172861	-41.75067877
P035	km -15.5	175.44769759	-41.72957349
P035	km -13	175.45388574	-41.76060304
P036	km 12	175.42574536	-41.77371017
P035	km 10	175.40166211	-41.78486387
P035	km 6	175.37962792	-41.79493840

They are also plotted as grey circles in the map (Figure 6.3.4.1).

Figures 6.3.4.4, 6.3.4.5 present data examples of the OBS recordings. A number of reflections can be seen between the first arrival and the multiple. In Figure 6.3.4.6 a 1-D velocity-depth function is shown, derived from OBS28 on line P035.

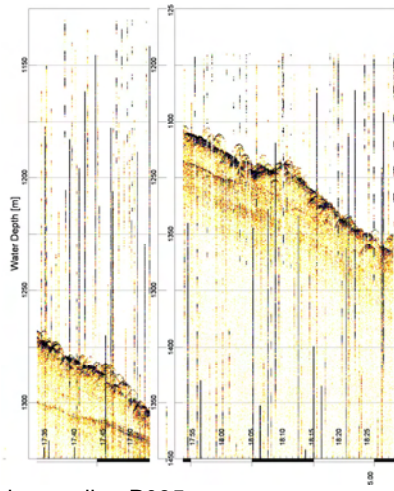


Figure 6.3.4.3a: Parasound record of vent sites on line P035

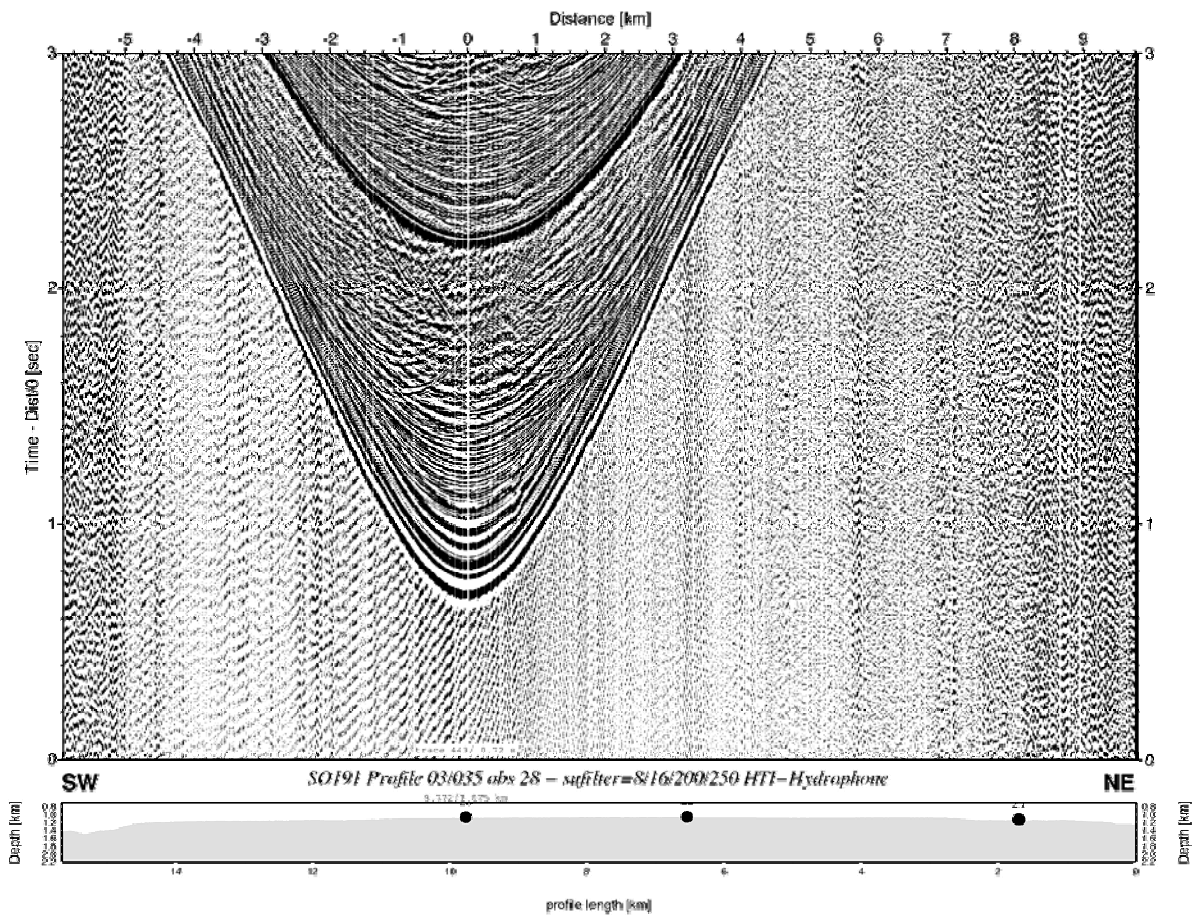


Figure 6.3.4.4: Record section from the hydrophone of OBS 28 recorded on line P035

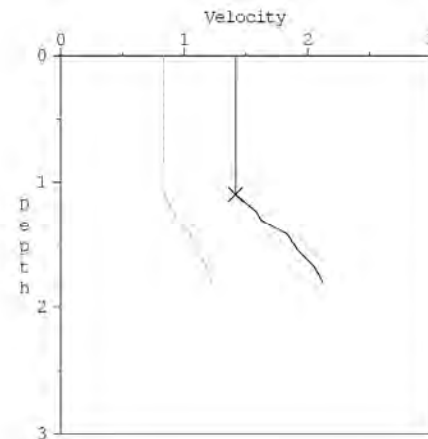


Figure 6.3.4.5: 1-D velocity-depth function from OBS28 on line P035.

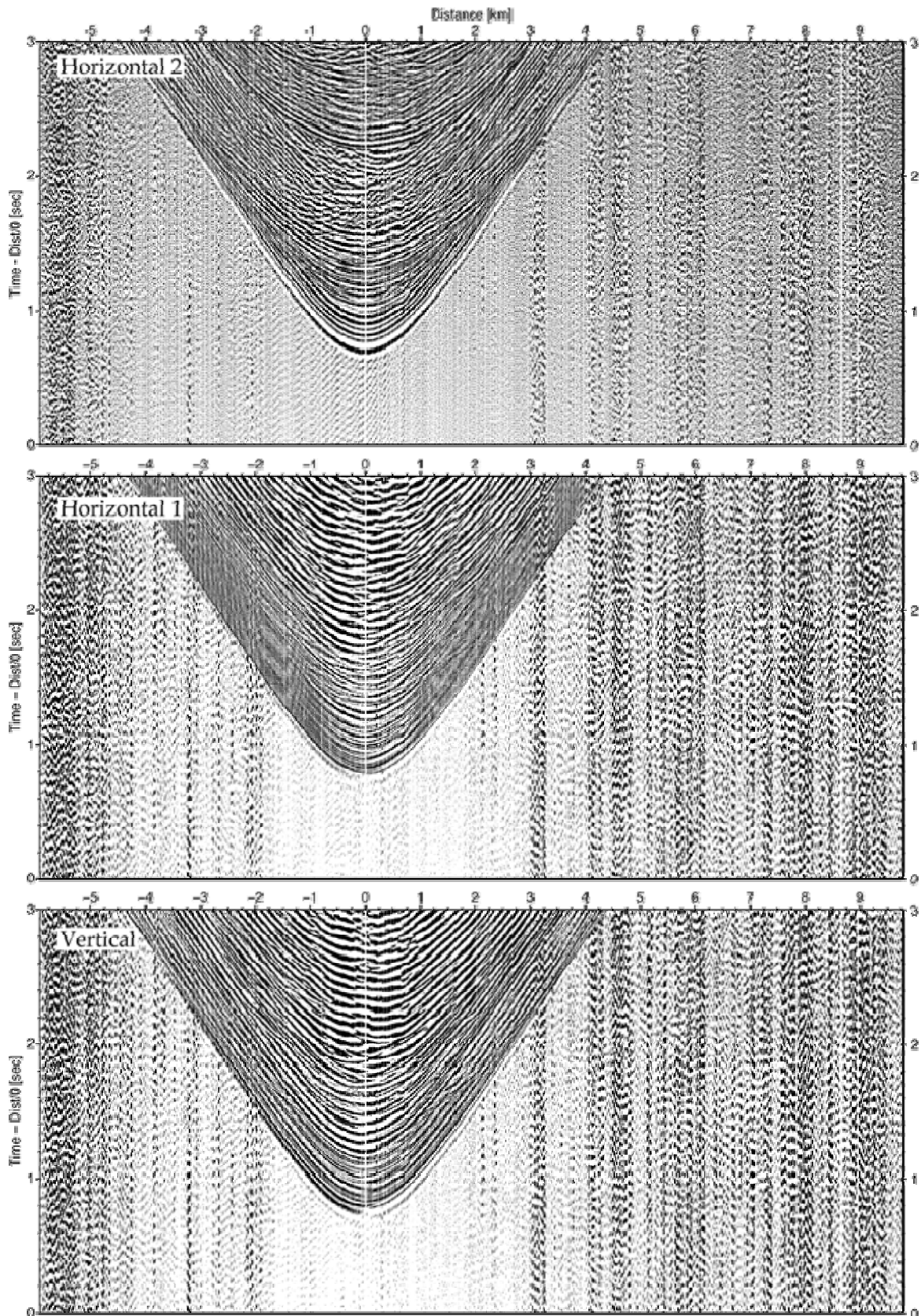


Figure 6.3.4.6: Record sections of the seismometer of OBS28 recorded on line 35

6.4 CSEM - Controlled Source Electro- Magnetics

K. Schwalenberg, D. Keen, P. Schroeder

During cruise SO191 Leg1 CSEM was deployed four times in three target areas. Table 6.4.1 comprises information about dates, deployment times, geometry, and number of sites for the respective deployment sites. Measurement locations are given in Table 6.4.2 to 6.4.5.

CSEM at Wairarapa

Survey area Wairarapa is located at the SE corner of the North Island in water depths between 1000m and 1100m. The survey area is characterized by several gas seep fields which have been identified in video observations, with sub-bottom profilers and in multibeam data as uprising gas flares. Gas flares are probably related to large amounts of free gas which is rising up to the seafloor through faults and fractures and may be transformed into gas hydrate of higher quantities at depth. CSEM has been deployed along two profiles at Wairarapa 1) to reveal the electrical signature associated with the gas seeps and 2) to derive information of the spatial distribution of gas hydrates.

Table 6.4.1: Overview of CSEM deployments during SO191 Leg 1. For the deployment on 24.01.2007 no data are available from receiver 1 (n.a.). On the 27.01.2007, the data from receiver 2 cannot be used in the analysis (n.u.), because the received signals are too small.

Date	Survey Site	Local Wake-up Time	Hours of Deployment	No. Of Sites	r_1 [m]	r_2 [m]	I [A]
21.01.2007	Wairarapa I	10:30pm	16h	23	171.91	275.33	5
24.01.2007	Wairarapa II	9:15pm	15h	12	171.91 (n.a.)	275.33	5
27.01.2007	Ingo's Site	10:30pm	15h	15	386.91	705.18 (n.u.)	8
30.01.2007	LM9	6:30am	8h	10	171.91	275.33	5

The map in Figure 6.4.1 displays the bathymetry of the target area, the seafloor locations of the gas seeps, and the midpoints of the CSEM array along the two profiles. The gas seeps are located on a bathymetric anticline. The seafloor drops abruptly towards SE and NW. Profile directions were chosen in order to cover the locations of the gas seeps and according to wind and swell conditions. This is because the array has to be stationary on the seafloor during measurements which is easier to achieve when the ship is pointing in the main wind or swell direction. The spacing between sites is about 150m over the seep sites, which is about the minimum spacing which can be practically achieved, and about 300m away from the seeps. Transmitter receiver separations are about 172m for Rx1 and 275m for Rx2, thus the maximum sensitivity of the array set up is expected to be at depth between approximately 50m and 250m.

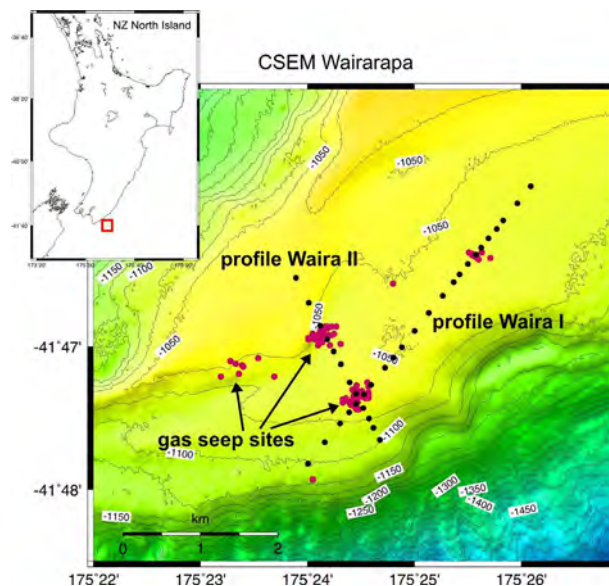


Figure 6.4.1: Bathymetry map of Wairarapa survey area with gas seeps sites and CSEM profiles Waira I and II.

Data from both receivers along profiles Waira I and II have been inverted to apparent resistivity profiles of the seafloor sediment section and subsequently to 1D-layered models. Figure 6.4.2 displays the apparent resistivity profiles projected on the map for profiles Waira I and II (top row) and two preliminary inversion results applying Marquardt Inversion and fixed model parameters for the deeper sediment section. Note, these are not true 2D models, but so-called stitched 1D models.

The results show clearly anomalous resistivities over the gas seeps. A smaller gas seep field located towards the NE end of profile Waira I does not cause any measurable signature in the CSEM data. The stitched 1D model applying Marquardt inversion of the data along profile Waira I shows a general increase of the resistivities with depth and a highly anomalous zone at approximately 70-80 m depth bsf below the gas seep field. The exact depth extend of this feature requires further modeling, but suggests that the highest resistivities are at depth rather than close to the seafloor and probably due to a highly enriched gas hydrate concentration rather than due to free gas.

Along profile Waira II data are only available from the second receiver, because a battery plug of the recording unit of receiver 1 got disconnected at the beginning of the deployment. The apparent resistivities calculated along this profile are generally higher than along profile Waira I. The two gas seep fields can be clearly correlated with locally increased resistivities. The preliminary 1D model shows a resistive layer above a halfspace with a fixed resistivity of 1 Ω m. The resistive layer itself has some inner structure, which can provide information on locally enhanced gas hydrate accumulations.

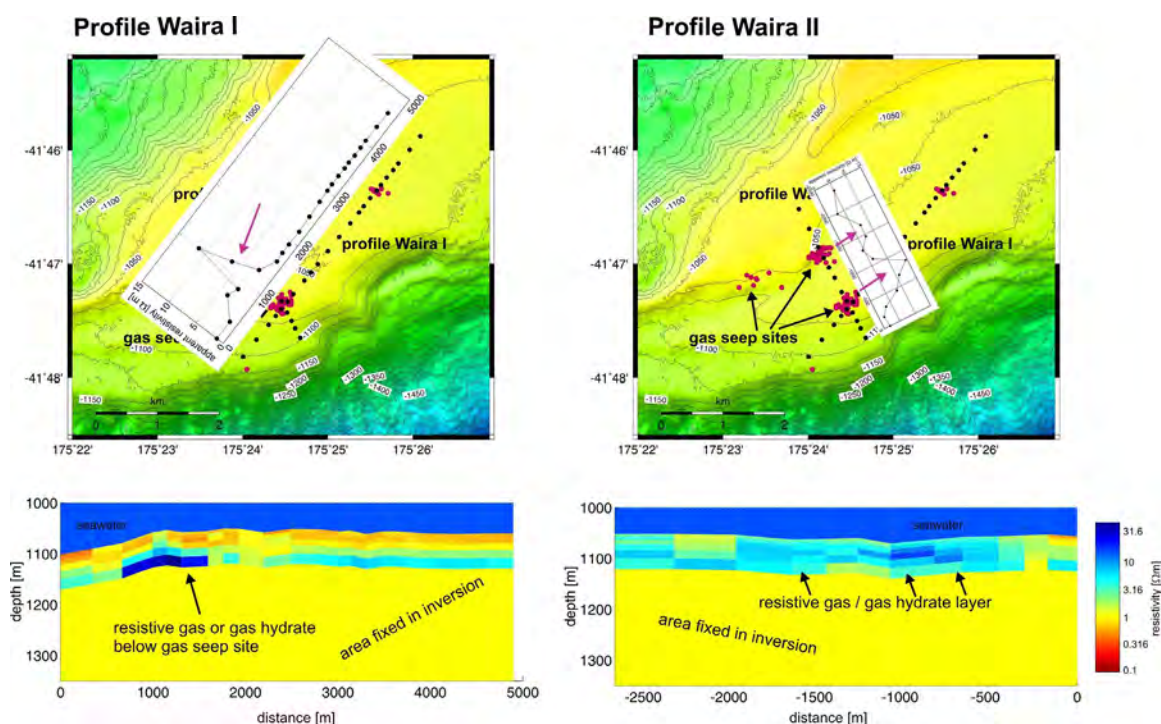


Figure 6.4.2: Preliminary results for profiles Waira I and II.

CSEM at LM9

LM9 is one of the gas seep sites described in Lewis and Marshall (1996). This target area is located off Hawke Bay in water depth around 1100-1200m. A short profile occupying 10 sites was deployed over a known gas seep fields. Figure 6.4.3 shows the bathymetric map, the locations of the seep sites (pink dots), the anticipated ship positions (blue dots), the ship track (black line) and the midpoints of the seafloor array. The inverted apparent resistivity profile calculated from data of both receivers has been projected on the profile and shows an anomaly over the western edge of the gas seep field. The first results obtained from 1D layered inversion (Figure 6.4.4) show a rather complicated distribution at depth around the gas seeps. However, the resistive anomalies seen in the CSEM are not necessarily an expression of the gas seeps seen on the seafloor. Where large amounts of free gas escapes on the seafloor probably triggered by faults, it is very likely that gas hydrate will form within the GHSZ. Thus the resistivity anomalies seen in the CSEM data are likely due to highly enriched zones of gas hydrate at depth. The presence of gas alone is unlikely to cause such a high anomaly, however, the presence of free gas is not excluded from the interpretation.

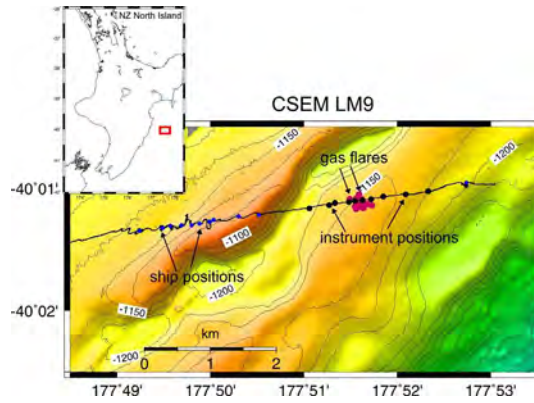


Figure 6.4.3: Bathymetry map of site LM9, CSEM ship and instrument positions, gas seeps at LM9 and apparent resistivities projected on the profile.

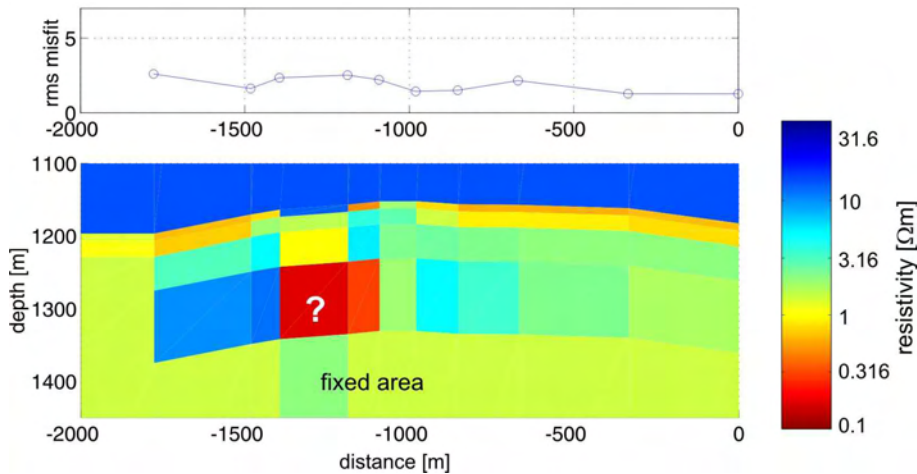


Figure 6.4.4: Preliminary result obtained from 1D inversion of data from both receivers along profile LM9. The model shows high resistivities below 100m depth next to a very conductive zone which is probably due to some equivalence problems during the inverse process.

6.5 Heatflow

Bear's Paw seep

Bear's Paw is a seep structure on the Omakere Ridge (LM9 area) that is well expressed on the side-scan sonar image and where cores have testified the presence of carbonate crusts and hydrate layers. In four stations up to five THP sensors were fixed to the corer: three stations turned out successful with core penetrations of 1-2 m. Station GC-17 was tilted by 41° and returned an empty corer, but temperature record showed a good penetration (Figure 6.5.1).

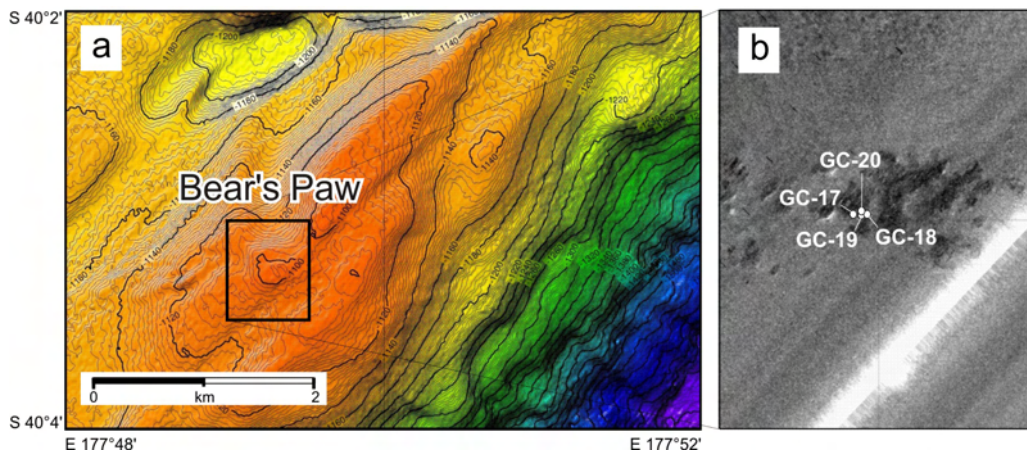


Figure 6.5.1: Geothermal stations in Bear's Paw seep: (a) swath bathymetry map of Omakere Ridge with location of Bear's Paw seep (frame); (b) side-scan sonar image of Bear's Paw structure with location of the geothermal stations.

All three successful stations show strongly enhanced thermal gradients, with values of 176-233 mK/m at the deepest interval. In stations GC-18 and GC-20 the temperature-depth profile in the sediments is nearly linear. In GC-17, however, the thermal gradient in the upper two intervals is reduced to only 30 mK/m. This may have been caused by water infiltration due to corer tilting.

The high thermal gradients in all stations of Bear's Paw point to a strong seepage activity. Extra heat can be brought up by warm migrating fluids or be released during formation of gas hydrates. Gas hydrates were visually observed in GC-20. The effect from BWT variation on the Bear's Paw stations appears to be minor.

Rock Garden

In Rock Garden four geothermal stations were deployed (Figure 6.5.2) along multi-channel seismic line TAN0607, which runs from the continental slope upwards across the northern part of the Rock Garden topographic high (slightly south of LM-3 site). Three THP sensors were set on the corer at one meter interval. Only two stations resulted in near-vertical penetration: GC-26 returned one gradient interval, GC-29 returned three intervals.

Along the slope a thermal gradient of 41 mK/m was measured in GC-26. This gradient was measured in a water depth of 1420 m, but there is no control on non-linearity because only one interval was obtained. In GC-29, located between the two topographic highs at 1007 m, a strongly non-linear temperature depth profile is obtained with a lower thermal gradient of 67 mK/m and an upper of -2 mK/m. This station might be strongly disturbed by BWT variations or high sedimentation rates. The limited amount of collected data does not allow to investigate a correlation with BSR features.

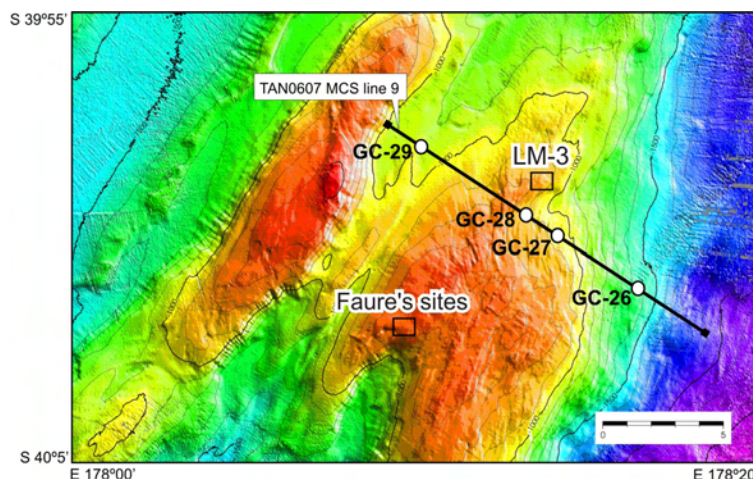


Figure 6.5.2: Geothermal stations in Rock Garden along TAN0607 MCS line 9 plotted on the swath bathymetry map (also major seep sites are indicated).

Wairarapa – Takahe seep

In Wairarapa eight stations were made (Figure 6.5.3) along the CSEM line Waira I, which crosses two seep structures (South Tower and Takahe) with clearly anomalous electrical resistivities. One more station was made near seep structure North Tower. Three THP sensors were fixed at the corer at 0.5 and 1 m interval. Except for one failed station, all deployments returned full (two gradient intervals) and near-vertical penetrations.

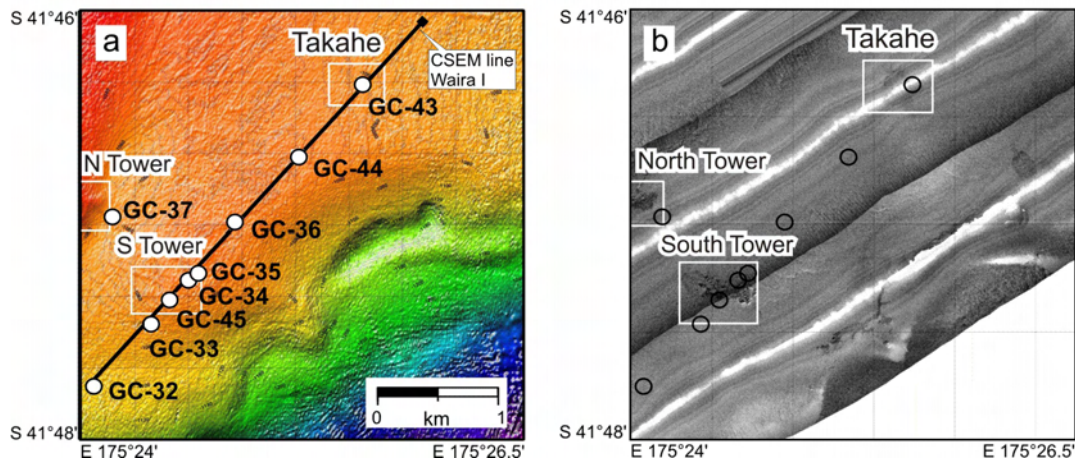


Figure 6.5.3: Geothermal stations in Wairarapa: (a) swath bathymetry map with stations and CSEM line Waira I; (b) side-scan sonar image to illustrate correlation with seep structures.

The thermal gradient in all seven stations outside seeps ranged from 24-49 mK/m and averaged to 40 mK/m at the deepest interval. The only station within a seep (Takahe seep) resulted in a gradient of 119 mK/m (Figure 6.5.4). All stations returned similar non-linear temperature-depth profiles with the upper thermal gradient smaller than the deeper. Temperature records and CTD data indicate that BWT variations are large in the area and may be the main reason for non-linearity.

The high thermal gradient in Takahe seep points to considerable seep activity, in terms of warm upward migrating fluids and/or hydrate formation. As in Bear's Paw, several gas hydrate layers were recovered in the high gradient core in Takahe. Outside the seeps, the thermal gradient is rather normal to low (40 ± 9 mK/m). This is exactly within the range of BSR-inferred regional heat flow of 35-45 mW/m² (Townend, 1997; Henrys et al., 2003) if we consider normal thermal conductivity values around 0.8-1.1 W/m/K and a minor effect of BWT variation on the deepest measured gradient intervals.

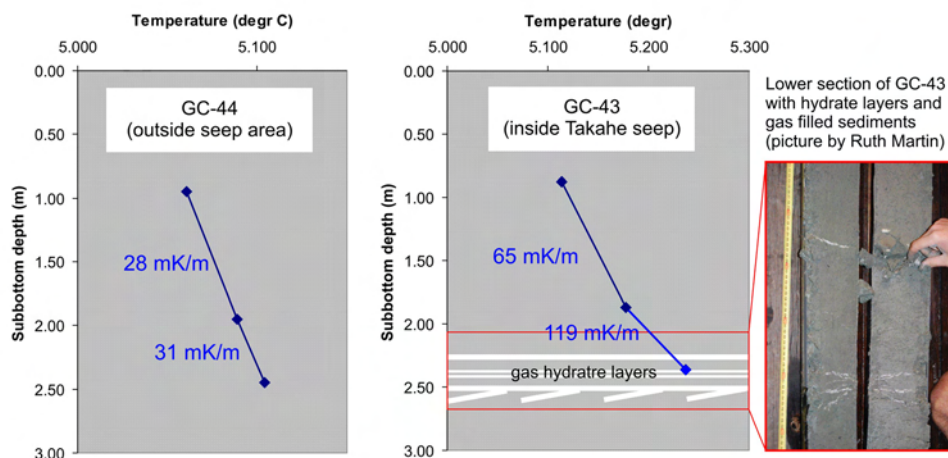


Figure 6.5.4: Example of two temperature-depth profiles from Wairarapa, with GC-44 having a normal near-linear thermal gradient and GC-43 a non-linear increased gradient. GC-43 was measured in the Takahe seep where gas hydrate layers were observed in the core.

6.6 OFOS Surveys

D. Bowden

A total of 19 OFOS deployments were performed during SO191-2 and subsequently 3 deployments during SO191-3 (Builder's Pencil, Pukeko and Piwakawaka). Total recorded bottom time during SO191-2 was 55h 44min, covering approximately 83,000 m² of seabed, and 8,400 still images were taken. Seep habitats with live fauna were restricted in area at all sites, extending for less than 30 m of transect in the majority of cases and were isolated from other sites by extensive areas of soft sediments (Omakere Ridge and Wairarapa) or bare rock (Rock Garden, LM3). Vestimentiferan tube worms (*Lamellibrachia* sp.) were the most conspicuous and widespread live macro-epifauna at all

sites, but dead clam shells (*Calyplogena* sp.) often covered large areas of the substratum. Bathymodiolid mussels were seen infrequently but appeared to be alive in all cases.

Rock Garden – LM3

Four OFOS deployments were made in this area: 1 covering Rock Garden and the Weka flare site; 2 at LM3, and 1 at a knoll feature south of LM3. Transects were largely devoid of active seep features except for occasional vestimentiferan worm tubes and scattered *Calyplogena* shell debris at Rock Garden and Weka. At LM3 itself, a single dense patch of live *Bathymodiolis* mussels, vestimentiferans and *Calyplogena* shells was observed (Figure 6.6.1). Cold water corals were present along the ridge between Rock Garden and Weka and on steep rock features to the northeast and southeast of LM3.

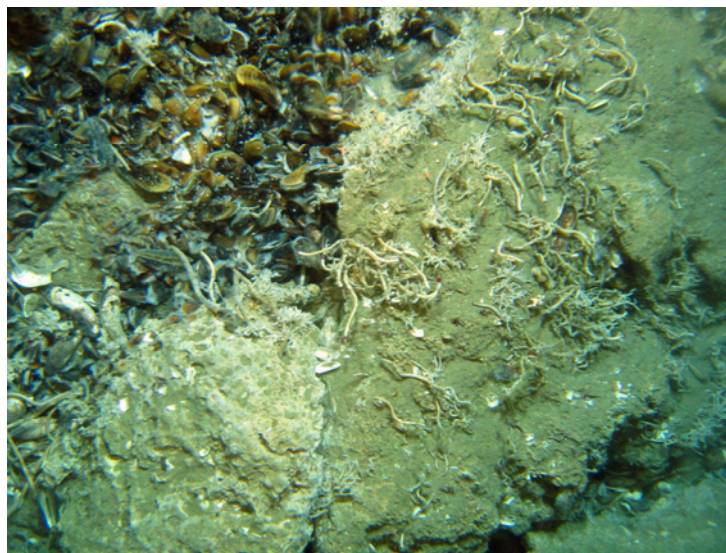


Figure 6.6.1: *Bathymodiolis* sp. Mussels at the LM3 seep site.

Omakere Ridge – LM9

Seven OFOS deployments were made in this area: 3 at the Kaka and Kea sites, 2 at the Bear's Paw and Moa sites; 1 from Kaka to Moa, and 1 on a crater feature NW of *Bear's Paw*. The crater was devoid of seep features but chemoherm habitats with abundant populations of vestimentiferan worms, extensive areas of *Calyplogena* sp. Clam shells, and patches of sulphidic sediment with apparently live *Calyplogena* were present at Bear's Paw, Moa, Kaka and Kea. Transects at these sites, particularly those at Bear's Paw, included areas with the highest concentrations of seep-related epifauna yet observed on the Hikurangi Margin (Figure 6.6.2). Cold water corals (*Solenosmilia* sp. and others) were abundant on hard substrata at Moa.

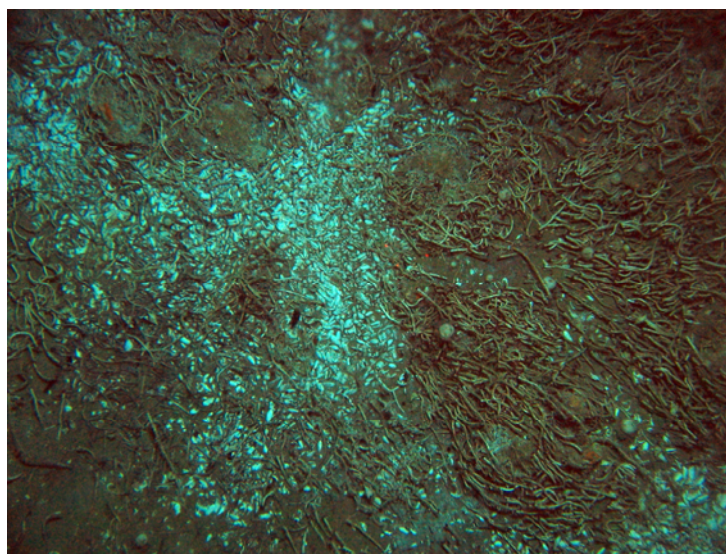


Figure 6.6.2: Dense assemblage of vestimentiferan worms (*Lamellibrachia* sp.) with clam shells (*Calyplogena* sp.) at Bear's Paw seep site.

Wairarapa

Eight OFOS deployments were made in this area: 3 at Tui, 2 around Pukeko, 1 at North Tower, 1 at Takahe, and 1 at Tuatara. Significant chemoherm habitats with seep-associated fauna were found only at North Tower and Tui. The transect across North Tower confirmed the findings of TAN0616: the site consists of scattered carbonate chemoherm with locally abundant vestimentiferans, *Calyptogena* sp. Shells, and numerous sulphidic sediment patches. At Tui, well-developed chemoherm habitats with abundant seep-related fauna were confined to areas on the summit of the knoll; the slopes being covered with soft sediment with abundant echinoid populations. Populations of vestimentiferans, fields of dead clam shells, and live *Bathymodiolis* sp. Mussels were found predominantly in areas in the northwest and the southeast quadrants of the knoll summit (Figs. 6.6.3 and 6.6.4).



Figure 6.6.3: Vestimentiferan tube worms (*Lamellibrachia* sp.) in chemoherm at Tui seep site.

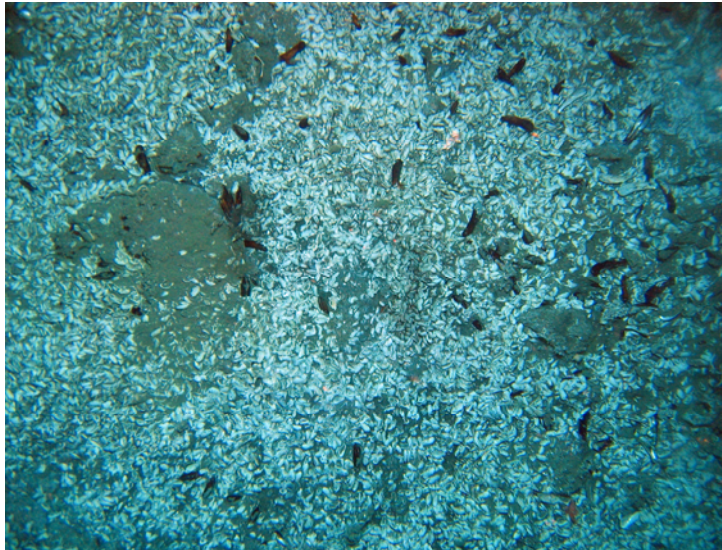


Figure 6.6.4: Live *Bathymodiolis* sp. Mussels amongst shells of *Calyptogena* sp. Clams at Tui seep site.

6.7 ROV Deployments

L. Naudts, J. Poort, D. Boone, J. Vercruyssen, W. Versteeg, J. Greinert, M. De Batist

All deployments, except for test dive ROV1 at Bear's Paw, were undertaken at the Rock Garden site (Table 6.7.1). For all dives the video from the black-and-white forward-looking camera was recorded with and without overlay. The forward-looking color video and still camera didn't function properly during the cruise; nevertheless color video footage was recorded during ROV6 with a Sony digital handycam provided by Dethlev Cordts and during ROV7 with RCMG's ROSS camera, which were sent over during the cruise and collected during a stop-over near Wellington. An important progress for the ROV navigation was made by integrating all online available position and direction data from the GAPS and ROV in the OFOP software package. This, together with the dynamic positioning and very accurate navigation of the vessel, allowed precise navigation and positioning of the ROV and online sea-floor characterization.

Table 6.7.1: Overview of the ROV dives with performed measurements and most important observations.

Dive	Area	Measurements	Remarks
1	LM9: Bear's Paw	/	test dive: tubeworms and clams
2	RG: Faure's Seep Site	/	localization of bubble site
3	RG: west of Faure's Seep Site	THP (0), Niskin bottles (2)	shell debris, carbonate platforms
4	RG: LM3	THP (2), Niskin bottles (2)	seep, clams, carbonates, tubeworms
5	RG: LM3	THP (7), Niskin bottles (2), CTD	clams, carbonates, raindrop site
6	RG : Faure's Seep Site	THP (6), Niskin bottles (2), CTD	seeps, BIGO & FLUFO landers
7	RG : Faure's Seep Site	THP (4), Niskin bottles (2), CTD	seeps, raindrop site, lander weights

Faure's site

At Faure's site three ROV deployments were made: ROV2, ROV6 and ROV7 (Figs. 6.7.1 and 6.7.2). A very important result was the precise localization of a seep site during ROV2, which allowed accurate planning for all other subsequent actions (landers, MUC's, etc.). Generally, at Faure's site, a flat sea floor with soft sediments was observed, which alternated with patches (sometimes very extensive) of porous semi-indurated sediments (carbonates?). These stand out in relief, either as small, isolated patches, or forming prominent, flat regional terraces, often showing a layered structure. Within the soft-sediment areas, often small holes were observed. It is unclear whether these represent non-active venting holes or whether they are due to bioturbation. The active venting sites, discovered during ROV2, were characterized by bubbles being released from 4-5 prominent depressions in the sea floor. Bubble-release activity was very variable in time, with periods of almost non-activity alternating with periods of violent outbursts. During the latter, sediment particles were entrained and formed a suspended particle cloud (possibly explaining the morphological expression of the venting holes). During ROV6 the BIGO 4 and FLUFO 4 landers were visited and checked up to a distance of 1.5 m. At the FLUFO lander (= seep site localized by ROV2) several bubbling seeps were observed and sampled with the Niskin bottles. Also temperature measurements with the TPH sensor were performed at both lander sites. The BIGO lander was observed in a tilted position; possibly indicating the presence of hard subsurface sediments which could not be penetrated by the sediment chamber. During ROV7 intensive seep activity was observed from a "raindrop site" (BIGO 4 site). Bubbles were being released from several small venting holes (that were virtually invisible prior to the start of the venting process), which formed a several-meter long lineament. Bubbles were often very large (ca. 2 cm in diameter). The venting process could be observed for nearly 15 minutes, during which period there were no signs of reduction in seep activity. Water samples and temperature measurements were taken from the venting sites.

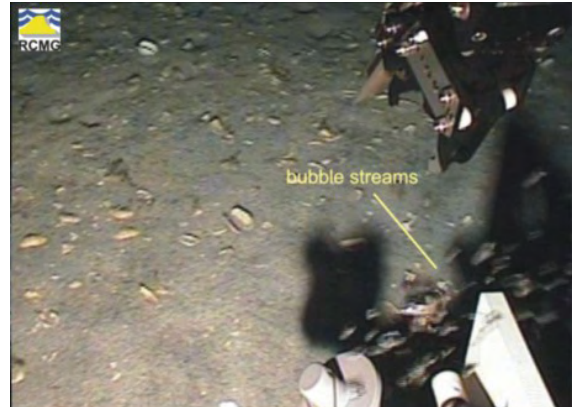
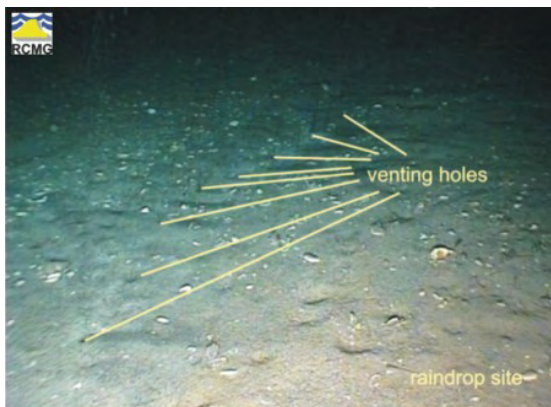
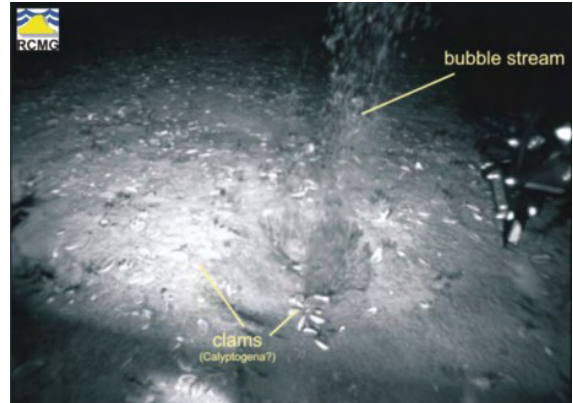
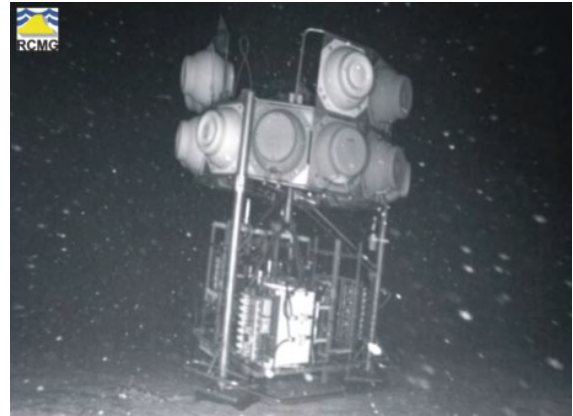


Figure 6.7.1: Screen captures from video recorded during dives ROV2, ROV6 and ROV7 at Faure's seep site.

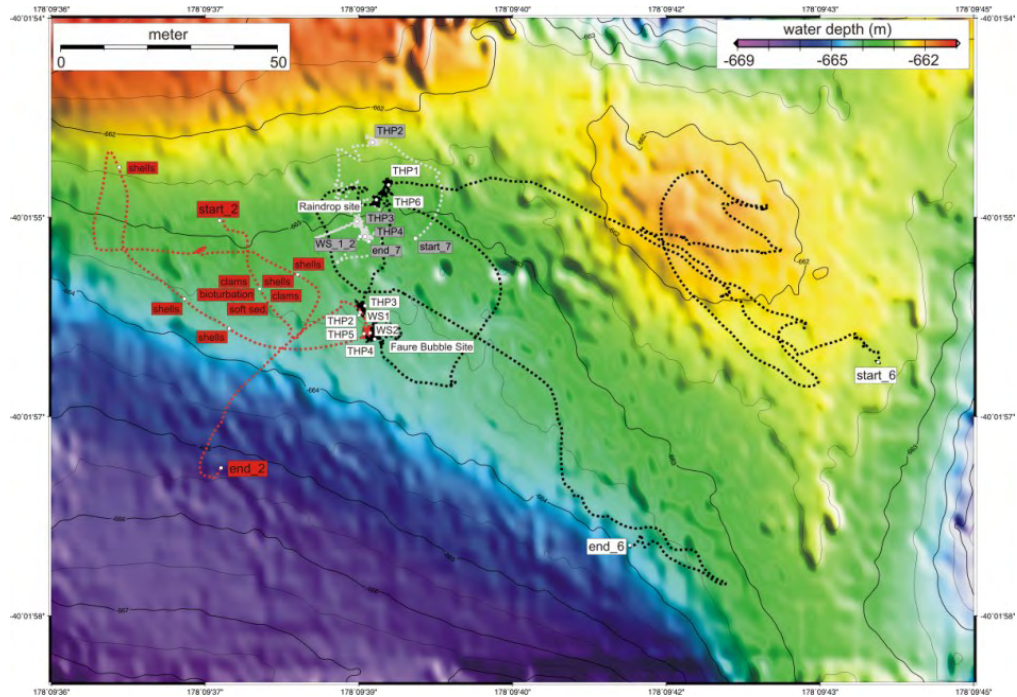


Figure 6.7.2: Dive track of ROV2, ROV6 and ROV7 at Faure's site plotted on swath bathymetry map with indication of the most important observations, temperature measurements (THP) and water-sampling stations (WS).

LM-3 site

During dives ROV4 and ROV5 at LM-3 site (Figure 6.7.3), several areas were discovered that were covered with dense fields of live *Calyptogena* and/or *Bathymodiolus* clams, often in association with tube worms, sponges and/or soft tissue corals (Figure 6.7.4). These clam fields often occurred on and between large carbonate structures (which appeared much more indurated than the porous semi-indurated sediments encountered at the Faure site), but some also on flat, soft-sediment sea floor. Temperature measurements and water samples were taken from within these clam fields, showing only slightly elevated methane concentration. During ROV4 a small bubbling seep was observed.

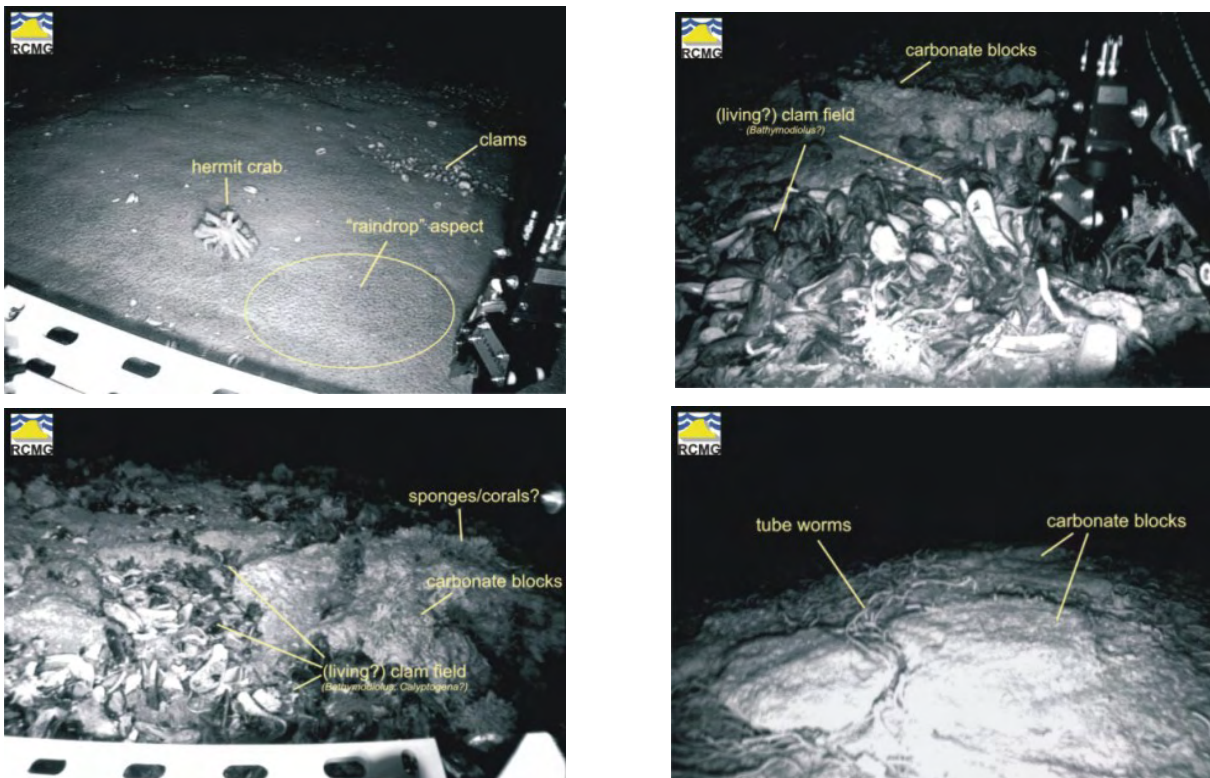


Figure 6.7.3: Screen captures from video recorded during dives ROV4 and ROV5 at LM-3 seep site.

During ROV5, a “raindrop site” (i.e., characterized by a peculiar spotted micromorphology and by the presence of dense populations of small polychaetes) was investigated in detail, with temperature measurements (showing an anomalous low sediment-temperature in comparison with the CTD-recorded bottom-water temperature) and a collection of water samples (revealing very high concentrations of methane). The THP sensor together with the CTD also revealed temperature fluctuations due to variations in ROV-depth, as well as a long-term (i.e. 1 hour) temperature variation that appears to be unrelated to location and/or movement of the ROV (Figure 6.7.5).

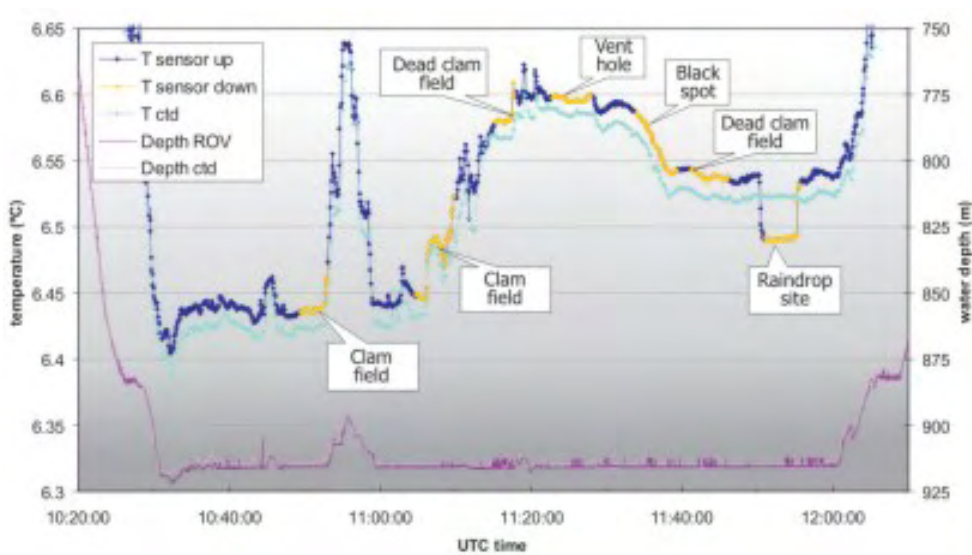


Figure 6.7.4: Measurements conducted during ROV5 with the ROV-mounted CTD and THP sensor.

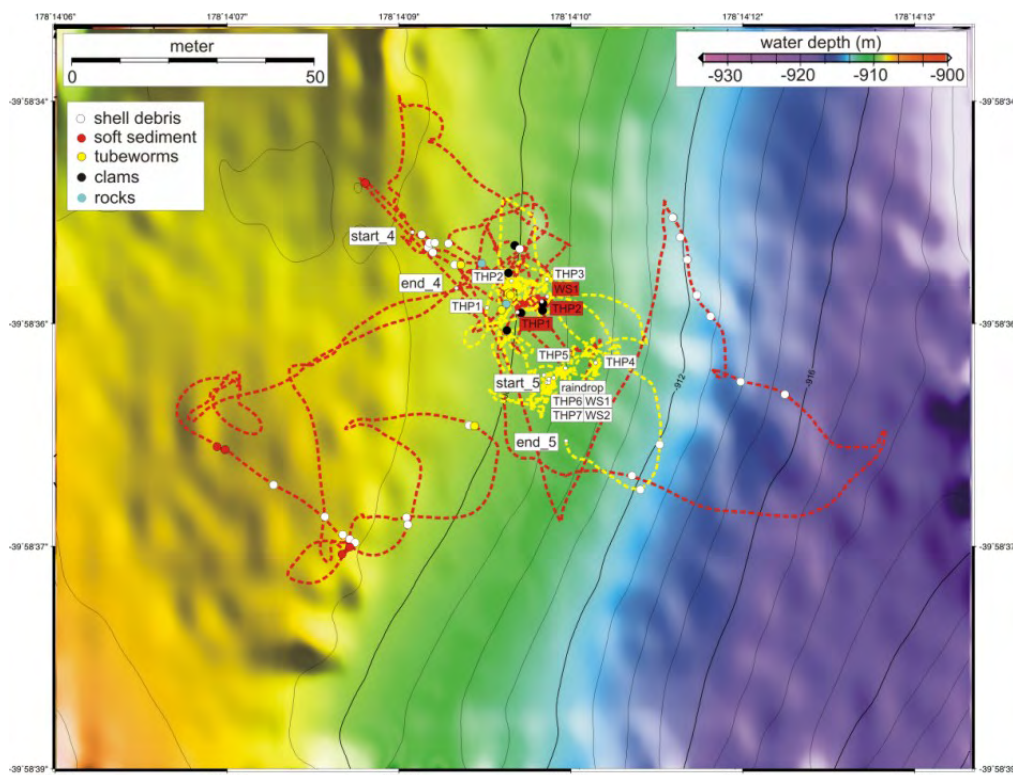


Figure 6.7.5: Dive track of ROV4 and ROV5 at LM-3 site plotted on swath bathymetry map with indication of the most important observations, temperature measurements (THP) and water sampling stations (WS).

West of Faure’s site

ROV3 was undertaken west of Faure’s seep site (Figure 6.7.6) where an undulating sea floor was observed. These changes in relief can probably be attributed to the observed carbonate platforms, be it massive carbonate rocks or semi-indurated, as at Faure’s site.

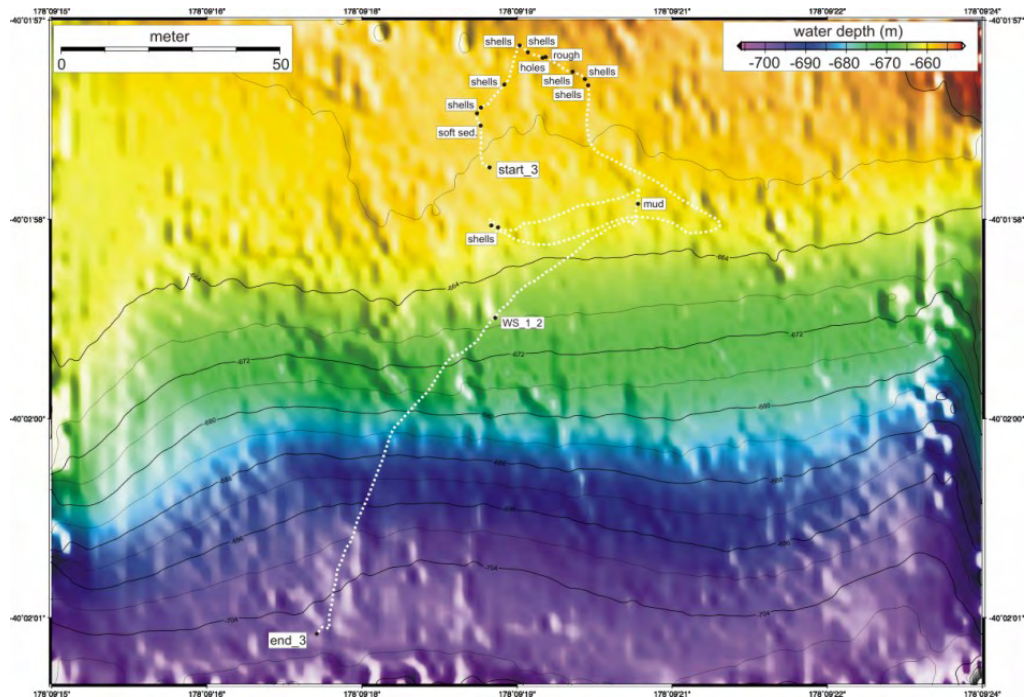


Figure 6.7.6: Dive track of ROV3 west of Faure's site plotted on swath bathymetry map with indication of the most important observations, temperature measurements (THP) and water sampling stations (WS).

6.8 Methane Measurements

6.8.1 Surface Methane Concentrations: Equilibrator Measurements

J. Greinert

For calculating the ppm of CH₄ and CO₂ the integrated peak areas of calibration gas 1 were used as reference. Data were corrected by a time dependant linear spline. Figure 6.8.1.1 depicts the calculated ppm values of calibration gas 2 over several weeks (= 9.78 ppmV CH₄; 5.15 times CG1). Due to pressure and temperature changes the measured raw area of the methane peak of CG2 varied over time quite drastically, which reflects the normal drift of the system. Calculating the ppmV of CG2 by using the area of CG1 as standard results in a constant concentration for CG2. This proves that the drift correction worked well and that fluctuations of the water and atmospheric concentrations after the correction are not caused by a drifting system.

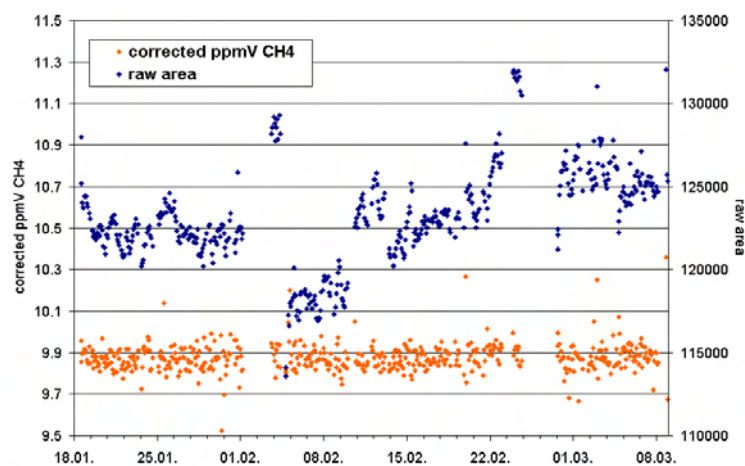


Figure 6.8.1.1: Result of the drift correction of calibration gas 2.

Sea surface methane concentrations are displayed in figures 6.8.1.2, 6.8.1.3 and 6.8.1.4 for the entire area covered during SO191. Detecting higher concentrations at the Faure Site is astonishing as the water depth at 700m is quite deep and bubbles would have been dissolved totally before reaching the sea surface. However, the massive bubble release at Faure Site as seen during ROV dives might be able to create a plume that stays stable over a longer time and transports methane to the sea surface. Unfortunately, we could not confirm these high concentrations during a 12h survey over

Faure Site at the end of the cruise. One reason might be that a storm directly before the survey equilibrated the surface water with the atmosphere, but contaminations from the ship during the time at station and a broken air pump might partly be responsible for the higher concentrations in the air and water (Figure 6.8.1.5).

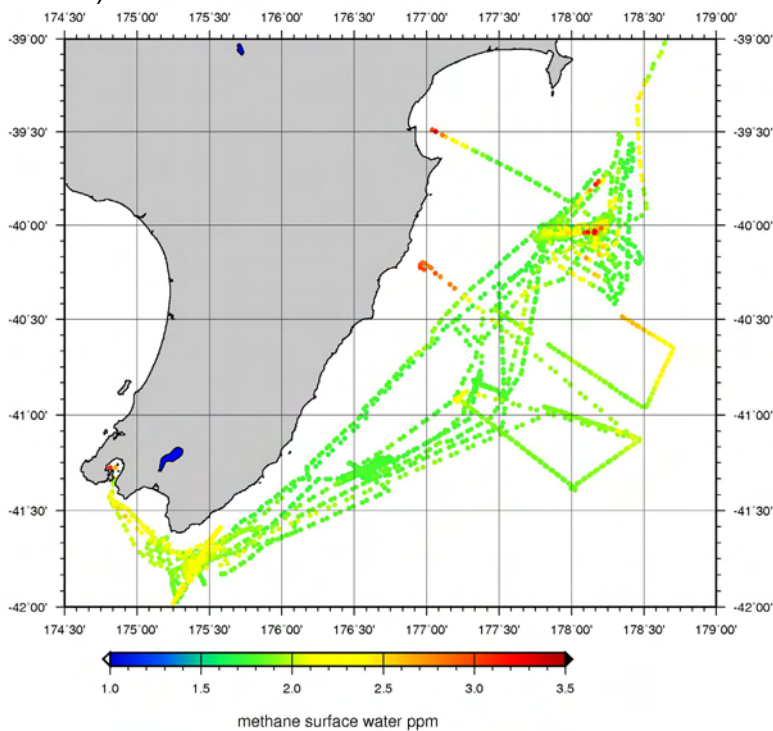


Figure 6.8.1.2: Methane concentrations of the sea surface in ppm during the cruise.

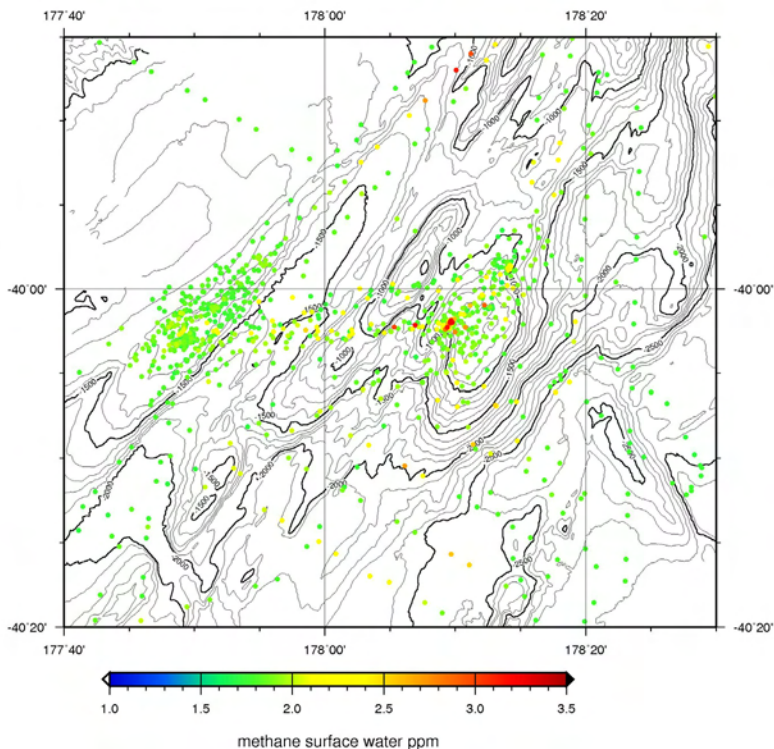


Figure 6.8.1.3: Methane sea surface concentrations in the Rock Garden – Omakere Ridge area with possible higher methane concentrations above Faure Site.

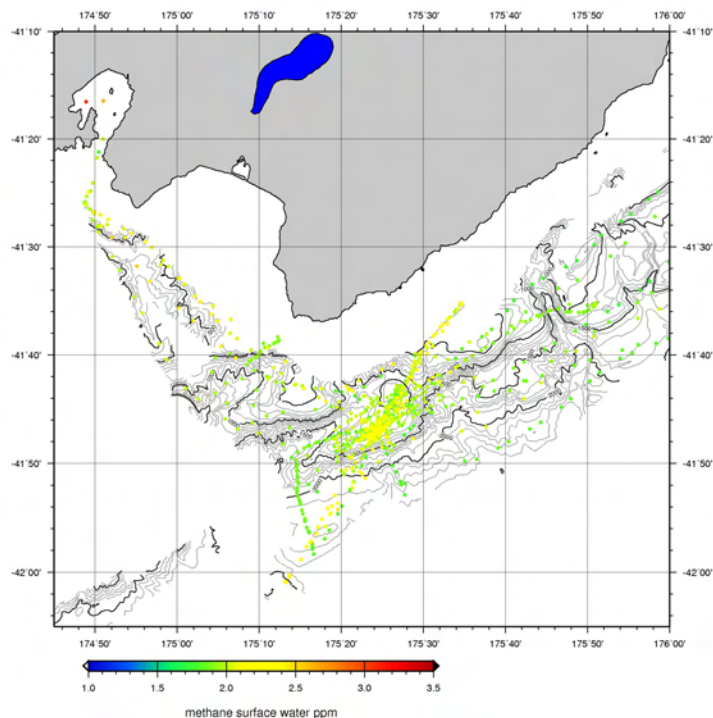


Figure 6.8.1.4: Methane sea surface concentrations in the Wairarapa area. No anomalies were detected.

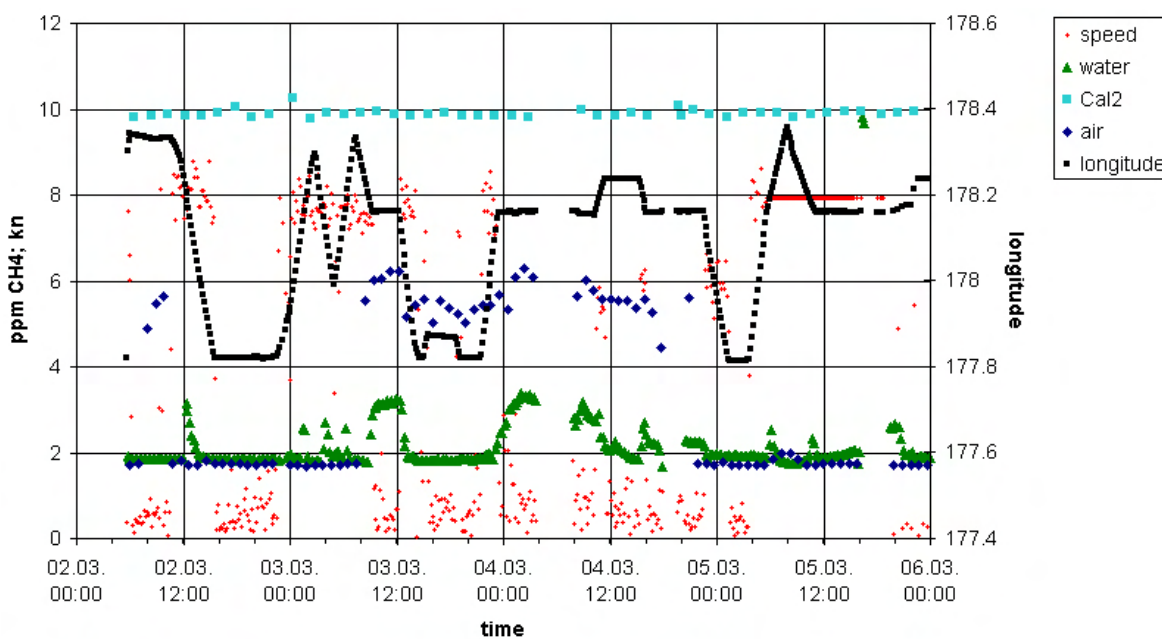


Figure 6.8.1.5: Time plot showing methane, speed and position data at the time the higher methane concentrations were recorded at Faure Site (178.18 longitude).

6.8.2 CTD and Water Column Methane Measurements

K. Faure, D. McGinnis, R. Kipfer, J. Schneider v. Deimling

Physical constituents

Figure 6.8.2.1 shows typical background values for temperature, salinity and dissolved oxygen (DO) obtained at LM9. Potential density shown in Figure 6.8.2.1 was calculated using the Oceans Toolbox, and accounts for pressure effects on density. The DO sensor was faulty for CTDs 1-8, and was replaced right before CTD 9. Three Winkler measurements were obtained during CTD 11 (Figure 6.8.2.2) with a good match, however, it is recommended that the sensor be further verified on Leg 3.

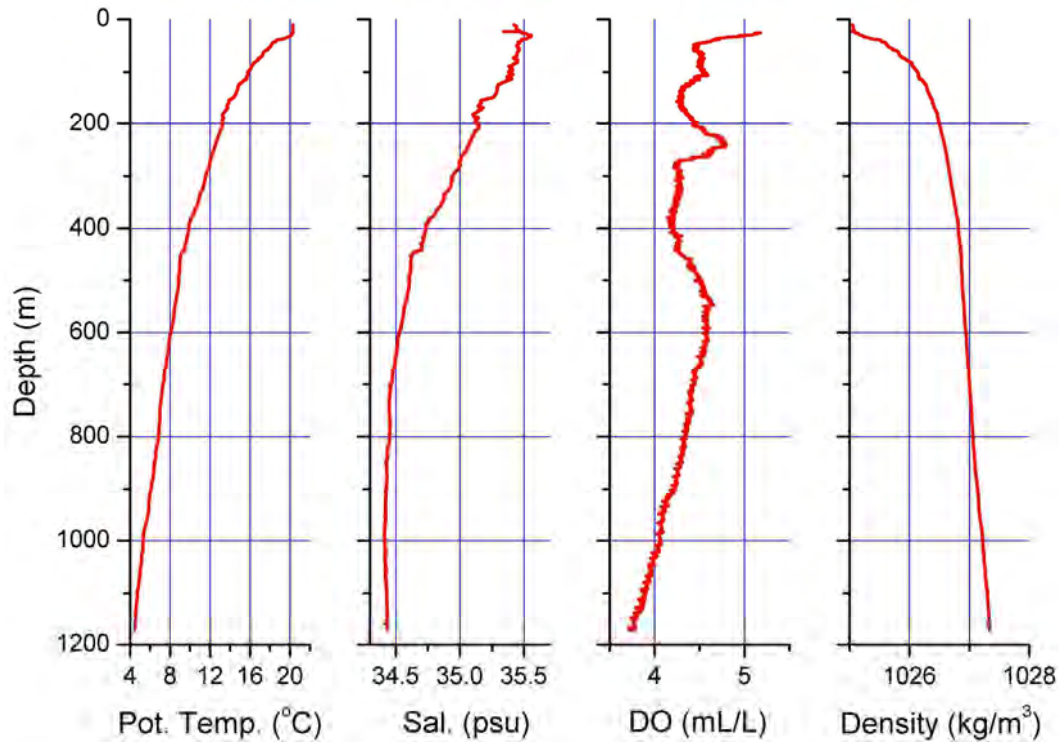


Figure 6.8.2.1: Background physical constituents at the study site. Potential density was calculated using Oceans Toolbox, and accounts for compressibility of fluid at great depths. Note that for the upper 700 meters, temperature acts to stabilize the water column, while salinity destabilizes.

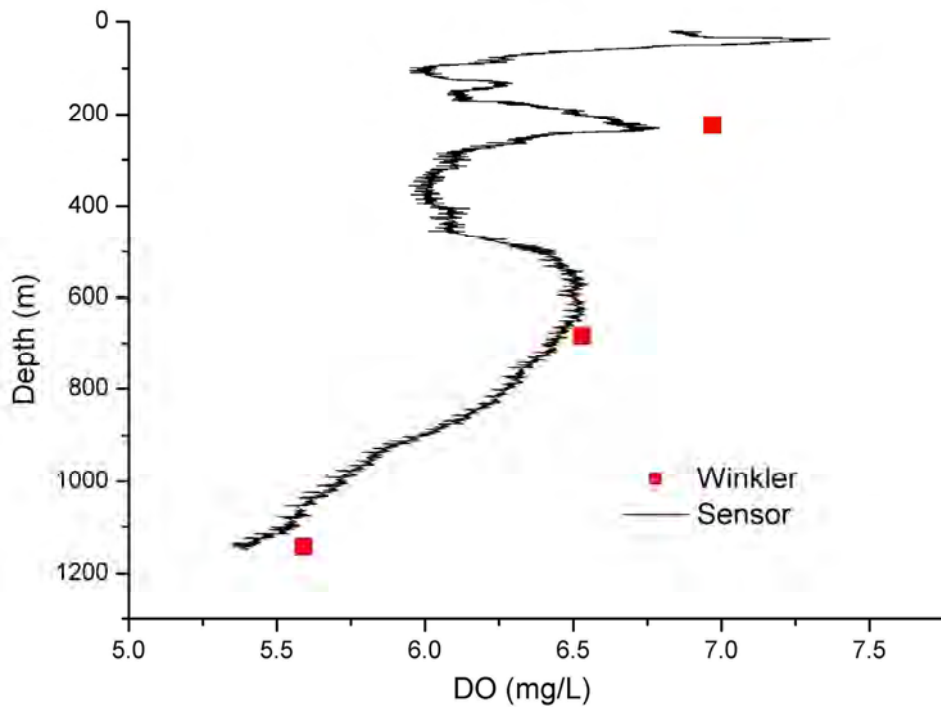


Figure 6.8.2.2: Comparison of Winkler with CTD 11 DO profiles.

Overall, the water body is weakly stratified, particularly at depth (Figure 6.8.2.1). The salinity acts to destabilize the stratification above 700m, with density ratios (not shown) on the order of 1. This indicates the potential for double diffusion, but it is doubtful the characteristic step profiles would be observed in the highly energetic location. Temperature acts as the primary component of stratification across the entire depth, and salinity almost plays no role below 700 m.

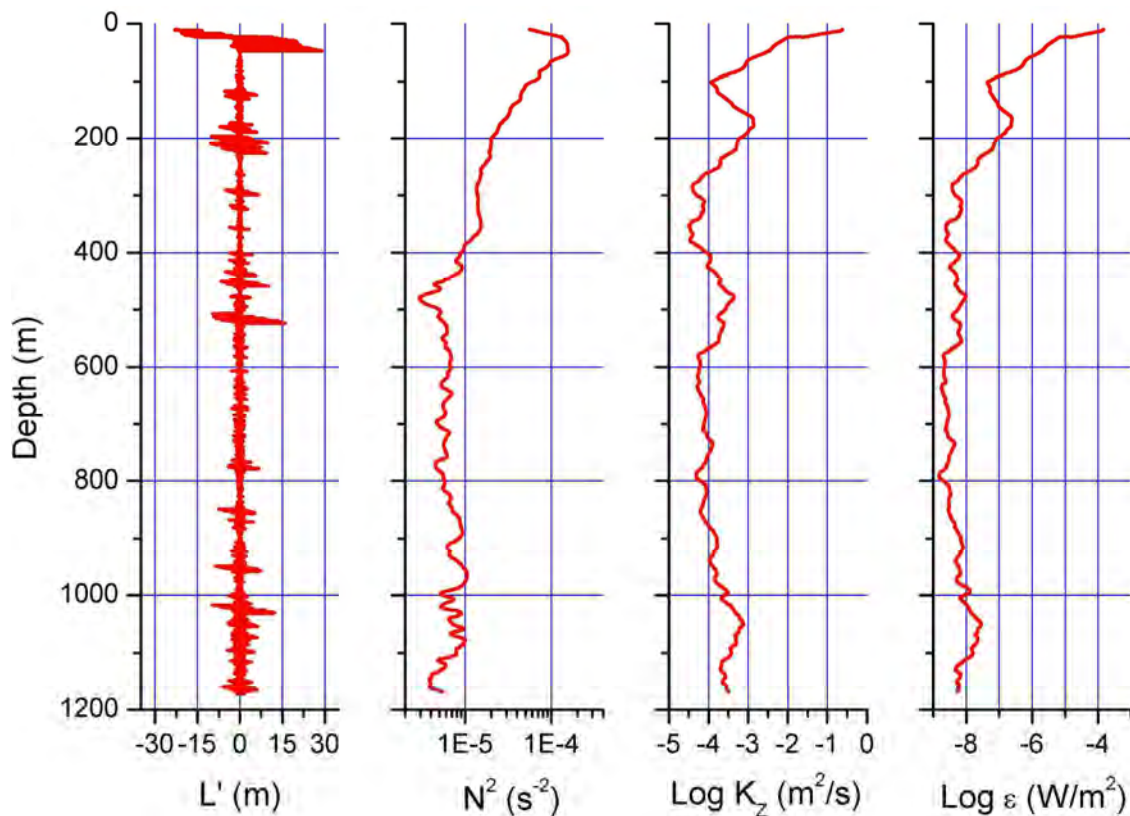


Figure 6.8.2.3: Calculated physical properties of water column showing characteristic mixing length L' , water column stability N^2 , turbulent eddy viscosity K_z , and dissipation of turbulent kinetic energy ϵ .

Preliminary calculations for basic physical properties and transport/mixing characteristics were performed for the study sites (Figure 6.8.2.3). These include the Thorpe mixing length L' , stability frequency N^2 , vertical turbulent diffusivity K_z , and the dissipation of TKE ϵ . Again, these values indicate a fairly weakly stratified, and energetic environment. The K_z values will be later used to determine the life time of methane signals, and the vertical flux, given as

$$F_{CH_4} = A_s K_z \left(\frac{\partial C_{CH_4}}{\partial z} \right)$$

where “ A_s ” is the cross-sectional area at a given depth, and the right-hand term in brackets is the methane concentration gradient. These results are very preliminary. All physical data must be processed and averaged for both areas to obtain representative values and the intermittency. This processing will be performed after the cruise by EAWAG.

Water Column Methane Measurements

The SO191-2,3 legs surveyed predominantly vent sites in the mid- and lower-Hikurangi margin, in particular the LM 9,/ Rock Garden, Uruti Ridge, Builders Pencil and the Wairarapa regions. In these areas individual vent sites have been identified with very high CH_4 concentrations in the water column, especially in the Wairarapa region (up to about 920 nM) and at the Faure site (Rock Garden, CTD 46). Here, a prominent subsurface signal of 22nM in 80 m depth was found. The reliability and sensitivity of the METS sensor (Figure 6.8.2.4) enabled high resolution sampling of the anomalous CH_4 zones. Unfortunately, the online voltage output of the CONTROS indicated, that the methane sensor did not respond to elevated methane concentration in the water. A summary of findings at the sites follow. CTDs with CH_4 concentrations greater than 100 nM are presented in Table 6.8.2.1.

Table 6.8.2.1: CTDs which had CH₄ concentrations greater than 100 nM.

LM Region			Wairarapa, Tui vent site			Wairarapa North Tower site		
	Depth (m)	CH ₄ (nM)		Depth (m)	CH ₄ (nM)		Depth (m)	CH ₄ (nM)
CTD6	1059	103.5	CTD24	775.0	189.8	CTD 33	971	118.9
CTD6	994	147.8	CTD24	762.0	377.7	CTD 66	928	265
CTD7	1059	103.5	CTD24	665.0	159.1			
CTD8	1050	21.9	CTD25	793.0	678.0			
CTD9	994	147.8	CTD25	787.0	271.0	Rock Garden		
CTD11	1021	142.8	CTD28a	740.0	288.0	CTD 46	662	3178
CTD12	1106	164.1	CTD28a	730.0	478.0			
CTD12	1085	102.9	CTD28a	724.0	648.0	Bears Paw		
CTD18	1047	320.0	CTD28a	716.0	447.8	CTD 42	1100	127
CTD19	1101	155.6	CTD28a	708.0	611.7	CTD 43	1111	282
CTD19	1097	130.8	CTD28a	687.0	294.8			
CTD19	904	160.0	CTD28a	642.0	180.0			
CTD21	860	107.39	CTD34b	818	525.31			
CTD39	1090	376.1	CTD34b	815	244.22			
CTD39	1092	247.3	CTD34b	812	177.43			
CTD39	1092	225.2	CTD36	830	728.6			
			CTD36	825	461.4			
			CTD36	821	231.8			
			CTD36	787	124.3			
			CTD36	737	174.4			
			CTD37	832	211.9			
			CTD37	824	295.8			

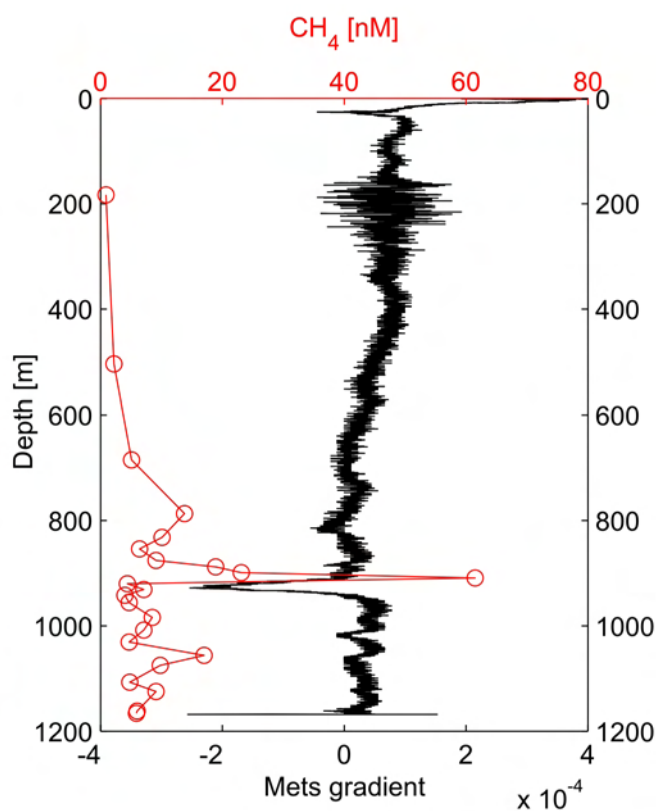


Figure 6.8.2.4: Methane concentration from CTD 7 (upcast) compared to the METS gradient of its voltage (downcast). A negative gradient corresponds to elevated methane concentration (signals above 400m are considered bad). The small depth offset between the highest methane concentration and the negative METS peak is caused by the response time of the sensor.

LM9-region

Seventeen CTD casts were deployed in the LM9 region (Figure 6.8.2.5). A cast (CTD 4) near the original LM9 site (Lewis and Marshall, 1996) revealed relatively low CH₄ concentrations. However, new vent sites in the LM9 region have been identified with CH₄ concentrations up to about 380 nM at depths varying between 800 and 1200 m (Figure 6.8.2.6). The most active site in this region is the Bear's Paw, but very high CH₄ concentrations (up to 150 nM) were also obtained in casts to the northeast (CTD 6) of LM 9 and also southwest of Bears Paw (CTD 5). Further exploration around these sites is recommended. A cross-section along the LM 9 "valley" illustrates the distribution of CH₄ concentrations in the water column (Figure 6.8.2.7).

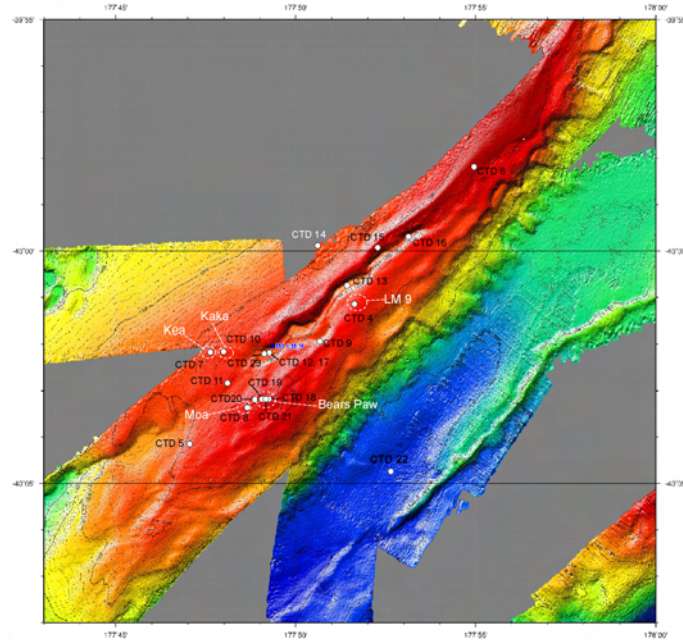


Figure 6.8.2.5: Map showing the localities of CTD casts and mooring sites within the LM9 region. One of the most active new vents sites is Bear's Paw.

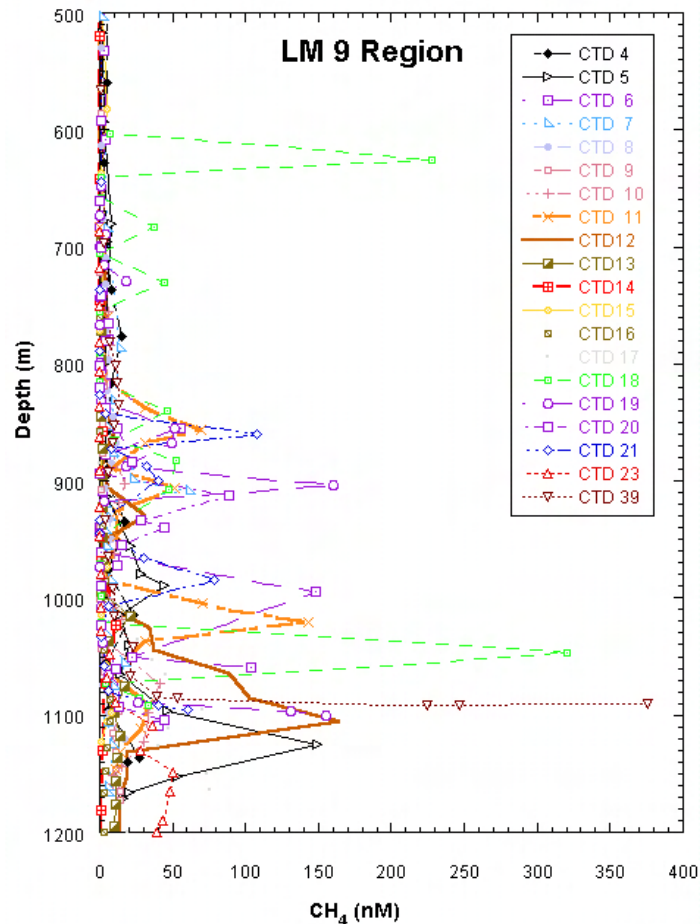


Figure 6.8.2.6: Plot of CH₄ concentration in the water column versus depth in the LM 9 region.

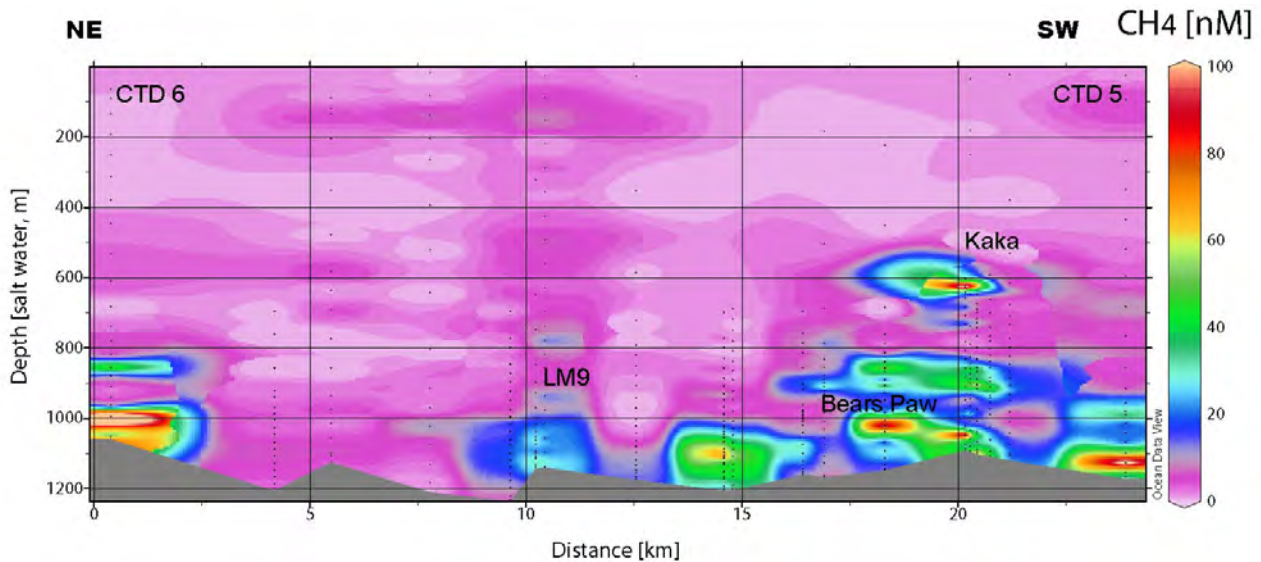


Figure 6.8.2.7: A cross-section (along a NE line) of CH₄ concentrations in the water column in the LM 9 region. Depicted is the high CH₄ activity at Bear's Paw and also the promising relatively un-explored regions to the northeast of LM9 and southwest of Bear's Paw sites.

A "time-series" experiment was carried-out at one site, by analysing the CH₄ concentrations on 3 occasions with approximately two day intervals between the casts (Figure 6.8.2.8). The first cast (CTD 12) revealed a 100 m thick CH₄ zone with the highest value (170 nM) at 1100 m. A second cast (CTD 17) revealed a lower CH₄ values for the 1100 m peak (similar shape) and a new CH₄ (80 nM) peak at 1160 m. A third cast (CTD 23) showed that the 1100 m CH₄ peak was still lower, but clearly discernible, and the 1160 m was lower (50 nM). The validity of the controls of the experiment can be questioned, however, empirically it would seem that an injection (assuming limited input, not continuous) of a CH₄ plume into the water column is preserved for at least 6 days and probably would last longer than 10 days.

CTD casts to determine background CH₄ concentrations proved to be quite difficult. CTD 16 was deployed ostensibly as a background cast about 5 km southwest of Bear's Paw and had values that ranged between 0.5 and 6.9 nM, the highest value occurring at about 1100 m (Figure 6.8.2.5).

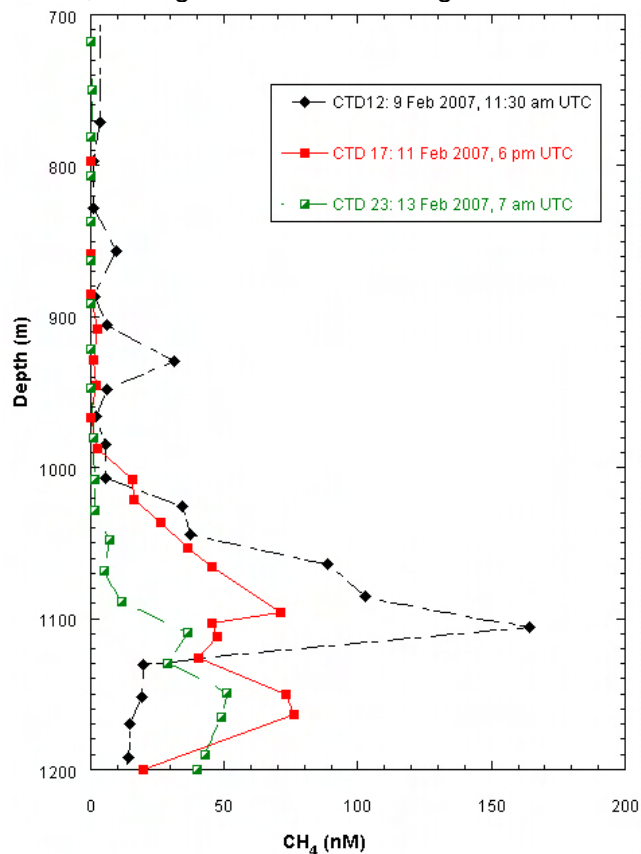


Figure 6.8.2.8: A plot of three CTD casts, in the same position, separated by approximately two days each.

Wairarapa region

In the Wairarapa region, CTD deployments were primarily at the Tui site and one on the North Tower site. A cast (CTD 31) to establish “background” CH₄ concentrations was deployed to the southeast of Tui. This was also the site of two moorings to establish “background” physical parameters for the area (Figure 6.8.2.9). The values in this cast varied between 0.7 and 4.4 nM.

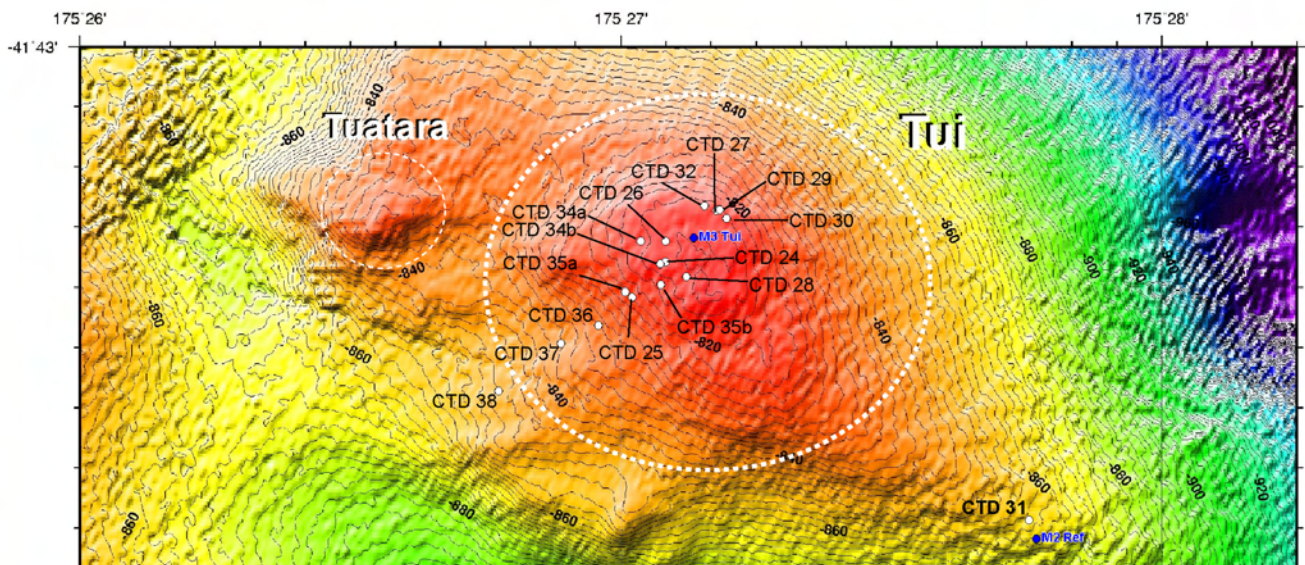


Figure 6.8.2.9: Map showing the localities of CTD casts and mooring sites at the Tui vent site.

Tui site

Eleven vertical and two “tow” CTD casts were deployed at the Tui site. The “tow” casts (CTD 34a,b and 35a,b) entailed tripping ½ the Niskin bottles in a vertical array at one site and tripping the other ½ at another site a short distance away, also in vertical array. Niskin bottles were tripped based on METS measurements suggesting elevated CH₄ concentrations.

Figure 6.8.2.10 is a plot of all the casts at Tui and show that CH₄ occurs at depths between 550 m and the seafloor (~800 m). The highest CH₄ concentrations measured along the Hikurangi margin, so far, have been measured at the Tui vent site (up to 920 nM).

A cross-section of CH₄ concentrations in the water column summarises distribution and concentrations at Tui (Figure 6.8.2.10). High concentrations of CH₄ (up to 600 nM) are found relatively high in the water column (~700 m depth) in the central part of Tui (e.g., CTD 24, 28), whereas on the south west slope of Tui very high concentrations (up to 920 nM) are found in water nearest the sediment contact (ca. 2 m above sediments). The tentative interpretation of the CH₄ distribution is that diffusive venting is taking place on the slopes through soft sediments (OFOS observations indicate soft sediment on slope) whereas plume injection of fluids is occurring at the top of Tui in a focused manner through more consolidated (carbonate) sediments (Figure 6.8.2.11).

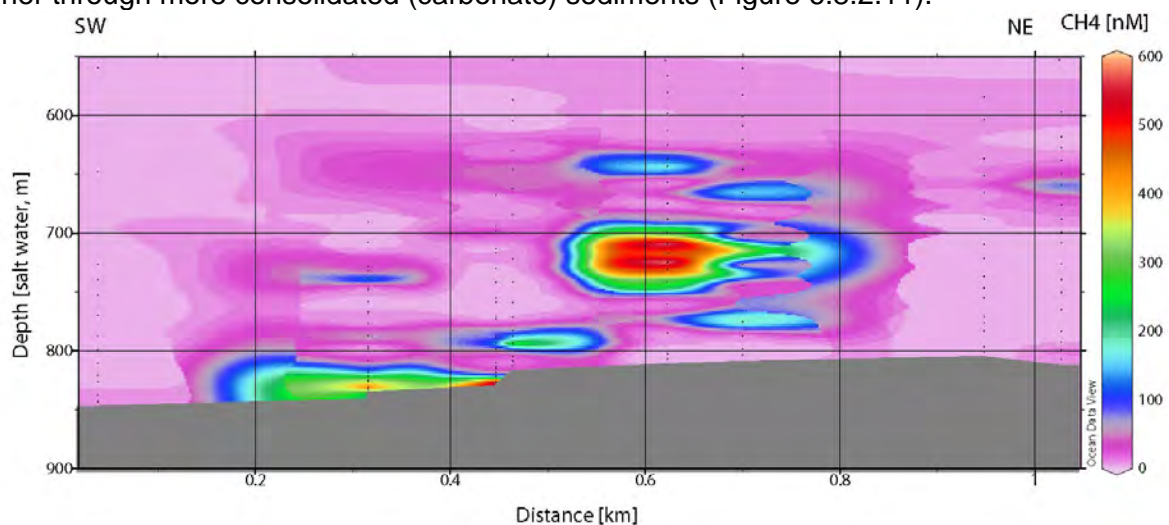


Figure 6.8.2.10 : Cross-section of CH₄ concentrations in the water column at Tui

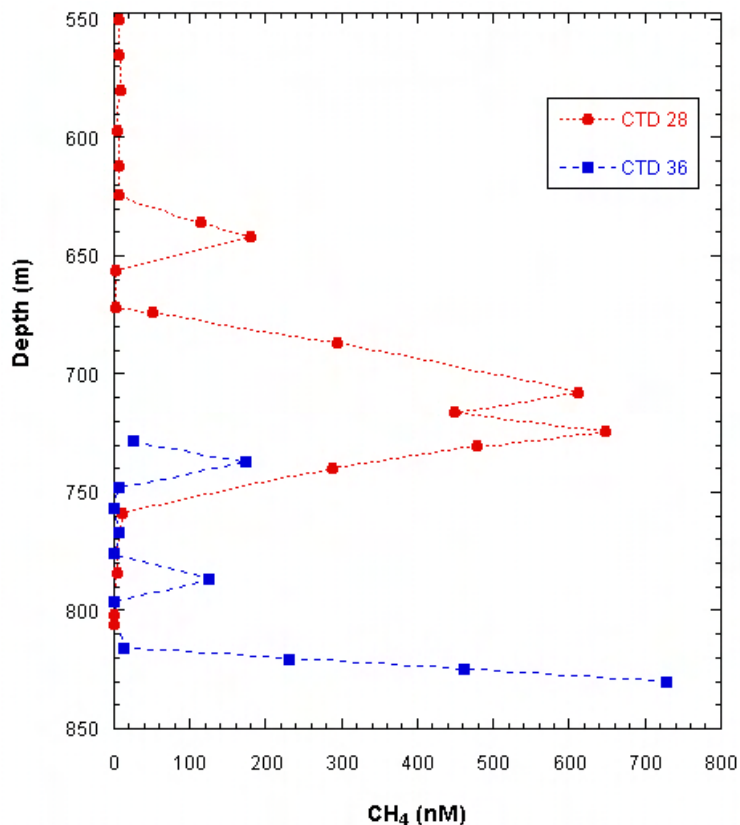


Figure 6.8.2.11 : Plot of methane concentrations at the top of Tui.

An interesting feature observed at Tui, not observed at LM 9 or North Tower sites, is that there appears to be a general elevated “Tui CH₄ background” deeper than 550 m depth (Figure 6.8.2.11). CH₄ concentrations above 550 m are generally less than 3 nM. CTDs that were cast at the perimeter of Tui have a relatively lower “Tui CH₄ background” concentrations (Figure 6.8.2.12). We suggest that oceanographic features at Tui (e.g., currents, tides, etc.) and the overall high concentrations of CH₄ are the cause of this feature. Further analysis of cruise data will be examined to try and understand the cause of this phenomenon.

CTD 34a which had a CH₄ concentration of 519 nM was analysed for higher hydrocarbon compounds (C1-C6). In addition to methane the only other hydrocarbon that was present in concentrations high enough to measure, was ethane (0.9 nM).

Evidence of a methane plume injection was obtained during CTD 28 (Figure 6.8.2.13). Here, a plume is defined as a vertical advective flow driven by a source of buoyancy (e.g., heat flux, bubbles, high dissolved methane concentration, etc.). A technique, called the Thorpe scale analysis, is used to reorder the temperature profiles to give a corresponding smooth profile [Thorpe, 1977] (Figure 6.8.2.13). This allows us to locate turbulent overturns and the associated small- to large-scale temperature inversions. Thorpe displacement analysis shows substantial overturns of ~30 m at around 720 m depth that perfectly corresponds with a large peak (~600 nM) of methane (Figure 6.8.2.13). This is likely from plume input (the final equilibrium depth of a plume originating on the sea floor); however, it is inconclusive which buoyancy source(s) are driving the plume (e.g. heat flux, bubbles, etc.). In the corresponding profiles, a completely well-mixed step (in T and Sal) is observed at this location which is ~35 m thick (Figure 6.8.2.14). This further suggests a local source nearby and a substantial energy input is required to maintain such a structure. In absence of a supporting energy source, this signal would be vertically diffusively smeared within 4 days ($t = z/K_z$), and much faster horizontally.

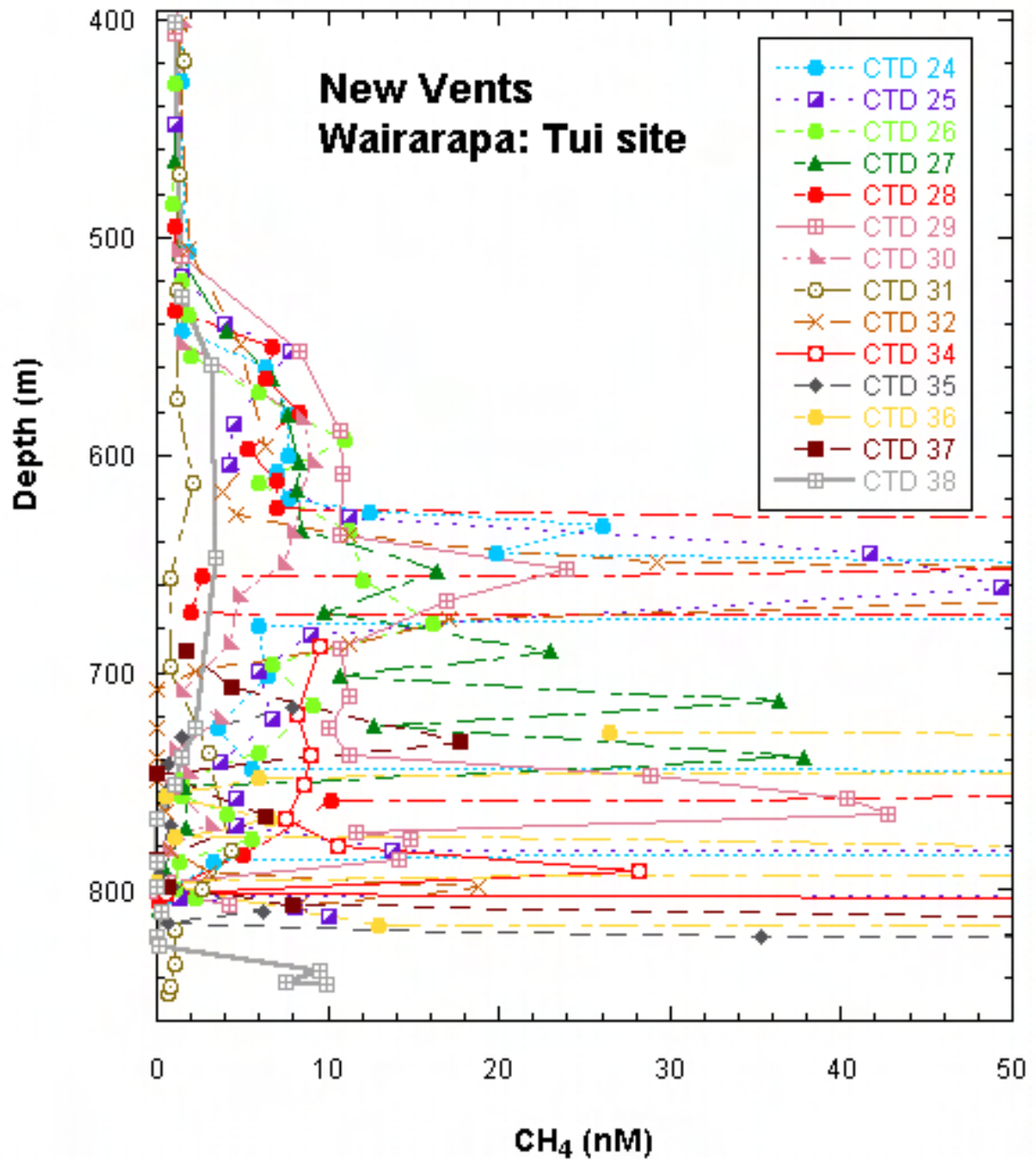


Figure 6.8.2.12: Plot of CH₄ in the water column versus depth at the Tui vent site.

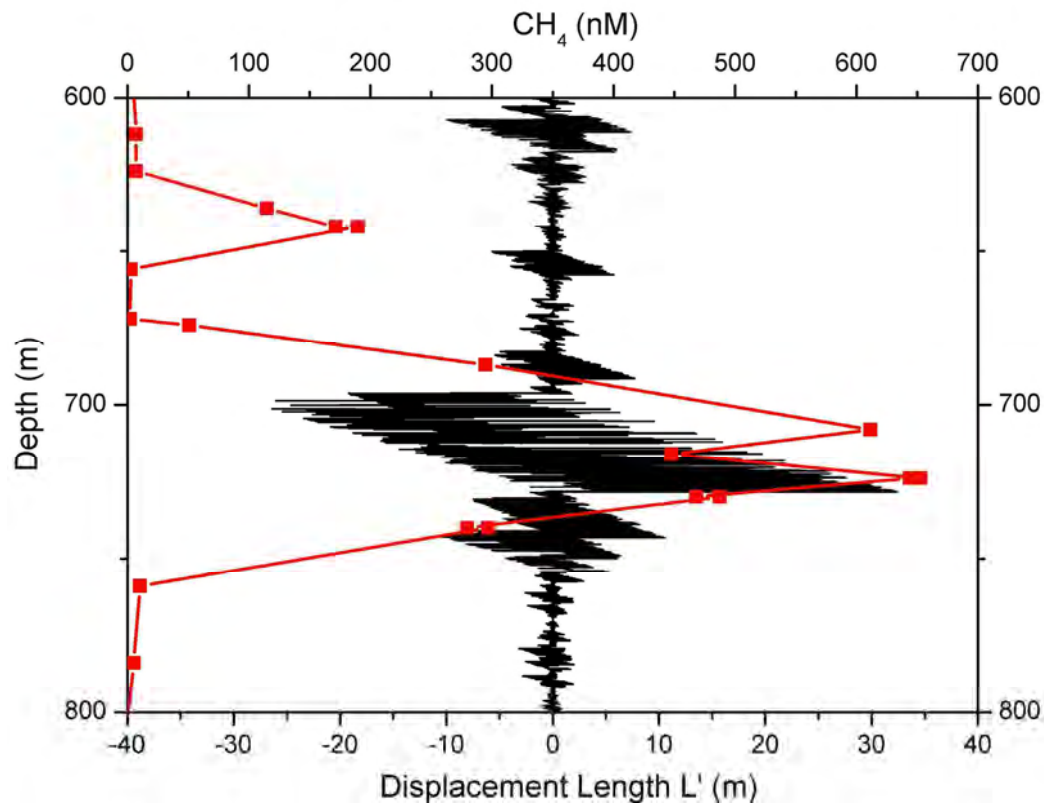


Figure 6.8.2.13: CTD 28 Thorpe displacement compared with peak of methane. The Thorpe displacements are abnormally large indicating a possible CH₄ – enriched fluid injection at this level.

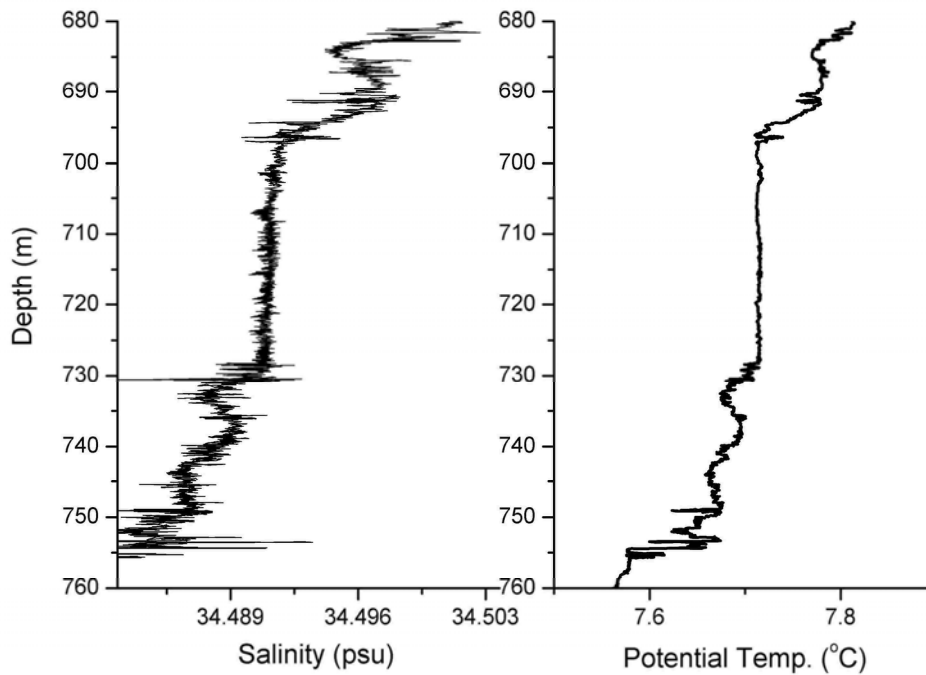


Figure 6.8.2.14: Deep mixed layer in salinity and temperature corresponding with Thorpe displacement shown in Figure 6.8.2.13. Such structures require an energy input to maintain their shape. It is estimated that such a feature would be diffusively smeared within 4 days.

North Tower

A single cast (CTD 33) was deployed at North Tower at the same site as deployment of the BIGO lander (#142). Samples analysed from this site showed elevated concentrations at the seafloor (40 nM) and a relatively thin (10-15 m thick) plume at about 970 m with CH₄ concentrations of up to 120 nM (Figure 6.8.2.15). Again, the convenience of having a reliable METS sensor has enabled high resolution sampling to distinguish between the separate CH₄ layers, which may not otherwise have been possible.

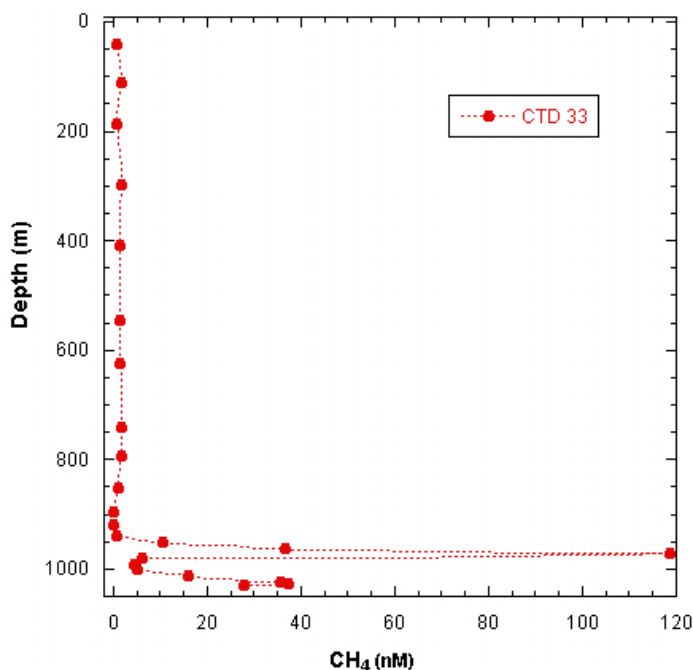


Figure 6.8.2.15: Plot of CH₄ in the water column versus depth at the North Tower site.

During leg 3 data gaps of formerly sampled working areas have been completed. Furthermore, a detailed vertical section over 30 km distance at the Wairarapa area was conducted. This allowed us to track the methane of two known sources in a tracer like manner over several kilometres (Figure 6.8.2.16). A third prominent signal of 20nM was found in the 2000 m deep water mass in this section. The origin of this elevated methane concentration remains unknown.

At the Faure site a prominent subsurface signal of 22 nM in only 80 m depth was found during leg 2 and we tried to confirm this high value by additional subsurface water sampling but could not confirm the high value.

Here, with the Parasound echosounder we could proof several flares rising at least 200 m from the seafloor. By means of the ROV the precise location of this gas seepage was localized and a discrete water sample was taken in the very vicinity of the releasing point source. The methane concentration of this sample achieved 5%.

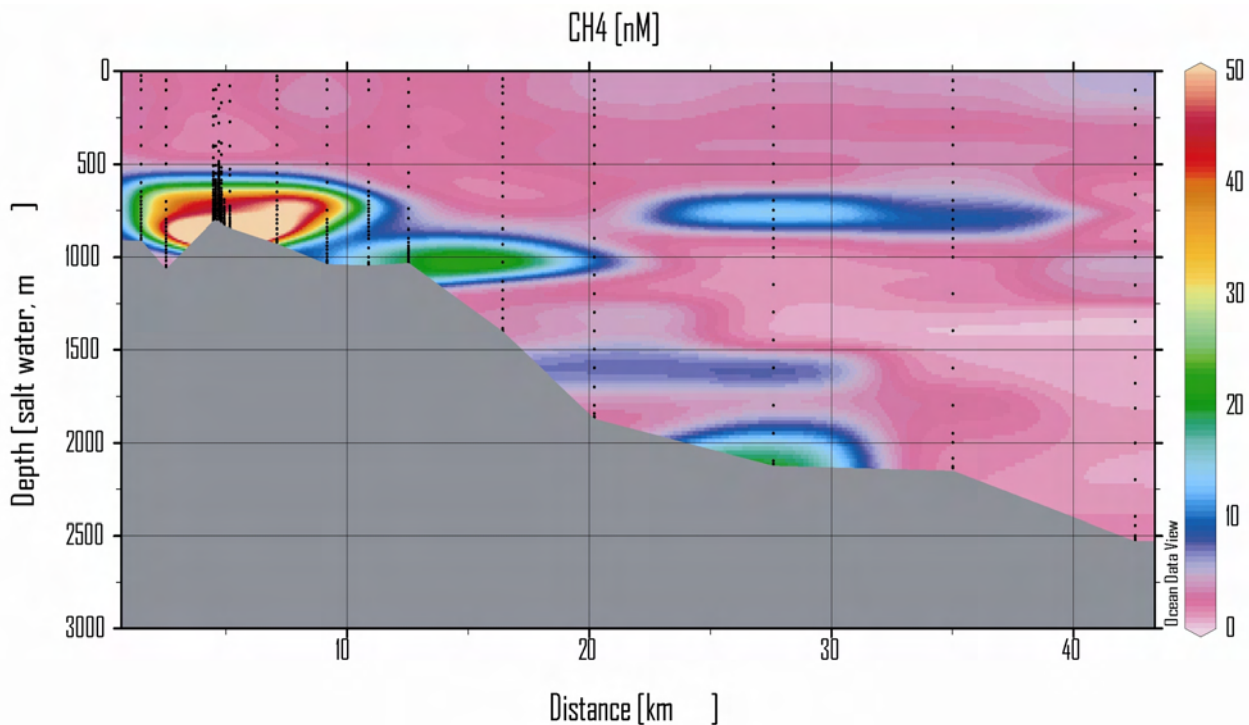


Figure 6.8.2.16 Vertical section of methane distribution from NNE to SSW in the Wairarapa area. The corresponding water samples of the fourteen CTDs are plotted as black dots.

Noble gas sampling

In total 37 water samples for noble gas analysis (concentration of He, Ne, Ar, Kr and Xe; $^3\text{He}/^4\text{He}$, $^{20}\text{Ne}/^{22}\text{Ne}$ and $^{40}\text{Ar}/^{36}\text{Ar}$) were taken and filled in copper tubes during Leg 3. About 30 samples were taken in close vicinity of previously identified active seep sites, where bubbles enter the overlaying water body. The rest of the samples were taken direct and within the root zone of bubbling seep sites by means of water sampler being mounted on a remote operated ROV.

The atmospheric noble gas abundances are expected to yield information about the possible interaction of the rising gas bubbles with the surrounding water mass, because the initially noble gas free gas phase will strip noble gas from the saturated water. This secondary gas exchange between gas and water phase will produce characteristic noble gas depletions in the water body that can be interpreted in terms of gas release. Similarly the noble gas abundances, especially that of He and the $^3\text{He}/^4\text{He}$ ratios have the potential to track the injection of pore water fluids into the open water body, e.g. the ascent and detrainment of pore waters might be determined.

Sediment analysis.

Three sediment cores were sampled for noble gas analysis in the pore water of the sediment (15 samples). These samples are the probably the first sediment samples ever taken in Pacific Ocean for noble gas analysis. Two cores were taken at active seep sites, whereas the third core was taken in a area that is not affected by bubble release ('reference'). The abundance, $^3\text{He}/^4\text{He}$ ratios as well as the respective spatial gradients will show whether He emissions are different between the reference and seep stations. In addition $^3\text{He}/^4\text{He}$ ratios are expected to identify the geochemical source of the emitted/accumulated He.

6.8.3 OBM Measurements at Seismic Profile P05

A. Krabbenhöft

Along the Wairarapa region, the five methane sensors were deployed again, see the map in chapter 6.3.4 for deployment locations. Here, an example of a station OBM49 is shown in Figure 6.8.3.1. Here, in this example, the curve for the methane concentration is missing in the upper part of the figure, because the methane concentration could not be calculated with the conversion formula from the methane voltage, U1, due to the drift of the sensor. However, variations in the methane concentration can be derived from the methane voltage (middle part of Figure 6.8.3.1, U1).

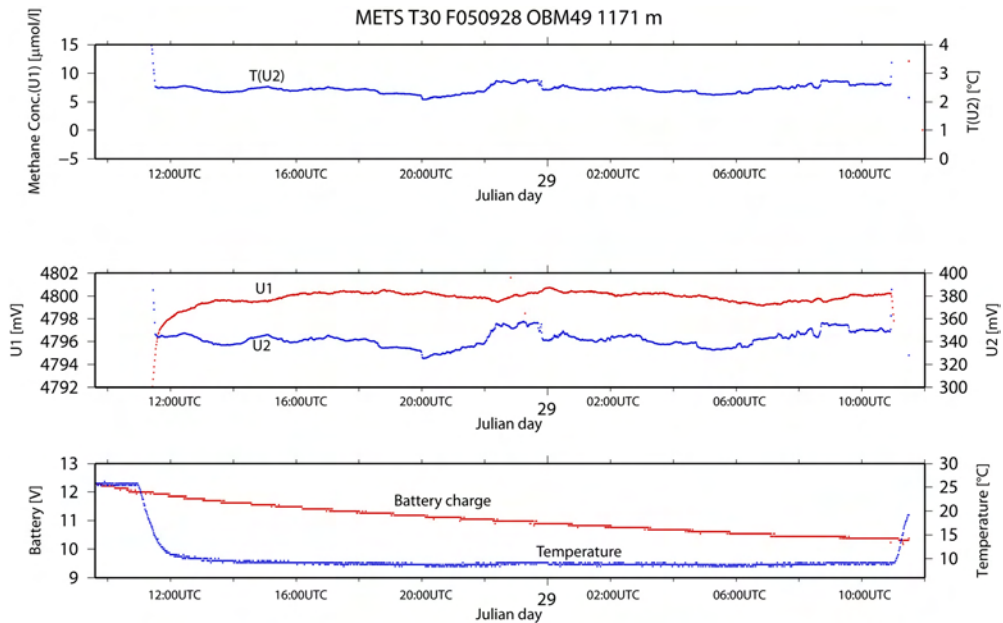


Figure 6.8.3.1: Raw data (bottom and middle, U [mV]), methane data (top, methane concentration [mmol/l]), OBM49.

6.9 Thermistor Moorings

D. McGinnis

For mooring locations, see Figure 6.8.2.9 and Figure 6.8.2.5 in CTD section. LM9 Mooring TM1 (Table 6.9.1): The data have been only preliminarily plotted (Figure 6.9.1), and as expected, show a dynamic system with the occurrence of high-frequency internal waves. BWS2 at LM9 (Table 6.9.2): The second (first were disregarded) BWS thermistors deployed at LM9 show a very small, well-mixed BBL of about 80 cm thick (Figure 6.9.2). This is surprising as it was thought that this should be much larger given the high bottom current velocities.

BWS3 at LM9 (Table 6.9.3): The third logger installation of the BWS. Data have yet to be analysed.

LM9 Moorings TM4 and TM5 (Table 6.9.4). Deployed as a reference (TM4) and seep site at Bear Paw (TM5). Should be deployed for duration of the 3rd Legs.

Tui Moorings 2 and 3 (Table 6.9.5): The pressure logger installed at 820 m deep on M2 show a huge pressure variation over time, with changes up to 15 dbar (15 meters; see Figure 6.9.3). It is thought that the mooring may have been leaning due to the large current velocities.

The analysis for all thermistor data is very preliminary at this stage. The loggers must be re-calibrated at EAWAG after the cruise. After the calibration, these data will be used to determine the water column energetics as well as overturn length and frequencies, and a mass transport phenomena.

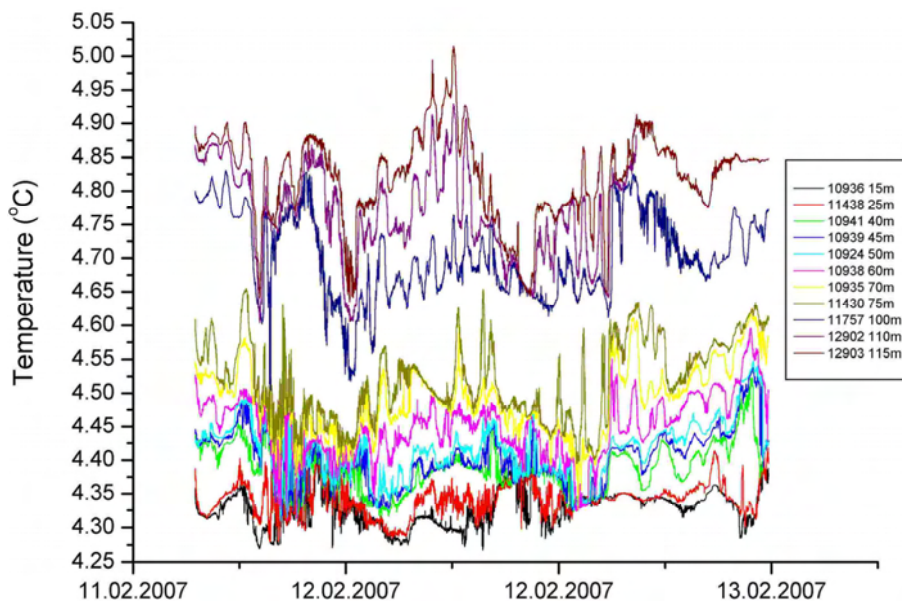


Figure 6.9.1: Temperature time series from M1 at LM9.

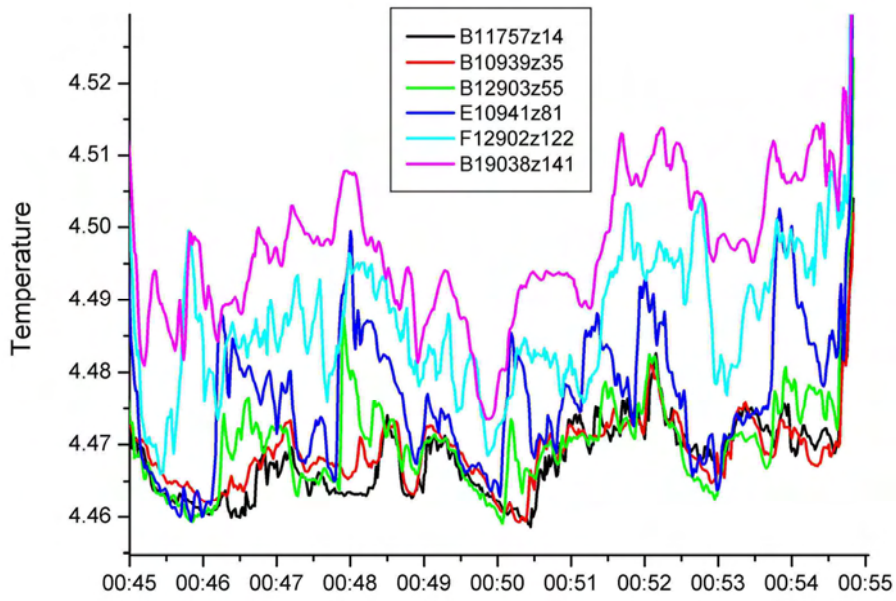


Figure 6.9.2: Temperature time series from BWS2 lander at LM9.

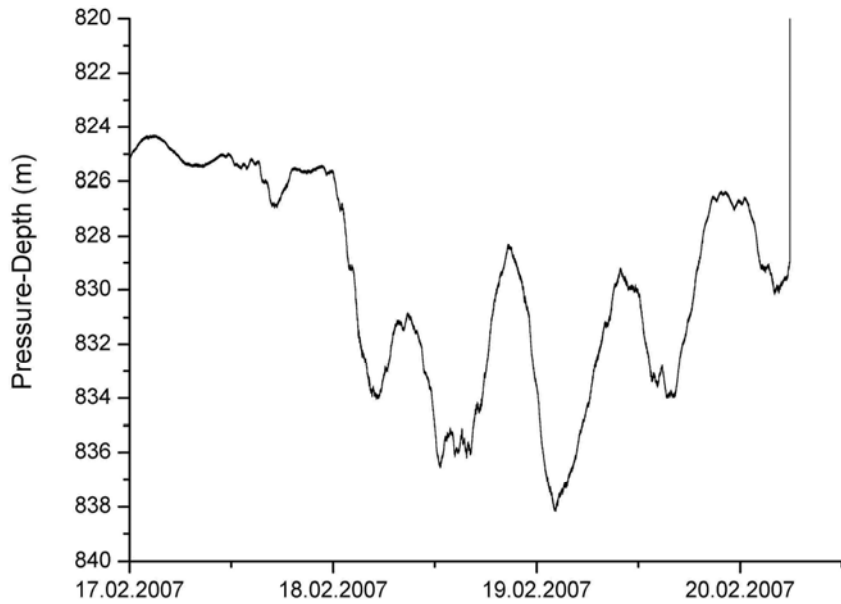


Figure 6.9.3: Pressure time series from M2 at Tui (Wairarapa). 15 m fluctuations suggest mooring was tilting due to large currents.

Table 6.9.1: Mooring configuration at LM9. Location was 177:49.344 40:2.042 with a water depth of 1215 m.

Mooring 1	CTD 17 prior to deployment
LM 9	CTD 22 after retrieval

Start	11 Feb 07 21:00 UTC
Stopped	13 Feb 07 ~08:00 UTC

Lander codes Mode A on both

SN 432		SN 361	
Enable	5967	3505	
Rel	5969	3501	3585

Thermistor	Height (m)	
8273	390	
8829	375	
8872	350	
8825	340	
8819	325	
8828	300	
8263	275	
8824	250	
8817	225	
8821	200	
8820	170	
8870	140	
12903	115	
12902	110	
TDR (silver)	100	Pressure
11430	75	
10935	70	
10938	60	
10924	50	
10939	45	
10941	40	
10923	30	Dead dead dead
11438	25	
10936	15	
8823	10	
8268	9	

Table 6.9.2: Configuration for BWS2 loggers at LM9. Location was 177:49.213, 40:3.199 and depth of 1113 m.

Mooring on Bottom Water Sampler. Thermistors were configured on leg.

Start time	09.02.2007 00:01	UTC
Stop time	10.02.2007 00:30	

Depth from bottom (cm)*	Serial No.	Comments
14	11757	Pressure
35	10939	
55	12903	
81	10941	
103	10923	No data, logger date reset - this one crushed on the next deployment
122	12902	TDO
141	10938	

*measured from the top of foot

Table 6.9.3: Configuration for BWS3 loggers at LM9.
Deployed 22 Feb

BWS 3		
Distance* (cm)	Type	Ser.No.
7	TR1000	8263
38	TR1000	8268
74	TDR	Silver
107	TR1000	8823
141	TR1000	8272

* measured up from foot

Table 6.9.4: Configuration for TM4 and TM5 at LM9. Mooring were retrieved at the end of Leg 3.
Deployed 22:00 23 Feb

40: 2.719 177:49.927

M4 Tui	Reference mooring		
Depth	Distance	Type	Ser.No.
1100	0	TR1000	8270
1080	20	TR1000	8824
1060	40	TR1000	8268
1040	60	TR1000	8821
1020	80	TR1000	8829
1000	100	TR1000	8823
980	120	TR1000	8817
960	140	TR1050	10938
940	160	TR1050	10939
920	180	TR1050	11438
900	200	TR1050	10941

Release codes Mode A on both Reference Mooring

SN 432		SN 361	
Enable	5967	3505	
Rel	5969	3501	3585

Deployed 22:40 23 Feb

40: 3.251 177:49.139

M5 Tui		Marking on		
Depth	Distance	Rope	Type	Ser.No.
1100	0	200	TR1000	8272
1080	20	220	TR1000	8820
1060	40	240	TR1000	8819
1040	60	260	TR1000	8825
1020	80	280	TR1000	8828
1000	100	300	TR1000	8263
980	120	320	TR1000	8827
960	140	340	TR1050	11430
940	160	360	TR1050	10935
920	180	380	TR1050	10936
900	200	400	TR1050	10924

Eawag releaser codes are on release deck unit.

SN 266	SN 265
RX 12.00	RX 12.00
TX 13.50	TX 14 00

Cmd D = release

Cmd B = enable

Table 6.9.5: Configuration for Tui moorings TM 2 and TM 3 with locations at 175:27.767, 41:43.682 and 175:27.134, 41:43.265, respectively.

M2 Tui	Reference mooring		
Depth	Distance	Type	Ser.No.
851	0	TR1000	8272
831	20	TR1000	8268
821	30	TDR	Pressure
791	60	TR1050	10939
761	90	TR1050	10924
741	110	TR1050	10936
721	130	TR1060	13696
711	140	TR1060	13688
701	150	TR1060	13690
681	170	TR1060	13694
651	200	TR1060	13691

M3 Tui	Marking on			
Depth	Distance	Rope	Type	Ser.No.
821	0	200	TR1050	10941
791	30	230	TR1050	11438
761	60	260	TR1050	10935
741	80	280	TR1050	10938
721	100	290	TR1050	11430
711	110	300	TR1060	13693
701	120	310	TR1060	13695
681	140	340	TR1060	13692
666	155	355	TR1060	13689
651	170	370	TR1060	13697

6.10 Lander Deployments

S. Sommer, P. Linke, O. Pfannkuche, J. Greinert, J. Schneider v Deimling

Three GasQuant deployments were performed, one at Tui and two at the Faure Site (#209 GQ2, #247 GQ3; Figures 6.10.1 and 6.10.2).

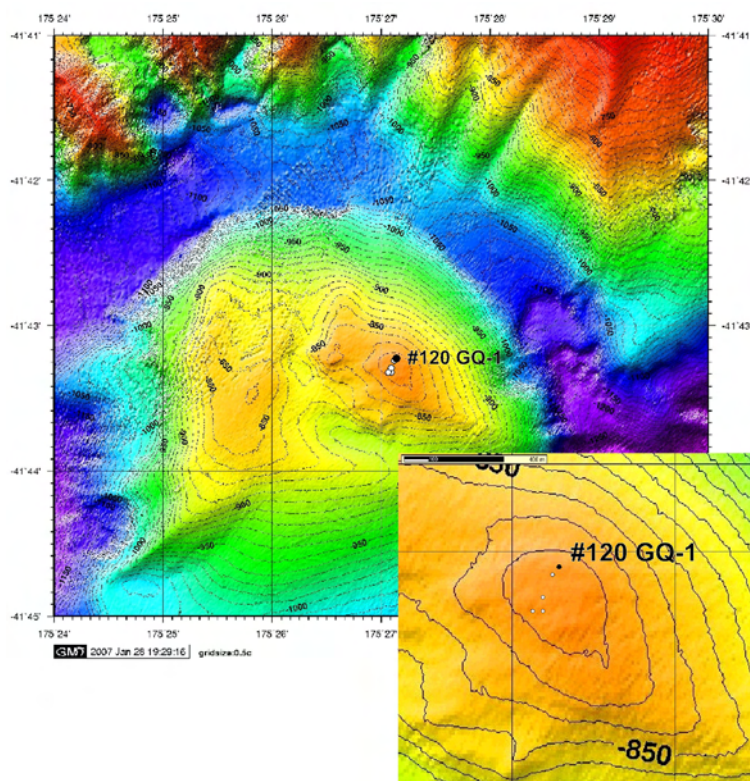


Figure 6.10.1: Map shows the Tui Site with flare positions (white dots) and the position of station #120 GasQuant-1.

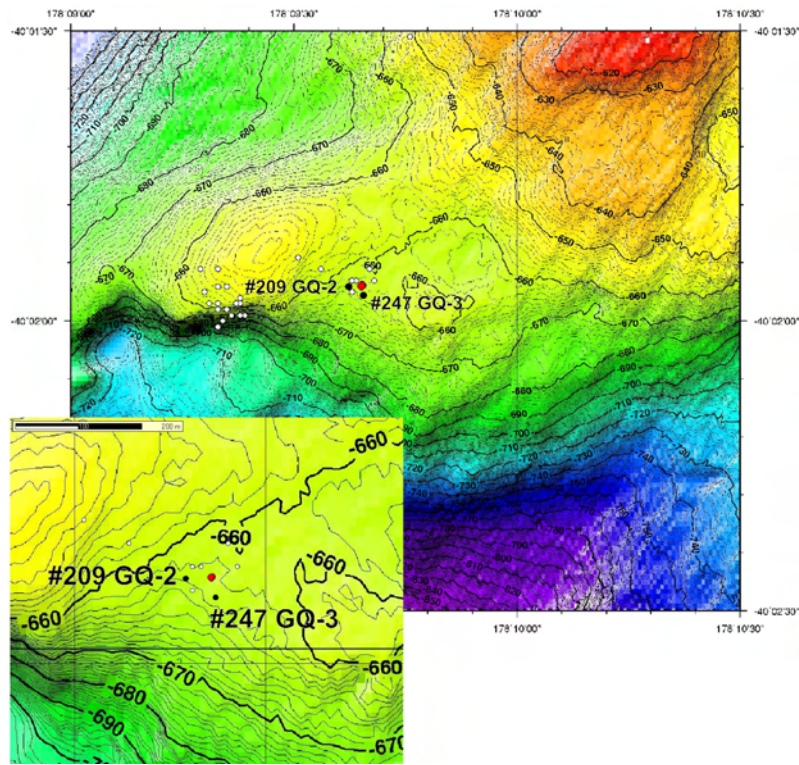


Figure 6.10.2: Map shows the Faure Site with flare positions (white dots) and the visually detected bubble release site (ROV 2; red dots) as well as the two GasQuant positions.

Figure 6.10.3 shows swath plots off all three deployments. Unfortunately GQ-3 doesn't show any indications of bubble release. One reason might be that the positioning wasn't accurate enough as during this deployment we had to use the ships HPR system which had an offset that we didn't correct accurately enough. Another reason might be that no bubbles have been released but we think this is more unlikely.

Swath plots from GQ 1 show several potential spots of bubble release events. However, looking into the data at these areas didn't reveal clear signs of bubble release events but more noise.

Changing the background detection to a moving average window of 2000 and decreasing the threshold to 1.6 times standard deviation obtains a complete different result (Figure 6.10.4). Trace plots (Figure 6.10.4a) of sample 120 to 180 of beam 14 show five significant events that occur about every 4 hours. The reason why these events were not picked up in Figure 6.10.4 is the much larger (longer) background window. Despite these clear changes in activity we are not absolutely sure if bubbles or system noise is the reason. It cannot be explained why strong signals occur all of a sudden from sample 124 to 125, hydroacoustically this cannot happen. Same is true for the end of the high intensity area from sample 248 to 249 where high signals suddenly do not occur anymore. Furthermore it is unclear why all five events spatially appear at the same position (sample 129) despite the fact that currents should have moved the bubbles over time to other samples.

However, we stacked the data shown in Figure 6.10.4a to get the overall activity of this potential seep site and plotted it in relation to ADCP data (Figure 6.10.5). Spectrum analysis via FFT show harmonic frequencies of 218 , 109, ~75, ~55, 45, 38 but no clear relation to tides. GasQuant 2 and 3 will be processed in a similar way with new processing techniques.

ADCP current data sets (RDI WorkHorse, 1200kHz) of all three GasQuant deployments are shown in Figure 6.10.6.

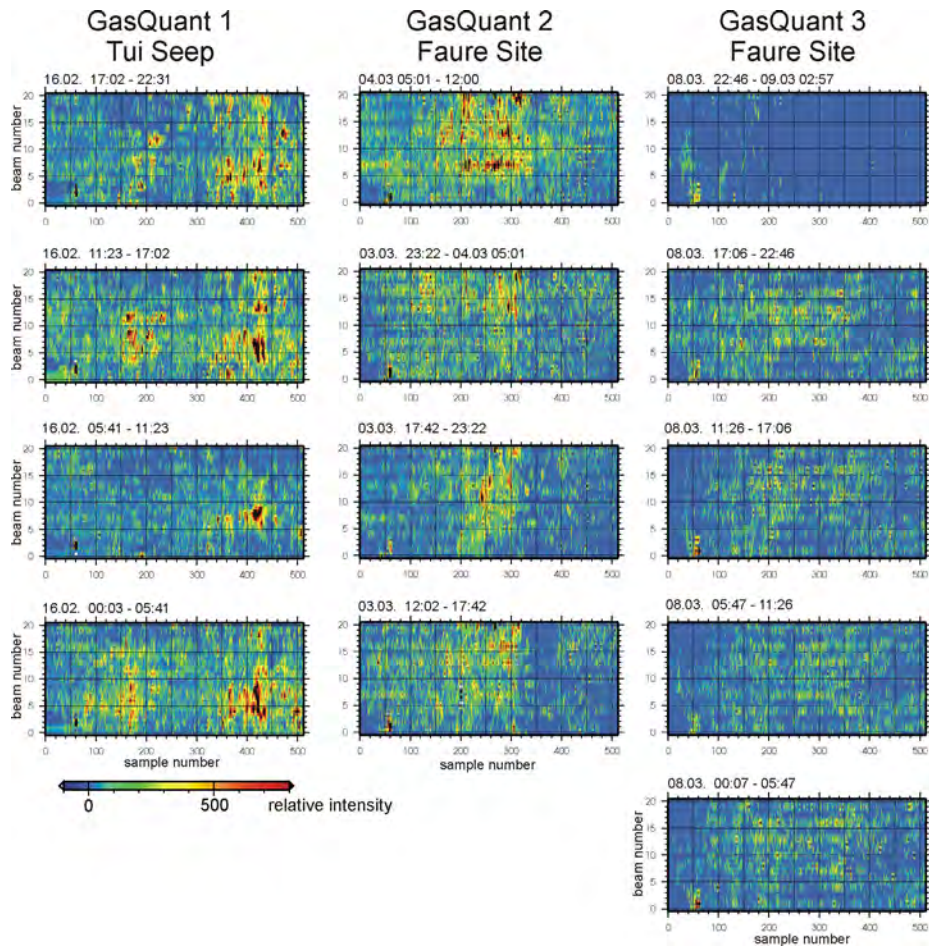


Figure 6.10.3: Swath plots of all three GasQuant deployments during SO191. GQ-1 at Tui shows few potential bubble release sites, a quite prominent one is in beam 6 to 9 and at sample 420 to 440. Data were processed with: background = moving average of 200 pings, target window of 4 pings, threshold = 2 times standard deviation of entire trace. These values gave very good results for GasQuant data from the Black Sea.

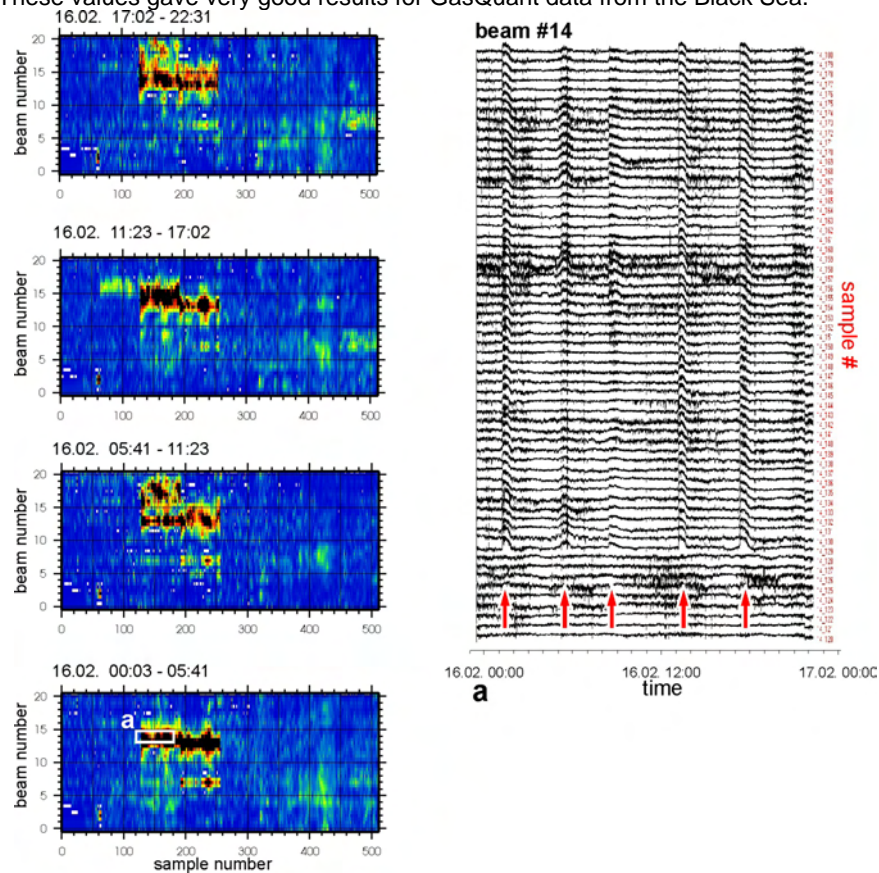


Figure 6.10.4: Swath plots of GQ-1 with: background = moving average of 2000 pings, target window of 4 pings, threshold = 1.6 times standard deviation of entire trace. Clearly shown are higher intensities in beam 13 to 15 between sample 125 and 248. The trace plot (a) is from beam 14, showing samples 120 to 180. Red arrows indicate potential bubble release events.

GasQuant 1, Tui Seep

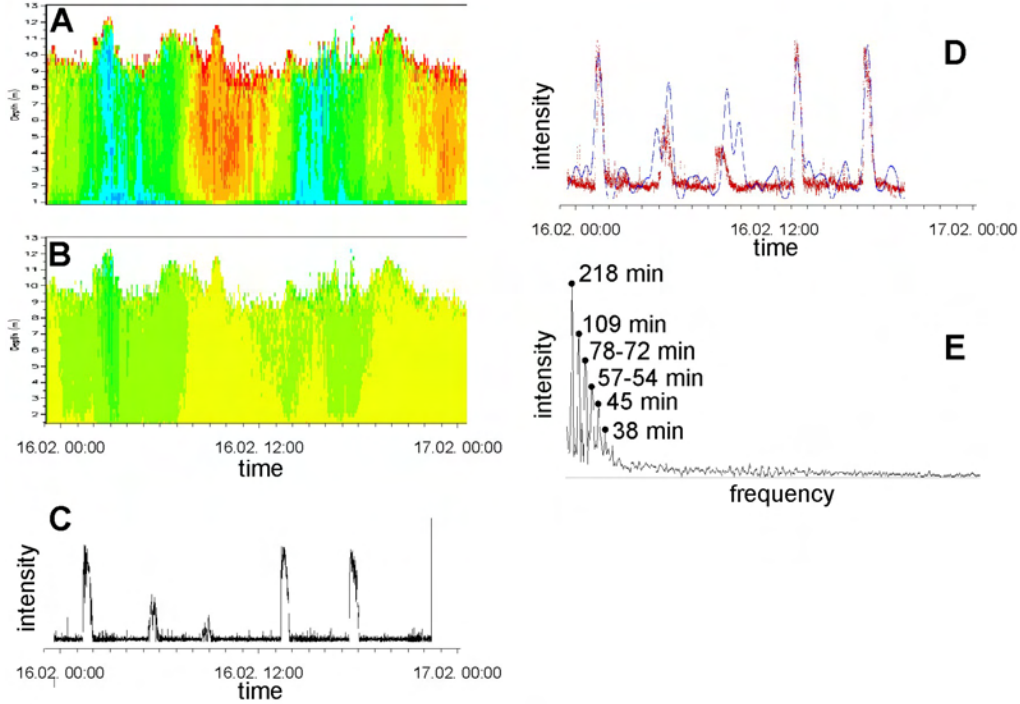


Figure 6.10.5: GasQuant 1 data set. A (velocity) and B (direction) are ADCP data (see Figure 6.10.6 for scale). C shows the stacked data of beam 14 as shown in Figure 6.10.4a. D depicts the data used during the FFT analysis (red) and the sum of the six main frequencies (blue) as shown in the power spectrum (E).

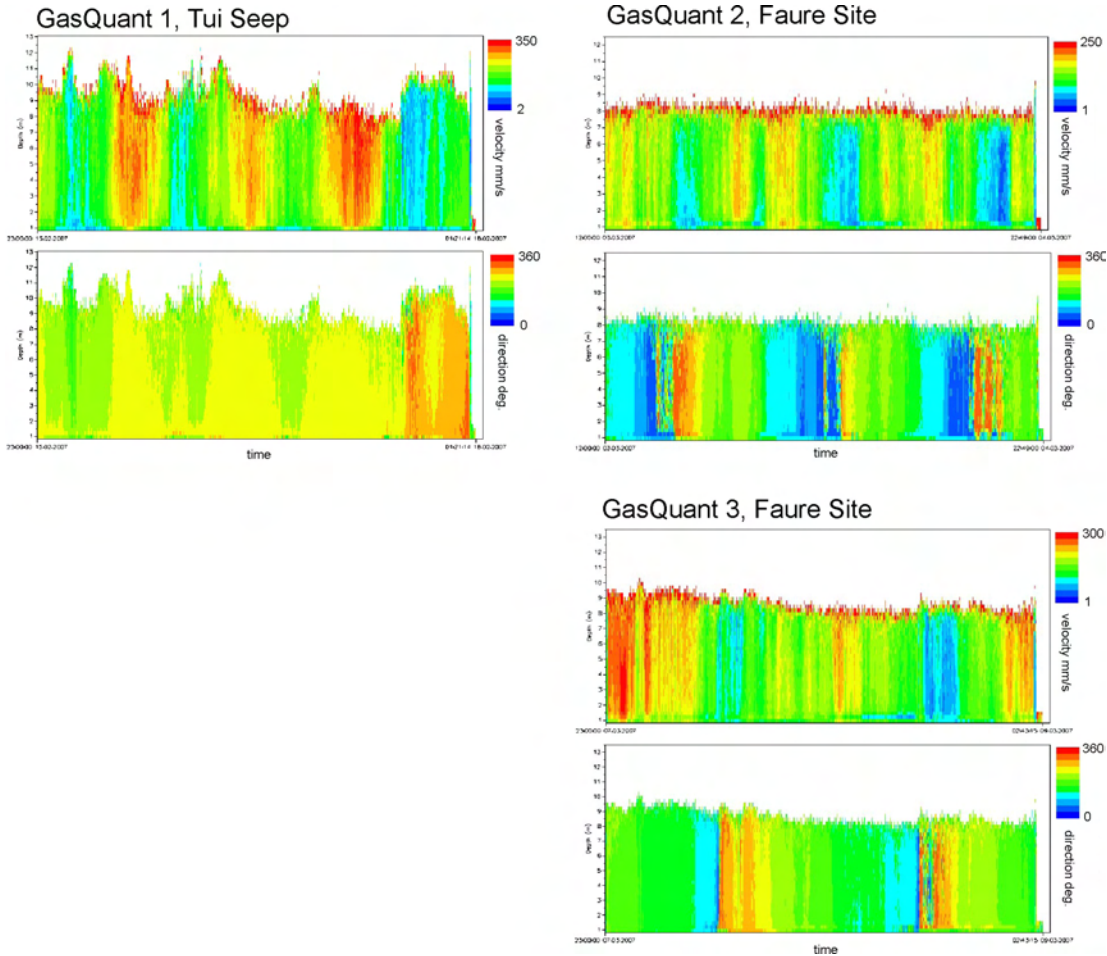


Figure 6.10.6: Current velocity and direction of the 300kHz ADCP recorded during the three GasQuant deployments.

Ecology and Geochemistry of Hikurangi margin seep sites

During leg 2 and leg 3 of Sonne cruise 191 we focused on 3 areas alongside the Hikurangi margin; the LM9 area (Bears Paw, depth ~1100 m), the Rock Garden area (~ 670 m) close to Hawkes Bay and Wairarapa (~ 1050 m) at the southern tip of the North Island of New Zealand. Table 6.10.1 (Appendix A) displays the gears and the biogeochemical parameters which were measured during the respective deployments.

High resolution side scan imaging (Weinrebe, Klauke et al., IFM-GEOMAR) revealed distinct carbonate concretions at all investigation areas. The carbonates as well as the transition zones between the carbonates and the sediment are densely populated by typical seep fauna (vestimentiferan tube worms, bivalve mollusks). At the fringes of these carbonate platforms prominent dark sediment spots were observed regularly. ROV observations (Naudts et al., RCMG) showed that gas seepage from these sites occurs. These sediment patches are hitherto referred to as rain drop sites. Sediment sampling and in situ seabed methane emission measurements were concentrated on these transition zones and the rain drop sites. In some cases we had difficulties to sample these spots. This was due to the presence of massive carbonates below a thin coverage of sediments (several centimeters) which did not allow the gears to deeply penetrate into the sea floor.

Ampharetid polychaetes constitute the key fauna of seep sediments

In all three areas extremely high abundances of polychaetes (up to 10320 ind. m⁻²) belonging to the family Ampharetidae were found to be associated with high pore water concentrations of methane, Figure 6.10.7c,d. Image analysis revealed that abundant colonization of these organisms is clearly associated with the above introduced rain drop sites, Figure 6.10.7a,b. The coloration of these spots varies from grey to dark-grey and is likely due to the precipitation of sulfides and is clearly set off from the light-brown non methane seepage affected sediment. On the surface of the sediment the presence of the worms/tubes cause darkish depressions in sediment leaving the impression of rain drops falling on mud surfaces. The ampharetids live in relatively thin-walled fibrous tubes of organic material which in some cases extend several millimeters out of the sediment surface into the water column. The outside of the tubes is covered with sediment particles. In some cases there are highly dense accumulations of polychaete tubes sticking out of the sediment forming polychaete lawns. In intact sediment cores with overlying bottom water which were kept under in situ temperature (LM 9, Bears Paw ~ 4.3 °C; Rock Garden ~ 7.5 °C; Wairarapa ~ 5.2 °C) we observed that these organisms predominantly remain in their tubes (Figure 6.10.7f) and only 4 pairs of tentacles extending into the bottom water and mouth parts are visible. Sometimes, probably when the oxygen concentration of the bottom water is too low they extend 2-3 cm into the bottom water or graze on elevated sediment structures (MUC 22), Figure 6.10.7e.

The tubes penetrate about 2-3 cm deep into the sediment. At several sites we observed highly dense accumulations of tubes largely contributing to the overall structure of the sediment, Figure 3g. Apparently, two different putative species of these Ampharetids colonize the investigated seep sediments. The length of these organisms varied between 11.1 and 23.8 mm, their width (posterior) was in the range between 0.7 to 1.6 mm.

These polychaetes possess a well established digestive tract and mouth parts. Ampharetids are deposit feeding organisms, with their retractile buccal tentacles they might graze on bacteria (cf. Figure 6.10.7e) or other small sized organisms. A series of respiration measurements of single ampharetids from different sites (MUC 12, 20, 22, 26) have been conducted to relate their oxygen demand to the TOU of their habitat.

In situ seabed methane emission and total oxygen uptake

Wairarapa

At North Tower area seabed methane emission varied between 0.3 to 264.6 mmol m⁻² d⁻¹ whereas at the sites with maximum seabed methane emission dense populations of ampharetid polychaetes were observed. The oxygen uptake varied between 14.1 to 291.05 mmol m⁻¹ d⁻¹. Contrastingly, at a nearby reference site (Takaha, BIGO 6) no methane emission was detected and total oxygen uptake was 3.2 mmol m⁻² d⁻¹.

Rock Garden

At Rock Garden similar to the North Tower area the maximum seafloor methane emission was 286.7 mmol m⁻² d⁻¹ and as observed at the Wairarapa sites again associated with extremely high abundances of ampharetids (FLUFO 5). Maximum total oxygen uptake at this site was 140.2 mmol m⁻² d⁻¹. At a site characterized with the sporadic occurrence of small tube worms and very low

abundance of ampharetids (BIGO 4) seabed methane emission was $5.1 \text{ mmol m}^{-2} \text{ d}^{-1}$ associated with a total oxygen uptake of $72.4 \text{ mmol m}^{-2} \text{ d}^{-1}$.

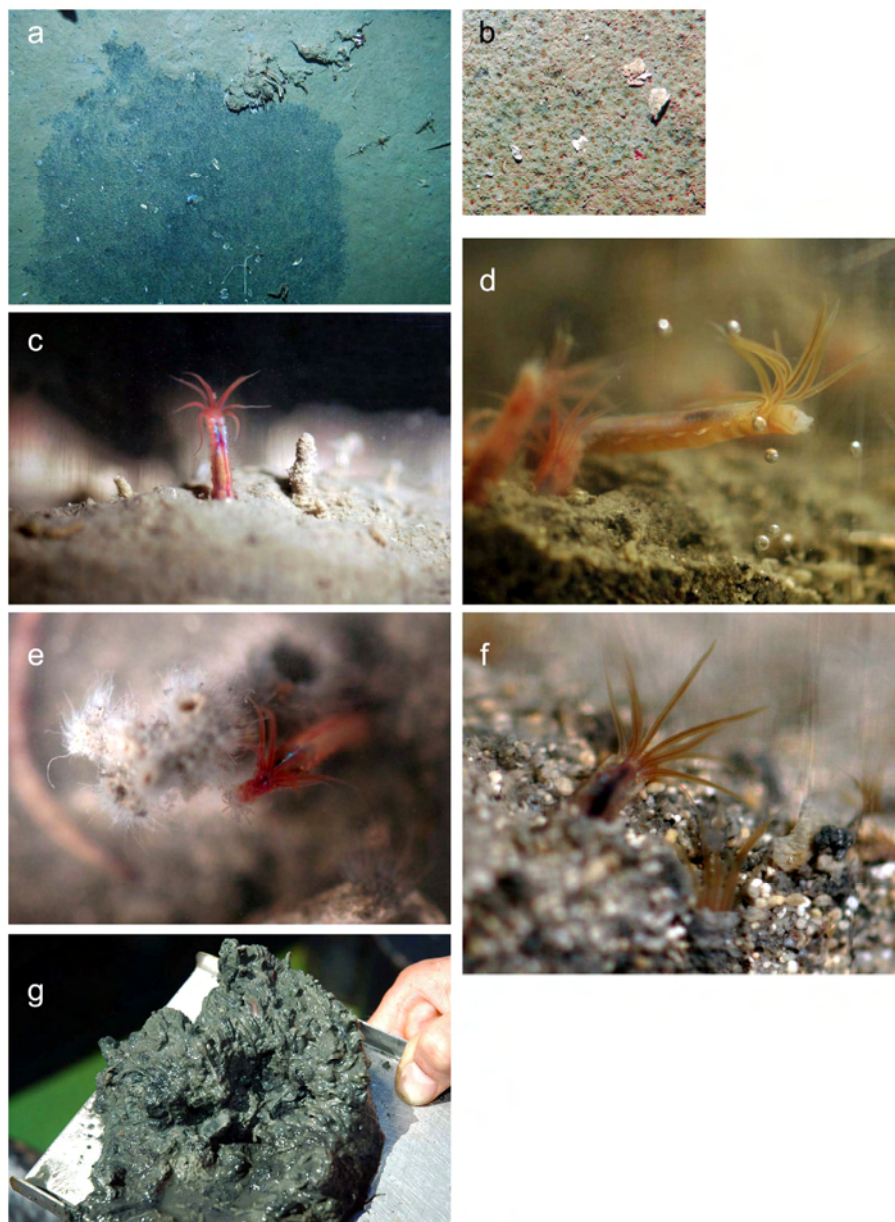


Figure 6.10.7a-g: a: Rain drop site at the Wairarapa region, b: close up of a rain drop site revealing that ampharetids forming the depressions in the sediment, c,d: two different putative species of ampharetids extending into the water column, e: ampharetid probably grazing on filamentous structures (bacteria?), f: often these organisms live drawn back into their tubes with only 4 pairs of tentacles and mouthparts visible on the sediment surface, g: massive occurrence of tubes largely contributing to the overall structure of the sediment. Photos credits: a/b: D. Bowden (NIWA), c-g: S. Sommer (IFM-GEOMAR).

LM9, Bears Paw

At this site seabed methane emission was measured at a weak methane seep site not associated with the occurrence of ampharetid polychaetes (FLUFO 1). Whereas in the FLUX chamber living typical seep organisms such as tube worms and juveniles of the bivalve mollusks *Acharax* and *Calyptogena* were retrieved, inside the backup chamber (BU) which is mounted only about 40 cm away from the FLUX chamber only shell debris and a few very small tube worms were recovered. Methane flux in the BU chamber was 0.01 compared to a maximum methane emission recorded in the FLUX chamber of $0.9 \text{ mmol m}^{-2} \text{ d}^{-1}$. The respective total oxygen uptake was 1.6 and $4.4 \text{ mmol m}^{-2} \text{ d}^{-1}$. Methane consumption experiments with the tube worms indicate that the tube worms and/or microbes attached to the tube are able to consume methane at a high rate of about $0.6 \text{ nmol ind}^{-1} \text{ h}^{-1}$. Time course of methane concentration in the FLUX chamber indicate that methane release from the sea floor was not constant but occurred in single events. An increase of the methane concentration of the FLUX chamber after $\sim 33 \text{ h}$ coincides with a high echo intensity recorded by the ADCP mounted on FLUFO indicating gas release from the sea floor.

Pore water gradients of methane, oxygen and sulfide

Please note that the data described in the following are preliminary and are not corrected yet for pH or porosity. Oxygen fluxes were only mentioned to highlight gross differences between the different sites.

At the reference sites (BIGO 6, MUC 6) not affected by methane seepage pore water methane concentrations of the surface sediments were below $1 \mu\text{mol dm}^{-3}\text{sed}$. Sulfide was not detected in the surface horizons. Oxygen penetrated $\sim 11 - 13 \text{ mm}$ deep into the sediments, diffusive oxygen fluxes were $1.9 - 2.3 \text{ mmol m}^{-2} \text{ d}^{-1}$, Figure 6.10.8.

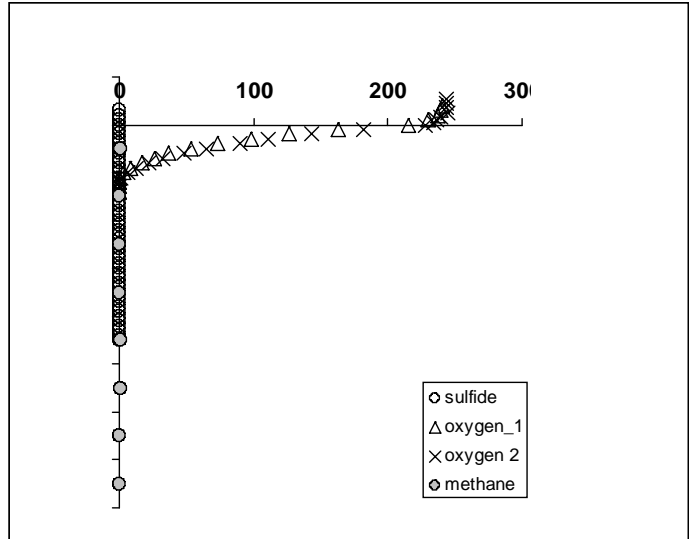


Figure 6.10.8: Pore water profiles of methane and micro profiles of sulfide and oxygen at the reference site Takahae (BIGO 6).

We investigated several sites with intermediate and high numbers of ampharetid polychaetes (MUC 3/5/12/13/15/22/26/29/40, BIGO 4, FLUFO 4/5/6). Common to all sites characterized by highly abundant ampharetids was that methane concentrations of the surface sediments are very high ($> 1 \text{ mmol dm}^{-3} \text{ sed}$) with still up to $330 \mu\text{mol dm}^{-3} \text{ sed}$ at the uppermost sediment layer (MUC 12, Wairarapa), Figure 6.10.9 right panel. At sites with less abundant ampharetids pore water methane concentrations were $< 1 \text{ mmol dm}^{-3} \text{ sed}$. In comparison to the reference sites oxygen penetration depth is strongly reduced in the methane seep sediments with intermediate (1.8 – 3.0 mm) and high abundances of ampharetids (1.0 – 1.3 mm). The maximum diffusive oxygen flux was measured at the site MUC 40 with $14.7 \text{ mmol m}^{-2} \text{ d}^{-1}$. At the sites with intermediate abundance of ampharetids the depth of the sulfide front was about 20 mm sediment depth with relatively low sulfide concentrations compared to the sites with dense populations where the onset of free sulfide in the porewater was in about 6 mm.

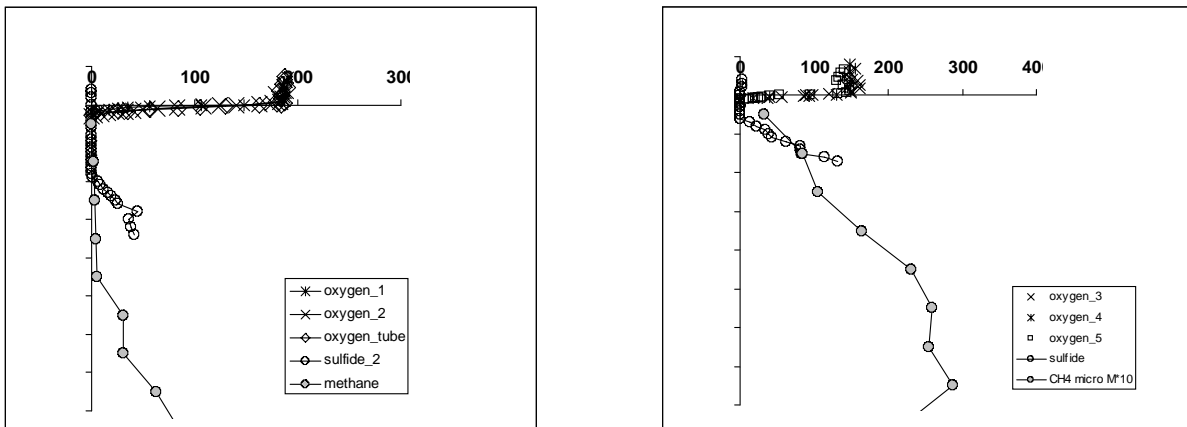


Figure 6.10.9: Pore water gradients of CH_4 and micro profiles of O_2 and HS^- . Left panel: site with intermediate abundances of ampharetids (MUC 15, Wairarapa); right panel: site with high abundances of ampharetids (MUC 12, Wairarapa). The sulfide profiles are not corrected yet for pH. Methane profiles not corrected for porosity.

Even on millimeter scales the seep sites were found to be highly variable and biologically diverse. At sites densely populated with ampharetids the topography of the sediment surface provided a range of micro-habitats, Figure 6.10.10.

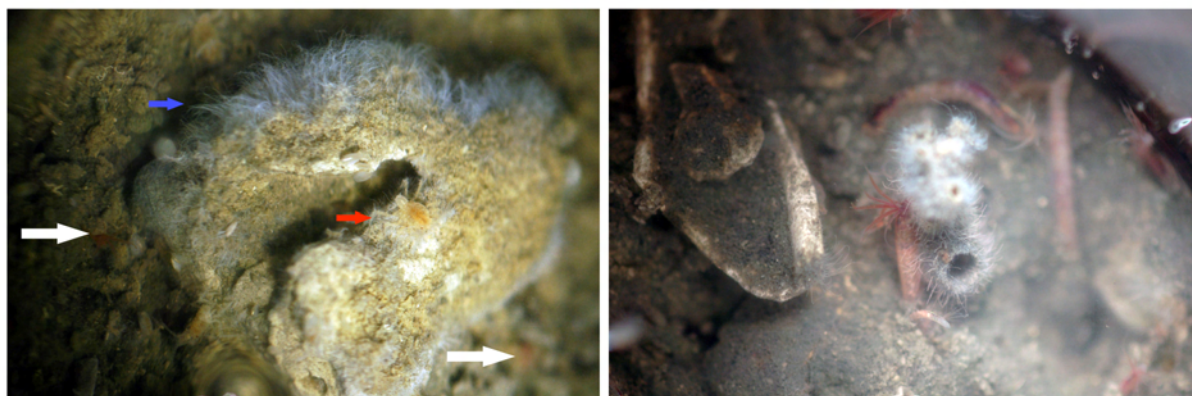


Figure 6.10.10: left panel: (MUC 40) chunk of carbonate densely covered with filaments (blue arrow, bacteria?), ampharetids (white arrows) are present but out of focus, an isopod (red arrow) can be detected on the surface of the carbonate; right panel: (MUC 22) tube structure covered with filaments (bacteria?) surrounded by several ampharetids (cf Figure 6.10.7e).

Along a transect across the tube structure displayed in Figures 6.10.7e and 6.10.10 vertical micro-gradients of oxygen and sulfide changed considerably. Further away from the tube structure oxygen penetrated 4 mm deep into the sediment and the sulfide front was located in a sediment depth of 8 mm (P1), Figure 6.10.11 right panel. Directly at the tube (P4) the oxygen concentration in the water column was close to zero and increased levels of sulfide were measured in the water column up to 6 mm above the sediment surface, Figure 6.10.11 left panel. Probably these empty tube structures might serve as escape routes for sulfide and other solutes such as methane from deeper sediment horizons to the water column. An ampharetid polychaete was observed to constantly move around this structure probably feeding on these white filaments which might be sulfide oxidizing bacteria.

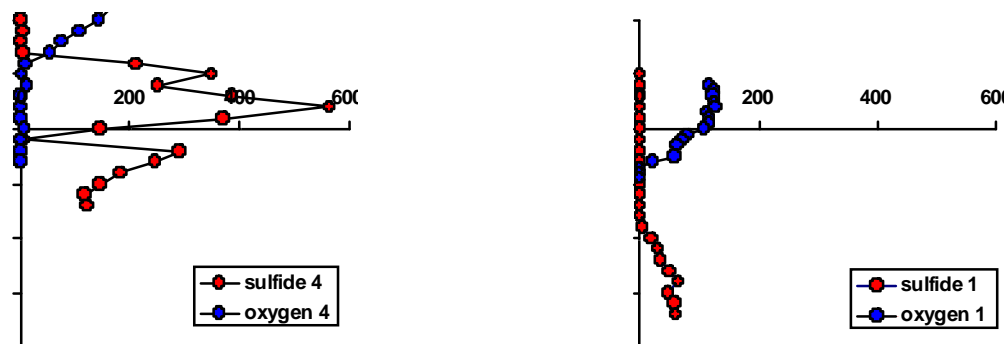


Figure 6.10.11: Micro profiles of oxygen and sulfide measured directly at the tube structure densely covered with filaments (bacteria?), left panel; and a few millimeter distant from this structure, right panel.

6.11 Foraminiferal and Metazoan Biology

A. Thurber, K. Kröger, R. Martin, L. Zemke-White, S. Boyd

A total of 232 megafaunal specimens belonging to 26 taxonomic groupings were collected during Leg 3. These include seep fauna such as *Bathymodiolus* mussels and *Lamellibrachia* polychaetes. These specimens will be identified by appropriate experts and genetic analyses will be carried out to corroborate their identification as well as address how genetically distinct they are from populations in other oceans.

The 11 multicore and lander samples (Tab. 6.11.1, 6.11.2) that were sorted live yielded a total of 2,625 specimens belonging to 98 putative species. A total of 333 were collected for stable isotopic analyses and 264 for fatty acid/ lipid analyses and will be used to construct a food web. The reference collection, which consists of 146 specimens will be distributed to their respective taxonomists. The quantitative megafaunal cores will be sorted and identified to species level and the species assemblage compared to that of other seeps around the world.

The ~500 foraminiferal samples collected during this cruise will be used to 1) compare living and dead foraminiferal assemblages in different seep microhabitats; 2) compare these assemblages with the fauna extant in other New Zealand waters and with seeps in other parts of the world (e.g. Hydrate Ridge, Blake Ridge, Gulf of Mexico); 3) measure carbon and oxygen isotope ratios to assess the influence of methane on foraminiferal tests, identify methane sources, and test the possibility of using these to identify hydrate dissociation; 4) perform Mg/Ca analyses to measure the extent of early diagenetic alteration to the tests; 5) use down-core data from both multicores and gravity cores to evaluate the evolution of seepage over time.

Table 6.11.1: Stations where samples were collected aboard RV Sonne cruise 191 leg 2

	Station	Equipment	Equipment No.	Location
Sediment Slabs				
	51	TV-BC	1	LM9
	66	TV-BC	2	LM9
	96	TV-BC	5	LM9 south
	98	TV-BC	7	LM9
	158	TV-MUC	16	Wairarapa - North Tower
Forams				
	66	TV-BC	2	LM9
	96	TV-BC	5	LM9 south
	98	TV-BC	7	LM9
	158	TV-MUC	16	Wairarapa - North Tower
Macrofauna				
	50	GC	1	LM9
	51	TV-BC	1	LM9
	54	TV-MUC	3	LM9
	56	TV-MUC	4	LM9
	66	TV-BC	2	LM9
	73	TV-MUC	5	LM9
	77	FLUFO	1	LM9
	78	TV-MUC	6	LM9
	85	TV-MUC	7	LM9 south
	86	TV-MUC	8	LM9 south
	87	TV-G	4	LM9
	95	GC	7	LM9 south
	96	TV-BC	5	LM9 south
	97	TV-BC	6	LM9 south
	98	TV-BC	7	LM9
	113	BC	8	Wairarapa
	114	BC	9	Wairarapa
	124	TV-MUC	12b	Wairarapa
	125	GC	10	Wairarapa
	127-3	BC	11b	Wairarapa
	137	TV-MUC	13	Wairarapa - North Tower
	138	TV-G	5	Wairarapa - North Tower
	142	BIGO	2	Wairarapa - North Tower
	148	TV-G	6	Wairarapa - Tui Flare
	149	TV-G	7	Wairarapa - South Tower
	150	FLUFO	2	Wairarapa - North Tower
	151	TV-G	8	Wairarapa - Pukeko
	158	TV-MUC	16	Wairarapa - North Tower
	162	BIGO	2	Wairarapa - North Tower
	164	TV-G	9	LM 9
	165	TV-G	10	LM 9

Table 6.11.2: Location, type of gear, and samples taken for Foraminiferal, Mega- and Macrobenthos studies aboard RV Sonne cruise 191 leg 3. Abbreviations include: TV-MUC (Video Guided Multicorer), GC (Gravity Core), BIGO and FLUFO (Lander deployments), TV-G (Video Guided Grab), Mega (Megafauna), Macro (Quantitative macrofauna), Foram (Foraminifera), Live (Sorted live and sub-sampled for genetic, reference, stable isotopic and lipid analyses), Gen (bulk preserved in 95% Ethanol for genetic analyses)

Station number/ Location	Gear & no.	Location		Depth (m)	Samples Taken
		Lat. (S.)	Long. (E.)		
Bear's Paw					
186	TV-MUC 19	40:03.18	177:49.20	1078	Macro, Foram, Live
197	TV-MUC 21	40:03.20	177:49.13	1104	Live
198	TV-MUC 22	40:03.173	177:49.58	1107	Macro, Foram, Live
LM-3					
216	TV-MUC 28	40:1.98	178:09.65	664	Macro, Foram, Live
238	TV-G 17	39:58.58	178:14.16	907	Mega
259	TV-MUC 36	40:01.90	178:09.65	659	Macro, Foram
260	TV-MUC 37	40:01.89	178:09.71	661	Macro, Foram
Moa					
227	TV-G 14	40:03.28	177:48.75	1120	Mega
Rock Garden					
229	TV-G 15	40:01.78	178:11.40	660	Mega
230	TV-G 16	40:01.58	178:11.01	655	Mega
239	TV-G 18	40:03.09	178:13.83	891	Mega
250	GC 26	40:00.91	178:16.46	1412	Foram
<i>Kaka</i>					
232	TV-MUC 32	40:02.15	177:47.98	1176	Live
242	TV-MUC 34	40:02.14	177:47.91	1175	Macro, Foram, Live
261	TV-MUC 38	40:02.12	177:47.66	1171	Macro, Foram, Live
262	TV-MUC 39	40:02.15	177:47.95	1167	Macro, Foram, Live
Faure Site					
265	FLUFO 5	40:01.98	178:09.42	661	Live, Gen, Macro
Wairarapa					
278	GC 32	41:47.76	175:24.10	1094	Foram
289	TV-MUC 42	41:46.93	175:24.13	1059	Failed Drop
290	TV-MUC 43	41:46.94	175:24.20	1059	Macro, Live
291	TV-MUC 44	41:46.93	175:24.16	1061	Macro, Foram
298	BIGO 5	41:46.93	175:24.35	1056	Live, Gen, Macro
302	GC 42	41:47.33	175:24.54	1053	Foram
277	FLUFO 6	41:46.90	175:24.10	1048	Live, Gen, Macro
307	BIGO 6	41:46.74	175:25.14	1051	Gen, Macro
Takahae					
304	GC 53	41:46.34	175:25.58	1054	Foram
309	TV-MUC 46	41:46.92	175:25.62	1054	Foram, Live
315	TV-MUC 47	41:46.32	175:25.69	1057	Foram, Macro
<i>Uruti</i>					
316	TV-G 19	41:17.53	176:32.87	756	Mega

6.12 Microbial Ecology

J. Arnds, V. Beier, H. Niemann, D.I Santillano, T. Treude, G. Wegener

Multicorer samples

Targets of TV-guided multicorers were so called "Black Spot- and Bacterial Mat Sites", "pogonophora Sites", "Raindrop Sites", and "Reference Sites".

Black Spot Sites were characterized by black surface sediments sometimes covered with small spots of white bacterial mats. Sampling of these sites was difficult because the spots had usually a small diameter, were rather scattered or surrounded by carbonates. At Station 137 we were able to confirm the presence of filamentous sulfide-oxidizing bacteria (probably *Beggiatoa*). They formed small white spots on the greenish-grey sediment surface (see Figure 6.12.1). Underneath the very thin (ca. 0.5

cm) greenish-grey surface the sediment turned black. Interestingly bacterial filaments were also found embedded into sediment below the top layer. Probably the bacteria are following the sulphide gradient deeper into the sediment.

Pogonophora Sites were characterized by high densities of symbiotic pogonophoran worms. These sites were characterised by bright grey sediments sometimes containing black layers in deeper sediment strata. The pogonophoran tubes extended vertically into the sediment and reached lengths of up to 20 cm.

Raindrop Sites had a blackish appearance on video footage with a high density of small depressions (like rain drops falling on flat sand). Each depression had a polychaet worm surrounded by a tube in its centre extending for about 1-2 cm into the water column as well as into the sediment. The activity of the worms caused an intense bioturbation in the first centimetres of the sediment. When exposed to oxygen limitation (closed cores) the worms left their tubes and climbed up the core walls.

The *Reference Site* was sampled outside the cold-seep area at a similar water depth. These sediments were bright grey with no visible seep-related fauna (Figure 6.12.2).

Gravity corer samples

GC's were sampled if gas hydrates were present in the sediment. At station 64 (GC 2), samples were taken to investigate the deeper layers under a *Pogonophora* Site in addition to MUC 2 (Station 45).

TV-Grab samples

Chemoherm carbonates were investigated to study the formation of authigenic carbonates during AOM activity. Here, four carbonate pieces and sediments attached to the chemoherm with aragonite precipitates were sampled to investigate microbial activity and diversity. One aim was to directly show ^{14}C - CaCO_3 precipitation from ^{14}C -methane incubations.

CTD samples

Selected water samples from depth profiles revealing high concentrations of methane were incubated with ^{14}C -methane to study aerobic methanotrophic activity and link them to methane gradients in the water column. Additionally (Station 171, 210 and 211), water was filtered for molecular studies of the microbial methanotrophic community. At the time of sampling and writing this report, the institutes / scientists who will work on these samples have not been identified.

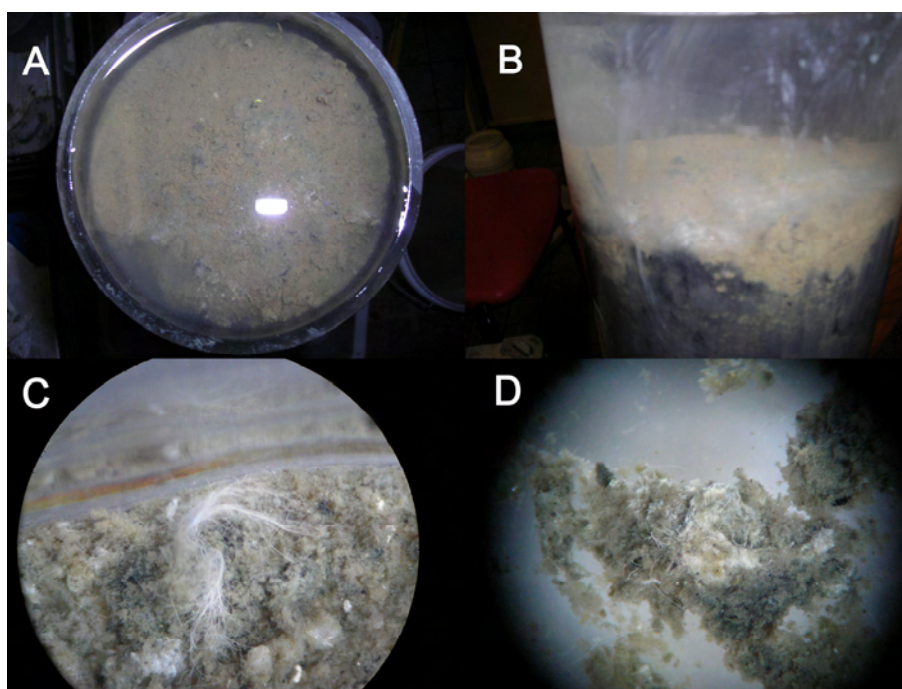


Figure 6.12.1: MUC Core G, Station 137 showing white spots of filamentous sulfide-oxidizing bacteria on the sediment surface (A). The very thin greenish grey surface sediment was followed by a black sediment layer (B). (C) White bacteria filament from the sediment surface, (D) filaments embedded into the top sediment layer.

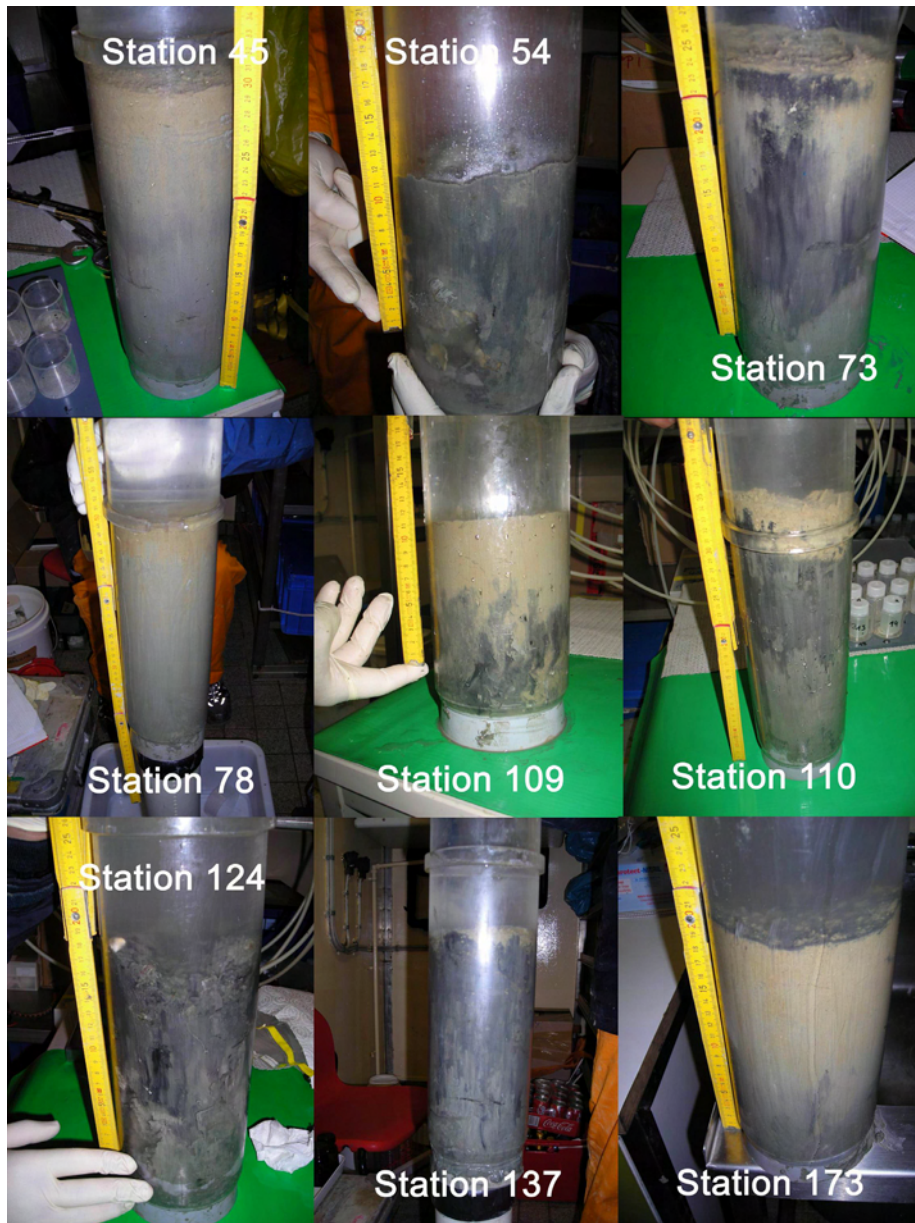


Figure 6.12.2: Selection of MUC cores.

Sediment samples were obtained from multi core and water samples were collected from CTD water columns. All samples were analyzed for methane oxidation rates. Microbial analysis of methanotrophs will also be performed through cultivation techniques and PCR. The following samples were analyzed.

Station	Sample source	Sample #
45	MUC	Core F
49	CTD 6	bottle 1, 3
54	MUC	Core A
S61	CTD 11	Bottle 8, 9, 17
S68	CTD 12	Bottle 7, 8
S73	MUC	Core H
S82	CTD 17	Bottle 1-8, 10-12, 14-24
S85	MUC	Core E
S89	CTD 18	Bottle 4, 22
S90	CTD 19	Bottle 1, 2, 10
S109	MUC	Core H
S110	MUC	Core B
S115	CTD 24	Bottle 5
S116	CTD 25	Bottle 4, 5
S119	CTD 28	Bottle 6, 9
S124	MUC	Core E
S137	MUC	Core G
S138	TV Grab	Rock sample
S144	CTD 35	Bottle 15
S145	CTD 36	Bottle 1
S146	CTD 37	Bottle 3
S157	MUC	Core C
S171	CTD	Bottle 1, 2, 4, 5, 6, 8, 10, 14, 18, 20, 22, 24
S173	MUC	Core B

6.13 Geochemistry

M. Haeckel, K. Krieger, M. Bausch, M. Marquardt (IFM-GEOMAR)

Rock Garden

At Rock Garden seep related sediments were generally extensively covered with (mostly dead) shells and shell debris as well as vestimentifera and carbonates. In between, small patches of black sediment or living clams and mussels occurred. Thus, sediment recovery was rather poor with ~10 cm for TV-MUC and ~1 m for GC deployments. Since it was impossible to retrieve sediment from the clam fields and carbonate areas, we concentrated on sampling the black sediment patches. The corresponding pore fluids show porewater bioirrigation in the top 4-5 cm that is probably attributed to the high abundances of polychaetes and pogonophorans (see chapter 6.10). Below this depth, sulfate is rapidly consumed by upward migrating methane. Hence, in these black sediment spots SO_4^{2-} generally declines rapidly below 5 cm and, correspondingly, total alkalinity and hydrogen sulfide values start to increase (Figure 6.13.1). In general, the seep influenced fluids are depleted in ammonium and show no deviations from seawater chloride and bromine concentrations, unless gas hydrate formation occurs near the sediment surface.

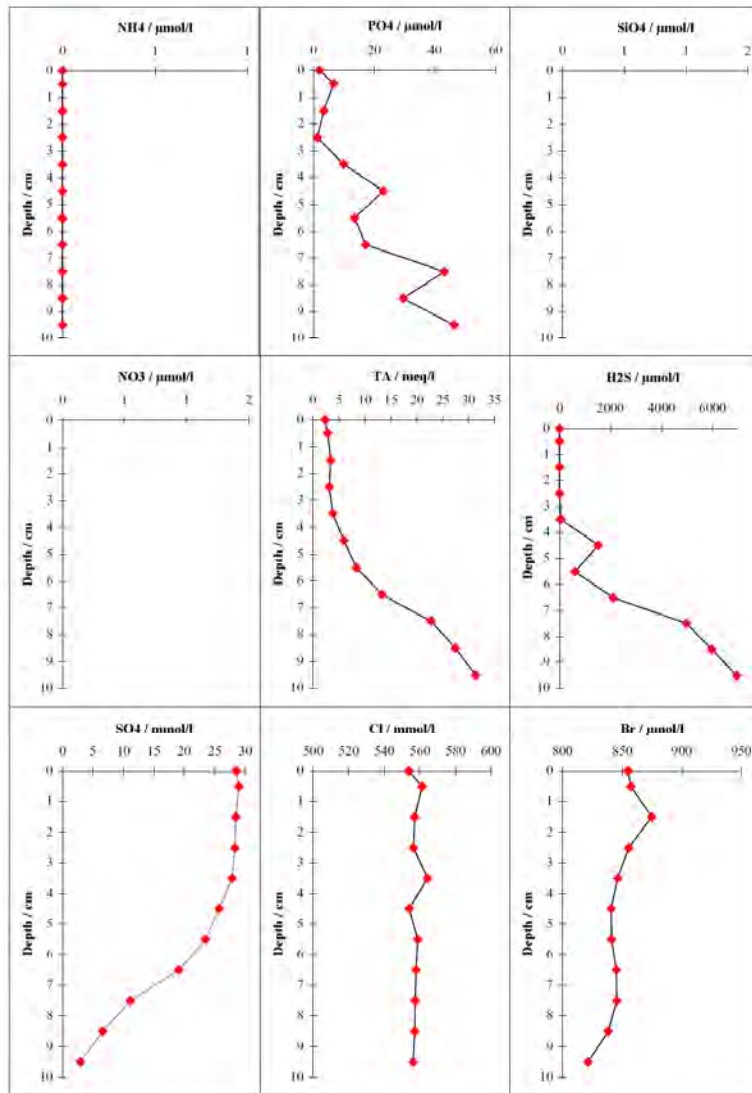


Figure 6.13.1: Porewater geochemistry of the black sediment spots at Rock Garden (258 MUC 35).

LM-9

M. Haeckel, K. Krieger, B. Domeyer, E. Hütten, M. Bausch, M. Marquardt, D. Müller (IFM-GEOMAR)

In the region of Okamere Ridge, we collected sediment samples from several seep areas, LM-9, Kaka, Moa, and Bear's Paw as well as 2 reference sites. All seep areas are extensively covered with (mostly dead) shells or shell debris and carbonate boulders and plates populated by vestimentifera tubes. In between, small patches of black sediment or living clams and mussels occurred. Again, we were more successful in sampling black sediment patches and areas only sparsely covered with shells, carbonates, and tubes.

The pore fluids of the black sediment patches show porewater bioirrigation in the top 4-5 cm that is probably attributed to the high abundances of polychaetes and pogonophorans (see chapter 6.10). Below this depth, sulfate is consumed by upward migrating methane and hence total alkalinity and hydrogen sulfide concentrations start to increase (Figure 6.13.2). From these porewater profiles a general trend of decreasing methane flux that is associated with the observed fauna can be deduced: polychaetes (black sediment) > pogonophora > clams & mussels > carbonates & vestimentifera > "normal" seep sediments. Maximum amounts of hydrogen sulphide reach concentrations of up to ~12 mM and alkalinity values of up to 23 meq/l. Ammonium contents are close to zero and chloride and bromine concentrations show only small deviations around the seawater value, unless gas hydrate formation occurs near the sediment surface.

At Bear's Paw we were also able to recover gas hydrates in several gravity cores. For example, in core 196 GC 20 (Figure 6.13.3) a gas hydrate layer with a thickness of ~1 cm was observed at a sediment depth of 105 cm. Two more discrete hydrate layers were observed at 93 and 125 cm. After complete decomposition, the core was processed leading to a chloride minimum of ~520 mM at 105

cm. This core was taken in close vicinity of a black sediment spot, as it showed greenish to black sediment in the uppermost 5 cm. A high methane flux is to be expected for this core causing the observed rapid consumption of sulfate within the top 40 cm. On deck, degassing of the sediment was observed below 60 cm and hydrate decomposition of 3 discrete hydrate layers at 93, 105, and 125 cm. Anaerobic methane oxidation (AMO) appears to be quite intense as sulfide and alkalinity values increase rapidly between 0-40 cm sediment depth and reach ~10 mM and ~28 meq/l, respectively. Ammonium concentrations stay low (<20 μM) within the core whereas phosphate concentrations increase almost linearly to ~100 μM at the base of the core (at 170 cm). Gravity cores that recovered sediment outside the black patches showed the typical deep porewater irrigation characteristic discussed in more detail for the Wairarapa area.

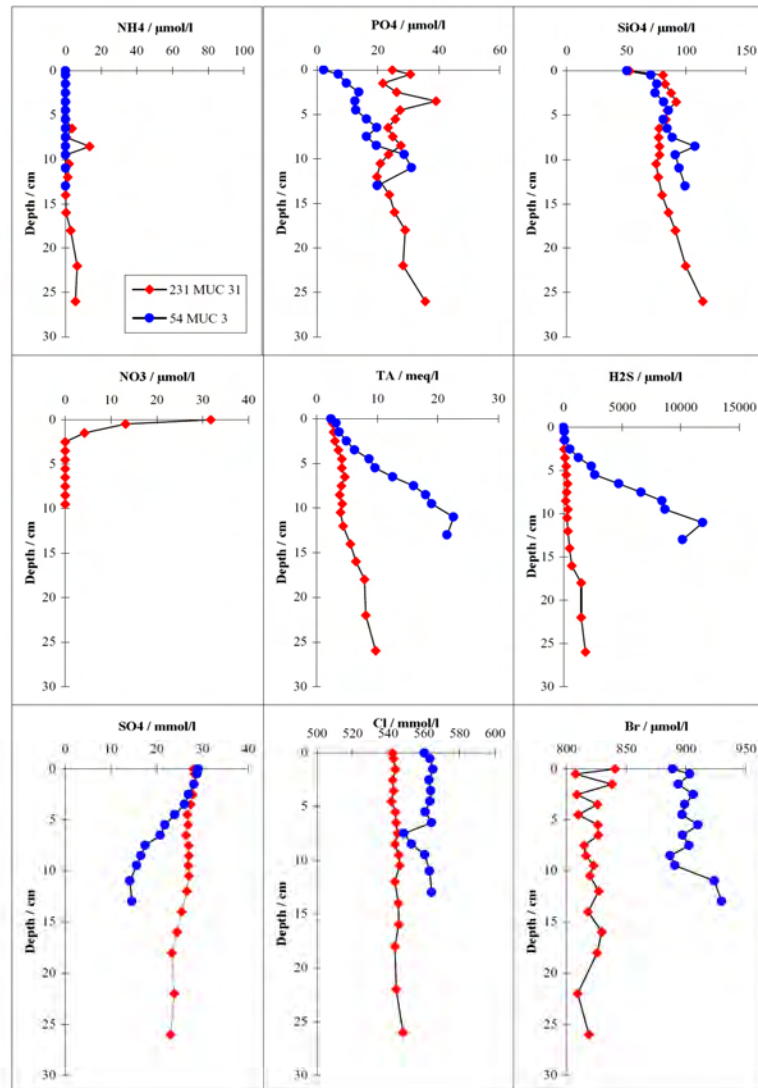


Figure 6.13.2: Porewater geochemistry of black sediment spots at Kaka. a) 54 MUC 3 (blue) - fauna dominated by polychaetes and b) 231 MUC 31 (red) - fauna dominated by pogonophorans.

At Okamere Ridge, we also collected gravity cores at 2 reference sites. The porewater profiles (Figure 6.13.4) show a linear decline of sulfate with an extrapolated penetration depth of ~650 cm, indicating a steady state situation dominated by sulfate consumption due to AMO. Correspondingly, total alkalinity increases linearly to >20 meq/l at the base of the core. Sulfide concentrations slowly start to increase below a sediment depth of 400 cm, such that only the beginning of the gradient could be recovered in the cores. Compared to the seep-influenced sediments, the reference porewaters are nutrient-rich: Ammonium and phosphate concentrations increase linearly with depth and reach ~1.4 mM and ~330 μM , respectively, at the base of the core (total length of the core: 540 cm).

196 GC 20

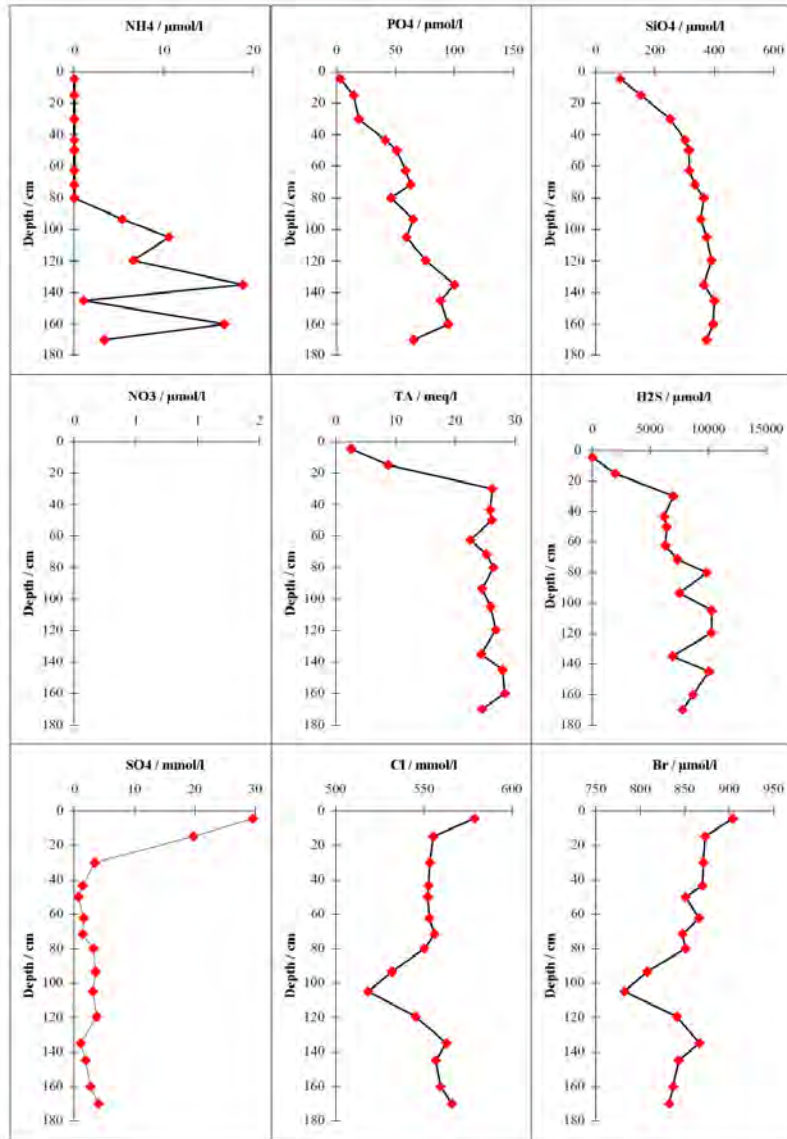


Figure 6.13.3: Porewater geochemistry of gas hydrate bearing sediments outside the black sediment spots (196 GC 20, Bear's Paw).

79 GC 4

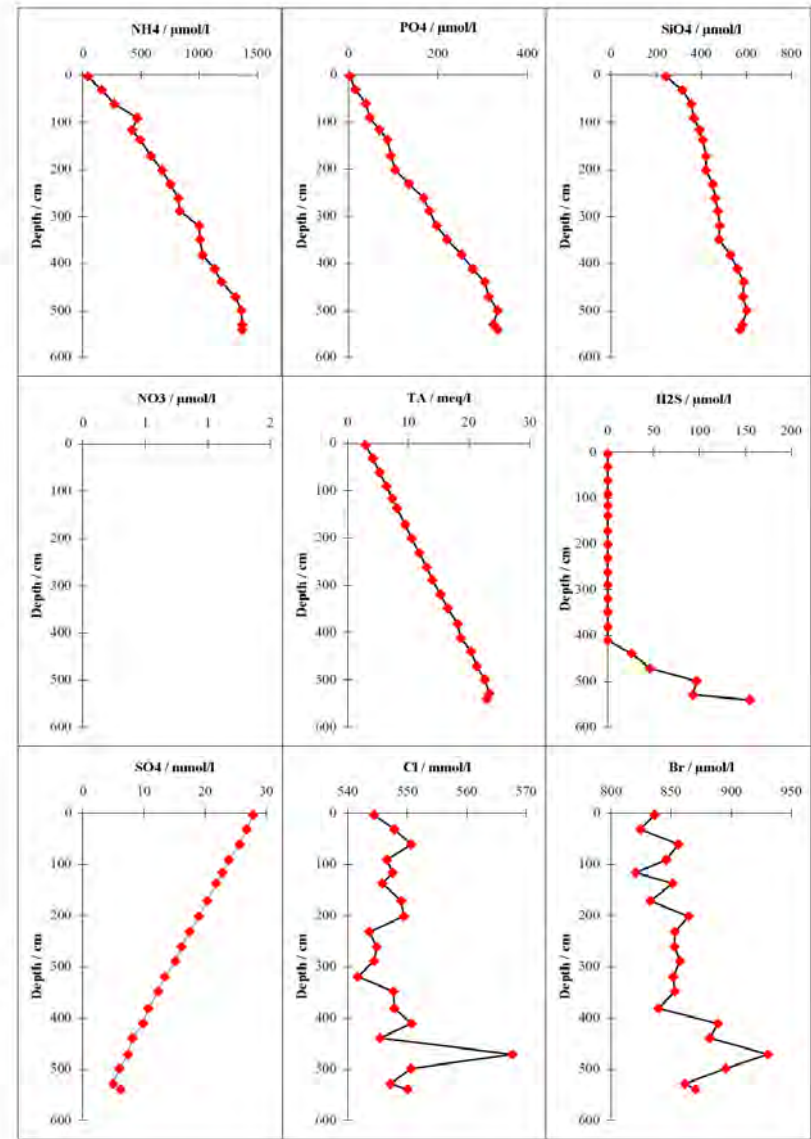


Figure 6.13.4: Porewater geochemistry of the reference sediment (no seep influence) close to LM-9 (79 GC 4).

Wairarapa

M. Haeckel, K. Krieger, B. Domeyer, E. Hütten, M. Bausch, M. Marquardt, D. Müller (IFM-GEOMAR)

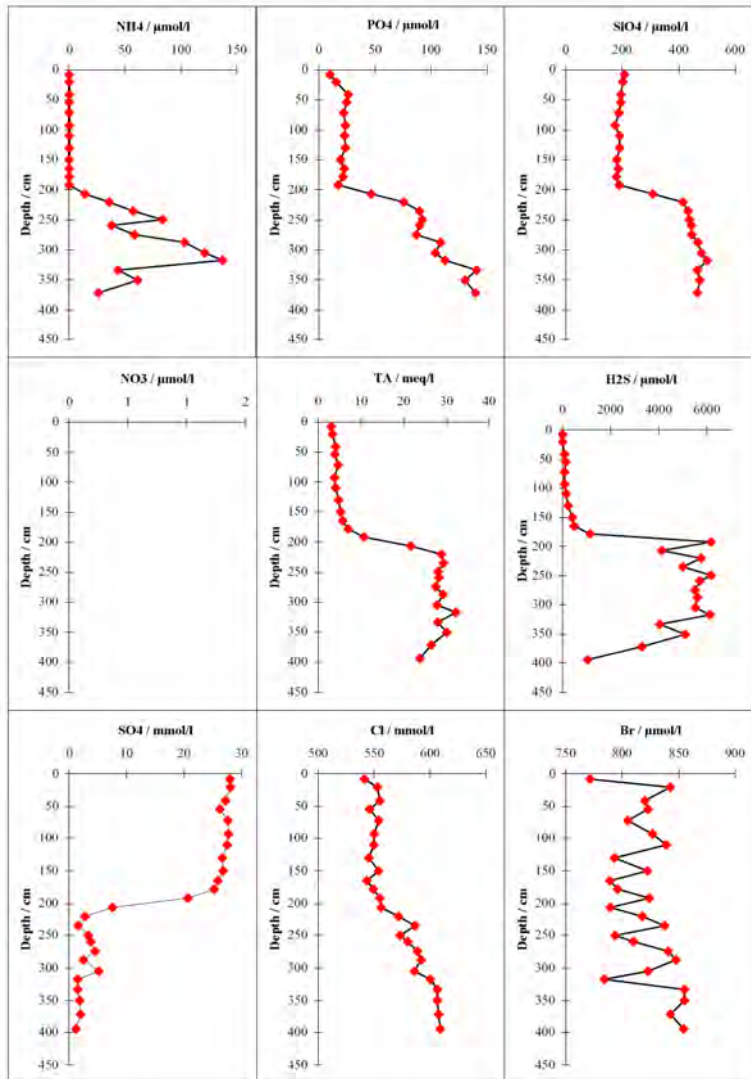
In the Wairarapa area, 2 seep sites, North Tower and South Tower, have been investigated as well as 1 reference site. A third seep site, Tui Flare, could not be sampled successfully because of a thick cover consisting of carbonates and shell debris. Our main focus was on the North Tower seep site that was most active southeast of the high backscatter reflections. Here, several black sediment patches with a white rim of *Beggiatoa* bacteria have been detected.

The corresponding pore fluids of the black sediment patches are similar to those in the other investigation areas. Porewater bioirrigation, probably from polychaetes, occurs in the top 3-4 cm (see chapter 6.10) followed by intense AMO. In the center of these patches sulfate is consumed within the top ~10 cm and hence total alkalinity and hydrogen sulfide concentrations are high (up to ~40 meq/l and ~13 mM, respectively; Figure 6.13.5). The depicted core, 273 MUC 40, was also degassing vigorously on retrieval, suggesting potential gas hydrate occurrences only a few centimeters below its penetration depth of 20 cm. Again, ammonium contents are low and chloride and bromine concentrations are about the seawater value, unless gas hydrate formation occurs near the sediment surface.

Porewater profiles from gravity cores that were deployed outside the black sediment patches, but within the seep area, showed deep irrigation of bottom water on a 1-to-3-m scale. This pattern is most likely caused by methane gas bubbles rising through the surface sediments, which induces an eddy-type diffusive mixing. In core 287 GC 39 (Figure 6.13.6), this bubble irrigation occurs down to a sediment depth of 200 cm and affects all porewater constituents. Subsequently, AMO completely consumes the sulfate within 10-20 cm leading to steep gradients in SO_4 , TA, and H_2S . In addition, chloride concentrations in 287 GC 39 gradually increase to ~610 mM, indicating active hydrate formation in the surface sediments, probably right below the penetration depth of the gravity core (i.e., 400 cm). In 111 GC 8, we were able to recover small gas hydrate pieces that were finely disseminated in the sediment matrix below a depth of 200 cm.

In contrast to Okamere Ridge, the reference core taken between North Tower and Tui Flare, close to the location of CSEM pig 9 (see chapter 6.5), showed only little sulfate reduction (Figure 6.13.7). Within the cored top 530 cm SO_4 concentrations only decrease by about 2 mM and thus, nutrient concentrations increase only moderately. Ammonium concentrations increase to ~300 μM and maximum phosphate values are ~70 μM . Due to the low sulfate reduction rates, total alkalinity does not increase above ~6 meq/l and sulphide concentrations are below ~40 μM .

287 GC 39



273 MUC 40

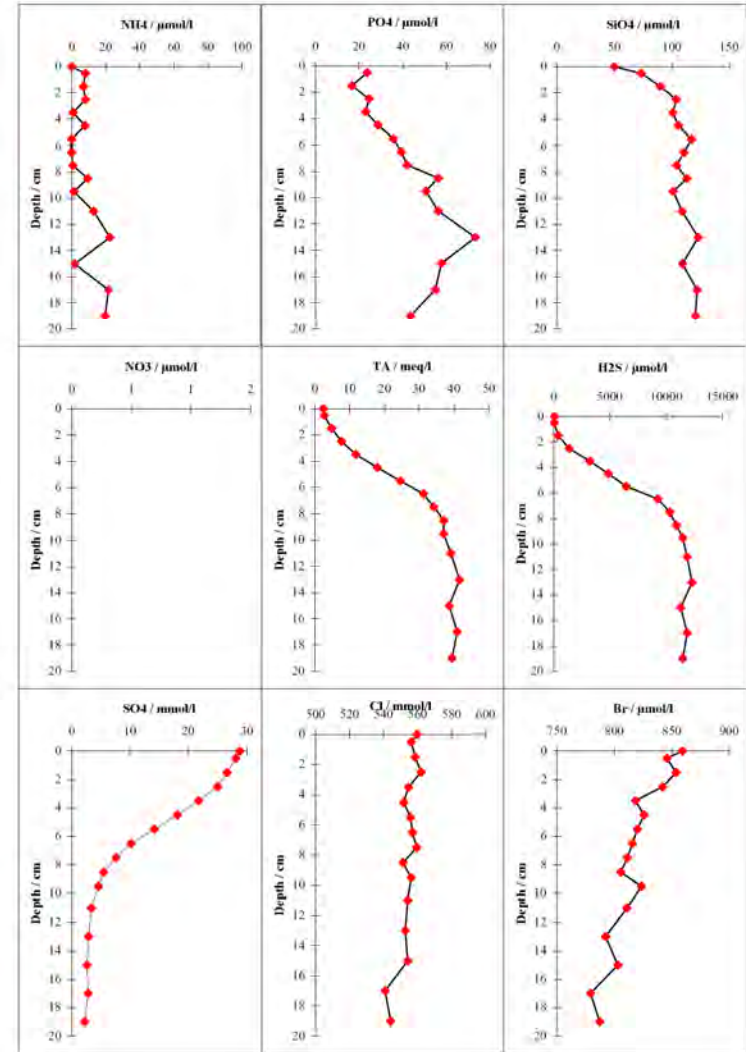


Figure 6.13.5: Porewater geochemistry of black sediment spots at Wairarapa North Tower (273 MUC 40).

Figure 6.13.6: Porewater geochemistry of seep sediments outside black sediment spots at Wairarapa North Tower (287 GC 39).

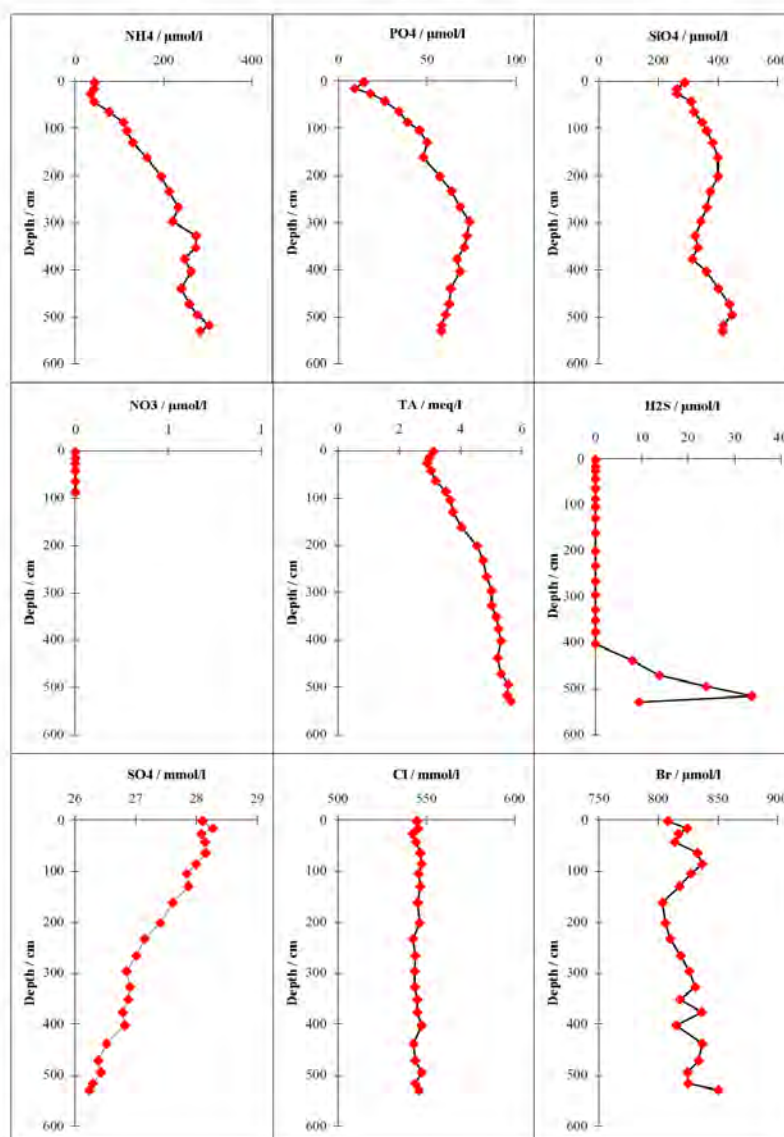


Figure 6.13.7: Porewater geochemistry of reference sediments in the Wairarapa area (153 GC 13).

6.14 Radon Measurements

A. Eisenhauer

In order to demonstrate the ²²²Rn results determined on boards SO191-2 we focused on results determined on a reference site (station 78). From the increase of the ²²²Rn concentrations (Figure 6.14.1) above the sediment column determined after about 900 and 1100 minutes a ²²²Rn production rate of about $\sim 10^{-4}$ cpm/(cm²xmin) can be determined.

Within the sediment column (Figure 6.14.2) the ²²²Rn concentrations (black dots) decrease from about 5 cpm/cm² (0-5 cm) to about 1 cpm/cm² (20-25 cm). About 48 hours later the ²²²Rn concentrations decreased markedly due to upward gas advection and radioactive decay from about 5 to 0,5 cpm/cm² at about 0 to 5 cm depth. Preliminary results and calculations applying the usual diffusion-advection model an advection rate for this reference sediment in the order of \sim mm/min can be determined. Whereas the diffusion rate is less than $\sim 10^{-3}$ cm²/min. These preliminary results will be accomplished and more precisely quantified by determination of the excess amount of ²²²Rn in pore-water and bottom-water samples. Re-measurements of the samples with a time gap equivalent of at least 6 half-lives allow to determine the amount of supported ²²²Rn in the samples, therefore, the activity of the dissolved mother isotope ²²⁶Ra of the ²³⁸U-series. Subtracting the supported ²²²Rn activity, measured in the lab, from the on-board measurements close to sampling, results in the amount of un-supported ²²²Rn_(excess) in the sample. This enrichment is an important additional tracer for estimation of residence time of pore-water and the advection rate in a cold vent system. These re-measurements are topic of actual laboratory work at the IFM-GEOMAR.

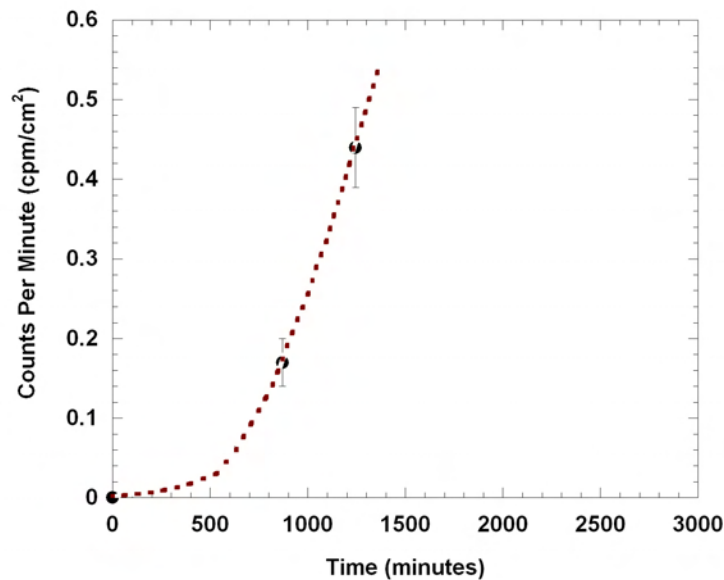


Figure 6.14.1: The ^{222}Rn -concentrations increase as a function of time above the sediments of MUC station 78 from 0 to about 0.15 cpm/cm after about 900 minutes, and to about 0.45 cpm/cm² after about 1100 minutes. From the increase of the concentrations a ^{222}Rn -production rate in the order of about 10^{-4} cpm/(cm²·min) can be estimated.

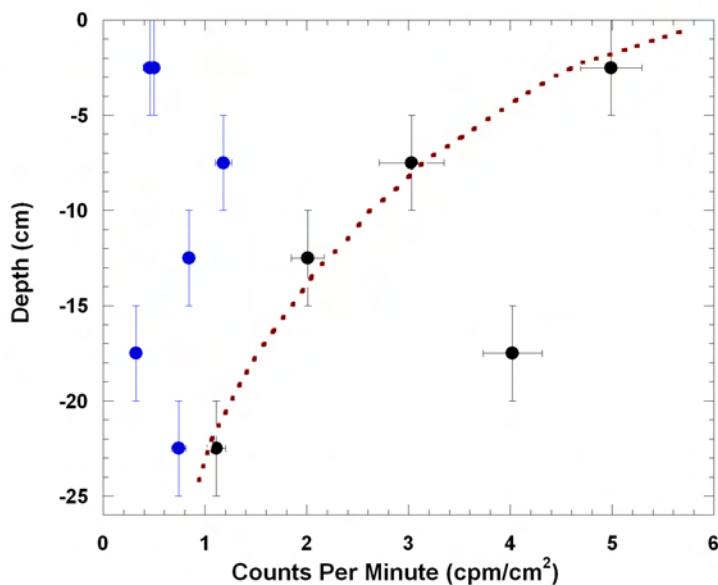


Figure 6.14.2: The ^{222}Rn -concentrations (black dots, red line) increase exponentially from ~ 1 cpm/cm² (20-25 cm) to about 5 cpm/cm². About 48 hours later, the ^{222}Rn -concentrations (blue dots) decreased due to upward advection of ^{222}Rn and radioactive decay. Latter profiles can be used in order to constrain diffusion and advection rates as a function of the geological settings.

6.15 Carbonates

A. Eisenhauer, V. Liebetrau

During various OFOS tracks different types of vent site carbonates were observed at the northern and southern area of interest. Most abundant are carbonates forming flat pavements on the sediment seawater transition. These carbonates are different from large brownish to blackish blocks characterized by a smooth and even surface not showing any remarkable biological overgrowth. Another type of light brown to white carbonates (chemoherm) erect directly into seawater and is marked by a porous and brecciated surface structure. In particular, the SO191 sampling strategy focused on the collection of these chemoherms as they are supposed to be excellent archives of the vent site history in high temporal resolution.

During two stations of SO191-2 (87, TVG-4 and 138, TVG-5) two massive chemoherm carbonates have been recovered from the ocean floor. In particular, the chemoherm recovered from the ocean floor during station 87 (Figure 6.15.1) is the largest vent site chemoherm carbonate recovered, at least within the Geotechnologien Program (height: 1 m; width: 1.4 m; length: 2.4 m). Preliminary inspection on deck of RV Sonne showed that this chemoherms but also the smaller one are heavily

overgrown by biological communities like tube worms, clams, solitary corals, sponges and other marine life. In particular the large chemoherm collected during station 138 showed still ongoing AOM activity at the base of the block. This is indicated by the observation that within the grayish to blackish mud white patches of carbonate could be detected probably produced by ongoing anaerobic methane oxidation. In order to verify this observation samples have been taken and frozen for further examination in the laboratories back home in Germany and New Zealand.



Figure 6.15.1: Massive chemoherm carbonate from LM9 (Stat. 87, TVG-4)

During SO191-3 a structurally comparable but smaller block of chemoherm carbonate precipitation was recovered from a carbonate platform of the Uruti Ridge, extending the sampling range of cold-vent related carbonates of the Hikurangi Margin significantly.

Due to the spread of sampling sites a comparison and reconstruction of cold vent activity for different geological settings of the Hikurangi seems achievable and is one aim of the on-going isotope geochemical investigation.

As important archive of chemical changes in the bottom water cold-water corals were additionally recovered. Solitary species are sampled from the chemoherm carbonates and two reef structures are sampled at the Moa Site, consisting of reef-building and solitary species (Figure 6.15.2).



Figure 6.15.2: Recovered fragments of a cold-water coral reef at the Moa site (Stat. 218, TVG-12)

As special advantage for chemical calibration approaches of this rare archive, reef-building as well as solitary corals were sampled alive.

Comparing isotope geochemical coral records from different sites (cold-vent and background) is a potential tool to reconstruct directly the impact of cold-vent related methane emanation on the bottom water chemistry through time.

7 Regional Work

7.1 Multichannel Seismic Reflection Study

Barnes, P, Gerring, P.K., Wilcox, S., Lamarche, G., Pecher, I., Crutchley, G.

Despite several decades of scientific research and exploration interest in the Hikurangi margin, there is surprisingly sparse coverage of good quality seismic reflection data from the continental slope. The Sonne SO191 voyage created an opportunity to acquire new multichannel seismic reflection profiles from the central margin accretionary wedge (Figures 7.1.1 and 7.1.2). Five regional seismic lines were acquired from the continental slope (SO191 –1, –3, –4, –6 and –9), together with two tie-lines in the Hikurangi Trough (SO191 –2 and 5) and one tie-line in a large mid-slope basin (SO191 –8).

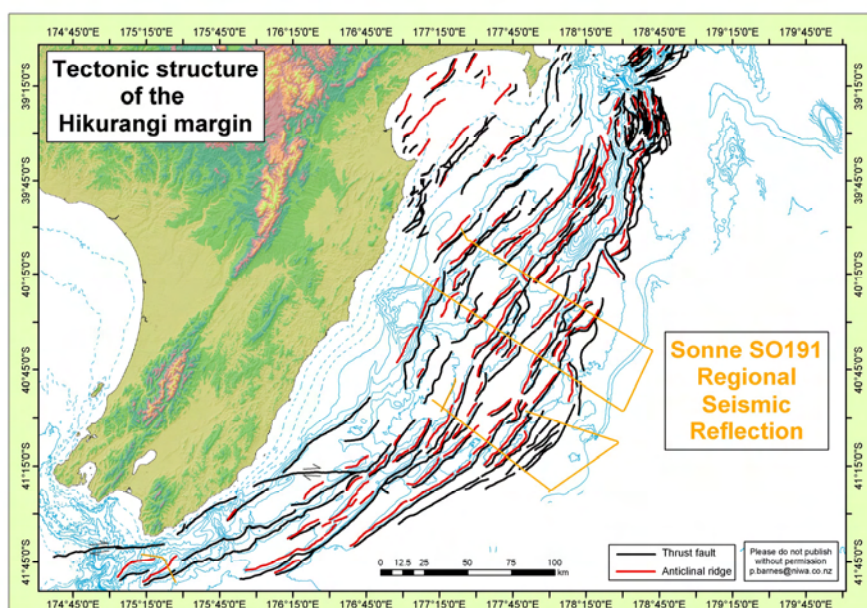


Figure 7.1.1 Regional tectonic structures. Major faults (black) and anticlinal ridges (red) interpreted from bathymetric and seismic reflection data in the central Hikurangi margin. Lines indicate the location of the new *Sonne* SO191 Leg 1 profiles.

Two of the regional lines (SO191 –1 and 3) extend across the entire margin from the shelf to the Hikurangi Trough, and tie into the 2005 NZ MED Crown Minerals data (Figure 7.1.2). SO191 –4 extends line GNS/MED–38 across the subduction deformation front, and was recorded with both towed streamer and with six OBS deployed along the line 5 NM apart. Line SO191-6 extends across the lower slope and trench. Line SO191 –9 was recorded across the Wairarapa seep site off Cape Palliser in the south of the margin.

The airgun source was a 2000 cubic inch G gun array on lines SO191 –1 to –6, and a 250/105 GI gun on lines SO191 –8 and –9. The streamer was 32 channels on all profiles. Lines SO191 –1 to –6 were processed onboard to post-stack time migrated sections, and preliminary interpretations were completed.

The aims of the study include:

- (1) Identification of the primary subduction décollement, upper plate and subducted sequence.
- (2) Evaluation of along-margin variations in regional tectonic structures and subduction processes, including the effects of subducting seamounts.
- (3) Establishing characteristics of the trench-fill sedimentary sequence entering the subduction system.
- (4) Determining amounts and rates of tectonic shortening, so that kinematic models of plate boundary deformation can be improved.
- (5) Evaluation of mechanisms of tectonic accretion and thrust fault evolution.

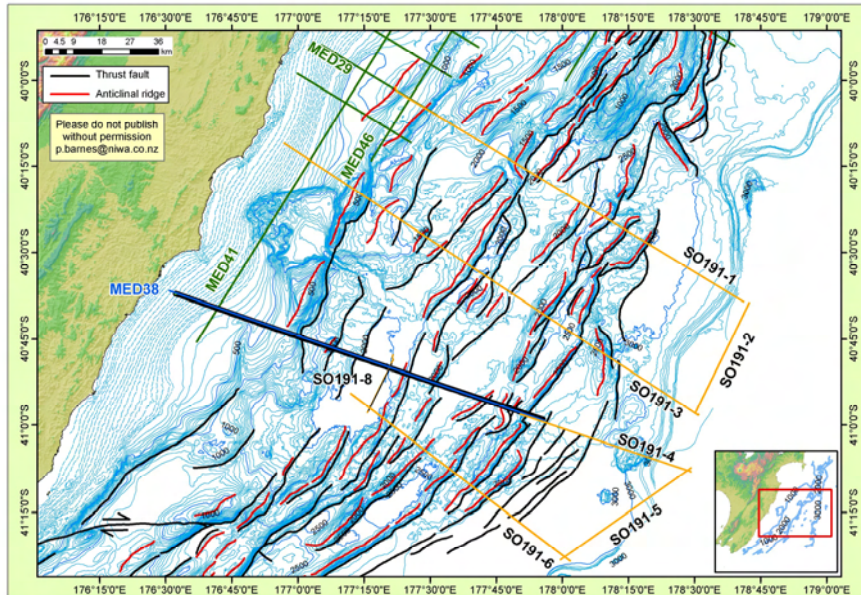


Figure 7.1.2 Tectonic structures of the central Hikurangi margin thrust wedge, showing the location of the new Sonne SO191 Leg 1 profiles and ties to the 2005 MED Crown Minerals lines. Bathymetric contours are at 10 m intervals on the continental shelf (grey) and 50 m intervals in water depths greater than 200 m.

The new regional seismic lines are of good quality, despite the short streamer, and typically image 3.0-3.5s two-way travel (TWT) beneath the seafloor (Figure 7.1.3). The trench-fill turbidite section, together with the pelagic sediments and oceanic crust of the Hikurangi Plateau are well imaged in the Hikurangi Trough, where up to 4.0s TWT of seismic penetration was achieved. The main subduction interplate thrust can be identified as a major décollement between the subducted sequence and the accretionary wedge. This décollement can be interpreted along the seismic sections to about 35-40 km down the dip of the subduction zone, where it becomes masked by the primary seafloor multiple at about 6.5s TWT.

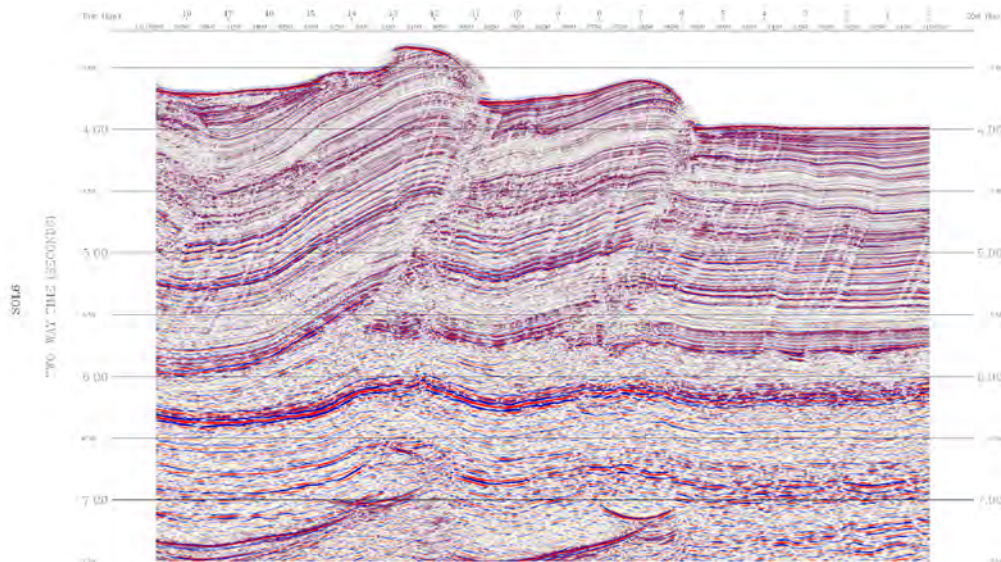


Figure 7.1.3 Example of seismic section (SO191-6) across the deformation front of the Hikurangi subduction zone. All profiles were processed onboard to post-stack time migrated sections, and were interpreted.

The structures in the upper plate thrust wedge are impressive, with many forward- and back-verging thrusts clearly imaged in the profiles. In the mid-slope region, there appears to be a significant tectonic buttress, with the upper margin sequences differing in their reflective characteristics from what are clearly accreted trench fill turbidites beneath the lower slope. Major thrusts faults typically coincide with bathymetric ridges, and can be traced along strike from multibeam bathymetric data (Figure 7.1.2). Slope basins between the ridges are variously infilled with sediments up to about 1.5-2.0 s TWT thick.

Across the principal deformation front there is a spectacular zone of “protothrust” deformation. These faults represent a zone of incipient deformation up to 25 km wide that has developed in advance of the main deformation front. The structures were recognised in previous surveys, but not with such clarity. The new data also reveal an interesting change in the vergence of the protothrusts along the strike of the margin.

Lines SO191–3 and –4 cross a 70 km long seamount ridge (including Bennett Knoll) that is entering the subduction zone in the centre of the margin. By comparing the structure and stratigraphy on these two lines with that on lines SO191–1 and –6, to the north and south respectively, we can identify the early deformation effects of subducting seamounts on accretionary wedges.

7.2 Higher-Resolution Imaging for Gas Hydrates

The gas hydrate zone in the first few hundred meters beneath the seafloor is ideally imaged with higher-frequency sources than the large G gun array used for the regional MCS. However, the sharp waveform of the gun array still made it possible to image the shallow sub-seafloor in surprising detail. Figure 7.2.1 shows a BSR beneath an anticline along MCS Line 6. The only significant difference to the processing used for the regional images was binning at 6.25 rather than 12.5 m. Numerous small-offset faults are resolved nicely. The image also displays two features that are typical for BSRs on the Hikurangi margin. The BSR is broken up, often with sharp lateral terminations. It often occurs in sediment packages with reduced reflectivity, which is likely to be caused by a destruction of the sediment frame by intense fracturing during deformation – although in this specific case, the decrease of reflection amplitudes at least beneath the eastern flank of the anticline may also be caused by the steep dips of the layer package. A comparison of BSR occurrences with stratigraphic and structural interpretations of the regional lines will prove invaluable for studying the sources and migration paths of gas for hydrate formation on the Hikurangi margin.

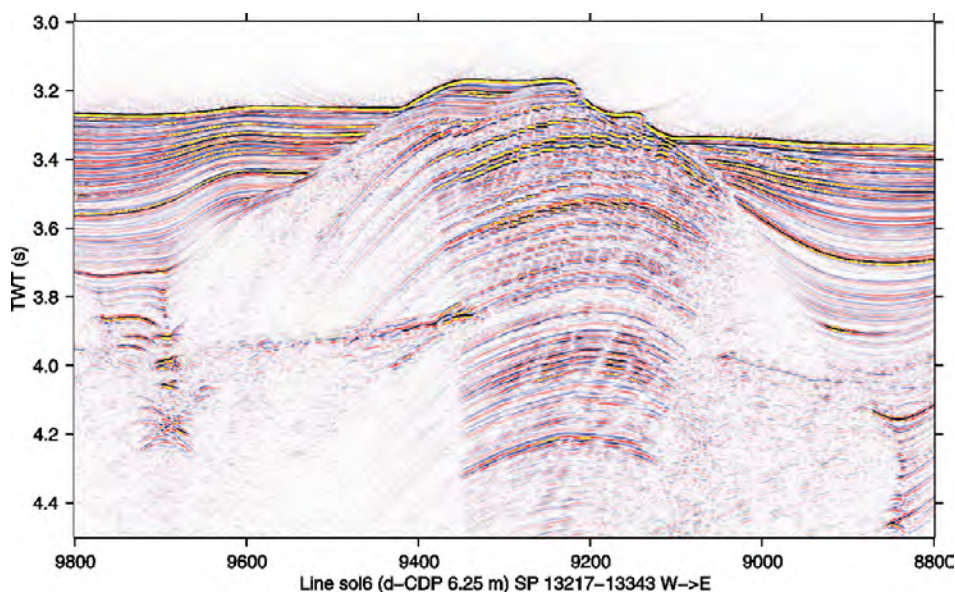


Figure 7.2.1: Image across an anticline along SO191-6. CDP numbers differ from that of the regional lines, but the corresponding shot numbers are the same (13217-13343).

7.3 Controlled Source Electro-Magnetics – Ingo’s Site

K. Schwalenberg, D. Keen, P. Schroeder

Ingo’s Site is a working title for the CSEM deployment off the coast of Wairarapa along seismic line 02 which has been obtained during cruise TAN0607 on R/V Tangaroa. Figure 7.3.1 shows the bathymetric map and the CSEM sites along the profile. The profile is crossing a NE-SW crossing ridge and is in water depths between 1900m and 2100m. Distance between sites was about 500m. The target was a zone of high reflectivity ascending from the BSR at the western edge of the ridge, probably associated with free gas or gas hydrate (see seismogram in Figure 7.3.2). To cover at least the upper part of the reflective zone the CSEM array on the seafloor was extended to transmitter receiver separations of 387m for the first receiver and 705m for the second receiver. The operation was extremely challenging and it was the first time that a bottom-towed array of that length has been deployed in more than 2km water depth. High quality data have been obtained from 15 sites with the

first receiver, however, the data collected with the second receiver cannot be analyzed, because the source signal wasn't strong enough for such large separations and the signal size was below the noise level. Figure 7.3.2 combines the seismic section along the profile, the inverted apparent resistivity profile and the data misfit, i.e. rms error for the respective sites along the profile. The ascending reflector in the seismogram can be clearly correlated with a big anomaly in the apparent resistivity profile. Further modeling and joint interpretation will give more insight in the inner structure and nature of this feature. However, this is another convincing example that CSEM is sensitive to the presence of gas hydrate and/or free gas.

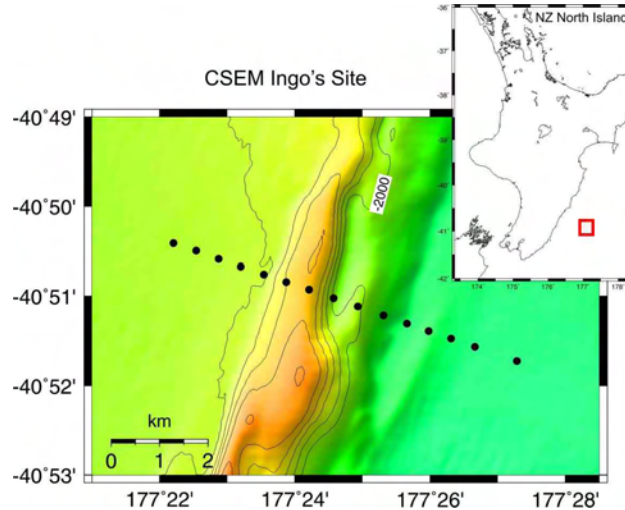


Figure 7.3.1: Bathymetry map for "Ingo's Site" off the Wairarapa and CSEM Sites

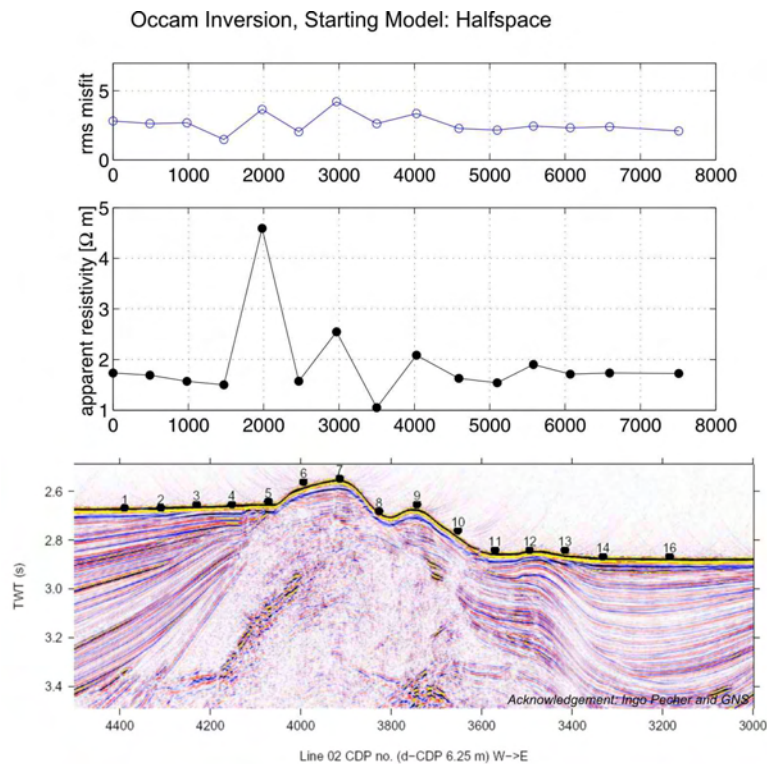


Figure 7.3.2: Seismic section along Line 02 TAN0607 (bottom), apparent resistivity profile derived from data at receiver 1 (Tx-Rx1: 387m, middle), and rms misfit. Ascending seismic reflector clearly correlates with resistivity anomaly.

8 Acknowledgements

The cruise SO191 Leg 1, 2 and 3 was financed within the project New Vents funded by the German Federal Ministry for Education and Research (Bundesministerium für Bildung und Forschung, BMBF) under project No. 03G0191. Funding for biogeochemical and microbial studies was provided by the GEOTECHNOLOGIEN programmes COMET and MUMM-II. We are grateful to the continuous support of marine sciences with an outstanding platform such as R/V SONNE. We acknowledge the support of the project by GNS and NIWA providing helpful information and data, which was made available for the conduction of the cruise. The authors wish to express their gratitude to all the colleagues who have supported the work before, during and after the cruise. Much of the work done during the cruise was only made possible by the scientists', technicians' and the crews' experience. Particular thanks are directed to Captain Oliver Meyer, Captain Lutz Mallon and to the entire crew of R/V SONNE for their excellent support throughout the cruise.

9 References:

- Boetius A, Ravenschlag K, Schubert C, Rickert D, Widdel F, Gieseke A, Amann R, Jørgensen BB, Witte U, Pfannkuche O (2000) A marine microbial consortium apparently mediating anaerobic oxidation of methane. *Nature* 407:623-626
- Brenwald, M.S., Hofer, M., Peeters, F., Aeschbach-Hertig, W., Strassmann, K., Kipfer, R., Imboden, D.M. (2003) Analysis of dissolved noble gases in the porewater of lacustrine sediments. *Limnology and Oceanography: Methods* 1, 51-62.
- Crutchley, G.J., I.A. Pecher, S.A. Henrys, and A.R. Gorman, Gas hydrate "sweet spots" on the Hikurangi margin, from recently acquired multi-channel seismic data, in Proc. New Zealand Petrol. Conf., pp. 7, Auckland, 2006.
- Faure, K.; Greinert, J.; Pecher, I.A.; Graham, I.J.; Massoth, G.J.; de Ronde, C.E.J.; Wright, I.C.; Baker, E.T.; Olson, E.J. (2006), Methane seepage and its relation to slumping and gas hydrate at the Hikurangi margin, New Zealand. *New Zealand Journal of Geology and geophysics*, 49(4): 503-516
- Grasshoff K., Ehrhardt M., and Kremling K. (1999) *Methods of Seawater Analysis*. Wiley-VCH, Weinheim.
- Henrys SA, Ellis S, Uruski C (2003) Conductive heat flow variations from bottom-simulating reflectors in the Hikurangi margin, New Zealand. *Geophysical Research Letters*, 30 (2), 1065, doi:10.1029/2002GL015772.
- Henrys, S.A., D. Woodward, D., and I.A. Pecher, Variation of bottom-simulating reflector (BSR) strength in a high-flux methane province, Hikurangi margin, New Zealand, submitted to AAPG Memoirs.
- Henrys, S.A., S. Ellis, and C. Uruski, Conductive heat flow variations from bottom simulating reflectors on the Hikurangi margin, New Zealand, *Geophys. Res. Lett.*, 30, doi:10.1029/2002GL015772, 2003.
- Hornbach, M.J., D.M. Saffer, and W.S. Holbrook, Critically pressured free-gas reservoirs below gas-hydrate provinces, *Nature*, 427, 542-544, 2004.
- Katz, H.R., Probable gas hydrate in continental slope east of the North Island, New Zealand, *J. Petrol. Geol.*, 3, 315-324, 1981.
- Lammers, S. and E. Suess (1994), An improved head-space analysis method for methane in seawater. *Mar. Chem.* 47: 115-125.
- Lewis KB, Marshall BA (1996) Seep faunas and other indicators of methane-rich dewatering on New Zealand convergent margins. *New Zealand Journal of Geology and Geophysics*, 39, 181-200.
- Lewis, K. B., and B. A. Marshall, Seep faunas and other indicators of methane-rich dewatering on the New Zealand convergent margins, *NZ J. Geol. Geophys.*, 39, 181– 200, 1996.
- Linke P, Wallman K, Suess E, Hensen C, Rehder G (2005) In situ benthic fluxes from an intermittently active mud volcano at the Costa Rica convergent margin. *Earth Planet Sci Lett*, 235: 79-95.
- Liu, X., and P. D. Flemings, Passing gas through the hydrate stability zone at southern Hydrate Ridge, offshore Oregon, *Earth Planet. Sci. Lett.*, 241, 211-226, 2006.
- Luff R, Wallmann K (2003) Fluid flow, methane fluxes, carbonate precipitation and biogeochemical turnover in hydrate-bearing sediments at Hydrate Ridge, Cascadia margin: Numerical modelling and mass balances. *Geochim Cosmochim Acta*, 67: 3403-3421.
- MacDonald IR, Sager WW, Peccini MB (2003) Gas hydrate and chemosynthetic biota in mounded bathymetry at mid-slope hydrocarbon seeps: Northern Gulf of Mexico, *Mar Geol*, 198: 133-158
- Morse JW, Boland G, Rowe GT (1999) A "gilled" benthic chamber for extended measurement of sediment water fluxes. *Mar Chem*, 66: 225-230.
- Niemann H, Elvert M, Hovland M, Orcutt B, Judd AG, Suck I, Gutt J, Joye SB, Damm E, Finster K, Boetius A (2005) Methane emission and consumption at a North Sea gas seep (Tommeliten area). *Biogeosciences* 2:335-351
- Niemann H, Lösekann T, de Beer D, Elvert M, Nadalig T, Knittel K, Amann R, Sauter EJ, Schlüter M, Klages M, Foucher JP, Boetius A (2006) Novel microbial communities of the Haakon Mosby mud volcano and their role as a methane sink. *Nature* 443:854-858
- Olu K, Lance S, Sibuet M, Henry P, Fiala-Médioni A, Dinert A (1997) Cold seep communities as indicators of fluid expulsion patterns through mud volcanoes seaward of the Barbados accretionary prism. *Deep Sea Res, Part I*, 44(5): 811-841.
- Pecher IA, Henrys SA, Ellis S, Chiswell SM, Kukowski N (2005) Erosion of the seafloor at the top of the gas hydrate stability zone on the Hikurangi margin, New Zealand. *Geophysical Research Letters*, 33, L24603, doi:10.1029/2005GL024687.
- Pecher, I.A., and S.A. Henrys, Potential gas reserves in gas hydrate sweet spots on the Hikurangi Margin, New Zealand, pp. 32, Institute of Geological and Nuclear Sciences, Lower Hutt, 2003.
- Pecher, I.A., S.A. Henrys, S. Ellis, S.M. Chiswell, and N. Kukowski, Erosion of the seafloor at the top of the gas hydrate stability zone on the Hikurangi Margin, New Zealand, *Geophys. Res. Lett.*, 32, L24603, 2005.
- Pfannkuche O, Linke P (2003) GEOMAR landers as long-term deep sea observatories. *Sea Technology*, 44, 50-55.
- Purkl S. and Eisenhauer A. (2004); Determination of radium isotopes and ²²²Rn in a groundwater affected coastal area of the Baltic Sea and the underlying sub-sea floor aquifer. *Marine Chemistry* 87, 137-149.
- Reeburgh WS (2003) Global methane biogeochemistry. *Treatise Geochem*, 4: 65-89.

- Reeburgh WS, Whalen SC, Alperin MJ (1993) The role of methanotrophy in the global methane budget. In *Microbial Growth on C-1 compounds*, edited by JC Murrell & DP Kelly, pp 1-14, Intercept Andover, U.K.
- Rehder, Gregor ; Keir, Robin ; Suess, Erwin ; Pohlmann, T.: The multiple sources and patterns of methane in North Sea waters .In: *Aquatic Geochemistry* 4 (1998), S.403-427
- Rehder, G., Erwin Suess, 2001 Methane and $p\text{CO}_2$ in the Kuroshio and the South China Sea during maximum summer surface temperatures. *Mar. Chem.*, 75: 89-108.
- Sahling H, Rickert D, Lee RW, Linke P, Suess E (2002) Macrofaunal community structure and the sulphide flux at gas hydrate deposits from the Cascadia convergent margin, NE Pacific. *Mar Ecol Prog Ser*, 231: 121-138
- Sommer S, Pfannkuche O, Linke P, Luff R, Greinert M, Drews M, Gubsch S, Pieper M, Poser M, Viergutz T (2006) Efficiency of the benthic filter: Biological control of the emission of dissolved methane from sediments containing shallow gas hydrates at Hydrate Ridge. *Global Biogeochem Cycles* 20, GB2019, doi:10.1029/2004GB002389.
- Sommer S, Türk M, Kriwanek S, Pfannkuche O (subm) Gas exchange system for extended in situ benthic chamber respiration and flux measurements under controlled oxygen conditions. *Limnol Oceanog Methods*.
- Tengberg A, Hovdenes J, Andersson HJ, Brocandel O, Diaz R, Hebert D, Arnerich T, Huber C, Körtzinger A, Khripounoff A, Rey F, Rönning C, Schimanski J, Sommer S, Stangelmayer A (2006) Evaluation of a lifetime-based optode to measure oxygen in aquatic systems. *Limnol Oceanog: Methods*, 4: 7-17.
- Thorpe, S.A. (1977), Turbulence and mixing in a Scottish Loch, *Phil. Trans. Roy. Soc. London, A.*, 286, 125-181.
- Torres ME, McManus J, Hammond DE, de Angelis MA, Heeschen KU, Colbert SL, Tyron MD, Brown KM, Suess E (2002) Fluid and chemical fluxes in and out of sediments hosting methane hydrate deposits on Hydrate Ridge, OR, I: Hydrological provinces. *Earth Planet Sci Lett*, 201: 525-540.
- Townend, J., Estimates of conductive heat flow through bottom-simulating reflectors on the Hikurangi and southwest Fiordland continental margins, New Zealand, *Mar. Geol.*, 141, 209–220, 1997.
- Treude T, Boetius A, Knittel K, Wallmann K, Jørgensen BB (2003) Anaerobic oxidation of methane above gas hydrates at Hydrate Ridge, NE Pacific Ocean. *Mar Ecol Prog Ser*, 264: 1-14.
- Valentine DL, Blanton DC, Reeburgh WS, Kastner M (2001) Water column methane oxidation adjacent to an area of active hydrate dissociation, Eel River Basin. *Geochim Cosmochim Acta* 65: 2633-2640.
- Weiss, R.F., 1981. Determinations of carbon dioxide and methane by Dual Catalyst Flame Ionisation Chromatography and nitrous oxide by Electron Capture Chromatography. *J. Chrom. Sci.*, 19: 611-616.
- Xu, W., and C. Ruppel, Predicting the occurrence, distribution, and evolution of methane gas hydrate in porous marine sediments, *J. Geophys. Res. Lett.*, 104, 5081-5095.

10. Appendices

10.1 List of Gears and Biogeochemical Parameters determined.

PW: Pore water chemistry; μ : determined using micro sensors

Area	Gear/Station	Biogeochemical parameters										
		PW	CH ₄	O ₂ (W)	pH	O ₂ (μ)	HS ⁻ (μ)	pH(μ)	Meiofauna	Photodoc	Pigments	Respiration
LM9												
Bears Paw	MUC2/45	+	+	-		+	-	-	+	+	+	-
Bears Paw	MUC3/54	+	+	-		+	+	+	+	+	+	-
Bears Paw	MUC5/73	+	+	-		+	+	+	+	+	+	-
Bears Paw	MUC6/78	+	+	-		+	-	-	+	+	+	-
Bears Paw	MUC18/172	+	+	-		+	+	-	+	+	-	-
Bears Paw	MUC20/187	-	-	-	-	-	-	-	-	-	-	+
Bears Paw	MUC22/198	+	+	-	-	+	+	+	+	+	-	+
Bears Paw	FLUFO 1	+	+	+	+	-	-	-	-	-	-	-
Bears Paw	FLUFO 3	+	+	+	+	-	-	-	+	+	+	-
Bears Paw	BIGO 3	-	+	+	+	-	-	-	-	-	-	-
Bears Paw	BC 7/89	-	+	-		-	-	-	-	-	-	-
Bears Paw	BWS 1	-	+	+	+	-	-	+	-	-	-	-
Bears Paw	BWS 2	no water samples retrieved										
Bears Paw	BWS 3	-	+	+	+	-	-	+	-	-	-	-
Bears Paw	BWS 4	-	+	+	+	-	-	+	-	-	-	-
Rock Garden												
	MUC26/214	+	+	-	-	+	-	-	+	+	+	+
	MUC29/221	+	+	-	-	+	+	+	+	+	+	-
	FLUFO 4	+	+	+	+	+	+	+	+	+	+	-
Faure site	FLUFO 5	+	+	+	+	+	-	-	+	+	+	-
Faure site	BIGO 4	-	+	+	+	-	-	-	-	+	-	-
Wairarapa												
Northern T.	MUC11/110	+	+	-	-	+	+	-	+	+	+	-
Northern T.	MUC12/124	+	+	-	-	+	+	+	+	+	+	+
Northern T.	MUC13/137	+	+	-	-	+	+	-	+	+	-	-
Northern T.	MUC15/157	+	+	-	-	+	+	+	+	+	+	-
Northern T.	MUC40/273	+	+	-	-	+	+	+	+	+	+	-
Northern T.	FLUFO 2	-	+	+	+	-	-	-	-	-	-	-
Northern T.	FLUFO 6		+	+	+	-	-	-	-	+	-	-
Northern T.	BIGO 2	+	+	+	+	+	+	+	+	+	+	-
Northern T.	BIGO 5	+	+	+	+	-	-	-	+	+	+	-
Northern T.	BIGO 6	+	+	+	+	+	+	+	+	+	+	-
KaKa												
	MUC38	-	-	-	-	+	+	+	-	-	-	-

Pogos

Poly

Table 10.2: Sample list (SO191-2, 3). Sediment cores were sampled for various biological and geochemical parameters during the R/V Sonne cruise 191. Core length and sampling intervals (cm) are indicated below (sampling depth/interval). The number following the sampling device is the sequential number given to the deployment of the instrument. Abbreviations include: Microbial rate measurements [AOM (anaerobic oxidation of methane), SR (sulfate reduction), Bicarb (bicarbonate reduction), acet (acetate reduction)], FISH (Fluorescent In Situ Hybridization), ARISA (Automated Ribosomal Intergenic Spacer Analysis), MUC (Multiple Corer), GC (Gravity Corer), CTD (Rosette Water Sampler). Animals 1: Vesicomya (bivalve); 2: Solemya (bivalve); 3: pogonophora (tubeworm). PW I: methane; II: sulphate; III: porosity; IV: bicarbonate; V: acetate. Other: carb (carbonate), MOx (aerobic oxidation of methane)

Location Device	Stat.	Core Length	AOM SR	Bicarb	Acet.	FISH DNA	ARISA	Biom.	Cult.	Anim.	PW	Other	Description
Bear's Paw													
MUC 18	173	16	0-16/1	-	-	0-16/1	0-16/1	0-16/2	-	-	I-III	-	Black Spot
MUC 20	187	10	-	-	-	bulk	bulk	bulk	-	1, 2	-	-	Raindrop, gassy, sulphidic
MUC 21	197	5	-	-	-	bulk	bulk	bulk	-	-	-	-	Raindrop, sulphidic
GC 17	193	-	-	-	-	carbonate	-	-	-	-	-	carb.	stiff sed. w carb. rubble
GC 20	196	120	0-120/10	0-120/10	0-120/10	0-120/10	-	0-120/10	-	-	-	-	grayish sed., gassy, GH at 70cm, sulphidic
Kaka													
MUC 32	232	21	0-21/1	0-21/1	0-21/1	0-21/1	0-21/1	0-21/2	-	-	I-V	-	Raindrop, gassy sulphidic, biv. & vest. fragm.
MUC 33	241	46	0-44/2	0-46/2	0-46/2	0-41/2	0-41/2	0-34/2	0-30/5	3 fragm.	I-V	-	<i>Pogonophora</i> , sulphidic, 0-2 pelagic, 2-15 black then grey sed
L.M. 9													
MUC 2	45	23	0-19/1	-	-	0-19/1	0-19/1	0-19/2	0-20/5	-	I-III	-	<i>Pogonophora</i> , 0-6 pelagic, biv. fragm.
MUC 3	54	13	0-8/1	-	-	0-8/1	0-8/1	0-8/2	0-2 aer.	-	I-III	-	Black spot; 0-1 yellow grey, 1-6 dark grey, 6-13 med 6-13 medium grey; foamy text.; polychaete tubes/clam
MUC 5	73	24	0-24/1	-	-	0-18/1	0-18/1	0-18/2	0-2 aer.	2,3	I-III	-	Transition sediment; near carbonates; foaming > 16cm strong oily smell
MUC 6	78	25	0-25/1	-	-	0-24/2	0-24/2	0-24/2	0-10 aer.	-	I-III	-	Reference Site
GC	64	450	0-450/50	-	-	-	-	-	-	-	-	-	Foaming from 2m to end; very small gas hydrates
TV Grab	87	-	-	-	-	-	-	-	-	-	-	-	Large Carbonate ~ 100 kg; full of tube worms
CTD	90	-	-	-	-	-	-	-	-	-	-	MOx	(from 699 – 1206 m depth; 13 Niskin bottles)
L.M. 9 (South)													
MUC 7	85	13	-	-	-	0-10/1	0-10/1	-	-	Acharax	I-III	-	Polych. site; live Acharax found 8-10cm, carb. 1-8cm
GC	95	118	0-101/15	-	-	0-115/15	-	0-101/15	-	-	I-III	-	0-80 carbonate rich clay, >80 greenish clay w/o carb.
GC	96	85	-	-	-	0-87/10	-	0-87/10	-	-	-	-	15-20 cm: above and within gas hydrate zone
74 cm: within old gas hydrates/g.h. sources carbonates													
Rock Garden													
MUC 27	215	15	0-11	-	-	0-8/1	0-8/1	0-15/1	0/15/5	-	-	-	Raindrop
MUC 30	222	11	0-11/1	-	-	0-10/1	0-10/1	0-10/1	0-10/10	-	-	-	0-2 pelagic, from 7 cm sulphidic
MUC 35	258	13	0-13/1	0-13/2	-	0-15/1	0-13/1	0-13/1	0-15/5	-	-	-	close to bubble site, cores degassing on deck
Raindrop, degassing on deck													

Table 10.2 (continued)

Location Device	Stat.	Core Length	AOM SR	Bicarb	Acet.	FISH DNA	ARISA	Biom.	Cult.	Anim.	PW	Other	Description
Rock Garden (continued)													
GC 21	217	120	-	-	-	0-120/10	0-120/10	0-120/5	-	-	-	-	Raindrop
CTD	210	-	-	-	-	24-656	-	-	-	-	-	MOx	above bubble site at Rock Garden (10 samples)
CTD	211	-	-	-	-	580	-	-	-	-	-	MOx	perpendicular to current at Stat. 210 (5 samples)
Wairarapa													
MUC 10	109	11	-	-	-	-	-	-	0-10	-	-	-	Black Spot; 0-7 greenish grey, 5-10 black polych. tubes, burrows; bioturbation
MUC 11	110	22	0-24/1	-	-	0-22/1	0-22/1	0-22/2	-	large. polych.	I-III	-	Black Spot; 0-6 yellow grey, >6 dark grey
Wairarapa (North Tower)													
MUC 12b	124	22	0-20/1	-	-	0-17/1	0-17/1	0-17/2	0-20/2	1,3	I-III	-	Raindrop Site; 0-2 "crunchy" carb., lots of animals, foamy
MUC 13	137	21	0-24/1	-	-	0-17/1	0-17/1	0-17/2	-	polychaetes, ostracodes	I-III	-	Black Spot/ <i>Beggiatoa</i>
MUC 40	273	22	0-23/2	-	-	0-28/5	-	-	0-35/5	-	-	carb	Raindrop, sulphidic, degassing on deck
MUC 41	274	20	0-20/2	0-22/2	0-22/2	0-19/1	0-14/1	0-20/2	0-20/5	-	I-V	carb	0-15 black, carbonate < 6-8 cm
MUC 44	291	-	-	-	-	0-15/1	0-15/1	0-22/2	-	-	I-V	carb	Bacterial mat, slightly sulphidic sampled near bacterial mat (none visible on deck)
Wairarapa (Tui)													
MUC 45a	309	37	0-38/2	0-35/2	-	0-36/1	-	0-30/2	0-35/5	-	I-V	-	polychaete sheath visible, strong sulphidic smell 1 cm pelagic, >17cm grayish
MUC 47	315	37	0-38/2	0-40/2	-	0-34/1	0-36/1	0-40/2	0-40/5	-	I-V	-	traces of bacteria visible on deck, strongly sulphidic 0-0.5 cm sulphidic, >0.5 black

10.3 List of Porewater Sampling Sites and Collected Sub-samples.

Station	Area	Latitude (S)	Longitude (E)	Water depth / m	TA	H ₂ S	NH ₄	PO ₄ /SiO ₂	Cl, Br, SO ₄	NO ₃	Poros / CNS	ICP-AES	¹³ C	¹⁸ O, ² H	CH ₄	IC	He	Length / cm	No. of samples
45 MUC 2	LM-9	40°01.079'	177°51.573'	1059	X	X	X	X	X	X	X	X	X	X	X	X	-	22	15
50 GC 1	LM-9	40°01.070'	177°51.585'	1059	X	X	X	X	X	-	X	X	X	X	X	X	-	430	14
54 MUC 3	Kaka	40°02.152'	177°48.047'	1160	X	X	X	X	X	X	X	X	X	X	X	X	-	14.5	13
56 MUC 4	Moa	40°03.291'	177°48.643'	1124	X	X	X	X	X	X	X	X	X	X	X	X	-	18	14
64 GC 2	LM-9	40°01.067'	177°51.581'	1150	X	X	X	X	X	-	X	X	X	X	X	X	-	490	15
65 GC 3	Kaka	40°02.160'	177°48.056'	1165	X	X	X	X	X	-	X	X	X	X	X	X	-	425	13
73 MUC 5	Bear's Paw	40°03.214'	177°49.238'	1111	X	X	X	X	X	X	X	X	X	X	X	X	-	25.5	18
77 FLUFO 1	Bear's Paw	40°03.214'	177°49.216'	1098	X	-	X	X	X	X	X	X	-	-	-	X	-	0 ; 0	21
78 MUC 6	LM-9 Ref	40°01.399'	177°48.944'	1177	X	X	X	X	X	X	X	X	X	X	X	X	-	32	19
79 GC 4	LM-9 Ref	40°01.401'	177°48.941'	1180	X	X	X	X	X	X	X	X	X	X	X	X	-	540	20
85 MUC 7	Bear's Paw	40°03.182'	177°49.191'	1099	X	X	X	X	X	X	X	X	X	X	X	X	-	10	11
93 GC 5	Bear's Paw	40°03.188'	177°49.162'	1100	X	X	X	X	X	-	X	X	X	X	X	X	-	170	9
94 GC 6	Bear's Paw	40°03.183'	177°49.182'	1101	X	X	X	X	X	-	X	X	X	X	X	X	-	116	9
95 GC 7	Bear's Paw	40°03.102'	177°49.174'	1100	X	X	X	X	X	-	X	X	X	X	X	X	-	90	7
109 MUC 10	W. N Tower	41°46.951'	175°24.169'	1059	X	X	X	X	X	X	X	X	X	X	X	X	-	11	8
110 MUC 11	W. N Tower	41°46.995'	175°24.226'	1059	X	X	X	X	X	X	X	X	X	X	X	X	-	24	16
111 GC 8	W. N Tower	41°46.955'	175°24.184'	1061	X	X	X	X	X	-	X	X	X	X	X	X	-	254	12
112 GC 9	W. Hill	41°43.299'	175°27.110'	815	X	X	X	X	X	-	X	X	X	X	X	X	-	47	4
124 MUC 12	W. N Tower	41°46.927'	175°23.988'	1048	X	X	X	X	X	X	X	X	X	X	X	X	-	17	15
125 GC 10	W. N Tower	41°46.932'	175°23.973'	1041	X	X	X	X	X	-	X	X	X	X	X	X	-	150	8
126 GC 11	W. N Tower	41°46.911'	175°23.984'	1042	-	-	-	-	-	-	-	-	-	-	-	-	-	10	0
133 FLUFO 2	W. Tui Flare	41°46.960'	175°24.043'	1060	-	-	-	X	X	X	-	X	-	-	-	X	-	0 ; 0	16
137 MUC 13	W. N Tower	41°46.895'	175°24.042'	1059	X	X	X	X	X	X	X	X	X	X	X	X	-	22.5	16
142 BIGO 2	W. N Tower	41°47.000'	175°24.069'	1067	X	X	X	X	X	X	X	X	X	X	X	X	-	14 ; 16	58
152 GC 12	W. N Tower	41°46.956'	175°24.182'	1065	X	X	X	X	X	-	X	X	X	X	X	X	-	490	19
153 GC 13	W. Ref	41°45.444'	175°26.536'	1057	X	X	X	X	X	X	X	X	X	X	X	X	-	535	22
157 MUC 15	W. N Tower	41°46.951'	175°24.211'	1060	X	X	X	X	X	X	X	X	X	X	X	X	-	10	8
169 GC 15	LM-9 Ref	40°01.415'	175°49.011'	1177	X	X	X	X	X	-	X	X	X	X	X	X	-	591	29
170 GC 16	LM-9 Ref	39°56.350'	177°55.350'	1155	X	X	X	X	X	-	X	X	X	X	X	X	-	584	26

GC = gravity corer; MUC = TV guided multi-corer; BIGO = biogeochemical observatory; FLUFO = fluid flux observatory; GKG = large box corer; LM-9 = Lewis & Marshall (1996) Site 9; W. = Wairarapa

Table 10.3: List of porewater sampling sites and collected sub-samples (continued).

Station	Area	Latitude (S)	Longitude (E)	Water depth / m	TA	H ₂ S	NH ₄	PO ₄ /SiO ₂	Cl, Br, SO ₄	NO ₃	Poros / CNS	ICP-AES	¹³ C	¹⁸ O, ² H	CH ₄	IC	He	Length / cm	No. of samples
179 FLUFO 3	Bear's Paw	40°03.183'	177°49.198'	1100	X	X	X	X	X	X	X	X	X	X	X	X	-	16	29
188 BIGO 3	Bear's Paw	40°03.189'	177°49.138'	1103	-	-	-	-	X	X	-	X	-	-	-	X	-	0	32
194 GC 18	Bear's Paw	40°03.195'	177°49.188'	1102	-	-	-	-	-	-	-	-	-	-	-	-	X	72	4
196 GC 20	Bear's Paw	40°03.196'	177°49.183'	1102	X	X	X	X	X	-	X	X	X	X	X	X	-	170	15
214 MUC 26	Rock Garden	40°01.926'	178°09.658'	660	X	X	X	X	X	X	X	X	X	X	X	X	-	8	10
215 MUC 27	Rock Garden	40°01.923'	178°09.651'	665	X	X	X	X	X	X	X	X	X	X	X	X	-	10.5	11
217 GC 21	Rock Garden	40°01.138'	178°09.703'	662	X	X	X	X	X	X	X	X	-	X	X	X	-	134	12
221 MUC 29	Rock Garden	40°01.936'	178°09.658'	660	X	X	X	X	X	X	X	X	X	X	X	X	-	8	8
223 FLUFO 4	Rock Garden	40°01.984'	178°09.662'	661	X	X	X	X	X	X	X	X	X	X	X	X	-	8 ; 0	24
228 BIGO 4	Rock Garden	40°02.003'	178°09.665'	659	-	-	X	X	X	X	X	X	-	-	-	X	-	0 ; 0	32
231 MUC 31	Kaka	40°02.145'	177°47.981'	1170	X	X	X	X	X	X	X	X	X	X	X	X	-	29	18
233 GC 22	LM-9 Ref	40°01.414'	177°48.953'	1179	-	-	-	-	-	-	-	-	-	-	-	-	X	535	5
243 GC 24	Kaka	40°02.158'	177°48.049'	1167	X	X	X	X	X	-	X	X	X	X	X	X	-	560	20
244 GC 25	LM-9	40°01.068'	177°51.583'	1152	X	X	X	X	X	-	X	X	X	X	X	X	-	477	22
248 FLUFO 5	Rock Garden	40°01.900'	178°09.619'	658	X	X	X	X	X	X	X	X	-	X	X	X	-	8 ; 0	24
258 MUC 35	Rock Garden	40°01.914'	178°09.685'	659	X	X	X	X/-	X	X	X	X	-	X	X	X	-	12	11
267 GC 27	Rock Garden	40°01.937'	178°09.653'	662	X	X	X	X	X	X	X	X	-	X	X	X	-	115	11
268 GC 28	Rock Garden	40°01.939'	178°09.654'	662	-	-	-	-	-	-	-	-	-	-	-	-	X	95	4
273 MUC 40	W. N Tower	41°46.962'	175°24.268'	1059	X	X	X	X	X	X	X	X	X	X	X	X	-	22	16
276 BIGO 5	W. N Tower	41°46.919'	175°24.097'	1059	-	-	X	X	X	X	X	X	-	-	-	X	-	5 ; 5	32
277 FLUFO 6	W. N Tower	41°46.900'	175°24.099'	1048	X	X	X	X	X	X	X	X	-	-	-	X	-	0 ; 4	16
285 GC 37	W. N Tower	41°46.956'	175°24.189'	1061	X	X	X	X	X	X	X	X	X	X	X	X	-	286	14
287 GC 39	W. N Tower	41°46.961'	175°24.233'	1059	X	X	X	X	X	X	X	X	X	X	X	X	-	400	25
295 GC 40	W. S Tower	41°47.595'	175°24.247'	1081	X	X	X	X	X	X	X	X	X	X	X	X	-	374	12
296 GC 41	W. S Tower	41°47.377'	175°24.473'	1056	X	X	X	X	X	X	X	X	X	X	X	X	-	360	14
302 GC 42	W. S Tower	41°47.327'	175°24.541'	1056	X	X	X	X	X	X	X	X	X	X	X	X	-	150	11
304 GC 43	W. S Tower	41°46.340'	175°25.580'	1054	-	-	-	-	-	-	-	-	-	-	-	-	-	280	2
307 BIGO 6	W. Ref	41°46.740'	175°25.140'	1051	X	X	X	X	X	X	X	X	X	X	X	X	-	15.5 ; 18	50

GC = gravity corer; MUC = TV guided multi-corer; BIGO = biogeochemical observatory; FLUFO = fluid flux observatory; GKG = large box corer; LM-9 = Lewis & Marshall (1996) Site 9; W. = Wairarapa

10.4 CSEM Measure Points

Waypoint	Longitude Rx1	Latitude Rx1	Longitude Rx2	Latitude Rx2	Water depth [m]
1	175.4003	-41.7968	175.3999	-41.7972	1101.4
2	175.4029	-41.7944	175.4025	-41.7947	1090.2
3	175.4053	-41.7921	175.4049	-41.7925	1079.3
4	175.4067	-41.7908	175.4063	-41.7912	1066.8
5	175.4078	-41.7898	175.4074	-41.7902	1058.1
6	175.4090	-41.7887	175.4086	-41.7891	1053.5
7	175.4101	-41.7876	175.4098	-41.7880	1057.7
8	175.4123	-41.7856	175.4119	-41.7860	1055.5
9	175.4136	-41.7844	175.4132	-41.7848	1050.4
10	175.4149	-41.7832	175.4145	-41.7836	1050.8
11	175.4168	-41.7814	175.4165	-41.7817	1058.3
12	175.4191	-41.7793	175.4187	-41.7796	1051.0
13	175.4213	-41.7772	175.4209	-41.7776	1051.9
14	175.4230	-41.7757	175.4226	-41.7760	1056.3
15	175.4239	-41.7748	175.4235	-41.7751	1054.8
16	175.4252	-41.7736	175.4248	-41.7739	1061.2
17	175.4264	-41.7724	175.4261	-41.7728	1056.4
18	175.4273	-41.7716	175.4269	-41.7720	1055.9
19	175.4284	-41.7706	175.4280	-41.7709	1057.5
20	175.4297	-41.7694	175.4293	-41.7698	1059.5
21	175.4307	-41.7684	175.4303	-41.7688	1060.3
22	175.4329	-41.7664	175.4325	-41.7668	1060.9
23	175.4350	-41.7644	175.4347	-41.7647	1059.9

Instrument locations, CSEM Wairarapa I, 21.01.2007

Way point	Longitude Rx2	Latitude Rx2	Water depth [m]	Way point	Longitude Rx1	Latitude Rx1	Water depth [m]
1	175.4113	-41.7942	1056.5	1	177.3701	-40.8402	1989.9
2	175.4103	-41.7928	1053.1	2	177.3757	-40.8416	1987.4
3	175.4096	-41.7917	1054.8	3	177.3812	-40.8431	1985.4
4	175.4087	-41.7905	1056.4	4	177.3867	-40.8445	1981.1
5	175.4076	-41.7888	1057.7	5	177.3924	-40.8460	1975.4
6	175.4066	-41.7875	1062.9	6	177.3979	-40.8474	1926.5
7	175.4052	-41.7854	1070.5	7	177.4035	-40.8488	1904.1
8	175.4041	-41.7839	1059.6	8	177.4096	-40.8504	2009.2
9	175.4031	-41.7825	1061.6	9	177.4155	-40.8519	1994.5
10	175.4020	-41.7809	1062.9	10	177.4218	-40.8536	2075.5
11	175.4002	-41.7782	1053.7	11	177.4276	-40.8551	2128.0
12	175.3982	-41.7753	1051.7	12	177.4330	-40.8565	2120.1
				13	177.4385	-40.8579	2132.8
				14	177.4444	-40.8594	2141.7
				15	177.4547	-40.8621	2143.0
Instrument locations, CSEM Wairarapa II, 24.01.2007				Instrument locations, CSEM "Ingo's Site", 27.01.2007			

Waypoint	Longitude Rx1	Latitude Rx1	Longitude Rx2	Latitude Rx2	Water depth [m]
1	177.8740	-40.0168	177.8746	-40.0168	1182.8
2	177.8700	-40.0173	177.8706	-40.0172	1162.0
3	177.8660	-40.0177	177.8666	-40.0176	1157.2
4	177.8638	-40.0179	177.8644	-40.0179	1156.5
5	177.8623	-40.0181	177.8629	-40.0180	1152.3
6	177.8610	-40.0182	177.8616	-40.0182	1152.6
7	177.8598	-40.0184	177.8604	-40.0183	1156.9
8	177.8574	-40.0186	177.8580	-40.0186	1163.8
9	177.8563	-40.0187	177.8569	-40.0187	1170.4
10	177.8528	-40.0191	177.8534	-40.0190	1196.9

Instrument locations, CSEM LM9, 30.01.2007

10.5 Table of OBS Deployments

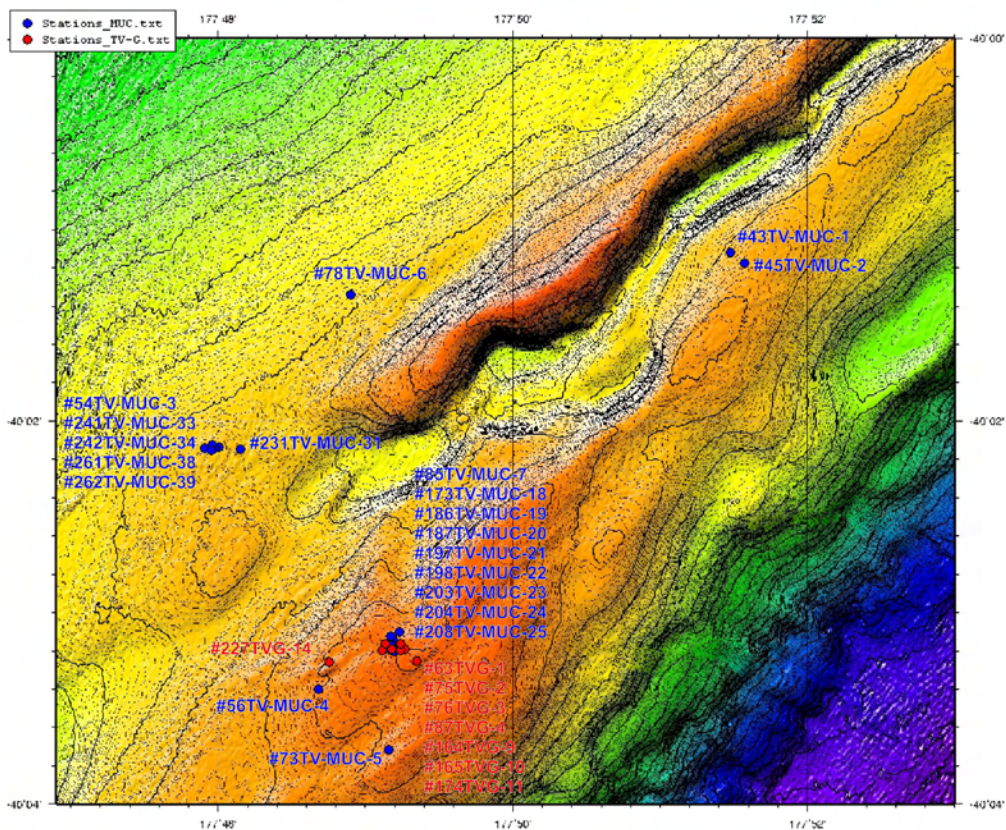
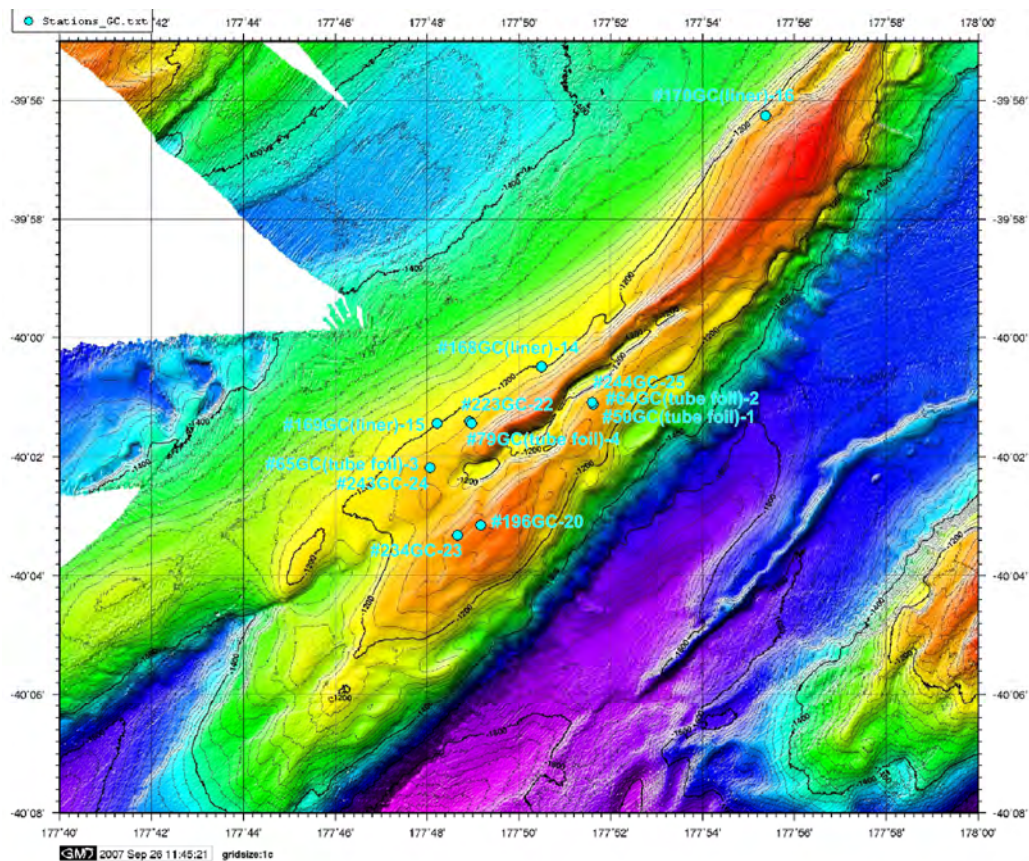
	INST.	LAT (N)	LON (E)	DEPTH	REC.	SKEW	SENSORS
		D:M	D:M	(m)	NO.	(ms)	
P 01	OBS 01	39°32,435' S	178°19,142' E	851	MBS 020509	9	HTI 79 + Owen 56
	OBS 02	39°32,575' S	178°19,660' E	835	MBS 020504	13	HTI 78 + Owen 80
	OBS 03	39°32,694' S	178°20,101' E	819	MBS 980907	-152	HTI 33 + Owen 58
	OBS 04	39°32,797' S	178°20,517' E	821	MBS 020505	2	HTI Riesling + Owen 78
	OBS 05	39°30,154' S	178°21,754' E	840	MBS 020508	13	HTI 65 + Owen 64
	OBS 06	39°26,401' S	178°23,491' E	1067	MBS 000610	-9	HTI 87 + Owen 79
	OBS 07	39°23,375' S	178°23,971' E	1275	MBS 990901		HTI 90 + Owen 61
	OBS 08	39°23,486' S	178°24,381' E	1260	MBS 001006	-150	HTI 77 + Owen 77
	OBS 09	39°23,629' S	178°24,812' E	1228	MBS 991292		HTI 76 + Owen 55
	OBS 10	39°23,749' S	178°25,186' E	1202	MBS 001005	7	HTI 48 + Owen 82

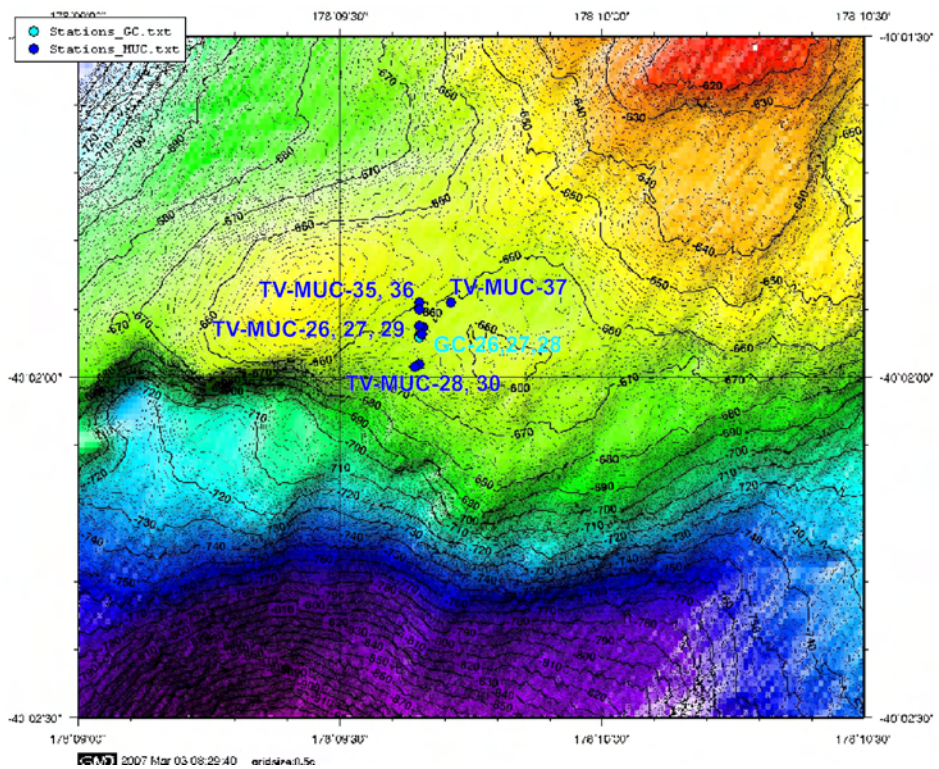
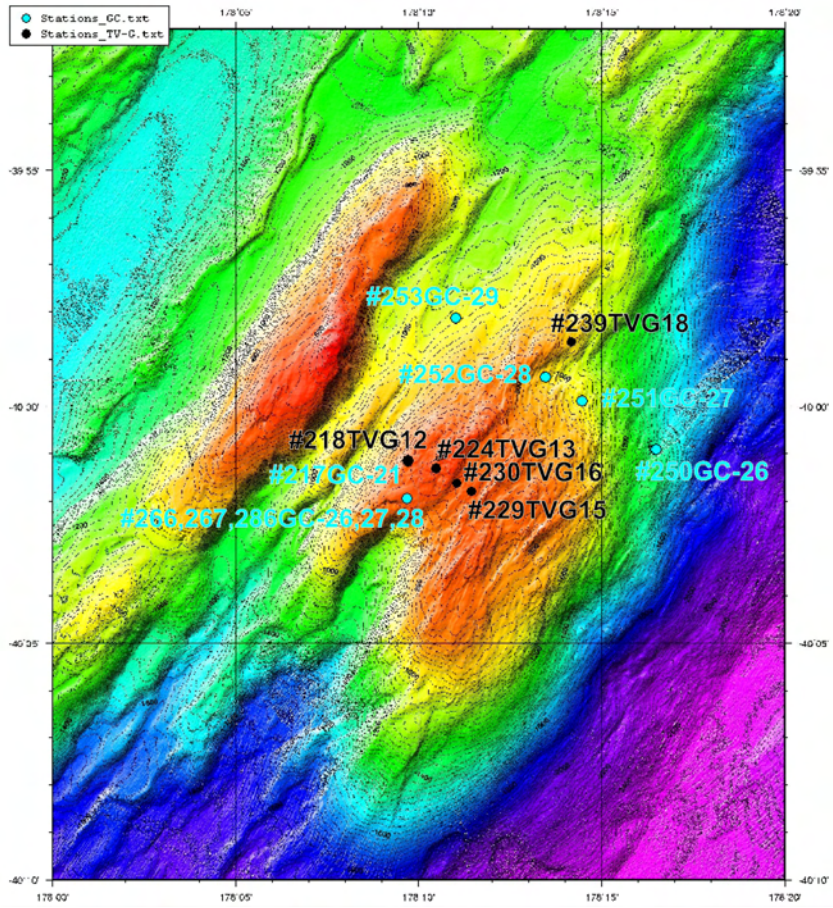
P 02	OBS 11	41°06,627' S	178°25,003' E	3117	MBS 001005	5	HTI 79 + Owen 75
	OBS 12	41°04,921' S	178°18,756' E	2898	MBS 000610	-5	HTI Riesling + Owen 78
	OBS 13	41°03,373' S	178°12,469' E	2968	MBS 020508	8	HTI 78 + Owen 80
	OBS 14	41° 1,876' S	178° 6,145' E	2818	MBS 991292	-11	HTI 90 + Owen 64
	OBS 15	41° 0,147' S	177° 59,832' E	2823	MBS 001006	-150	HTI 76 + Owen 55
	OBS 16	40° 58,506' S	177° 53,604' E	2746	MBS 990901		HTI 77 + Owen 77

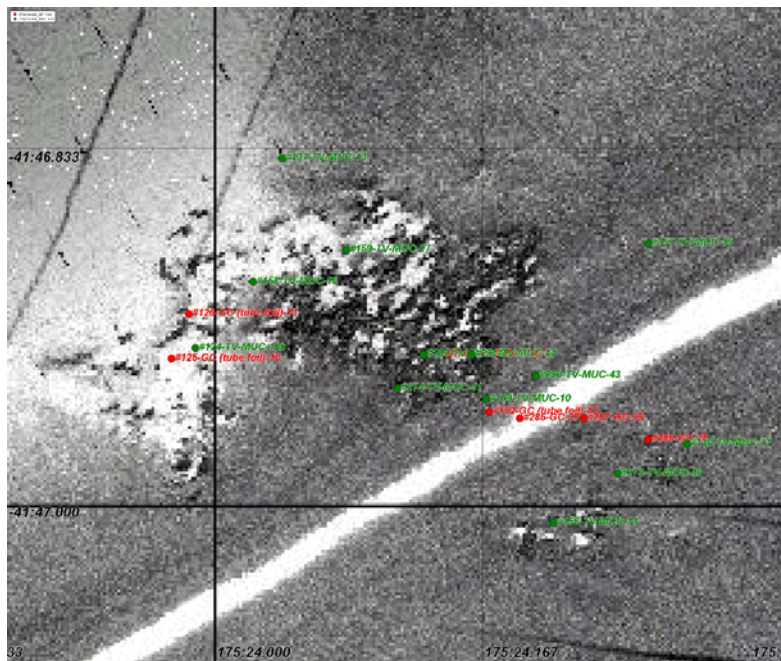
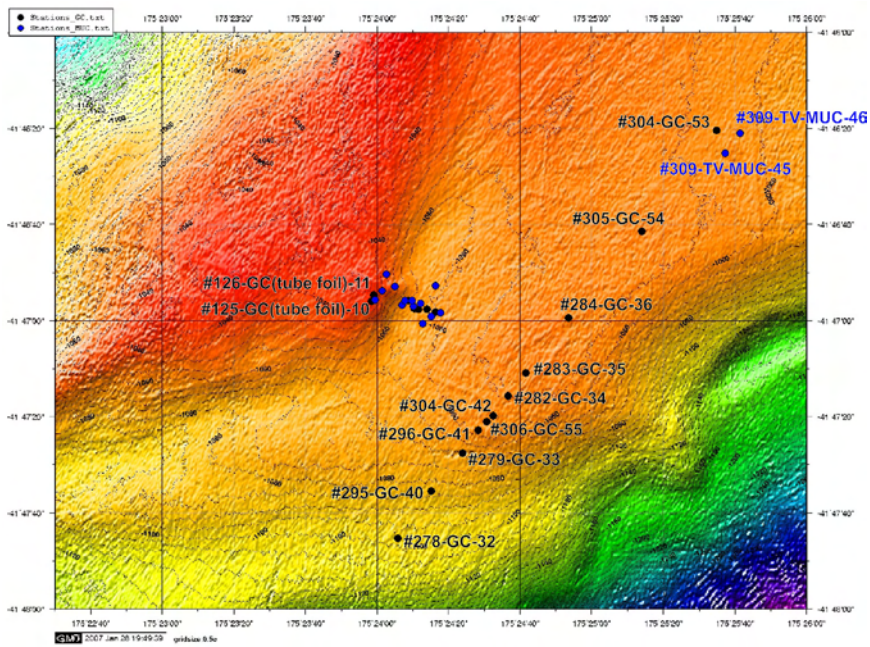
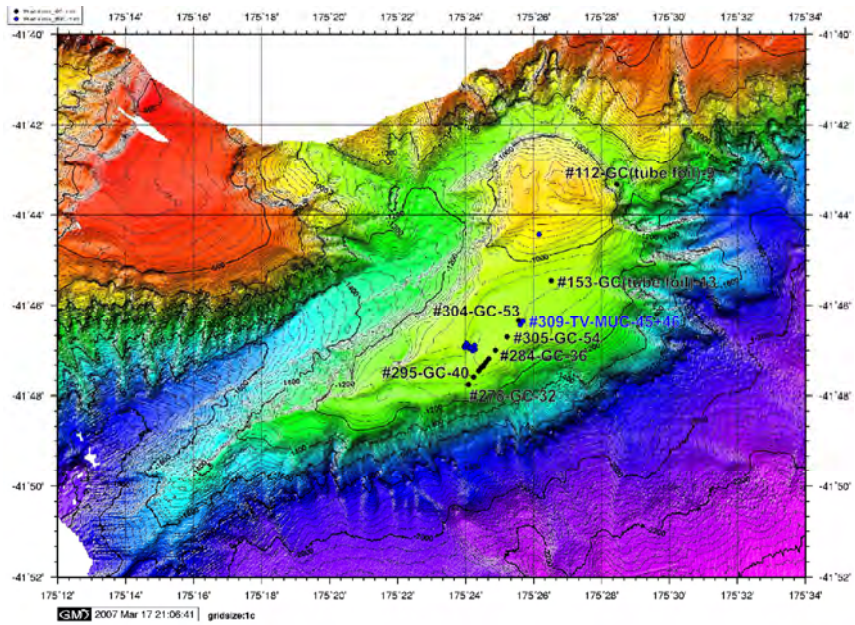
P 03	OBS 17	41°43,080' S	175°26,841' E	832	MBS 000613	-30	HTI 76 + Owen 55
	OBS/M 18	41°43,232' S	175°27,025' E	816	MBS 980901 / B	13	HTI 90 + Owen 64 + T31
	OBS/M 19	41°43,404' S	175°27,204' E	819	MBS 001006 / D	-149	HTI 78 + Owen 80 + T27
	OBS 20	41°43,604' S	175°27,384' E	857	MBS 980904	3	HTI Riesling + Owen 78
	OBS 21	41°44,974' S	175°28,625' E	1133	MBS 000614	-16	HTI 88 + Owen 71
	OBS/M 22	41°46,852' S	175°24,609' E	1054	MBS 000616 / F	-39	HTI 79 + Owen + T30
	OBS 23	41°46,970' S	175°24,380' E	1057	MBS 990901	-252	HTI 68 + Owen 81
	OBS 24	41°47,398' S	175°24,567' E	1058	MBS 020501	5	HTI 64 + Owen 79
	OBS/M 25	41°47,219' S	175°24,372' E	1056	MBS 020504 / A	12	HTI 48 +Owen ? + T29
	OBS 26	41°47,062' S	175°24,151' E	1066	MBS 020509		HTI 58 + Owen 58
	OBS 27	41°47,181' S	175°23,901' E	1065	MBS 980907	-2	HTI 82 +Owen 56
	OBS 28	41°47,282' S	175°23,699' E	1074	MBS 020515	2	HTI 83 + Owen 57
	OBS/M 29	41°46,862' S	175°24,015' E	1040	MBS 001005 / C	6	HTI 77 + Owen 77 + T28
	OBS 30	41°46,640' S	175°23,601' E	1030	MBS 000610	-7	HTI 87 + Owen 61
	OBS 31	41°46,530' S	175°23,656' E	1036	MBS 020508	11	HTI 86 + Owen 19
	OBS 32	41°45,981' S	175°22,938' E	1154	MBS 991299	-151	HTI 85 + Owen 63

P 04	OBS 33	41°19,124' S	176°28,419' E	1071	MBS 020509		HTI 82 +Owen 61
	OBS 34	41°19,181' S	176°31,365' E	829	MBS 020515		HTI 58 + Owen 77
	OBS 35	41°15,968' S	176°30,040' E	1052	MBS 980904		HTI 78 + Owen 80
	OBS 36	41°16,522' S	176°31,189' E	1023	MBS 020501		HTI 32 +Owen 79
	OBS 37	41°17,071' S	176°32,310' E	808	MBS 990901		HTI 68 + Owen 81
	OBS/M 38	41°17,301' S	176°32,795' E	769	MBS 980901 / B		HTI 48 + Owen ? + T29
	OBS/M 39	41°17,442' S	176°32,991' E	733	MBS 001006 / D		HTI 77 + Owen 58 + T30
	OBS/M 40	41°17,557' S	176°33,242' E	761	MBS 000616 / F		HTI 79 + Owen ? + T28
	OBS/M 41	41°17,682' S	176°33,490' E	750	MBS 020504 / A		HTI 89 + Owen 55 + T27
	OBS 42	41°17,791' S	176°33,740' E	808	MBS 980907		HTI 86 + Owen 19
	OBS 43	41°18,151' S	176°34,454' E	917	MBS 000610		HTI 83 + Owen 57
	OBH 44	41°18,570' S	176°35,313' E	1082	MBS 020508		HTI 87
	OBS/M 45	41°17,153' S	176°35,381' E	735	MBS 001005 / C		HTI 33 + Owen 64 + T31
	OBS 46	41°16,674' S	176°35,928' E	900	MBS 991299		HTI 22 + Owen ?
	OBS 47	41°16,177' S	176°36,408' E	840	MBS 000613		HTI Riesling + Owen 78 (?)
	OBS 48	41°16,287' S	176°37,143' E	881	MBS 000614		HTI 88 + Owen 71

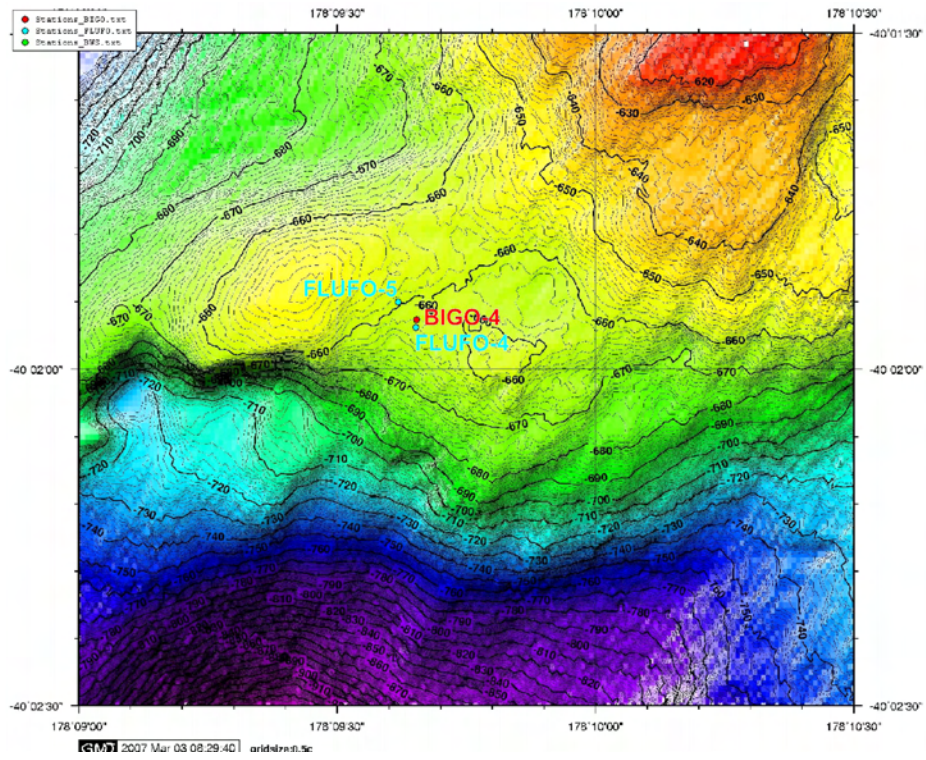
10.6 Maps of Coring Stations







10.7 Map of Lander and Mooring Stations



11 Station Lists

11.1 Station list Leg 1

Station	Datum	UTC	PositionLat	PositionLon	Tiefe [m]	Windstärke [m/s]	Kurs [°]	v [kn]	Gerät	Geräte Kürzel
SO191/001-1	11.01.07	22:16	41° 46,80' S	175° 17,47' E	1541	SW 4	95,5	6,7	Vermessung	EM / PS
SO191/001-1	11.01.07	23:42	41° 40,75' S	175° 30,42' E	658	SSW 3	84,3	6,7	Vermessung	EM / PS
SO191/001-1	11.01.07	23:56	41° 42,15' S	175° 31,80' E	1125	SSW 4	199,6	6,3	Vermessung	EM / PS
SO191/001-1	12.01.07	01:26	41° 48,43' S	175° 18,68' E	1228	SSE 2	206,7	5,8	Vermessung	EM / PS
SO191/001-1	12.01.07	01:40	41° 49,78' S	175° 20,01' E	1842	SSW 5	109,7	7,8	Vermessung	EM / PS
SO191/001-1	12.01.07	03:40	41° 43,57' S	175° 33,29' E	1760	ESE 2	110	7,1	Vermessung	EM / PS
SO191/001-1	12.01.07	03:59	41° 43,75' S	175° 36,98' E	1471	ENE 2	63	9,1	Vermessung	EM / PS
SO191/001-1	12.01.07	04:58	41° 37,33' S	175° 46,10' E	1601	E 2	54	9,1	Vermessung	EM / PS
SO191/001-1	12.01.07	05:50	41° 31,89' S	175° 55,52' E	1114	E 3	50,2	10,1	Vermessung	EM / PS
SO191/001-1	12.01.07	07:06	41° 22,86' S	176° 8,02' E	907	E 5	46,5	10,4	Vermessung	EM / PS
SO191/001-1	12.01.07	10:00	41° 22,54' S	176° 36,49' E	1022	ENE 4	59,9	10,1	Vermessung	EM / PS
SO191/001-1	12.01.07	12:31	40° 53,81' S	177° 6,00' E	1955	NE 3	71,2	9,3	Vermessung	EM / PS
SO191/001-1	12.01.07	13:33	40° 54,75' S	177° 18,12' E	2009	NNE 6	93,4	8,9	Vermessung	EM / PS
SO191/001-1	12.01.07	15:49	40° 58,72' S	177° 43,86' E	2337	N 10	94	8,9	Vermessung	EM / PS
SO191/001-1	12.01.07	21:00	40° 39,10' S	178° 42,50' E	3137	NNE 11	16,3	1,9	Vermessung	EM / PS
SO191/002-1	12.01.07	21:02	40° 39,08' S	178° 42,50' E	3134	NNE 12	187,9	0,6	CTD	CTD
SO191/002-1	12.01.07	21:05	40° 39,10' S	178° 42,50' E	3136	NNE 11	150	0,6	CTD	CTD
SO191/002-1	12.01.07	22:16	40° 39,06' S	178° 42,49' E	3132	NNE 10	179	0,2	CTD	CTD
SO191/002-1	13.01.07	00:31	40° 39,08' S	178° 42,51' E	3134	NNE 10	203,4	0,6	CTD	CTD
SO191/002-1	13.01.07	00:51	40° 39,09' S	178° 42,50' E	3137	NNE 10	261,1	0,2	CTD	CTD
SO191/002-1	13.01.07	00:57	40° 39,06' S	178° 42,49' E	3132	NNE 10	332,9	1,7	CTD	CTD
SO191/003-1	13.01.07	01:22	40° 41,15' S	178° 43,61' E	3133	NE 10	49,7	1,1	Profil	PR
SO191/003-1	13.01.07	01:43	40° 40,72' S	178° 43,91' E	3130	NNE 9	37,5	1,8	Profil	PR
SO191/003-1	13.01.07	01:47	40° 40,62' S	178° 43,97' E	3134	NNE 9	32	1,7	Profil	PR
SO191/003-1	13.01.07	02:52	40° 38,30' S	178° 45,29' E	3112	NNE 10	14	2,4	Profil	PR
SO191/003-1	13.01.07	03:35	40° 39,43' S	178° 47,98' E	2705	NNE 13	165,2	4	Profil	PR
SO191/003-1	13.01.07	04:14	40° 42,01' S	178° 48,55' E	2979	NNE 13	178,6	5,2	Profil	PR
SO191/003-1	13.01.07	05:30	40° 40,43' S	178° 44,23' E	3126	NE 12	305,3	2,1	Profil	PR
SO191/003-1	13.01.07	06:03	40° 39,45' S	178° 43,24' E	3127	NE 13	309,8	2,1	Profil	PR
SO191/003-1	13.01.07	06:15	40° 38,96' S	178° 42,49' E	3134	NNE 12	302,9	5,9	Profil	PR
SO191/003-1	13.01.07	06:19	40° 38,82' S	178° 42,10' E	3140	NE 13	301,8	4,5	Profil	PR
SO191/003-1	13.01.07	06:53	40° 38,48' S	178° 40,88' E	3141	NNE 11	106,4	1	Profil	PR
SO191/003-1	13.01.07	07:00	40° 38,54' S	178° 40,95' E	3142	NNE 10	149	1,2	Profil	PR
SO191/003-1	13.01.07	07:00	40° 38,54' S	178° 40,95' E	3142	NNE 10	149	1,2	Profil	PR
SO191/004-1	13.01.07	08:43	40° 40,05' S	178° 20,27' E	2991	NW 10	182,8	8,7	Vermessung	EM / PS
SO191/004-1	13.01.07	11:23	41° 00,54' S	178° 10,92' E	2939	NNE 7	205,3	8,5	Vermessung	EM / PS
SO191/004-1	13.01.07	12:12	40° 59,65' S	178° 6,87' E	2846	NNE 13	36,2	5	Vermessung	EM / PS
SO191/004-1	13.01.07	15:02	40° 39,04' S	178° 16,35' E	3011	NNE 10	0,2	7,6	Vermessung	EM / PS
SO191/004-1	13.01.07	15:25	40° 37,93' S	178° 12,64' E	2900	NNE 14	290,7	8,4	Vermessung	EM / PS

Station	Datum	UTC	PositionLat	PositionLon	Tiefe [m]	Windstärke [m/s]	Kurs [°]	v [kn]	Gerät	Geräte Kürzel
SO191/004-1	13.01.07	17:33	40° 53,87' S	178° 5,26' E	2748	NNE 8	222,9	7,4	Vermessung	EM / PS
SO191/004-1	13.01.07	17:58	40° 52,78' S	178° 1,24' E	2794	NE 10	343,7	5,4	Vermessung	EM / PS
SO191/004-1	13.01.07	20:01	40° 36,89' S	178° 8,50' E	2940	N 2	19,7	7,5	Vermessung	EM / PS
SO191/004-1	13.01.07	22:37	40° 13,32' S	177° 51,15' E	1600	NE 16	331,1	9,9	Vermessung	EM / PS
SO191/004-1	13.01.07	23:21	40° 08,28' S	177° 58,16' E	1566	NNE 13	43,3	10,6	Vermessung	EM / PS
SO191/004-1	14.01.07	00:00	40° 03,60' S	178° 4,03' E	1239	NNE 12	43,6	11,3	Vermessung	EM / PS
SO191/004-1	14.01.07	01:57	39° 51,38' S	178° 16,76' E	1077	NNE 13	45,4	10,1	Vermessung	EM / PS
SO191/004-1	14.01.07	02:31	39° 45,69' S	178° 17,59' E	797	NNE 12	6,4	9,8	Vermessung	EM / PS
SO191/004-1	14.01.07	03:23	39° 37,04' S	178° 19,66' E	900	NNE 11	16,2	9,6	Vermessung	EM / PS
SO191/005-1	14.01.07	03:57	39° 32,47' S	178° 19,12' E	852	NNE 11	0,5	2,6	OBS/OBH	OBS/OBH
SO191/005-1	14.01.07	03:59	39° 32,44' S	178° 19,14' E	851	NNE 13	58,6	1	OBS/OBH	OBS/OBH
SO191/005-1	14.01.07	04:21	39° 32,57' S	178° 19,66' E	834	NNE 12	91,7	0,9	OBS/OBH	OBS/OBH
SO191/005-1	14.01.07	04:34	39° 32,70' S	178° 20,10' E	819	N 12	148,2	0,5	OBS/OBH	OBS/OBH
SO191/005-1	14.01.07	04:47	39° 32,80' S	178° 20,52' E	824	N 13	155,4	0,2	OBS/OBH	OBS/OBH
SO191/005-1	14.01.07	05:22	39° 30,15' S	178° 21,75' E	842	NNE 13	47,8	0,7	OBS/OBH	OBS/OBH
SO191/005-1	14.01.07	05:55	39° 26,41' S	178° 23,49' E	1062	N 14	115,4	1	OBS/OBH	OBS/OBH
SO191/005-1	14.01.07	06:23	39° 23,37' S	178° 23,97' E	1275	NNE 14	6,6	1,2	OBS/OBH	OBS/OBH
SO191/005-1	14.01.07	06:33	39° 23,48' S	178° 24,39' E	1260	NW 13	100,9	1,4	OBS/OBH	OBS/OBH
SO191/005-1	14.01.07	06:43	39° 23,62' S	178° 24,79' E	1230	NNW 14	102,3	1,4	OBS/OBH	OBS/OBH
SO191/005-1	14.01.07	06:50	39° 23,74' S	178° 25,17' E	1208	NNW 12	90,2	2,6	OBS/OBH	OBS/OBH
SO191/005-1	14.01.07	06:50	39° 23,74' S	178° 25,17' E	1208	NNW 12	90,2	2,6	OBS/OBH	OBS/OBH
SO191/006-1	14.01.07	08:54	39° 38,52' S	178° 19,79' E	919	NNE 13	107,7	0,3	Profil	PR
SO191/006-1	14.01.07	09:26	39° 38,56' S	178° 19,77' E	916	NNW 12	71,7	1	Profil	PR
SO191/006-1	14.01.07	09:45	39° 38,11' S	178° 20,03' E	2863	N 12	23,1	1,2	Profil	PR
SO191/006-1	14.01.07	10:13	39° 37,52' S	178° 20,27' E	896	N 11	42,5	0,8	Profil	PR
SO191/006-1	14.01.07	12:37	39° 37,39' S	178° 20,41' E	883	N 8	353,1	1,6	Profil	PR
SO191/006-1	14.01.07	13:10	39° 36,42' S	178° 20,80' E	845	NNW 7	31,5	2	Profil	PR
SO191/006-1	14.01.07	13:10	39° 36,42' S	178° 20,80' E	845	NNW 7	31,5	2	Profil	PR
SO191/006-1	14.01.07	13:40	39° 35,36' S	178° 21,27' E	787	N 6	13,8	2,5	Profil	PR
SO191/006-1	14.01.07	13:55	39° 34,69' S	178° 21,57' E	758	N 7	7,1	3,9	Profil	PR
SO191/006-1	14.01.07	15:05	39° 31,41' S	178° 23,09' E	865	N 7	15,2	3	Profil	PR
SO191/006-1	14.01.07	17:44	39° 23,90' S	178° 26,55' E	1151	N 6	23,5	3,3	Profil	PR
SO191/006-1	14.01.07	18:05	39° 22,92' S	178° 26,99' E	1158	N 6	38	2,8	Profil	PR
SO191/006-1	14.01.07	18:05	39° 22,92' S	178° 26,99' E	1158	N 6	38	2,8	Profil	PR
SO191/006-1	14.01.07	19:33	39° 23,64' S	178° 24,76' E	1229	N 6	203,7	2,6	Profil	PR
SO191/006-1	14.01.07	19:50	39° 24,45' S	178° 24,39' E	1233	N 6	202,4	2,9	Profil	PR
SO191/006-1	15.01.07	00:07	39° 36,61' S	178° 18,76' E	1026	N 5	202,8	2,9	Profil	PR
SO191/006-1	15.01.07	00:19	39° 37,15' S	178° 18,51' E	1026	N 5	202,8	2,9	Profil	PR
SO191/006-1	15.01.07	01:33	39° 35,34' S	178° 17,43' E	1054	NNE 6	12,3	3	Profil	PR
SO191/006-1	15.01.07	01:36	39° 35,19' S	178° 17,51' E	1056	NNE 6	30,3	2,9	Profil	PR
SO191/006-1	15.01.07	06:13	39° 22,30' S	178° 23,53' E	1312	ENE 4	13,5	3	Profil	PR
SO191/006-1	15.01.07	06:13	39° 22,30' S	178° 23,53' E	1312	ENE 4	13,5	3	Profil	PR

Station	Datum	UTC	PositionLat	PositionLon	Tiefe [m]	Windstärke [m/s]	Kurs [°]	v [kn]	Gerät	Geräte Kürzel
SO191/006-1	15.01.07	07:56	39° 23,62' S	178° 25,72' E	1171	ENE 5	223,8	3,3	Profil	PR
SO191/006-1	15.01.07	08:21	39° 24,78' S	178° 25,19' E	1171	ESE 2	192,2	2,4	Profil	PR
SO191/006-1	15.01.07	12:28	39° 36,17' S	178° 19,96' E	897	E 6	199,8	3,2	Profil	PR
SO191/006-1	15.01.07	12:30	39° 36,26' S	178° 19,91' E	897	E 6	199,8	3,2	Profil	PR
SO191/006-1	15.01.07	13:18	39° 35,56' S	178° 18,28' E	1057	ESE 4	27,3	3,4	Profil	PR
SO191/006-1	15.01.07	13:33	39° 34,87' S	178° 18,59' E	1015	ESE 5	14,9	2,6	Profil	PR
SO191/006-1	15.01.07	18:23	39° 21,29' S	178° 24,96' E	1341	SE 4	26	2,9	Profil	PR
SO191/006-1	15.01.07	18:23	39° 21,29' S	178° 24,96' E	1341	SE 4	26	2,9	Profil	PR
SO191/006-1	15.01.07	20:48	39° 22,63' S	178° 21,53' E	1282	WSW 0	121,3	2,9	Profil	PR
SO191/006-1	15.01.07	21:29	39° 23,40' S	178° 24,06' E	1271	WSW 3	113,1	2,6	Profil	PR
SO191/006-1	15.01.07	22:29	39° 24,56' S	178° 27,88' E	1326	SW 3	112,4	3,5	Profil	PR
SO191/006-1	15.01.07	22:29	39° 24,56' S	178° 27,88' E	1326	SW 3	112,4	3,5	Profil	PR
SO191/006-1	15.01.07	23:49	39° 26,03' S	178° 26,12' E	1198	SSE 1	255,9	3,2	Profil	PR
SO191/006-1	15.01.07	23:57	39° 26,11' S	178° 25,62' E	996	SSE 1	247	3,3	Profil	PR
SO191/006-1	16.01.07	02:10	39° 27,27' S	178° 17,31' E	804	NE 2	258,6	3,1	Profil	PR
SO191/006-1	16.01.07	02:10	39° 27,27' S	178° 17,31' E	804	NE 2	258,6	3,1	Profil	PR
SO191/006-1	16.01.07	02:54	39° 28,87' S	178° 17,26' E	785	N 3	109,6	2,9	Profil	PR
SO191/006-1	16.01.07	02:55	39° 28,89' S	178° 17,32' E	789	N 3	103,6	2,3	Profil	PR
SO191/006-1	16.01.07	05:07	39° 31,26' S	178° 25,39' E	1216	NNE 9	118,1	3	Profil	PR
SO191/006-1	16.01.07	05:07	39° 31,26' S	178° 25,39' E	1216	NNE 9	118,1	3	Profil	PR
SO191/006-1	16.01.07	06:30	39° 33,55' S	178° 23,22' E	773	NNE 10	275,6	3,5	Profil	PR
SO191/006-1	16.01.07	08:12	39° 31,85' S	178° 16,92' E	889	ENE 2	294,7	2,7	Profil	PR
SO191/006-1	16.01.07	08:43	39° 31,28' S	178° 15,10' E	791	ENE 3	287,2	2,8	Profil	PR
SO191/006-1	16.01.07	08:44	39° 31,26' S	178° 15,04' E	788	ENE 3	292,5	3,5	Profil	PR
SO191/006-1	16.01.07	08:45	39° 31,24' S	178° 14,98' E	782	ENE 3	284,7	3	Profil	PR
SO191/006-1	16.01.07	08:53	39° 31,06' S	178° 14,49' E	724	E 2	270,8	3,5	Profil	PR
SO191/006-1	16.01.07	09:19	39° 30,36' S	178° 15,02' E	729	E 3	102,5	2,3	Profil	PR
SO191/006-1	16.01.07	09:32	39° 30,44' S	178° 15,29' E	750	ENE 3	103,5	1,1	Profil	PR
SO191/007-1	16.01.07	09:48	39° 31,56' S	178° 16,98' E	868	ENE 2	127,8	9,3	OBS/OBH	OBS/OBH
SO191/007-1	16.01.07	09:50	39° 31,77' S	178° 17,28' E	883	ENE 2	130,4	9	OBS/OBH	OBS/OBH
SO191/007-1	16.01.07	10:00	39° 32,34' S	178° 18,70' E	862	ESE 1	101,4	5,4	OBS/OBH	OBS/OBH
SO191/007-1	16.01.07	10:23	39° 32,67' S	178° 19,19' E	855	ESE 1	122,2	0,8	OBS/OBH	OBS/OBH
SO191/007-1	16.01.07	10:25	39° 32,69' S	178° 19,23' E	853	ESE 1	108,1	1	OBS/OBH	OBS/OBH
SO191/007-1	16.01.07	10:34	39° 32,62' S	178° 19,57' E	838	SSE 1	64,6	0,8	OBS/OBH	OBS/OBH
SO191/007-1	16.01.07	11:23	39° 32,80' S	178° 19,98' E	830	SW 3	138,2	2,2	OBS/OBH	OBS/OBH
SO191/007-1	16.01.07	11:30	39° 32,94' S	178° 20,14' E	812	WSW 4	189,5	3	OBS/OBH	OBS/OBH
SO191/007-1	16.01.07	11:37	39° 32,80' S	178° 19,64' E	853	WSW 4	321	4	OBS/OBH	OBS/OBH
SO191/007-1	16.01.07	11:47	39° 32,72' S	178° 20,13' E	824	SSW 4	137,6	1,8	OBS/OBH	OBS/OBH
SO191/007-1	16.01.07	11:49	39° 32,75' S	178° 20,18' E	817	SSW 3	135,2	0,9	OBS/OBH	OBS/OBH
SO191/007-1	16.01.07	12:01	39° 32,75' S	178° 20,14' E	820	SW 4	149,4	1,3	OBS/OBH	OBS/OBH
SO191/007-1	16.01.07	12:22	39° 32,81' S	178° 20,65' E	827	SW 3	130,2	1,1	OBS/OBH	OBS/OBH
SO191/007-1	16.01.07	12:39	39° 31,34' S	178° 21,44' E	788	SW 5	16,9	9,9	OBS/OBH	OBS/OBH

Station	Datum	UTC	PositionLat	PositionLon	Tiefe [m]	Windstärke [m/s]	Kurs [°]	v [kn]	Gerät	Geräte Kürzel
SO191/007-1	16.01.07	12:48	39° 30,47' S	178° 21,76' E	840	SW 6	20,6	3,4	OBS/OBH	OBS/OBH
SO191/007-1	16.01.07	13:01	39° 30,17' S	178° 21,85' E	841	WSW 5	131,6	1,3	OBS/OBH	OBS/OBH
SO191/007-1	16.01.07	13:21	39° 28,19' S	178° 23,01' E	998	SW 8	24,6	10,2	OBS/OBH	OBS/OBH
SO191/007-1	16.01.07	13:54	39° 26,53' S	178° 23,76' E	0	SSW 8	126,6	1,1	OBS/OBH	OBS/OBH
SO191/007-1	16.01.07	14:10	39° 26,45' S	178° 23,68' E	0	WSW 8	139,4	1,1	OBS/OBH	OBS/OBH
SO191/007-1	16.01.07	14:25	39° 25,24' S	178° 24,49' E	0	SSW 8	26,2	10,8	OBS/OBH	OBS/OBH
SO191/007-1	16.01.07	14:41	39° 23,95' S	178° 25,33' E	0	SSW 6	42,4	1,4	OBS/OBH	OBS/OBH
SO191/007-1	16.01.07	15:00	39° 23,86' S	178° 25,30' E	0	SSW 8	267,7	0,6	OBS/OBH	OBS/OBH
SO191/007-1	16.01.07	15:02	39° 23,86' S	178° 25,29' E	0	S 7	308,3	0,3	OBS/OBH	OBS/OBH
SO191/007-1	16.01.07	15:16	39° 23,84' S	178° 25,26' E	0	S 7	141,8	0,4	OBS/OBH	OBS/OBH
SO191/007-1	16.01.07	15:16	39° 23,84' S	178° 25,26' E	0	S 7	141,8	0,4	OBS/OBH	OBS/OBH
SO191/007-1	16.01.07	15:32	39° 23,67' S	178° 24,92' E	0	S 8	303,2	0,6	OBS/OBH	OBS/OBH
SO191/007-1	16.01.07	15:34	39° 23,67' S	178° 24,92' E	0	S 7	114,2	0,4	OBS/OBH	OBS/OBH
SO191/007-1	16.01.07	15:34	39° 23,67' S	178° 24,92' E	0	S 7	114,2	0,4	OBS/OBH	OBS/OBH
SO191/007-1	16.01.07	15:45	39° 23,54' S	178° 24,51' E	1254	S 8	248,8	0,8	OBS/OBH	OBS/OBH
SO191/007-1	16.01.07	15:53	39° 23,52' S	178° 24,42' E	1255	S 7	261,9	1,2	OBS/OBH	OBS/OBH
SO191/007-1	16.01.07	16:05	39° 23,39' S	178° 24,07' E	1271	S 9	132	0,3	OBS/OBH	OBS/OBH
SO191/007-1	16.01.07	16:05	39° 23,39' S	178° 24,07' E	1271	S 9	132	0,3	OBS/OBH	OBS/OBH
SO191/008-1	16.01.07	20:28	40° 10,81' S	178° 28,98' E	3038	SSW 12	117,7	1,4	MT	MT
SO191/008-1	16.01.07	20:30	40° 10,82' S	178° 28,97' E	3040	SSW 10	186,3	0,8	MT	MT
SO191/008-2	16.01.07	20:55	40° 12,05' S	178° 28,34' E	3131	S 11	202	3,4	Profil	PR
SO191/008-2	16.01.07	21:38	40° 14,95' S	178° 25,65' E	2791	S 10	227,7	2,9	Profil	PR
SO191/008-2	16.01.07	21:59	40° 15,83' S	178° 24,49' E	2842	SSW 11	215,3	3,9	Profil	PR
SO191/008-3	16.01.07	23:20	40° 5,08' S	178° 18,20' E	2433	S 9	320,1	1,1	MT	MT
SO191/008-3	17.01.07	00:32	39° 59,43' S	178° 7,41' E	531	SSW 10	11,4	1,5	MT	MT
SO191/008-3	17.01.07	01:30	39° 53,88' S	177° 56,55' E	1316	SW 10	303,5	1,4	MT	MT
SO191/008-3	17.01.07	02:28	39° 48,29' S	177° 45,82' E	1160	SSW 10	296,6	1,1	MT	MT
SO191/008-3	17.01.07	03:29	39° 42,76' S	177° 35,04' E	316	SSW 11	205,4	1,2	MT	MT
SO191/008-3	17.01.07	03:29	39° 42,76' S	177° 35,04' E	316	SSW 11	205,4	1,2	MT	MT
SO191/009-1	17.01.07	12:36	39° 58,38' S	177° 23,90' E	395	SSW 9	176,7	1,5	Profil	PR
SO191/009-1	17.01.07	12:48	39° 58,75' S	177° 23,94' E	378	S 9	188,9	1,7	Profil	PR
SO191/009-1	17.01.07	13:12	39° 59,62' S	177° 23,93' E	350	S 10	176	1,6	Profil	PR
SO191/009-1	17.01.07	13:20	39° 59,98' S	177° 23,92' E	344	S 10	174	3,9	Profil	PR
SO191/009-1	17.01.07	14:38	40° 4,62' S	177° 28,42' E	946	SSW 9	116,6	4,5	Profil	PR
SO191/009-1	18.01.07	04:02	40° 38,96' S	178° 42,23' E	3139	WSW 4	146,2	5,9	Profil	PR
SO191/009-1	18.01.07	08:09	40° 57,24' S	178° 30,97' E	3128	NW 2	204,4	4,5	Profil	PR
SO191/009-1	19.01.07	01:01	40° 12,07' S	176° 58,99' E	151	ENE 2	294,1	5	Profil	PR
SO191/009-1	19.01.07	01:42	40° 13,00' S	176° 57,28' E	131	N 3	209,2	2	Profil	PR
SO191/009-1	19.01.07	01:48	40° 13,18' S	176° 57,20' E	132	N 2	198,1	1,7	Profil	PR
SO191/009-1	19.01.07	01:52	40° 13,35' S	176° 57,20' E	136	NW 3	128	3,8	Profil	PR
SO191/010-1	19.01.07	08:59	41° 6,62' S	178° 25,01' E	3116	S 2	271,5	1,4	OBS/OBH	OBS/OBH
SO191/010-1	19.01.07	09:02	41° 6,63' S	178° 25,01' E	3117	SSW 2	1,8	0,6	OBS/OBH	OBS/OBH

Station	Datum	UTC	PositionLat	PositionLon	Tiefe [m]	Windstärke [m/s]	Kurs [°]	v [kn]	Gerät	Geräte Kürzel
SO191/010-1	19.01.07	09:38	41° 4,92' S	178° 18,77' E	2901	WSW 2	232,6	1,2	OBS/OBH	OBS/OBH
SO191/010-1	19.01.07	10:17	41° 3,37' S	178° 12,48' E	2984	WSW 3	255,2	1,2	OBS/OBH	OBS/OBH
SO191/010-1	19.01.07	10:54	41° 1,88' S	178° 6,13' E	2816	WNW 4	283,9	1,2	OBS/OBH	OBS/OBH
SO191/010-1	19.01.07	11:33	41° 0,15' S	177° 59,83' E	2823	WNW 5	282,8	0,7	OBS/OBH	OBS/OBH
SO191/010-1	19.01.07	12:07	40° 58,51' S	177° 53,61' E	2745	NW 6	295	1,2	OBS/OBH	OBS/OBH
SO191/010-1	19.01.07	12:08	40° 58,50' S	177° 53,59' E	2746	NW 6	287	2	OBS/OBH	OBS/OBH
SO191/011-1	19.01.07	12:36	40° 57,29' S	177° 48,49' E	2383	NNW 5	96,8	3,2	Profil	PR
SO191/011-1	19.01.07	12:43	40° 57,34' S	177° 48,81' E	2308	WNW 3	94,6	2,6	Profil	PR
SO191/011-1	19.01.07	13:12	40° 57,74' S	177° 50,30' E	2372	WSW 2	110,1	2	Profil	PR
SO191/011-1	19.01.07	13:13	40° 57,77' S	177° 50,43' E	2370	WSW 3	98,3	2,4	Profil	PR
SO191/011-1	19.01.07	19:16	41° 7,20' S	178° 27,56' E	3122	WSW 1	108,2	5	Profil	PR
SO191/011-1	20.01.07	00:42	41° 22,94' S	177° 59,99' E	2958	N 4	209	5,7	Profil	PR
SO191/011-1	20.01.07	10:38	40° 54,48' S	177° 12,62' E	2017	NW 12	305,6	4,7	Profil	PR
SO191/011-1	20.01.07	11:10	40° 55,60' S	177° 12,76' E	2017	W 12	36	3,6	Profil	PR
SO191/011-1	20.01.07	11:41	40° 54,49' S	177° 13,82' E	2014	W 17	57,6	1,8	Profil	PR
SO191/011-1	20.01.07	12:07	40° 53,71' S	177° 14,78' E	2016	W 14	60,8	1,2	Profil	PR
SO191/011-1	20.01.07	12:11	40° 53,54' S	177° 14,93' E	2022	W 14	21,9	3,3	Profil	PR
SO191/012-1	20.01.07	16:13	41° 4,68' S	178° 13,02' E	2779	WNW 11	110,5	12,4	OBS/OBH	OBS/OBH
SO191/012-1	20.01.07	16:37	41° 6,05' S	178° 19,38' E	3261	W 10	105,2	12,5	OBS/OBH	OBS/OBH
SO191/012-1	20.01.07	17:44	41° 7,04' S	178° 26,14' E	3118	WNW 11	201,2	4,3	OBS/OBH	OBS/OBH
SO191/012-1	20.01.07	17:48	41° 7,39' S	178° 26,04' E	3119	WNW 11	186,7	5,1	OBS/OBH	OBS/OBH
SO191/012-1	20.01.07	17:53	41° 7,48' S	178° 25,95' E	3120	W 13	76,7	2,3	OBS/OBH	OBS/OBH
SO191/012-1	20.01.07	18:49	41° 5,12' S	178° 19,38' E	3255	W 13	280,7	0,1	OBS/OBH	OBS/OBH
SO191/012-1	20.01.07	18:50	41° 5,12' S	178° 19,37' E	3257	W 13	253,5	1,6	OBS/OBH	OBS/OBH
SO191/012-1	20.01.07	18:57	41° 5,16' S	178° 19,27' E	3238	WSW 13	120,1	1,3	OBS/OBH	OBS/OBH
SO191/012-1	20.01.07	19:38	41° 3,57' S	178° 13,28' E	2836	W 13	282,6	4,3	OBS/OBH	OBS/OBH
SO191/012-1	20.01.07	19:58	41° 3,42' S	178° 12,45' E	2996	W 12	51,5	1,2	OBS/OBH	OBS/OBH
SO191/012-1	20.01.07	20:00	41° 3,42' S	178° 12,51' E	2937	W 14	37,4	1,7	OBS/OBH	OBS/OBH
SO191/012-1	20.01.07	20:41	41° 1,99' S	178° 6,95' E	2842	W 15	288,1	5,1	OBS/OBH	OBS/OBH
SO191/012-1	20.01.07	20:53	41° 1,84' S	178° 6,35' E	2832	W 12	64	1,2	OBS/OBH	OBS/OBH
SO191/012-1	20.01.07	20:54	41° 1,83' S	178° 6,37' E	2838	W 13	66,4	1,4	OBS/OBH	OBS/OBH
SO191/012-1	20.01.07	21:44	41° 0,22' S	178° 0,05' E	2820	W 12	288,7	2	OBS/OBH	OBS/OBH
SO191/012-1	20.01.07	21:54	40° 59,87' S	177° 59,73' E	2819	S 12	276,5	1,2	OBS/OBH	OBS/OBH
SO191/012-1	20.01.07	21:55	40° 59,93' S	177° 59,80' E	2817	W 12	51,1	1,1	OBS/OBH	OBS/OBH
SO191/012-1	20.01.07	22:46	40° 58,46' S	177° 53,75' E	2750	WSW 10	288,7	2,1	OBS/OBH	OBS/OBH
SO191/012-1	20.01.07	22:55	40° 58,34' S	177° 53,45' E	2744	W 12	2,6	1,3	OBS/OBH	OBS/OBH
SO191/012-1	20.01.07	22:58	40° 58,32' S	177° 53,51' E	2746	W 10	86,6	1,8	OBS/OBH	OBS/OBH
SO191/013-1	21.01.07	09:08	41° 48,33' S	175° 23,49' E	1257	E 5	92,2	0,3	Controlled Source Electro-Magnetic	CSEM
SO191/013-1	21.01.07	09:33	41° 48,32' S	175° 23,50' E	1260	E 4	138,1	0,3	Controlled Source Electro-Magnetic	CSEM
SO191/013-1	21.01.07	09:46	41° 48,33' S	175° 23,41' E	1244	E 5	190,1	0	Controlled Source Electro-Magnetic	CSEM
SO191/013-1	21.01.07	10:13	41° 48,32' S	175° 23,47' E	1254	E 5	230,6	0,2	Controlled Source Electro-Magnetic	CSEM
SO191/013-1	21.01.07	10:18	41° 48,32' S	175° 23,44' E	1237	E 5	35,3	0,3	Controlled Source Electro-Magnetic	CSEM

Station	Datum	UTC	PositionLat	PositionLon	Tiefe [m]	Windstärke [m/s]	Kurs [°]	v [kn]	Gerät	Geräte Kürzel
SO191/013-1	21.01.07	10:47	41° 48,33' S	175° 23,45' E	1257	ENE 4	235,6	0,5	Controlled Source Electro-Magnetic	CSEM
SO191/013-1	21.01.07	11:06	41° 48,34' S	175° 23,52' E	1283	ENE 5	207	0,3	Controlled Source Electro-Magnetic	CSEM
SO191/013-1	21.01.07	11:33	41° 48,35' S	175° 23,45' E	1258	NE 5	301,8	0,2	Controlled Source Electro-Magnetic	CSEM
SO191/013-1	21.01.07	12:47	41° 47,33' S	175° 24,54' E	1054	NE 5	27,1	1,5	Controlled Source Electro-Magnetic	CSEM
SO191/013-1	21.01.07	13:28	41° 46,60' S	175° 25,33' E	1053	NE 5	5,7	0,2	Controlled Source Electro-Magnetic	CSEM
SO191/013-1	21.01.07	13:35	41° 46,61' S	175° 25,28' E	1055	NE 4	159,8	0,2	Controlled Source Electro-Magnetic	CSEM
SO191/013-1	21.01.07	13:44	41° 46,62' S	175° 25,30' E	1052	ENE 5	174,2	0,3	Controlled Source Electro-Magnetic	CSEM
SO191/013-1	21.01.07	13:47	41° 46,62' S	175° 25,32' E	1052	ENE 4	71,8	0,7	Controlled Source Electro-Magnetic	CSEM
SO191/013-1	21.01.07	13:51	41° 46,59' S	175° 25,36' E	1052	ENE 5	13,9	0,9	Controlled Source Electro-Magnetic	CSEM
SO191/013-1	21.01.07	13:57	41° 46,52' S	175° 25,42' E	1054	ENE 4	41,9	1,4	Controlled Source Electro-Magnetic	CSEM
SO191/013-1	21.01.07	14:07	41° 46,47' S	175° 25,42' E	1054	NE 4	56	0,8	Controlled Source Electro-Magnetic	CSEM
SO191/013-1	21.01.07	14:17	41° 46,49' S	175° 25,43' E	1054	NE 5	106,5	0,4	Controlled Source Electro-Magnetic	CSEM
SO191/013-1	21.01.07	14:17	41° 46,49' S	175° 25,43' E	1054	NE 5	106,5	0,4	Controlled Source Electro-Magnetic	CSEM
SO191/013-1	21.01.07	14:22	41° 46,43' S	175° 25,50' E	1055	NE 5	6,7	1,1	Controlled Source Electro-Magnetic	CSEM
SO191/013-1	21.01.07	14:30	41° 46,33' S	175° 25,58' E	1056	NE 5	278,2	0,6	Controlled Source Electro-Magnetic	CSEM
SO191/013-1	21.01.07	14:36	41° 46,32' S	175° 25,57' E	1056	NE 5	28,2	0,6	Controlled Source Electro-Magnetic	CSEM
SO191/013-1	21.01.07	14:46	41° 46,33' S	175° 25,58' E	1056	NE 4	201,9	0,4	Controlled Source Electro-Magnetic	CSEM
SO191/013-1	21.01.07	14:48	41° 46,34' S	175° 25,58' E	1056	NNE 4	9	0,6	Controlled Source Electro-Magnetic	CSEM
SO191/013-1	21.01.07	14:54	41° 46,29' S	175° 25,65' E	1057	NE 4	2,4	0,6	Controlled Source Electro-Magnetic	CSEM
SO191/013-1	21.01.07	15:05	41° 46,27' S	175° 25,65' E	1058	ENE 4	0,3	0,6	Controlled Source Electro-Magnetic	CSEM
SO191/013-1	21.01.07	15:13	41° 46,27' S	175° 25,58' E	1058	NE 4	274,2	0,4	Controlled Source Electro-Magnetic	CSEM
SO191/013-1	21.01.07	15:24	41° 46,25' S	175° 25,60' E	1058	NE 4	36,9	0,2	Controlled Source Electro-Magnetic	CSEM
SO191/013-1	21.01.07	15:25	41° 46,25' S	175° 25,60' E	1058	NE 5	356	0,6	Controlled Source Electro-Magnetic	CSEM
SO191/013-1	21.01.07	15:31	41° 46,23' S	175° 25,67' E	1058	NE 5	96,1	0,5	Controlled Source Electro-Magnetic	CSEM
SO191/013-1	21.01.07	15:37	41° 46,21' S	175° 25,73' E	1058	ENE 5	355,3	0,5	Controlled Source Electro-Magnetic	CSEM
SO191/013-1	21.01.07	15:38	41° 46,21' S	175° 25,73' E	1058	ENE 5	132,6	0,4	Controlled Source Electro-Magnetic	CSEM
SO191/013-1	21.01.07	15:43	41° 46,21' S	175° 25,73' E	1058	NE 5	55,7	0,4	Controlled Source Electro-Magnetic	CSEM
SO191/013-1	21.01.07	15:52	41° 46,21' S	175° 25,74' E	1060	NE 4	310,5	0,6	Controlled Source Electro-Magnetic	CSEM
SO191/013-1	21.01.07	15:52	41° 46,21' S	175° 25,74' E	1060	NE 4	310,5	0,6	Controlled Source Electro-Magnetic	CSEM
SO191/013-1	21.01.07	16:00	41° 46,19' S	175° 25,77' E	1059	NE 4	39,8	0,3	Controlled Source Electro-Magnetic	CSEM
SO191/013-1	21.01.07	16:10	41° 46,16' S	175° 25,80' E	1060	NNE 4	122,7	0,2	Controlled Source Electro-Magnetic	CSEM
SO191/013-1	21.01.07	16:11	41° 46,16' S	175° 25,80' E	1060	NNE 4	179,5	0,4	Controlled Source Electro-Magnetic	CSEM
SO191/013-1	21.01.07	16:16	41° 46,16' S	175° 25,81' E	1060	NNE 4	254,3	0,3	Controlled Source Electro-Magnetic	CSEM
SO191/013-1	21.01.07	16:25	41° 46,16' S	175° 25,81' E	1060	NNE 2	193,1	0,6	Controlled Source Electro-Magnetic	CSEM
SO191/013-1	21.01.07	16:25	41° 46,16' S	175° 25,81' E	1060	NNE 2	193,1	0,6	Controlled Source Electro-Magnetic	CSEM
SO191/013-1	21.01.07	16:33	41° 46,12' S	175° 25,83' E	1060	NNE 3	19,2	0,5	Controlled Source Electro-Magnetic	CSEM
SO191/013-1	21.01.07	16:40	41° 46,08' S	175° 25,87' E	1060	NNE 3	86,5	0,2	Controlled Source Electro-Magnetic	CSEM
SO191/013-1	21.01.07	16:40	41° 46,08' S	175° 25,87' E	1060	NNE 3	86,5	0,2	Controlled Source Electro-Magnetic	CSEM
SO191/013-1	21.01.07	16:46	41° 46,08' S	175° 25,88' E	1059	NE 3	116,1	0,1	Controlled Source Electro-Magnetic	CSEM
SO191/013-1	21.01.07	16:56	41° 46,07' S	175° 25,87' E	1061	NE 2	307,3	0,3	Controlled Source Electro-Magnetic	CSEM
SO191/013-1	21.01.07	16:56	41° 46,07' S	175° 25,87' E	1061	NE 2	307,3	0,3	Controlled Source Electro-Magnetic	CSEM
SO191/013-1	21.01.07	17:05	41° 46,00' S	175° 25,97' E	1061	NNE 2	357,6	0,7	Controlled Source Electro-Magnetic	CSEM

Station	Datum	UTC	PositionLat	PositionLon	Tiefe [m]	Windstärke [m/s]	Kurs [°]	v [kn]	Gerät	Geräte Kürzel
SO191/013-1	21.01.07	17:11	41° 45,95' S	175° 26,00' E	1060	ENE 3	31	0,8	Controlled Source Electro-Magnetic	CSEM
SO191/013-1	21.01.07	17:11	41° 45,95' S	175° 26,00' E	1060	ENE 3	31	0,8	Controlled Source Electro-Magnetic	CSEM
SO191/013-1	21.01.07	17:17	41° 45,94' S	175° 26,01' E	1060	ENE 2	123,5	0,4	Controlled Source Electro-Magnetic	CSEM
SO191/013-1	21.01.07	17:26	41° 45,95' S	175° 26,01' E	1060	ENE 2	189,7	0,3	Controlled Source Electro-Magnetic	CSEM
SO191/013-1	21.01.07	17:26	41° 45,95' S	175° 26,01' E	1062	ENE 2	189,7	0,3	Controlled Source Electro-Magnetic	CSEM
SO191/013-1	21.01.07	17:34	41° 45,89' S	175° 26,06' E	1060	ENE 3	96,9	0,4	Controlled Source Electro-Magnetic	CSEM
SO191/013-1	21.01.07	17:35	41° 45,89' S	175° 26,06' E	1060	ENE 3	98,1	0,2	Controlled Source Electro-Magnetic	CSEM
SO191/013-1	21.01.07	17:35	41° 45,89' S	175° 26,06' E	1060	ENE 3	98,1	0,2	Controlled Source Electro-Magnetic	CSEM
SO191/013-1	21.01.07	17:40	41° 45,89' S	175° 26,08' E	1060	ENE 3	51,2	0,3	Controlled Source Electro-Magnetic	CSEM
SO191/013-1	21.01.07	17:50	41° 45,89' S	175° 26,08' E	1060	E 3	176,4	0,4	Controlled Source Electro-Magnetic	CSEM
SO191/013-1	21.01.07	17:51	41° 45,89' S	175° 26,08' E	1060	E 3	83,6	0,3	Controlled Source Electro-Magnetic	CSEM
SO191/013-1	21.01.07	17:58	41° 45,83' S	175° 26,14' E	1060	E 3	59,1	0,5	Controlled Source Electro-Magnetic	CSEM
SO191/013-1	21.01.07	17:59	41° 45,82' S	175° 26,15' E	1060	E 4	34,2	0,6	Controlled Source Electro-Magnetic	CSEM
SO191/013-1	21.01.07	17:59	41° 45,82' S	175° 26,15' E	1060	E 4	34,2	0,6	Controlled Source Electro-Magnetic	CSEM
SO191/013-1	21.01.07	18:05	41° 45,82' S	175° 26,16' E	1060	ENE 4	279,1	0,4	Controlled Source Electro-Magnetic	CSEM
SO191/013-1	21.01.07	18:15	41° 45,83' S	175° 26,15' E	1060	ENE 3	312,4	0,2	Controlled Source Electro-Magnetic	CSEM
SO191/013-1	21.01.07	18:15	41° 45,83' S	175° 26,15' E	1060	ENE 3	312,4	0,2	Controlled Source Electro-Magnetic	CSEM
SO191/013-1	21.01.07	18:23	41° 45,77' S	175° 26,22' E	1059	ENE 4	57	0,8	Controlled Source Electro-Magnetic	CSEM
SO191/013-1	21.01.07	18:29	41° 45,71' S	175° 26,28' E	1070	ENE 4	351,2	0,5	Controlled Source Electro-Magnetic	CSEM
SO191/013-1	21.01.07	18:29	41° 45,71' S	175° 26,28' E	1070	ENE 4	351,2	0,5	Controlled Source Electro-Magnetic	CSEM
SO191/013-1	21.01.07	18:36	41° 45,71' S	175° 26,28' E	1059	NE 4	287,5	0,2	Controlled Source Electro-Magnetic	CSEM
SO191/013-1	21.01.07	18:44	41° 45,71' S	175° 26,28' E	1059	ENE 3	68,7	0,2	Controlled Source Electro-Magnetic	CSEM
SO191/013-1	21.01.07	18:44	41° 45,71' S	175° 26,28' E	1059	ENE 3	68,7	0,2	Controlled Source Electro-Magnetic	CSEM
SO191/013-1	21.01.07	18:53	41° 45,64' S	175° 26,35' E	1057	ENE 4	18,7	1,1	Controlled Source Electro-Magnetic	CSEM
SO191/013-1	21.01.07	19:00	41° 45,58' S	175° 26,40' E	1058	NE 3	65,7	0,5	Controlled Source Electro-Magnetic	CSEM
SO191/013-1	21.01.07	19:00	41° 45,58' S	175° 26,40' E	1058	NE 3	65,7	0,5	Controlled Source Electro-Magnetic	CSEM
SO191/013-1	21.01.07	19:08	41° 45,57' S	175° 26,43' E	1057	NE 3	302,9	0,2	Controlled Source Electro-Magnetic	CSEM
SO191/013-1	21.01.07	19:19	41° 45,53' S	175° 26,33' E	1055	NE 4	257,8	0,8	Controlled Source Electro-Magnetic	CSEM
SO191/013-1	21.01.07	19:19	41° 45,53' S	175° 26,33' E	1055	NE 4	257,8	0,8	Controlled Source Electro-Magnetic	CSEM
SO191/013-1	21.01.07	19:34	41° 45,47' S	175° 26,59' E	1056	ENE 4	182,4	0,7	Controlled Source Electro-Magnetic	CSEM
SO191/013-1	21.01.07	19:42	41° 45,48' S	175° 26,57' E	1056	ENE 3	337,4	0,3	Controlled Source Electro-Magnetic	CSEM
SO191/013-1	21.01.07	19:43	41° 45,48' S	175° 26,56' E	1056	ENE 3	275,1	0,2	Controlled Source Electro-Magnetic	CSEM
SO191/013-1	21.01.07	19:52	41° 45,49' S	175° 26,57' E	1056	NNE 3	34,4	0,8	Controlled Source Electro-Magnetic	CSEM
SO191/013-1	21.01.07	19:52	41° 45,49' S	175° 26,57' E	1056	NNE 3	34,4	0,8	Controlled Source Electro-Magnetic	CSEM
SO191/013-1	21.01.07	20:04	41° 45,39' S	175° 26,65' E	1056	ENE 3	329,5	0,6	Controlled Source Electro-Magnetic	CSEM
SO191/013-1	21.01.07	20:11	41° 45,39' S	175° 26,64' E	1050	ENE 3	195,5	0,3	Controlled Source Electro-Magnetic	CSEM
SO191/013-1	21.01.07	20:12	41° 45,39' S	175° 26,64' E	1051	ENE 3	97	0,2	Controlled Source Electro-Magnetic	CSEM
SO191/013-1	21.01.07	20:20	41° 45,40' S	175° 26,63' E	1052	NE 2	224,8	0,7	Controlled Source Electro-Magnetic	CSEM
SO191/013-1	21.01.07	20:20	41° 45,40' S	175° 26,63' E	1052	NE 2	224,8	0,7	Controlled Source Electro-Magnetic	CSEM
SO191/013-1	21.01.07	20:31	41° 45,32' S	175° 26,70' E	1051	E 2	204,4	0,8	Controlled Source Electro-Magnetic	CSEM
SO191/013-1	21.01.07	20:38	41° 45,33' S	175° 26,70' E	1051	NE 2	58,1	0,6	Controlled Source Electro-Magnetic	CSEM
SO191/013-1	21.01.07	20:39	41° 45,33' S	175° 26,70' E	1051	NE 2	94,1	0,1	Controlled Source Electro-Magnetic	CSEM

Station	Datum	UTC	PositionLat	PositionLon	Tiefe [m]	Windstärke [m/s]	Kurs [°]	v [kn]	Gerät	Geräte Kürzel
SO191/013-1	21.01.07	20:46	41° 45,33' S	175° 26,71' E	1051	NNE 1	330,5	0,3	Controlled Source Electro-Magnetic	CSEM
SO191/013-1	21.01.07	20:47	41° 45,33' S	175° 26,71' E	1051	NE 2	359,1	0,9	Controlled Source Electro-Magnetic	CSEM
SO191/013-1	21.01.07	20:57	41° 45,26' S	175° 26,77' E	1051	NE 3	36,2	0	Controlled Source Electro-Magnetic	CSEM
SO191/013-1	21.01.07	21:03	41° 45,27' S	175° 26,78' E	1044	ENE 2	204,3	0,4	Controlled Source Electro-Magnetic	CSEM
SO191/013-1	21.01.07	21:04	41° 45,27' S	175° 26,78' E	1046	NE 2	225,9	0,6	Controlled Source Electro-Magnetic	CSEM
SO191/013-1	21.01.07	21:12	41° 45,27' S	175° 26,77' E	1042	E 1	145,4	0,6	Controlled Source Electro-Magnetic	CSEM
SO191/013-1	21.01.07	21:12	41° 45,27' S	175° 26,77' E	1042	E 1	145,4	0,6	Controlled Source Electro-Magnetic	CSEM
SO191/013-1	21.01.07	21:21	41° 45,19' S	175° 26,85' E	1041	ENE 2	243,7	0,1	Controlled Source Electro-Magnetic	CSEM
SO191/013-1	21.01.07	21:28	41° 45,20' S	175° 26,84' E	1041	NE 2	171,4	0,1	Controlled Source Electro-Magnetic	CSEM
SO191/013-1	21.01.07	21:29	41° 45,20' S	175° 26,83' E	1041	NE 3	295,2	0,6	Controlled Source Electro-Magnetic	CSEM
SO191/013-1	21.01.07	21:37	41° 45,20' S	175° 26,84' E	1041	NW 2	61	0,7	Controlled Source Electro-Magnetic	CSEM
SO191/013-1	21.01.07	21:37	41° 45,20' S	175° 26,84' E	1041	NW 2	61	0,7	Controlled Source Electro-Magnetic	CSEM
SO191/013-1	21.01.07	21:46	41° 45,14' S	175° 26,91' E	1041	NW 5	182	1,3	Controlled Source Electro-Magnetic	CSEM
SO191/013-1	21.01.07	21:52	41° 45,15' S	175° 26,90' E	1039	WNW 5	22,1	0,6	Controlled Source Electro-Magnetic	CSEM
SO191/013-1	21.01.07	21:53	41° 45,15' S	175° 26,90' E	1052	WNW 5	67,8	0,6	Controlled Source Electro-Magnetic	CSEM
SO191/013-1	21.01.07	22:01	41° 45,15' S	175° 26,92' E	1036	WNW 7	61,7	0,4	Controlled Source Electro-Magnetic	CSEM
SO191/013-1	21.01.07	22:01	41° 45,15' S	175° 26,92' E	1036	WNW 7	61,7	0,4	Controlled Source Electro-Magnetic	CSEM
SO191/013-1	21.01.07	22:12	41° 45,07' S	175° 26,99' E	1032	WNW 7	198,8	0,7	Controlled Source Electro-Magnetic	CSEM
SO191/013-1	21.01.07	22:18	41° 45,09' S	175° 27,00' E	1032	WNW 11	285,4	0,3	Controlled Source Electro-Magnetic	CSEM
SO191/013-1	21.01.07	22:19	41° 45,09' S	175° 27,00' E	1032	WNW 9	212,7	0,4	Controlled Source Electro-Magnetic	CSEM
SO191/013-1	21.01.07	22:25	41° 45,10' S	175° 27,01' E	1032	WNW 8	309,3	0,3	Controlled Source Electro-Magnetic	CSEM
SO191/013-1	21.01.07	22:25	41° 45,10' S	175° 27,01' E	1032	WNW 8	309,3	0,3	Controlled Source Electro-Magnetic	CSEM
SO191/013-1	21.01.07	22:39	41° 45,01' S	175° 27,04' E	1032	NW 9	175,7	0,7	Controlled Source Electro-Magnetic	CSEM
SO191/013-1	21.01.07	22:45	41° 45,00' S	175° 27,07' E	1031	NW 7	122,2	0,6	Controlled Source Electro-Magnetic	CSEM
SO191/013-1	21.01.07	22:46	41° 45,01' S	175° 27,07' E	1025	NW 7	150,9	0,7	Controlled Source Electro-Magnetic	CSEM
SO191/013-1	21.01.07	22:54	41° 45,01' S	175° 27,05' E	1025	NW 7	272,5	0,5	Controlled Source Electro-Magnetic	CSEM
SO191/013-1	21.01.07	22:54	41° 45,01' S	175° 27,05' E	1025	NW 7	272,5	0,5	Controlled Source Electro-Magnetic	CSEM
SO191/013-1	21.01.07	23:06	41° 44,94' S	175° 27,11' E	1025	WNW 8	284	0,2	Controlled Source Electro-Magnetic	CSEM
SO191/013-1	21.01.07	23:12	41° 44,93' S	175° 27,11' E	1018	NW 7	344,4	0,6	Controlled Source Electro-Magnetic	CSEM
SO191/013-1	21.01.07	23:13	41° 44,93' S	175° 27,10' E	1024	NW 9	246,9	0,4	Controlled Source Electro-Magnetic	CSEM
SO191/013-1	21.01.07	23:26	41° 44,95' S	175° 27,10' E	1020	NNW 4	34,6	0,2	Controlled Source Electro-Magnetic	CSEM
SO191/013-1	21.01.07	23:28	41° 44,94' S	175° 27,10' E	1019	N 5	83,9	0,1	Controlled Source Electro-Magnetic	CSEM
SO191/013-1	21.01.07	23:33	41° 44,84' S	175° 27,12' E	1019	NNW 4	25,9	0,9	Controlled Source Electro-Magnetic	CSEM
SO191/013-1	21.01.07	23:48	41° 44,81' S	175° 27,27' E	1019	NW 6	19,1	0,6	Controlled Source Electro-Magnetic	CSEM
SO191/013-1	21.01.07	23:52	41° 44,81' S	175° 27,27' E	1019	NNW 5	222,5	0,3	Controlled Source Electro-Magnetic	CSEM
SO191/013-1	22.01.07	00:06	41° 44,81' S	175° 27,28' E	1001	NW 5	165,3	0,9	Controlled Source Electro-Magnetic	CSEM
SO191/013-1	22.01.07	00:07	41° 44,81' S	175° 27,28' E	1001	NW 8	93,8	0,5	Controlled Source Electro-Magnetic	CSEM
SO191/013-1	22.01.07	00:14	41° 44,70' S	175° 27,34' E	1001	NW 9	112,9	0,7	Controlled Source Electro-Magnetic	CSEM
SO191/013-1	22.01.07	00:17	41° 44,69' S	175° 27,37' E	1000	NW 8	12,6	1,3	Controlled Source Electro-Magnetic	CSEM
SO191/013-1	22.01.07	00:24	41° 44,68' S	175° 27,41' E	1000	NW 8	227,3	0,2	Controlled Source Electro-Magnetic	CSEM
SO191/013-1	22.01.07	00:37	41° 44,68' S	175° 27,42' E	1000	NNW 10	42	0,3	Controlled Source Electro-Magnetic	CSEM
SO191/013-1	22.01.07	01:58	41° 44,27' S	175° 27,28' E	936	NW 6	302,2	1,4	Controlled Source Electro-Magnetic	CSEM

Station	Datum	UTC	PositionLat	PositionLon	Tiefe [m]	Windstärke [m/s]	Kurs [°]	v [kn]	Gerät	Geräte Kürzel
SO191/013-1	22.01.07	02:34	41° 43,27' S	175° 27,40' E	835	NE 2	33,4	0,8	Controlled Source Electro-Magnetic	CSEM
SO191/013-1	22.01.07	02:40	41° 43,06' S	175° 27,43' E	856	ESE 1	4,6	0,9	Controlled Source Electro-Magnetic	CSEM
SO191/014-1	22.01.07	03:00	41° 43,01' S	175° 26,72' E	838	WNW 3	113,7	1,8	OBS/OBH	OBS/OBH
SO191/014-1	22.01.07	03:05	41° 43,08' S	175° 26,84' E	832	NW 2	292,6	0,6	OBS/OBH	OBS/OBH
SO191/014-1	22.01.07	03:14	41° 43,23' S	175° 27,02' E	816	SSE 1	18,9	0,2	OBS/OBH	OBS/OBH
SO191/014-1	22.01.07	03:24	41° 43,40' S	175° 27,21' E	819	ESE 1	288,6	0,3	OBS/OBH	OBS/OBH
SO191/014-1	22.01.07	03:32	41° 43,60' S	175° 27,38' E	845	E 2	204,3	0,4	OBS/OBH	OBS/OBH
SO191/014-1	22.01.07	03:55	41° 44,97' S	175° 28,64' E	1136	ENE 5	312,5	0,3	OBS/OBH	OBS/OBH
SO191/014-1	22.01.07	04:26	41° 46,85' S	175° 24,61' E	1057	N 13	219	0,7	OBS/OBH	OBS/OBH
SO191/014-1	22.01.07	04:39	41° 46,97' S	175° 24,38' E	1057	N 13	244,3	0,8	OBS/OBH	OBS/OBH
SO191/014-1	22.01.07	05:17	41° 47,40' S	175° 24,56' E	1060	NNW 12	235,8	0,8	OBS/OBH	OBS/OBH
SO191/014-1	22.01.07	05:25	41° 47,22' S	175° 24,37' E	1056	N 11	115	0,1	OBS/OBH	OBS/OBH
SO191/014-1	22.01.07	05:40	41° 47,06' S	175° 24,15' E	1063	N 12	325,2	0,8	OBS/OBH	OBS/OBH
SO191/014-1	22.01.07	05:56	41° 47,18' S	175° 23,90' E	1065	N 13	314,4	0,7	OBS/OBH	OBS/OBH
SO191/014-1	22.01.07	06:13	41° 47,28' S	175° 23,68' E	1074	N 11	181,9	0,5	OBS/OBH	OBS/OBH
SO191/014-1	22.01.07	06:26	41° 46,90' S	175° 24,01' E	1038	NW 12	62,7	1,3	OBS/OBH	OBS/OBH
SO191/014-1	22.01.07	06:35	41° 46,75' S	175° 23,83' E	1034	NNW 13	187,7	0,4	OBS/OBH	OBS/OBH
SO191/014-1	22.01.07	06:51	41° 46,53' S	175° 23,56' E	1036	NW 14	279,5	0,2	OBS/OBH	OBS/OBH
SO191/014-1	22.01.07	07:10	41° 45,98' S	175° 22,94' E	1154	NW 20	224,3	0,4	OBS/OBH	OBS/OBH
SO191/014-1	22.01.07	07:11	41° 45,99' S	175° 22,95' E	1152	NW 18	193	0,5	OBS/OBH	OBS/OBH
SO191/015-1	22.01.07	14:37	41° 42,73' S	175° 21,07' E	987	NW 13	65,3	9,5	Vermessung	EM / PS
SO191/015-1	22.01.07	15:42	41° 39,35' S	175° 30,73' E	554	NW 21	104,2	6,5	Vermessung	EM / PS
SO191/015-1	22.01.07	16:25	41° 41,92' S	175° 36,16' E	1422	NW 10	120,6	6,2	Vermessung	EM / PS
SO191/016-1	22.01.07	18:00	41° 46,81' S	175° 24,65' E	1055	NW 15	342,6	1,2	Kalibrierung	KAL
SO191/016-1	22.01.07	19:28	41° 46,33' S	175° 24,50' E	1049	NW 14	326,1	1,3	Kalibrierung	KAL
SO191/016-1	22.01.07	20:03	41° 46,29' S	175° 24,76' E	1050	WNW 13	190,6	2,3	Kalibrierung	KAL
SO191/016-1	22.01.07	21:23	41° 46,72' S	175° 24,63' E	1059	WNW 16	79,8	2,9	Kalibrierung	KAL
SO191/016-1	22.01.07	21:32	41° 46,57' S	175° 24,63' E	1053	NW 12	283,5	0,9	Kalibrierung	KAL
SO191/016-1	22.01.07	22:01	41° 46,44' S	175° 24,09' E	1049	WNW 13	334,1	0,6	Kalibrierung	KAL
SO191/016-1	22.01.07	22:01	41° 46,44' S	175° 24,09' E	1049	WNW 13	334,1	0,6	Kalibrierung	KAL
SO191/017-1	23.01.07	00:10	41° 41,54' S	175° 34,57' E	1252	WSW 10	231,7	7,2	Profil	PR
SO191/017-1	23.01.07	00:20	41° 41,46' S	175° 34,58' E	1197	W 10	48,7	0,4	Profil	PR
SO191/017-1	23.01.07	00:50	41° 41,43' S	175° 33,78' E	1139	SW 13	264,4	2,8	Profil	PR
SO191/017-1	23.01.07	00:55	41° 41,42' S	175° 33,52' E	1019	SW 13	257,7	2,6	Profil	PR
SO191/017-1	23.01.07	01:07	41° 41,46' S	175° 32,87' E	1041	WSW 11	267,5	2,2	Profil	PR
SO191/017-1	23.01.07	02:27	41° 43,43' S	175° 28,35' E	1044	SW 7	239,5	2,7	Profil	PR
SO191/017-1	23.01.07	04:55	41° 47,41' S	175° 19,92' E	1345	SSW 6	241	2,6	Profil	PR
SO191/017-1	23.01.07	04:55	41° 47,41' S	175° 19,92' E	1345	SSW 6	241	2,6	Profil	PR
SO191/017-1	23.01.07	06:13	41° 48,92' S	175° 21,96' E	1426	S 6	61,5	3	Profil	PR
SO191/017-1	23.01.07	06:50	41° 47,98' S	175° 23,96' E	1130	S 4	61,1	3,1	Profil	PR
SO191/017-1	23.01.07	09:02	41° 44,47' S	175° 31,50' E	1743	SSE 5	59,6	3	Profil	PR
SO191/017-1	23.01.07	09:02	41° 44,47' S	175° 31,50' E	1743	SSE 5	59,6	3	Profil	PR

Station	Datum	UTC	PositionLat	PositionLon	Tiefe [m]	Windstärke [m/s]	Kurs [°]	v [kn]	Gerät	Geräte Kürzel
SO191/017-1	23.01.07	09:39	41° 42,81' S	175° 32,17' E	1480	SSE 3	331,5	3,1	Profil	PR
SO191/017-1	23.01.07	10:41	41° 43,99' S	175° 28,92' E	1292	ESE 4	238	2,9	Profil	PR
SO191/017-1	23.01.07	10:42	41° 44,02' S	175° 28,86' E	1278	ESE 5	232,2	3,1	Profil	PR
SO191/017-1	23.01.07	10:55	41° 44,39' S	175° 28,13' E	1000	E 4	238,7	2,7	Profil	PR
SO191/017-1	23.01.07	13:15	41° 48,07' S	175° 20,28' E	1139	NE 4	237,1	3,1	Profil	PR
SO191/017-1	23.01.07	13:15	41° 48,07' S	175° 20,28' E	1139	NE 4	237,1	3,1	Profil	PR
SO191/017-1	23.01.07	14:08	41° 46,53' S	175° 20,03' E	1444	E 5	51,4	3,4	Profil	PR
SO191/017-1	23.01.07	14:28	41° 46,04' S	175° 21,06' E	1382	ENE 5	70,2	2,9	Profil	PR
SO191/017-1	23.01.07	16:38	41° 42,62' S	175° 28,38' E	1085	NE 5	60,2	3,8	Profil	PR
SO191/017-1	23.01.07	16:38	41° 42,62' S	175° 28,38' E	1085	NE 5	60,2	3,8	Profil	PR
SO191/017-1	23.01.07	17:37	41° 44,58' S	175° 29,49' E	1261	NE 5	242,7	2,7	Profil	PR
SO191/017-1	23.01.07	17:37	41° 44,58' S	175° 29,49' E	1261	NE 5	242,7	2,7	Profil	PR
SO191/017-1	23.01.07	20:19	41° 48,97' S	175° 20,12' E	1469	ENE 5	257,4	3,2	Profil	PR
SO191/017-1	23.01.07	20:19	41° 48,97' S	175° 20,12' E	1469	ENE 5	257,4	3,2	Profil	PR
SO191/017-1	23.01.07	22:02	41° 49,35' S	175° 22,62' E	1729	ENE 11	21,7	3,1	Profil	PR
SO191/017-1	23.01.07	22:14	41° 48,84' S	175° 23,01' E	1459	ENE 12	22,9	3	Profil	PR
SO191/017-1	24.01.07	01:02	41° 41,40' S	175° 28,66' E	788	ENE 14	247,7	15,8	Profil	PR
SO191/017-1	24.01.07	01:06	41° 41,23' S	175° 28,81' E	733	ENE 13	37,9	3,1	Profil	PR
SO191/017-1	24.01.07	01:16	41° 40,87' S	175° 29,09' E	631	ENE 15	40,2	3	Profil	PR
SO191/017-1	24.01.07	01:30	41° 40,45' S	175° 29,39' E	597	ENE 14	19,9	1,3	Profil	PR
SO191/017-1	24.01.07	01:52	41° 39,81' S	175° 29,75' E	578	ENE 15	29,4	2,7	Profil	PR
SO191/018-1	24.01.07	02:10	41° 40,12' S	175° 29,73' E	640	NE 17	203,7	5,8	OBS/OBH	OBS/OBH
SO191/018-1	24.01.07	02:12	41° 40,31' S	175° 29,59' E	624	NE 16	211,4	7,3	OBS/OBH	OBS/OBH
SO191/018-1	24.01.07	02:38	41° 42,91' S	175° 27,24' E	0	NE 13	220,7	7,6	OBS/OBH	OBS/OBH
SO191/018-1	24.01.07	03:04	41° 43,44' S	175° 26,20' E	0	ENE 13	182,3	1,1	OBS/OBH	OBS/OBH
SO191/018-1	24.01.07	03:08	41° 43,51' S	175° 26,16' E	0	NE 13	177,9	1,7	OBS/OBH	OBS/OBH
SO191/018-1	24.01.07	03:21	41° 43,67' S	175° 26,25' E	0	NE 12	67,8	4	OBS/OBH	OBS/OBH
SO191/018-1	24.01.07	03:31	41° 43,39' S	175° 26,61' E	0	NNE 16	208,1	1,4	OBS/OBH	OBS/OBH
SO191/018-1	24.01.07	03:32	41° 43,41' S	175° 26,59' E	0	NE 14	238,2	2,3	OBS/OBH	OBS/OBH
SO191/018-1	24.01.07	03:42	41° 43,50' S	175° 26,65' E	0	NE 14	152,4	1	OBS/OBH	OBS/OBH
SO191/018-1	24.01.07	03:43	41° 43,51' S	175° 26,66' E	0	NE 13	136,8	0,5	OBS/OBH	OBS/OBH
SO191/018-1	24.01.07	03:49	41° 43,57' S	175° 26,82' E	0	NNE 15	177,3	1,4	OBS/OBH	OBS/OBH
SO191/018-1	24.01.07	03:54	41° 43,65' S	175° 26,84' E	0	NNE 13	83,3	1,7	OBS/OBH	OBS/OBH
SO191/018-1	24.01.07	03:57	41° 43,68' S	175° 26,92' E	0	E 14	134,8	2,4	OBS/OBH	OBS/OBH
SO191/018-1	24.01.07	04:01	41° 43,80' S	175° 26,92' E	0	NNE 13	227,8	2,4	OBS/OBH	OBS/OBH
SO191/018-1	24.01.07	04:10	41° 44,43' S	175° 27,25' E	0	NE 14	157,4	7,1	OBS/OBH	OBS/OBH
SO191/018-1	24.01.07	04:23	41° 45,26' S	175° 27,98' E	0	NE 13	138,9	1,4	OBS/OBH	OBS/OBH
SO191/018-1	24.01.07	04:40	41° 45,67' S	175° 25,97' E	0	NE 13	263,6	8,1	OBS/OBH	OBS/OBH
SO191/018-1	24.01.07	05:01	41° 45,91' S	175° 22,54' E	0	NE 12	256,6	5,9	OBS/OBH	OBS/OBH
SO191/018-1	24.01.07	05:09	41° 46,20' S	175° 22,54' E	0	NNE 13	175,4	1,1	OBS/OBH	OBS/OBH
SO191/018-1	24.01.07	05:11	41° 46,23' S	175° 22,53' E	0	NE 9	191,5	1,1	OBS/OBH	OBS/OBH
SO191/018-1	24.01.07	05:23	41° 46,76' S	175° 22,89' E	0	NNE 12	165,2	1,4	OBS/OBH	OBS/OBH

Station	Datum	UTC	PositionLat	PositionLon	Tiefe [m]	Windstärke [m/s]	Kurs [°]	v [kn]	Gerät	Geräte Kürzel
SO191/018-1	24.01.07	05:29	41° 46,78' S	175° 23,10' E	0	NE 13	68,3	1,6	OBS/OBH	OBS/OBH
SO191/018-1	24.01.07	05:33	41° 46,81' S	175° 23,16' E	0	NE 12	141,8	0,5	OBS/OBH	OBS/OBH
SO191/018-1	24.01.07	05:40	41° 46,97' S	175° 23,11' E	0	NNE 11	196,5	1,1	OBS/OBH	OBS/OBH
SO191/018-1	24.01.07	05:44	41° 46,96' S	175° 23,29' E	0	ENE 10	74,9	2,6	OBS/OBH	OBS/OBH
SO191/018-1	24.01.07	05:48	41° 47,03' S	175° 23,41' E	0	ENE 13	217,5	2,6	OBS/OBH	OBS/OBH
SO191/018-1	24.01.07	05:59	41° 47,18' S	175° 23,34' E	0	ENE 11	192,4	1,1	OBS/OBH	OBS/OBH
SO191/018-1	24.01.07	06:00	41° 47,18' S	175° 23,35' E	0	ENE 11	60,2	0,7	OBS/OBH	OBS/OBH
SO191/018-1	24.01.07	06:05	41° 47,26' S	175° 23,46' E	0	NNE 13	197,1	1,7	OBS/OBH	OBS/OBH
SO191/018-1	24.01.07	06:11	41° 47,36' S	175° 23,26' E	0	NE 10	263,6	1,8	OBS/OBH	OBS/OBH
SO191/018-1	24.01.07	06:12	41° 47,37' S	175° 23,23' E	0	NE 12	178,9	2	OBS/OBH	OBS/OBH
SO191/018-1	24.01.07	06:18	41° 47,58' S	175° 23,25' E	0	NNE 11	163,5	2,1	OBS/OBH	OBS/OBH
SO191/018-1	24.01.07	06:24	41° 47,57' S	175° 23,34' E	0	ENE 9	32,8	2,5	OBS/OBH	OBS/OBH
SO191/018-1	24.01.07	06:26	41° 47,51' S	175° 23,38' E	0	NE 11	348,8	3,2	OBS/OBH	OBS/OBH
SO191/018-1	24.01.07	06:32	41° 47,49' S	175° 23,44' E	0	ENE 10	197,3	1,5	OBS/OBH	OBS/OBH
SO191/018-1	24.01.07	06:38	41° 47,49' S	175° 23,51' E	0	NE 9	31,4	3,3	OBS/OBH	OBS/OBH
SO191/018-1	24.01.07	06:40	41° 47,41' S	175° 23,56' E	0	NE 10	19,7	3,4	OBS/OBH	OBS/OBH
SO191/018-1	24.01.07	06:46	41° 47,36' S	175° 23,73' E	0	NE 11	182,4	1,6	OBS/OBH	OBS/OBH
SO191/018-1	24.01.07	06:54	41° 47,45' S	175° 23,83' E	0	NE 10	57,6	1,2	OBS/OBH	OBS/OBH
SO191/018-1	24.01.07	06:55	41° 47,44' S	175° 23,85' E	0	NE 9	36,7	0,5	OBS/OBH	OBS/OBH
SO191/018-1	24.01.07	07:00	41° 47,56' S	175° 23,86' E	0	NNE 9	159	1,6	OBS/OBH	OBS/OBH
SO191/018-1	24.01.07	07:06	41° 47,68' S	175° 23,84' E	0	N 7	80,4	1,1	OBS/OBH	OBS/OBH
SO191/018-1	24.01.07	07:08	41° 47,63' S	175° 23,92' E	0	NE 6	60,3	2,5	OBS/OBH	OBS/OBH
SO191/018-1	24.01.07	07:16	41° 47,73' S	175° 24,11' E	0	N 5	192,1	1,4	OBS/OBH	OBS/OBH
SO191/018-1	24.01.07	07:23	41° 47,87' S	175° 24,00' E	0	NNW 5	121,6	1,1	OBS/OBH	OBS/OBH
SO191/018-1	24.01.07	07:26	41° 47,80' S	175° 23,97' E	0	N 5	329,9	3,8	OBS/OBH	OBS/OBH
SO191/018-1	24.01.07	07:40	41° 47,36' S	175° 23,93' E	0	N 4	177,9	1,4	OBS/OBH	OBS/OBH
SO191/018-1	24.01.07	07:49	41° 47,30' S	175° 24,11' E	0	NNE 5	10,1	3,2	OBS/OBH	OBS/OBH
SO191/018-1	24.01.07	08:04	41° 47,30' S	175° 24,01' E	0	NE 2	221,1	0,4	OBS/OBH	OBS/OBH
SO191/018-1	24.01.07	08:05	41° 47,31' S	175° 24,01' E	0	NE 2	160,7	0,4	OBS/OBH	OBS/OBH
SO191/019-1	24.01.07	08:38	41° 47,46' S	175° 22,61' E	1096	N 3	127,2	0,2	Controlled Source Electro-Magnetic	CSEM
SO191/019-1	24.01.07	08:42	41° 47,48' S	175° 22,61' E	1096	N 3	183,1	0,2	Controlled Source Electro-Magnetic	CSEM
SO191/019-1	24.01.07	08:54	41° 47,41' S	175° 22,60' E	1096	WNW 7	215,2	0,3	Controlled Source Electro-Magnetic	CSEM
SO191/019-1	24.01.07	09:08	41° 47,46' S	175° 22,63' E	1096	NNW 1	90	0,6	Controlled Source Electro-Magnetic	CSEM
SO191/019-1	24.01.07	09:14	41° 47,46' S	175° 22,65' E	1096	NE 3	137,8	0,6	Controlled Source Electro-Magnetic	CSEM
SO191/019-1	24.01.07	09:57	41° 47,51' S	175° 22,77' E	1096	NW 10	157	1,2	Controlled Source Electro-Magnetic	CSEM
SO191/019-1	24.01.07	11:35	41° 46,48' S	175° 24,96' E	1055	NNW 11	63,9	0,5	Controlled Source Electro-Magnetic	CSEM
SO191/019-1	24.01.07	12:24	41° 45,99' S	175° 24,80' E	1045	NNW 15	135,8	0,9	Controlled Source Electro-Magnetic	CSEM
SO191/019-1	24.01.07	13:01	41° 45,76' S	175° 24,56' E	1040	NW 14	307,4	1,8	Controlled Source Electro-Magnetic	CSEM
SO191/019-1	24.01.07	15:23	41° 48,14' S	175° 25,01' E	1380	NW 13	354,7	0,3	Controlled Source Electro-Magnetic	CSEM
SO191/019-1	24.01.07	16:55	41° 46,96' S	175° 24,19' E	1064	WNW 12	328,2	2,4	Controlled Source Electro-Magnetic	CSEM
SO191/019-1	24.01.07	17:31	41° 46,31' S	175° 23,73' E	1052	WNW 12	327	0,6	Controlled Source Electro-Magnetic	CSEM
SO191/019-1	24.01.07	17:32	41° 46,31' S	175° 23,73' E	1036	WNW 12	353,2	0,3	Controlled Source Electro-Magnetic	CSEM

Station	Datum	UTC	PositionLat	PositionLon	Tiefe [m]	Windstärke [m/s]	Kurs [°]	v [kn]	Gerät	Geräte Kürzel
SO191/019-1	24.01.07	17:37	41° 46,30' S	175° 23,72' E	1036	WNW 12	213,3	0,2	Controlled Source Electro-Magnetic	CSEM
SO191/019-1	24.01.07	17:45	41° 46,31' S	175° 23,71' E	1036	NW 15	239	0,3	Controlled Source Electro-Magnetic	CSEM
SO191/019-1	24.01.07	17:45	41° 46,31' S	175° 23,71' E	1036	NW 15	239	0,3	Controlled Source Electro-Magnetic	CSEM
SO191/019-1	24.01.07	17:52	41° 46,26' S	175° 23,70' E	1037	WNW 14	309,3	1,2	Controlled Source Electro-Magnetic	CSEM
SO191/019-1	24.01.07	17:56	41° 46,24' S	175° 23,68' E	1039	WNW 13	320	0,7	Controlled Source Electro-Magnetic	CSEM
SO191/019-1	24.01.07	17:56	41° 46,24' S	175° 23,68' E	1039	WNW 13	320	0,7	Controlled Source Electro-Magnetic	CSEM
SO191/019-1	24.01.07	18:02	41° 46,24' S	175° 23,68' E	1038	WNW 13	224,6	0,2	Controlled Source Electro-Magnetic	CSEM
SO191/019-1	24.01.07	18:11	41° 46,24' S	175° 23,67' E	1040	WNW 13	276,4	0,3	Controlled Source Electro-Magnetic	CSEM
SO191/019-1	24.01.07	18:11	41° 46,24' S	175° 23,67' E	1040	WNW 13	276,4	0,3	Controlled Source Electro-Magnetic	CSEM
SO191/019-1	24.01.07	18:19	41° 46,17' S	175° 23,64' E	1042	WNW 14	326,7	1	Controlled Source Electro-Magnetic	CSEM
SO191/019-1	24.01.07	18:19	41° 46,17' S	175° 23,64' E	1042	WNW 14	326,7	1	Controlled Source Electro-Magnetic	CSEM
SO191/019-1	24.01.07	18:19	41° 46,17' S	175° 23,64' E	1042	WNW 14	326,7	1	Controlled Source Electro-Magnetic	CSEM
SO191/019-1	24.01.07	18:25	41° 46,17' S	175° 23,63' E	1049	WNW 12	294,8	0,6	Controlled Source Electro-Magnetic	CSEM
SO191/019-1	24.01.07	18:34	41° 46,17' S	175° 23,61' E	1056	NW 13	73,5	0,6	Controlled Source Electro-Magnetic	CSEM
SO191/019-1	24.01.07	18:34	41° 46,17' S	175° 23,61' E	1056	NW 13	73,5	0,6	Controlled Source Electro-Magnetic	CSEM
SO191/019-1	24.01.07	18:42	41° 46,10' S	175° 23,57' E	1060	NW 12	31,9	0,6	Controlled Source Electro-Magnetic	CSEM
SO191/019-1	24.01.07	18:42	41° 46,10' S	175° 23,57' E	1060	NW 12	31,9	0,6	Controlled Source Electro-Magnetic	CSEM
SO191/019-1	24.01.07	18:42	41° 46,10' S	175° 23,57' E	1060	NW 12	31,9	0,6	Controlled Source Electro-Magnetic	CSEM
SO191/019-1	24.01.07	18:49	41° 46,09' S	175° 23,59' E	1067	WNW 11	120,5	0,2	Controlled Source Electro-Magnetic	CSEM
SO191/019-1	24.01.07	18:57	41° 46,08' S	175° 23,60' E	1064	WNW 9	174,5	0,2	Controlled Source Electro-Magnetic	CSEM
SO191/019-1	24.01.07	18:57	41° 46,08' S	175° 23,60' E	1064	WNW 9	174,5	0,2	Controlled Source Electro-Magnetic	CSEM
SO191/019-1	24.01.07	19:05	41° 46,03' S	175° 23,52' E	1067	WNW 10	4,4	0,5	Controlled Source Electro-Magnetic	CSEM
SO191/019-1	24.01.07	19:08	41° 46,01' S	175° 23,51' E	1078	W 10	288,6	0,5	Controlled Source Electro-Magnetic	CSEM
SO191/019-1	24.01.07	19:08	41° 46,01' S	175° 23,51' E	1078	W 10	288,6	0,5	Controlled Source Electro-Magnetic	CSEM
SO191/019-1	24.01.07	19:15	41° 45,98' S	175° 23,51' E	1078	WNW 11	96,4	0,3	Controlled Source Electro-Magnetic	CSEM
SO191/019-1	24.01.07	19:25	41° 45,95' S	175° 23,51' E	1078	WNW 12	313,8	0,7	Controlled Source Electro-Magnetic	CSEM
SO191/019-1	24.01.07	19:26	41° 45,94' S	175° 23,50' E	1078	WNW 12	307,1	0,8	Controlled Source Electro-Magnetic	CSEM
SO191/019-1	24.01.07	19:32	41° 45,95' S	175° 23,41' E	1078	NW 11	294,6	1,2	Controlled Source Electro-Magnetic	CSEM
SO191/019-1	24.01.07	19:56	41° 45,81' S	175° 23,36' E	1157	W 10	338,7	1	Controlled Source Electro-Magnetic	CSEM
SO191/019-1	24.01.07	19:57	41° 45,80' S	175° 23,36' E	1157	W 10	257	0,2	Controlled Source Electro-Magnetic	CSEM
SO191/019-1	24.01.07	20:04	41° 45,79' S	175° 23,38' E	1157	W 9	175,2	0,1	Controlled Source Electro-Magnetic	CSEM
SO191/019-1	24.01.07	20:09	41° 45,77' S	175° 23,39' E	1153	W 11	338,9	0,9	Controlled Source Electro-Magnetic	CSEM
SO191/019-1	24.01.07	20:09	41° 45,77' S	175° 23,39' E	1153	W 11	338,9	0,9	Controlled Source Electro-Magnetic	CSEM
SO191/019-1	24.01.07	20:20	41° 45,74' S	175° 23,34' E	1171	W 9	218,9	1	Controlled Source Electro-Magnetic	CSEM
SO191/019-1	24.01.07	20:22	41° 45,75' S	175° 23,32' E	1182	WNW 11	43,9	0,3	Controlled Source Electro-Magnetic	CSEM
SO191/019-1	24.01.07	20:23	41° 45,75' S	175° 23,32' E	1180	WNW 10	81,8	0,1	Controlled Source Electro-Magnetic	CSEM
SO191/019-1	24.01.07	20:30	41° 45,73' S	175° 23,31' E	1180	W 9	255,3	0,7	Controlled Source Electro-Magnetic	CSEM
SO191/019-1	24.01.07	20:37	41° 45,72' S	175° 23,30' E	1187	WSW 10	252,5	0,5	Controlled Source Electro-Magnetic	CSEM
SO191/019-1	24.01.07	20:38	41° 45,72' S	175° 23,30' E	1184	WSW 11	36,4	0,1	Controlled Source Electro-Magnetic	CSEM
SO191/019-1	24.01.07	20:45	41° 45,68' S	175° 23,28' E	1199	WSW 10	313,8	0,9	Controlled Source Electro-Magnetic	CSEM
SO191/019-1	24.01.07	20:47	41° 45,66' S	175° 23,26' E	1202	WSW 9	9,7	0,3	Controlled Source Electro-Magnetic	CSEM
SO191/019-1	24.01.07	20:47	41° 45,66' S	175° 23,26' E	1202	WSW 9	9,7	0,3	Controlled Source Electro-Magnetic	CSEM

Station	Datum	UTC	PositionLat	PositionLon	Tiefe [m]	Windstärke [m/s]	Kurs [°]	v [kn]	Gerät	Geräte Kürzel
SO191/019-1	24.01.07	20:54	41° 45,63' S	175° 23,23' E	1202	WSW 10	292,5	1	Controlled Source Electro-Magnetic	CSEM
SO191/019-1	24.01.07	21:02	41° 45,64' S	175° 23,18' E	1216	W 10	302,5	0,3	Controlled Source Electro-Magnetic	CSEM
SO191/019-1	24.01.07	21:02	41° 45,64' S	175° 23,18' E	1216	W 10	302,5	0,3	Controlled Source Electro-Magnetic	CSEM
SO191/019-1	24.01.07	21:12	41° 45,61' S	175° 23,22' E	1211	SW 8	6,8	0,4	Controlled Source Electro-Magnetic	CSEM
SO191/019-1	24.01.07	21:12	41° 45,61' S	175° 23,22' E	1211	SW 8	6,8	0,4	Controlled Source Electro-Magnetic	CSEM
SO191/019-1	24.01.07	21:15	41° 45,59' S	175° 23,20' E	1223	SW 9	15,5	0,3	Controlled Source Electro-Magnetic	CSEM
SO191/019-1	24.01.07	21:23	41° 45,56' S	175° 23,14' E	1224	WSW 9	324,5	0,6	Controlled Source Electro-Magnetic	CSEM
SO191/019-1	24.01.07	21:33	41° 45,56' S	175° 23,15' E	1223	WSW 10	153,5	0,2	Controlled Source Electro-Magnetic	CSEM
SO191/019-1	24.01.07	21:33	41° 45,56' S	175° 23,15' E	1223	WSW 10	153,5	0,2	Controlled Source Electro-Magnetic	CSEM
SO191/019-1	24.01.07	21:42	41° 45,49' S	175° 23,08' E	1233	WSW 9	295,8	0,7	Controlled Source Electro-Magnetic	CSEM
SO191/019-1	24.01.07	21:42	41° 45,49' S	175° 23,08' E	1233	WSW 9	295,8	0,7	Controlled Source Electro-Magnetic	CSEM
SO191/019-1	24.01.07	21:42	41° 45,49' S	175° 23,08' E	1233	WSW 9	295,8	0,7	Controlled Source Electro-Magnetic	CSEM
SO191/019-1	24.01.07	21:54	41° 45,55' S	175° 23,03' E	1233	WSW 11	184,9	0,7	Controlled Source Electro-Magnetic	CSEM
SO191/019-1	24.01.07	22:02	41° 45,56' S	175° 23,02' E	1238	SW 9	339,2	0,4	Controlled Source Electro-Magnetic	CSEM
SO191/019-1	24.01.07	22:02	41° 45,56' S	175° 23,02' E	1238	SW 9	339,2	0,4	Controlled Source Electro-Magnetic	CSEM
SO191/019-1	24.01.07	22:11	41° 45,48' S	175° 22,99' E	1236	SSW 10	347,7	0,6	Controlled Source Electro-Magnetic	CSEM
SO191/019-1	24.01.07	22:15	41° 45,44' S	175° 23,00' E	1238	SSW 8	352,6	1	Controlled Source Electro-Magnetic	CSEM
SO191/019-1	24.01.07	22:27	41° 45,39' S	175° 22,81' E	1262	SSW 11	21,3	1,2	Controlled Source Electro-Magnetic	CSEM
SO191/019-1	24.01.07	22:34	41° 45,35' S	175° 22,87' E	1262	SW 14	44,5	0,4	Controlled Source Electro-Magnetic	CSEM
SO191/019-1	24.01.07	22:46	41° 45,31' S	175° 22,88' E	1289	SSW 8	40,6	0,3	Controlled Source Electro-Magnetic	CSEM
SO191/019-1	24.01.07	23:45	41° 44,69' S	175° 23,36' E	1263	SW 5	38,8	0,9	Controlled Source Electro-Magnetic	CSEM
SO191/019-1	25.01.07	00:00	41° 44,46' S	175° 23,65' E	1245	WSW 6	54,1	1,8	Controlled Source Electro-Magnetic	CSEM
SO191/019-1	25.01.07	00:29	41° 44,04' S	175° 24,31' E	1099	SW 4	70	1	Controlled Source Electro-Magnetic	CSEM
SO191/019-1	25.01.07	00:41	41° 43,87' S	175° 24,52' E	1045	WSW 6	36,8	1,3	Controlled Source Electro-Magnetic	CSEM
SO191/020-1	25.01.07	01:43	41° 45,21' S	175° 32,20' E	1611	SSW 7	57,7	6,5	Vermessung	EM / PS
SO191/020-1	25.01.07	04:38	41° 34,51' S	175° 55,67' E	1700	SSW 5	58	7,4	Vermessung	EM / PS
SO191/020-1	25.01.07	07:14	41° 20,15' S	176° 15,16' E	1017	S 5	52,5	7,4	Vermessung	EM / PS
SO191/020-1	25.01.07	08:35	41° 20,02' S	176° 28,66' E	1048	SSE 3	91,4	7,6	Vermessung	EM / PS
SO191/021-1	25.01.07	08:54	41° 19,13' S	176° 28,42' E	1072	SSW 1	290	0,1	OBS/OBH	OBS/OBH
SO191/021-1	25.01.07	08:55	41° 19,12' S	176° 28,42' E	1075	SE 2	34,4	0,2	OBS/OBH	OBS/OBH
SO191/021-1	25.01.07	09:50	41° 18,18' S	176° 31,36' E	829	SE 5	241	0,2	OBS/OBH	OBS/OBH
SO191/021-1	25.01.07	10:26	41° 15,97' S	176° 30,04' E	1049	E 5	255,9	0,2	OBS/OBH	OBS/OBH
SO191/021-1	25.01.07	10:50	41° 16,52' S	176° 31,19' E	1023	E 3	33,8	0,2	OBS/OBH	OBS/OBH
SO191/021-1	25.01.07	11:07	41° 17,07' S	176° 32,30' E	806	NE 4	56,3	1	OBS/OBH	OBS/OBH
SO191/021-1	25.01.07	11:18	41° 17,30' S	176° 32,79' E	769	NE 4	104,7	0,8	OBS/OBH	OBS/OBH
SO191/021-1	25.01.07	11:25	41° 17,44' S	176° 32,99' E	734	E 4	178,3	0,3	OBS/OBH	OBS/OBH
SO191/021-1	25.01.07	11:36	41° 17,56' S	176° 33,24' E	762	NE 3	164,3	0,8	OBS/OBH	OBS/OBH
SO191/021-1	25.01.07	11:43	41° 17,68' S	176° 33,48' E	750	ENE 4	67,6	1	OBS/OBH	OBS/OBH
SO191/021-1	25.01.07	11:52	41° 17,79' S	176° 33,74' E	809	E 3	17,3	0,5	OBS/OBH	OBS/OBH
SO191/021-1	25.01.07	12:10	41° 18,15' S	176° 34,45' E	915	ENE 3	106,4	0,6	OBS/OBH	OBS/OBH
SO191/021-1	25.01.07	12:30	41° 18,57' S	176° 35,32' E	1083	NE 4	81,8	0,6	OBS/OBH	OBS/OBH
SO191/021-1	25.01.07	12:54	41° 17,15' S	176° 35,38' E	734	ENE 4	353	0,5	OBS/OBH	OBS/OBH

Station	Datum	UTC	PositionLat	PositionLon	Tiefe [m]	Windstärke [m/s]	Kurs [°]	v [kn]	Gerät	Geräte Kürzel
SO191/021-1	25.01.07	13:06	41° 16,67' S	176° 35,93' E	900	ENE 4	20,2	1	OBS/OBH	OBS/OBH
SO191/021-1	25.01.07	13:16	41° 16,18' S	176° 36,41' E	840	NE 4	17,3	1,2	OBS/OBH	OBS/OBH
SO191/021-1	25.01.07	13:30	41° 16,29' S	176° 37,14' E	882	ENE 4	35,9	0,3	OBS/OBH	OBS/OBH
SO191/021-1	25.01.07	13:31	41° 16,28' S	176° 37,15' E	877	ENE 4	46,7	0,5	OBS/OBH	OBS/OBH
SO191/022-1	25.01.07	15:25	41° 21,67' S	176° 23,14' E	1026	E 1	75,6	0,9	Profil	PR
SO191/022-1	25.01.07	15:25	41° 21,67' S	176° 23,14' E	1026	E 1	75,6	0,9	Profil	PR
SO191/022-1	25.01.07	15:30	41° 21,62' S	176° 23,25' E	1028	ESE 1	74	1,1	Profil	PR
SO191/022-1	25.01.07	15:35	41° 21,56' S	176° 23,40' E	1027	SE 1	67,2	2,5	Profil	PR
SO191/022-1	25.01.07	15:44	41° 21,43' S	176° 23,86' E	1016	ESE 2	63	2,6	Profil	PR
SO191/022-1	25.01.07	16:19	41° 20,80' S	176° 25,82' E	986	E 3	74,4	3,2	Profil	PR
SO191/022-1	25.01.07	16:19	41° 20,80' S	176° 25,82' E	986	E 3	74,4	3,2	Profil	PR
SO191/022-1	25.01.07	21:22	41° 14,66' S	176° 44,44' E	945	ENE 2	67,6	2,8	Profil	PR
SO191/022-1	25.01.07	21:30	41° 14,49' S	176° 44,92' E	991	ENE 2	63,1	3	Profil	PR
SO191/022-1	25.01.07	22:20	41° 13,32' S	176° 43,91' E	942	N 2	242,4	3	Profil	PR
SO191/022-1	25.01.07	22:25	41° 13,42' S	176° 43,62' E	928	NNE 2	245,1	3	Profil	PR
SO191/022-1	26.01.07	03:17	41° 19,25' S	176° 26,23' E	1131	NE 2	240,6	2,9	Profil	PR
SO191/022-1	26.01.07	03:17	41° 19,25' S	176° 26,23' E	1131	NE 2	240,6	2,9	Profil	PR
SO191/022-1	26.01.07	04:36	41° 19,49' S	176° 27,32' E	1153	SE 3	68	2,3	Profil	PR
SO191/022-1	26.01.07	04:36	41° 19,49' S	176° 27,32' E	1153	SE 3	68	2,3	Profil	PR
SO191/022-1	26.01.07	08:19	41° 15,01' S	176° 41,06' E	832	SSW 4	64,1	2,9	Profil	PR
SO191/022-1	26.01.07	08:35	41° 14,77' S	176° 41,85' E	763	SW 3	71,4	1,4	Profil	PR
SO191/022-1	26.01.07	08:54	41° 14,57' S	176° 42,55' E	813	SW 5	66,6	1,4	Profil	PR
SO191/022-1	26.01.07	08:58	41° 14,56' S	176° 42,67' E	821	SW 5	74,9	1,2	Profil	PR
SO191/022-2	26.01.07	10:06	41° 14,87' S	176° 41,46' E	793	SW 3	51,6	1,8	Profil	PR
SO191/022-2	26.01.07	10:07	41° 14,84' S	176° 41,51' E	795	SW 3	64	3,6	Profil	PR
SO191/022-2	26.01.07	10:38	41° 14,19' S	176° 43,52' E	878	SW 4	69,6	3,3	Profil	PR
SO191/022-2	26.01.07	10:38	41° 14,19' S	176° 43,52' E	878	SW 4	69,6	3,3	Profil	PR
SO191/022-2	26.01.07	12:22	41° 14,10' S	176° 38,55' E	936	WSW 8	217,7	2,3	Profil	PR
SO191/022-2	26.01.07	14:36	41° 19,12' S	176° 33,44' E	976	SW 7	215,2	3	Profil	PR
SO191/022-2	26.01.07	14:36	41° 19,12' S	176° 33,44' E	976	SW 7	215,2	3	Profil	PR
SO191/022-2	26.01.07	15:47	41° 18,90' S	176° 35,93' E	1528	S 7	298,7	3,5	Profil	PR
SO191/022-2	26.01.07	18:00	41° 15,20' S	176° 28,51' E	1160	SSW 7	302	2,7	Profil	PR
SO191/022-2	26.01.07	18:03	41° 15,11' S	176° 28,35' E	1164	S 6	312,9	2,9	Profil	PR
SO191/022-2	26.01.07	18:08	41° 14,98' S	176° 28,12' E	1170	S 7	317,3	2,2	Profil	PR
SO191/022-2	26.01.07	18:08	41° 14,98' S	176° 28,12' E	1170	S 7	317,3	2,2	Profil	PR
SO191/023-1	26.01.07	18:21	41° 15,05' S	176° 27,71' E	1179	SSW 6	25,9	2,6	OBS/OBH	OBS/OBH
SO191/023-1	26.01.07	18:27	41° 15,20' S	176° 28,07' E	1168	SSW 8	101,3	5,6	OBS/OBH	OBS/OBH
SO191/023-1	26.01.07	18:39	41° 15,38' S	176° 29,34' E	1131	SSW 8	95	4,2	OBS/OBH	OBS/OBH
SO191/023-1	26.01.07	18:52	41° 15,66' S	176° 30,33' E	1073	SW 7	265,6	2,3	OBS/OBH	OBS/OBH
SO191/023-1	26.01.07	18:55	41° 15,65' S	176° 30,23' E	1080	S 8	301,9	1,1	OBS/OBH	OBS/OBH
SO191/023-1	26.01.07	19:15	41° 16,18' S	176° 31,20' E	1004	SSW 5	100,2	1,9	OBS/OBH	OBS/OBH
SO191/023-1	26.01.07	19:25	41° 16,36' S	176° 31,22' E	1013	S 6	275	0,9	OBS/OBH	OBS/OBH

Station	Datum	UTC	PositionLat	PositionLon	Tiefe [m]	Windstärke [m/s]	Kurs [°]	v [kn]	Gerät	Geräte Kürzel
SO191/023-1	26.01.07	19:26	41° 16,37' S	176° 31,19' E	1013	S 6	257,4	1,2	OBS/OBH	OBS/OBH
SO191/023-1	26.01.07	19:55	41° 18,65' S	176° 28,92' E	1014	S 7	214	5	OBS/OBH	OBS/OBH
SO191/023-1	26.01.07	20:04	41° 18,85' S	176° 28,45' E	1063	SSE 7	301,7	1	OBS/OBH	OBS/OBH
SO191/023-1	26.01.07	20:05	41° 18,84' S	176° 28,43' E	1068	SSE 6	287,4	0,6	OBS/OBH	OBS/OBH
SO191/023-1	26.01.07	20:34	41° 17,83' S	176° 31,38' E	837	SSW 4	75,8	5,5	OBS/OBH	OBS/OBH
SO191/023-1	26.01.07	20:42	41° 17,90' S	176° 31,54' E	821	SSE 6	276,9	0,4	OBS/OBH	OBS/OBH
SO191/023-1	26.01.07	21:06	41° 16,94' S	176° 34,31' E	1025	SSW 6	68,9	8,4	OBS/OBH	OBS/OBH
SO191/023-1	26.01.07	21:20	41° 16,29' S	176° 36,47' E	845	SSW 5	70,6	6,1	OBS/OBH	OBS/OBH
SO191/023-1	26.01.07	21:28	41° 16,07' S	176° 37,39' E	840	SW 5	119	1,9	OBS/OBH	OBS/OBH
SO191/023-1	26.01.07	21:41	41° 15,95' S	176° 37,38' E	822	SE 9	332,5	0,8	OBS/OBH	OBS/OBH
SO191/023-1	26.01.07	21:49	41° 16,00' S	176° 37,02' E	795	SSE 7	253,4	3	OBS/OBH	OBS/OBH
SO191/023-1	26.01.07	21:50	41° 16,01' S	176° 36,94' E	798	SSW 6	283,5	3,7	OBS/OBH	OBS/OBH
SO191/023-1	26.01.07	22:03	41° 15,81' S	176° 36,76' E	790	SSE 7	7,1	1	OBS/OBH	OBS/OBH
SO191/023-1	26.01.07	22:10	41° 15,89' S	176° 36,71' E	795	S 5	184	3,6	OBS/OBH	OBS/OBH
SO191/023-1	26.01.07	22:20	41° 16,39' S	176° 36,29' E	853	S 6	218,4	2	OBS/OBH	OBS/OBH
SO191/023-1	26.01.07	22:23	41° 16,43' S	176° 36,20' E	861	S 5	233,8	0,4	OBS/OBH	OBS/OBH
SO191/023-1	26.01.07	22:31	41° 16,75' S	176° 36,01' E	887	S 6	207,7	3,6	OBS/OBH	OBS/OBH
SO191/023-1	26.01.07	22:41	41° 16,98' S	176° 35,59' E	775	SSE 6	258	0,8	OBS/OBH	OBS/OBH
SO191/023-1	26.01.07	22:42	41° 16,98' S	176° 35,58' E	771	SSE 6	284,5	0,4	OBS/OBH	OBS/OBH
SO191/023-1	26.01.07	22:55	41° 17,76' S	176° 35,61' E	879	S 5	177,8	6,2	OBS/OBH	OBS/OBH
SO191/023-1	26.01.07	23:06	41° 18,39' S	176° 35,49' E	1049	S 6	161	0,6	OBS/OBH	OBS/OBH
SO191/023-1	26.01.07	23:07	41° 18,40' S	176° 35,49' E	1051	S 5	178,6	0,4	OBS/OBH	OBS/OBH
SO191/023-1	26.01.07	23:21	41° 18,25' S	176° 34,77' E	987	SSE 5	293,3	2,8	OBS/OBH	OBS/OBH
SO191/023-1	26.01.07	23:22	41° 18,24' S	176° 34,72' E	960	SSE 5	280,6	2,4	OBS/OBH	OBS/OBH
SO191/023-1	26.01.07	23:30	41° 17,95' S	176° 34,60' E	887	SSW 6	14,5	1	OBS/OBH	OBS/OBH
SO191/023-1	26.01.07	23:43	41° 17,73' S	176° 34,25' E	813	S 6	277,6	2,3	OBS/OBH	OBS/OBH
SO191/023-1	26.01.07	23:45	41° 17,69' S	176° 34,17' E	802	SSW 6	308,5	1,8	OBS/OBH	OBS/OBH
SO191/023-1	26.01.07	23:53	41° 17,51' S	176° 33,91' E	788	S 5	326,1	1,5	OBS/OBH	OBS/OBH
SO191/023-1	26.01.07	23:58	41° 17,39' S	176° 33,84' E	818	SSW 5	0,8	2,7	OBS/OBH	OBS/OBH
SO191/023-1	27.01.07	00:04	41° 17,40' S	176° 33,92' E	818	WSW 4	266,2	2,8	OBS/OBH	OBS/OBH
SO191/023-1	27.01.07	00:10	41° 17,37' S	176° 33,72' E	817	SSW 7	326,1	1,1	OBS/OBH	OBS/OBH
SO191/023-1	27.01.07	00:14	41° 17,32' S	176° 33,76' E	833	S 5	64,8	1,4	OBS/OBH	OBS/OBH
SO191/023-1	27.01.07	00:18	41° 17,29' S	176° 33,70' E	838	SE 6	255,2	2,4	OBS/OBH	OBS/OBH
SO191/023-1	27.01.07	00:24	41° 17,34' S	176° 33,44' E	807	SSW 6	310,4	0,8	OBS/OBH	OBS/OBH
SO191/023-1	27.01.07	00:30	41° 17,26' S	176° 33,44' E	836	S 7	53,2	1,3	OBS/OBH	OBS/OBH
SO191/023-1	27.01.07	00:33	41° 17,22' S	176° 33,38' E	840	SSE 6	271,7	2,7	OBS/OBH	OBS/OBH
SO191/023-1	27.01.07	00:38	41° 17,27' S	176° 33,26' E	803	SW 6	328,9	0,6	OBS/OBH	OBS/OBH
SO191/023-1	27.01.07	00:45	41° 17,17' S	176° 33,28' E	841	S 5	58,4	0,6	OBS/OBH	OBS/OBH
SO191/023-1	27.01.07	00:48	41° 17,14' S	176° 33,20' E	849	S 6	281,2	3,2	OBS/OBH	OBS/OBH
SO191/023-1	27.01.07	00:53	41° 17,10' S	176° 32,96' E	820	SSW 6	326,1	1,8	OBS/OBH	OBS/OBH
SO191/023-1	27.01.07	00:57	41° 17,02' S	176° 32,89' E	844	SSE 7	276,4	1,6	OBS/OBH	OBS/OBH
SO191/023-1	27.01.07	01:07	41° 16,90' S	176° 32,43' E	877	SSW 6	346,9	1,3	OBS/OBH	OBS/OBH

Station	Datum	UTC	PositionLat	PositionLon	Tiefe [m]	Windstärke [m/s]	Kurs [°]	v [kn]	Gerät	Geräte Kürzel
SO191/023-1	27.01.07	01:20	41° 16,69' S	176° 32,37' E	1050	S 6	6,9	0,8	OBS/OBH	OBS/OBH
SO191/024-1	27.01.07	02:07	41° 20,78' S	176° 35,97' E	1868	S 6	71,7	7,4	Vermessung	EM / PS
SO191/024-1	27.01.07	02:54	41° 18,17' S	176° 43,55' E	1890	S 5	59,8	7,8	Vermessung	EM / PS
SO191/024-1	27.01.07	03:27	41° 14,50' S	176° 46,75' E	1299	SSE 6	50,5	8,1	Vermessung	EM / PS
SO191/024-1	27.01.07	06:55	41° 1,08' S	177° 17,91' E	1807	SE 6	57,9	7,3	Vermessung	EM / PS
SO191/025-1	27.01.07	08:36	40° 50,19' S	177° 21,12' E	2001	ENE 2	196,9	0,5	Controlled Source Electro-Magnetic	CSEM
SO191/025-1	27.01.07	08:38	40° 50,20' S	177° 21,14' E	1999	ENE 2	166,8	0,4	Controlled Source Electro-Magnetic	CSEM
SO191/025-1	27.01.07	09:06	40° 50,20' S	177° 21,22' E	2000	E 2	158,9	0,6	Controlled Source Electro-Magnetic	CSEM
SO191/025-1	27.01.07	09:46	40° 50,12' S	177° 21,63' E	1996	ESE 2	179,5	0,2	Controlled Source Electro-Magnetic	CSEM
SO191/025-1	27.01.07	09:48	40° 50,11' S	177° 21,64' E	1997	ESE 3	81,2	0,2	Controlled Source Electro-Magnetic	CSEM
SO191/025-1	27.01.07	13:08	40° 51,02' S	177° 24,52' E	1999	E 3	128,4	2	Controlled Source Electro-Magnetic	CSEM
SO191/025-1	27.01.07	13:30	40° 51,17' S	177° 25,12' E	2042	ENE 3	110,8	0,9	Controlled Source Electro-Magnetic	CSEM
SO191/025-1	27.01.07	13:31	40° 51,18' S	177° 25,15' E	2046	ENE 3	119,8	1,8	Controlled Source Electro-Magnetic	CSEM
SO191/025-1	27.01.07	13:39	40° 51,20' S	177° 25,21' E	2046	ENE 4	125,4	0,5	Controlled Source Electro-Magnetic	CSEM
SO191/025-1	27.01.07	13:52	40° 51,19' S	177° 25,20' E	2046	E 4	106,4	0,8	Controlled Source Electro-Magnetic	CSEM
SO191/025-1	27.01.07	13:53	40° 51,19' S	177° 25,21' E	2046	E 4	342	0,3	Controlled Source Electro-Magnetic	CSEM
SO191/025-1	27.01.07	14:02	40° 51,24' S	177° 25,39' E	2114	E 5	118,5	1,8	Controlled Source Electro-Magnetic	CSEM
SO191/025-1	27.01.07	14:08	40° 51,25' S	177° 25,47' E	2129	E 5	140,8	0,7	Controlled Source Electro-Magnetic	CSEM
SO191/025-1	27.01.07	14:09	40° 51,25' S	177° 25,47' E	2129	E 5	106,6	0,2	Controlled Source Electro-Magnetic	CSEM
SO191/025-1	27.01.07	14:14	40° 51,24' S	177° 25,45' E	2129	ENE 4	311,7	0,3	Controlled Source Electro-Magnetic	CSEM
SO191/025-1	27.01.07	14:24	40° 51,23' S	177° 25,47' E	2113	E 5	345,6	0,6	Controlled Source Electro-Magnetic	CSEM
SO191/025-1	27.01.07	14:25	40° 51,23' S	177° 25,46' E	2134	E 4	172,5	0,1	Controlled Source Electro-Magnetic	CSEM
SO191/025-1	27.01.07	14:31	40° 51,26' S	177° 25,56' E	2131	E 5	137,8	1	Controlled Source Electro-Magnetic	CSEM
SO191/025-1	27.01.07	14:43	40° 51,34' S	177° 25,79' E	2131	ENE 5	146,8	0,9	Controlled Source Electro-Magnetic	CSEM
SO191/025-1	27.01.07	14:44	40° 51,34' S	177° 25,80' E	2133	ENE 5	210,9	0,2	Controlled Source Electro-Magnetic	CSEM
SO191/025-1	27.01.07	14:50	40° 51,35' S	177° 25,80' E	2133	ENE 5	200,8	0,6	Controlled Source Electro-Magnetic	CSEM
SO191/025-1	27.01.07	15:04	40° 51,34' S	177° 25,77' E	2135	NE 6	73,6	1	Controlled Source Electro-Magnetic	CSEM
SO191/025-1	27.01.07	15:04	40° 51,34' S	177° 25,77' E	2135	NE 6	73,6	1	Controlled Source Electro-Magnetic	CSEM
SO191/025-1	27.01.07	15:21	40° 51,42' S	177° 26,06' E	2126	ENE 5	91,2	0,6	Controlled Source Electro-Magnetic	CSEM
SO191/025-1	27.01.07	15:29	40° 51,44' S	177° 26,12' E	2130	ENE 5	129,7	0,5	Controlled Source Electro-Magnetic	CSEM
SO191/025-1	27.01.07	15:29	40° 51,44' S	177° 26,12' E	2130	ENE 5	129,7	0,5	Controlled Source Electro-Magnetic	CSEM
SO191/025-1	27.01.07	15:35	40° 51,44' S	177° 26,16' E	2130	ENE 5	58	0,8	Controlled Source Electro-Magnetic	CSEM
SO191/025-1	27.01.07	15:44	40° 51,44' S	177° 26,15' E	2128	ENE 5	116,9	0,6	Controlled Source Electro-Magnetic	CSEM
SO191/025-1	27.01.07	15:44	40° 51,44' S	177° 26,15' E	2128	ENE 5	116,9	0,6	Controlled Source Electro-Magnetic	CSEM
SO191/025-1	27.01.07	15:51	40° 51,46' S	177° 26,25' E	2137	ENE 5	114,1	1,3	Controlled Source Electro-Magnetic	CSEM
SO191/025-1	27.01.07	16:07	40° 51,52' S	177° 26,48' E	2143	ENE 5	111	0,9	Controlled Source Electro-Magnetic	CSEM
SO191/025-1	27.01.07	16:07	40° 51,52' S	177° 26,48' E	2143	ENE 5	111	0,9	Controlled Source Electro-Magnetic	CSEM
SO191/025-1	27.01.07	16:13	40° 51,54' S	177° 26,49' E	2143	ENE 5	295,7	0,4	Controlled Source Electro-Magnetic	CSEM
SO191/025-1	27.01.07	16:22	40° 51,53' S	177° 26,49' E	2145	ENE 5	32,1	0,1	Controlled Source Electro-Magnetic	CSEM
SO191/025-1	27.01.07	16:22	40° 51,53' S	177° 26,49' E	2145	ENE 5	32,1	0,1	Controlled Source Electro-Magnetic	CSEM
SO191/025-1	27.01.07	16:30	40° 51,57' S	177° 26,63' E	2147	ENE 6	110,2	1,1	Controlled Source Electro-Magnetic	CSEM
SO191/025-1	27.01.07	16:42	40° 51,62' S	177° 26,82' E	2147	ENE 5	86,2	0,7	Controlled Source Electro-Magnetic	CSEM

Station	Datum	UTC	PositionLat	PositionLon	Tiefe [m]	Windstärke [m/s]	Kurs [°]	v [kn]	Gerät	Geräte Kürzel
SO191/025-1	27.01.07	16:42	40° 51,62' S	177° 26,82' E	2147	ENE 5	86,2	0,7	Controlled Source Electro-Magnetic	CSEM
SO191/025-1	27.01.07	16:48	40° 51,62' S	177° 26,86' E	2147	ENE 6	269,3	0,4	Controlled Source Electro-Magnetic	CSEM
SO191/025-1	27.01.07	16:57	40° 51,63' S	177° 26,85' E	2148	ENE 6	264,1	0,1	Controlled Source Electro-Magnetic	CSEM
SO191/025-1	27.01.07	16:57	40° 51,63' S	177° 26,85' E	2148	ENE 6	264,1	0,1	Controlled Source Electro-Magnetic	CSEM
SO191/025-1	27.01.07	17:05	40° 51,65' S	177° 26,98' E	2149	ENE 6	104,7	1,3	Controlled Source Electro-Magnetic	CSEM
SO191/025-1	27.01.07	17:14	40° 51,69' S	177° 27,17' E	2148	ENE 6	105,8	0,7	Controlled Source Electro-Magnetic	CSEM
SO191/025-1	27.01.07	17:14	40° 51,69' S	177° 27,17' E	2148	ENE 6	105,8	0,7	Controlled Source Electro-Magnetic	CSEM
SO191/025-1	27.01.07	17:20	40° 51,70' S	177° 27,19' E	2148	ENE 6	302,2	0,1	Controlled Source Electro-Magnetic	CSEM
SO191/025-1	27.01.07	17:28	40° 51,70' S	177° 27,19' E	2147	ENE 6	112,9	0,2	Controlled Source Electro-Magnetic	CSEM
SO191/025-1	27.01.07	17:28	40° 51,70' S	177° 27,19' E	2147	ENE 6	112,9	0,2	Controlled Source Electro-Magnetic	CSEM
SO191/025-1	27.01.07	17:36	40° 51,73' S	177° 27,33' E	2150	ENE 5	120,7	1,6	Controlled Source Electro-Magnetic	CSEM
SO191/025-1	27.01.07	17:45	40° 51,78' S	177° 27,50' E	2153	ENE 6	132,1	0,3	Controlled Source Electro-Magnetic	CSEM
SO191/025-1	27.01.07	17:45	40° 51,78' S	177° 27,50' E	2153	ENE 6	132,1	0,3	Controlled Source Electro-Magnetic	CSEM
SO191/025-1	27.01.07	17:51	40° 51,78' S	177° 27,52' E	2153	ENE 6	281,6	0,6	Controlled Source Electro-Magnetic	CSEM
SO191/025-1	27.01.07	17:59	40° 51,79' S	177° 27,51' E	2151	ENE 5	326,4	0,7	Controlled Source Electro-Magnetic	CSEM
SO191/025-1	27.01.07	17:59	40° 51,79' S	177° 27,51' E	2151	ENE 5	326,4	0,7	Controlled Source Electro-Magnetic	CSEM
SO191/025-1	27.01.07	18:07	40° 51,82' S	177° 27,66' E	2151	ENE 5	80,9	2	Controlled Source Electro-Magnetic	CSEM
SO191/025-1	27.01.07	18:17	40° 51,87' S	177° 27,85' E	2149	NE 5	116,7	0,1	Controlled Source Electro-Magnetic	CSEM
SO191/025-1	27.01.07	18:17	40° 51,87' S	177° 27,85' E	2149	NE 5	116,7	0,1	Controlled Source Electro-Magnetic	CSEM
SO191/025-1	27.01.07	18:24	40° 51,87' S	177° 27,85' E	2149	ENE 5	154,1	0,3	Controlled Source Electro-Magnetic	CSEM
SO191/025-1	27.01.07	18:35	40° 51,87' S	177° 27,85' E	2149	ENE 5	90,7	0,5	Controlled Source Electro-Magnetic	CSEM
SO191/025-1	27.01.07	18:35	40° 51,87' S	177° 27,85' E	2149	ENE 5	90,7	0,5	Controlled Source Electro-Magnetic	CSEM
SO191/025-1	27.01.07	18:44	40° 51,91' S	177° 28,04' E	2149	NE 5	107,8	0,5	Controlled Source Electro-Magnetic	CSEM
SO191/025-1	27.01.07	18:51	40° 51,95' S	177° 28,20' E	2148	NE 5	132,8	1,3	Controlled Source Electro-Magnetic	CSEM
SO191/025-1	27.01.07	18:51	40° 51,95' S	177° 28,20' E	2148	NE 5	132,8	1,3	Controlled Source Electro-Magnetic	CSEM
SO191/025-1	27.01.07	18:58	40° 51,96' S	177° 28,21' E	2148	NE 5	87,8	0,3	Controlled Source Electro-Magnetic	CSEM
SO191/025-1	27.01.07	19:07	40° 51,97' S	177° 28,19' E	2148	NE 4	169,2	0,6	Controlled Source Electro-Magnetic	CSEM
SO191/025-1	27.01.07	19:08	40° 51,98' S	177° 28,19' E	2148	NE 5	232,4	0,4	Controlled Source Electro-Magnetic	CSEM
SO191/025-1	27.01.07	19:16	40° 51,99' S	177° 28,33' E	2148	NE 4	93,2	1,8	Controlled Source Electro-Magnetic	CSEM
SO191/025-1	27.01.07	19:34	40° 52,05' S	177° 28,55' E	2145	NNE 5	81,6	0,6	Controlled Source Electro-Magnetic	CSEM
SO191/025-1	27.01.07	19:35	40° 52,05' S	177° 28,55' E	2144	NNE 6	41,9	0,2	Controlled Source Electro-Magnetic	CSEM
SO191/025-1	27.01.07	19:42	40° 52,07' S	177° 28,57' E	2144	NNE 5	46,3	0,1	Controlled Source Electro-Magnetic	CSEM
SO191/025-1	27.01.07	19:50	40° 52,07' S	177° 28,60' E	2145	NNE 5	81,7	0,2	Controlled Source Electro-Magnetic	CSEM
SO191/025-1	27.01.07	19:50	40° 52,07' S	177° 28,60' E	2145	NNE 5	81,7	0,2	Controlled Source Electro-Magnetic	CSEM
SO191/025-1	27.01.07	19:58	40° 52,11' S	177° 28,75' E	2141	N 6	144,8	1	Controlled Source Electro-Magnetic	CSEM
SO191/025-1	27.01.07	20:06	40° 52,14' S	177° 28,85' E	2143	NNE 5	128,6	0,4	Controlled Source Electro-Magnetic	CSEM
SO191/025-1	27.01.07	20:07	40° 52,15' S	177° 28,86' E	2142	NNE 5	103,4	0,3	Controlled Source Electro-Magnetic	CSEM
SO191/025-1	27.01.07	20:14	40° 52,14' S	177° 28,89' E	2145	NNE 5	109,1	0,8	Controlled Source Electro-Magnetic	CSEM
SO191/025-1	27.01.07	20:22	40° 52,15' S	177° 28,91' E	2142	NNE 5	119,9	0,8	Controlled Source Electro-Magnetic	CSEM
SO191/025-1	27.01.07	20:23	40° 52,15' S	177° 28,91' E	2142	NNE 5	142	0,4	Controlled Source Electro-Magnetic	CSEM
SO191/025-1	27.01.07	20:30	40° 52,16' S	177° 29,02' E	2141	N 5	107,7	1,2	Controlled Source Electro-Magnetic	CSEM
SO191/025-1	27.01.07	20:42	40° 52,21' S	177° 29,22' E	2140	NE 4	138,8	0,4	Controlled Source Electro-Magnetic	CSEM

Station	Datum	UTC	PositionLat	PositionLon	Tiefe [m]	Windstärke [m/s]	Kurs [°]	v [kn]	Gerät	Geräte Kürzel
SO191/025-1	27.01.07	20:43	40° 52,21' S	177° 29,22' E	2140	NE 4	39,3	0,5	Controlled Source Electro-Magnetic	CSEM
SO191/025-1	27.01.07	20:48	40° 52,20' S	177° 29,24' E	2138	NE 5	134,8	0,2	Controlled Source Electro-Magnetic	CSEM
SO191/025-1	27.01.07	20:59	40° 52,21' S	177° 29,26' E	2139	NE 5	144,8	0,6	Controlled Source Electro-Magnetic	CSEM
SO191/025-1	27.01.07	20:59	40° 52,21' S	177° 29,26' E	2139	NE 5	144,8	0,6	Controlled Source Electro-Magnetic	CSEM
SO191/025-1	27.01.07	21:08	40° 52,24' S	177° 29,41' E	2138	NE 4	80,6	1,4	Controlled Source Electro-Magnetic	CSEM
SO191/025-1	27.01.07	21:19	40° 52,30' S	177° 29,53' E	2138	NE 5	162,9	0,5	Controlled Source Electro-Magnetic	CSEM
SO191/025-1	27.01.07	21:19	40° 52,30' S	177° 29,53' E	2138	NE 5	162,9	0,5	Controlled Source Electro-Magnetic	CSEM
SO191/025-1	27.01.07	21:27	40° 52,31' S	177° 29,55' E	2138	NE 6	300,5	0,3	Controlled Source Electro-Magnetic	CSEM
SO191/025-1	27.01.07	21:37	40° 52,30' S	177° 29,57' E	2138	NE 7	22	0,7	Controlled Source Electro-Magnetic	CSEM
SO191/025-1	27.01.07	21:38	40° 52,30' S	177° 29,57' E	2138	NE 7	106	0,4	Controlled Source Electro-Magnetic	CSEM
SO191/025-1	27.01.07	21:45	40° 52,35' S	177° 29,77' E	2135	NNE 6	114,5	1,6	Controlled Source Electro-Magnetic	CSEM
SO191/025-1	27.01.07	22:04	40° 52,48' S	177° 30,21' E	2077	NNE 6	92,4	0,4	Controlled Source Electro-Magnetic	CSEM
SO191/025-1	27.01.07	22:05	40° 52,48' S	177° 30,22' E	2081	NE 7	67,7	0,3	Controlled Source Electro-Magnetic	CSEM
SO191/025-1	27.01.07	22:11	40° 52,49' S	177° 30,22' E	2081	NE 7	133,9	0,1	Controlled Source Electro-Magnetic	CSEM
SO191/025-1	27.01.07	22:22	40° 52,48' S	177° 30,22' E	2077	NNE 6	39,2	0,4	Controlled Source Electro-Magnetic	CSEM
SO191/025-1	27.01.07	23:56	40° 52,77' S	177° 30,35' E	2106	NNE 8	184,3	0,9	Controlled Source Electro-Magnetic	CSEM
SO191/025-1	28.01.07	00:47	40° 53,31' S	177° 30,29' E	2225	NNE 7	196,2	0,7	Controlled Source Electro-Magnetic	CSEM
SO191/025-1	28.01.07	01:48	40° 55,08' S	177° 31,39' E	2386	NNE 11	139,6	1,6	Controlled Source Electro-Magnetic	CSEM
SO191/025-1	28.01.07	02:00	40° 55,11' S	177° 31,61' E	2408	NE 10	16,3	10,1	Controlled Source Electro-Magnetic	CSEM
SO191/026-1	28.01.07	03:33	40° 44,35' S	177° 31,77' E	2084	NE 10	1	6,6	Vermessung	EM / PS
SO191/026-1	28.01.07	06:45	40° 20,89' S	177° 29,96' E	1867	NE 11	357,4	7,2	Vermessung	EM / PS
SO191/026-1	28.01.07	08:16	40° 13,42' S	177° 40,84' E	1955	N 10	46,9	7,5	Vermessung	EM / PS
SO191/026-1	28.01.07	09:38	40° 5,82' S	177° 48,89' E	1480	NNW 10	33,7	7,3	Vermessung	EM / PS
SO191/027-1	28.01.07	10:52	39° 59,35' S	177° 54,36' E	1165	N 13	351,8	0,6	OBS/OBH	OBS/OBH
SO191/027-1	28.01.07	10:58	39° 59,33' S	177° 54,35' E	1165	N 12	194,1	0,2	OBS/OBH	OBS/OBH
SO191/027-1	28.01.07	11:29	40° 0,36' S	177° 53,07' E	1177	N 12	227,3	0,4	OBS/OBH	OBS/OBH
SO191/027-1	28.01.07	11:59	40° 2,06' S	177° 53,97' E	1563	N 11	283,5	0,4	OBS/OBH	OBS/OBH
SO191/027-1	28.01.07	12:18	40° 1,61' S	177° 52,79' E	1277	N 13	36,4	0,6	OBS/OBH	OBS/OBH
SO191/027-1	28.01.07	12:34	40° 1,29' S	177° 51,91' E	1167	N 11	62,6	0,2	OBS/OBH	OBS/OBH
SO191/027-1	28.01.07	12:44	40° 1,20' S	177° 51,67' E	1148	N 13	86,2	0,6	OBS/OBH	OBS/OBH
SO191/027-1	28.01.07	12:53	40° 1,10' S	177° 51,43' E	1163	N 11	174,6	0,9	OBS/OBH	OBS/OBH
SO191/027-1	28.01.07	13:03	40° 0,97' S	177° 51,03' E	1205	NNE 12	349,1	2,9	OBS/OBH	OBS/OBH
SO191/027-1	28.01.07	13:14	40° 0,79' S	177° 50,60' E	1143	N 9	318,3	0,8	OBS/OBH	OBS/OBH
SO191/027-1	28.01.07	13:24	40° 0,62' S	177° 50,13' E	1196	NNE 12	309,9	0,1	OBS/OBH	OBS/OBH
SO191/027-1	28.01.07	13:38	40° 0,31' S	177° 49,30' E	1244	NNE 7	151,9	0,2	OBS/OBH	OBS/OBH
SO191/027-1	28.01.07	14:14	40° 3,05' S	177° 49,66' E	1102	NNE 10	164,4	0,9	OBS/OBH	OBS/OBH
SO191/027-1	28.01.07	14:15	40° 3,06' S	177° 49,66' E	1100	NNE 9	158,6	1,2	OBS/OBH	OBS/OBH
SO191/028-1	28.01.07	15:00	40° 7,32' S	177° 47,79' E	1864	NNW 10	265,2	1,3	Profil	PR
SO191/028-1	28.01.07	15:12	40° 7,23' S	177° 47,60' E	1756	NW 8	48,3	0,2	Profil	PR
SO191/028-1	28.01.07	15:14	40° 7,22' S	177° 47,56' E	1725	NW 8	303,6	1,5	Profil	PR
SO191/028-1	28.01.07	15:17	40° 7,16' S	177° 47,48' E	1671	NW 7	327,9	2,8	Profil	PR
SO191/028-1	28.01.07	15:27	40° 6,85' S	177° 47,16' E	1424	NW 7	316,3	2,4	Profil	PR

Station	Datum	UTC	PositionLat	PositionLon	Tiefe [m]	Windstärke [m/s]	Kurs [°]	v [kn]	Gerät	Geräte Kürzel
SO191/028-1	28.01.07	15:55	40° 5,97' S	177° 47,22' E	1253	WNW 7	2,2	2,3	Profil	PR
SO191/028-1	28.01.07	16:59	40° 3,37' S	177° 49,25' E	1107	N 6	46,5	3,1	Profil	PR
SO191/028-1	28.01.07	19:20	39° 58,49' S	177° 55,45' E	1123	N 10	52,9	2,4	Profil	PR
SO191/028-1	28.01.07	19:37	39° 57,86' S	177° 56,22' E	1122	N 11	40,6	3	Profil	PR
SO191/028-1	28.01.07	20:35	39° 58,04' S	177° 53,35' E	1205	N 11	234,2	3,5	Profil	PR
SO191/028-1	28.01.07	21:05	39° 59,21' S	177° 51,91' E	1215	N 9	222,3	2,8	Profil	PR
SO191/028-1	28.01.07	22:47	40° 3,02' S	177° 47,25' E	1172	NNW 6	223,7	3,6	Profil	PR
SO191/028-1	28.01.07	23:00	40° 3,49' S	177° 46,68' E	1214	N 6	227	2,8	Profil	PR
SO191/028-1	29.01.07	00:23	40° 4,14' S	177° 49,57' E	1202	NNW 7	43,1	1,9	Profil	PR
SO191/028-1	29.01.07	01:11	40° 2,76' S	177° 51,36' E	1265	N 8	44,8	2,2	Profil	PR
SO191/028-1	29.01.07	01:52	40° 1,30' S	177° 53,21' E	1275	N 8	48	3	Profil	PR
SO191/028-1	29.01.07	01:53	40° 1,26' S	177° 53,26' E	1278	N 8	44,8	3,5	Profil	PR
SO191/028-1	29.01.07	01:58	40° 1,10' S	177° 53,47' E	1265	N 8	62,2	1,5	Profil	PR
SO191/028-1	29.01.07	02:23	40° 0,59' S	177° 53,85' E	1234	N 8	334,8	0,6	Profil	PR
SO191/028-2	29.01.07	03:05	40° 1,22' S	177° 54,94' E	1506	N 11	156,1	2,1	Profil	PR
SO191/028-2	29.01.07	03:43	40° 2,17' S	177° 54,30' E	1588	NNE 8	289	3,1	Profil	PR
SO191/028-2	29.01.07	05:25	39° 59,95' S	177° 48,37' E	1321	NNE 8	288,3	3,2	Profil	PR
SO191/028-3	29.01.07	05:35	39° 59,87' S	177° 47,95' E	1339	NNE 7	245,5	1,1	OBS/OBH	OBS/OBH
SO191/028-2	29.01.07	05:40	39° 59,88' S	177° 47,81' E	1339	NNE 7	262,8	1,4	Profil	PR
SO191/028-3	29.01.07	06:09	40° 0,31' S	177° 47,88' E	1308	N 11	205,2	1,2	OBS/OBH	OBS/OBH
SO191/028-2	29.01.07	06:24	40° 0,48' S	177° 47,64' E	1293	NNE 9	242,5	1,2	Profil	PR
SO191/028-3	29.01.07	06:45	40° 0,69' S	177° 48,27' E	1252	NNE 8	90,8	4,2	OBS/OBH	OBS/OBH
SO191/028-3	29.01.07	07:00	40° 0,69' S	177° 49,09' E	1228	NE 8	96,2	0,6	OBS/OBH	OBS/OBH
SO191/028-3	29.01.07	07:06	40° 0,74' S	177° 49,16' E	1216	NNE 8	80,2	2,2	OBS/OBH	OBS/OBH
SO191/028-3	29.01.07	07:08	40° 0,74' S	177° 49,27' E	1221	NE 7	90,3	2,7	OBS/OBH	OBS/OBH
SO191/028-3	29.01.07	07:20	40° 0,75' S	177° 49,99' E	1186	N 9	124,7	0,8	OBS/OBH	OBS/OBH
SO191/028-3	29.01.07	07:31	40° 0,81' S	177° 50,23' E	1159	N 10	181,2	0,3	OBS/OBH	OBS/OBH
SO191/028-3	29.01.07	07:34	40° 0,82' S	177° 50,32' E	1168	NNW 10	73	1,6	OBS/OBH	OBS/OBH
SO191/028-3	29.01.07	07:41	40° 1,02' S	177° 50,48' E	1111	NNW 12	211,4	1,2	OBS/OBH	OBS/OBH
SO191/028-3	29.01.07	07:51	40° 1,15' S	177° 50,45' E	1092	NNW 9	112,5	1,3	OBS/OBH	OBS/OBH
SO191/028-3	29.01.07	07:56	40° 1,06' S	177° 50,73' E	1107	NNW 11	58,8	4,7	OBS/OBH	OBS/OBH
SO191/028-3	29.01.07	08:06	40° 0,86' S	177° 51,15' E	1245	NW 11	121	0,5	OBS/OBH	OBS/OBH
SO191/028-3	29.01.07	08:12	40° 0,94' S	177° 51,14' E	1218	NW 9	151,9	1,2	OBS/OBH	OBS/OBH
SO191/028-3	29.01.07	08:15	40° 0,97' S	177° 51,20' E	1211	NNW 10	141,7	2,7	OBS/OBH	OBS/OBH
SO191/028-3	29.01.07	08:25	40° 1,24' S	177° 51,36' E	1156	NW 9	168,9	0,7	OBS/OBH	OBS/OBH
SO191/028-3	29.01.07	08:31	40° 1,30' S	177° 51,33' E	1155	NW 7	202,9	0,9	OBS/OBH	OBS/OBH
SO191/028-3	29.01.07	08:31	40° 1,30' S	177° 51,33' E	1155	NW 7	202,9	0,9	OBS/OBH	OBS/OBH
SO191/028-3	29.01.07	08:44	40° 1,26' S	177° 51,54' E	1145	NW 8	179,7	0,5	OBS/OBH	OBS/OBH
SO191/028-3	29.01.07	08:49	40° 1,26' S	177° 51,56' E	1144	NNW 8	54,9	1	OBS/OBH	OBS/OBH
SO191/028-3	29.01.07	08:52	40° 1,26' S	177° 51,65' E	1141	NNW 7	110,6	2	OBS/OBH	OBS/OBH
SO191/028-3	29.01.07	08:58	40° 1,32' S	177° 51,81' E	1157	NW 8	92,8	0,3	OBS/OBH	OBS/OBH
SO191/028-3	29.01.07	09:09	40° 1,44' S	177° 52,10' E	1197	NNW 7	105,8	3,2	OBS/OBH	OBS/OBH

Station	Datum	UTC	PositionLat	PositionLon	Tiefe [m]	Windstärke [m/s]	Kurs [°]	v [kn]	Gerät	Geräte Kürzel
SO191/028-3	29.01.07	09:09	40° 1,44' S	177° 52,10' E	1197	NNW 7	105,8	3,2	OBS/OBH	OBS/OBH
SO191/028-3	29.01.07	09:21	40° 1,59' S	177° 52,69' E	1274	WNW 8	90,9	0,2	OBS/OBH	OBS/OBH
SO191/028-3	29.01.07	09:27	40° 1,61' S	177° 52,82' E	1273	N 7	118,5	3,4	OBS/OBH	OBS/OBH
SO191/028-3	29.01.07	09:43	40° 2,06' S	177° 53,78' E	1538	WNW 4	169,8	0,4	OBS/OBH	OBS/OBH
SO191/028-3	29.01.07	09:45	40° 2,07' S	177° 53,79' E	1542	W 4	136,8	0,2	OBS/OBH	OBS/OBH
SO191/028-3	29.01.07	10:45	40° 0,28' S	177° 52,93' E	1162	SSW 5	198,4	0,9	OBS/OBH	OBS/OBH
SO191/028-3	29.01.07	10:47	40° 0,29' S	177° 52,91' E	1163	SSW 3	274	1,4	OBS/OBH	OBS/OBH
SO191/028-3	29.01.07	10:58	40° 0,33' S	177° 52,95' E	1169	SSW 4	184,7	0,7	OBS/OBH	OBS/OBH
SO191/028-3	29.01.07	11:10	39° 59,97' S	177° 53,37' E	1159	SW 4	43	6,7	OBS/OBH	OBS/OBH
SO191/028-3	29.01.07	11:26	39° 59,29' S	177° 54,25' E	1162	WNW 2	135,3	0,7	OBS/OBH	OBS/OBH
SO191/028-3	29.01.07	11:46	40° 0,60' S	177° 52,60' E	1167	WSW 2	227,6	7,7	OBS/OBH	OBS/OBH
SO191/028-3	29.01.07	11:59	40° 1,80' S	177° 51,00' E	1143	SW 1	226,8	7,8	OBS/OBH	OBS/OBH
SO191/028-3	29.01.07	12:33	40° 3,03' S	177° 49,28' E	1117	W 2	121,1	0,8	OBS/OBH	OBS/OBH
SO191/028-4	29.01.07	12:52	40° 3,12' S	177° 49,12' E	1106	WSW 2	235,7	0,8	Profil	PR
SO191/028-4	29.01.07	13:34	40° 3,33' S	177° 48,83' E	1116	NW 10	216,1	1,7	Profil	PR
SO191/028-4	29.01.07	13:35	40° 3,34' S	177° 48,83' E	1115	NW 11	105,3	0,6	Profil	PR
SO191/029-1	29.01.07	14:01	39° 59,93' S	177° 49,64' E	1254	WNW 7	50,1	12,3	Vermessung	EM / PS
SO191/029-1	29.01.07	14:36	39° 55,24' S	177° 56,82' E	1177	NW 7	47,4	12,8	Vermessung	EM / PS
SO191/029-1	29.01.07	15:52	39° 42,97' S	178° 11,35' E	985	WSW 7	44,3	13,2	Vermessung	EM / PS
SO191/030-1	29.01.07	18:00	40° 0,97' S	177° 53,04' E	1230	WNW 16	229,3	1,1	Controlled Source Electro-Magnetic	CSEM
SO191/030-1	29.01.07	18:05	40° 0,97' S	177° 53,00' E	1223	WNW 15	251,6	1	Controlled Source Electro-Magnetic	CSEM
SO191/030-1	29.01.07	18:10	40° 0,97' S	177° 52,93' E	1223	WNW 13	204,9	0,3	Controlled Source Electro-Magnetic	CSEM
SO191/030-1	29.01.07	18:26	40° 0,95' S	177° 52,78' E	1203	WNW 14	224,5	1,1	Controlled Source Electro-Magnetic	CSEM
SO191/030-1	29.01.07	19:23	40° 0,97' S	177° 52,70' E	1199	W 11	31,1	0,4	Controlled Source Electro-Magnetic	CSEM
SO191/030-1	29.01.07	19:24	40° 0,96' S	177° 52,70' E	1197	W 12	286,6	0,7	Controlled Source Electro-Magnetic	CSEM
SO191/030-1	29.01.07	20:25	40° 1,19' S	177° 50,76' E	1174	W 9	274,2	1	Controlled Source Electro-Magnetic	CSEM
SO191/030-1	29.01.07	20:38	40° 1,22' S	177° 50,53' E	1587	W 10	138,3	0,5	Controlled Source Electro-Magnetic	CSEM
SO191/030-1	29.01.07	20:38	40° 1,22' S	177° 50,53' E	1587	W 10	138,3	0,5	Controlled Source Electro-Magnetic	CSEM
SO191/030-1	29.01.07	20:45	40° 1,21' S	177° 50,52' E	1587	W 12	93,8	0,6	Controlled Source Electro-Magnetic	CSEM
SO191/030-1	29.01.07	20:54	40° 1,20' S	177° 50,51' E	1086	W 11	181,8	0,5	Controlled Source Electro-Magnetic	CSEM
SO191/030-1	29.01.07	20:55	40° 1,20' S	177° 50,50' E	1087	W 11	279,1	1,1	Controlled Source Electro-Magnetic	CSEM
SO191/030-1	29.01.07	21:02	40° 1,24' S	177° 50,34' E	1087	WNW 11	323,4	0,6	Controlled Source Electro-Magnetic	CSEM
SO191/030-1	29.01.07	21:05	40° 1,23' S	177° 50,31' E	1094	W 12	14	0	Controlled Source Electro-Magnetic	CSEM
SO191/030-1	29.01.07	21:06	40° 1,23' S	177° 50,30' E	1098	W 11	319,9	0,5	Controlled Source Electro-Magnetic	CSEM
SO191/030-1	29.01.07	21:12	40° 1,22' S	177° 50,30' E	1098	W 11	15	0,6	Controlled Source Electro-Magnetic	CSEM
SO191/030-1	29.01.07	21:21	40° 1,22' S	177° 50,30' E	1093	W 10	79,4	0,5	Controlled Source Electro-Magnetic	CSEM
SO191/030-1	29.01.07	21:21	40° 1,22' S	177° 50,30' E	1093	W 10	79,4	0,5	Controlled Source Electro-Magnetic	CSEM
SO191/030-1	29.01.07	21:28	40° 1,27' S	177° 50,14' E	1104	WNW 12	313,8	0,3	Controlled Source Electro-Magnetic	CSEM
SO191/030-1	29.01.07	21:31	40° 1,26' S	177° 50,10' E	1105	W 11	299,4	0,4	Controlled Source Electro-Magnetic	CSEM
SO191/030-1	29.01.07	21:32	40° 1,26' S	177° 50,10' E	1106	W 12	62,1	0,8	Controlled Source Electro-Magnetic	CSEM
SO191/030-1	29.01.07	21:38	40° 1,26' S	177° 50,10' E	1588	W 11	9,3	0,5	Controlled Source Electro-Magnetic	CSEM
SO191/030-1	29.01.07	21:46	40° 1,26' S	177° 50,08' E	1107	W 10	252,3	0,2	Controlled Source Electro-Magnetic	CSEM

Station	Datum	UTC	PositionLat	PositionLon	Tiefe [m]	Windstärke [m/s]	Kurs [°]	v [kn]	Gerät	Geräte Kürzel
SO191/030-1	29.01.07	21:46	40° 1,26' S	177° 50,08' E	1107	W 10	252,3	0,2	Controlled Source Electro-Magnetic	CSEM
SO191/030-1	29.01.07	21:53	40° 1,27' S	177° 49,99' E	1110	WNW 11	36	0,1	Controlled Source Electro-Magnetic	CSEM
SO191/030-1	29.01.07	21:53	40° 1,27' S	177° 49,99' E	1110	WNW 11	36	0,1	Controlled Source Electro-Magnetic	CSEM
SO191/030-1	29.01.07	21:54	40° 1,27' S	177° 49,99' E	1107	W 9	136,6	0,1	Controlled Source Electro-Magnetic	CSEM
SO191/030-1	29.01.07	22:01	40° 1,28' S	177° 50,01' E	1106	W 12	86,5	0,3	Controlled Source Electro-Magnetic	CSEM
SO191/030-1	29.01.07	22:08	40° 1,30' S	177° 50,00' E	1101	W 12	197,2	1	Controlled Source Electro-Magnetic	CSEM
SO191/030-1	29.01.07	22:09	40° 1,32' S	177° 50,00' E	1101	W 12	177,6	1,2	Controlled Source Electro-Magnetic	CSEM
SO191/030-1	29.01.07	22:20	40° 1,27' S	177° 49,92' E	1116	W 11	185,9	0,5	Controlled Source Electro-Magnetic	CSEM
SO191/030-1	29.01.07	22:25	40° 1,29' S	177° 49,89' E	1118	W 11	48,2	0,3	Controlled Source Electro-Magnetic	CSEM
SO191/030-1	29.01.07	22:32	40° 1,29' S	177° 49,90' E	1122	W 12	185,2	0,3	Controlled Source Electro-Magnetic	CSEM
SO191/030-1	29.01.07	22:39	40° 1,29' S	177° 49,89' E	1113	W 13	217,9	0,6	Controlled Source Electro-Magnetic	CSEM
SO191/030-1	29.01.07	22:39	40° 1,29' S	177° 49,89' E	1113	W 13	217,9	0,6	Controlled Source Electro-Magnetic	CSEM
SO191/030-1	29.01.07	22:47	40° 1,30' S	177° 49,80' E	1130	WNW 11	278,8	0,8	Controlled Source Electro-Magnetic	CSEM
SO191/030-1	29.01.07	22:47	40° 1,30' S	177° 49,80' E	1130	WNW 11	278,8	0,8	Controlled Source Electro-Magnetic	CSEM
SO191/030-1	29.01.07	22:47	40° 1,30' S	177° 49,80' E	1130	WNW 11	278,8	0,8	Controlled Source Electro-Magnetic	CSEM
SO191/030-1	29.01.07	22:54	40° 1,29' S	177° 49,79' E	1135	W 13	45,3	0,2	Controlled Source Electro-Magnetic	CSEM
SO191/030-1	29.01.07	23:04	40° 1,24' S	177° 49,75' E	1157	W 12	47,8	0,8	Controlled Source Electro-Magnetic	CSEM
SO191/030-1	29.01.07	23:04	40° 1,24' S	177° 49,75' E	1157	W 12	47,8	0,8	Controlled Source Electro-Magnetic	CSEM
SO191/030-1	29.01.07	23:11	40° 1,22' S	177° 49,75' E	1170	W 11	101,6	0,5	Controlled Source Electro-Magnetic	CSEM
SO191/030-1	29.01.07	23:27	40° 1,30' S	177° 49,67' E	1587	W 12	348,3	0,2	Controlled Source Electro-Magnetic	CSEM
SO191/030-1	29.01.07	23:28	40° 1,31' S	177° 49,67' E	1585	WSW 11	133,9	0,6	Controlled Source Electro-Magnetic	CSEM
SO191/030-1	29.01.07	23:30	40° 1,32' S	177° 49,66' E	1587	W 13	89,7	0,4	Controlled Source Electro-Magnetic	CSEM
SO191/030-1	29.01.07	23:39	40° 1,33' S	177° 49,66' E	1585	WSW 11	223,3	0,9	Controlled Source Electro-Magnetic	CSEM
SO191/030-1	29.01.07	23:39	40° 1,33' S	177° 49,66' E	1585	WSW 11	223,3	0,9	Controlled Source Electro-Magnetic	CSEM
SO191/030-1	29.01.07	23:46	40° 1,31' S	177° 49,58' E	1162	WSW 12	209,8	0,3	Controlled Source Electro-Magnetic	CSEM
SO191/030-1	30.01.07	00:00	40° 1,31' S	177° 49,58' E	1586	WSW 14	75,6	0,6	Controlled Source Electro-Magnetic	CSEM
SO191/030-1	30.01.07	00:00	40° 1,31' S	177° 49,58' E	1586	WSW 14	75,6	0,6	Controlled Source Electro-Magnetic	CSEM
SO191/030-1	30.01.07	00:15	40° 1,31' S	177° 49,58' E	1172	W 12	33,4	1,3	Controlled Source Electro-Magnetic	CSEM
SO191/030-1	30.01.07	00:15	40° 1,31' S	177° 49,58' E	1172	W 12	33,4	1,3	Controlled Source Electro-Magnetic	CSEM
SO191/030-1	30.01.07	00:22	40° 1,31' S	177° 49,53' E	1168	WSW 13	103,4	0,2	Controlled Source Electro-Magnetic	CSEM
SO191/030-1	30.01.07	00:28	40° 1,33' S	177° 49,48' E	1172	WSW 14	43,2	1,2	Controlled Source Electro-Magnetic	CSEM
SO191/030-1	30.01.07	00:28	40° 1,33' S	177° 49,48' E	1172	WSW 14	43,2	1,2	Controlled Source Electro-Magnetic	CSEM
SO191/030-1	30.01.07	00:34	40° 1,34' S	177° 49,47' E	1589	WSW 14	49,5	0,7	Controlled Source Electro-Magnetic	CSEM
SO191/030-1	30.01.07	00:45	40° 1,31' S	177° 49,46' E	1177	WSW 12	97,8	0,3	Controlled Source Electro-Magnetic	CSEM
SO191/030-1	30.01.07	00:45	40° 1,31' S	177° 49,46' E	1177	WSW 12	97,8	0,3	Controlled Source Electro-Magnetic	CSEM
SO191/030-1	30.01.07	00:53	40° 1,33' S	177° 49,32' E	1174	WSW 12	243,8	1,1	Controlled Source Electro-Magnetic	CSEM
SO191/030-1	30.01.07	00:58	40° 1,36' S	177° 49,26' E	1175	WSW 13	36,2	0,6	Controlled Source Electro-Magnetic	CSEM
SO191/030-1	30.01.07	00:59	40° 1,36' S	177° 49,26' E	1585	W 14	329,1	0,5	Controlled Source Electro-Magnetic	CSEM
SO191/030-1	30.01.07	01:03	40° 1,35' S	177° 49,26' E	1587	W 15	351,2	0,7	Controlled Source Electro-Magnetic	CSEM
SO191/030-1	30.01.07	01:16	40° 1,35' S	177° 49,22' E	1175	WSW 13	253,5	0,3	Controlled Source Electro-Magnetic	CSEM
SO191/030-1	30.01.07	02:05	40° 1,42' S	177° 48,60' E	1190	WSW 12	289,3	0,8	Controlled Source Electro-Magnetic	CSEM
SO191/030-1	30.01.07	02:25	40° 1,43' S	177° 48,09' E	1210	WSW 11	334,4	0,9	Controlled Source Electro-Magnetic	CSEM

Station	Datum	UTC	PositionLat	PositionLon	Tiefe [m]	Windstärke [m/s]	Kurs [°]	v [kn]	Gerät	Geräte Kürzel
SO191/030-1	30.01.07	03:00	40° 0,67' S	177° 46,86' E	1317	SW 13	321,9	1,9	Controlled Source Electro-Magnetic	CSEM
SO191/031-1	30.01.07	03:55	40° 7,39' S	177° 50,61' E	1812	WSW 8	228,6	10,5	Vermessung	EM / PS
SO191/031-1	30.01.07	04:40	40° 14,78' S	177° 43,53' E	2037	WSW 5	213,9	12,8	Vermessung	EM / PS
SO191/031-1	30.01.07	06:25	40° 30,20' S	177° 22,84' E	1498	SW 4	224,2	12,1	Vermessung	EM / PS
SO191/031-1	30.01.07	07:28	40° 43,54' S	177° 22,90' E	1968	WSW 5	180,1	12,7	Vermessung	EM / PS
SO191/032-1	30.01.07	07:47	40° 46,39' S	177° 22,12' E	1986	WSW 6	212,6	1,6	Profil	PR
SO191/032-1	30.01.07	08:16	40° 47,48' S	177° 21,79' E	1990	WSW 4	193,8	2,5	Profil	PR
SO191/032-1	30.01.07	08:24	40° 47,82' S	177° 21,70' E	1993	WSW 4	190,1	2,8	Profil	PR
SO191/032-1	30.01.07	10:31	40° 48,76' S	177° 21,63' E	1995	NW 5	205,1	4,3	Profil	PR
SO191/032-1	30.01.07	12:38	40° 58,02' S	177° 15,69' E	2013	WNW 7	201,1	4,1	Profil	PR
SO191/032-1	30.01.07	12:40	40° 58,13' S	177° 15,62' E	2013	WNW 6	201,9	3,3	Profil	PR
SO191/032-1	30.01.07	13:04	40° 59,19' S	177° 15,43' E	2014	WNW 5	185,2	2,8	Profil	PR
SO191/032-1	30.01.07	13:07	40° 59,32' S	177° 15,42' E	2013	WNW 5	187,4	3	Profil	PR
SO191/033-1	30.01.07	13:07	40° 59,32' S	177° 15,42' E	2013	WNW 5	187,4	3	Vermessung	EM / PS
SO191/033-1	30.01.07	14:06	41° 6,06' S	177° 5,85' E	1573	NW 6	235,2	12,1	Vermessung	EM / PS
SO191/033-1	30.01.07	14:40	41° 9,71' S	176° 58,03' E	1738	NW 8	236,7	11,9	Vermessung	EM / PS
SO191/033-1	30.01.07	15:29	41° 13,94' S	176° 46,83' E	1225	NW 9	239,4	11,4	Vermessung	EM / PS
SO191/033-1	30.01.07	15:52	41° 16,88' S	176° 42,67' E	1838	NW 7	245,5	10,9	Vermessung	EM / PS
SO191/033-1	30.01.07	16:54	41° 20,98' S	176° 28,37' E	1147	NNW 7	247,1	10,7	Vermessung	EM / PS
SO191/033-1	30.01.07	19:00	41° 33,43' S	176° 0,38' E	1269	NE 6	239	11,9	Vermessung	EM / PS
SO191/033-1	30.01.07	19:46	41° 34,17' S	175° 48,14' E	932	NNW 9	266	11,9	Vermessung	EM / PS
SO191/033-1	30.01.07	20:37	41° 40,86' S	175° 37,34' E	882	NE 7	235,7	12,4	Vermessung	EM / PS
SO191/033-1	30.01.07	21:06	41° 43,10' S	175° 29,60' E	1035	NE 8	249,4	13,2	Vermessung	EM / PS
SO191/034-1	30.01.07	22:05	41° 52,29' S	175° 27,57' E	2271	NE 7	335,9	2,9	Profil	PR
SO191/034-1	30.01.07	22:32	41° 51,47' S	175° 27,09' E	2138	NE 3	329,2	1,8	Profil	PR
SO191/034-1	30.01.07	22:36	41° 51,33' S	175° 27,01' E	2116	N 2	335,6	2,6	Profil	PR
SO191/034-1	30.01.07	22:40	41° 51,12' S	175° 26,87' E	2091	NNW 2	330,2	4,6	Profil	PR
SO191/034-1	31.01.07	00:32	41° 44,37' S	175° 22,53' E	1265	SSE 2	335,5	3,7	Profil	PR
SO191/034-1	31.01.07	02:40	41° 42,49' S	175° 12,15' E	712	NNW 18	283,2	3,8	Profil	PR
SO191/034-1	31.01.07	02:46	41° 42,41' S	175° 11,83' E	790	NNW 18	294,6	1,1	Profil	PR
SO191/034-1	31.01.07	03:12	41° 41,99' S	175° 10,85' E	979	NNW 17	287,6	1,2	Profil	PR
SO191/034-1	31.01.07	03:12	41° 41,99' S	175° 10,85' E	979	NNW 17	287,6	1,2	Profil	PR
SO191/035-1	31.01.07	08:22	41° 40,29' S	175° 4,71' E	585	WSW 17	133,9	8	Vermessung	EM / PS
SO191/035-1	31.01.07	09:07	41° 45,07' S	175° 12,74' E	659	NNW 19	131,3	10,5	Vermessung	EM / PS
SO191/035-1	31.01.07	09:22	41° 47,29' S	175° 14,08' E	1501	NNW 14	151,1	9,7	Vermessung	EM / PS
SO191/035-1	31.01.07	09:56	41° 51,97' S	175° 18,31' E	2043	NNW 15	175,9	9,7	Vermessung	EM / PS
SO191/035-1	31.01.07	10:06	41° 52,64' S	175° 16,93' E	2355	NNW 14	262,8	8,4	Vermessung	EM / PS
SO191/035-1	31.01.07	10:45	41° 47,89' S	175° 12,61' E	1560	NNW 21	325	9,6	Vermessung	EM / PS
SO191/035-1	31.01.07	10:58	41° 46,05' S	175° 11,56' E	839	NW 18	332,5	9,8	Vermessung	EM / PS
SO191/035-1	31.01.07	11:42	41° 41,36' S	175° 3,82' E	919	NNW 17	259,5	9,3	Vermessung	EM / PS
SO191/035-1	31.01.07	11:49	41° 42,27' S	175° 2,74' E	853	NW 21	162,4	12,5	Vermessung	EM / PS
SO191/035-1	31.01.07	12:33	41° 46,89' S	175° 10,11' E	1282	NNW 17	181,4	7,8	Vermessung	EM / PS

Station	Datum	UTC	PositionLat	PositionLon	Tiefe [m]	Windstärke [m/s]	Kurs [°]	v [kn]	Gerät	Geräte Kürzel
SO191/035-1	31.01.07	12:43	41° 47,81' S	175° 9,18' E	1664	N 23	249,3	5,8	Vermessung	EM / PS
SO191/035-1	31.01.07	13:38	41° 42,58' S	175° 0,20' E	840	NNW 17	307	10,1	Vermessung	EM / PS
SO191/035-1	31.01.07	15:39	41° 26,04' S	174° 48,62' E	85	N 17	335	7,8	Vermessung	EM / PS

11.2 Station list Leg 2

SO 191#	Gear	No.	Location	Date 2007	Start Station Time (UTC)	Lat. [S]	Long. [E]	Depth (m)	Gear at bottom Time (UTC)	Lat. [S]	Long. [E]	Depth (m)	End Station Time (UTC)	Lat. [S]	Long. [E]	Depth (m)
37	POSIDONIA calibration	1	Rock Garden	03.02.	19:50	39:57.77	178:05.38	1200	22:03	39:57.9	178:5.3	1198	16:01	39:58.3	178:5.29	1173
38	DTS	5	Rock Garden	04.02.	4:02	40:4.62	178:6.21	1289	5:07	40:2.81	178:8.05	873	1:07	40:6.75	178:11.34	1221
39	CTD	2	Rock Garden	05.02.	2:03	40:3.307	178:11.517	644	2:51	40:3.354	178:11.579	644	3:07	40:3.336	178:11.599	648
40	CTD	3	Rock Garden	05.02.	4:44	40:1.997	178:9.384	673	5:30	40:1.991	178:9.354	666	5:48	40:1.988	178:9.359	657
41	OFOS	1	Rock Garden	05.02.	7:43	40:1.870	178:10.582	658	8:04	40:1.841	178:10.586	655	20:03	39:59.81	178:12.35	731
42	OFOS	2	Rock Garden	05.02.	21:05	39:58.117	178:13.234	897	22:39	39:58.811	178:14.570	1059	23:06	39:58.770	178:14.553	1055
43	TV-MUC	1	LM9	06.02.	1:50	40:1.064	177:51.374	1172	02:17*	40:1.072	177:51.443	1160	3:49	40:1.087	177:51.515	1151
44	CTD	4	LM9	06.02.	4:40	40:1.120	177:51.571	1151	5:25	40:1.124	177:51.601	1152	5:50	40:1.142	177:51.588	1152
45	TV-MUC	2	LM9	06.02.	6:15	40:1.168	177:51.539	1156	7:10	40:1.079	177:51.573	1159	7:48	40:1.066	177:51.595	1157
46	DTS	6	LM9	06.02.	8:45	40:4.3	177:46.9	1205					9:05	40:4.300	177:46.900	1175
47	CTD	5	LM9	06.02.	9:46	40:4.142	177:47.047	1184	10:31	40:4.144	177:47.063	1183	11:06	40:4.135	177:47.046	1181
48	DTS	6	LM9	06.02.	12:04	40:4.15	177:47.06	1183	13:00	40:2.52	177:49.07	1166	19:50	40:6.6	177:47.000	1307
49	CTD	6	LM9	06.02.	23:35	39:58.180	177:54.960	1060	00:24	39:58.184	177:54.946	1060	0:59	39:58.186	177:54.939	1060
50	GC (tube foil)	1	LM9	07.02.	1:45	40:1.090	177:51.558	1154	2:21	40:1.070	177:51.585	1053	2:51	40:1.064	177:51.593	1150
51	TV-BC	1	LM9	07.02.	4:26	40:1.065	177:51.570	1151	4:56	40:1.076	177:51.586	1151	5:27	40:1.068	177:51.583	1149
52-1	OFOS	3	LM9	07.02.	6:30	40:2.168	177:48.288	1165	6:57	40:2.161	177:48.273	1168	10:07	40:2.218	177:47.710	1170
52-2	OFOS	4	LM9	07.02.	10:59	40:2.09	177:50.40	1150	11:26	40:2.11	177:50.40	1152	13:57	40:1.86	177:50.46	1202
52-3	OFOS	5	LM9	07.02.	14:21	40:3.266	177:49.344	74	14:44	40:3.267	177:49.377	1099	17:20	40:3.176	177:48.800	1119
53	CTD	7	LM9	07.02.	17:44	40:2.176	177:47.610	1173	18:45	40:2.169	177:47.611	1168	19:19	40:2.168	177:47.607	1176
54	TV-MUC	3	LM9	07.02.	19:46	40:2.116	177:47.981	1175	21:47	40:2.152	177:48.047	1166	22:22	40:2.16	177:48.05	1164
55	CTD	8	LM9	07.02.	22:53	40:3.374	177:48.602	1123	23:42	40:3.370	177:48.620	1126	0:18	40:3.369	177:48.640	1122
56	TV-MUC	4	LM9	08.02.	0:18	40:3.371	177:48.634	1122	1:16	40:3.291	177:48.643	1122	1:52	40:3.287	177:48.696	1123

SO 191#	Gear	No.	Location	Date 2007	Start Station Time (UTC)	Lat. [S]	Long. [E]	Depth (m)	Gear at bottom Time (UTC)	Lat. [S]	Long. [E]	Depth (m)	End Station Time (UTC)	Lat. [S]	Long. [E]	Depth (m)
57	CTD	9	LM9	08.02.	2:29	40:1.894	177:50.556	1186	4:20	40:1.931	177:50.662	1176	4:41	40:1.931	177:50.668	1173
58	BWS	1	LM9	08.02.	6:20	40:3.371	177:48.616	1122	7:19	40:3.348	177:48.726	1121	8:10	40:3.33	177:48.77	1121
59	CTD	10	LM9	08.02.	8:36	40:2.156	177:47.989	1168	9:30	40:2.156	177:47.986	1168	10:15	40:2.162	177:48.011	1167
60	DTS	7	LM9	08.02.	11:05	40:4.2	177:45.3	1225	12:26	40:1.84	177:48.09	1186	20:00	39:58.9	177:54.6	1128
61	CTD	11	LM9	08.02.	21:19	40:2.851	177:48.112	1158	22:08	40:2.852	177:48.115	1154	22:46	40:2.839	177:48.106	1159
62	BWS	2	LM9	08.02.	23:38	40:3.216	177:49.288	1099	0:43	40:3.199	177:49.213	1096	1:50	40:3.214	177:49.291	1097
63	TV-G	1	LM9	09.02.	2:45	40:3.215	177:49.290	1096	3:34	40:3.199	177:49.181	1103	4:28	40:3.194	177:49.193	1098
64	GC (tube foil)	2	LM9	09.02.	5:10	40:1.083	177:51.579	1150	5:47	40:1.067	177:51.581	1160	6:17	40:1.000	177:51.500	1153
65	GC (tube foil)	3	LM9	09.02.	7:00	40:2.141	177:48.067	1169	7:43	40:2.160	177:48.056	1168	8:18	40:2.000	177:48.000	1166
66	TV-BC	2	LM9	09.02.	8:43	40:3.220	177:49.343	1099	9:18	40:3.223	177:49.293	1097	9:18	40:3.223	177:49.320	1098
67	TV-BC	3	LM9	09.02.	9:48	40:3.229	177:49.289	1097	10:10	40:3.206	177:49.293	1097	11:00	40:3.17	177:49.31	1102
68	CTD	12	LM9	09.02.	11:23	40:2.149	177:49.252	1212	12:03	40:2.162	177:49.266	1213	12:37	40:2.141	177:49.284	1215
69	CTD	13	LM9	09.02.	13:08	40:0.745	177:51.411	1243	14:02	40:0.713	177:51.435	1250	14:35	40:0.687	177:51.404	1230
70	CTD	14	LM9	09.02.	15:00	39:59.883	177:50.625	1218	15:57	39:59.872	177:50.650	1219	16:30	39:59.881	177:50.613	1216
71	CTD	15	LM9	09.02.	17:23	39:59.917	177:52.251	1132	18:01	39:59.909	177:52.269	1136	18:25	39:59.922	177:52.257	1136
72	CTD	16	LM9	09.02.	19:22	39:59.685	177:53.136	1213	20:00	39:59.683	177:53.133	1214	20:28	39:59.679	177:53.177	1214
73	TV-MUC	5	LM9	09.02.	21:53	40:3.183	177:48.120	1105	22:34	40:3.214	177:49.238	1101	23:16	40:3.288	177:49.047	1115
74	Multibeam	n/a	LM9	10.02.	0:06	40:6.06	177:52.49	1748	07:42	39:44.93	178:19.00	794	17:07	40:5.44	178:4.20	1516
75	TV-G	2	LM9	10.02.	19:51	40:3.195	177:49.116	1108	20:43	40:3.187	177:49.264	1089	21:08	40:3.195	177:49.261	1099
76	TV-G	3	LM9	10.02.	21:09	40:3.195	177:49.179	1092	23:25	40:3.191	177:49.232	1098	23:56	40:3.220	177:49.226	1100
77	FLUFO	1	LM9	11.02.	1:46	40:3.188	177:49.183	1100	2:37	40:3.214	177:49.216	1098	3:08	40:3.183	177:49.199	1001
78	TV-MUC	6	LM9	11.02.	3:52	40:1.349	177:1.350	1188	4:30	40:1.399	177:48.944	1182	5:02	40:1.40	177:48.94	1186
79	GC (tube foil)	4	LM9	11.02.	5:44	40:1.397	177:48.953	1180	6:13	40:1.401	177:48.941	1180	6:43	40:1.435	177:48.961	1176
80	OFOS	6	LM9 west	11.02.	7:23	40:2.248	177:48.490	1173	7:59	40:2.248	177:48.490	1175	12:45	40:2.17	177:47.54	1177
81	OFOS	7	LM9 west	11.02.	13:18	40:3.42	177:48.59	1125	14:04	40:3.42	177:48.48	1125	18:09	40:3.18	177:49.39	1101
82	CTD	17	LM9	11.02.	18:43	40:2.161	177:49.283	1210	19:19	40:2.177	177:49.266	1211	19:47	40:2.178	177:49.243	1211
83	TM	1	LM9	11.02.	20:14	40:2.042	177:49.344	1106	21:09	40:2.215	177:49.307	1215	21:44	40:2.249	177:49.214	1212
84	BWS	3	LM9	11.02.	22:39	40:3.185	177:49.177	1101	23:50	40:3.189	177:49.244	1100	00:45	40:3.189	177:49.199	1100
85	TV-MUC	7	LM9 south	12.02.	1:30	40:3.200	177:49.195	1102	2:08	40:3.182	177:49.191	1099	2:46	40:3.17	177:49.26	1100

SO 191#	Gear	No.	Location	Date 2007	Start Station Time (UTC)	Lat. [S]	Long. [E]	Depth (m)	Gear at bottom Time (UTC)	Lat. [S]	Long. [E]	Depth (m)	End Station Time (UTC)	Lat. [S]	Long. [E]	Depth (m)
86	TV-MUC	8	LM9 south	12.02.	2:54	40:3.183	177:49.170	1100	4:03	40:3.197	177:49.141	1104	4:37	40:3.19	177:49.20	1101
87	TV-G	4	LM9	12.02.	5:17	40:3.189	177:44.116	1106	6:09	40:3.198	177:49.231	1099	6:37	40:3.216	177:49.228	1098
88	TV-BC	4	LM9	12.02.	7:28	40:3.182	177:49.174	1102	8:20	40:3.22	177:49.25	1099	8:44	40:3.18	177:49.18	1099
89	CTD	18	LM9 south	12.02.	9:01	40:3.182	177:49.233	1096	10:15	40:3.177	177:49.237	1097	10:45	40:3.186	177:49.236	1099
90	CTD	19	LM9	12.02.	11:30	40:3.195	177:49.051	1110	12:02	40:3.170	177:49.057	1108	12:35	40:3.192	177:49.032	1114
91	CTD	20	LM9 south	12.02.	13:37	40:3.194	177:48.856	1119	14:12	40:3.211	177:48.871	1112	14:45	40:3.211	177:48.871	1115
92	CTD	21	LM9 south	12.02.	14:49	40:3.168	177:49.175	1114	16:15	40:3.186	177:49.149	1102	16:35	46:3.187	177:49.167	1101
93	GC (tube foil)	5	LM9 south	12.02.	16:36	40:3.196	177:49.175	1101	18:00	40:3.188	177:49.162	1100	18:52	40:3.184	177:49.145	1103
94	GC (tube foil)	6	LM9 south	12.02.	18:53	40:3.171	177:49.133	1104	19:40	40:3.183	177:49.182	1101	20:00	40:3.200	177:49.178	1100
95	GC (tube foil)	7	LM9 south	12.02.	20:08	40:3.166	177:49.181	1102	21:15	40:3.192	177:49.174	1100	21:45	40:3.212	177:49.261	1099
96	TV-BC	5	LM9 south	12.02.	21:46	40:3.215	177:49.243	1096	22:45	40:3.223	177:49.256	1100	23:13	40:3.211	177:49.238	1099
97	TV-BC	6	LM9 south	12.02.	23:38	40:3.184	177:49.199	1100	0:19	40:3.201	177:49.180	1099	0:49	40:3.20	177:49.21	1103
98	TV-BC	7	LM9	13.02.	0:58	40:3.202	177:49.184	1101	1:35	40:3.205	177:49.187	1099	2:08	40:3.207	177:49.157	1104
99	FLUFO (see stat. # 77)	1	LM9	13.02.	2:33	40:03:00	177:49:08	1108	2:37	40:3.018	177:49.105	1110	3:15	40:3.142	177:49.168	1102
100	CTD	22	LM9	13.02.	3:57	40:4.761	177:52.629	1743	4:40	40:4.809	177:52.630	1734	5:08	40:4.864	177:52.615	1736
101	TM (see # 83)	1	LM9	13.02.	5:54	40:02:06	177:49:08	1175	5:59	40:2.08	177:49.06	1185	6:54	40:2.08	177:49.00	1184
102	CTD	23	LM9	13.02.	6:55	40:2.257	177:49.211	1181	7:51	40:2.209	177:49.157	1215	8:22	40:2.169	177:49.217	1212
103	Multibeam	2	Wairarapa	13.02.	8:59	40:1.84	177:44.94	1299	20:23	41:2.67	176:29.95	640	6:40	41:46.90	175:24.14	1060
104	TV-MUC	9	Wairarapa	14.02.	6:14	41:46.924	175:24.142	1058	07:28	41:46.92	175:24.15	1061	7:53	41:46.916	175:24.134	1062
105	OFOS	8	Wairarapa	14.02.	8:26	41:47.671	175:22.143	1107	8:57	41:47.688	177:22.136	1107	12:30	41:47.277	175:23.102	1098
106	OFOS	9	Wairarapa	14.02.	12:54	41:46.911	175:23.82	1051	13:37	41:46.657	175:23.456	1042	15:48	41:47.037	175:24.346	1059
107	OFOS	10	Wairarapa	14.02.	16:37	41:46.438	175:25.326	1054	17:02	41:46.392	175:25.445	1060	18:26	41:46.529	175:25.873	1065
108	OFOS	11	Wairarapa	14.02.	19:23	41:43.287	175:26.978	821	19:45	41:43.300	175:26.975	822	22:07	41:43.309	175:27.322	890
109	TV-MUC	10	Wairarapa	14.02.	22:49	41:46.951	175:24.031	1060	0:01	41:46.959	175:24.277	1060	0:36	41:47.000	175:24.314	1063
110	TV-MUC	11	Wairarapa	15.02.	0:50	41:46.946	175:24.160	1061	1:45	41:96.995	175:24.226	1067	2:24	41:47.000	175:24.256	1057
111	GC (tube foil)	8	Wairarapa	15.02.	2:41	41:46.969	175:24.142	1063	3:32	41:46.955	175:24.184	1061	4:07	41:46.957	175:24.158	1068
112	GC (tube foil)	9	Wairarapa	15.02.	4:57	41:43.273	175:27.146	815	5:24	41:43.299	175:27.110	815	5:45	41:43.316	175:27.101	815

SO 191#	Gear	No.	Location	Date 2007	Start Station Time (UTC)	Lat. [S]	Long. [E]	Depth (m)	Gear at bottom Time (UTC)	Lat. [S]	Long. [E]	Depth (m)	End Station Time (UTC)	Lat. [S]	Long. [E]	Depth (m)
113	BC	8	Wairarapa	15.02.	5:46	41:43.308	175:27.072	815	6:39	41:43.305	175:27.087	814	7:00	41:43.290	175:27.066	817
114	BC	9	Wairarapa	15.02.	7:01	41:43.308	175:27.056	816	7:50	41:43.306	175:27.082	816	8:12	41:43.286	175:27.036	817
114-2	BC	10	Wairarapa	15.02.	8:28	41:43.289	175:27.023	818	8:50	41:43.303	175:27.097	814	9:17	41:43.284	175:27.069	815
115	CTD	24	Wairarapa	15.02.	9:25	41:43.299	175:27.068	816	10:00	41:43.299	175:27.084	815	10:20	41:43.301	175:27.086	815
116	CTD	25	Wairarapa	15.02.	12:00	41:43.333	175:27.006	823	12:30	41:43.338	175:27.008	828	12:58	41:43.348	175:27.012	822
117	CTD	26	Wairarapa	15.02.	14:06	41:43.270	175:27.083	816	14:40	41:43.272	175:27.098	816	15:06	41:43.279	175:27.121	818
118	CTD	27	Wairarapa	15.02.	16:28	41:43.227	175:27.177	815	17:00	41:43.229	175:27.184	816	17:20	41:43.229	175:27.179	815
119	CTD	28	Wairarapa	15.02.	19:30	41:43.291	175:27.127	814	19:58	41:43.319	175:27.120	815	20:23	41:43.315	175:27.111	815
120	GQ	1	Wairarapa - Tui Flare	15.02.	21:05	41:43.373	175:27.048	813	23:04	41:43.221	175:27.223	823	23:50	41:43.246	175:27.064	855
121	TV-MUC	12a	Wairarapa - Tui Flare	15.02.	0:45	41:46.907	175:24.193	1057	0:49	41:46.90	175:24.09	1054	0:45	41:46.911	175:23.922	1042
122	CTD	29	Wairarapa - Tui Flare	16.02.	19:2=:00	41:43.219	175:27.165	819	19:55	41:43.255	175:27.181	815	20:18	41:43.229	175:27.122	815
123	Parasound Flare Imaging	1	Wairarapa - Tui Flare	16.02.	20:44	41:43.22	175:26:89	831	23:57	41:46.93	175:24.05	1054	22:03	41:43:43	175:26:88	838
124	TV-MUC	12b	Wairarapa	16.02.	23:15	41:46.862	175:23.991	1048	23:56	41:46.908	175:24.024	1054	0:33	41:46.952	175:24.047	1046
125	GC (tube foil)	10	Wairarapa	17.02.	2:26	41:46.993	175:23.998	1038	3:20	41:46.920	175:24.001	1039	3:44	41:46.940	175:23.005	1042
126	GC (tube foil)	11	Wairarapa	17.02.	3:45	41:46.938	175:24.005	1042	4:22	41:46.931	175:24.000	1045	4:45	41:46.914	175:23.989	1040
127-1	BC	11	Wairarapa	17.02.	4:46	41:46.929	175:23.989	1040	5:41	41:46.927	175:24.005	1046	6:09	41:46.928	175:24.056	1053
127-2	BC	11a	Wairarapa	17.02.	6:31	41:46.930	175:24.002	1037	7:05	41:46.921	175:23.991	1037	7:31	41:46.907	175:23.971	1032
127-3	BC	11b	Wairarapa	17.02.	7:33	41:46.902	175:23.974	1036	8:12	41:46.950	175:24.042	1057	8:37	41:46.956	175:23.964	1038
128	CTD	30	Wairarapa - Tui Flare	17.02.	9:54	41:43.221	175:27.150	815	10:32	41:43.238	175:27.195	814	10:54	41:43.243	175:27.170	814
129	OFOS	12	Wairarapa - Tui Flare	17.02.	10:56	41:43.213	175:27.156	815	11:23	41:43.251	175:27:00	815	15:39	41:43.295	175:26.880	825
130	OFOS	13	Wairarapa - Tui Flare	17.02.	15:40	41:43.189	175:26.724	828	16:48	41:43.189	175:26.730	830	18:21	41:43.186	175:26.668	829
131	CTD	31	Wairarapa	17.02.	18:51	41:43.656	175:27.754	859	19:19	41:43.65	175:27.80	862	19:43	41:43.674	175:27.781	862
132	TM	2	Wairarapa - Tui Flare	17.02.	20:07	41:43.682	175:27.767	903	20:32	41:43.674	175:27.690	861	20:33	41:43.613	175:27.654	865
133	FLUFO	2	Wairarapa - North	17.02.	21:25	41:69.919	175:24.07	1056	23:23	41:46.825	175:24.181	1061	23:54	41:46.889	175:24.183	1059
134	GQ (see # 120)	1	Wairarapa - Tui Flare	18.02.	0:37	41:43.123	175:27.000	826	0:54	41:43.217	175:27.236	819	1:19	41:43.246	175:27.095	834
135	CTD	32	Wairarapa -	18.02.	1:40	41:43.225	175:27.139	815	2:11	41:43.220	175:27.155	816	2:37	41:43.231	175:27.161	815

SO 191#	Gear	No.	Location	Date 2007	Start Station Time (UTC)	Lat. [S]	Long. [E]	Depth (m)	Gear at bottom Time (UTC)	Lat. [S]	Long. [E]	Depth (m)	End Station Time (UTC)	Lat. [S]	Long. [E]	Depth (m)
			Tui Flare													
136	TM	3	Wairarapa - Tui Flare	18.02.	2:50	41:42.81	175:27.42	918	3:15	41:43.265	175:27.134	814	3:17	41:43.307	175:27.163	814
137	TV-MUC	13	Wairarapa - North	18.02.	4:13	41:46.858	175:23.926	1034	5:52	41:46.838	175:24.042	1041	6:27	41:46.812	175:24.032	1041
138	TV-G	5	Wairarapa - North	18.02.	6:28	41:46.821	175:24.046	1043	7:40	41:46.908	175:24.092	1047	8:05	41:46.962	175:24.181	1059
139	DTS	8	Wairarapa	18.02.	9:20	41:45.133	175:28.363	1063	13:57	41:46.88	175:24.20	1060	0:47	41:44.800	175:28.700	1105
140	CTD	33	Wairarapa - North	19.02.	1:28	41:46.895	175:24.051	1046	1:58	41:46.902	175:24.014	1043	2:27	41:46.948	175:23.922	1039
141	BIGO	1	Wairarapa - North	19.02.	2:37	41:46.897	175:23.998	1042	n/a	n/a	n/a	n/a	4:17	41:46.90	175:23.94	1037
142	BIGO	2	Wairarapa - North	19.02.	7:29	41:46.917	175:24.132	1064	8:49	41:46.850	175:24.290	1062	9:27	41:46.939	175:24.221	1060
143	CTD	34a	Wairarapa - Tui Flare	19.02.	10:55	41:43.246	175:27.089	813	11:25	41:43.270	175:27.036	814	12:31	41:43.29	175:27.07	813
143	CTD	34b	Wairarapa - Tui Flare	19.02.	11:59	41:43.307	175:17.064	814	12:04	41:43.301	175:27.073	814	12:12	41:43.302	175:27.074	814
144	CTD	35a	Wairarapa - Tui Flare	19.02.	14:01	41:43.338	175:26.995	820	14:33	41:43.347	175:27.020	821	14:40	41:43:34	175:27:02	820
144	CTD	35b	Wairarapa - Tui Flare	19.02.	14:57	41:43.334	175:27.078	815	15:04	41:43.330	175:27.074	820	15:24	41:43.34	175:27.04	818
145	CTD	36	Wairarapa - Tui Flare	19.02.	16:35	41:43.387	175:26.938	835	17:03	41:43.386	175:26.958	834	17:21	41:43.382	175:26.945	835
146	CTD	37	Wairarapa - Tui Flare	19.02.	17:46	41:43.418	175:26.884	840	18:10	41:43.411	175:26.889	837	18:33	41:43.416	175:26.893	839
147	CTD	38	Wairarapa - Tui Flare	19.02.	19:00	41:43.476	175:26.786	845	19:26	41:43.477	175:26.774	846	19:48	43.468	175:26.786	845
148	TV-G	6	Wairarapa - Tui Flare	19.02.	20:11	41:43.394	175:26.523	830	22:01	41:43.232	175:26.556	826	22:25	41:43.228	175:26.630	826
149	TV-G	7	Wairarapa - South	19.02.	23:11	41:47.314	175:24.421	1055	00:50 (20.02.)	41:47.317	175:24.487	1053	1:27	41:47.374	175:24.321	1055
150	FLUFO (see #133)	2	Wairarapa - North	20.02.	1:41	41:47.090	175:23.737	1054	02:03	41:47.06	175:23.79	1055	2:19	41:47.299	175:23.383	1062
151	TV-G	8	Wairarapa - Pukeko	20.02.	2:31	41:47.248	175:23.276	1059	4:08	41:47.101	175:23.520	1060	4:36	41:47.082	175:23.582	1040
152	GC (tube foil)	12	Wairarapa - North	20.02.	5:48	41:46.954	175:24.180	1067	6:17	41:46.956	175:24.182	1065	6:41	41:46.955	175:24.196	1060
153	GC (tube foil)	13	Wairarapa	20.02.	7:31	41:45.422	175:26.536	1052	7:55	41:45.444	175:26.536	1057	8:19	41:45.452	175:26.551	1053
154	OFOS	14	Wairarapa - Tui Flare	20.02.	9:00	41:43.519	175:26.643	859	9:26	41:43.528	175:26.645	861	14:11	41:43.635	175:27.098	854
155	OFOS	15	Wairarapa	20.02.	15:00	41:47.410	175:22.743	1086	15:28	41:47.450	175:22.759	1100	19:27	41:47.294	175:23.265	1081
156	TV-MUC	14	Wairarapa - North	20.02.	20:16	41:47.062	175:24.342	1058	21:05	41:46.915	175:24.228	1072	21:42	41:46.902	175:24.141	1063

SO 191#	Gear	No.	Location	Date 2007	Start Station Time (UTC)	Lat. [S]	Long. [E]	Depth (m)	Gear at bottom Time (UTC)	Lat. [S]	Long. [E]	Depth (m)	End Station Time (UTC)	Lat. [S]	Long. [E]	Depth (m)
			Tower													
157	TV-MUC	15	Wairarapa - North	20.02.	21:43	41:46.880	175:24.117	1058	22:11	41:46.851	175:24.107	1056	22:47	41:46.856	175:24.090	1052
158	TV-MUC	16	Wairarapa - North	20.02.	22:57	41:46.877	175:24.105	1053	23:51	41:46.850	175:24.192	1060	0:24	41:46.839	175:24.192	1060
159	TV-MUC	17	Wairarapa - North	21.02.	0:36	41:46.846	175:24.180	1059	1:27	41:46.915	175:24.256	1058	2:05	41:46.874	175:24.239	1058
160	TM (see #132)	2	Wairarapa - Tui Flare	21.02.	2:49	41:43.612	175:27.253	854	3:02	41:43:58	175:27:17	844	3:23	41:43.62	175:27.43	847
161	TM (see #136)	3	Wairarapa - Tui Flare	21.02.	3:23	41:43.571	175:27.362	847	03:45	41:43.21	175:26.84	830	3:50	41:43.20	175:26.78	830
162	BIGO (see #142)	2	Wairarapa - North	21.02.	5:00	41:46.676	175:23.620	1033	05:27	41:46.72	175:23.70	1032	5:47	41:47.316	175:23.468	1055
163	Multibeam survey	3	Wairarapa to LM 9	21.02.	6:24	41:51.05	175:23.54	2025	18:12	41:8.69	177:5.43'	1175	5:19	40:3.25	177:49.30	1096
164	TV-G	9	LM 9	22.02.	5:20	40:3.248	177:49.293	1097	6:33	40:3.147	177:49.239	1080	7:00	40:3.196	177:49.107	1110
165	TV-G	10	LM 9	22.02.	7:01	40:3.191	177:49.092	1109	8:28	40:3.185	177:49.264	1102	9:06	40:3.193	177:49.136	1112
166	OFOS	16	LM 9	22.02.	9:28	40:2.415	177:48.270	1169	10:21	40:2.429	177:48.264	1168	15:23	40:3.346	177:48.866	1116
167	OFOS	17	LM 9	22.02.	15:47	40:2.291	177:47.888	1161	16:18	40:2.297	177:47.887	1153	19:00	40:2.095	177:48.080	1165
168	GC (liner)	14	LM 9	22.02.	19:37	40:0.454	177:50.482	1196	20:40	40:0.454	177:50.842	1199	21:09	40:0.549	177:50.511	1201
169	GC (liner)	15	LM 9	22.02.	21:37	40:1.436	177:48.834	1181	22:13	40:1.415	177:49.011	1177	22:00	40:1.401	177:49.025	1179
170	GC (liner)	16	LM 9	22.02.	23:46	39:56.272	177:55.350	1156	0:19	39:56.262	177:55.350	1155	0:48	39:56.259	177:55.342	1150
171	CTD	39	LM 9	23.02.	2:02	40:3.192	177:49.141	1101	2:59	40:3.183	177:49.215	1111	3:46	41:3.173	177:49.211	1098
172	BWS	4	LM 9	23.02.	3:47	40:3.176	177:49.210	1099	4:51	40:3.185	177:49.236	1098	5:42	40:3.192	177:49.196	1099
173	TV-MUC	18	LM 9	23.02.	5:43	40:3.187	177:49.204	1098	7:00	40:3.197	177:49.190	1099	7:34	40:3.210	177:49.150	1101
174	TV-G	11	LM 9	23.02.	8:00	40:3.197	177:49.216	1098	8:36	40:3.194	177:49.239	1055	9:09	40:3.185	177:49.252	1104
175	OFOS	18	LM 3	23.02.	11:43	40:1.116	178:12.258	685	12:03	40:1.18	178:12.26	684	14:07	40:0.956	178:12.976	716
176	OFOS	19	LM 3	23.02.	14:41	39:58.718	178:13.385	798	15:04	39:58.748	178:13.401	795	18:06	39:58.328	178:14.366	902
177	TM	4	LM 9	23.02.	21:17	40:2.68	177:49.34	1149	21:45	40:2.719	177:49.927	1105	21:57	40:2.762	177:50.002	1106
178	TM	5	LM 9	23.02.	22:17	40:3.23	177:48.58	1134	22:39	40:3.251	177:49.139	1106	22:41	40:3.25	177:49.16	1102
179	FLUFO	3	LM 9	24.02.	00:29	40°03.15	177° 49.14	1105	01:28	40° 3.19	177° 49.19	1095	02:48	40° 3.02	177° 49.15	1112
180-1	OBMT	4		24.02.	04:26	39° 53.45	177° 56.59	1318	04:34	39° 53.49	177° 56.49	1314	05:28	39° 54.00	177° 56.30	1328
180-2	OBMT	5		24.02.	06:18	39° 49.69	177° 49.20						07:00	39° 48.12	177° 45.92	
180-3	OBMT	6		24.02.	07:52	39° 42.87	177° 36.26						08:10	39° 42.67	177° 35.01	314
181	Multibeam	4		24.02.	08:31	39° 43.21	177° 35.18	347	12:37	39:43:70	177:34:71	366	14:48	39° 59.29	177° 48.90	1348

11.3 Station list Leg 3

SO191#	Gear	No.	Location	Date 2007	Start Station Time (UTC)	Lat. [S]	Long. [E]	Depth (m)	Gear at bottom Time (UTC)	Lat. [S]	Long. [E]	Depth (m)	End Station Time (UTC)	Lat. [S]	Long. [E]	Depth (m)
182	MB Mapping	1		27.02.	10:17	39:42:28	177:35:60	291	13:00	39:52:17	177:58:60	1272	16:22	40:6:91	178:26:53	2851
183-1	OBMT	1		27.02.	16:23	40:6:98	178:26:64	2854	16:30	40:10:82	178:28:97	3041	18:39	40:11:72	178:28:12	3112
183-2	CTD	40		27.02.	18:54	40:11:82	178:28:04	3125	19:17	40:12:00	178:28:15	3136	19:48	40:12:27	178:28:11	3137
184	OBMT	2		27.02.	20:45	40:08:24	178:22:23	2462	20:55	40:05:07	178:18:19	2496	22:23	40:5:66	178:17:44	2479
185	OBMT	3		27.02.	23:24	40:1:62	178:10:29	630	23:37	39:59:42	178:07:41	970	0:39	39:59:79	178:6:85	556
186	TV-MUC	19	Bear's Paw	28.02.	2:32	40:03:14	177:49:24	1102	3:39	40:3:18	177:49:20	1078	4:10	40:03:20	177:49:17	0
187	TV-MUC	20	Bear's Paw	28.02.	4:30	40:3:12	177:49:22	1101	5:50	40:3:17	177:49:12	1118	6:23	40:03:17	177:49:14	1107
188	BIGO Depl.	3	Bear's Paw	28.02.	9:28	40:3:20	177:49:12	1111	10:05	40:3:18	177:49:14	1108	10:35	40:3:23	177:49:18	1102
189	CTD	41	Bear's Paw	28.02.	15:52	40:3:23	177:49:18	1104	12:11	40:3:22	177:49:18	1100	14:40	40:3:28	177:49:19	1107
190	CTD	42	Bear's Paw	28.02.	14:41	40:3:28	177:49:098	1107	16:30	40:03:30	177:49:16	1112	18:12	40:03:33	177:49:24	1105
191	CTD	43	Bear's Paw	28.02.	18:13	40:03:199	177:49:13	1105	20:00	40:03:16	177:49:18	1112	20:53	40:03:34	177:49:37	1108
192	ROV	1	Bear's Paw	28.02.	21:15	40:03:20	177:49:12	1108	23:03	40:03:8	177:49:20	1112	2:12	40:03:40	177:48:98	1110
193	GC	17	Bear's Paw	01.03.	2:13	40:03:213	177:49:179	1113	2:56	40:03:195	177:49:166	1103	3:28	40:03:194	177:49:17	1103
194	GC	18	Bear's Paw	01.03.	3:29	40:03:19	177:49:170	1101	4:02	40:03:195	177:49:188	1104	4:33	40:03:191	177:49:180	1102
195	GC	19	Bear's Paw	01.03.	4:34	40:03:190	177:49:180	1103	5:36	40:03:193	177:49:178	1104	6:09	40:03:21	177:49:18	1102
196	GC	20	Bear's Paw	01.03.	6:10	40:03:192	177:49:186	1103	6:50	40:03:193	177:49:175	1102	7:22	40:03:191	177:49:182	1104
197	TV-MUC	21	Bear's Paw	01.03.	7:23	40:03:17	177:49:17	1104	8:42	40:03:168	177:49:169	1102	9:26	40:03:172	177:49:148	1103
198	TV-MUC	22	Bear's Paw	01.03.	9:27	40:03:17	177:49:16	1104	10:19	40:03:173	177:49:258	1102	11:08	40:03:195	177:49:261	1100
199	OFOS	20	Builder's Pencil	01.03.	17:00	39:32:019	178:20:410	825	19:47	39:31:013	178:19:747	802	20:08	39:31:013	178:19:728	803
200	CTD	44	Builder's Pencil	01.03.	20:35	39:32:64	178:19:91	796	20:58	39:32:64	178:19:91	795	21:20	39:32:64	178:19:90	797
201	CTD	45	Bear's Paw	02.03.	2:35	40:03:211	177:49:223	1102	2:53	40:03:20	177:49:22	1104	3:19	40:03:20	177:49:20	1102
202	FLUFO Retr.	3	Bear's Paw	02.03.	3:20	40:03:20	177:49:20	1100	3:45	40:03:29	177:49:21	1101	4:00	40:03:26	177:49:21	1101
203	TV-MUC	23	Bear's Paw	02.03.	4:01	40:03:27	177:49:22	1102	6:38	40:03:174	177:49:318	1104	7:08	40:03:138	177:49:341	1102
204	TV-MUC	24	Bear's Paw	02.03.	7:09	40:03:167	177:49:171	1102	8:04	40:03:167	177:49:171	1102	9:22	40:2:76	177:49:49	1123
205	MB Mapping			02.03.	11:00	40:09:59	177:56:56	1964	15:47	40:07:59	177:59:47	1480	18:13	40:12:53	178:20:07	2743
206	ROV	2	Bear's Paw	02.03.	20:19	40:02:01	178:09:61	670	21:01	40:1:87	178:9:68	659	22:48	40:1:91	178:9:69	660
207	BIGO Retr.	3	Bear's Paw	03.03.	1:03	40:02:976	177:50:535	1151	1:27	40:3:01	177:49:22	1117	1:45	40:3:21	177:49:14	1104
208	TV-MUC	25	Bear's Paw	03.03.	6:35	40:03:129	177:49:155	1104	7:13	40:3:113	177:49:176	1102	8:12	40:3:13	177:49:24	1098

SO191#	Gear	No.	Location	Date 2007	Start Station Time (UTC)	Lat. [S]	Long. [E]	Depth (m)	Gear at bottom Time (UTC)	Lat. [S]	Long. [E]	Depth (m)	End Station Time (UTC)	Lat. [S]	Long. [E]	Depth (m)
209	GQ Depl.	2	Rock Garden	03.03.	10:24	40:01.840	178:09.543	657	11:24	40:1.940	178:9.623	661	11:45	40:1.93	178:9.64	661
210	CTD	46	Rock Garden	03.03.	12:41	40:01.96	178:09.64	662	13:16	40:1.939	178:9.654	662	13:36	40:1.944	178:9.661	661
211	CTD	47	Rock Garden	03.03.	13:37	40:01.95	178:09.66	661	16:46	40:1:96	178:9:68	662	18:29	40:01.999	178:09.632	666
212	ROV	3	Rock Garden	03.03.	18:30	40:02.00	178:09.63	667	20:20	40.01:99	178.09:31	662	21:06	40:02:53	178:09:22	932
213	ROV	4	Rock Garden	03.03.	22:23	39:58.59	178:14.22	915	4:48	39.58:61	178.14:21	915	2:01	39:58.622	178:14.18	908
214	TV-MUC	26	Rock Garden LM3	04.03.	3:00	40:02.06	1780:9.45	694	3:33	40:1.97	178:9.46	660	5:34	40:1.368	178:9.631	663
215	TV-MUC	27	Rock Garden LM3	05.03.	5:35	40:01.948	178:09.624	663	6:45	40:2.07	178:9.65	661	6:46	40:1.973	178:9.644	664
216	TV-MUC	28	Rock Garden LM3	04.03.	6:47	40:01.986	1780:9.642	665	7:15	40:1.98	178:9.65	664	7:57	40:1.516	178:9.645	662
217	GC	21	Rock Garden LM3	04.03.	7:58	40:01.920	178:09.641	664	8:59	40:1.92	178:9.65	676	9:16	40:1.921	178:9.673	669
218	TV-G	12	Moa-corals	04.03.	12:13	40:03.326	178:40.891	1110	12:57	40:03.27	178:48.77	1107	13:27	40:03.330	177:48.807	1115
219	MB Mapping		Rock Garden		16:31	0116:02.33	10:09.44	791	18:42	16:17.17	10:21.43	2874	19:30	40:22.78	178:17.91	2892
220	GQ Retr.	2	Rock Garden	04.03.	22:14	40:02.120	178:09.631	700	22:27	40:2.08	178:9.45	700	22:41	40:02.10	178:09.66	681
221	TV-MUC	29	Rock Garden	04.03.	22:42	40:02.11	178:09.65	690	1:40	40:1.91	178:9.64	661	2:02	40:1.949	178:9.637	662
222	TV-MUC	30		05.03.	2:03	40:01.979	178:09.612	662	2:41	40:1.91	178:9.66	661	3:07	16:01.92	10:09.65	664
223	FLUFO Depl.	4	Rock Garden	05.03.	6:10	40:01.97	178:09.65	664	6:45	40:1.92	178:9.64	661	7:06	40:01.924	178:09.656	663
224	TV-G	13	Rock Garden	05.03.	7:30	40:01.281	178:10.464	615	8:12	40:1.25	178:10.47	610	8:35	40:1.246	178:10.463	610
225	ROV	5	LM3	05.03.	9:35	39:50.599	178:14.179	908	10:33	39:58.55	178:14.18	907	12:57	39:58.653	178:14.087	904
226	CTD	48	Moa	05.03.	15:00	40:03.26	177:48.70	1124	16:12	40:03.23	177:48.71	1120	16:36	40:03.264	177:48.71	1123
227	TV-G	14	Moa	05.03.	16:37	40:03.242	177:48.736	1124	17:57	40:03.28	177:48.75	1120	19:00	40:03.2921	177:48.774	1119
228	BIGO Depl.	4	Rock Garden	05.03.	22:34	40:01.983	178:09.666	663	23:15	40:01.91	178:09.65	659	23:35	40:01.887	178:09.650	659
229	TV-G	15	Rock Garden	06.03.	0:05	40:01.806	178:11.45	660	0:36	40:01.78	178:11.40	660	0:59	40:1.76	178:11.37	660
230	TV-G	16	Rock Garden	06.03.	1:12	40:01.576	178:11.033	653	1:35	40:01.58	178:11.01	655	1:57	40:01.614	178:11.004	657
231	TV-MUC	31	Kaka	06.03.	3:42	40:02.174	177:48.127	1165	4:41	40:02.14	177:47.96	1170	5:16	40:02.14	177:48.14	1170

SO191#	Gear	No.	Location	Date 2007	Start Station Time (UTC)	Lat. [S]	Long. [E]	Depth (m)	Gear at bottom Time (UTC)	Lat. [S]	Long. [E]	Depth (m)	End Station Time (UTC)	Lat. [S]	Long. [E]	Depth (m)
232	TV-MUC	32	Kaka	06.03.	5:17	40:02.1421	177:48.143	1168	6:24	40:02.15	177:47.95	1172	7:00	40:02.151	177:47.983	1169
233	GC	22	LM9 reference	06.03.	7:33	40:01.41	177:41.94	1186	8:05	40:1.40	177:48.94	1180	8:00	40:01.4	177:48.96	1189
234	GC	23	Moa	06.03.	9:15	40:03.295	177:48.651	1125	9:47	40:03.30	177:48.65	1125	10:09	40:03.296	177:48.649	1125
235	CTD	49	LM3	06.03.	12:20	39:58:68	178.14:326	944	14:20	39:58.61	178:14.24	920	16:00	39:58:536	178.14:20	907
236	CTD	50	Rock Garden	06.03.	17:15	40:1.99	178:9.76	661	17:38	40:1.97	178:9.76	660	17:59	40:1.98	178:9.77	662
237	ROV	6	Faure site	06.03.	18:39	40:01.904	178:09.745	660	19:05	40:01.91	178:09.75	662	22:12	40:01.961	178:09.754	660
238	TV-G	17	Rock Garden LM3	06.03.	23:18	39:58.65	178:14.13	907	0:31	39:58.58	178:14.16	907	1:01	39:58.619	178:14.158	908
239	TV-G	18	Rock Garden	07.03.	1:57	40:03.11	178:13.86	902	2:46	40:03.09	178:13.83	891	2:48	40:3.08	178:13.83	882
240	FLUFO Retr..	4		07.03.	3:20	40:2.26	178:9.63	741	3:24	40:02.26	178:09.63	743	3:50	40:2.15	178:9.73	682
241	TV-MUC	33	Kaka	07.03.	5:49	40:02.225	177:48.077	1169	6:33	40:02.14	177:47.97	1172	7:06	40	177	1169
242	TV-MUC	34	Kaka	07.03.	7:28	40:02.51	177.:47.948	1169	8:04	40:02.14	177:47.91	1175	8:36	40:02.150	177:47.946	1172
243	GC	24	Kaka	07.03.	8:39	40:02.15	177:47.95	1167	9:43	40:02.16	177:48.05	1166	10:07	40:02.159	177:48.07	1164
244	GC	25	LM9	07.03.	10:44	40:01.09	177:51.60	1155	11:12	40:01.07	177:51.58	1155	11:42	40:01:08	177:51:59	1153
245	CTD	51	LM3	07.03.	13:33	39:58.656	178:14.2	916	14:48	39:58.58	178:14.17	907	16:02	39:58.62	178:14.15	907
246	ROV	7	Rock Garden LM3	07.03.	10:03	39:58.62	178:14.14	907	17:56	39:58.60	178:14.7	909	18:18	39:58.60	178:14.18	908
247	GQ Depl.	3	Faure site	07.03.	22:25	40:1.97	178:9.784	659	23:06	40:1.99	178:09.61	664	23:26	40:1.990	178:09.61	666
248	FLUFO Depl.	5	Faure site	08.03.	1:23	40:01.991	178:09.64	666	2:14	40:1.88	178:09.62	658	2:35	40:01.915	178:09.68	660
249	BIGO Retr.	4	Rock Garden	08.03.	2:35	40:2.05	178:09.68	660	3:00	40:02.05	178:09.90	667	3:30	40:2.03	178:9.43	696
250	GC	26	Rock Garden	08.03.	4:42	40:01.075	178:36.449	1398	5:11	40:00.91	178:16.46	1412	5:48	40:00.92	178:16.46	1422
251	GC	27	Rock Garden	08.03.	6:20	39:58.879	178:19.449	976	6:45	39:59.88	178:14.45	982	7:16	39:59.87	178:14.44	975
252	GC	28	Rock Garden	08.03.	7:47	39:59.307	178:13.429	907	8:19	39:59.36	178:13.44	904	8:47	39:59.350	178:13.452	908
253	GC	29	Rock Garden	08.03.	9:20	39:58.132	178:11.00	1006	9:45	39:58.13	178:11.00	1016	10:13	39:58.13	178:11.01	1006
254	multibeam				11:03	39:53.53	178:19.21	1612	15:41	40:17.35	178:22.99	2881	19:34	40:12.59	177:54.33	2056
255-1	TM	4	Bear's Paw	08.03.	20:32	40:02.944	177:49.938	1107	21:17	40:3.11	177:49.27	1109	21:35	40:3.35	177:49.12	1110
255-2	TM		Bear's Paw	08.03.	21:44	40:3.25	177:49.13	1107	22:14	40:3.24	177:49.12	1108	22:38	40:3.26	177:49.17	1104
256	CTD	53	Bear's Paw	08.03.	23:00	40:02.68	177:49.89	1106	0:10	40:02.94	177:49.76	1097	0:33	40:02.98	177:49.81	1102

SO191#	Gear	No.	Location	Date 2007	Start Station Time (UTC)	Lat. [S]	Long. [E]	Depth (m)	Gear at bottom Time (UTC)	Lat. [S]	Long. [E]	Depth (m)	End Station Time (UTC)	Lat. [S]	Long. [E]	Depth (m)
256 #1	TM	5	Bear's Paw	08.03.	23:00	40:02.68	177:49.89	1106	23:04	40.2:67	177:49:87	1106	23:35	40:02.88	177:49.82	1100
256 #2	CTD	54	Bear's Paw	08.03.	23:36	40:2.88	177:49.81	1101	0:10	40:02.94	177:49.76	1097	0:33	40:02.976	177:49.809	1102
257	GQ Retr.	3			2:09	40:02.24	178:09.19	734	2:23	40.2:21	178.9:34	715	2:36	40:02.22	178:09.52	736
258	TV-MUC	35	Rock Garden	09.03.	3:09	40:02.05	177:09.57	679	4:02	40:01.89	178:09.65	659	4:27	40:01.94	177:09.58	660
259	TV-MUC	36	LM3	09.03.	4:28	40:02.008	178:09.613	659	5:33	40:01.90	178:09.65	659	5:57	40:01.90	178:09.71	660
260	TV-MUC	37	LM3	09.03.	5:58	40:01.896	178:09.71	661	6:27	40:01.89	178:09.71	661	6:51	40:01.888	178:09.718	661
261	TV-MUC	38	Kaka	09.03.	8:23	40:02.17	177:47:98	1175	9:25	40:02.12	177:47.96	1171	9:55	40:02.12	177:48.93	1165
262	TV-MUC	39	Kaka	09.03.	9:56	40:02.128	177:47.927	1169	10:50	40:02.15	177:47.95	1167	11:24	40:02.12	177:47.884	1169
263	CTD	55	Faure site		13:47	40:00.994	178:11.072	584	14:55	40.0:93	178.11:21	601	15:50	40:00.938	178:11.298	631
264	CTD	56	Faure site	09.03.	16:32	40:01.947	178:09.636	661	16:59	40:01.95	178:09.63	662	17:18	40.1:95	178.9:62	661
265	FLUFO Retr.	5	Faure site	09.03.	19:00	40:01.98	178:09.41	668	19:02	40:01.98	178:09.42	661	19:28	40:02.07	178:09.48	697
266	GC	26	Rock Garden	09.03.	20:43	40:01.933	178:09.641	662	20:59	40:01.94	178:09.65	662	21:14	40:1.937	178:09.650	662
267	GC	27	Rock Garden	09.03.	21:15	40:01.938	178:09.649	662	21:44	40:01.938	178:09.65	662	21:58	40:01.938	178:09.64	662
268	GC	28	Rock Garden	09.03.	21:59	40:01.939	178:09.656	662	22:28	40:01.94	178:09.65	662	22:42	40:01.943	178:09.653	663
269	MB Mapping		underway	10.03.	0:47	40:15.68	177:43.44	1990	5:53	41.3:65	177.31:31	2459	10:58	41:17.48	176:33.18	742
270	CTD	57	Uruti Ridge	10.03.	11:12	41:17.464	176:33.093	750	11:34	41:17.37	176:33.15	753	11:51	41:17.252	176:33.190	808
271	MB Mapping		underway	10.03.	11:52	41:17.22	176:33.22	817	16:24	41.36:97	176.4:68	1922	19:42	41:46.98	175:23.99	1044
272	OFOS	21	Pukeko	10.03.	20:06	41:46.941	175:23.324	1034	20:31	41:46.93	175:23.31	1033	23:14	41:47.02	175:23.59	1055
273	TV-MUC	40	North Tower	11.03.	23:15	41:47.03	175:24.61	1053	0:48	41:46.986	175:24.251	1059	1:15	41:46.985	175:24.265	1061
274	TV-MUC	41	North Tower	11.03.	1:16	41:46.980	175:24.299	1061	2:04	41:46.946	175:24.114	1060	2:35	41:46.939	175:24.072	1048
275	CTD	58	Wairarapa	11.03.	3:23	41:50.384	175:21.174	1858	4:00	41:50.37	175:21.22	1862	4:37	41:50.386	175:21.228	1856
276	BIGO Depl.	5	North Tower	11.03.	5:51	41:46.994	175:21.289	1057	7:17	41:46.919	175:24.097	1059	7:48	41:46.927	175:24.104	1054
277	FLUFO Depl.	6	North Tower	11.03.	7:49	41:46.999	175:24.287	1052	9:43	41:46.900	175:24.099	1048	10:09	41:46.90	175:24.11	1053
278	GC	32	Wairarapa	11.03.	10:49	41:47.755	175:24.108	1098	11:29	41:47.755	175:24.096	1094	11:52	41:47.74	175:24.10	1096
279	GC	33	Wairarapa	11.03.	11:53	41:47.73	175:24.10	1069	13:00	41:47.458	175:24.398	1068	13:24	41:47.45	175:24.37	1067
280	CTD	59	Wairarapa	11.03.	14:11	41:45.41	175:25.46	1038	14:36	41:45.39	175:25.51	1034	14:57	41:45.385	175:25.490	1032
281	CTD	60	Wairarapa	11.03.	16:21	41:42.33	1175:28.00 0	1065	16:44	41:42.35	175:28.02	1066	17:07	41:42.371	175:28.00	1065

SO191#	Gear	No.	Location	Date 2007	Start Station Time (UTC)	Lat. [S]	Long. [E]	Depth (m)	Gear at bottom Time (UTC)	Lat. [S]	Long. [E]	Depth (m)	End Station Time (UTC)	Lat. [S]	Long. [E]	Depth (m)
282	GC	34	Wairarapa	11.03.	18:14	41:47.282	175:24.652	1053	18:40	41:47.26	175:24.61	1053	19:08	47:47.262	175:24.63	1056
283	GC	35	Wairarapa	11.03.	19:09	47:47.27	175:24.63	1056	20:11	41:47.18	175:24.69	1051	20:41	47:47.17	175:24.69	1051
284	GC	36	Wairarapa	11.03.	20:53	47:57.98	175:24.93	1050	21:34	41:46.99	175:24.89	1050	22:05	47:47.057	175:24.853	1053
285	GC	37	Wairarapa North	11.03.	22:24	41:46.94	175:24.14	1061	23:11	41:46.96	175:24.19	1062	23:42	41:46.96	175:24.16	1061
286	GC	38	Wairarapa North	12.03.	23:43	41:46.96	175:24.16	1061	0:38	41:46.97	175:24.27	1060	1:03	432	175:24.29	1059
287	GC	39	Wairarapa North	12.03.	1:04	41:46.94	175:24.29	1061	2:08	41:46.96	175:24.23	1060	2:33	41:46.94	175:24.24	1060
288	Profiler	1	North T	12.03.	3:00	41:46.98	175:24.27	1060	6:21	41:46.98	175:24.28	1066	6:49	41:43.980	175:24.282	1063
289	TV-MUC	42	North T	12.03.	6:50	41:47.020	175:24.223	1065	8:17	41:46.93	175:24.13	1059	8:51	41:46.953	175:24.105	1059
290	TV-MUC	43	North T	12.03.	8:52	41:46.95	175:24.10	1055	9:41	41:46.94	175:24.20	1059	10:08	41:46.983	175:24.268	1059
291	TV-MUC	44	North T.	12.03.	10:10	41:46.98	175:24.27	1059	11:00	41:46.93	175:24.16	1061	11:28	41:46.91	175:24.14	1058
292	OFOS	22	Piwakaw.	12.03.	12:06	41:47.79	175:22.36	1113	12:38	41:47.76	175:22.32	1111	14:31	41:47.624	175: 266	1103
293	CTD	61	Wairarapa	12.03.	16:01	41:53.930	175:18.612	2125	17:05	41:53.90	175:18.63	2133	17:45	41:53.906	175:18.630	2126
294	CTD	62		12.03.	18:42	41:57.443	178:16.103	2151	19:27	41:57.41	1175:16.12	2147	20:11	41:57.42	175:16.11	2151
295	GC	40	Wairarapa North	12.03.	22:00	41:47.590	175:24.255	1083	22:29	41:47.59	175:24.25	1083	22:55	41:47.594	175:24.247	1084
296	GC	41	Wairarapa North	12.03.	22:56	41:47.60	175:24.25	1082	23:43	41:47.38	175:24.47	1058	0:07	41:47.43	175:14.52	1063
297	Profiler Retr.	1	North T	14.03.	18:45	41:46.942	175:24.528	1057	19:00	41:46.94	175:24.53	1052	19:19	41:46.92	175:24.32	1059
298	Bigo Retr.	5	North T	14.03.	19:19	41:46.92	175:24.32	1059	19:29	41:46.93	175:24.35	1056	20:00	41:46.95	175:24.18	1059
299	FLUFO Retr.	6	North T	14.03.	20:01	41:46.948	175:24.306	1059	20:06	41:46.95	175:24.29	1057	20:36	41:46.95	175:24.27	1058
300	CTD	63	Wairarapa	14.03.	22:04	41:47.519	175:75.536	1173	22:30	14:47.52	175:25.51	1147	22:55	41:47.58	175:25.52	1183
301	CTD	64	Cook St. (Rocky)	14.03.	1:01	41:00.887	175:13.259	2529	1:49	42:00.86	175:13.18	2532	2:38	42:00.85	175:13.13	2529
302	GC	42	Wairarapa South	15.03.	4:19	41:47.319	175:24.56	1055	4:45	41:47.33	175:24.54	1053	5:09	41:47.327	175:24.547	1055
303	CTD	65	Wairarapa	15.03.	5:44	41:48.661	175:22.63	1403	6:13	41:48.66	175:22.60	1409	6:41	41:48.659	175:22.588	1408
304	GC	43	Wairarapa	15.03.	7:16	41:46.29	175:25.66	1055	7:50	41:46.34	175:25.58	1054	8:21	41:46.315	175:25.560	1055
305	GC	44	Wairarapa	15.03.	8:42	41:46.699	175:25.223	1050	9:12	41:46.69	175:25.23	1051	9:40	41:46.689	175:25.25	1051
306	GC	45	Wairarapa	16.03.	10:06	41:47.36	175:29.505	1058	10:36	41:47.35	175:24.51	1055	11:15	41:47.24	175:24.81	1051
307	BIGO Depl.	6	Wairarapa Takahae	16.03.	0:05	41:46.83	175:25.13	1052	1:31	41:46.74	175:25.14	1051	1:58	41:46.722	175:25.084	1058
308	Profiler	2	Wairarapa Takahae	16.03.	1:59	41:46.72	175:25.06	1053	4:57	41:36.34	175:25.60	1055	7:42	41:46.47	175:25.70	1056

SO191#	Gear	No.	Location	Date 2007	Start Station Time (UTC)	Lat. [S]	Long. [E]	Depth (m)	Gear at bottom Time (UTC)	Lat. [S]	Long. [E]	Depth (m)	End Station Time (UTC)	Lat. [S]	Long. [E]	Depth (m)
308 2nd try	Profiler Depl..	2	Wairarapa Takahae	16.03.	6:18	41:46.356	175:25.600	1054	7:12	41:46.31	175:25.75	1058	7:42	41:46.473	175:25.688	1056
309	TV-MUC	45	Wairarapa Takahae	16.03.	7:43	41:46.47	175:25.699	1056	8:42	41:46.42	175:25.62	1054	10:57	41:46.34	175:25.68	1056
309 2nd try	TV-MUC	46	Wairarapa Takahae	16.03.	9:12	41:46.417	175:25.465	1054	10:29	41:46.35	175:25.69	1057	10:52	41:46.336	175:25.681	1056
310	CTD	66	Wairarapa	16.03.	11:58	41:44.39	175:26.205	920	12:23	41:44.43	175:26.16	928	12:49	41:44.474	175:26.181	932
311	CTD	67	Wairarapa	16.03.	13:43	41:46.18	175:24.81	1046	14:42	41:46.18	175:24.81	1052	15:05	41:46.19	175:24.82	1045
312	CTD	68	Wairarapa	16.03.	17:11	41:41.91	175:28.54	914	17:29	41:41.94	175:28.53	925	17:48	41:41.78	175:28.56	869
313	Profiler Retr.	2	Takahae	17.03.	17:52	41:46.138	175:26.26	1066	17:58	41:46.14	175:26.28	1067	18:35	41:43.23	175:25.76	1057
314	BIGO Retr.	6	Takahae	17.03.	18:36	41:46.069	175:25.940	1059	18:53	41:46.08	175:25.91	1059	19:24	41:46.74	175:25.10	1050
315	TV-MUC	47	Takahae	17.03.	19:59	41:46.285	175:25.785	1058	20:37	41:46.32	175:25.69	1057	21:10	41:46.21	175:25.54	1053
316	TV-G	19	Uruti	18.03.	3:30	41:17.46	176:33.04	728	5:05	41:17.53	176:32.87	756	5:33	41:17.45	176:32.88	762
317	Multi-beam			18.03.	6:33	41:14.98	176:34.03	988	13:18	40:30.07	177:12.43	1371	20:02	40:02.19	178:09.81	722
318	ROV	8		18.03.	20:15	40:01.89	178:09.73	661	22:45	40:1.94	178:9.63	662	23:55	40:01.91	178:09.56	657
319	CTD	69	Faure site	19.03.	23:56	40:01.91	178:09.56	659	1:01	40:01.92	178:09.68	660	1:18	40:01.94	178:09.67	662
320	CTD	70	Faure site	19.03.	1:18	40:01.94	178:09.67	662	3:03	40:1.92	178:9.69	660	5:33	40:01.91	178:09.67	662
321	CTD	71	Faure site	19.03.	6:00	40:02.80	178:03.12	1090	6:56	40:02.82	178:09.12	1091	7:21	40:02.82	178:09.10	1091
322	Multi-beam			19.03.	7:50	40:03.39	178:10.42	749	13:16	40:1.94	178:7.37	1073	18:21	40:03.07	178:11.12	667
323	CTD	72		19.03.	19:00	40:03.72	178:08.60	1258	19:30	40:03.74	178:08.57	1269	19:59	40:03.74	178:08.54	1266
324	CTD	73		19.03.	20:41	40:05.522	178:07.478	1584	22:12	40:05.55	178:07.47	1582	22:47	40:05.542	178:07.483	1582
325	Multi-beam			20.03.	0:35	39:55.92	178:31.26	2743	2:24	39:38.74	178:28.16	1367	4:24	39:19.89	178:27.34	1132

- 12 Appendices (electrical)**
- 12.1 Captain's report Leg 1 (Winch operation, Station book)**
- 12.2 Captain's report Leg 2 (Winch operation, Station book)**
- 12.3 Captain's report Leg 3 (Winch operation, Station book)**
- 13 Press clippings (electrical)**



IFM-GEOMAR

Leibniz-Institut für Meereswissenschaften
an der Universität Kiel

Das Leibniz-Institut für Meereswissenschaften
ist ein Institut der Wissenschaftsgemeinschaft
Gottfried Wilhelm Leibniz (WGL)

The Leibniz-Institute of Marine Sciences is a
member of the Leibniz Association
(Wissenschaftsgemeinschaft Gottfried
Wilhelm Leibniz).

Leibniz-Institut für Meereswissenschaften / Leibniz-Institute of Marine Sciences

IFM-GEOMAR
Dienstgebäude Westufer / West Shore Building
Düsternbrooker Weg 20
D-24105 Kiel
Germany

Leibniz-Institut für Meereswissenschaften / Leibniz-Institute of Marine Sciences

IFM-GEOMAR
Dienstgebäude Ostufer / East Shore Building
Wischhofstr. 1-3
D-24148 Kiel
Germany

Tel.: ++49 431 600-0
Fax: ++49 431 600-2805
www.ifm-geomar.de

Rücken (nur bei umfangreicheren Dokumenten)

IFM - GEOMAR REPORT Nr. 9 - FS Sonne Fahrtbericht / Cruise Report SO 191 New Vents